NEW ADVANCES IN GENETIC STUDIES TO UNDERSTAND YEAST ADAPTATION TO EXTREME AND FERMENTATIVE ENVIRONMENTS

EDITED BY: Francisco A. Cubillos, Amparo Querol, Cecile Fairhead, Roberto Nespolo and Roberto Pérez-Torrado

PUBLISHED IN: Frontiers in Genetics and Frontiers in Microbiology

frontiers Research Topics

frontiers

ISSN 1664-8714
ISBN 978-2-88966-727-7
DOI 10.3389/978-2-88966-727-7

About Frontiers

Frontiers is more than just an open-access publisher of scholarly articles: it is a pioneering approach to the world of academia, radically improving the way scholarly research is managed. The grand vision of Frontiers is a world where all people have an equal opportunity to seek, share and generate knowledge. Frontiers provides immediate and permanent online open access to all its publications, but this alone is not enough to realize our grand goals.

Frontiers Journal Series

The Frontiers Journal Series is a multi-tier and interdisciplinary set of open-access, online journals, promising a paradigm shift from the current review, selection and dissemination processes in academic publishing. All Frontiers journals are driven by researchers for researchers; therefore, they constitute a service to the scholarly community. At the same time, the Frontiers Journal Series operates on a revolutionary invention, the tiered publishing system, initially addressing specific communities of scholars, and gradually climbing up to broader public understanding, thus serving the interests of the lay society, too.

Dedication to Quality

Each Frontiers article is a landmark of the highest quality, thanks to genuinely collaborative interactions between authors and review editors, who include some of the world's best academicians. Research must be certified by peers before entering a stream of knowledge that may eventually reach the public - and shape society; therefore, Frontiers only applies the most rigorous and unbiased reviews.
Frontiers revolutionizes research publishing by freely delivering the most outstanding research, evaluated with no bias from both the academic and social point of view. By applying the most advanced information technologies, Frontiers is catapulting scholarly publishing into a new generation.

What are Frontiers Research Topics?

Frontiers Research Topics are very popular trademarks of the Frontiers Journals Series: they are collections of at least ten articles, all centered on a particular subject. With their unique mix of varied contributions from Original Research to Review Articles, Frontiers Research Topics unify the most influential researchers, the latest key findings and historical advances in a hot research area! Find out more on how to host your own Frontiers Research Topic or contribute to one as an author by contacting the Frontiers Editorial Office: frontiersin.org/about/contact

NEW ADVANCES IN GENETIC STUDIES TO UNDERSTAND YEAST ADAPTATION TO EXTREME AND FERMENTATIVE ENVIRONMENTS

Topic Editors:
Francisco A. Cubillos, University of Santiago, Chile
Amparo Querol, Consejo Superior de Investigaciones Científicas (CSIC), Spain
Cecile Fairhead, Université Paris-Sud, France
Roberto Nespolo, Austral University of Chile, Chile
Roberto Pérez-Torrado, Consejo Superior de Investigaciones Científicas (CSIC), Spain

Citation: Cubillos, F. A., Querol, A., Fairhead, C., Nespolo, R., Pérez-Torrado, R., eds. (2021). New Advances in Genetic Studies to Understand Yeast Adaptation to Extreme and Fermentative Environments. Lausanne: Frontiers Media SA.
doi: 10.3389/978-2-88966-727-7

Table of Contents

frontiers in Genetics

EDITORIAL
published: 11 March 2021
doi: 10.3389/fgene.2021.663641

Editorial: New Advances in Genetic Studies to Understand Yeast Adaptation to Extreme and Fermentative Environments

Roberto Pérez-Torrado[1]* *and Francisco A. Cubillos*[2,3]*

[1] *Food Biotechnology Department, Instituto de Agroquímica y Tecnología de los Alimentos–Consejo Superior de Investigaciones Científicas, Valencia, Spain,* [2] *Departamento de Biología, Facultad de Química y Biología, Universidad de Santiago de Chile, Santiago, Chile,* [3] *Agencia Nacional de Investigación y Desarrollo (ANID)–Millennium Science Initiative Program–Millennium Institute for Integrative Biology (iBIO), Santiago, Chile*

Keywords: yeast, adaptive evolution, extreme enviroment, fermentation, wine, beer

Editorial on the Research Topic

New Advances in Genetic Studies to Understand Yeast Adaptation to Extreme and Fermentative Environments

OPEN ACCESS

Edited and reviewed by:
Ludmila Chistoserdova, University of Washington, United States

***Correspondence:**
Roberto Pérez-Torrado
rober@iata.csic.es
Francisco A. Cubillos
francisco.cubillos.r@usach.cl

Specialty section:
This article was submitted to Evolutionary and Genomic Microbiology, a section of the journal Frontiers in Genetics

Received: *03 February 2021*
Accepted: *22 February 2021*
Published: *11 March 2021*

Citation:
Pérez-Torrado R and Cubillos FA (2021) Editorial: New Advances in Genetic Studies to Understand Yeast Adaptation to Extreme and Fermentative Environments. Front. Genet. 12:663641. doi: 10.3389/fgene.2021.663641

This Research Topic features recent advances in research on the mechanisms involved in yeast genetic adaptations. It highlights the tremendous importance of using and applying these advances to the enhancement and optimization of industrial fermentative processes. This *Frontiers eBook* includes studies related to the production of some of the most popular drinks, such as wine or beer, by conventional (i.e., *Saccharomyces* sp) and non-conventional yeast species (non-*Saccharomyces* sp). In particular, it includes recent work on the study of yeast physiological adaptations to extreme and fermentative environments aided by the increasing power of new high-throughput phenotyping and sequencing technologies, the latter including genome re-sequencing projects and RNA-seq studies. Yeast adaptations to those environments increases industrial yeasts' diversity and comprises several genetic mechanisms, including horizontal gene transfer (HGT), chromosomal rearrangements, hybridizations, and genome duplications. A literature review on these mechanisms is included in this Research Topic (Giannakou et al.).

An area of significant interest is the physiological study and optimization of yeast to brewing environments. The collection includes a study that highlights the potential of non-conventional yeast, such as *Lachancea fermentati* strains isolated from Kombucha, to produce low alcohol beer (Bellut et al.). Bellut et al. demonstrated the potential of *L. fermentati* to substantially decrease ethanol concentration in beer due to the metabolic deviation toward the production of lactic acid. This work attracted significant attention because of its impact on the generation of low-alcohol drinks, a topic that is currently of research interest in the industry.

In a study focused on brewing yeast optimization, de Vries et al. describe an elegant new methodology to generate strain diversity based on engineering chromosome copy number variation (CCNV) through centromere-silencing. The authors noticed that variable CCNV in industrial *Saccharomyces* generates phenotypic diversity, allowed them to select for ethanol tolerant mutants. Another study in this collection, examining yeast tolerance to high ethanol concentrations in high gravity fermentations, suggests that this tolerance is dependent on the unfolded protein response and proteostasis (Telini et al.), a finding that is in agreement with previous reports (Miyagawa et al., 2014; Navarro-Tapia et al., 2017).

Another topic covered in this *Frontiers eBook* is the identification of genetic and molecular evidence of adaptation and optimization of *Saccharomyces cerevisiae* yeast strains to wine environments. A pivotal study by Devia et al. demonstrates the role of new genes acquired through HGT in wine fermentation. Here, the authors carried out a systematic analysis of the promoter activity and protein levels of 30 genes located within three different horizontally acquired regions found across various wine strains. The authors highlight ORF A9, an ortholog of a thiamine (vitamin B1) transporter, which appears to impact biomass and fermentation capacity traits. These findings are complemented in this collection with a literature review on the adaptive advantages provided by an oligopeptide transporter family acquired in *S. cerevisiae* wine strains by horizontal gene transfer from *Torulaspora microellipsoides* (Becerra-Rodriguez et al.).

Chromosomal rearrangements around *SSU1* promoters are known to provide higher sulfite tolerance to enological *S. cerevisiae* strains under wine environments. In this context, Marullo et al. applied a novel multiplex PCR method (*SSU1* checkup) to analyze nearly 600 wine strains from vineyards and cellars, observing an enrichment of rearranged *SSU1* promoters in commercial strains.

Another hallmark of wine yeasts is efficient nitrogen assimilation. Molinet et al. studied the different *S. cerevisiae* allelic variants of *GTR1*, a GTPase that participates in the EGO complex responsible for *TORC1* activation in response to amino acids availability. The authors conducted a series of elegant experiments, including allelic swapping, and demonstrated that polymorphisms in the coding region of *GTR1* in a specific subpopulation were relevant for TORC1 activity, impacting nitrogen consumption under wine fermentation conditions. In another study on vineyard-associated environments, conducted by Cheng et al., the authors reported a predominance of *S. cerevisiae* and some *S. uvarum* strains in spontaneous Pinot Noir fermentations. The authors identified a specific anthocyanin and flavonoid profile in fermented wines representative of this viticultural area. In another study included in the collection, the molecular underpinning of the velum stage, which is particular to sherry-wines, was also investigated, via RNA-seq (Mardanov et al.). The authors found a complex response during biofilm formation in response to this stressful environment, including strong upregulation of the flocculation gene *FLO11*. Altogether, these studies demonstrate how genetic hallmarks in different yeast strains are responsible for their improved fermentative capacity.

This Research Topic also includes studies on non-conventional yeasts and how HGT can mediate the reestablishment of alcoholic fermentation. The study by Gonçalves et al. on the evolutionary history of the *Wickerhamiella* and *Starmerella* genera (W/S clade) demonstrates that these fructophilic species have a preference to produce mannitol to compensate for a probable ancient loss of capacity to perform alcoholic fermentation.

Finally, the collection includes a review on the cellular responses induced by Msn2-mediated proline incorporation, which represents an important yeast adaptation to many suboptimal environmental conditions (Mat Nanyan and Takagi).

This Research Topic highlights recent key findings on yeast adaptations to extreme and industrial environments. Besides the crucial basic knowledge reported and discussed here, these discoveries can help various industrial processes, such as wine or beer production, by allowing the enhancement and optimization of the yeasts involved in popular food products.

AUTHOR CONTRIBUTIONS

RP-T and FC fulfill the standard requirements for authorship and read and approved the final manuscript. Both authors contributed to the article and approved the submitted version.

FUNDING

RP-T received a grant from the Spanish government PID2019-104113RB-I00. FC is funded by Comisión Nacional de Investigación Científica y Tecnológica CONICYT FONDECYT (1180161) and Millennium Institute for Integrative Biology (iBio).

ACKNOWLEDGMENTS

We thank Dr. Alejandro Montenegro-Montero for editorial support.

REFERENCES

Miyagawa, K. I., Ishiwata-Kimata, Y., Kohna, H., and Kimata, Y. (2014). Ethanol stress impairs protein folding in the endoplasmic reticulum and activates Ire1 in *Saccharomyces cerevisiae*. *Biosci. Biotech. Biochem.* 78, 1389–1391. doi: 10.1080/09168451.2014.921561

Navarro-Tapia, E., Pérez-Torrado, R., and Querol, A. (2017). Ethanol effects involve non-canonical unfolded protein response activation in yeast cells. *Front. Microbiol.* 8:383. doi: 10.3389/fmicb.2017.00383

Conflict of Interest: The authors declare that the research was conducted in the absence of any commercial or financial relationships that could be construed as a potential conflict of interest.

frontiers in Microbiology

ORIGINAL RESEARCH
published: 01 November 2019
doi: 10.3389/fmicb.2019.02510

A New Pathway for Mannitol Metabolism in Yeasts Suggests a Link to the Evolution of Alcoholic Fermentation

*Carla Gonçalves[1†], Carolina Ferreira[1†], Luís G. Gonçalves[2], David L. Turner[2], Maria José Leandro[2], Madalena Salema-Oom[1,3], Helena Santos[2] and Paula Gonçalves[1]**

[1] UCIBIO-REQUIMTE, Departamento de Ciências da Vida, Faculdade de Ciências e Tecnologia, Universidade Nova de Lisboa, Caparica, Portugal, [2] Instituto de Tecnologia Química e Biológica António Xavier, Universidade Nova de Lisboa, Oeiras, Portugal, [3] Centro de Investigação Interdisciplinar Egas Moniz (CiiEM), Instituto Universitário Egas Moniz, Caparica, Portugal

OPEN ACCESS

Edited by:
Amparo Querol,
Spanish National Research Council (CSIC), Spain

Reviewed by:
Raul Raya,
CONICET Centro de Referencia para Lactobacilos (CERELA), Argentina
Elvira Maria Hebert,
National Scientific and Technical Research Council (CONICET), Argentina

***Correspondence:**
Paula Gonçalves
pmz@fct.unl.pt

[†] These authors have contributed equally to this work

Specialty section:
This article was submitted to Evolutionary and Genomic Microbiology, a section of the journal Frontiers in Microbiology

Received: 21 August 2019
Accepted: 18 October 2019
Published: 01 November 2019

Citation:
Gonçalves C, Ferreira C, Gonçalves LG, Turner DL, Leandro MJ, Salema-Oom M, Santos H and Gonçalves P (2019) A New Pathway for Mannitol Metabolism in Yeasts Suggests a Link to the Evolution of Alcoholic Fermentation. Front. Microbiol. 10:2510. doi: 10.3389/fmicb.2019.02510

The yeasts belonging to the *Wickerhamiella* and *Starmerella* genera (W/S clade) share a distinctive evolutionary history marked by loss and subsequent reinstatement of alcoholic fermentation mediated by horizontal gene transfer events. Species in this clade also share unusual features of metabolism, namely the preference for fructose over glucose as carbon source, a rare trait known as fructophily. Here we show that fructose may be the preferred sugar in W/S-clade species because, unlike glucose, it can be converted directly to mannitol in a reaction with impact on redox balance. According to our results, mannitol is excreted to the growth medium in appreciable amounts along with other fermentation products such as glycerol and ethanol but unlike the latter metabolites mannitol production increases with temperature. We used comparative genomics to find genes involved in mannitol metabolism and established the mannitol biosynthesis pathway in W/S-clade species *Starmerella bombicola* using molecular genetics tools. Surprisingly, mannitol production seems to be so important that *St. bombicola* (and other W/S-clade species) deploys a novel pathway to mediate the conversion of glucose to fructose, thereby allowing cells to produce mannitol even when glucose is the sole carbon source. Using targeted mutations and ^{13}C-labeled glucose followed by NMR analysis of end-products, we showed that the novel mannitol biosynthesis pathway involves fructose-6-phosphate as an intermediate, implying a key role for a yet unknown fructose-6-P phosphatase. We hypothesize that mannitol production contributed to mitigate the negative effects on redox balance of the ancient loss of alcoholic fermentation in the W/S clade. Presently, mannitol also seems to play a role in stress protection.

Keywords: alcoholic fermentation, yeast metabolism, mannitol metabolism, *Starmerella*, fructophily

INTRODUCTION

Fungi are excellent models in which to explore the evolution of metabolism, as shown by multiple studies focused chiefly on secondary metabolite production by filamentous fungi (Spatafora and Bushley, 2015; Wisecaver and Rokas, 2015; Theobald et al., 2018; Keller, 2019). Ascomycetous yeasts (Saccharomycotina) produce very few secondary metabolites and are mainly known for their

ability to convert sugars into ethanol, a trait of wide biotechnological relevance. However, central carbon and nitrogen metabolisms are in fact quite diverse in yeasts, accounting for the utilization of very different carbon and nitrogen sources and different regulation of energy production processes (Kurtzman et al., 2011). Comparative genomics of a large and ever-increasing number of yeast genomes is beginning to shed light on the evolution of metabolic traits in this sub-phylum, thus far revealing a general trend of loss of metabolic capabilities that implies a common ancestor metabolically more complex than most extant species (Shen et al., 2018). These losses most often resulted in narrowing spectra of nutrient assimilation, but we reported recently that even a central metabolic feature like alcoholic fermentation, which usually plays a crucial role in the metabolism of yeasts, either as the main pathway for energy production or as a means to circumvent oxygen shortage, was lost in a lineage within the Saccharomycotina currently comprising approximately 100 species belonging to the genera *Wickerhamiella* and *Starmerella* (referred to as the W/S clade) (Gonçalves et al., 2018). An ancestor of this clade seems to have lost the genes required for alcoholic fermentation, encoding pyruvate decarboxylase and alcohol dehydrogenase, which are also absent in at least one extant species, *Candida* (*Wickerhamiella*) *galacta* (Gonçalves et al., 2018). Reinstatement of alcoholic fermentation was subsequently made possible through horizontal acquisition of a bacterial alcohol dehydrogenase, and co-option of a new decarboxylase to accept pyruvate as a substrate (Gonçalves et al., 2018). Alcohol dehydrogenase genes were among the more than 500 bacterial genes detected in W/S-clade genomes. Although this remains to be empirically demonstrated, the unusually high number of horizontally acquired genes in the W/S clade suggests that other aspects of metabolism were also impacted during evolution of the lineage (Gonçalves et al., 2018; Shen et al., 2018; Kominek et al., 2019).

One additional unusual trait in common between W/S-clade species is their preference for fructose over glucose when both carbon sources are present at high concentrations, a trait named fructophily. The preference for fructose relies on a highly unusual specific fructose transporter, Ffz1 (Pina et al., 2004; Leandro et al., 2011, 2014), present only in fructophilic yeasts, which does not belong to the sugar transporter family and was horizontally acquired from filamentous fungi by a W/S-clade ancestor (Gonçalves et al., 2016). Ffz1, like fructophily, is present in most W/S-clade species examined and was shown to be indispensable for preferred fructose metabolism in at least one species in this clade (Gonçalves et al., 2018). However, while Ffz1 ensures that cells can take up large amounts of fructose in a selective manner, it remained unclear why the preferential utilization of fructose was beneficial for W/S-clade yeasts. Most species included in the *Wickerhamiella* and *Starmerella* genera have an ecological association with the floral niche, being often isolated from flowers or insects that visit flowers (Lachance et al., 2001; Canto et al., 2017; de Vega et al., 2017). In floral nectars, overall sugar concentrations are very high and fructose is usually roughly as abundant as glucose, sucrose being frequently the main sugar present (Canto et al., 2017; de Vega et al., 2017). Why, in this kind of environment, fructose assimilation should be more advantageous than that of other equally available sugars remained unknown. However, the metabolism of fructophilic bacteria that are also associated with the floral niche (Endo et al., 2009, 2010; Neveling et al., 2012) provides a useful clue. In fructophilic bacteria, the loss of alcoholic fermentation appeared to be linked to acquisition of fructophily because fructose can function both as carbon source and as an electron acceptor (in a reaction that converts fructose to mannitol), ensuring redox balance in the absence of alcoholic fermentation (Maeno et al., 2016, 2019). Interestingly, some fructophilic yeasts from the W/S clade are also known to produce large amounts of mannitol (Savergave et al., 2013), suggesting a possible link between mannitol metabolism and the evolutionary history of alcoholic fermentation in this lineage. On the other hand, mannitol often plays stress protective roles, namely as compatible solute (Chaturvedi et al., 1996; Solomon et al., 2007; Wyatt et al., 2014; Zahid and Deppenmeier, 2016), and W/S-clade yeasts are known to be osmotolerant (Rosa and Lachance, 1998).

To shed light on the role played by mannitol in the metabolism of W/S-clade yeasts, we used comparative genomics and metabolic characterization of mutants constructed in the genetically amenable W/S-clade species *Starmerella bombicola.*

Our findings suggest that mannitol metabolism was important to the fulfillment of redox balance in the absence of alcoholic fermentation, because direct conversion of fructose into mannitol regenerates $NADP^+$. In support of this, we uncovered a novel biochemical pathway promoting the conversion of glucose to fructose. This pathway, which to our knowledge has not been reported before, enables mannitol production even when glucose is the only sugar available. Hence, we unraveled further the biochemical basis for fructophily in these yeasts and present a model for the evolution of metabolism in the W/S clade in which fructophily is linked to mannitol production and possibly to the ancient loss of alcoholic fermentation in this lineage.

MATERIALS AND METHODS

Yeast Strains and Culture Conditions

St. bombicola PYCC 5882, *Candida magnoliae* PYCC 2903, *Starmerella bacillaris* PYCC 3044, *St. bacillaris* PYCC 6282 and *Wickerhamiella domercqiae* PYCC 3067 were obtained from the Portuguese Yeast Culture Collection (PYCC). *Wickerhamiella versatilis* JCM 5958 was obtained from the Division of Genomic Technologies, RIKEN Center for Life Science Technologies, Japan. All strains were maintained in YPD medium [1% (w/v) yeast extract, 2% (w/v) peptone and 2% (w/v) glucose)].

Assessment of Mannitol Production in W/S-Clade Species

W/S-clade species (*St. bombicola*, *St. bacillaris*, *C. magnoliae, W. domercqiae* and *W. versatilis*) were cultivated in rich medium [YP, 1% (w/v) yeast extract and 2% (w/v) peptone] supplemented with 10% (w/v) glucose or 10% (w/v) fructose at 30°C until late exponential phase (when most of the sugar was consumed). Extracellular concentrations of fructose, glucose

and other extracellular metabolites including mannitol were determined by HPLC using a carbohydrate analysis column (300 mm × 7.8 mm, Aminex HPX-87P, Biorad) and a differential refractometer (LKB 2142). The column was kept at 80°C and H_2O was used as the mobile phase at 0.6 mL min^{-1}. The results were treated and integrated using the software Chromeleon v6.8 (Dionex).

Identification of Genes Involved in Mannitol Biosynthesis in W/S Genomes and Construction of Phylogenies

Genes possibly involved in mannitol biosynthesis, namely mannitol dehydrogenase (*MtDH*), mannitol-1P dehydrogenase (*M1PDH*) and mannitol-1P phosphatase (*MPP*), were searched in W/S-clade genomes by tBLASTx, using as query *MtDH* from *Yarrowia lipolytica* (*YlSDR*, accession number: Q6CEE9.1), *M1PDH* from *Aspergillus fumigatus* (KEY81154.1) and *MPP* from *Saccharina japonica* (AIC75600.1). An *E*-value cutoff of e^{-10} was considered for the tBLASTx search. The best hits were used as queries for BLASTp against the NCBI nr database to identify the closest related protein sequences in other yeasts (Saccharomycotina). No hits were obtained for genes other than *MtDH* and for that reason a detailed Maximum Likelihood (ML) phylogeny was constructed for the protein encoded by this gene. To that end, the top 750 hits BLASTp hits using the Mtdh-like protein from *St. bombicola* in UniprotKB (reference proteomes database) were selected to construct a ML phylogeny. Mtdh sequences from other W/S-clade species were retrieved by tBLASTx searches in local genome databases. The resulting protein sequences were aligned using an iterative refinement method (L-INS-i) in *MAFFT* v.6.956 (Katoh and Standley, 2014) and poorly aligned regions were removed with the *trimAl* (Capella-Gutierrez et al., 2009) software using the 'gappyout' option. An ML phylogeny was constructed with *IQ-TREE* v 1.4.3 (Nguyen et al., 2015) using the ultra-fast bootstrap method and the LG + I + G model of substitution (found as the best-fitting model). Accession numbers for W/S-clade genomes are the following: GCA_003033765.1 (*St. bacillaris* PYCC 3044), GCA_001005415.1 (*Candida apicola* NRRL Y-50540), GCA_003033435.1 (*St. bombicola* PYCC 5882), GCA_003033705.1 (C. *magnoliae* PYCC 2903), GCA_001600375.1 (*W. domercqiae* PYCC 3067), GCA_001005415.1 (*W. versatilis* JCM 5958) and NW_020193984.1 (*Wickerhamiella sorbophila* DS02). Complete phylogeny and alignment files can be accessed in figshare (doi: 10.6084/m9.figshare.9959693).

Construction of *Starmerella bombicola* Deletion Mutants

Construction of deletion mutants was performed as described in Gonçalves et al. (2018). For *mtdh1*Δ and *mtdh2*Δ, the coding sequence (CDS) with ∼1 kb upstream and downstream were amplified from genomic DNA using the primer pairs listed in **Supplementary Table S1**. For the double mutant (*mtdh1*Δ*mtdh2*Δ), the same strategy was used as the two genes are located next to each other in the genome separated by a small intergenic region (∼1 kb). The three disruption cassettes were subsequently used to transform *St. bombicola* PYCC 5882 as previously described in Gonçalves et al. (2018). Two different transformants from each gene disruption transformation were subsequently used for the phenotypic assays.

For the construction of *mtdh1*Δ*sor1*Δ, the *SOR1* gene was searched in the genome of *St. bombicola* PYCC 5882 using *Y. lipolytica* sorbitol dehydrogenase as query (XM_503864.1). The putative *SOR1* gene was deleted in the *mtdh1:HYG* background using a zeocin resistance cassette (consisting in the *ble* gene from *Staphylococcus aureus* under control of the *GPD* promoter from *St. bombicola* and the *CYC* terminator from *Saccharomyces cerevisiae*). Transformants were selected in YPD plates (pH = 6.8) supplemented with 650 μg/mL zeocin (Invivogen, San Diego, CA, United States). For the construction of the *hxk1*Δ*glk1*Δ mutant, *HXK1* and *GLK1* from *S. cerevisiae* (YCL040W and YFR053C) were used to search for the respective orthologs in *St. bombicola* PYCC 5882 genome. A similar strategy as aforementioned was employed, starting with the construction of the *glk1:ZEO* mutant followed by disruption of the *HXK1* in the *glk1:ZEO* background using a hygromycin resistance cassette.

Enzymatic Assays

For the preparation of cell-free extracts, the cells were collected by centrifugation (3,000 × *g* for 5 min), washed twice with cold 100 mM Tris-HCl buffer (pH = 7.5) and disrupted with glass beads in 500 μL of Lysis Buffer (0.1 M triethanolamine hydrochloride, 2 mM $MgCl_2$, 1 mM DTT and 1 μM PMSF) with six cycles of 60 s vortex-ice. Cell debris were removed by centrifugation at 4°C, 16,000× *g* for 20 min and the cleared raw extracts were stored at −20°C. Protein was quantified using the QUBIT fluorimeter following the manufacturer's guidelines. The mannitol dehydrogenase (Mtdh) assay was performed in both the reductive and the oxidative directions at 25°C. For the oxidative reaction, 500 μL of reaction mixture was used containing 50 mM Tris-HCl (pH = 8.5), 1 mM of NADH or NADPH and 25 μL of protein extract (200–500 ng/μL of total protein). The reaction was started by the addition of fructose to a final concentration of 200 mM and oxidation of NADH or NADPH was monitored by the decrease in absorbance at 340 nm. For the reductive reaction, 50 mM of Tris-HCl (pH = 10) buffer and 1 mM of NAD^+ or $NADP^+$ were used instead. The reaction was started by adding mannitol to a final concentration of 50 mM and reduction of NAD^+ or $NADP^+$ was monitored by the increase in absorbance at 340 nm.

For the hexokinase assay (used as a control for the quality of the extracts when testing for the lack of Mtdh activity in the *St. bombicola mtdh* deletion mutants), a reaction mixture was prepared containing 50 mM Tris buffer (pH = 7.5), 10 mM $MgCl_2$, 1 mM ATP, 1 mM $NADP^+$, 0.2 U of glucose-6-P dehydrogenase (Sigma Aldrich, St. Louis, MO, United States) and 1 U phosphoglucose isomerase (Sigma Aldrich, St. Louis, MO, United States). Enzymatic assays were performed at 25°C

in a total volume of 500 μL and 25 μL of cell-free extract (200–500 ng/μL of total protein) was used. The reaction was started by the addition of fructose to a final concentration of 100 mM and reduction of $NADP^+$ was monitored spectrophotometrically by the increase in absorbance at 340 nm for 2 min.

For the detection of $NADP^+$-dependent glycerol dehydrogenase activity a reaction mixture containing 50 mM Tris-HCl (pH = 8.5) buffer, 1 mM $NADP^+$ and 25 μL of cell-free extract was prepared. The reaction was started by the addition of 100 mM of glycerol, and NADPH formation was monitored spectrophotometrically for 2 min.

For the detection of glucose isomerase activity, a protocol based on Sayyed et al. (2010) was used. Cells of both the wild type *St. bombicola* and the *mtdh1*Δ*mtdh2*Δ mutant were cultivated for 24 or 76 h in YP supplemented with 20% (w/v) of glucose and cell-free extracts were obtained as described above. Glucose isomerase activity was measured in a 2.4 mL reaction mixture containing 20–50 μg of total protein, 0.5 mL 50 mM of KPi (pH = 7.2), 2 mM $CaCl_2$, 20 mM glucose, 10 mM $MgSO_4.7H_2O$. Different temperatures (25, 30, and 60°C) and reaction times (1, 3, and 24 h) were tested. The eventual formation of fructose was assessed by HPLC.

For the detection of fructose-6-phosphate phosphatase activity, the *mtdh1*Δ*mtdh2*Δ mutant was grown in YP medium supplemented with 20% (w/v) glucose for 24 h at 25°C. Cell-free extracts were obtained as previously described. A solution containing 20–50 μg of total protein was incubated at 25°C in 100 mM of Tris Buffer (pH = 7.5) for 3 min. The reaction was started by the addition of fructose-6-phosphate to a final concentration of 50 mM or glucose-6-phosphate (used as a control) and left to proceed for 25 min. Two controls were also included, one in which no substrate was added and another one in which no extract was added. 300 μL samples were taken at different time points (0, 5, 10, and 20 min) and were immediately subjected to a procedure for the detection of inorganic phosphate based on Ames (1966). Briefly, 700 μL of a reagent mix (consisting in six parts of a solution of 0.42% (w/v) ammonium molybdate prepared in 1 N H_2SO_4 and one part of a solution of 10% (w/v) ascorbic acid prepared in milli-Q water) was added to each of the samples. The reaction was left to proceed for 1 h at 37°C. Absorbance at 820 nm was then measured.

Growth Assays and Sugar Consumption

For growth assays, *St. bombicola* wild type and *MtDH* deletion mutants were pre-grown overnight in 100 mL flasks containing 20 mL of culture medium at the temperature of choice. This inoculum was diluted to OD_{640} = 0.2 in 30 mL of YP (1% (w/v) yeast extract and 2% (w/v) peptone) supplemented with the different carbon sources tested in 250 mL flasks. Growth was monitored for 96–150 h.

To assess sugar consumption and metabolite production, wild type, *mtdh1*Δ and *mtdh1*Δ*mtdh2*Δ were grown as described before in YP supplemented with 10% (w/v) glucose and 10% (w/v) fructose at 30°C. Samples of 1 mL were collected from culture supernatants, centrifuged at 16,000 x *g* for 1 min and analyzed by HPLC as described previously. Data was visualized using GraphPad Prism version 6 for Windows, GraphPad Software, San Diego, CA, United States, www.graphpad.com.

Quantification of Extracellular and Intracellular Metabolites

Starmerella bombicola wild type was cultivated for 72 h in 30 mL of YP medium supplemented with 10% (w/v) fructose and 10% (w/v) glucose (20FG medium) at 20, 25, and 30°C at 180 r.p.m. After this period, cells were harvest by centrifugation (4°C, 10 min, 8,000 × *g*) and 1 mL of supernatant was collected to quantify extracellular metabolites by HPLC as described previously.

Cell-free extracts for intracellular metabolite analysis were obtained as described for the enzymatic assays. The samples were filtered using a nylon filter with a pore diameter of 0.2 μm and subsequently eluted with 0.6 M NaOH at 0.4 mL/min at 25°C in a CarboPac MA1 column and the peaks were identified with a pulsed amperometric detector.

To determine the total dry weight 2 mL of culture broth were centrifuged for 5 min at 9,000 × *g*. Pellets were washed twice and resuspended in distilled water. The suspension was filtered onto a nitrocellulose filter with a pore diameter of 0.45 μm and was dried at 80°C until a constant weight was attained.

To estimate the intracellular concentration of mannitol per cell (mM), the total amount of mannitol in the cell-free extracts was determined and divided by the number of cells used to produce the extract. We estimate that the volume of one cell of *St. bombicola* would be $\sim 4 \times 10^{-10}$ mL [half the volume of *S. cerevisiae*, Zakhartsev and Reuss (2018)]. Statistical significance was tested using a one-way ANOVA using the Bonferroni's correction for multiple testing, implemented in GraphPad Prism v6.

^{13}C-NMR Analysis of ^{13}C-Labeled Glucose Metabolism by Resting Cells

Cells were grown in YP medium supplemented with 20% (w/v) glucose (YP20G) for 24 h at 30°C. Cells were harvested, washed twice with 50 mM KPi buffer (pH = 7) and kept on ice. The cells were resuspended in 5 mL of KPi buffer (50 mM, pH = 7), to a final $OD_{640}\sim$50. The cell suspension was incubated at 30°C and approximately 50 mM of [1-^{13}C]glucose or [2-^{13}C]glucose was provided at time point zero; aliquots of 750 μL were withdrawn at different time points (0, 15, 30, 45, 60, and 120 min). The collected samples were centrifuged, and the supernatant solutions stored at −20°C until further analysis. NMR samples were prepared by adding 75 μL of deuterated water containing trimethylsilylpropanoic acid (TSP, final concentration of 0.44 mM) to 475 μL of each supernatant solution. All spectra were acquired at 30°C in a Bruker Avance II$^+$ 500 spectrometer, equipped with a 5 mm TCI H/C/N Prodigy Cryoprobe. For each sample the following spectra were acquired: one-dimensional ^{1}H-NMR (noesygppr1d, 64 free induction decays, with 64 k complex points, spectral window of 20 ppm, 5 s relaxation delay and 10 ms mixing time); ^{13}C-NMR with inverse gated proton decoupling (zgig, 1k free induction decays, with 64 k complex points, spectral window

of 248.5 ppm and 60 s relaxation delay). Whenever needed for spectral assignment, extra spectra were acquired: quantitative ^{1}H-NMR spectra (zgprde, 64 free induction decays, with 64 k complex points, spectral window of 20 ppm, 4 s relaxation delay and 60 s extra relaxation delay) and two-dimensional ^{13}C-^{1}H HSQC spectra (hsqcetgpsisp2 pulse sequence, 256 points in F1 and 2048 points in F2; 32 free induction decays; relaxation delay of 1.5 s; sweep width of 25153.695 Hz in F1 and 8012.820 Hz in F2). Spectra acquisition and processing was performed using TopSpin 3.2. The concentration of β-[2-^{13}C]glucose and [2-^{13}C]ethanol was determined in the fully relaxed ^{1}H-NMR spectra using the TSP signal as an internal concentration standard; this information was used to determine ^{13}C concentrations from ^{13}C-NMR spectra. Assignment of spectra was performed resorting to the HMDB[1] and BMRB[2] databases.

Analysis of Metabolic Fluxes

The essential features of the model required for flux analysis were determined by the metabolites which were observed (shown in bold in **Figure 3B**) and the standard routes into the TCA cycle. The appearance of significant amounts of fructose with reversed label (e.g., [6-^{13}C]fructose from [1-^{13}C]glucose) required the inclusion of a reverse flux from the triose pool to fructose. Numerical values were obtained by assuming that the fructose concentration reached an approximate steady state after 30 min, i.e., that the fluxes into and out of the fructose pool are then equal. The ratio of original and reversed label is then given by $(2 \times f_{IN} + f_R)/f_R$, where f_R is the back-flux and f_{IN} is the inward flux of labeled glucose, obtained from its approximately linear consumption.

The flux through the pentose phosphate pathway (PPP) was obtained from the concentrations of [1-^{13}C]fructose and [1,3-^{13}C]fructose observed in experiments starting with [2-^{13}C]glucose. In the first cycle of PPP, three molecules of [2-^{13}C]glucose will produce one of [1-^{13}C]fructose-6-P and one of [1,3-^{13}C]fructose-6-P. The mole fractions of fructose with carbon 1, 2 or 5 labeled (m_1, m_2 and m_5) are approximately constant, and reflects its origin either directly from [2-^{13}C]glucose (with back-flux) or via PPP. The flux into PPP is then $1.5\ m_1 f_{IN}/(1.5\ m_1 + m_2 + m_5)$, allowing for the production of two fructose molecules from three of glucose in PPP. Consumption of [1,3-^{13}C]fructose in a second PPP cycle produced a small amount of [2,3-^{13}C]fructose which was not used in the estimation of fluxes. A small but significant amount of [3-^{13}C]fructose was also generated but its origin remains obscure.

RESULTS

Identification of Putative Mannitol Biosynthetic Genes in W/S-Clade Species

Mannitol production in appreciable amounts, an unusual feature in yeasts, was previously detected in at least one W/S-clade species, *C. magnoliae* (Baek et al., 2003; Lee et al., 2003). To find out whether mannitol production is a widespread trait in the W/S clade, we quantified mannitol in the culture supernatants of representatives of five W/S-clade species, namely *C. magnoliae*, *St. bacillaris*, *St. bombicola*, *W. domercqiae* and *W. versatilis*, cultivated in rich medium containing either 10% glucose or 10% fructose as carbon and energy source. We found that all species but one produced variable amounts of mannitol in addition to ethanol and glycerol, and that more mannitol was produced from fructose than from glucose (**Figure 1A**). In *St. bacillaris* neither of the two strains tested (PYCC 3044 and PYCC 6282) produced mannitol; in this species glycerol, erythritol and ethanol were produced instead.

In fungi, mannitol can be produced from fructose through two distinct pathways. The first, usually found in filamentous fungi (Solomon et al., 2007), involves the NADH dependent conversion of fructose-6-phosphate (fructose-6-P) to mannitol-1-phosphate (mannitol-1P), followed by dephosphorylation to yield mannitol. The second, previously shown to operate in the oleaginous yeast *Y. lipolytica* (Napora et al., 2013), involves the direct conversion of fructose to mannitol through an NADPH dependent mannitol dehydrogenase (**Figure 1B**). The two pathways may coexist, in which case they form a cycle that may interconvert NAD(H) and NADP(H) (Hult et al., 1980). The fact that W/S-clade species produce mannitol when glucose is the only carbon and energy source, suggests that the pathway involving the conversion of fructose-6-P to mannitol-1P is operating in these yeasts, since the direct conversion pathway is specific for fructose. This specificity was demonstrated for the purified mannitol dehydrogenase from W/S-clade species *C. magnoliae* (Lee et al., 2003).

To obtain a first insight into the pathway(s) involved in mannitol production in the W/S clade, the genomes of six W/S-clade species were surveyed for the presence of genes likely to encode components of the mannitol biosynthetic pathways. Hence, tBLASTx searches were performed using available fungal protein sequences for the various components of the mannitol biosynthetic pathways as queries. The results (**Supplementary Table S2**) showed that genes encoding mannitol-1P dehydrogenase and mannitol-1P phosphatase seem to be absent in all genomes examined, leading to the unanticipated conclusion that in the W/S clade biosynthesis of mannitol from glucose most probably does not proceed through the pathway involving these two enzymes. On the contrary, homologs of the *Y. lipolytica* mannitol dehydrogenase (*YlSDR*) gene responsible for the direct conversion of fructose to mannitol (Napora et al., 2013; Dulermo et al., 2015) were readily found in all genomes examined. Among the genes identified was the previously characterized *MtDH1* from *C. magnoliae* (Lee et al., 2003). In *St. bombicola,* we also found next to *MtDH1* gene (**Supplementary Figure S1**), a second, very similar gene (encoding a protein with ∼63% similarity to Mtdh1) that we named *MtDH2*.

To shed light on the evolutionary origin of the Mtdh-like proteins identified in W/S-clade genomes, a ML phylogeny was

[1] www.hmdb.ca

[2] http://www.bmrb.wisc.edu/metabolomics/database

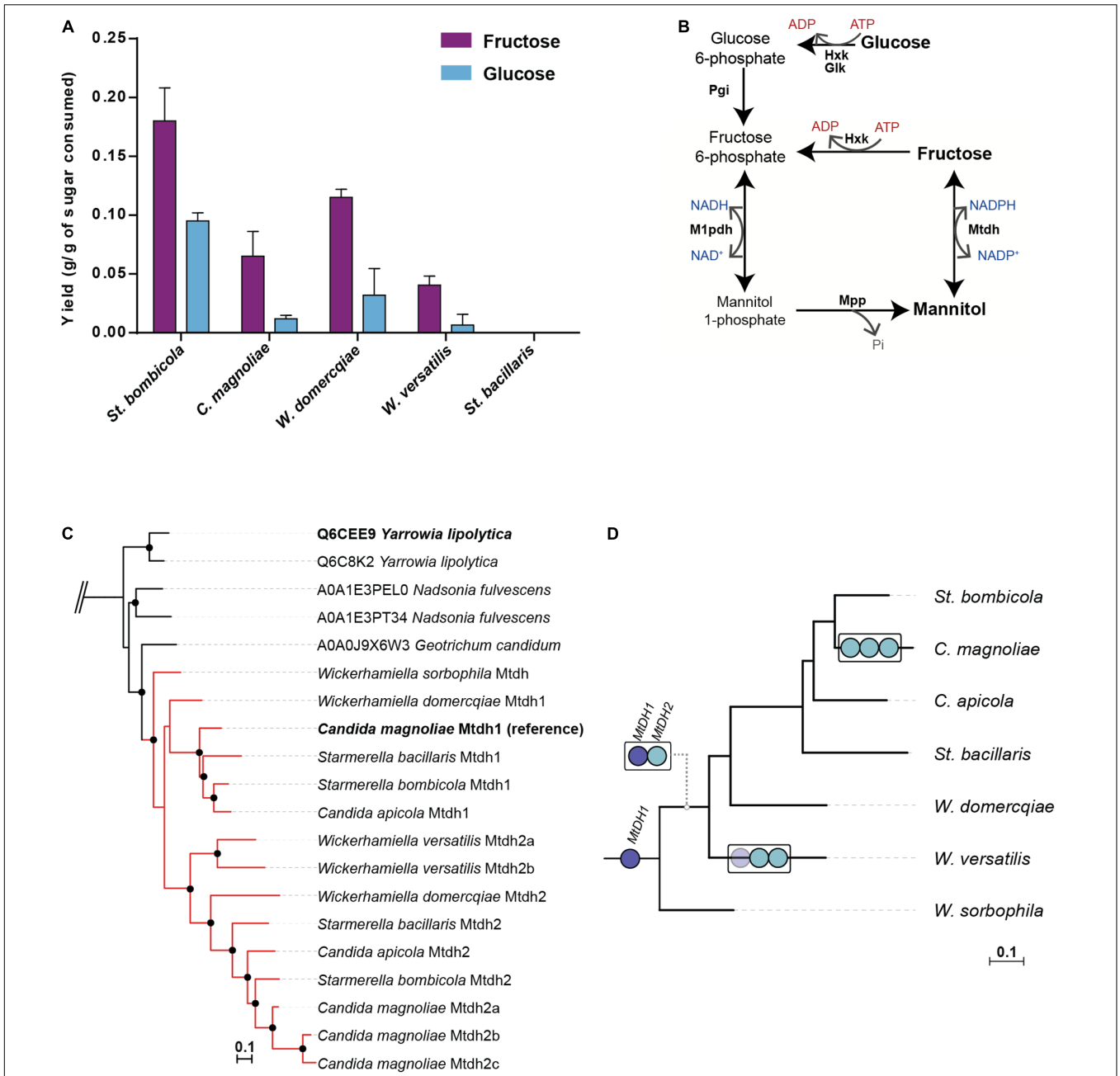

FIGURE 1 | Mannitol production and phylogenetic analyses of mannitol-related genes in W/S-clade species. **(A)** Mannitol yields determined after 72–150 h of growth on YP medium supplemented with 10% (w/v) glucose or 10% (w/v) fructose at 30°C in several W/S-clade species (*Starmerella bombicola*, *Candida magnoliae*, *Starmerella bacillaris*, *Wickerhamiella domercqiae* and *Wickerhamiella versatilis*). Assays were performed in duplicate and the error bars represent the standard deviation. **(B)** Mannitol biosynthetic pathways in Fungi as described by Hult et al. (1980). Glk – Glucokinase, Hxk – Hexokinase, Pgi – Phosphoglucose isomerase, Mtdh – mannitol dehydrogenase, Mpp – mannitol-1-phosphate phosphatase, M1pdh – mannitol-1-phosphate dehydrogenase. **(C)** Pruned Maximum Likelihood (ML) phylogeny of Mtdh-like proteins using the top 750 hits (UniprotKB database) to *St. bombicola* Mtdh1. Branches with support higher than 95% are indicated by black dots. W/S-clade proteins are shown in red. Complete phylogeny can be accessed in Figshare doi: 10.6084/m9.figshare.9959693. **(D)** Schematic representation of the phylogenetic relationships between W/S-clade species based on Gonçalves et al. (2018). *MtDH* genes are represented by blue circles (dark blue- *MtDH1*, light blue- *MtDH2*). The duplication events are represented by white boxes in the respective branches in which they were assumed to have occurred. In *W. versatilis*, *MtDH1* seems to have been lost (faded dark blue circle).

constructed including all the Mtdh proteins identified in W/S-clade genomes as well as the 750 best BLASTp hits in UniprotKB (reference proteomes database) obtained using *St. bombicola* Mtdh1 as a bait (**Figure 1C**). This phylogeny suggests that Mtdh1 and Mtdh2 are derived from a duplication event that took place in a common ancestor of the W/S clade (**Figure 1D**).

Each examined species possesses a single gene of each type, with the exception of *C. magnoliae,* which possesses three *MtDH2*-like genes and *W. versatilis* that lacks the *MtDH1* gene. *Wickerhamiella sorbophila* (formerly *Candida infanticola)* does not exhibit the duplication (**Figures 1C,D**).

Direct Conversion of Fructose to Mannitol in W/S-Clade Yeasts

Comparative genomic analyses showed in the previous section that W/S-clade genomes encoded two (or more) putative paralogous mannitol dehydrogenases, which potentially catalyze the interconversion between fructose and mannitol. To consubstantiate this finding and demonstrate that mannitol is produced directly from fructose in W/S-clade species, we assayed Mtdh activity in cell-free extracts of the species under study. In line with the absence of mannitol in culture supernatants, no Mtdh activity was detected in *St. bacillaris* irrespective of the cofactor (NADH or NADPH) used, although the *MtDH1* and *MtDH2* genes are also present in this species (**Figure 1C** and **Supplementary Figure S1**). For all other W/S-clade species, NADPH-dependent Mtdh activity was readily detected (**Supplementary Figure S2**), while no activity could be measured when NADH was supplied as a cofactor. *St. bacillaris* does not produce mannitol but rather glycerol and erythritol. Interestingly, in *St. bacillaris* glycerol synthesis involves $NADP^+$ recycling since it requires NADPH as cofactor (**Supplementary Figure S2B**) while in the other W/S-clade species this cofactor was apparently not used.

Genetic Dissection of Mannitol Production in *St. bombicola*

In order to find out which of the two *MtDH* genes, if any, was responsible for mannitol production in W/S-clade yeasts, single and double *MtDH* deletion mutants were constructed in the genetically amenable species *St. bombicola,* which encodes one Mtdh1 and one Mtdh2. As shown in **Figure 2**, in the *mtdh1*Δ and *mtdh1*Δ*mtdh2*Δ mutants no mannitol was detected in culture supernatants (**Figure 2A**) and no mannitol dehydrogenase activity could be measured in cell free extracts of *mtdh1*Δ (**Figure 2C**), suggesting that Mtdh1 is the main enzyme responsible for mannitol synthesis in this yeast. This agrees with the fact that mannitol biosynthesis seems to be unaffected in the *mtdh2*Δ mutant (**Figure 2A**).

Notably, mannitol production from glucose is also hampered in the mutants lacking *MtDH1* (**Figure 2B**). This result can only be explained by the existence of a yet unknown pathway mediating conversion of glucose to mannitol. Our genetic evidence suggests that such a pathway must include the reaction catalyzed by Mtdh1. Corroborating this, we found considerable amounts of fructose (∼10 g/L; **Figure 2B**) in the culture supernatants of *mtdh1*Δ and *mtdh1*Δ*mtdh2*Δ mutants cultivated on glucose. Therefore, we conclude that fructose is an intermediate in a novel pathway responsible for the biosynthesis of mannitol from glucose in *St. bombicola* and that fructose accumulates and is excreted when the fructose —> mannitol conversion is genetically prevented.

Conversion of Glucose to Fructose in W/S-Clade Yeasts

To examine whether the observed conversion of glucose to fructose was likely to be occurring as well in wild type *St. bombicola*, we examined the culture supernatants of the wild type strain for the presence of fructose. Although in much lower amounts than in the *mtdh1*Δ mutant (∼0.24 g/L in the wild type vs. ∼10 g/L in the mutant), fructose could also be detected in the supernatants of the wild type strain cultivated on 200 g/L glucose. The same was observed for wild type *W. versatilis* (1 g/L fructose detected by HPLC after ∼200 h of growth at 30°C), another W/S-clade species that produces mannitol (**Figure 1A**), showing that the glucose to fructose conversion was not an artifact of the *St. bombicola* mutant. Instead, this reaction seems to be part of a new pathway likely shared by W/S-clade yeasts that produce mannitol from glucose.

Conversion of glucose to fructose has not been described in yeasts so far but many bacteria and a few fungal species conduct this direct conversion using a glucose isomerase, an enzyme of exceptional biotechnological interest (Bhosale et al., 1996). Examples in fungi are found in species belonging to the genera *Piromyces* (Lee et al., 2017), *Aspergillus* (Sayyed et al., 2010) and *Penicillium* (Kathiresan and Manivannan, 2006). We searched for the presence of a glucose isomerase in the *St. bombicola* genome and the genomes of other W/S-clade species using fungal and bacterial glucose isomerases as queries in tBLASTx searches (AJ249909.1 and FJ858195.1, respectively), but no candidate genes could be found (*e*-value $>1e^{-3}$, **Supplementary Figure S3**). Importantly, we also failed to detect glucose to fructose conversion in cell free extracts.

Since no evidence could be found for the presence of a gene encoding a glucose isomerase, we searched for other known biochemical routes that could potentially be used by *St. bombicola* to produce fructose from glucose. A two-step conversion can be envisioned involving an aldose reductase to convert glucose to sorbitol and then a sorbitol dehydrogenase to convert sorbitol to fructose (**Supplementary Figure S3A**), a pathway that has been previously described (Muntz and Carroll, 1960). A candidate gene for a sorbitol dehydrogenase could be readily retrieved from the genome of *St. bombicola* by tBLASTx using a sorbitol dehydrogenase sequence from *Y. lipolytica* (YALI0E12463, XM_503864.1) while the results for the aldose reductase (XM_502540.1) were not clear (**Supplementary Figure S3B**). Nevertheless, disruption of the sorbitol dehydrogenase (*SOR1*) gene in *St. bombicola* was performed and we observed that this mutant was unable to grow on sorbitol as carbon source confirming the presumed function of the *St. bombicola* Sor1 protein. However, deletion of *SOR1* in the *mtdh1*Δ mutant background (*mtdh1*Δ*sor1*Δ) did not affect glucose conversion to fructose, since similar

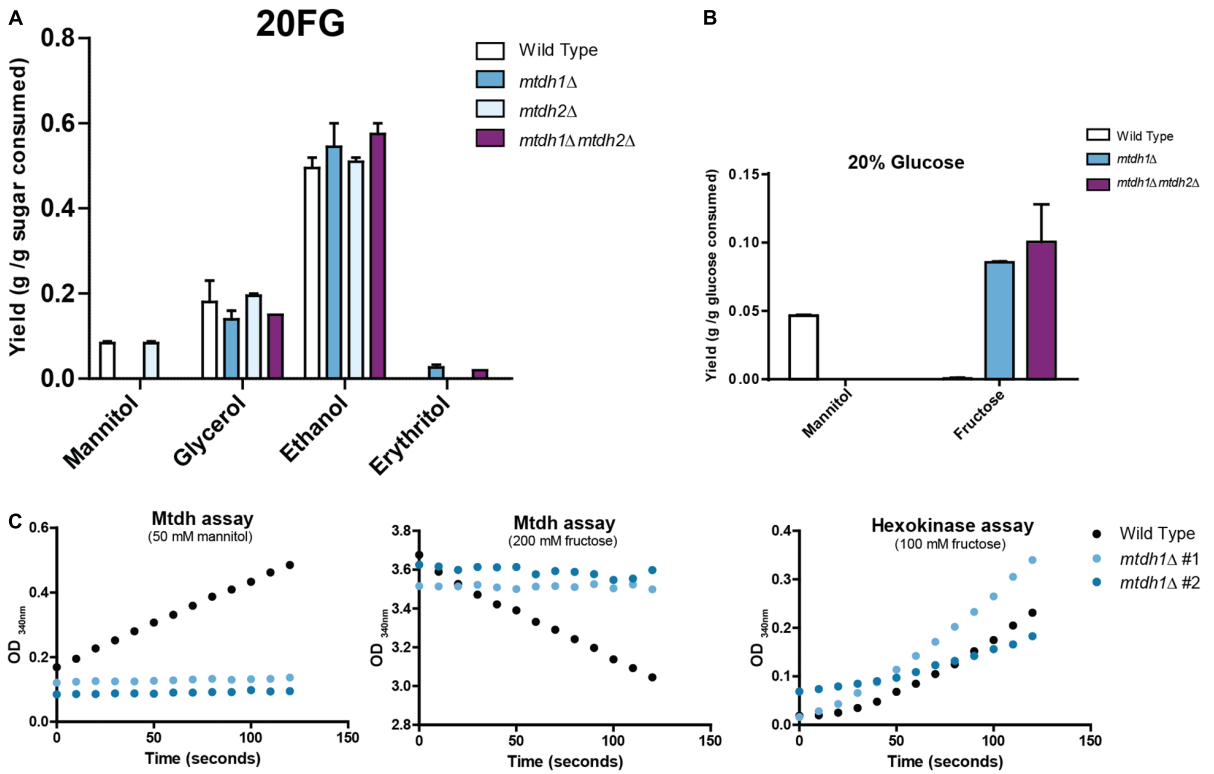

FIGURE 2 | Metabolite production and mannitol dehydrogenase (Mtdh) activities in *St. bombicola* wild type and deletion mutants. **(A)** Metabolite production in *St. bombicola* wild type and deletion mutants (*mtdh1*Δ, *mtdh2*Δ, *mtdh1*Δ*mtdh2*Δ) cultivated in YP supplemented with 10% (w/v) glucose and 10% (w/v) fructose (20FG) at 30°C for 76 h. **(B)** Mannitol and fructose production in *St. bombicola* wild type, *mtdh1*Δ, *mtdh1*Δ*mtdh2*Δ cultivated in YP medium supplemented with 20% (w/v) glucose at 30°C for 76 h. **(C)** Mtdh activities in cell-free extracts of wild type *St. bombicola* (black dotted line) and *mtdh1*Δ (blue lines represent two biological replicates). The hexokinase assay served as a control for the quality of the extracts.

levels of fructose were measured in the supernatants of the *mtdh1*Δ and *mtdh1*Δ*sor1*Δ mutants (∼10 g/L and ∼8 g/L, respectively) leading to the conclusion that this pathway is not involved in the conversion. Finally, we considered the possibility that fructose might be generated by dephosphorylation of the glycolytic intermediate fructose-6-phosphate (fructose-6P). Very few references are found in the literature to fructose-6P phosphatases in fungi but the activity has been studied in connection with mannitol metabolism in mushrooms (Kulkarni, 1990). Since genes that can be used as baits in tBLASTx searches are unavailable, we decided to use ^{13}C-labeled glucose and NMR analysis of end-products to obtain definite evidence for the occurrence of this novel metabolic pathway.

A Fructose-6-Phosphate Phosphatase Is the Key to Mannitol Production From Glucose

To trace the metabolic fate of glucose in the *mtdh1*Δ*mtdh2*Δ mutant, where considerable accumulation of fructose in the growth medium was observed, we first established that resting cells of this mutant, pre-grown on glucose and resuspended in phosphate buffer, produced ∼3 g/L of fructose when given a glucose pulse (∼50 mM). We subsequently performed similar experiments but using pulses of ^{13}C-glucose labeled on C_2 ([2-^{13}C]glucose) or labeled on C_1 ([1-^{13}C]glucose) to allow for tracing the metabolic fate of glucose by NMR. The label from [2-^{13}C]glucose was retrieved mainly in fructose and ethanol (**Figure 3A** and **Supplementary Table S3**); minor amounts of [2-^{13}C]pyruvate, [1-^{13}C]acetate, [2-^{13}C]glycerol and [2-^{13}C]dihydroxyacetone were also detected (**Supplementary Table S3**). If a direct conversion of glucose into fructose would occur, [1-^{13}C]glucose and [2-^{13}C]glucose would yield exclusively [1-^{13}C]fructose and [2-^{13}C]fructose, respectively. However, the fructose pool contained a substantial fraction (∼10%) of [6-^{13}C]fructose derived from [1-^{13}C]glucose and [5-^{13}C]fructose from [2-^{13}C]glucose (**Figure 3A** and **Supplementary Table S3**). This label diversion implies the occurrence of a reversed flux from the triose phosphate pool toward fructose-1,6-bisphosphate through aldolase (**Supplementary Figure S4**) and has been amply illustrated in early *in vivo* ^{13}C-NMR studies of central metabolism in *Lactococcus lactis* (Neves et al., 1999). This reversed flux is especially apparent when there is a metabolic constraint such as that created by a deficiency in activities that are key for the fulfillment of the redox balance (Neves et al., 2000). In the case of *St. bombicola* the observed label diversion unequivocally shows that there is fructose-6P phosphatase

activity in addition to the gluconeogenic enzyme, fructose-bisphosphatase; unfortunately, we were unable to detect such activity in crude cell-free extracts of the *mtdh1*Δ*mtdh2*Δ using a standard methodology for detection of inorganic phosphate (Ames, 1966).

While these results show that a phosphatase is implicated in the conversion of glucose to fructose in *St. bombicola*, they do not exclude the involvement of an isomerase (see **Supplementary Figure S4**). To investigate this, we constructed a *St. bombicola* mutant in which the hexokinase (*HXK1*) and glucokinase (*GLK1*) genes were disrupted, completely precluding hexose phosphorylation. We envisaged that in this mutant, glucose to fructose conversion could still take place only if an isomerase was involved, but not if a fructose-6P phosphatase was required (**Supplementary Figure S5A**). When the *hxk1*Δ*glk1*Δ mutant was grown in 10 g/L glycerol and 10 g/L fructose, mannitol was normally produced yielding ∼10 g/L (**Supplementary Figure S5B**). On the other hand, when the mutant was grown in a mixture of glycerol and glucose no mannitol or fructose production and no glucose consumption were observed (**Supplementary Figure S5B**), indicating that the inability to produce fructose-6P impedes mannitol formation from glucose and that the direct conversion of glucose to fructose, if present, is negligible and undetectable using this methodology. Altogether, our results led us to postulate that in *St. bombicola* glucose is converted into fructose via the intermediate metabolites glucose-6P and fructose-6P and the action of a yet unknown fructose-6P phosphatase.

On the basis of the ^{13}C-labeling patterns observed on the fructose pool the relevant carbon fluxes around the fructose-6P node were estimated (**Figure 3B**; for details on flux analysis see section "Materials and Methods"). Glucose was consumed at a rate of 1.47 ± 0.22 mM/min while fructose was produced at a rate of 0.68 ± 0.16 mM/min. The flux from fructose-6P toward the Pentose Phosphate Pathway (f_{PPP}) was small, only 0.08 mM/min. On the other hand, the reversed flux from the triose phosphate pool to fructose-6P was about half (48%) of the forward glycolytic flux. It is worth noting that there is a substantial flux from fructose-6P to fructose, in fact amounting to 86% of the net flux from fructose-6P to glycolysis.

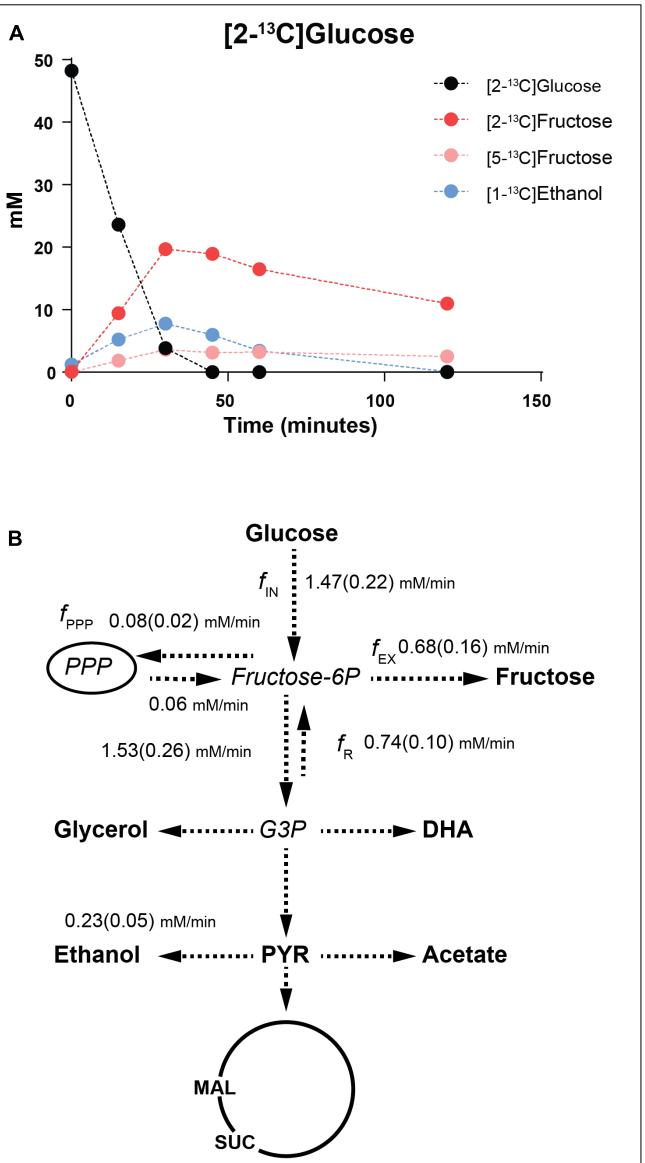

FIGURE 3 | ^{13}C-NMR analyses of [2-^{13}C]glucose metabolism in *St. bombicola mtdh1*Δ*mtdh2*Δ mutant. **(A)** Time course of ^{13}C-labeled glucose consumption and product formation by resting cell suspensions of the *St. bombicola mtdh1*Δ*mtdh2*Δ mutant. End products were quantified by ^{13}C-NMR in supernatants after a pulse (at time zero) of [2-^{13}C]glucose to a final concentration of approximately 50 mM. A comprehensive list of labeled end-product concentrations for this and similar assays is shown in **Supplementary Table S3**. **(B)** Metabolic fluxes deduced from experiments with ^{13}C-labeled glucose. Observed metabolites are shown in bold (DHA: dihydroxyacetone; PYR: pyruvate; MAL: malate; SUC: succinate) and inferred intermediates in italic (G3P: glyceraldehyde-3-phosphate). PPP represents the reactions of the pentose phosphate pathway. Each conversion, shown by dashed lines, may involve multiple steps. Standard deviations are shown in brackets.

Mannitol Production Contributes to Fructophily

As shown in the previous sections, mannitol production seems to be a key reaction in the metabolism of W/S-clade yeasts, which is best illustrated by the diversion of fructose-6P to mannitol production during growth on glucose. Mannitol production from glucose demands ATP expenditure but this is not the case when fructose is the substrate (**Figure 1B**). This is in line with the higher mannitol yield obtained from fructose when compared to the mannitol yield when glucose is used as the sole carbon source (**Figure 1A**) and could explain why fructose is preferred over glucose in these yeasts. Hence, we set out to investigate whether deletion of the *MtDH1* gene affected fructophily, by cultivating the mutant under the conditions where fructophily is usually observed (YP medium supplemented with 10% glucose + 10% fructose; henceforth referred to as 20FG). The results, shown in **Figure 4A** revealed an effect of the *MtDH1* gene deletion on the consumption rates of

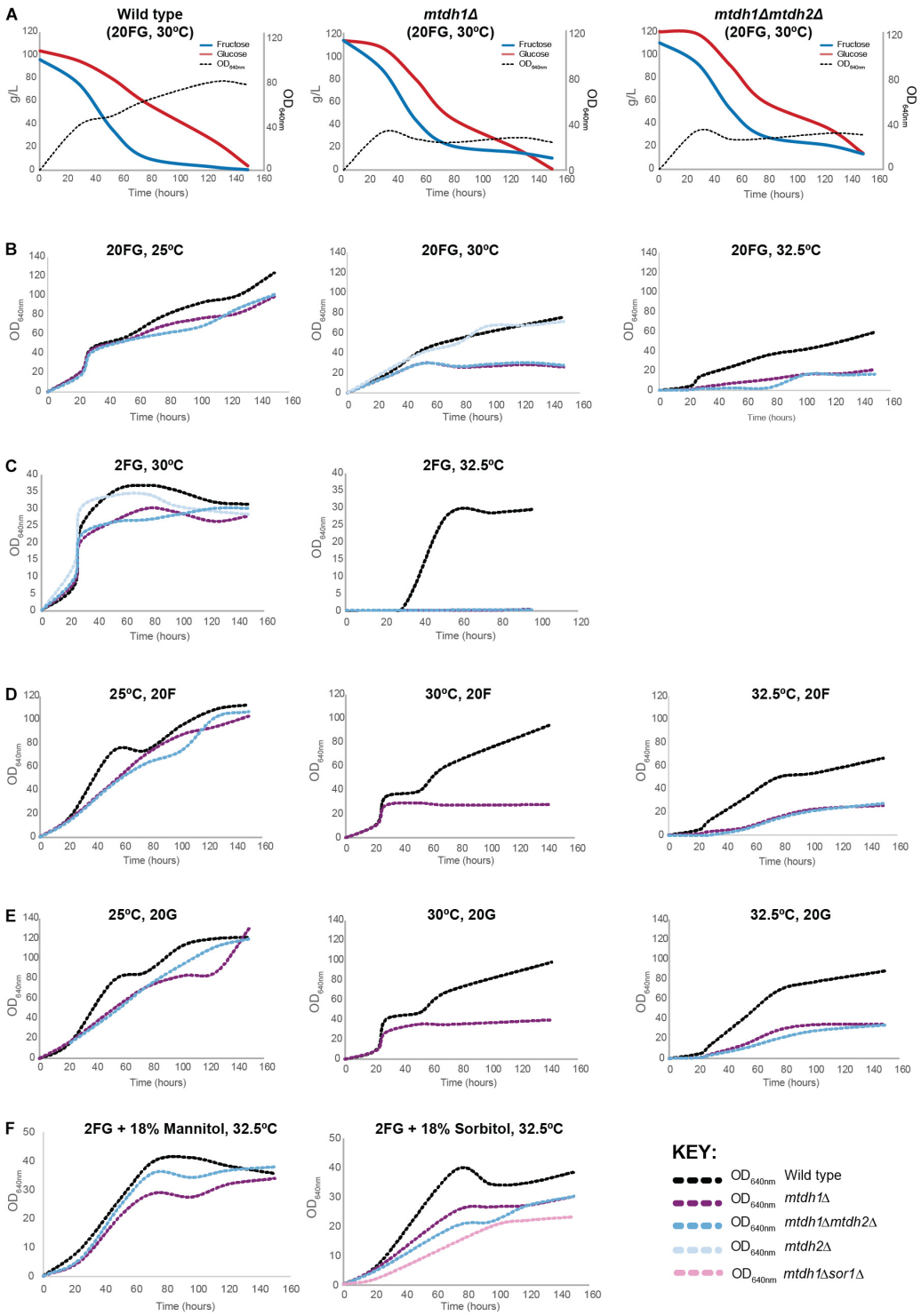

FIGURE 4 | Effect of *MtDH* deletion on fructophily and on biomass yield at different growth temperatures. **(A)** Sugar consumption profiles of *St. bombicola* wild type, *mtdh1*Δ and *mtdh1*Δ*mtdh2*Δ mutants. Strains were cultivated in YP supplemented with 10% (w/v) glucose and 10% (w/v) fructose (20FG) for 150 h at 30°C. Experiments were performed with two biological replicates. **(B)** Growth of wild type, *mtdh1*Δ, *mtdh2*Δ and *mtdh1*Δ*mtdh2*Δ in YP supplemented with 10% (w/v) glucose and 10% (w/v) fructose (20FG) for 150 h at different temperatures: 25, 30, and 32.5°C. **(C)** Growth of *St. bombicola* wild type, *mtdh1*Δ and *mtdh1*Δ*mtdh2*Δ in YP supplemented with 1% (w/v) glucose and 1% (w/v) fructose (2FG) at 30 and 32.5°C. **(D,E)** Growth of *St. bombicola* wild type, *mtdh1*Δ and *mtdh1*Δ*mtdh2*Δ in YP supplemented with 20% (w/v) fructose (20F) **(D)** or 20% (w/v) glucose (20G) **(E)** for 150 h at 25, 30, and 32.5°C. **(F)** Growth of *St. bombicola* wild type, *mtdh1*Δ, *mtdh1*Δ*mtdh2*Δ in (2FG) supplemented with 18% (w/v) mannitol (left) or 18% (w/v) sorbitol (right) at 32.5°C. *St. bombicola mtdh1*Δ*sor1*Δ was only grown in 2FG supplemented with 18% (w/v) sorbitol. Raw data can be found in **Supplementary Data S1**.

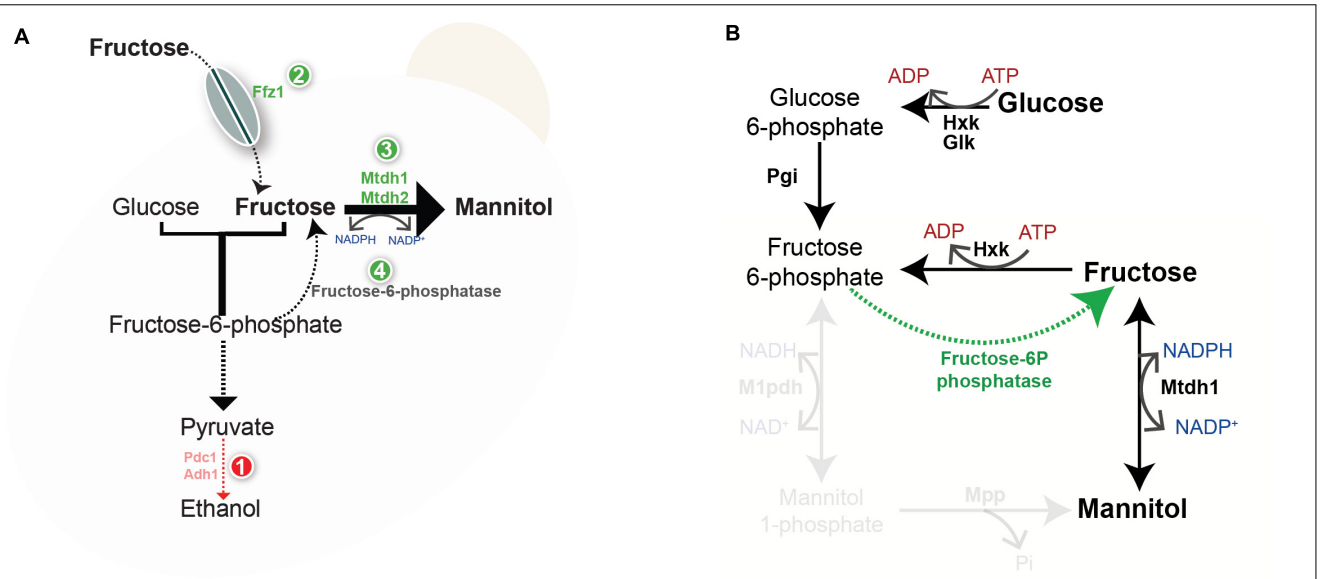

FIGURE 5 | Working model for the evolution of mannitol metabolism. **(A)** Lack of or inefficient alcoholic fermentation (1) causes redox constraints that can be partly alleviated by oxidized cofactor recycling by the mannitol dehydrogenase reaction. Acquisition of Ffz1 (2) and duplication of the *MtDH* gene (3) may have supported an increase in the flux toward mannitol production. In order to harvest the advantages of mannitol production also when glucose is the sole carbon and energy source a novel pathway (4) emerged converting fructose-6-P to fructose. **(B)** Novel pathway mediating the production of mannitol from glucose in W/S-clade yeasts; Hxk- Hexokinase, Glk- Glucokinase; Pgi- Phosphoglucose isomerase, Mtdh1- Mannitol dehydrogenase. Reactions involving M1pdh and Mpp are faded to indicate that they are absent in W/S-clade species.

both fructose and glucose, decreasing the first and increasing the latter, which results in attenuation of the preference for fructose. In the culture supernatants of the two mutants that fail to produce mannitol (*mtdh1*Δ and *mtdh1*Δ*mtdh2*Δ), small amounts of erythritol were detected, while ethanol and glycerol yields on sugar remained virtually unaltered (**Figure 2A**). Since erythritol production regenerates $NADP^+$, this result suggests that abolition of mannitol synthesis causes a redox imbalance at least partly compensated by an increase in erythritol production.

A Possible Role for Mannitol in Thermal Protection

Loss of the ability to synthesize mannitol was accompanied by a drop in the biomass yield on sugar, when compared with the wild type (**Figure 4A**). We first hypothesized that this decrease in biomass yield in the mutants incapable of producing mannitol could be due to a role of mannitol as a compatible solute, required to cope with osmotic stress in the high sugar concentration medium. In line with this possibility, we observed that the *mtdh1*Δ and *mtdh1*Δ *mtdh2*Δ mutants grew as well as the wt in medium containing 2% sugar (1% glucose + 1% fructose; henceforth referred to as 2FG), attaining similar cell densities (**Figure 4C**). However, when we grew the mutants in low sugar concentrations (2FG) but at 32.5°C instead of the previous 30°C, the *mtdh1*Δ and *mtdh1*Δ*mtdh2*Δ mutants did not grow (**Figure 4C**), suggesting that mannitol might rather play a role in adaptation to thermal stress.

To assess the possibility that mannitol might function as a thermal protector in *St. bombicola*, we revisited the performance of the single and double *mtdh* mutants in high sugar medium (20FG), at three different temperatures. The results, shown in **Figure 4B** demonstrate that also in 20FG medium, the growth defect is more pronounced at 32.5°C than at 30°C, although in this medium the mutants are still capable of growing at 32.5°C. Since at 25°C, only a mild effect of the inability to synthesize mannitol on growth was observed (**Figure 4B**) irrespective of the osmolarity of the growth medium it seems unlikely that mannitol plays a major role in osmoprotection. The effects produced by the increase in temperature were not specific for one of the sugars in particular (**Figures 4D,E**).

Next, we examined whether mannitol production increased with temperature in the wild type, which we anticipated should occur if it has a thermo-protective role. Relative internal (in cell-free extracts) and external mannitol concentrations were measured at different temperatures. An increase in extracellular mannitol concentration was readily observed with increasing temperatures (**Supplementary Figure S6A**), which does not happen for other fermentation products like ethanol and glycerol (**Supplementary Figure S6B**). We estimated intracellular mannitol concentrations per cell to vary between 5 and 40 mM, which might be sufficient to fulfill a role in thermal protection, but we did not see a clear increase in intracellular concentrations (**Supplementary Figures S6C,D**). Nevertheless, this represents a small fraction (approximately 1–5%) of the total amount of mannitol produced.

Starmerella bombicola does not grow well on mannitol, requiring up to 1 week of lag phase, but since it does eventually grow, this means that it possesses a transport system that enables it to take up mannitol. We reasoned that if mannitol itself, and not (only) the mannitol producing reaction was important for growth of the *mtdh1*Δ mutants at high temperatures, we might be able to ameliorate the growth defect by adding mannitol to the culture medium. In fact, when we added 18% (w/v) mannitol to the 2FG medium in which the mutants fail to grow at 32.5°C, the *MtDH1* mutants were able to achieve near wild type cell densities, albeit somewhat slower (**Figure 4F**). To find out whether this might also hold true for other polyols, we performed the same experiment using sorbitol, with similar results (**Figure 4F**). Moreover, when we used a mutant rendered unable to use sorbitol as carbon and energy source because of the deletion of a gene encoding an essential enzyme of sorbitol metabolism (*SOR1*) and lacking also *MtDH1*, growth was still observed (**Figure 4F**), showing that growth rescue is not dependent on sorbitol metabolization.

DISCUSSION

We showed recently that fructophily arose in yeasts in the W/S clade, a lineage that comprises yeast species sharing a recent common ancestor that lost the ability to conduct alcoholic fermentation. This central metabolic pathway was later reacquired by incorporation of an alcohol dehydrogenase of bacterial origin (Gonçalves et al., 2018). We also showed previously that the molecular basis for fructophily was established in a W/S-clade ancestor through the horizontal acquisition of a high capacity specific fructose transporter, Ffz1, from filamentous fungi (Gonçalves et al., 2016). Hence, two events with impact on metabolism, both unique in the evolutionary history of yeasts, took place in the same lineage and as far as can be currently judged, at not too distant a moment in evolution from each other. One pressing question arising from this observation is whether the two events might be somehow related. In order to explore this possibility, we sought to gather additional information on the fate of fructose in fructophilic yeasts, once it is taken up by the Ffz1 transporter. Here we showed that a significant amount of fructose is converted to mannitol in most W/S-clade yeasts tested.

Role of the Mannitol Biosynthetic Pathway in the W/S-Clade

Contrary to what was suggested previously for the yeast *Y. lipolytica*, our evidence does not support a role for mannitol as transient carbon storage (Dulermo et al., 2015). The fact that most of the mannitol produced is excreted to the growth medium and not reutilized, and that the mannitol biosynthesis reaction is associated with cofactor recycling, rather suggests that mannitol is mainly a fermentation product and that its production has a role in redox balance. Consistent with this, we found that the pathway for mannitol production consists in a direct conversion of fructose to mannitol with $NADP^+$ regeneration, mediated by an NADPH-dependent mannitol dehydrogenase and that all W/S-clade genomes examined lacked genes encoding the enzymes involved in the alternative pathway that converts fructose-6P to mannitol-1P. In *St. bombicola*, we obtained genetic evidence for the involvement of a mannitol dehydrogenase only, since elimination of *MtDH1* obliterates detectable mannitol production, notably also when glucose is the carbon source. Most importantly, we demonstrated that in spite of the absence of the mannitol-1P dehydrogenase pathway, glucose is also efficiently converted to mannitol through a novel pathway involving a fructose-6P phosphatase but not a glucose isomerase.

The role of a second gene, presumably paralogous to *MtDH1* could not be established with certainty. This gene, named *MtDH2* is phylogenetically closely related to *MtDH1* but its deletion has no measurable impact on the amount of mannitol produced. However, it seems likely that *MtDH2* has a role in mannitol metabolism in at least some W/S-clade species because *W. versatilis* lacks the *MtDH1* type of gene, possessing only several copies of the *MtDH2* type, but still produces mannitol. On the other hand, *St. bacillaris* has intact *MtDH1* and *MtDH2* genes but did not produce mannitol under the conditions tested, rather directing an important part of the carbon flux to glycerol. Therefore, either mannitol production occurs in this species under conditions distinct from those presently tested or these genes acquired a different function in *St. bacillaris*.

The fact that the production of the main polyol (either mannitol or glycerol) seems to be associated in W/S-clade species with $NADP^+$ recycling suggests that their production plays a role in dealing with excess NADPH, which may result from the Pentose Phosphate Pathway (PPP) carrying a higher relative flux than for example in *S. cerevisiae*, where it seems to be finely tuned to the needs of NADPH for biosynthesis (Frick and Wittmann, 2005). In the oleaginous yeast *Y. lipolytica*, which is more closely related to the W/S clade, this pathway was shown to be overactive, providing also the NADPH required for lipid production (Wasylenko et al., 2015). The fact that erythritol was present in measurable amounts in the culture supernatant of the *mtdh* mutants but not of the wt, suggests a compensation as is normally observed in glycerol synthesis when ethanol production is impaired in yeasts (Drewke et al., 1990; Gonçalves et al., 2018).

Characterization of *St. bombicola* mutants unable to produce mannitol also suggested a role for mannitol as thermo protector, which we showed could be taken over by a similar compound as sorbitol. The growth rescue by external polyols is only partial, probably reflecting that redox balance is not optimal under these conditions. The effect of temperature on the growth defect phenotype of the *mtdh* mutants as well as the increase in mannitol production at higher temperatures consubstantiate the role of mannitol as thermo protector. Similar substances, like trehalose have been suggested to fulfill a thermo-protective role in *S. cerevisiae* by stabilizing the membrane when present on both sides (Magalhães et al., 2018). The fact that the *mtdh1*Δ mutants are capable of some growth at 32.5°C in 20FG medium but not in 2FG medium could suggest that the sugars, which are structurally similar to sugar alcohols, might contribute to ameliorate the thermo sensitive phenotype when present at higher concentrations (Corry, 1976; Henle et al., 1985).

A New Pathway for the Conversion of Glucose Into Fructose Ensures Mannitol Biosynthesis in the Absence of Fructose

Taken together our findings point to mannitol playing an important role in central carbon metabolism in *St. bombicola* and also a possible role in stress protection (Wyatt et al., 2013), suggesting that fructose is preferred by this and other W/S-clade yeasts because it can be converted directly to mannitol. Our most striking finding that greatly emphasizes the importance of mannitol production for this yeast is the fact that it features a new pathway to convert glucose to fructose capable of carrying a considerable flux, therefore being able to operate the mannitol dehydrogenase reaction efficiently also when glucose is the only sugar available. In all documented cases so far in fungi, mannitol production from glucose relied on the mannitol-1P pathway (Solomon et al., 2007). As far as we could investigate taking advantage of the available W/S-clade genomes, the new pathway here reported is probably widespread in the W/S clade, a lineage that comprises presently close to 10% of all known yeast species, because all species examined are capable of producing mannitol from glucose and the only pathway for mannitol production seems to involve the fructose-specific Mtdh.

A Possible Link Between Mannitol Metabolism and Evolution of Alcoholic Fermentation

We propose a model (**Figure 5**) in which the advantage of preferential utilization of fructose would have arisen first in a background of lack of, or inefficient alcoholic fermentation, similarly to what is currently observed in fructophilic bacteria (Maeno et al., 2016, 2019). The advantage of fructose under these circumstances would be likewise to provide a means to alleviate redox imbalance by facilitating cofactor recycling through mannitol synthesis, which concomitantly oxidizes NADPH. Although alcoholic fermentation in yeasts in general oxidizes only NADH, extant W/S-clade species have alcohol dehydrogenases that operate using both NADH and NADPH as cofactors (Gonçalves et al., 2018). The likelihood of the proposed model depends on whether fructose reduction to mannitol was capable of minimizing redox balance problems resulting from loss of alcoholic fermentation. This would require either that the cofactors involved in both processes were the same in the W/S ancestor that lost alcoholic fermentation or that mechanisms existed for the equilibration of phosphorylated and unphosphorylated nicotinamide adenine cofactors. Such mechanisms have not been identified in extant yeast species (Bruinenberg et al., 1983). In this model, mannitol may have acquired later a role in stress protection in addition to its role in redox balancing. Evidence for the ancestral importance of mannitol synthesis, in addition to the evolutionary novelty of the pathway mediating glucose to fructose conversion, resides in the duplication of the mannitol dehydrogenase gene, which occurred in the W/S lineage. After efficient alcoholic fermentation was again in place, through acquisition of a bacterial gene and recruitment of the Aro10 decarboxylase for alcoholic fermentation (Gonçalves et al., 2018), the contribution of mannitol biosynthesis to redox balance may have become less important, possibly allowing one of the paralogous genes, *MtDH2*, to acquire a different main function. In conclusion, the surprisingly high flux through the novel pathway involving a fructose-6P phosphatase further underscores the link between fructophily and mannitol synthesis, since it ensures a supply of fructose even when it is not available in the environment, apparently solely for the purpose of mannitol production.

DATA AVAILABILITY STATEMENT

Publicly available datasets were analyzed in this study. This data can be found here: Bioproject PRJNA416493.

AUTHOR CONTRIBUTIONS

PG, HS, CG, MS-O, and LG designed the research. CG, CF, LG, and ML performed the experiments and analyzed the data. DT built the metabolic model and calculated the fluxes. PG wrote the manuscript with the assistance from HS, CG, and MS-O. DT, ML, and LG proofread the manuscript. PG and HS were responsible for funding acquisition. All authors read and approved the final manuscript.

FUNDING

This work was supported by the Applied Molecular Biosciences Unit – UCIBIO which is financed by national funds from FCT/MCTES (UID/Multi/04378/2019), by grant FructYEAST – LISBOA-01-0145-FEDER-029529/PTDC/BIA-MIC/29529/2017 from FCT/MCTES, Portugal (https://www.fct.pt/) and by project LISBOA-01-0145-FEDER-007660 (Microbiologia Molecular, Estrutural e Celular) funded by FEDER through COMPETE2020 – POCI and by national funds through FCT. The NMR data was acquired at CERMAX (Centro de Ressonância Magnética António Xavier) ITQB-NOVA, Oeiras, Portugal with equipment funded by FCT, project AAC 01/SAICT/2016. CG, LG, and ML were recipients of grants (SFRH/BD/89489/2012, SFRH/BPD/111100/2015, and SFRH/BPD/102803/2014, respectively) from FCT, Portugal.

ACKNOWLEDGMENTS

The authors would like to acknowledge PYCC for providing the strains used for this work and members of the Yeast Genomics Lab for helpful discussions.

SUPPLEMENTARY MATERIAL

The Supplementary Material for this article can be found online at: https://www.frontiersin.org/articles/10.3389/fmicb.2019.02510/full#supplementary-material

REFERENCES

Ames, B. N. (1966). Assay of inorganic phosphate, total phosphate and phosphatases. *Methods Enzymol.* 8, 115–118.

Baek, H., Song, K. H., Park, S. M., Kim, S. Y., and Hyun, H. H. (2003). Role of glucose in the bioconversion of fructose into mannitol by *Candida magnoliae*. *Biotechnol. Lett.* 25, 761–765.

Bhosale, S. H., Rao, M. B., and Deshpande, V. V. (1996). Molecular and industrial aspects of glucose isomerase. *Microbiol. Rev.* 60, 280–300.

Bruinenberg, P. M., van Dijken, J. P., and Scheffers, W. A. (1983). An enzymic analysis of NADPH production and consumption in *Candida utilis*. *J. Gen. Microbiol.* 129, 965–971. doi: 10.1099/00221287-129-4-965

Canto, A., Herrera, C. M., and Rodriguez, R. (2017). Nectar-living yeasts of a tropical host plant community: diversity and effects on community-wide floral nectar traits. *PeerJ* 5:e3517. doi: 10.7717/peerj.3517

Capella-Gutierrez, S., Silla-Martinez, J. M., and Gabaldon, T. (2009). trimAl: a tool for automated alignment trimming in large-scale phylogenetic analyses. *Bioinformatics* 25, 1972–1973. doi: 10.1093/bioinformatics/btp348

Chaturvedi, V., Flynn, T., Niehaus, W. G., and Wong, B. (1996). Stress tolerance and pathogenic potential of a mannitol mutant of *Cryptococcus neoformans*. *Microbiology* 142, 937–943. doi: 10.1099/00221287-142-4-937

Corry, J. E. (1976). The effect of sugars and polyols on the heat resistance and morphology of osmophilic yeasts. *J. Appl. Bacteriol.* 40, 269–276.

de Vega, C., Albaladejo, R. G., Guzman, B., Steenhuisen, S. L., Johnson, S. D., Herrera, C. M., et al. (2017). Flowers as a reservoir of yeast diversity: description of *Wickerhamiella* nectarea f.a. sp. nov., and Wickerhamiella natalensis f.a. sp. nov. from South African flowers and pollinators, and transfer of related *Candida* species to the genus wickerhamiella as new combinations. *FEMS Yeast Res.* 17:fox054. doi: 10.1093/femsyr/fox054

Drewke, C., Thielen, J., and Ciriacy, M. (1990). Ethanol formation in adh0 mutants reveals the existence of a novel acetaldehyde-reducing activity in *Saccharomyces cerevisiae*. *J. Bacteriol.* 172, 3909–3917. doi: 10.1128/jb.172.7.3909-3917.1990

Dulermo, T., Lazar, Z., Dulermo, R., Rakicka, M., Haddouche, R., and Nicaud, J. M. (2015). Analysis of ATP-citrate lyase and malic enzyme mutants of *Yarrowia lipolytica* points out the importance of mannitol metabolism in fatty acid synthesis. *Biochim. Biophys. Acta* 1851, 1107–1117. doi: 10.1016/j.bbalip.2015.04.007

Endo, A., Futagawa-Endo, Y., and Dicks, L. M. (2009). Isolation and characterization of fructophilic lactic acid bacteria from fructose-rich niches. *Syst. Appl. Microbiol.* 32, 593–600. doi: 10.1016/j.syapm.2009.08.002

Endo, A., Futagawa-Endo, Y., Sakamoto, M., Kitahara, M., and Dicks, L. M. (2010). Lactobacillus florum sp. nov., *a fructophilic species isolated from flowers*. *Int. J. Syst. Evol. Microbiol.* 60(Pt 10), 2478–2482. doi: 10.1099/ijs.0.019067-0

Frick, O., and Wittmann, C. (2005). Characterization of the metabolic shift between oxidative and fermentative growth in *Saccharomyces cerevisiae* by comparative 13C flux analysis. *Microb. Cell. Fact.* 4:30. doi: 10.1186/1475-2859-4-30

Gonçalves, C., Coelho, M. A., Salema-Oom, M., and Gonçalves, P. (2016). Stepwise functional evolution in a fungal sugar transporter family. *Mol. Biol. Evol.* 33, 352–366. doi: 10.1093/molbev/msv220

Gonçalves, C., Wisecaver, J. H., Kominek, J., Oom, M. S., Leandro, M. J., Shen, X. X., et al. (2018). Evidence for loss and reacquisition of alcoholic fermentation in a fructophilic yeast lineage. *eLife* 7:e33034. doi: 10.7554/eLife.33034

Henle, K. J., Monson, T. P., Nagle, W. A., and Moss, A. J. (1985). Heat protection by sugars and sugar analogues. *Int. J. Hyperthermia* 1, 371–382.

Hult, K., Veide, A., and Gatenbeck, S. (1980). The distribution of the NADPH regenerating mannitol cycle among fungal species. *Arch. Microbiol.* 128, 253–255.

Kathiresan, K., and Manivannan, S. (2006). Glucose isomerase production by *Penicillium fellutanum* isolated from mangrove sediment. *Trends Appl. Sci. Res.* 1, 524–528.

Katoh, K., and Standley, D. M. (2014). MAFFT: iterative refinement and additional methods. *Methods Mol. Biol.* 1079, 131–146. doi: 10.1007/978-1-62703-646-7_8

Keller, N. P. (2019). Fungal secondary metabolism: regulation, function and drug discovery. *Nat. Rev. Microbiol.* 17, 167–180. doi: 10.1038/s41579-018-0121-1

Kominek, J., Doering, D. T., Opulente, D. A., Shen, X. X., Zhou, X., DeVirgilio, J., et al. (2019). Eukaryotic acquisition of a bacterial operon. *Cell* 176, 1356.e10–1366.e10. doi: 10.1016/j.cell.2019.01.034

Kulkarni, R. K. (1990). Mannitol metabolism in *Lentinus edodes*, the shiitake mushroom. *Appl. Environ. Microbiol.* 56, 250–253.

Kurtzman, C. P., Fell, J. W., and Boekhout, T. (2011). *The Yeasts: A Taxonomic Study*, 5th Edn. Amsterdam: Elsevier, 1–2354.

Lachance, M. A., Starmer, W. T., Rosa, C. A., Bowles, J. M., Barker, J. S., and Janzen, D. H. (2001). Biogeography of the yeasts of ephemeral flowers and their insects. *FEMS Yeast Res.* 1, 1–8. doi: 10.1111/j.1567-1364.2001.tb00007.x

Leandro, M. J., Cabral, S., Prista, C., Loureiro-Dias, M. C., and Sychrova, H. (2014). The high-capacity specific fructose facilitator ZrFfz1 is essential for the fructophilic behavior of *Zygosaccharomyces rouxii* CBS 732T. *Eukaryot. Cell* 13, 1371–1379. doi: 10.1128/ec.00137-14

Leandro, M. J., Sychrova, H., Prista, C., and Loureiro-Dias, M. C. (2011). The osmotolerant fructophilic yeast *Zygosaccharomyces rouxii* employs two plasma-membrane fructose uptake systems belonging to a new family of yeast sugar transporters. *Microbiology* 157(Pt 2), 601–608. doi: 10.1099/mic.0.044446-0

Lee, J. K., Koo, B. S., Kim, S. Y., and Hyun, H. H. (2003). Purification and characterization of a novel mannitol dehydrogenase from a newly isolated strain of *Candida magnoliae*. *Appl. Environ. Microbiol.* 69, 4438–4447. doi: 10.1128/aem.69.8.4438-4447.2003

Lee, M., Rozeboom, H. J., de Waal, P. P., de Jong, R. M., Dudek, H. M., and Janssen, D. B. (2017). Metal dependence of the xylose isomerase from *Piromyces* sp. E2 explored by activity profiling and protein crystallography. *Biochemistry* 56, 5991–6005. doi: 10.1021/acs.biochem.7b00777

Maeno, S., Kajikawa, A., Dicks, L., and Endo, A. (2019). Introduction of bifunctional alcohol/acetaldehyde dehydrogenase gene (adhE) in *Fructobacillus fructosus* settled its fructophilic characteristics. *Res. Microbiol.* 170, 35–42. doi: 10.1016/j.resmic.2018.09.004

Maeno, S., Tanizawa, Y., Kanesaki, Y., Kubota, E., Kumar, H., Dicks, L., et al. (2016). Genomic characterization of a fructophilic bee symbiont *Lactobacillus kunkeei* reveals its niche-specific adaptation. *Syst. Appl. Microbiol.* 39, 516–526. doi: 10.1016/j.syapm.2016.09.006

Magalhães, R. S. S., Popova, B., Braus, G. H., Outeiro, T. F., and Eleutherio, E. C. A. (2018). The trehalose protective mechanism during thermal stress in *Saccharomyces cerevisiae*: the roles of Ath1 and Agt1. *FEMS Yeast Res.* 18:foy066. doi: 10.1093/femsyr/foy066

Muntz, J. A., and Carroll, R. E. (1960). A method for converting glucose to fructose. *J. Biol. Chem.* 235, 1258–1260.

Napora, K., Wrodnigg, T. M., Kosmus, P., Thonhofer, M., Robins, K., and Winkler, M. (2013). *Yarrowia lipolytica* dehydrogenase/reductase: an enzyme tolerant for lipophilic compounds and carbohydrate substrates. *Bioorg. Med. Chem. Lett.* 23, 3393–3395. doi: 10.1016/j.bmcl.2013.03.064

Neveling, D. P., Endo, A., and Dicks, L. M. (2012). Fructophilic *Lactobacillus kunkeei* and *Lactobacillus brevis* isolated from fresh flowers, bees and bee-hives. *Curr. Microbiol.* 65, 507–515. doi: 10.1007/s00284-012-0186-4

Neves, A. R., Ramos, A., Nunes, M. C., Kleerebezem, M., Hugenholtz, J., de Vos, W. M., et al. (1999). In vivo nuclear magnetic resonance studies of glycolytic kinetics in *Lactococcus lactis*. *Biotechnol. Bioeng.* 64, 200–212.

Neves, A. R., Ramos, A., Shearman, C., Gasson, M. J., Almeida, J. S., and Santos, H. (2000). Metabolic characterization of *Lactococcus lactis* deficient in lactate dehydrogenase using *in vivo* 13C-NMR. *Eur. J. Biochem.* 267, 3859–3868.

Nguyen, L. T., Schmidt, H. A., von Haeseler, A., and Minh, B. Q. (2015). IQ-TREE: a fast and effective stochastic algorithm for estimating maximum-likelihood phylogenies. *Mol. Biol. Evol.* 32, 268–274. doi: 10.1093/molbev/msu300

Pina, C., Goncalves, P., Prista, C., and Loureiro-Dias, M. C. (2004). Ffz1, a new transporter specific for fructose from *Zygosaccharomyces bailii*. *Microbiology* 150(Pt 7), 2429–2433. doi: 10.1099/mic.0.26979-0

Rosa, C. A., and Lachance, M. A. (1998). The yeast genus *Starmerella* gen. nov. and starmerella bombicola sp. nov., the teleomorph of *Candida bombicola* (Spencer, Gorin & Tullock) meyer & yarrow. *Int. J. Syst. Bacteriol.* 48(Pt 4), 1413–1417. doi: 10.1099/00207713-48-4-1413

Savergave, L. S., Gadre, R. V., Vaidya, B. K., and Jogdand, V. V. (2013). Two-stage fermentation process for enhanced mannitol production using *Candida magnoliae* mutant R9. *Bioprocess Biosyst. Eng.* 36, 193–203. doi: 10.1007/s00449-012-0775-4

Sayyed, R. Z., Shimpi, G. B., and Chincholkar, S. B. (2010). Constitutive production of extracellular glucose isomerase by an osmophillic *Aspergillus* sp. *under submerged conditions*. *J. Food Sci. Technol.* 47, 496–500. doi: 10.1007/s13197-010-0084-3

Shen, X. X., Opulente, D. A., Kominek, J., Zhou, X., Steenwyk, J. L., Buh, K. V., et al. (2018). Tempo and mode of genome evolution in the budding yeast subphylum. *Cell* 175, 1533.e20–1545.e20. doi: 10.1016/j.cell.2018.10.023

Solomon, P. S., Waters, O. D., and Oliver, R. P. (2007). Decoding the mannitol enigma in filamentous fungi. *Trends Microbiol.* 15, 257–262. doi: 10.1016/j.tim.2007.04.002

Spatafora, J. W., and Bushley, K. E. (2015). Phylogenomics and evolution of secondary metabolism in plant-associated fungi. *Curr. Opin. Plant Biol.* 26, 37–44. doi: 10.1016/j.pbi.2015.05.030

Theobald, S., Vesth, T. C., Rendsvig, J. K., Nielsen, K. F., Riley, R., de Abreu, L. M., et al. (2018). Uncovering secondary metabolite evolution and biosynthesis using gene cluster networks and genetic dereplication. *Sci. Rep.* 8:17957. doi: 10.1038/s41598-018-36561-3

Wasylenko, T. M., Ahn, W. S., and Stephanopoulos, G. (2015). The oxidative pentose phosphate pathway is the primary source of NADPH for lipid overproduction from glucose in *Yarrowia lipolytica*. *Metab. Eng.* 30, 27–39. doi: 10.1016/j.ymben.2015.02.007

Wisecaver, J. H., and Rokas, A. (2015). Fungal metabolic gene clusters-caravans traveling across genomes and environments. *Front. Microbiol.* 6:161. doi: 10.3389/fmicb.2015.00161

Wyatt, T. T., van Leeuwen, M. R., Wosten, H. A., and Dijksterhuis, J. (2014). Mannitol is essential for the development of stress-resistant ascospores in *Neosartorya fischeri* (*Aspergillus fischeri*). *Fungal Genet. Biol.* 64, 11–24. doi: 10.1016/j.fgb.2013.12.010

Wyatt, T. T., Wosten, H. A., and Dijksterhuis, J. (2013). Fungal spores for dispersion in space and time. *Adv. Appl. Microbiol.* 85, 43–91. doi: 10.1016/B978-0-12-407672-3.00002-2

Zahid, N., and Deppenmeier, U. (2016). Role of mannitol dehydrogenases in osmoprotection of *Gluconobacter oxydans*. *Appl. Microbiol. Biotechnol.* 100, 9967–9978.

Zakhartsev, M., and Reuss, M. (2018). Cell size and morphological properties of yeast *Saccharomyces cerevisiae* in relation to growth temperature. *FEMS Yeast Res.* 18:foy052. doi: 10.1093/femsyr/foy052

Conflict of Interest: The authors declare that the research was conducted in the absence of any commercial or financial relationships that could be construed as a potential conflict of interest.

frontiers in Genetics

HYPOTHESIS AND THEORY
published: 31 January 2020
doi: 10.3389/fgene.2020.00002

Does Inter-Organellar Proteostasis Impact Yeast Quality and Performance During Beer Fermentation?

Bianca de Paula Telini, Marcelo Menoncin and Diego Bonatto *

Brewing Yeast Research Group, Centro de Biotecnologia da UFRGS, Departamento de Biologia Molecular e Biotecnologia, Universidade Federal do Rio Grande do Sul, Porto Alegre, Rio Grande do Sul, Brazil

OPEN ACCESS

Edited by:
Francisco A. Cubillos, Universidad de Santiago de Chile, Chile

Reviewed by:
Brian Gibson, VTT Technical Research Centre of Finland Ltd, Finland
David Peris Navarro, University of Oslo, Norway

***Correspondence:**
Diego Bonatto
diegobonatto@gmail.com

Specialty section:
This article was submitted to Evolutionary and Genomic Microbiology, a section of the journal Frontiers in Genetics

Received: *11 October 2019*
Accepted: *06 January 2020*
Published: *31 January 2020*

Citation:
Telini BdP, Menoncin M and Bonatto D (2020) Does Inter-Organellar Proteostasis Impact Yeast Quality and Performance During Beer Fermentation? Front. Genet. 11:2. doi: 10.3389/fgene.2020.00002

During beer production, yeast generate ethanol that is exported to the extracellular environment where it accumulates. Depending on the initial carbohydrate concentration in the wort, the amount of yeast biomass inoculated, the fermentation temperature, and the yeast attenuation capacity, a high concentration of ethanol can be achieved in beer. The increase in ethanol concentration as a consequence of the fermentation of high gravity (HG) or very high gravity (VHG) worts promotes deleterious pleiotropic effects on the yeast cells. Moderate concentrations of ethanol (5% v/v) change the enzymatic kinetics of proteins and affect biological processes, such as the cell cycle and metabolism, impacting the reuse of yeast for subsequent fermentation. However, high concentrations of ethanol (> 5% v/v) dramatically alter protein structure, leading to unfolded proteins as well as amorphous protein aggregates. It is noteworthy that the effects of elevated ethanol concentrations generated during beer fermentation resemble those of heat shock stress, with similar responses observed in both situations, such as the activation of proteostasis and protein quality control mechanisms in different cell compartments, including endoplasmic reticulum (ER), mitochondria, and cytosol. Despite the extensive published molecular and biochemical data regarding the roles of proteostasis in different organelles of yeast cells, little is known about how this mechanism impacts beer fermentation and how different proteostasis mechanisms found in ER, mitochondria, and cytosol communicate with each other during ethanol/fermentative stress. Supporting this integrative view, transcriptome data analysis was applied using publicly available information for a lager yeast strain grown under beer production conditions. The transcriptome data indicated upregulation of genes that encode chaperones, co-chaperones, unfolded protein response elements in ER and mitochondria, ubiquitin ligases, proteasome components, *N*-glycosylation quality control pathway proteins, and components of processing bodies (p-bodies) and stress granules (SGs) during lager beer fermentation. Thus, the main purpose of this hypothesis and theory manuscript is to provide a concise picture of how inter-organellar proteostasis mechanisms are connected

with one another and with biological processes that may modulate the viability and/or vitality of yeast populations during HG/VHG beer fermentation and serial repitching.

Keywords: proteostasis, brewing yeasts, ethanol stress, beer fermentation, inter-organellar communication, transcriptome

INTRODUCTION

During beer production, ethanol generated as a by-product of fermentation is exported to the extracellular environment, where it accumulates. Depending on the initial mono-, di-, and trisaccharide concentrations present in the wort, the amount of yeast cell biomass inoculated, fermentation temperature, and the attenuative capability of yeast strains employed by the brewer, a high concentration of ethanol can be achieved in beer (Puligundla et al., 2011).

At present, the brewing industry is trying to implement the use of very high gravity (VHG) worts (24°P or approximately 1.101 kg · L^{-1} dissolved solids) to produce beer, which can save energy, time, labor, and capital costs, and improve plant efficiency (Silva et al., 2008; Puligundla et al., 2011). Beer produced from VHG worts contains high quantities of ethanol and other volatiles, which are dissolved in oxygen-free water to produce regular beers with 5% (v/v) ethanol (Stewart, 2010). However, the use of VHG worts imposes challenges for serial repitching due to the osmotic and oxidative stresses that yeast cells experience in the first hours of fermentation, which are followed by ethanol, nutritional, and thermal (cold shock) stresses in the later phases of fermentation and the beginning of cold maturation (Gibson et al., 2007). These stress conditions can lead to yeast slurries that display sluggish fermentation and poor viability, which precludes their use in subsequent fermentations (Huuskonen et al., 2010).

The increase in ethanol concentrations, as a consequence of VHG wort fermentation, can have pleiotropic effects in yeast. Ethanol is a chaotropic substance that affects cell macromolecular structures by reducing hydration (Hallsworth, 1998; Cray et al., 2015). Moderate concentrations of ethanol (around 5% v/v) can alter the enzymatic kinetics of proteins associated with primary metabolism (e.g. glycolysis), and affect different biological processes, such as the cell cycle (Hallsworth, 1998). In comparison, high concentrations of ethanol (> 5% v/v) can cause substantial changes in the structure and composition of hydrophobic molecules within the cell (Hallsworth, 1998). Thus, by reducing the water activity in the cell, ethanol promotes a water stress condition (Hallsworth, 1998). In a general sense, the effects of high concentrations of ethanol resemble those observed during heat shock conditions (defined as exposure to temperatures >35°C), and similar responses are observed in response to both stress situations, such as changes in membrane composition and synthesis of small protective osmolytes (e.g. glycerol and trehalose) (Piper, 1995). Interestingly, it was recently demonstrated by transcriptome analysis using RNA-seq data that ethanol tolerance in different *Saccharomyces cerevisiae* strains also depends on a series of environmental conditions (e.g. the presence or absence of dissolved oxygen), pointing to a strain-by-oxygen-by-alcohol interactions that lead to ethanol tolerance (Sardi et al., 2018).

Protein folding and activity, key features of "proteostasis", are strongly affected by ethanol. In this review, proteostasis mechanisms are defined as all steps required for a protein to exert its function(s), from protein biogenesis to degradation, including all post-translational changes that the protein experiences in between.

In mammalian models, it has been shown that post-translational modifications of proteins, like mannosylation and galactosylation, are substantially changed in ER and Golgi after ethanol shock (Ghosh et al., 1995; Esteban-Pretel et al., 2011). In yeast, there is limited available data on how ethanol affects post-translational modification of proteins, but it is clear that protein structure and activity change in the presence of ethanol (Hallsworth, 1998). It has been observed that ethanol can induce heat shock proteins like Hsp104p, Hsp70p, and Hsp26p, and oxidative stress-response proteins, like Ctt1p, Sod1, and Sod2p under moderate concentrations of ethanol (6% v/v) (Stanley et al., 2010). DNA microarray data supports the idea of a fermentative stress response associated with ethanol toxicity in industrial lager fermentations (Gibson et al., 2007).

Despite the paucity of data regarding the effects of ethanol toxicity in the modulation of yeast proteostasis mechanisms during VHG beer fermentation and serial repitching by using publicly available DNA microarray data (**Table S1** and **Figure S1**), we observed the upregulation of genes linked to lager beer fermentation (**Figures S2A, B**), including differentially expressed genes (DEGs) associated to organellar proteostasis mechanisms in DNA microarray single analysis (**Figures S3A, B** and **S4A, B**) and DNA microarray meta-analysis (**Figures S5A, B** and **S6A, B**). The Pan-DEGs resulting from both DNA microarray analyses (**Figures S1** and **S9A, B**) include genes linked to ER-associated unfolded protein response (UPR), endoplasmic reticulum-associated protein degradation (ERAD) responses (**Figures 1A, B**), and mitochondria-associated proteostasis (**Figures 2A, B**), suggesting cellular cross-talk among organellar proteostasis mechanisms. It is important to note that all three gene expression datasets (GSEs) analyzed in this work (**Table S1**) employed the Affymetrix Yeast Genome 2.0 Array for transcript detection of both *S. cerevisiae* and *Schizosaccharomyces pombe* yeast species (https://www.ncbi.nlm.nih.gov/geo/query/acc.cgi?acc = GPL2529), which can potentially introduce a bias when transcripts of *Saccharomyces pastorianus* are evaluated due to the hybrid genome of this species (Okuno et al., 2016). In order to evaluate if the parental genomes of *S. pastorianus* display some specific expression pattern, Horinouchi et al. (2010) designated a

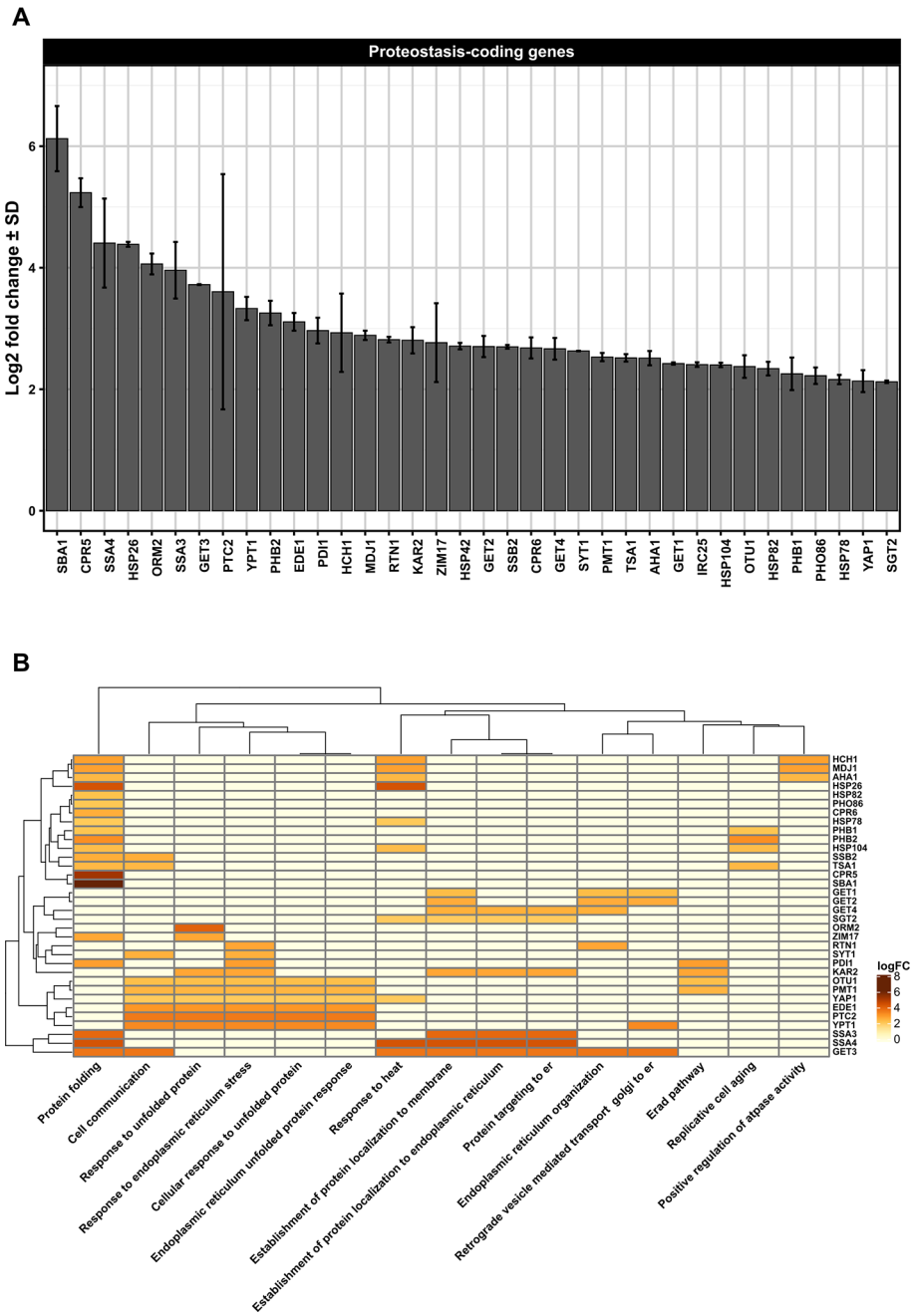

FIGURE 1 | (A) Differentially upregulated Pan-genes associated with proteostasis observed in the lager yeast CB11 strain during beer fermentation. The mean expression values are indicated by log2 fold change ± standard deviation (SD) on the y-axis and in the inset. Gene names are indicated on the x-axis. **(B)** Heatmap plot showing the clustered differentially upregulated genes associated with proteostasis observed in CB11 during beer fermentation and the associated clustered biological processes from gene ontology analysis (**Figure S1**). Heatmap rows and columns were grouped using the Euclidean distance method and complete linkage.

custom DNA microarray platform for *S. pastorianus* transcriptome analysis containing probes for both *S. cerevisiae* and *Saccharomyces bayanus* genomes. This custom DNA microarray was employed to evaluate gene expression pattern in the lager brewing strain Weihenstephan 34/7 during a pilot-scale fermentation condition. The transcriptome data gathered by the authors indicated a strong correlation between the expression levels of *S. cerevisiae* and *S. bayanus* orthologous genes during fermentation, allowing discriminate only a small set of *S. cerevisiae* or S. *bayanus* DEGs (Horinouchi et al., 2010). On

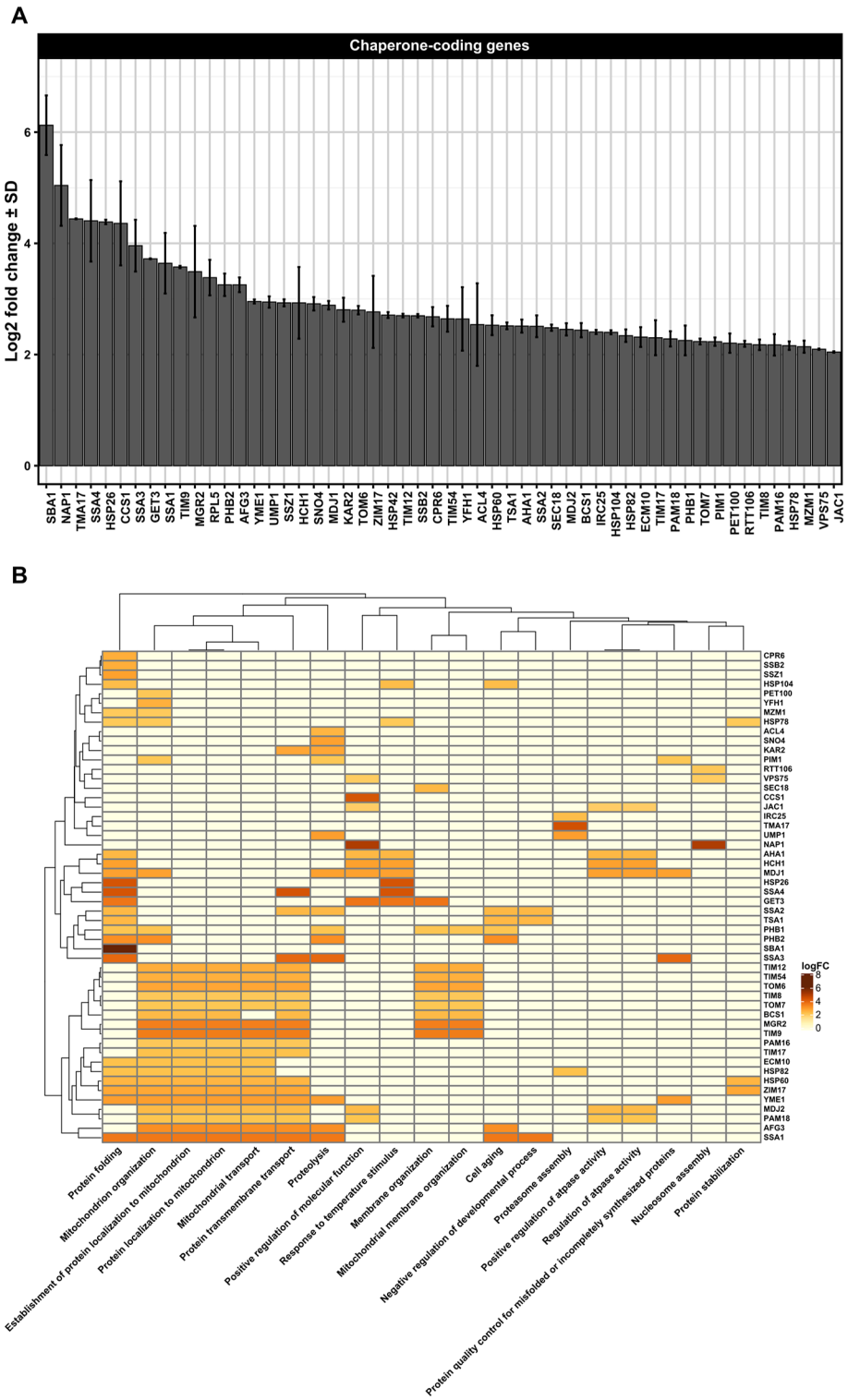

FIGURE 2 | (A) Differentially upregulated Pan-genes associated with chaperones and folding proteins observed in the lager yeast CB11 strain during beer fermentation. The mean expression values are indicated by log2 fold change ± standard deviation (SD) on the y-axis and in the inset. Gene names are indicated on the x-axis. **(B)** Heatmap plot showing the clustered differentially upregulated genes associated with chaperones and folding proteins observed in CB11 during beer fermentation and the associated clustered biological processes from gene ontology analysis (**Figure S1**). Heatmap rows and columns were grouped using the Euclidean distance method and complete linkage.

the other hand, the use of RNA sequencing technologies for evaluation of gene expression in *S. pastorianus* strains during beer production is virtually absent, making it difficult to understand the contribution of parental genomes of *S. pastorianus* in ethanol tolerance and proteostasis. Thus, considering the importance of *S. pastorianus* for brewing industry in general and for hybrid yeast species research (Gorter de Vries et al., 2019a; Gorter de Vries et al., 2019b), it is imperative to design new experimental procedures for the analysis of the influence of hybrid genomes in proteostasis and ethanol tolerance.

YEAST ER PROTEOSTASIS AND ETHANOL TOLERANCE

The endoplasmic reticulum (ER) consists of an extensive network of membranes that originates at the nuclear envelope and flows through the cytoplasm (English and Voeltz, 2013). It is the site of secretory, membrane, lysosomal, and vacuolar protein synthesis. Besides proteins, the ER is also fundamental for the synthesis of lipids and the assembly of lipid bilayers (van Meer et al., 2008). In the ER, proteins are structurally modified, which involves cleavage of signal sequences, *N*-linked glycosylation, disulfide bond formation, folding of monomers, and oligomerization (Braakman and Hebert, 2013). Correct protein folding is facilitated by different molecular chaperones and folding enzymes present in the ER, such as protein disulfide isomerases (PDIs). When a protein is unable to fold correctly, an ER quality control (ERQC) system is activated, comprised of both UPR and ERAD mechanisms (Brodsky and Wojcikiewicz, 2009).

Considering that many proteins found in the ER contain *N*-linked glycans, it is logical to consider that proteostasis mechanisms are largely associated with *N*-glycan synthesis in the ER. In fact, *N*-glycan modification by different glycanases found in ER defines the final destination of polypeptides, and the trimming of glucose residues recruit lectin chaperones that facilitate protein folding (Molinari, 2007; Ferris et al., 2014). Until now, data regarding *N*-glycan processing in yeast during VHG beer fermentation or yeast reuse has been extremely limited. However, our transcriptome data single- and meta-analysis (**Figure S1**) of the proprietary lager yeast CB11 strain (Coors Brewing Limited (Burton on Trent, UK) (Lawrence et al., 2012) under fermentation conditions, when compared to propagation conditions, point to upregulation of genes related to *N*-glycan processing, like *PDI1* and *PMT1*, which are also important components of the ERAD response (**Figures 1A, B**). ERAD components export unfolded proteins to the cytosol, which are ubiquitinated and degraded by the 26S proteasome (Brodsky and Wojcikiewicz, 2009; Hetz et al., 2015). The recognition step of unfolded protein can occur either on the luminal side (ERAD-L), the cytosolic side (ERAD-C), or inside of the ER membrane (ERAD-M) (Thibault and Ng, 2012). Protein disulfide isomerase 1, or Pdi1p, is essential for cell viability and is highly abundant in the ER (Mizunaga et al., 1990; Pfeiffer et al., 2016). Pdi1p is also involved in the removal of aberrant disulfide bridges (Gilbert, 1997; Pfeiffer et al., 2016). Interestingly, Pdi1p has chaperone activity, even with proteins that do not form disulfide bridges (Pfeiffer et al., 2016), assisting in the unfolding and the export of ERAD-client proteins from the ER (Weissman and Kimt, 1993). Finally, Pmt1p is an *O*-mannosyltransferase that, together with Pmt2p, exerts proteostasis control of ER proteins. Pmt1p interacts with Pdi1p in order to promote the correct folding of ER-resident proteins or to target misfolded proteins to Hrd1p, a major ERAD-associated E3 ubiquitin-protein ligase (Goder and Melero, 2011). It is worth noting that Pdi1p interacts with Htm1p/Mnl1p, an alpha-1,2-specific exomannosidase that generates Man7GlcNac2, an oligosaccharide structure on glycoproteins target for ERAD (Clerc et al., 2009). Moreover, Htm1p/Mnl1p is required for Yos9p activity (Clerc et al., 2009), a 75 kDa soluble ER glycoprotein (Friedmann et al., 2002) that has been shown to have an important role in glycoprotein degradation (Szathmary et al., 2005). It should be point that *YOS9* gene was found overexpressed in DNA microarray single analysis only (**Figures S4A, B**). The roles of Htm1p/Mnl1p in yeast cells subjected to VHG beer fermentation and/or ethanol stress are poorly understood, but it has been demonstrated that ethanol can impair the biosynthesis of *N*-glycans in liver cell models *in vitro* (Welti and Hülsmeier, 2014). This indicates that *N*-glycan biosynthesis and processing may be negatively affected by ethanol/fermentation stress during VHG or even high gravity (HG) beer production.

In addition to *N*-glycan structural alterations promoted by ethanol, the presence of unfolded proteins in ER reduces or even stops the translation of new proteins, and also exposes sticky hydrophobic amino acids in unfolded proteins, promoting so-called proteotoxicity (Ron, 2002; Mori, 2015), which is sensed by the transmembrane protein Ire1. Ire1p undergoes oligomerization and autophosphorylation and activates the endoribonuclease domain on the cytosolic side of the membrane that removes a regulatory intron in the *HAC1* mRNA (Chapman and Walter, 1997; Sidrauski and Walter, 1997), leading to the translation of active Hac1p, a bZip transcription factor associated with ER proteostasis (Liu and Chang, 2008). Noteworthy, Navarro-Tapia et al. (2017) showed that low to high concentrations of ethanol (≤ 8% v/v) did not promote protein unfolding in yeast cells, but did trigger UPR through an unknown mechanism in laboratory yeast strains cultured in synthetic medium. However, Miyagawa et al. (2014) showed that an increase in ethanol concentration, from 8 to 16% (v/v) in a synthetic culture medium, promoted the constant expression of *HAC1* spliced form mRNA, which demonstrated that UPR can become chronically activated. In addition, the same authors verified that Kar2p associated with unfolded protein aggregates in the ER when yeast cells were challenged with ethanol at a concentration of 16% (v/v), supporting the idea that very high concentrations of ethanol potentially induce protein aggregates in the ER and trigger ERQC (Miyagawa et al., 2014).

Our transcriptome data indicated that Pan-DEGs related to the classical UPR pathway, like *KAR2, PTC2,* and *YPT1*, are upregulated in lager beer fermentation compared to the yeast propagation step (**Figures 1A, B**). Ptc2p is a type 2C serine/threonine phosphatase that downregulates the UPR mechanism

by dephosphorylating Ire2p (Welihinda et al., 1998), while Ypt1p is a yeast Rab1 homolog that interacts with unspliced *HAC1* mRNA and regulates the UPR by promoting the decay of *HAC1* mRNA (Tsvetanova et al., 2012). Ypt1p has been linked to the maintenance of Golgi morphology and protein composition, participates in ER to Golgi anterograde/retrograde transport, and is necessary for intra Golgi transport (Kamena et al., 2008). While anterograde/retrograde ER to Golgi responses have been extensively studied in yeast and other model organisms, and the functions of a number of different protein complexes involved in these processes have been discerned (Lee et al., 2004), the influence of anterograde/retrograde ER to Golgi transport in brewing yeast vitality or beer fermentation is unknown. However, we hypothesize that this mechanism may be negatively modulated by high ethanol concentrations during VHG beer fermentation or yeast reuse. In support of this idea, it was previously shown that the rat PC12 cell line, when subjected *in vitro* to a low alcohol concentration (30 mM), exhibited delayed anterograde ER to Golgi transport, fragmented Golgi morphology, and a decreased number of secretory vesicles (Tomás et al., 2012). Interestingly, 5% of all eukaryotic proteins (referred to as tail-anchored (TA) proteins) possess a unique carboxy-terminal transmembrane region that targets them to the ER membrane (Stefanovic and Hegde, 2007). Considering that these proteins contain a hydrophobic domain that makes them prone to aggregation in the aqueous environment of the ER lumen, they should be targeted to the ER membrane to avoid the formation of protein aggregates. Thus, in order to guide the entry of TA proteins into the ER membrane, the guided entry of TA proteins (GET) pathway mediates the process, also acting in vesicle fusion and retrograde Golgi to ER responses (Denic et al., 2013). Moreover, the GET pathway is necessary for the retrieval of the Erd2p HDEL receptor from the Golgi to the ER (Schuldiner et al., 2005). Erd2p is an important component that retain proteins bearing a C-terminal tetrapeptide HDEL sequence in the ER, like the ER chaperone Kar2p (Semenza et al., 1990), invertase, and many other secreted proteins. In our transcriptome data analysis, we found that during lager beer fermentation, the Pan-DEGs *GET1*, *GET2*, *GET3*, *GET4*, and *SGT2* are significantly upregulated (**Figures 1A, B**). GET proteins are core components of GET pathway that promote the transfer of TA proteins from ribosomes to the Get4p/Get5p/Sgt2p complex and to the chaperone Get3p (Chartron et al., 2012). Then, Get1p and Get2p, which comprise a transmembrane complex, drive a conformational change that enables the release of TA proteins from Get3p and, as a consequence, insertion into the ER membrane (Wang et al., 2014). In the context of beer fermentation and ethanol stress, we speculate that ethanol generated during fermentation induces conformational changes in *N*-glycans and secreted proteins that potentially leads to the formation of aggregates in the ER, followed by modification of the structure and function of Golgi. This may result in the activation of ERQC mechanisms and promote the retrograde response of Golgi to ER by stimulating the function of the GET pathway (**Figure 4**). Finally, the induction of ERQC due to ethanol generated during beer fermentation may also occur in cytoplasm and mitochondria, especially due to the activity of multi-organellar ubiquitin ligases and chaperones.

CYTOSOL PROTEOSTASIS IN BREWING YEAST AND THE IMPACT ON BEER FERMENTATION

In the cytosol, misfolded proteins that have exposed hydrophobic amino acid residues are recognized by protein quality control mechanisms (Buchberger et al., 2010). The cytoplasmic proteostasis mechanism in yeast comprises the heat shock response (HSR) (Mager and Ferreira, 1993), which promotes the expression of molecular chaperones and the proteasome system (Parsell et al., 1993). Similar to UPR, the HSR is induced by different stress conditions that lead to proteotoxicity. In *S. cerevisiae*, the HSR is regulated by the heat shock factor 1 (Hsf1p) transcription factor, encoded by the *HSF1* gene (Weindling and Bar-Nun, 2015). Hsf1p promotes an adaptive response to different stressor agents, including ethanol (Weindling and Bar-Nun, 2015). Yeast cells treated with 6% (v/v) ethanol show induction of Hsf1p activity (Lee et al., 2000), while Hsf1p mutants were defective in ethanol stress-induced target gene expression (Takemori et al., 2006). Interestingly, the ER oxidoreductin, which is encoded by *ERO1* and induces protein disulfide bonds, was upregulated by Hsf1p in yeast cells exposed to ethanol (Takemori et al., 2006), pointing to a crosstalk between HSR and ERQC mechanisms. Unfortunately, the activity of HSR and ERQC in conditions of VHG beer fermentation or yeast serial repitching is not well understood, but we speculate that modulation of the crosstalk between HSR and ERQC mechanisms may promote ethanol tolerance and cell adaptability during beer fermentation. In line with this hypothesis, ubiquitin ligases, which function by transferring ubiquitin to misfolded/unfolded proteins thus targeting them to the 26S proteasome complex, are key components that regulate both HSR and ERQC (Szoradi et al., 2018). It is well known that different organelles have their own specific ubiquitin ligases, such as Hrd1p and Doa10p in the ER (Ruggiano et al., 2014), San1p in the nucleus (Gardner et al., 2005), and Ubr1p, Ubr2p, Hul5p, and Rsp5p in the cytosol (Prasad et al., 2018). However, different ubiquitin ligases have overlapping functions, such as Doa10p in nucleus and cytosol, San1p in cytoplasm, and Ubr1p in the ER (Szoradi et al., 2018). This ubiquitin ligase network is an essential component of inter-organellar proteostasis, yet very little is known about how this communication is mediated. For example, the overexpression of cytosolic Rsp5p, a NEDD4 family E3 ubiquitin ligase, improve thermoresistance and stress tolerance in yeast strains used for bioethanol production (Hiraishi et al., 2006; Shahsavarani et al., 2012). Disruption of *RSP5* increase the production of isoamyl alcohol and isoamyl acetate in laboratory yeast strains (Abe and Horikoshi, 2005). Rsp5p is part of the so-called "Rsp5-ART ubiquitin ligase adaptor network", which acts to promote the endocytosis and degradation of misfolded integral membrane proteins found in the ER, Golgi, and plasma membrane (Zhao et al., 2013). Additionally, Rsp5p

interacts with another important cytosolic E3 ubiquitin ligase named Ubr1p, which is a component of the stress-induced homeostatically-regulated protein degradation (SHRED) pathway (Szoradi et al., 2018).

The SHRED pathway is initially activated by transcription of the hydrophilin-coding gene *ROQ1* by different stress conditions due to the presence of Msn2p/4p and Hsf1p-associated stress response elements in the *ROQ1* promoter (Yamamoto et al., 2005; Verghese et al., 2012; Szoradi et al., 2018). Once translated, Roq1p is cleaved by the endopeptidase Ynm3p, and cleaved Roq1p binds to Ubr1p changing its substrate specificity and promoting the degradation of misfolded proteins at the ER membrane and in the cytosol by the proteasome (Szoradi et al., 2018). Ubr1p interacts with the chaperone Hsp70p and with Sse1p, the ATPase component of the heat shock protein Hsp90 chaperone complex (Nillegoda et al., 2010). Moreover, it has been demonstrated that Ubr1p is a fundamental component of ERAD when yeast cells are exposed to heat or ethanol stress, bypassing the functions of the canonical Hrd1p/Der3p and Doa10p (Stolz et al., 2013). Thus, considering the importance of Rsp5p and Ubr1p in heat and ethanol stress response, we hypothesize that under conditions of VHG/HG beer fermentation, the Rsp5-ART ubiquitin ligase adaptor network and SHRED pathway actively target protein aggregates present in the ER and cytosol to ERAD (**Figure 4**).

Besides ubiquitin ligases, many chaperones are essential to repair and/or prevent misfolded proteins even before they can be targeted to ERAD. In yeast, chaperones are classified in eight distinct families, which are the small heat-shock proteins (SMALL), the AAA+ family, the CCT/TRiC complex, the prefoldin/GimC (PFD) complex, Hsp40, Hsp60, Hsp70, and Hsp90 families (Gong et al., 2009). From transcriptome data analysis, we observed the upregulation of 54 Pan-DEGs linked to chaperone activity (**Figures 2A, B**) in the lager yeast strain during beer fermentationas compared to the propagation step. Of these 54 Pan-DEGs linked to chaperone activity, 21 Pan-DEGs encode for chaperone proteins that are found in the cytoplasm and mitochondria (**Figure 3A**) and belong to the HSP70, HSP40, SMALL, AAA+, HSP60, and HSP90 families (**Figure 3B**).

Considering the chaperones found in cytoplasm that belong to the Hsp70 family, we found that the Pan-DEGs *SSA1-4*, *SSZ1*, and *SSB2* were upregulated during beer fermentation in comparison to propagation (**Figures 2A, B**). The roles of Hsp70s proteins in yeast subjected to ethanol stress are extensively documented, including in beer production. For example, it was reported that *FES1, SSA2, SSA3, SSA4*, and *SSE1* are upregulated in a synthetic wort that mimicked a VHG beer fermentation (Qing et al., 2012). Other studies based on proteomics and quantitative RT-qPCR also confirmed the expression of cytosolic Hsp70p during the early phases of beer fermentation in different lager strains (Brejning et al., 2005; Smart, 2007), and it was clearly demonstrated that moderate concentrations of ethanol (> 4% v/v) induce the expression of Hsp70 proteins (Piper et al., 1994). In fact, proteins of the Hsp70 family display important functions not only as chaperones, but also in targeting misfolded proteins for proteasome degradation (Kettern et al., 2010; Kim et al., 2013). In addition, Hsp70 proteins form a bi-chaperone system with Hsp104p, a heat shock protein belonging to the AAA+ family

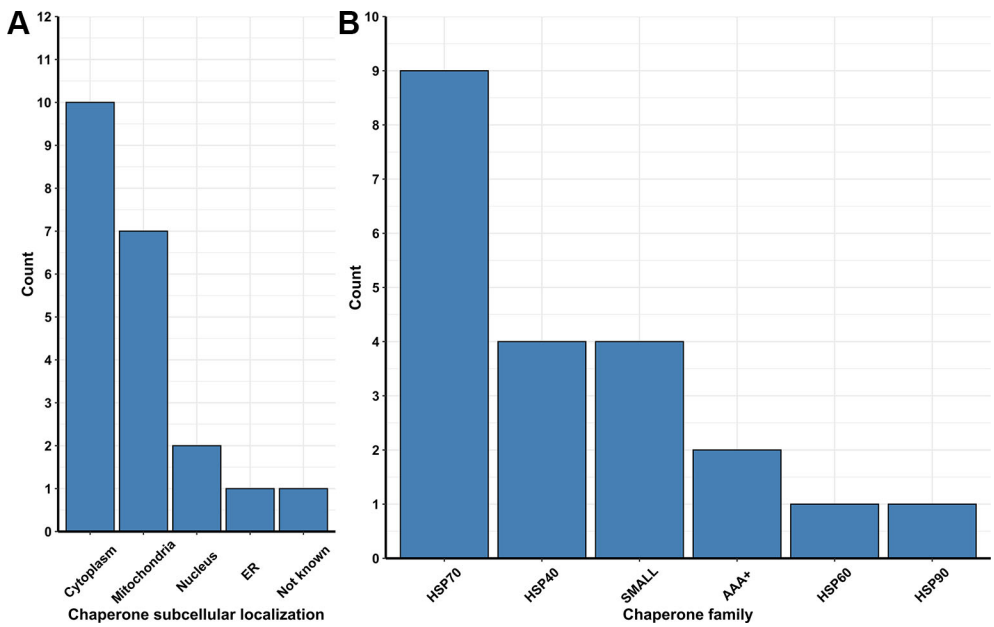

FIGURE 3 | (A) Number of chaperones and folding protein coding Pan-genes found to be upregulated in different organelles of the lager yeast CB11 strain during beer fermentation, in comparison to yeast propagation. **(B)** Number of coding Pan-genes upregulated in CB11 during beer fermentation, in comparison to yeast propagation, that are linked to the major chaperone protein families.

(Zolkiewski et al., 2012), and promote the disaggregation and resolubilization of misfolded proteins (Weibezahn et al., 2005). The transcriptome data also indicated that *HSP104* is upregulated during beer fermentation compared to propagation (**Figures 2A, B**), supporting our hypothesis that ethanol may promote the formation of misfolded protein aggregates in lager yeast strains during beer fermentation, which likely triggers the activity of Hsp70p and Hsp104p to refold and resolubilize the protein aggregates or target them to the proteasome.

Corroborating the importance of *HSP104* for VHG beer fermentation, Rautio et al. (2007) showed that *HSP104* is induced in the first 10 to 30 h of fermentation together with *TPS1*, which encodes trehalose phosphate synthase, a key enzyme involved in trehalose biosynthesis and ethanol stress protection (Alexandre et al., 2001) during beer fermentation. The roles of trehalose as a molecular chaperone in protecting yeast cells against protein aggregation are well understood (Singer and Lindquist, 1998) and a synergistic effect of Hsp104p on trehalose accumulation and degradation has been observed (Iwahashi et al., 1998). However, trehalose and Hsp104p are both required when protein aggregation can be reversible in yeast cells (Sethi et al., 2018). It will be interesting to determine if Hsp104p and trehalose act synergistically in VHG beer protecting yeast cells in the early phases of the fermentation process.

In addition to Hsp70 and AAA+ families, we also observed two additional HSP members with high expression in the cytosol of lager yeast cell during beer fermentation compared to cell propagation, which were the SMALL and Hsp40 proteins (**Figure 3B**). The SMALL or small heat shock proteins/α-crystallin (sHSP) family is comprised of Hsp26p and Hsp42p in *S. cerevisiae,* two proteins important for preventing unfolded protein aggregation that have overlapping functions in non-stressed and stressed yeast cells (Haslbeck et al., 2004). It was previously demonstrated that Hsp26p co-assembles with misfolded proteins and allows the Hsp104p/Hsp70p/Hsp40p complex to disaggregate them (Cashikar et al., 2005). Interestingly, *HSP26* and other HSP-coding genes were found to be upregulated in yeast strains isolated from sherry wines (Aranda et al., 2002), as well as in lager yeast cells in 16 °P and 24 °P wort after 24 h of fermentation (Odumeru et al., 1992). In addition, it was shown that Hsp26P is a key HSP for ethanol production (Sharma, 2001).

Another interesting target of our transcriptome analysis was the *HSP82* Pan-DEG, which was found to be upregulated in lager yeast during beer fermentation (**Figures 2A, B**), corroborating the previous data of Gibson et al. (2008). Additionally, in brewing yeast, it has been demonstrated by proteomics and transcriptomics that ethanol stress induces the expression of Hsp82p in wine yeasts (Aranda et al., 2002; Navarro-Tapia et al., 2016) and bioethanol yeast strains (Li et al., 2010). The Hsp82 protein, which belongs to the HSP90 family, is an abundant and essential dimeric ATP-dependent chaperone (Borkovich et al., 1989; Richter et al., 2001). It is required to reactivate proteins damaged by heat without participating in *de novo* folding of most proteins (Nathan et al., 1997). Hsp82 target proteins include steroid hormone receptors and kinases (Mayr et al., 2000). It has been demonstrated that Hsp82p is regulated by several co-chaperones, including Aha1p and Hch1p, both of which activate the ATPase function of Hsp82p (Panaretou et al., 2002) and whose Pan-DEGs were found upregulated in lager yeast during beer fermentation (**Figures 2A, B**). A third co-chaperone named Cpr6p, a peptidyl-prolyl cis-trans isomerase (cyclophilin) that interacts with Hsp82p, and together with Cpr7p, is required for normal yeast growth (Zuehlke and Johnson, 2012). *CPR6* was found to be upregulated in our transcriptome analysis during beer fermentation (**Figures 2A, B**), but little is known about its roles during beer fermentation. However, protein-protein interaction data (**Figure S10**) indicate that Cpr6p interacts with Pbp1p, a component of processing bodies (p-bodies) and stress granules (SGs), which may be induced by severe ethanol stress, heat shock, or glucose deprivation (Kato et al., 2011). Induction of p-bodies and SGs by UPR, which has been observed in mammalian cells (Harding et al., 2000; Anderson and Kedersha, 2008) may also occur in yeast cells. In fact, it would be interesting to determine whether p-bodies/SGs are formed during beer fermentation and if they are associated with proteostasis in cytosol and/or the ER. Cpr6p also interacts with Rpd3p (**Figure S10**), a conserved histone deacetylase that together with Sin3p and Ume1p comprise the Sin3 complex, a global regulator of transcription that is linked to a series of physiological conditions in yeast and other organisms (Silverstein and Ekwall, 2005), such as ethanol stress (Ma and Liu, 2012). Thus, Cpr6p could be an important co-chaperone that together with Hsp82 may serve as a hub for p-bodies/SGs and epigenetic regulation of genes linked to beer fermentation and proteostasis.

MITOCHONDRIAL PROTEOSTASIS IN BREWING YEAST

During beer production, yeast mitochondria exert important functions despite the catabolic repression of nuclear genes encoding mitochondrial proteins linked to respiration (O'Connor-Cox et al., 1996). In fact, mitochondria are not only the primary site of lipid and ergosterol synthesis, but they also provide a series of metabolites originating from central carbon and proline-arginine metabolism (Kitagaki and Takagi, 2014). A large proportion of cellular radical molecules are produced as a result of mitochondrial metabolism, which can strongly affect yeast physiology (Kitagaki and Takagi, 2014). Despite the metabolic and physiological importance of mitochondria, mutations linked to the mitochondrial genome that result in *petite* phenotypes can result in the production of off-flavors (related to synthesis of esters and fusel alcohols) in beer fermentation (Ernandes et al., 1993). Finally, in lager yeasts and possibly in ale strains, mitotype can have a strong influence on temperature tolerance (Baker et al., 2019).

Proteostasis in mitochondria includes different chaperones and proteases, as well as proteins that participate in inter-organellar communication, where defects in mitochondrial proteostasis impacts health and aging (Moehle et al., 2019).

Similar to ER, mitochondria have a so-called "mitochondrial unfolded protein response" or mtUPR, which was initially characterized in mammalian cells (Zhao, 2002).

Considering that mitochondria have distinct subcompartments within the organelle (e.g. matrix, outer membrane, and intermembrane space), protein import and sorting processes are very complex (Neupert and Herrmann, 2007). Most mitochondrial proteins are imported as unfolded precursors by means of the translocase of outer membrane (TOM) and translocase of inner membrane (TIM) complexes. Upon translocation into the mitochondria, the proteins undergo chaperone-assisted folding (Neupert and Herrmann, 2007).

The transcriptome analysis of lager yeast cells during beer fermentation revealed that TIM-related Pan-DEGs including *TIM8*, *TIM9*, *TIM12*, *TIM17*, and *TIM54* are upregulated (**Figures 2A, B**). Tim8p and Tim9p belong to the mitochondrial intermembrane space protein transporter complex, which together with Tim10p, Tim12p, and Tim13p, mediates the transit of proteins destined for the inner membrane across the mitochondria intermembrane space (Davis et al., 2007). Tim9p/Tim10p and Tim9p/Tim10p/Tim12p interact with Tim22p, comprising a multioligomeric complex with Tim54p, Tim22p, Tim18p, and Sdh3p (Gebert et al., 2011). The Tim22 complex mediates the insertion of large hydrophobic proteins, like carrier proteins with multiple transmembrane segments, as well as Tim23p, Tim17p, and Tim22p into the inner membrane (Mokranjac and Neupert, 2009). Tim17p is a component of the Tim23 complex, which promotes the translocation and insertion of proteins into the inner mitochondrial membrane (Mokranjac and Neupert, 2009). The Tim23 complex is composed of a membrane-embedded part, which forms the import motor. This component is formed by Tim14p (Pam18p), Tim16 (Pam16p), Tim44p, Mge1p, and mitochondrial Hsp70p (Mokranjac and Neupert, 2009). The Pan-DEGs encoding Pam16p and Pam18p were found to be upregulated in our transcriptome analysis (**Figures 2A, B**). Despite the large amount of data collected so far about the roles of Tim22 and Tim23 complexes in yeast mitochondria, considerably less is known about their roles in yeast fermentation/ethanol stress. However, Short et al. (2012) showed that yeast temperature sensitive mutant strains for *PAM16* have defects in fermentation linked to lipid metabolism. Moreover, an upregulated Pan-DEG in our transcriptome analysis, *MDJ2,* encode a chaperone belonging to the HSP40 family that regulates Hsp70 chaperone activity and interacts with Pam18p (Mokranjac et al., 2005). In addition, the transcriptome analysis of lager yeast cells revealed upregulation of *TOM6* and *TOM7* Pan-DEGs (**Figures 2A, B**), both encoding small protein components of the TOM complex (Dekker et al., 1998). At present, the roles of Tom6p and Tom7p in yeast fermentation/ethanol stress remain unknown.

Two important Pan-DEGs found to be upregulated in our transcriptome analysis, *PHB1* and *PHB2* (**Figures 2A, B**), encode the proteins prohibitin 1 (Phb1p) and 2 (Phb2p), which are part of a large chaperone complex that stabilizes protein structures and is involved in the regulation of yeast replicative life span and mtUPR (Coates et al., 1997; Nijtmans, 2000). In the context of aging and replicative life span, the impact of Phb1p/2p expression during VHG/HG beer fermentation and/or yeast reuse is unknown, despite the fact that a mixed aged yeast population is commonly observed in mostly ale/lager fermentations (Smart et al., 2000; Powell et al., 2003). Moreover, yeast *phb1* and *phb2* mutants are defective in mitochondrial segregation from mother cells to daughter cells, resulting in delayed segregation of mitochondria (Piper et al., 2002). Interestingly, loss of the orthologous prohibitin in *Caenorhabditis elegans* affected the morphology of mitochondria, resulting in fragmented and disorganized structures (Sanz et al., 2003), a phenotype previously observed in yeast strains used for sake (Kitagaki and Shimoi, 2007) and cider (Lloyd et al., 1996) after prolonged anaerobiosis under high concentration of ethanol (> 10% v/v). In animal cells, mitochondrial fragmentation is a feature of mitochondrial proteostasis that is activated in response to a high number of misfolded proteins, but that is also observed during mitophagy and programmed cell death (Moehle et al., 2019). Similarly, Fis1p, a protein involved in mitochondria and peroxisome maintenance in yeast, is upregulated when cells are subjected to high ethanol concentrations, thereby promoting mitochondrial fragmentation and inhibition of apoptosis (Kitagaki et al., 2007).

Taking into account mitochondria structure, *YME1* and *AFG3* were also found to be upregulated in lager yeast cells (**Figures 2A, B**). These Pan-DEGs encode the mitochondrial ATP-dependent metallopeptidase (AAA protease) Yme1p and Afg3p, respectively, which are necessary for degradation of unfolded or misfolded proteins associated with the mitochondrial inner membrane (Arlt et al., 1996; Schreiner et al., 2012). Despite the fact that the specific roles of Yme1p and Afg3p in VHG/HG beer fermentation or yeast reuse are currently unknown, data regarding the modulation of mitochondria activity upon ethanol exposure indicates that ethanol increases oxidative stress and induces the formation of mitochondrial permeability transition (MPT). MPT is a protein structure that forms a pore across the inner and outer membranes of mitochondria, leading to the depolarization of membrane potential, uncoupling of oxidative phosphorylation and ATP depletion, rupture of the outer mitochondrial membrane, and apoptosis induction (Pastorino et al., 1999; Hoek et al., 2002). Interestingly, AAA proteases seem to be essential to coordinate many functions within mitochondria, including mitochondrial genome stability, respiratory chain complexes synthesis, and the mitochondrial membrane metabolism (Patron et al., 2018). Moreover, AAA proteases are essential to modulate the activity of the mitochondrial Ca^{2+} uniporter (MCU) complex. Mutations in mammalian mitochondrial AAA proteases induce constitutive MCU activity and deregulated mitochondrial Ca^{2+} influx, leading to cell death (König et al., 2016). This suggests that yeast AAA proteases may have essential roles in maintaining mitochondrial structure and function during beer fermentation and ethanol stress, and dysfunctions in mitochondrial AAA proteases are likely to affect brewing yeast viability and vitality.

Besides the protein complexes linked to mitochondrial structure and function, our transcriptome analysis revealed an additional eight upregulated genes during beer fermentation (**Figure 3A**) that encode for mitochondrial molecular chaperones. These included three upregulated Pan-DEGs belonging to the HSP40 family (*MDJ1*, *MDJ2*, and *JAC1*), one to the HSP60 family (*HSP60*), one to the HSP70 family (*ECM10*), and one to the AAA+ family (*HSP78*) (**Figures 2A, B**). The interaction between mitochondrial Hsp40 and Hsp70 proteins has been extensively documented, being involved in the translocation of proteins to the matrix and folding (Liu et al., 2001). The chaperone Hsp60p is a fundamental protein required to assist the folding and import of different target proteins to the mitochondrial matrix (Reading et al., 1989), also being important for the replication of mitochondrial DNA in yeast (Kaufman et al., 2003). Finally, Hsp78p is a chaperone that displays similar functions with those of the mitochondrial Hsp70 system (Schmitt et al., 1995). Biochemical studies have indicated cooperation between the Hsp70 system and Hsp78p, forming a bichaperone Hsp70-Hsp78 system that assists in protein refolding after stress induction (Krzewska et al., 2001). Similar to Hsp60p, available evidence suggests that Hsp78p is required for the maintenance of mitochondrial genome integrity (Schmitt, 1996). Thus, it is clear that proteostasis mechanisms in mitochondria play a central role in the maintenance of both proteins and mitochondria nucleoid structure and function, the latter of which profoundly affects beer fermentation (Smart, 2007) and hybrid brewing yeast strain adaptability to temperature (Baker et al., 2019).

DISCUSSION

Different organelles such as ER, cytosol, and mitochondria display a set of molecules/proteins that are essential for proteostasis under environmental conditions that are prone to induce protein misfolding/unfolding and amorphous aggregate formation, both potentially leading to proteotoxicity. One such condition is beer fermentation, where brewing yeast strains require protection from the toxic and pleiotropic effects of ethanol. In order to deal with ethanol and maintain proteostasis during beer fermentation, the major cellular compartments (e.g. mitochondria, ER, and cytosol) must communicate with one another to mount a systemic cell response (**Figure 4**).

Multiple lines of evidence indicate that organellar proteostasis is a concerted process that is directly connected with different biological processes, such as metabolism and aging (Raimundo and Kriško, 2018). This so-called "inter-organellar/cross-organellar communication/response" or CORE is dependent on a series of signaling-associated and/or protein networks that include HSPs and their target molecules (Raimundo and Kriško, 2018). Interestingly, one hallmark of the CORE is the

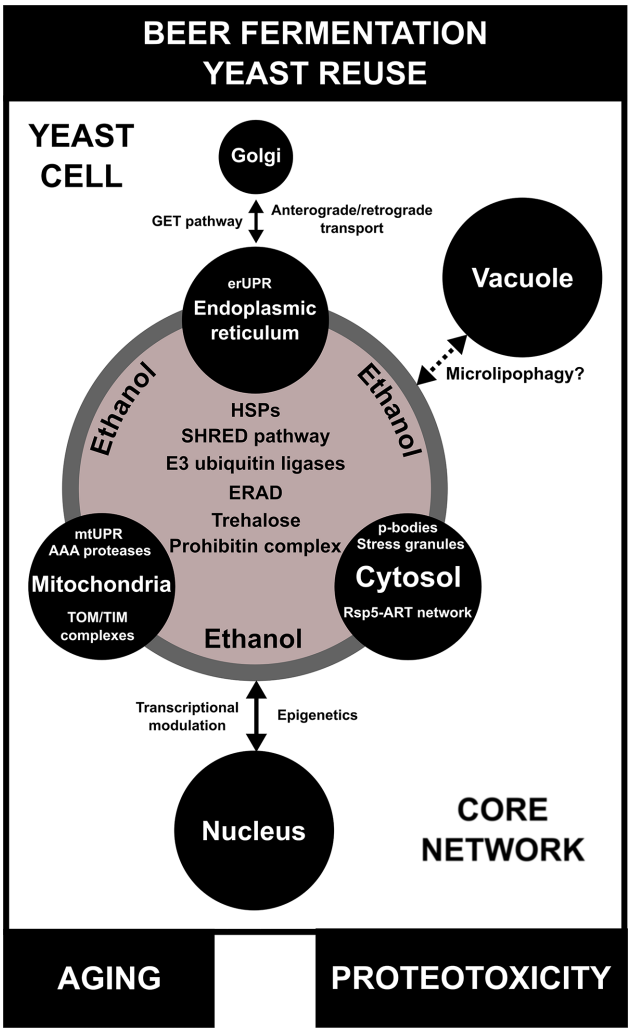

FIGURE 4 | A model for inter-organellar/cross-organellar communication/response proteostasis (CORE network) in brewing yeast. During beer fermentation and/or yeast reuse, the endoplasmic reticulum (ER), mitochondria, and cytosol regulate proteostasis/protein quality by monitoring their environments and communicating with one another by means of the CORE network. In conditions of proteotoxicity induced by ethanol during beer fermentation, the CORE network is activated and is composed of different proteins/pathways, such as heat shock proteins (HSPs), endoplasmic reticulum-associated protein degradation (ERAD), the stress-induced, homeostatically regulated protein degradation (SHRED) pathway, E3 ubiquitin ligases, and the prohibitin complex. Trehalose, a molecular chaperone necessary for proteotoxic response, is also part of the CORE network. Additionally, each organelle has its own particular mechanisms of protein quality control/proteostasis. The impact of the CORE network in the proteostasis response of vacuoles of brewing yeast is not well understood, but may be associated with microlipophagy. Finally, proteotoxicity induced by ethanol regulates transcriptional activity and epigenetic mechanisms in the nucleus, which are influenced by CORE network components. Moreover, the CORE network activity and proteotoxicity are potentially linked to aging in brewing yeast cells.

upregulation of multiple genes and proteins linked to proteostasis, including *PDI1*, *HSP26*, and *HSP90* (Perić et al., 2016). However, we speculate that other protein and small molecule networks, such as those composed of E3 ubiquitin ligases, the SHRED pathway, trehalose biosynthesis, ERAD, and the prohibitin complex, could be essential components of a larger CORE network that is upregulated during beer fermentation (**Figure 4**). The activation of a CORE network may impact different aspects of fermentative metabolism that are crucial for yeast viability and/or vitality and further use in serial repitching. For example, it was observed in *C. elegans* that mitochondrial proteotoxicity increases fatty acid synthesis and promotes lipid accumulation, a condition associated with mitochondrial-to-cytosolic stress response that is essential for *C. elegans* survival (Kim et al., 2016). Similarly, we observed in our transcriptome analysis an increase in the expression of genes related to lipid biosynthesis in lager yeast (**Figures S11** and **S12**), pointing to a potentially conserved CORE network in eukaryotes. Furthermore, the roles of inter-organellar proteostasis mechanisms in the replicative and chronological life span of yeast cells have been demonstrated previously (Perić et al., 2016; Chadwick et al., 2019), which are very likely to affect brewing. Finally, a number of important questions remain about how the CORE network may modulate other organelles (e.g. nucleus and vacuole) during beer fermentation (**Figure 4**). As described above, some components of organellar proteostasis influence transcriptional activity in the nucleus. Recently, Andréasson et al. (2019) demonstrated an important connection between mitochondria and nucleus for proteostasis and cell metabolism. However, little is known about epigenetic modulation during proteotoxic stress induced by ethanol. In the same sense, how the CORE network connects with vacuoles is an open question (**Figure 4**). Noteworthy, it was demonstrated that in conditions of lipid imbalance, unfolded ER proteins can be removed by lipid droplets and targeted to the vacuole for degradation by microlipophagy (Vevea et al., 2015). However, the impact of this mechanism remains to be determined in beer fermentation.

To evaluate the importance of each component of the CORE network for beer fermentation, it is indispensable to get high quality RNA-seq data from different *S. pastorianus* strains in conditions of industrial yeast propagation and beer fermentation. It can be potentially achieved by tagging the major genes of *S. cerevisiae* and *S. eubayanus* linked to the CORE network followed by interspecies hybridization to generate *S. pastorianus* strains by different techniques, like HyPr (Alexander et al., 2016), and testing them in brewery environment. On the other hand, the use of different proteome techniques to evaluate the contribution of CORE components is also welcome as well as the generation of *S. pastorianus* mutant strains for CORE components by uding CRISPR-Cas9 technology (de Vries et al., 2017).

In conclusion, a better understanding of the CORE network in the context of beer fermentation and/or ethanol stress will allow us to improve different aspects of brewing, from ethanol tolerance in VHG/HG fermentation to yeast reuse, potentially allowing us to select yeast strains with high tolerance to ethanol or diminished aging, which will ultimately improve beer yield and quality.

DATA AVAILABILITY STATEMENT

Publicly available datasets were analyzed in this study. These data can be found at Gene Expression Omnibus (GSE9423, GSE10205, and GSE16376).

AUTHOR CONTRIBUTIONS

DB contributed to the design, acquisition, analysis, and interpretation of data for the work. DB, BT, and MM contributed to drafting the work and prepared the final work. DB prepared the figures and all authors approved the final manuscript.

SUPPLEMENTARY MATERIAL

The Supplementary Material for this article can be found online at: https://www.frontiersin.org/articles/10.3389/fgene.2020.00002/full#supplementary-material

REFERENCES

Abe, F., and Horikoshi, K. (2005). Enhanced production of isoamyl alcohol and isoamyl acetate by ubiquitination-deficient *Saccharomyces cerevisiae* mutants. *Cell. Mol. Biol. Lett.* 10, 383–388.

Alexander, W. G., Peris, D., Pfannenstiel, B. T., Opulente, D. A., Kuang, M., and Hittinger, C. T. (2016). Efficient engineering of marker-free synthetic allotetraploids of *Saccharomyces*. *Fungal Genet. Biol. FG B.* 89, 10–17. doi: 10.1016/j.fgb.2015.11.002

Alexandre, H., Ansanay-Galeote, V., Dequin, S., and Blondin, B. (2001). Global gene expression during short-term ethanol stress in *Saccharomyces cerevisiae*. *FEBS Lett.* 498, 98–103. doi: 10.1016/S0014-5793(01)02503-0

Anderson, P., and Kedersha, N. (2008). Stress granules: the Tao of RNA triage. *Trends Biochem. Sci.* 33, 141–150. doi: 10.1016/j.tibs.2007.12.003

Andréasson, C., Ott, M., and Büttner, S. (2019). Mitochondria orchestrate proteostatic and metabolic stress responses. *EMBO Rep.* 20, e47865. doi: 10.15252/embr.201947865

Aranda, A., Querol, A., and del Olmo, M. L. (2002). Correlation between acetaldehyde and ethanol resistance and expression of HSP genes in yeast strains isolated during the biological aging of sherry wines. *Arch. Microbiol.* 177, 304–312. doi: 10.1007/s00203-001-0391-1

Arlt, H., Tauer, R., Feldmann, H., Neupert, W., and Langer, T. (1996). The YTA10–12 complex, an AAA protease with chaperone-like activity in the inner membrane of mitochondria. *Cell* 85, 875–885. doi: 10.1016/S0092-8674(00)81271-4

Baker, E. P., Peris, D., Moriarty, R. V., Li, X. C., Fay, J. C., and Hittinger, C. T. (2019). Mitochondrial DNA and temperature tolerance in lager yeasts. *Sci. Adv.* 5, eaav1869. doi: 10.1126/sciadv.aav1869

Borkovich, K. A., Farrelly, F. W., Finkelstein, D. B., Taulien, J., and Lindquist, S. (1989). Hsp82 is an essential protein that is required in higher concentrations for growth of cells at higher temperatures. *Mol. Cell. Biol.* 9, 3919–3930. doi: 10.1128/MCB.9.9.3919

Braakman, I., and Hebert, D. N. (2013). Protein folding in the endoplasmic reticulum. *Cold Spring Harb. Perspect. Biol.* 5, a013201–a013201. doi: 10.1101/cshperspect.a013201

Brejning, J., Arneborg, N., and Jespersen, L. (2005). Identification of genes and proteins induced during the lag and early exponential phase of lager brewing yeasts. *J. Appl. Microbiol.* 98, 261–271. doi: 10.1111/j.1365-2672.2004.02472.x

Brodsky, J. L., and Wojcikiewicz, R. J. (2009). Substrate-specific mediators of ER associated degradation (ERAD). *Curr. Opin. Cell Biol.* 21, 516–521. doi: 10.1016/j.ceb.2009.04.006

Buchberger, A., Bukau, B., and Sommer, T. (2010). Protein quality control in the cytosol and the endoplasmic reticulum: brothers in arms. *Mol. Cell* 40, 238–252. doi: 10.1016/j.molcel.2010.10.001

Cashikar, A. G., Duennwald, M., and Lindquist, S. L. (2005). A chaperone pathway in protein disaggregation: Hsp26 alters the nature of protein aggregates to facilitate reactivation by Hsp104. *J. Biol. Chem.* 280, 23869–23875. doi: 10.1074/jbc.M502854200

Chadwick, S. R., Fazio, E. N., Etedali-Zadeh, P., Genereaux, J., Duennwald, M. L., and Lajoie, P. (2019). A functional unfolded protein response is required for chronological aging in Saccharomyces cerevisiae. *Curr. Genet*. doi: 10.1007/s00294-019-01019-0

Chapman, R. E., and Walter, P. (1997). Translational attenuation mediated by an mRNA intron. *Curr. Biol.* 7, 850–859. doi: 10.1016/S0960-9822(06)00373-3

Chartron, J. W., Clemons, W. M., and Suloway, C. J. (2012). The complex process of GETting tail-anchored membrane proteins to the ER. *Curr. Opin. Struct. Biol.* 22, 217–224. doi: 10.1016/j.sbi.2012.03.001

Clerc, S., Hirsch, C., Oggier, D. M., Deprez, P., Jakob, C., Sommer, T., et al. (2009). Htm1 protein generates the N-glycan signal for glycoprotein degradation in the endoplasmic reticulum. *J. Cell Biol.* 184, 159–172. doi: 10.1083/jcb.200809198

Coates, P. J., Jamieson, D. J., Smart, K., Prescott, A. R., and Hall, P. A. (1997). The prohibitin family of mitochondrial proteins regulate replicative lifespan. *Curr. Biol.* 7, 607–610. doi: 10.1016/S0960-9822(06)00261-2

Cray, J. A., Stevenson, A., Ball, P., Bankar, S. B., Eleutherio, E. C., Ezeji, T. C., et al. (2015). Chaotropicity: a key factor in product tolerance of biofuel-producing microorganisms. *Curr. Opin. Biotechnol.* 33, 228–259. doi: 10.1016/j.copbio.2015.02.010

Davis, A. J., Alder, N. N., Jensen, R. E., and Johnson, A. E. (2007). The Tim9p/10p and Tim8p/13p complexes bind to specific sites on Tim23p during mitochondrial protein import. *Mol. Biol. Cell* 18, 475–486. doi: 10.1091/mbc.e06-06-0546

de Vries, A. R. G., de Groot, P. A., van den Broek, M., and Daran, J.-M. G. (2017). CRISPR-Cas9 mediated gene deletions in lager yeast. *Saccharomyces pastorianus. Microb. Cell Factories* 16. doi: 10.1186/s12934-017-0835-1

Dekker, P. J. T., Ryan, M. T., Brix, J., Müller, H., Hönlinger, A., and Pfanner, N. (1998). Preprotein translocase of the outer mitochondrial membrane: molecular dissection and assembly of the general import pore complex. *Mol. Cell. Biol.* 18, 6515–6524. doi: 10.1128/MCB.18.11.6515

Denic, V., Dotsch, V., and Sinning, I. (2013). Endoplasmic reticulum targeting and insertion of tail-anchored membrane proteins by the GET pathway. *Cold Spring Harb. Perspect. Biol.* 5, a013334–a013334. doi: 10.1101/cshperspect.a013334

English, A. R., and Voeltz, G. K. (2013). Endoplasmic reticulum structure and interconnections with other organelles. *Cold Spring Harb. Perspect. Biol.* 5, a013227–a013227. doi: 10.1101/cshperspect.a013227

Ernandes, J. R., Williams, J. W., Russell, I., and Stewart, G. G. (1993). Respiratory deficiency in brewing yeast strains—effects on fermentation, flocculation, and beer flavor components. *J. Am. Soc Brew. Chem.* 51, 16–20. doi: 10.1094/ASBCJ-51-0016

Esteban-Pretel, G., Marín, M. P., Romero, A. M., Ponsoda, X., Ballestin, R., Canales, J. J., et al. (2011). Protein traffic is an intracellular target in alcohol toxicity. *Pharmaceuticals* 4, 741–757. doi: 10.3390/ph4050741

Ferris, S. P., Kodali, V. K., and Kaufman, R. J. (2014). Glycoprotein folding and quality-control mechanisms in protein-folding diseases. *Dis. Model. Mech.* 7, 331–341. doi: 10.1242/dmm.014589

Friedmann, E., Salzberg, Y., Weinberger, A., Shaltiel, S., and Gerst, J. E. (2002). YOS9, the putative yeast homolog of a gene amplified in osteosarcomas, is involved in the endoplasmic reticulum (ER)-Golgi transport of GPI-anchored proteins. *J. Biol. Chem.* 277, 35274–35281. doi: 10.1074/jbc.M201044200

Gardner, R. G., Nelson, Z. W., and Gottschling, D. E. (2005). Degradation-mediated protein quality control in the nucleus. *Cell* 120, 803–815. doi: 10.1016/j.cell.2005.01.016

Gebert, N., Gebert, M., Oeljeklaus, S., von der Malsburg, K., Stroud, D. A., Kulawiak, B., et al. (2011). Dual function of Sdh3 in the respiratory chain and TIM22 protein translocase of the mitochondrial inner membrane. *Mol. Cell* 44, 811–818. doi: 10.1016/j.molcel.2011.09.025

Ghosh, P., Liu, Q.-H., and Lakshman, M. R. (1995). Long-term ethanol exposure impairs glycosylation of both N- and O-glycosylated proteins in rat liver. *Metabolism* 44, 890–898. doi: 10.1016/0026-0495(95)90242-2

Gibson, B. R., Lawrence, S. J., Leclaire, J. P. R., Powell, C. D., and Smart, K. A. (2007). Yeast responses to stresses associated with industrial brewery handling. *FEMS Microbiol. Rev.* 31, 535–569. doi: 10.1111/j.1574-6976.2007.00076.x

Gibson, B. R., Lawrence, S. J., Boulton, C. A., Box, W. G., Graham, N. S., Linforth, R. S. T., et al. (2008). The oxidative stress response of a lager brewing yeast strain during industrial propagation and fermentation: oxidative stress response of lager brewing yeast. *FEMS Yeast Res.* 8, 574–585. doi: 10.1111/j.1567-1364.2008.00371.x

Gilbert, H. F. (1997). Protein disulfide isomerase and assisted protein folding. *J. Biol. Chem.* 272, 29399–29402. doi: 10.1074/jbc.272.47.29399

Goder, V., and Melero, A. (2011). Protein O-mannosyltransferases participate in ER protein quality control. *J. Cell Sci.* 124, 144–153. doi: 10.1242/jcs.072181

Gong, Y., Kakihara, Y., Krogan, N., Greenblatt, J., Emili, A., Zhang, Z., et al. (2009). An atlas of chaperone–protein interactions in *Saccharomyces cerevisiae* : implications to protein folding pathways in the cell. *Mol. Syst. Biol.* 5, 275. doi: 10.1038/msb.2009.26

Gorter de Vries, A. R., Voskamp, M. A., van Aalst, A. C. A., Kristensen, L. H., Jansen, L., van den Broek, M., et al. (2019a). Laboratory evolution of a *Saccharomyces cerevisiae* × *S. eubayanus* hybrid under simulated lager-brewing conditions. *Front. Genet.* 10. 1–18. doi: 10.3389/fgene.2019.00242

Gorter de Vries, A. R., Pronk, J. T., and Daran, J.-M. G. (2019b). Lager-brewing yeasts in the era of modern genetics. *FEMS Yeast Res.* 19 1–17. doi: 10.1093/femsyr/foz063

Hallsworth, J. E. (1998). Ethanol-induced water stress in yeast. *J. Ferment. Bioeng.* 85, 125–137. doi: 10.1016/S0922-338X(97)86756-6

Harding, H. P., Zhang, Y., Bertolotti, A., Zeng, H., and Ron, D. (2000). Perk is essential for translational regulation and cell survival during the unfolded protein response. *Mol. Cell* 5, 897–904. doi: 10.1016/S1097-2765(00)80330-5

Haslbeck, M., Braun, N., Stromer, T., Richter, B., Model, N., Weinkauf, S., et al. (2004). Hsp42 is the general small heat shock protein in the cytosol of *Saccharomyces cerevisiae*. *EMBO J.* 23, 638–649. doi: 10.1038/sj.emboj.7600080

Hetz, C., Chevet, E., and Oakes, S. A. (2015). Proteostasis control by the unfolded protein response. *Nat. Cell Biol.* 17, 829–838. doi: 10.1038/ncb3184

Hiraishi, H., Mochizuki, M., and Takagi, H. (2006). Enhancement of stress tolerance in *Saccharomyces cerevisiae* by overexpression of ubiquitin ligase Rsp5 and ubiquitin-conjugating enzymes. *Biosci. Biotechnol. Biochem.* 70, 2762–2765. doi: 10.1271/bbb.60250

Hoek, J. B., Cahill, A., and Pastorino, J. G. (2002). Alcohol and mitochondria: a dysfunctional relationship. *Gastroenterology* 122, 2049–2063. doi: 10.1053/gast.2002.33613

Horinouchi, T., Yoshikawa, K., Kawaide, R., Furusawa, C., Nakao, Y., Hirasawa, T., et al. (2010). Genome-wide expression analysis of *Saccharomyces pastorianus* orthologous genes using oligonucleotide microarrays. *J. Biosci. Bioeng.* 110, 602–607. doi: 10.1016/j.jbiosc.2010.05.011

Huuskonen, A., Markkula, T., Vidgren, V., Lima, L., Mulder, L., Geurts, W., et al. (2010). Selection from industrial lager yeast strains of variants with improved fermentation performance in very-high-gravity worts. *Appl. Environ. Microbiol.* 76, 1563–1573. doi: 10.1128/AEM.03153-09

Iwahashi, H., Nwaka, S., Obuchi, K., and Komatsu, Y. (1998). Evidence for the interplay between trehalose metabolism and Hsp104 in yeast. *Appl. Environ. Microbiol.* 64, 4614–4617. doi: 10.1128/AEM.64.11.4614-4617.1998

König, T., Tröder, S. E., Bakka, K., Korwitz, A., Richter-Dennerlein, R., Lampe, P. A., et al. (2016). The m-AAA protease associated with neurodegeneration

limits MCU activity in mitochondria. *Mol. Cell* 64, 148–162. doi: 10.1016/j.molcel.2016.08.020

Kamena, F., Diefenbacher, M., Kilchert, C., Schwarz, H., and Spang, A. (2008). Ypt1p is essential for retrograde Golgi-ER transport and for Golgi maintenance in. *S. cerevisiae. J. Cell Sci*. 121, 1293–1302. doi: 10.1242/jcs.016998

Kato, K., Yamamoto, Y., and Izawa, S. (2011). Severe ethanol stress induces assembly of stress granules in. *Saccharomyces cerevisiae. Yeast* 28, 339–347. doi: 10.1002/yea.1842

Kaufman, B. A., Kolesar, J. E., Perlman, P. S., and Butow, R. A. (2003). A function for the mitochondrial chaperonin Hsp60 in the structure and transmission of mitochondrial DNA nucleoids in *Saccharomyces cerevisiae*. *J. Cell Biol.* 163, 457–461. doi: 10.1083/jcb.200306132

Kettern, N., Dreiseidler, M., Tawo, R., and Höhfeld, J. (2010). Chaperone-assisted degradation: multiple paths to destruction. *Biol. Chem.* 391, 481–489. doi: 10.1515/bc.2010.058

Kim, Y. E., Hipp, M. S., Bracher, A., Hayer-Hartl, M., and Ulrich Hartl, F. (2013). Molecular chaperone functions in protein folding and proteostasis. *Annu. Rev. Biochem.* 82, 323–355. doi: 10.1146/annurev-biochem-060208-092442

Kim, H.-E., Grant, A. R., Simic, M. S., Kohnz, R. A., Nomura, D. K., Durieux, J., et al. (2016). Lipid biosynthesis coordinates a mitochondrial-to-cytosolic stress response. *Cell* 166, 1539–1552.e16. doi: 10.1016/j.cell.2016.08.027

Kitagaki, H., and Shimoi, H. (2007). Mitochondrial dynamics of yeast during sake brewing. *J. Biosci. Bioeng.* 104, 227–230. doi: 10.1263/jbb.104.227

Kitagaki, H., and Takagi, H. (2014). Mitochondrial metabolism and stress response of yeast: applications in fermentation technologies. *J. Biosci. Bioeng.* 117, 383–393. doi: 10.1016/j.jbiosc.2013.09.011

Kitagaki, H., Araki, Y., Funato, K., and Shimoi, H. (2007). Ethanol-induced death in yeast exhibits features of apoptosis mediated by mitochondrial fission pathway. *FEBS Lett.* 581, 2935–2942. doi: 10.1016/j.febslet.2007.05.048

Krzewska, J., Langer, T., and Liberek, K. (2001). Mitochondrial Hsp78, a member of the Clp/Hsp100 family in *Saccharomyces cerevisiae*, cooperates with Hsp70 in protein refolding. *FEBS Lett.* 489, 92–96. doi: 10.1016/S0014-5793(00)02423-6

Lawrence, S. J., Wimalasena, T. T., Nicholls, S. M., Box, W. G., Boulton, C., and Smart, K. A. (2012). Incidence and characterization of petites isolated from lager brewing yeast *Saccharomyces cerevisiae* populations. *J. Am. Soc Brew. Chem.* 70, 268–274. doi: 10.1094/ASBCJ-2012-0917-01

Lee, S., Carlson, T., Christian, N., Lea, K., Kedzie, J., Reilly, J. P., et al. (2000). The Yeast heat shock transcription factor changes conformation in response to superoxide and temperature. *Mol. Biol. Cell* 11, 1753–1764. doi: 10.1091/mbc.11.5.1753

Lee, M. C. S., Miller, E. A., Goldberg, J., Orci, L., and Schekman, R. (2004). Bi-directional protein transport between the ER and Golgi. *Annu. Rev. Cell Dev. Biol.* 20, 87–123. doi: 10.1146/annurev.cellbio.20.010403.105307

Li, B.-Z., Cheng, J.-S., Qiao, B., and Yuan, Y.-J. (2010). Genome-wide transcriptional analysis of Saccharomyces cerevisiae during industrial bioethanol fermentation. *J. Ind. Microbiol. Biotechnol.* 37, 43–55. doi: 10.1007/s10295-009-0646-4

Liu, Y., and Chang, A. (2008). Heat shock response relieves ER stress. *EMBO J.* 27, 1049–1059. doi: 10.1038/emboj.2008.42

Liu, Q., Krzewska, J., Liberek, K., and Craig, E. A. (2001). Mitochondrial Hsp70 Ssc1: role in protein folding. *J. Biol. Chem.* 276, 6112–6118. doi: 10.1074/jbc.M009519200

Lloyd, D., Moran, C. A., Suller, M. T. E., Dinsdale, M. G., and Hayes, A. J. (1996). Flow cytometric monitoring of rhodamine 123 and a cyanine dye uptake by yeast during cider fermentation. *J. Inst. Brew.* 102, 251–259. doi: 10.1002/j.2050-0416.1996.tb00910.x

Ma, M., and Liu, Z. L. (2012). "Molecular mechanisms of ethanol tolerance in *Saccharomyces cerevisiae*,," in *Microbial Stress Tolerance for Biofuels*. Ed. Z. L. Liu (Berlin, Heidelberg: Springer Berlin Heidelberg), 77–115. doi: 10.1007/978-3-642-21467-7_4

Mager, W. H., and Ferreira, P. M. (1993). Stress response of yeast. *Biochem. J.* 290, 1–13. doi: 10.1042/bj2900001

Mayr, C., Richter, K., Lilie, H., and Buchner, J. (2000). Cpr6 and Cpr7, two closely related Hsp90-associated immunophilins from *Saccharomyces cerevisiae*, differ in their functional properties. *J. Biol. Chem.* 275, 34140–34146. doi: 10.1074/jbc.M005251200

Miyagawa, K.-I., Ishiwata-Kimata, Y., Kohno, K., and Kimata, Y. (2014). Ethanol stress impairs protein folding in the endoplasmic reticulum and activates Ire1 in *Saccharomyces cerevisiae*. *Biosci. Biotechnol. Biochem.* 78, 1389–1391. doi: 10.1080/09168451.2014.921561

Mizunaga, T., Katakura, Y., Miura, T., and Maruyama, Y. (1990). Purification and characterization of yeast protein disulfide isomerase. *J. Biochem. (Tokyo)* 108, 846–851. doi: 10.1093/oxfordjournals.jbchem.a123291

Moehle, E. A., Shen, K., and Dillin, A. (2019). Mitochondrial proteostasis in the context of cellular and organismal health and aging. *J. Biol. Chem.* 294, 5396–5407. doi: 10.1074/jbc.TM117.000893

Mokranjac, D., and Neupert, W. (2009). Thirty years of protein translocation into mitochondria: unexpectedly complex and still puzzling. *Biochim. Biophys. Acta BBA Mol. Cell Res.* 1793, 33–41. doi: 10.1016/j.bbamcr.2008.06.021

Mokranjac, D., Sichting, M., Popov-Čeleketič, D., Berg, A., Hell, K., and Neupert, W. (2005). The import motor of the yeast mitochondrial TIM23 preprotein translocase contains two different J proteins, Tim14 and Mdj2. *J. Biol. Chem.* 280, 31608–31614. doi: 10.1074/jbc.M502397200

Molinari, M. (2007). N-glycan structure dictates extension of protein folding or onset of disposal. *Nat. Chem. Biol.* 3, 313–320. doi: 10.1038/nchembio880

Mori, K. (2015). The unfolded protein response: the dawn of a new field. *Proc. Jpn. Acad. Ser. B.* 91, 469–480. doi: 10.2183/pjab.91.469

Nathan, D. F., Vos, M. H., and Lindquist, S. (1997). In vivo functions of the *Saccharomyces cerevisiae* Hsp90 chaperone. *Proc. Natl. Acad. Sci.* 94, 12949–12956. doi: 10.1073/pnas.94.24.12949

Navarro-Tapia, E., Nana, R. K., Querol, A., and Pérez-Torrado, R. (2016). Ethanol cellular defense induce unfolded protein response in yeast. *Front. Microbiol.* 7, 1–12. doi: 10.3389/fmicb.2016.00189

Navarro-Tapia, E., Pérez-Torrado, R., and Querol, A. (2017). Ethanol effects involve non-canonical unfolded protein response activation in yeast cells. *Front. Microbiol.* 8. doi: 10.3389/fmicb.2017.00383

Neupert, W., and Herrmann, J. M. (2007). Translocation of Proteins into Mitochondria. *Annu. Rev. Biochem.* 76, 723–749. doi: 10.1146/annurev.biochem.76.052705.163409

Nijtmans, L. G. J. (2000). Prohibitins act as a membrane-bound chaperone for the stabilization of mitochondrial proteins. *EMBO J.* 19, 2444–2451. doi: 10.1093/emboj/19.11.2444

Nillegoda, N. B., Theodoraki, M. A., Mandal, A. K., Mayo, K. J., Ren, H. Y., Sultana, R., et al. (2010). Ubr1 and Ubr2 function in a quality control pathway for degradation of unfolded cytosolic proteins. *Mol. Biol. Cell* 21, 2102–2116. doi: 10.1091/mbc.e10-02-0098

O'Connor-Cox, E. S. C., Lodolo, E. J., and Axcell, B. C. (1996). Mitochondrial relevance to yeast fermentative performance: a review. *J. Inst. Brew.* 102, 19–25. doi: 10.1002/j.2050-0416.1996.tb00890.x

Odumeru, J. A., D'Amore, T., Russell, I., and Stewart, G. G. (1992). Effects of heat shock and ethanol stress on the viability of aSaccharomyces uvarum (carlsbergensis) brewing yeast strain during fermentation of high gravity wort. *J. Ind. Microbiol.* 10, 111–116. doi: 10.1007/BF01583843

Okuno, M., Kajitani, R., Ryusui, R., Morimoto, H., Kodama, Y., and Itoh, Y. T. (2016). Next-generation sequencing analysis of lager brewing yeast strains reveals the evolutionary history of interspecies hybridization. *DNA Res.* 23, 67–82. doi: 10.1093/dnares/dsv037

Panaretou, B., Siligardi, G., Meyer, P., Maloney, A., Sullivan, J. K., Singh, S., et al. (2002). Activation of the ATPase activity of Hsp90 by the stress-regulated cochaperone Aha1. *Mol. Cell* 10, 1307–1318. doi: 10.1016/S1097-2765(02)00785-2

Parsell, D. A., Taulien, J., Lindquist, S. L., Viitanen, P., Jaenicke, R., Horwich, A., et al. (1993). The role of heat-shock proteins in thermotolerance. *Philos. Trans. R. Soc Lond. B. Biol. Sci.* 339, 279–286. doi: 10.1098/rstb.1993.0026

Pastorino, J. G., Marcineviciute, A., Cahill, A., and Hoek, J. B. (1999). Potentiation by chronic ethanol treatment of the mitochondrial permeability transition. *Biochem. Biophys. Res. Commun.* 265, 405–409. doi: 10.1006/bbrc.1999.1696

Patron, M., Sprenger, H.-G., and Langer, T. (2018). m-AAA proteases, mitochondrial calcium homeostasis and neurodegeneration. *Cell Res.* 28, 296–306. doi: 10.1038/cr.2018.17

Perić, M., Dib, P. B., Dennerlein, S., Musa, M., Rudan, M., Lovrić, A., et al. (2016). Crosstalk between cellular compartments protects against proteotoxicity and extends lifespan. *Sci. Rep.* 6, 28751. doi: 10.1038/srep28751

Pfeiffer, A., Stephanowitz, H., Krause, E., Volkwein, C., Hirsch, C., Jarosch, E., et al. (2016). A Complex of Htm1 and the oxidoreductase Pdi1 accelerates degradation of misfolded glycoproteins. *J. Biol. Chem.* 291, 12195–12207. doi: 10.1074/jbc.M115.703256

Piper, P. W., Talreja, K., Panaretou, B., Moradas-Ferreira, P., Byrne, K., Praekelt, U. M., et al. (1994). Induction of major heat-shock proteins of *Saccharomyces cerevisiae,* including plasma membrane Hsp30, by ethanol levels above a critical threshold. *Microbiology* 140, 3031–3038. doi: 10.1099/13500872-140-11-3031

Piper, P. W., Jones, G. W., Bringloe, D., Harris, N., MacLean, M., and Mollapour, M. (2002). The shortened replicative life span of prohibitin mutants of yeast appears to be due to defective mitochondrial segregation in old mother cells: prohibitin influence on yeast aging, p. w. piper et al. *Aging Cell* 1, 149–157. doi: 10.1046/j.1474-9728.2002.00018.x

Piper, P. W. (1995). The heat shock and ethanol stress responses of yeast exhibit extensive similarity and functional overlap. *FEMS Microbiol. Lett.* 134, 121–127. doi: 10.1111/j.1574-6968.1995.tb07925.x

Powell, C., Quain, D., and Smart, K. (2003). The impact of brewing yeast cell age on fermentation performance, attenuation and flocculation. *FEMS Yeast Res.* 3, 149–157. doi: 10.1016/S1567-1356(03)00002-3

Prasad, R., Xu, C., and Ng, D. T. W. (2018). Hsp40/70/110 chaperones adapt nuclear protein quality control to serve cytosolic clients. *J. Cell Biol.* 217, 2019–2032. doi: 10.1083/jcb.201706091

Puligundla, P., Smogrovicova, D., Obulam, V. S. R., and Ko, S. (2011). Very high gravity (VHG) ethanolic brewing and fermentation: a research update. *J. Ind. Microbiol. Biotechnol.* 38, 1133–1144. doi: 10.1007/s10295-011-0999-3

Qing, Z., Hai, Z., Guohua, Z., Kaize, H., Zhirong, Y., and Yanling, J. (2012). Transcriptome analysis of *Saccharomyces cerevisiae* at the late stage of very high gravity (VHG) fermentation. *Afr. J. Biotechnol.* 11, 9641–9648. doi: 10.5897/AJB12.268

Raimundo, N., and Kriško, A. (2018). Cross-organelle communication at the core of longevity. *Aging* 10, 15–16. doi: 10.18632/aging.101373

Rautio, J. J., Huuskonen, A., Vuokko, H., Vidgren, V., and Londesborough, J. (2007). Monitoring yeast physiology during very high gravity wort fermentations by frequent analysis of gene expression. *Yeast* 24, 741–760. doi: 10.1002/yea.1510

Reading, D. S., Hallberg, R. L., and Myers, A. M. (1989). Characterization of the yeast *HSP60* gene coding for a mitochondrial assembly factor. *Nature* 337, 655–659. doi: 10.1038/337655a0

Richter, K., Muschler, P., Hainzl, O., and Buchner, J. (2001). Coordinated ATP hydrolysis by the Hsp90 dimer. *J. Biol. Chem.* 276, 33689–33696. doi: 10.1074/jbc.M103832200

Ron, D. (2002). Translational control in the endoplasmic reticulum stress response. *J. Clin. Invest.* 110, 1383–1388. doi: 10.1172/JCI0216784

Ruggiano, A., Foresti, O., and Carvalho, P. (2014). ER-associated degradation: protein quality control and beyond. *J. Cell Biol.* 204, 869–879. doi: 10.1083/jcb.201312042

Sanz, M. A., Tsang, W. Y., Willems, E. M., Grivell, L. A., Lemire, B. D., van der Spek, H., et al. (2003). The mitochondrial prohibitin complex is essential for embryonic viability and germline function in *Caenorhabditis elegans*. *J. Biol. Chem.* 278, 32091–32099. doi: 10.1074/jbc.M304877200

Sardi, M., Krause, M., Heilberger, J., and Gasch, A. P. (2018). Genotype-by-environment-by-environment interactions in the *Saccharomyces cerevisiae* transcriptomic response to alcohols and anaerobiosis. *G3. GenesGenomesGenetics* 8, 3881–3890. doi: 10.1534/g3.118.200677

Schmitt, M., Neupert, W., and Langer, T. (1995). Hsp78, a Clp homologue within mitochondria, can substitute for chaperone functions of mt-hsp70. *EMBO J.* 14, 3434–3444. doi: 10.1002/j.1460-2075.1995.tb07349.x

Schmitt, M. (1996). The molecular chaperone Hsp78 confers compartment-specific thermotolerance to mitochondria. *J. Cell Biol.* 134, 1375–1386. doi: 10.1083/jcb.134.6.1375

Schreiner, B., Westerburg, H., Forné, I., Imhof, A., Neupert, W., and Mokranjac, D. (2012). Role of the AAA protease Yme1 in folding of proteins in the intermembrane space of mitochondria. *Mol. Biol. Cell* 23, 4335–4346. doi: 10.1091/mbc.e12-05-0420

Schuldiner, M., Collins, S. R., Thompson, N. J., Denic, V., Bhamidipati, A., Punna, T., et al. (2005). Exploration of the function and organization of the yeast early secretory pathway through an epistatic miniarray profile. *Cell* 123, 507–519. doi: 10.1016/j.cell.2005.08.031

Semenza, J. C., Hardwick, K. G., Dean, N., and Pelham, H. R. B. (1990). ERD2, a yeast gene required for the receptor-mediated retrieval of luminal ER proteins from the secretory pathway. *Cell* 61, 1349–1357. doi: 10.1016/0092-8674(90)90698-E

Sethi, R., Iyer, S. S., Das, E., and Roy, I. (2018). Discrete roles of trehalose and Hsp104 in inhibition of protein aggregation in yeast cells. *FEMS Yeast Res.* 18, 1–11. doi: 10.1093/femsyr/foy058

Shahsavarani, H., Sugiyama, M., Kaneko, Y., Chuenchit, B., and Harashima, S. (2012). Superior thermotolerance of *Saccharomyces cerevisiae* for efficient bioethanol fermentation can be achieved by overexpression of RSP5 ubiquitin ligase. *Biotechnol. Adv.* 30, 1289–1300. doi: 10.1016/j.biotechadv.2011.09.002

Sharma, V. M. (2001). Quantitative target display: a method to screen yeast mutants conferring quantitative phenotypes by mutant DNA fingerprints. *Nucleic Acids Res.* 29, 86e–886. doi: 10.1093/nar/29.17.e86

Short, M. K., Hallett, J. P., Tar, K., Dange, T., Schmidt, M., Moir, R., et al. (2012). The yeast magmas ortholog Pam16 has an essential function in fermentative growth that involves sphingolipid metabolism. *PloS One* 7, e39428. doi: 10.1371/journal.pone.0039428

Sidrauski, C., and Walter, P. (1997). The transmembrane kinase Ire1p is a site-specific endonuclease that initiates mRNA splicing in the unfolded protein response. *Cell* 90, 1031–1039. doi: 10.1016/S0092-8674(00)80369-4

Silva, D., Bránylk, T., Dragone, G., Vicente, A., Teixeira, J., and Almeida e Silva, J. (2008). High gravity batch and continuous processes for beer production: evaluation of fermentation performance and beer quality. *Chem. Pap.* 62, 34–41. doi: 10.2478/s11696-007-0076-6

Silverstein, R. A., and Ekwall, K. (2005). Sin3: a flexible regulator of global gene expression and genome stability. *Curr. Genet.* 47, 1–17. doi: 10.1007/s00294-004-0541-5

Singer, M. A., and Lindquist, S. (1998). Multiple effects of trehalose on protein folding *in vitro* and. *In vivo. Mol. Cell* 1, 639–648. doi: 10.1016/S1097-2765(00)80064-7

Smart, K. A., Quain, D. E., Powell, C. D., and Van Zandycke, S. M. (2000). Replicative ageing and senescence in *Saccharomyces cerevisiae* and the impact on brewing fermentations. *Microbiology* 146, 1023–1034. doi: 10.1099/00221287-146-5-1023

Smart, K. A. (2007). Brewing yeast genomes and genome-wide expression and proteome profiling during fermentation. *Yeast* 24, 993–1013. doi: 10.1002/yea.1553

Stanley, D., Bandara, A., Fraser, S., Chambers, P. J., and Stanley, G. A. (2010). The ethanol stress response and ethanol tolerance of *Saccharomyces cerevisiae*. *J. Appl. Microbiol.* 109, 13–24. doi: 10.1111/j.1365-2672.2009.04657.x

Stefanovic, S., and Hegde, R. S. (2007). Identification of a targeting factor for posttranslational membrane protein insertion into the ER. *Cell* 128, 1147–1159. doi: 10.1016/j.cell.2007.01.036

Stewart, G. G. (2010). High-gravity brewing and distilling—past experiences and future prospects. *J. Am. Soc Brew. Chem.* 68, 1–9. doi: 10.1094/ASBCJ-2009-1214-01

Stolz, A., Besser, S., Hottmann, H., and Wolf, D. H. (2013). Previously unknown role for the ubiquitin ligase Ubr1 in endoplasmic reticulum-associated protein degradation. *Proc. Natl. Acad. Sci.* 110, 15271–15276. doi: 10.1073/pnas.1304928110

Szathmary, R., Bielmann, R., Nita-Lazar, M., Burda, P., and Jakob, C. A. (2005). Yos9 protein is essential for degradation of misfolded glycoproteins and may function as lectin in ERAD. *Mol. Cell* 19, 765–775. doi: 10.1016/j.molcel.2005.08.015

Szoradi, T., Schaeff, K., Garcia-Rivera, E. M., Itzhak, D. N., Schmidt, R. M., Bircham, P. W., et al. (2018). SHRED is a regulatory cascade that reprograms Ubr1 substrate specificity for enhanced protein quality control during stress. *Mol. Cell* 70, 1025–1037.e5. doi: 10.1016/j.molcel.2018.04.027

Takemori, Y., Sakaguchi, A., Matsuda, S., Mizukami, Y., and Sakurai, H. (2006). Stress-induced transcription of the endoplasmic reticulum oxidoreductin gene *ERO1* in the yeast *Saccharomyces cerevisiae*. *Mol. Genet. Genomics* 275, 89–96. doi: 10.1007/s00438-005-0065-9

Thibault, G., and Ng, D. T. W. (2012). The endoplasmic reticulum-associated degradation pathways of budding yeast. *Cold Spring Harb. Perspect. Biol.* 4, a013193–a013193. doi: 10.1101/cshperspect.a013193

Tomás, M., Marín, M. P., Martínez-Alonso, E., Esteban-Pretel, G., Díaz-Ruiz, A., Vázquez-Martínez, R., et al. (2012). Alcohol induces Golgi fragmentation in differentiated PC12 cells by deregulating Rab1-dependent ER-to-Golgi transport. *Histochem. Cell Biol.* 138, 489–501. doi: 10.1007/s00418-012-0970-z

Tsvetanova, N. G., Riordan, D. P., and Brown, P. O. (2012). The yeast Rab GTPase Ypt1 modulates unfolded protein response dynamics by regulating the stability of *HAC1* RNA. *PloS Genet.* 8, e1002862. doi: 10.1371/journal.pgen.1002862

van Meer, G., Voelker, D. R., and Feigenson, G. W. (2008). Membrane lipids: where they are and how they behave. *Nat. Rev. Mol. Cell Biol.* 9, 112–124. doi: 10.1038/nrm2330

Verghese, J., Abrams, J., Wang, Y., and Morano, K. A. (2012). Biology of the heat shock response and protein chaperones: budding yeast (*Saccharomyces cerevisiae*) as a model system. *Microbiol. Mol. Biol. Rev.* 76, 115–158. doi: 10.1128/MMBR.05018-11

Vevea, J. D., Garcia, E. J., Chan, R. B., Zhou, B., Schultz, M., Di Paolo, G., et al. (2015). Role for lipid droplet biogenesis and microlipophagy in adaptation to lipid imbalance in yeast. *Dev. Cell* 35, 584–599. doi: 10.1016/j.devcel.2015.11.010

Wang, F., Chan, C., Weir, N. R., and Denic, V. (2014). The Get1/2 transmembrane complex is an endoplasmic-reticulum membrane protein insertase. *Nature* 512, 441–444. doi: 10.1038/nature13471

Weibezahn, J., Schlieker, C., Tessarz, P., Mogk, A., and Bukau, B. (2005). Novel insights into the mechanism of chaperone-assisted protein disaggregation. *Biol. Chem.* 386., 739–744. doi: 10.1515/BC.2005.086

Weindling, E., and Bar-Nun, S. (2015). Sir2 links the unfolded protein response and the heat shock response in a stress response network. *Biochem. Biophys. Res. Commun.* 457, 473–478. doi: 10.1016/j.bbrc.2015.01.021

Weissman, J. S., and Kimt, P. S. (1993). Efficient catalysis of disulphide bond rearrangements by protein disulphide isomerase. *Nature* 365, 185–188. doi: 10.1038/365185a0

Welihinda, A. A., Tirasophon, W., Green, S. R., and Kaufman, R. J. (1998). Protein serine/threonine phosphatase Ptc2p negatively regulates the unfolded-protein response by dephosphorylating Ire1p kinase. *Mol. Cell. Biol.* 18, 1967–1977. doi: 10.1128/MCB.18.4.1967

Welti, M., and Hülsmeier, A. J. (2014). Ethanol-induced impairment in the biosynthesis of n-linked glycosylation: ethanol interference with N-linked glycosylation. *J. Cell. Biochem.* 115, 754–762. doi: 10.1002/jcb.24713

Yamamoto, A., Mizukami, Y., and Sakurai, H. (2005). Identification of a novel class of target genes and a novel type of binding sequence of heat shock transcription factor in *Saccharomyces cerevisiae*. *J. Biol. Chem.* 280, 11911–11919. doi: 10.1074/jbc.M411256200

Zhao, Y., MacGurn, J. A., Liu, M., and Emr, S. (2013). The ART-Rsp5 ubiquitin ligase network comprises a plasma membrane quality control system that protects yeast cells from proteotoxic stress. *eLife* 2, e00459. doi: 10.7554/eLife.00459

Zhao, Q. (2002). A mitochondrial specific stress response in mammalian cells. *EMBO J.* 21, 4411–4419. doi: 10.1093/emboj/cdf445

Zolkiewski, M., Zhang, T., and Nagy, M. (2012). Aggregate reactivation mediated by the Hsp100 chaperones. *Arch. Biochem. Biophys.* 520, 1–6. doi: 10.1016/j.abb.2012.01.012

Zuehlke, A. D., and Johnson, J. L. (2012). Chaperoning the chaperone: a role for the co-chaperone cpr7 in modulating Hsp90 function in *Saccharomyces cerevisiae*. *Genetics* 191, 805–814. doi: 10.1534/genetics.112.140319

Conflict of Interest: The authors declare that this work was conducted in the absence of any commercial or financial relationships that could be construed as a potential conflict of interest.

frontiers in Microbiology

ORIGINAL RESEARCH
published: 03 April 2020
doi: 10.3389/fmicb.2020.00538

Transcriptome Profile of Yeast Strain Used for Biological Wine Aging Revealed Dynamic Changes of Gene Expression in Course of Flor Development

Andrey V. Mardanov[1], Mikhail A. Eldarov[1], Alexey V. Beletsky[1], Tatiana N. Tanashchuk[2], Svetlana A. Kishkovskaya[2] and Nikolai V. Ravin[1]*

[1] *Institute of Bioengineering, Research Center of Biotechnology of the Russian Academy of Sciences, Moscow, Russia,*
[2] *Research Institute of Viticulture and Winemaking "Magarach" of the Russian Academy of Sciences, Yalta, Russia*

OPEN ACCESS

Edited by:
Roberto Pérez-Torrado, Spanish National Research Council, Spain

Reviewed by:
Jean-luc Legras, INRA Institut National de la Recherche Agronomique Centre Montpellier, France
Juan Carlos Mauricio, Universidad de Córdoba, Spain
Severino Zara, University of Sassari, Italy

***Correspondence:**
Andrey V. Mardanov
mardanov@biengi.ac.ru

Specialty section:
This article was submitted to Evolutionary and Genomic Microbiology, a section of the journal Frontiers in Microbiology

Received: *03 December 2019*
Accepted: *12 March 2020*
Published: *03 April 2020*

Citation:
Mardanov AV, Eldarov MA, Beletsky AV, Tanashchuk TN, Kishkovskaya SA and Ravin NV (2020) Transcriptome Profile of Yeast Strain Used for Biological Wine Aging Revealed Dynamic Changes of Gene Expression in Course of Flor Development. Front. Microbiol. 11:538. doi: 10.3389/fmicb.2020.00538

Flor strains of *Saccharomyces cerevisiae* are principal microbial agents responsible for biological wine aging used for production of sherry-like wines. The flor yeast velum formed on the surface of fortified fermented must is a major adaptive and technological characteristic of flor yeasts that helps them to withstanding stressful winemaking conditions and ensures specific biochemical and sensory oxidative alterations typical for sherry wines. We have applied RNAseq technology for transcriptome analysis of an industrial flor yeast strain at different steps of velum development over 71 days under experimental winemaking conditions. Velum growth and maturation was accompanied by accumulation of aldehydes and acetales. We have identified 1490 differentially expressed genes including 816 genes upregulated and 674 downregulated more than 2-fold at mature biofilm stage as compared to the early biofilm. Distinct expression patterns of genes involved in carbon and nitrogen metabolism, respiration, cell cycle, DNA repair, cell adhesion, response to various stresses were observed. Many genes involved in response to different stresses, oxidative carbon metabolism, high affinity transport of sugars, glycerol utilization, sulfur metabolism, protein quality control and recycling, cell wall biogenesis, apoptosis were induced at the mature biofilm stage. Strong upregulation was observed for *FLO11* flocculin while expression of other flocculins remained unaltered or moderately downregulated. Downregulated genes included those for proteins involved in glycolysis, transportation of ions, metals, aminoacids, sugars, indicating repression of some major transport and metabolic process at the mature biofilm stage. Presented results are important for in-depth understanding of cell response elicited by velum formation and sherry wine manufacturing conditions, and for the comprehension of relevant regulatory mechanisms. Such knowledge may help to better understand the molecular mechanisms that flor yeasts use to adapt to winemaking environments, establish the functions of previously uncharacterized genes, improve the technology of sherry- wine production, and find target genes for strain improvement.

Keywords: *Saccharomyces cerevisiae*, flor yeast, sherry, genetic diversity, comparative genomics, biofilm, SNP

INTRODUCTION

Biological wine aging is a multistep technological process used in several countries for production of sherry type wines. The essence of this process is the use of a special race of *Saccharomyces cerevisiae*, the flor yeast that are responsible for the majority of biochemical changes affecting composition and sensory properties of these wines. Biochemical and physiological conditions of biological wine aging are different from those in the course of fermentation. Flor yeast strains that form a biofilm on the surface of fortified fermented must display drastic alterations in carbon and nitrogen metabolism. In the absence of fermentable sugars flor yeast use ethanol and glycerol as major carbon sources through oxidative catabolism. They shift to use poor nitrogen sources and withstand harsh and stressful conditions of biological wine aging with high ethanol and acetaldehyde concentrations, oxidative damage and limitations of many essential nutrients (Alexandre, 2013; Legras et al., 2016). Velum formation is considered to be a major adaptive property of flor yeast ensuring oxygen access and protecting them from various stresses (Esteve-Zarzoso et al., 2001).

Specific phenotypic and biochemical properties of flor yeast are thought to be the result of domestication and artificial selection that were fixed in the course of separation of flor yeast as a sister branch from Wine/European clade (Legras et al., 2014). Recent extensive comparative genomic analysis supports and extends this view. Comparison of wine and flor yeast genomes have revealed a complex landscape of genetic variation specific for flor yeast including hundreds of SNPs, InDels, chromosomal rearrangements, gene content alterations (Coi et al., 2017; Eldarov et al., 2018; Legras et al., 2018). Many of these structural variations have affected key regulatory molecules (transcription factors, signal transduction molecules), suggesting direct influence on gene expression patterns of target genes, involved in metabolic and morphological changes specific for flor yeast (Coi et al., 2017; Eldarov et al., 2018).

Comparative transcriptome analysis is a powerful tool for the study of global dynamics of yeast gene expression in response to various environmental, genetics and chemicals cues. In recent years hundreds of transcriptome studies performed either with microarray or RNAseq platforms provided enormous resource for understanding the whole-genome regulatory networks and mechanisms of yeast gene expression in response to various stresses (Taymaz-Nikerel et al., 2016). While majority of these reports use laboratory strains and artificial conditions, several directly address the dynamics of gene expression in industrial conditions related to wine, beer, and bioethanol production. In one of the first studies significant alterations in the expression of more than 2000 genes were detected in the course of adaptation of wine yeast strain EC1118 to changing physiological and biochemical conditions of wine fermentation (Rossignol et al., 2003). Genes involved in many metabolic and signaling pathways underwent coordinated regulation, including genes associated with wine fermentation, genes involved in nitrogen catabolism and others. Under conditions of low-temperature fermentation, important to improve wine quality, cold shock genes, genes involved in cell cycle progression and cell proliferation were upregulated (Beltran et al., 2006). These and other transcriptional changes correlated with increased cell viability, improved ethanol tolerance, increased production of short chain fatty acids and esters (Tronchoni et al., 2017). Significant inter-strain differences in the expression patterns of about 30% of genes responsible for aroma formation were detected in 3 yeast strains in the course of wine fermentation at normal (28°C) and low (12°C) temperatures (Gamero et al., 2014). Notably, altered expression was observed for many genes important for winemaking, encoding acyl acetyltransferases, decarboxylases, aldehyde dehydrogenases, alcohol dehydrogenases, enzymes involved in amino acid transport and metabolism. This and many other studies, in particular for the analysis of gene expression in wine yeast strains depending from the availability of nitrogen sources (Rossignol et al., 2003; Barbosa et al., 2015) clearly show that variations in gene expression is closely associated with phenotypic variation of wine strains (Salvado et al., 2008; Walker et al., 2014; García-Ríos and Guillamón, 2019).

Significant changes in wine yeast transcriptome occur during the transition to the stationary phase. Thus, the 223 genes dramatically induced at different stages of fermentation have been allocated to a specific group of Fermentation stress response (FSR) genes, wherein more than 60% of these genes has previously unknown functions (Marks et al., 2008).

Studies of differential protein expression in the course of sherry-wine formation is limited, however recently several reports documenting semi-quantitative proteomic analysis of cytosolic, cell-wall and mitochondrial proteins of industrial flor strain under laboratory "non-biofilm" and "biofilm" conditions have been carried out (Moreno-García et al., 2015, 2016, 2017, 2018a). These studies revealed alterations in the abundance of proteins involved in respiration, translation, stress damage prevention, DNA reparation, carbon and amino acid metabolism, some interesting finding associated with the changes in abundance of flor yeast enzymes affecting sensory properties of sherry wine.

Here, we report a comprehensive transcriptome analysis of *flor yeast gene expression* using RNA-seq data. We generated transcriptomic data for a recently sequenced flor yeast strain I-329, for which detailed microbiological, biochemical, physiological data is also available (Kishkovskaia et al., 2017; Eldarov et al., 2018). This strain was grown under conditions mimicking biological wine aging, at three consecutive stages of velum formation and growth. This dataset was used to determine the expression levels of each of the genes at different stages of velum formation, to reveal novel regulatory networks and expression patterns, including those for previously uncharacterized genes. We observed distinct expression patterns of genes involved in carbon and nitrogen metabolism, respiration, cell cycle, DNA repair, cell adhesion, response to various stresses etc., illuminating the complex landscape of gene expression associated with specific oenological conditions. These data will help to better understand flor yeast physiology and adaptive evolutionary changes pertinent to their oenological properties, establish the functions of previously uncharacterized yeast genes, improve the technology of sherry wine production, find target genes for subsequent strain improvement programs.

MATERIALS AND METHODS

Cultivation of Flor Yeast and Sampling

The strain used was *S. cerevisiae* I-329, industrial flor yeast from the culture collection of the Research Institute of Viticulture and Winemaking "Magarach" of the Russian Academy of Sciences (Kishkovskaia et al., 2017).

Sterilized Albillo grape must (concentration of sugars 230 g/l, concentration of titratable acids 5.4 g/l, pH 3.5) was inoculated with a pure culture of strain I-329 with a seed dose of 2×10^6 cells/ml and fermented for 28 days at room temperature in a 3 l glass balloon. At the end of fermentation the wine was fortified to 14.5% ethanol and incubation was continued. The firm yeast velum, covering about 90% of the entire surface became formed 10 days after adding alcohol (**Supplementary Figure S1**). At this point the first sample of floating flor ("early biofilm," **Table 1**) was taken. 45 days later completion of continuous film growth was observed and at this point the second sample ("thin biofilm," **Supplementary Figure S1**) was taken. The third, "mature biofilm," sample was taken 26 days after the second sample, at this point the mature folded biofilm (**Supplementary Figure S1**) was formed (**Table 1**). Sampling at each time point was carried out in triplicate. Samples were taken with a small spoon at three points of the floating biofilm covering the surface of the balloon (pieces about 2–5 cm in diameter weighting 100–300 mg). The samples included the entire film thickness, from the upper layer exposed in air to the lower layer in contact with the liquid. Biofilm samples were immediately placed in the RNA later solution (Invitrogen, United States) and kept at −20°C until RNA isolation.

Chemical Analysis of Wine Samples

At the time of sampling aliquots of wine were also taken for chemical analyzes. The content of volatile and titratable acids, alcohol, aldehydes and acetals was determined using standard methods adopted in winemaking (Compendium of international methods of wine and must analysis, 2018) and as described earlier (Kishkovskaia et al., 2017).

TABLE 1 | Chemical composition of wine samples.

Sample designation	Early biofilm	Thin biofilm	Mature biofilm
Days from inoculation to sampling	38	83	109
Ethanol% (v/v)	12.4	10.8	9.6
Volatile acidity (g/l)*	0.2	0.2	0.1
Total acidity (g/l)**	7.8	7.4	7.0
Aldehydes (mg/l)	382.8	531.3	668.8
Acetals (mg/l)	147.2	253.7	280.3
pH	3.6	3.6	3.6
Glucose (g/l)	0.2	0.1	<0.1
Fructose (g/l)	<0.1	<0.1	<0.1
Oligosaccharides (g/l)	0.3	0.2	0.2
Glycerol (g/l)	8.5	7.9	6.8

**Expressed in grams of tartaric acid per liter. **Expressed in grams of acetic acid per liter.*

Ethanol content was measured with a hydrometer. Total acidity was measured by titration with bromothymol blue as indicator and comparison with an end-point color standard and expressed in grams of tartaric acid. Volatile acids, derived from the acids of the acetic series, were separated from the wine by steam distillation and titrated using standard sodium hydroxide and expressed in grams of acetic acid per liter. The mass concentration of aldehydes was determined by a method based on the ability of aldehydes to bind to sodium hydrosulfite in a complex non-volatile compound. Excess of hydrosulfite was oxidized with iodine and then the aldehyde sulfite compound was decomposed with alkali. The liberated sulfur aldehyde was titrated with a 0.005 M iodine solution. Acetaldehyde accounted for more than 90% of all aldehydes. The mass concentration of acetals was determined by the method based on vacuum distillation of aldehydes and volatile acetals of wine with further acid cleavage of the acetals remaining in the flask and determination of the released volatile aldehydes by iodometric titration.

Glucose, fructose, oligosaccharides, and glycerol were determined by liquid chromatography with a Shimadzu LC-20AD chromatograph (Shimadzu, Japan).

Transcriptome Sequencing and Analysis of Gene Expression

Nine RNA samples (three sampling points, each in three replications) were used for transcriptome analysis of strain I-329 in course of flor maturation. The total RNA was extracted employing a hot phenol method (Schmitt et al., 1990) followed by purification using RNeasy Mini Kit (Qiagen GmbH, Germany). mRNA library preparation was performed using an NEBNext mRNA Library Prep Reagent Set for Illumina according to the manufacturer's instructions (New England Bio-Labs Inc., Ipswich, MA, United States). The libraries were sequenced using the Illumina HiSeq 2500 platform (Illumina, San Diego, CA, United States). Six to nine million of 50-bp single-end reads were generated for each sample. The previously assembled genome of *S. cerevisiae* strain I-329 (GenBank PTER00000000, Eldarov et al., 2018) was used as a reference for the expression analysis.

Gene expression levels were estimated using RSEM v.1.3.1 software (Li and Dewey, 2011) and recorded in reads per kilobase per million mapped reads (RPKM). Mapping of RNA-seq reads to genes (excluding introns) was performed using program Bowtie2 (Langmead and Salzberg, 2012), with parameters selected by RSEM script. Statistical analysis of differential expression was performed using EBSeq v. 1.2.0 package (Leng and Kendziorski, 2019), invoked by RSEM script. To quantify evidence in favor of differential expression EBSeq provide posterior probabilities of differential expression (PPDE), PPDE values above 0.95 were considered as statistically significant. Note that EBSeq is more conservative method for identification of differentially expressed genes than DESeq program (Anders and Huber, 2010) which provides *P*-values adjusted for multiple testing using Benjamini–Hochberg method (Leng et al., 2013).

For the analysis of gene expression in flor yeast strain CECT10094 (the dataset obtained on AB SOLiD 4 System, retrieved from SRR9027083; Ibáñez et al., 2017) we used SHRiMP v.2.2.3 (Rumble et al., 2009) to map colorspace. The reads were mapped on strain I-329 genome and RSEM v.1.3.1 software was used for the following expression analysis.

Volcano plots were generated using custom perl and R scripts, using RSEM results as an input. To visualize expression on KEGG pathways we used Pathview and KEGGREST Bioconductor v.3.8 packages run with custom scripts in R environment v.3.6.0 (Luo and Brouwer, 2013; Tenenbaum, 2019).

Gene Ontology Functional Categories Analysis

Gene ontology (GO) enrichment analysis of differentially expressed genes was performed using PANTHER database (Mi et al., 2019). Fischer's exact test with Bonferroni correction and a p-value < 0.05 were used to filter the results. For submission to database gene names were converted from LOCUS_TAGs to UNIPROT_IDs using online DAVID Gene ID Conversion Tool v.6.8 (Jiao et al., 2012) available at https://david.ncifcrf.gov/conversion.jsp. The concise list of terms was obtained after removing redundant GO terms with the help of ReViGo web tool (Supek et al., 2011). Search and analysis of transcription factors (TF) and TF-binding sites was done using the Yeasttract database (Teixeira et al., 2018).

Nucleotide Sequence Accession Numbers

This BioProject has been deposited in GenBank under accession number PRJNA592304. The sequences obtained in this project have been deposited in the NCBI Sequence Read Archive under the accession numbers SRR10551657-SRR10551665 (**Supplementary Table S1**).

RESULTS

Changes of Composition of Fortified Fermented Must in Course of Flor Growth

To gain insight into the dynamics of transcriptional responses of industrial flor yeast strain at stage of biofilm formation we used the previously sequenced flor strain I-329 (Eldarov et al., 2018). This strain was chosen because it is used for industrial production of sherry-like wine in Russia, it is tolerant to high ethanol concentration (16–17%) and could retain high viability at the biofilm stage (Kishkovskaia et al., 2017).

The strain I-329 was used to ferment the must and upon completion of fermentation the must was fortified by addition of ethanol to 14.5%. In course of further incubation the yeasts appeared on the surface and 10 days after ethanol addition formed a tiny biofilm covering about 90% of the surface of the balloon. At this point the first biofilm sample (early biofilm) was taken. The second sample (thin biofilm) was collected when the flor covered the whole surface of the balloon, and the third sample was obtained after formation of mature biofilm (**Table 1**). Throughout all three stages chemical composition of wine was monitored (**Table 1**). In the course of velum growth volumetric ethanol concentration dropped from 12.4% to 9.6%, while the concentration of aldehydes and acetals almost doubled reaching, respectively, 668.8 mg/l and 280.3 mg/l, illustrating the typical dynamics of ethanol oxidation by yeast during biofilm maturation.

Global Transcriptome Variation at Different Steps of Flor Development

For nine samples a total of 64 million reads were obtained with at least 5.9 million reads for each sample (**Supplementary Table S1**). Of 5323 protein-coding genes annotated in the nuclear genome, 5320 genes were expressed in at least one sample. Analysis of RNA-seq data revealed a global gene expression profile of I-329 strain in the course of flor biofilm maturation (**Supplementary Table S2**).

Volcanic plot shows that in the process of flor growth there was a notable increase in the amount of differentially expressed genes (DEGs) upregulated or downregulated in the course of flor growth as compared to the early biofilm stage (**Figure 1**). In total we have identified 1490 DEGs with more than 2-fold statistically significant (PPDE > 0.95) difference of expression level between the mature biofilm stage and the early stage. Of these 565 genes were upregulated 2–4 fold (Up2), and 528 genes (Dn2) showed 2–4 fold decline in the expression level (**Table 2**). A group of 397 DEGs with more pronounced differences in gene expression levels included 251 genes upregulated more than 4-fold (Up4) and 146 genes downregulated more than 4-fold (Dn4) at the mature biofilm stage as compared to the early stage. Five genes, namely *YJL218W* (acetyltransferase), *AIF1* (apoptosis-inducing factor 1), *ENB1* (siderophore iron transporter), *REE1* (regulator of enolase expression), *CSS3* (hypothetical protein) were found to be expressed only at the mature biofilm stage.

GO analysis was performed for these four gene sets. For the Up2 set there was notable diversity of enriched terms in all 3 GO categories (**Supplementary Table S3**). The most prevalent in the "Biological process" category were such terms as "cell-redox homeostasis," "mitochondrial respiratory chain complex assembly," various terms related to mitochondrial protein synthesis, proteasome-mediated protein degradation etc. Gene products of these DEGs were predicted to have mitochondrial and proteasomal localization ("TCA complex," "mitochondrial ribosome," "proteasome complex") with "molecular functions" related to "structural constituent of ribosome" and "structural molecule activity" (**Supplementary Table S3**). For the Up4 set enriched the "Biological Process" terms were those related to sulfur metabolism, biosynthesis of sulfur-containing aminoacids, protein refolding etc. In the "Cellular Component" and "Molecular Function" categories the number of enriched terms was much smaller and limited to "mitochondrial intermembrane space," "organelle envelope lumen" and "unfolded protein binding" (**Supplementary Table S4**).

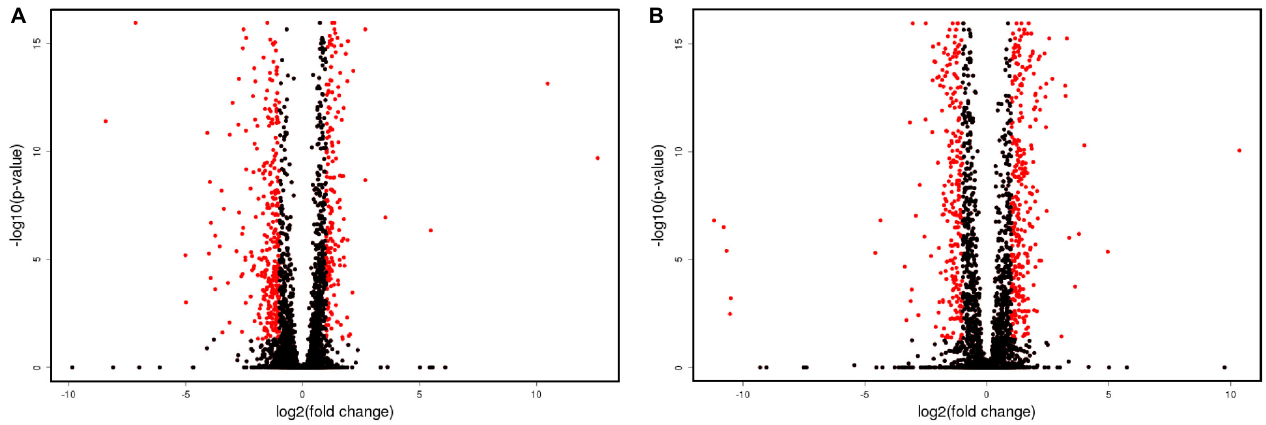

FIGURE 1 | Volcanic plot representation of changes in gene expression. Genes up-regulated or down-regulated more than 2-fold are shown in red. **(A)** Sample 2 vs. sample 1; **(B)** sample 3 vs. sample 1.

The Dn2 group of 528 moderately downregulated DEGs (**Supplementary Table S5**) was enriched in genes for proteins with organelle membrane localization, with functions related to binding and transportation of ions, metals and small molecules. In the "Biological Process" category overrepresented were terms related to "regulation of transcription from RNA polymerase II promoter in response to oxidative stress," "glycolytic process," "ATP generation from ADP," etc. Altogether these data indicates downregulation of several transport and metabolic process at the mature biofilm stage. This trend was more evident in the Dn4 group of 146 DEGs (**Supplementary Table S6**). This group includes genes for proteins involved in metabolism of nucleotides and sugars. In particular, strong downregulation was observed for low affinity glucose transporter *HXT1* (150-fold), *OPT1* oligopeptide transporter (40-fold), *TPO4* and *VBA1* polyamine and general amino acid transporters (∼16-fold), some enzymes involved in glycolysis (*PGK1, ENO2, TDH1*).

Differentially expressed genes within the four sets (Up2, Up4, Dn2, Dn4) represented a wide range of KEGG functional categories. To gain more detailed insight in the nature of transcriptional responses in the course of growth and maturation of flor yeast velum we have analyzed expression levels of genes assigned to various functional KEGG groups and categories.

KEGG pathway analysis showed major alterations in expression levels of genes belonging to the categories of "Energy metabolism" and "Carbohydrate metabolism," reflecting changes in yeast metabolism during biofilm growth as related to exhaustion of sugars and shift to ethanol oxidation (**Figure 2**).

For the vast majority of DEGs, a unidirectional trend (up- or downregulation) in the expression level was observed from the early biofilm stage to the thin biofilm, and further to the mature biofilm stage. Nevertheless, a small group of genes had a maximum (64 genes) or a minimum (87 genes) of expression level at the second stage, which was more than two times different from the expression levels in both the early and mature biofilm stages (**Supplementary Table S7**). Therefore, in the following sections we compared the expression levels in the first and the last flor samples; genes most activated or repressed at the thin biofilm stage are described in the last section of the "Results."

Transcription Profiles of Genes Carrying Flor Yeast Specific SNPs

Previous taxonomic and comparative genomic studies of wine and flor yeast strains showed that flor yeasts form a separate phylogenetic group artificially selected in the course of domestication and possessing unique physiological and genetic properties (Legras et al., 2014; Coi et al., 2017; Eldarov et al., 2018). Genome-wide comparative analysis of wine and flor strains revealed 2270 flor-yeast specific SNPs located in 1337 loci (Eldarov et al., 2018) with 73 SNP located in intergenic regions and the rest in 1334 protein-coding genes. Transcriptome analysis of these genes revealed 369 DEGs (27.7%) with more than 2-fold alterations in expression levels, 188 upregulated and 181 downregulated (**Table 2**). Since the shares of up- and downregulated genes were nearly the same for the whole genome (28%), these data did not support the hypothesis that genes carrying flor-specific SNPs should be preferentially differently expressed in course of flor growth.

Top Highly Expressed Genes

Quantification of the expression levels of analyzed DEGs enabled to select groups of highly expressed genes at the early biofilm and mature biofilm stages. Superposition of the lists of top 250 genes with highest expression level at these two stages revealed a group of 121 common highly expressed genes and genes, specifically expressed at one or another stage (**Supplementary Table S8**).

The list of 121 common highly expressed genes is a mixed collection of those for some heat-shock proteins, components of mitochondrial electron transfer chain and ATP generation machinery, enzymes of glycolytic pathway and sugar transporters, transcription and translation elongation factors etc. Despite relatively high expression level at two stages many genes showed notable alteration in transcription. For instance, genes for many HSP proteins showed 5–10 fold upregulation at the mature

TABLE 2 | Numbers of up- and down-regulated genes during flor development.

Expression pattern	Set	Regulation range	Thin biofilm vs. early biofilm		Mature biofilm vs. thin biofilm		Mature biofilm vs. early biofilm	
			All genes	Genes containing flor yeast specific SNPs*	All genes	Genes containing flor yeast specific SNPs*	All genes	Genes containing flor yeast specific SNPs*
Up-regulated	Up4	$X \geq 4$	84	21	122	34	251	55
	Up2	$4 > X \geq 2$	398	81	458	121	565	133
Down-regulated	Dn2	$0.25 < X \leq 0.5$	355	105	340	85	528	148
	Dn4	$X \leq 0.25$	66	19	52	10	146	33
Total DEG			903	226	972	250	1490	369

*1334 protein-coding genes containing flor-yeast specific SNPs (Eldarov et al., 2018).

biofilm stage, genes involved in oxidative phosphorylation were upregulated 2–4 fold at this stage, while strong downregulation was observed for genes for glycolytic enzymes, plasma membrane ATPase gene *PMA1*, and low affinity glucose transporter gene *HXT3* (**Supplementary Table S8**).

We have also compared the list of 121 genes highly expressed at both early and mature biofilm stages and the list of top 250 genes highly expressed during alcoholic fermentation using the recently published RNA-seq data obtained for flor yeast strain CECT10094 after 7 days of fermentation in synthetic must media (Ibáñez et al., 2017). We found 79 common genes between these sets (**Supplementary Table S9**). This common set included genes for glycolysis and gluconeogenesis, transport of sugars, glycogen and trehalose metabolism, heat-shock and oxidative stress response, ATP generation machinery. It is interesting to note that the *YML131W* gene, which encodes a protein with an unknown function, has a constantly high expression level both under fermentation conditions and in biofilm-grown cells. According to SGD description[1] this protein is similar to medium chain dehydrogenase/reductases and was induced by various stresses including osmotic shock, DNA damaging agents, and other chemicals.

Possible Transcriptional Control of Differentially Expressed Genes

Numerous data concerning transcriptional responses of yeast cells to different environmental perturbations revealed the key role of stress-responsive transcriptional factors (TFs) in sensing and protection against environmental damage (Causton et al., 2001; Roberts and Hudson, 2006; Berry and Gasch, 2008; Taymaz-Nikerel et al., 2016). Using the data available at YeasTract database we have counted TF-binding sites in the promoters of highly upregulated (Up4) and downregulated (Dn4) genes and selected TF with most frequent sites (**Supplementary Table S10**). Most numerous in the promoters of Up4 genes were sites for TFs with established role in regulating stress-responsive genes (Cin5, Msn2, Msn4, Hsf1, Yap1), TF regulating genes for carbon and nitrogen utilization (Adr1, Gcn4), control of cellular morphogenesis (Fkh1, Tec1, Ste12), confirming the role of these TF and their targets in stress resistance and metabolic and morphological changes of yeast cells specific to biofilm stage.

The genes for selected TF showed variable patterns of regulation, but majority of TF genes showed induction at the mature biofilm stage, with the highest upregulation level observed for *SWI5* (about 30-fold induction) coding for TF binding at stress response elements of responsive genes and for *MET4, MET28, MET32* regulating biosynthesis of sulfur-containing aminoacids. *MSN2* and *MSN4* were downregulated at the mature biofilm stage (**Supplementary Table S10**).

This TF set partially overlapped with the list of TF identified as possessing most frequent sites in the promoters of strongly downregulated genes (**Supplementary Table S10**). Msn2, Rap1, Ste12, Sok2, Yap1 sites were among the most frequent. Specific for this set were sites for Gln3, Hap1, Ino4, Pdr1, Skn7 and Yox1

[1]https://www.yeastgenome.org/locus/S000004600#paragraph

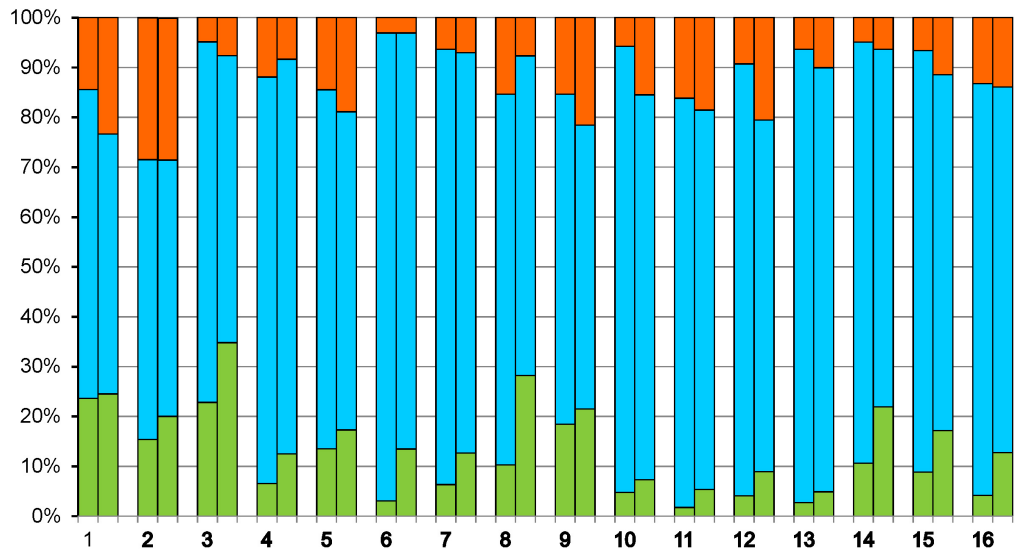

FIGURE 2 | Up-regulation and down-regulation of genes distributed to various KEGG categories. Metabolism: 1 – Carbohydrate metabolism, 2 – Energy metabolism, 3 – Lipid metabolism, 4 – Nucleotide metabolism, 5 – Amino acid metabolism, 6 – Glycan biosynthesis and metabolism, 7 – Metabolism of cofactors and vitamins, 8 – Biosynthesis of other secondary metabolites, 9 – Xenobiotic biodegradation and metabolism. Genetic Information Processing: 10 – Transcription, 11 – Translation, 12 – Folding, sorting and degradation, 13 – Replication and repair. Environmental Information Processing: 14 – Signal transduction. Cellular Processes: 15 – Transport and catabolism, 16 – Cell growth and death. Fractions of up-regulated genes are shown in red, down-regulated in green, and genes without significant changes in expression in blue. In each category, the left and right parts of the column indicate the changes of gene expression in the second and in the third sample, respectively, relative to the first sample.

regulating amino acid biosynthesis, oxidative stress response, regulation of cell cycle, and pseudohyphal growth.

Carbohydrates and Energy Metabolism

According to KEGG functional analysis most notable transcriptional changes during flor yeast biofilm development were observed for genes belonging to the categories of "Carbohydrate Metabolism" and "Energy Metabolism." Glycolysis is the central route of carbohydrate metabolism in yeast. During velum development expression levels of almost all glycolytic genes (*HXK2, PGI1, PFK1, FBA1, TPI1, TDH1, TDH2, PGK1, GPM1, GPM2, ENO1, ENO2, PYK2,* and *CDC19)* decreased more than 2-fold (**Figure 3** and **Supplementary Table S11**). This trend reflected an exhaustion of glucose in the growth medium (**Table 1**) and a switch of flor yeasts to other carbon sources.

Contrary to decreased transcription of the majority of glycolytic genes, expression of key genes involved in gluconeogenesis - phosphoenolpyruvate carboxykinase (*PCK1*) and fructose-1,6-bisphosphatase (*FBP1*) increased significantly (**Supplementary Table S11**). Apparently, their induction is required for biosynthesis of sugars under conditions of glucose exhaustion.

The transcription of most genes of the pentose-phosphate pathway (PPP) was not changed significantly, except that for 6-phosphogluconate dehydrogenase (*GND1* and *GND2*), transketolase (*TKL2*), and glucose-6-phosphate dehydrogenase (*ZWF1*). Levels of *GND1* mRNA decreased more than 5-fold at the mature biofilm stage. This data corresponds to previous observation (Zhang et al., 2004), showing a decrease in *GND1* expression upon growth on ethanol and lactic acid as carbon sources. Significantly increased were expression levels of *ZWF1* and *TKL2* genes. *TKL2* upregulation may be related to known patterns of induction of this gene in carbon-limited cultures and in the course of diauxic shift (Boer et al., 2003). *ZWF1* is the first PPP enzyme, catalyzing the rate-limiting and irreversible step (Nogae and Johnston, 1990). *ZWF1* is known to be important for adaptation to oxidative stress (Juhnke et al., 1996).

Expression changes of genes for key pyruvate metabolic enzymes were variable. While the expression of pyruvate carboxylases (*PYC1* and *PYC2*) more than doubled, the expression of pyruvate decarboxylases (*PDC1, PDC5, PDC6*) decreases several fold. *PYC1* and *PYC2* convert pyruvate to oxaloacetate, the substrate important for anaplerosis and gluconeogenesis (Pronk et al., 1996). Pyruvate decarboxylases are key enzymes for alcoholic fermentation, degrading pyruvate to acetaldehyde and carbon dioxide, and also important for oxidation of other 2-oxo acids (Flikweert et al., 1996). Downregulation of these genes likely reflected suppression of fermentative metabolism in course of biofilm growth. Likewise, strong down-regulation was observed for alcohol dehydrogenase *ADH1*, fermentative isozyme, required for the reduction of acetaldehyde to ethanol. The switch of yeasts to ethanol consumption was also reflected by strong up-regulation of aldehyde dehydrogenases (*ALD4, ALD5, ALD6*), required for growth on ethanol and conversion of acetaldehyde to acetate. No significant changes of expression were observed for *ACS1* gene coding for acetate-CoA ligase 1, known to be expressed during growth on non-fermentable carbon sources and under aerobic conditions, while *ACS2* gene coding for the acetate-CoA ligase

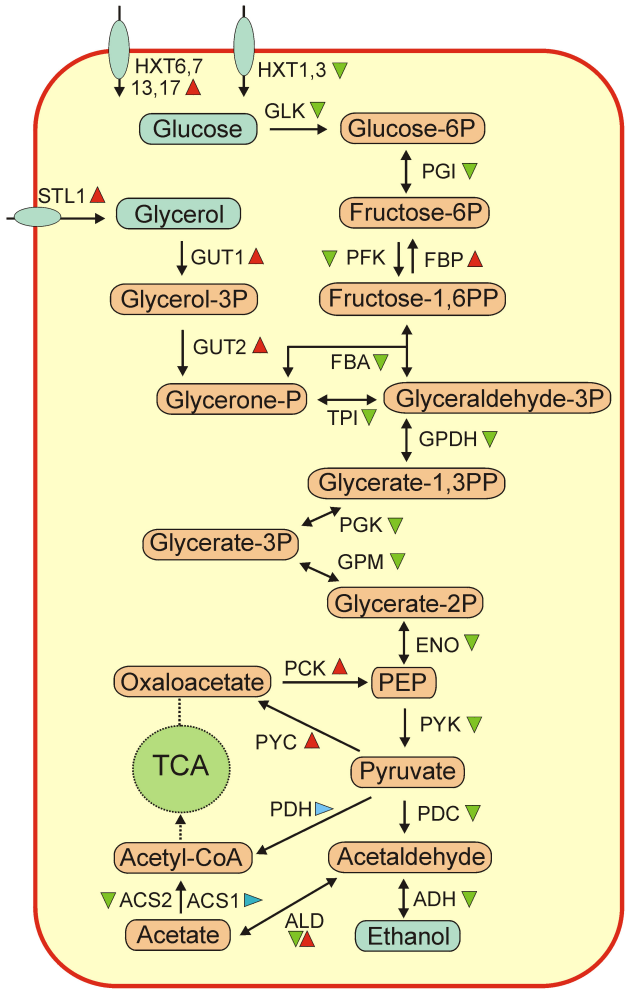

FIGURE 3 | An overview of changes of expression of genes involved in central metabolic pathways. Abbreviations: GLK, glucokinase; PGI, glucose-6-phosphate isomerase; PFK, 6-phosphofructokinase; FBP, fructose 1,6-bisphosphate 1-phosphatase; FBA, fructose-bisphosphate aldolase; TPI, triose-phosphate isomerase; GPDH, glyceraldehyde-3-phosphate dehydrogenase; PGK, phosphoglycerate kinase; GPM, phosphoglycerate mutase; ENO, enolase; PCK, phosphoenolpyruvate carboxykinase; PYK, pyruvate kinase; PYC, pyruvate carboxylase; PDH, pyruvate dehydrogenase; PDC, pyruvate decarboxylase; ADH, alcohol dehydrogenase; ALS, aldehyde dehydrogenase; ACS, acetate- CoA ligase; TCA, tricarboxylic acids cycle; STL1, glycerol proton symporter; HXT, hexose transporter. Genes, up-regulated more than 2-fold at the mature biofilm stage relative to the early biofilm are marker by red triangles, ones down-regulated more than 2-fold, – by green triangles, and ones without significant changes in expression, – by blue triangles. Note that most of ALD genes were up-regulated (*ALD 1, 3, 4, 5*) while *ALD2* was down-regulated.

2 required for growth on glucose under anaerobic conditions was downregulated.

Under aerobic conditions *S. cerevisiae* can use glycerol as a sole carbon and energy source. At the mature biofilm stage two key genes for glycerol catabolism, glycerol kinase *GUT1* and glycerol-3-phosphate dehydrogenase *GUT2*, were induced more than 8-fold. These genes are known to be repressed when cells are grown on fermentable carbon sources and upregulated on non-fermentable carbon sources such as glycerol or ethanol (Sprague and Cronan, 1977; Grauslund and Rønnow, 2000). Gene *STL1* encoding glycerol proton symporter was upregulated more than 5-fold. Probably, upon exhaustion of glucose in the medium the yeasts switched to the use of remaining glycerol. This is consistent with the observed decrease in glycerol concentration in wine as the velum grew (**Table 1**).

Most genes for mitochondrially located TCA enzymes showed increased expression at the mature biofilm stage, while paralogous genes for proteins with cytosolic and peroxisomal localization involved in other pathways showed decreased expression, as seen, for instance for mitochondrial (*MDH1*) and cytoplasmic (*MDH2*) malate dehydrogenases.

Expression of genes relevant to the electron transport chain shows different dynamics. Moderate up-regulation was observed for genes coding for subunits of the mitochondrial F_1F_0 ATP synthase, the ubiquinol cytochrome c reductase, and the NADH-ubiquinone reductase, while no clear trend was observed for cytochrome c oxidase and succinate dehydrogenase subunits (**Supplementary Table S11**).

DNA Repair

It is generally supposed that under biological wine aging conditions flor yeast experience chronic genotoxic stress due to mutagenic action of elevated ethanol and acetaldehyde concentrations. Concentration of aldehydes considerably increased in course of biofilm growth while ethanol concentration moderately decreased (**Table 1**). Acetaldehyde can form DNA-protein and DNA–DNA crosslinks and adducts that interfere with DNA replication. As shown in recent comprehensive study in fission yeast, acetaldehyde causes a variety of DNA damage and induces different DNA repair pathways (Noguchi et al., 2017). Comparison of mRNA levels of DNA repair genes at the early and mature biofilm stages showed mild induction of some nucleotide excision repair (NER) and mismatch repair (MMR) genes at mature biofilm stage, suggesting that cell has already adapted to this type of DNA damage in the beginning of the experiment (**Supplementary Table S12**). More notable induction was observed for the majority of genes involved in homologous recombination, highest upregulation observed for *RAD59, RAD54, RDH54,* involved in DNA double strand break repair and overcoming barriers to DNA replication fork progression due to DNA damage. Perhaps, elevation of concentration of acetaldehyde in course of flor maturation induces this type of DNA damage thus activating homologous recombination pathway.

Cell Wall Structure and Biogenesis

Biofilm formation of flor yeast on the surface of fortified wine materials is a critical prerequisite for efficient biological wine aging. Fungal biofilms are complex structures composed of cells and extracellular matrix. Genetic control of yeast biofilm formation is best studied in *Candida albicans*, and capacity for biofilm formation is directly linked to virulence in this human pathogen (Chandra et al., 2001). Surprisingly, the data about genetic and biochemical control of biofilm formation in yeast

are rather limited. The involvement of small heat-shock protein Hsp12 (Zara et al., 2002), v-snare protein Btn2 (Espinazo-Romeu et al., 2008), as well as the dominant role of Flo11 cell surface adhesion molecule for biofilm formation was established using gene knockout and/or overexpression approaches (Fidalgo et al., 2006; Brückner et al., 2012). Recent proteomic study compared abundance of various groups of proteins in flor yeast at biofilm and non-biofilm stage. Notable overrepresentation of several cell wall proteins at the biofilm stage was detected (Moreno-García et al., 2017). The role of some of identified cell surface proteins (Ccw14, Ygp1) in velum formation was confirmed in subsequent gene-knockout experiments with haploid flor yeast strain (Moreno-García et al., 2018b).

We have compared expression levels of the genes for 60 proteins known as cell wall components and enzymes involved in cell wall modification (**Supplementary Table S13**). The most significant upregulation at the mature biofilm stage relative to the early biofilm stage was observed for *FLO11* (39-fold induction). The genes for other structural GPI-anchored PIR-proteins were also significantly induced, including *CIS3* (19-fold), *PIR1* (15-fold), *PIR3* (3-fold), *SRL1*(14-fold). Also induced were genes for several cell-wall localized heat-shock proteins – *HSP150* and *SSA2*. Along with upregulation of genes for structural cell wall proteins we observed upregulation of genes coding for some enzymes potentially involved in cell-wall restructuring and ECM formation, e.g., *SCW10* family 17 glucosidase (7-fold), *SIM1* glucosidase (6-fold), endo-1,3(4) beta glucanase *ENG1* (6-fold). Some structural and enzymatic cell wall components were downregulated. Strongly downregulatåd was the mannoprotein gene *DAN4* (3-fold) known to be repressed under aerobic growth conditions (Mrsa et al., 1999). These observations show that biofilm formation was accompanied by notable reorganization of the flor yeast cell wall.

Expression of genes coding for 6 types of flocculins was detected at all three stages of biofilm development (**Figure 4**). At the early biofilm stage expression levels of all flocculins were comparable but at later stages all flocculin genes except *FLO11* were moderately down-regulated (*FLO5, FLO8*, and *FLO10*) or did not significantly changed their level of transcription (*FLO1* and *FLO9*). On the contrary, gene coding for Flo11-like adhesin was strongly up-regulated and its expression level reached maximum at the mature biofilm stage, accounting for more than 99% of all flocculins transcripts. Notably, *FLO11* was the fourth most highly expressed gene in the mature biofilm. Thus, these results show that Flo11 flocculin plays a key role in flor growth and maturation.

Increased requirements for structural and enzymatic cell wall components at the biofilm stage suggests upregulation of the major pathways for protein secretion and export. In the secretory pathway we observed upregulation of the genes for components of SEC61 translocon, the Srp14, Srp102 components of the signal recognition particle and signal peptidase, and Kar2 - the endoplasmic reticulum (ER) chaperone and unfolded protein response (UPR) regulator. Meanwhile, expression of genes for proteins involved in vesicle targeting, fusion and endocytosis did not show obvious alterations, majority of these genes were expressed at similar levels at the two compared stages (**Supplementary Table S12**).

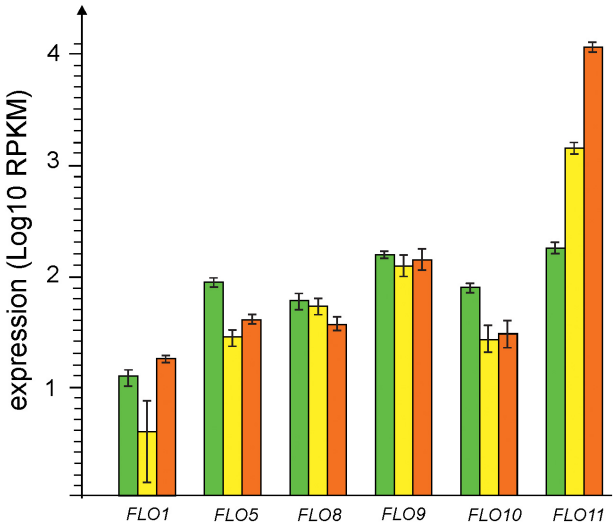

FIGURE 4 | Changes in expression of genes of flocculins, – *FLO1* (gene 4857), *FLO5* (gene 3725), *FLO8* (gene 2945), *FLO9* (gene 5324), *FLO10* (gene 1874), and *FLO11* (gene 5300). Transcription levels observed at the stages of early, thin and mature biofilms are shown by green, yellow and red bars, respectively.

Endoplasmic Reticulum and Cytosolic Protein Quality Control

High ethanol and acetaldehyde concentrations in the course of biological wine aging impose significant burden on flor yeast physiology and metabolism and require activation of cellular defense mechanisms to ensure resistance and survival (Martínez et al., 1997; Esteve-Zarzoso et al., 2001; Castrejón et al., 2002; Aranda and del Olmo, 2003; Alexandre, 2013; Fierro-Risco et al., 2013). Under conditions of our experiment ethanol concentration was high already at the early biofilm stage and than slightly decreased, while concentration of acetaldehyde increased almost twice (**Table 1**).

Acetaldehyde is a highly reactive toxic compound for all organisms. Acetaldehyde-protein and acetaldehyde-DNA adducts cause conformational changes and inactivation of celluar targets, stoping cellular growth and inhibiting various cellular metabolic activities (Jones, 1990). Acetaldehyde-mediated accumulation of unfolded/misfolded proteins in ER may induce ER stress and trigger UPR as adaptive response to maintain cellular proteostasis (Ji, 2012). UPR is a complex interplay of activities like chaperones, glycosylation enzymes, trafficking pathways, endoplasmic-reticulum-associated protein degradation (ERAD) components etc, regulating the balance between protein synthesis, degradation and export and inducing apoptosis in conditions of unreleived stress (Cao and Kaufman, 2012).

Among the genes required for ER protein quality control most significantly upregulated were various chaperones, but

not the ER ubiquitin ligases. Regarding ubiquitin-proteasomal system we found that many structural and regulatory proteasome subunit genes (*RPN1, RPN2, RNP10, RPN11, PRE6, PRE7* etc.) were upregulated at the mature biofilm stage (**Supplementary Table S12**). Thus, our gene expression analysis suggests that at the mature biofilm stage flor yeast cells do not experience more pronounced UPR stress relative to the early biofilm stage, but do induce the ERAD pathway as reflected by notable upregulation of the proteasomal genes and ER chaperone genes.

Yeast transcriptional responses to acetaldehyde exposure have been the subject of several studies (Aranda et al., 2002; Aranda and del Olmo, 2003, 2004). Under conditions of short-term acetaldehyde stress in the lab strain (Aranda and del Olmo, 2004) upregulated were genes for heat-shock proteins, sulfur metabolism, polyamine transporters, mediated by Met4 and Haa1 transcription factors, while downregulated were many genes involved in cellular division and cell-cycle progression. We have found that 75% of genes described as acetaldehyde-inducble by Aranda and del Olmo (2004) were also upregulated in our experimental conditions at mature biofilm stage (**Supplementary Table S14**). This common list includes *HSP* and *MET* genes, but not *TPO* genes for polyamine transporters. Upregulation of *MET* genes may be required for acetaldehyde detoxification through the synthesis of non-toxic compound.

Autophagy and Cell Death

The specific environment of biological wine aging is characterized by nutrient starvation – a condition, potentially capable to induce both for authophagy and apoptosis. Evaluation of the known genes involved in micro and macro autophagy in yeast revealed that most of them were down-regulated at the mature biofilm stage. Notably, this downregulation was accompanied by a strong upregulation of *PCL5,* coding for a cyclin that in complex with Pho80 is known to negatively regulate autophagy (Measday et al., 1997). In contrast, many genes, known to be involved in apoptosis in yeast, were upregulated at this stage (**Supplementary Table S12**). These findings indicate opposing roles of autophagy and apoptosis in course of biofilm development.

Gene expression comparison revealed no clear pattern of up- or downregulation of genes involved in mitophagy. Most of mitophagy-related genes showed minor alterations in expression levels (**Supplementary Table S12**). Some positive mitophagy regulators, like *MDM34* and *ATG33* were upregulated and some negative regulators (*TOR1*, *TOR2*, *PTC6*) were downregulated. On the other hand, some important mitophagy mediators, mitophagy receptor *ATG32* and *MMM1* subunit of ERMES complex, were downregulated (**Supplementary Table S12**).

Apoptosis induction was accompanied by upregulation of the TF known to control apoptotic processes in yeast. Analysis of expression level of various vacuolar peptidases and nucleases indicated that apoptotic process is accompanied by extensive degradation of intracellular molecules and autolysis (Carmona-Gutierrez et al., 2010). Downregulation of many genes involved in peroxisome biogenesis in combination with downregulation of fatty acid and steroid biosynthetic processes suggests that fatty acid catabolism is suppressed at biofilm stage (**Supplementary Table S15**).

Transport Protein Genes

There are almost 300 genes for established or predicted transmembrane transporters in *S. cerevisiae* genome, encoding proteins that facilitate the transport of a very wide variety of small compounds across the plasma and internal membranes, - amino acid, sugars, ions etc, that are differentially regulated depending on metabolic and physiological status of yeast cells, in nutrient-rich and starvation condition etc.

Yeast transport protein database (Brohée et al., 2010) is a resource dedicated to the precise classification and annotation of yeast transport protein genes (YTP genes). Of the 303 YTP genes stored at YTP database 287 were found in our RNA-seq data. For these genes we have compared the expression levels at different biofilm growth stages (**Supplementary Table S16**).

We observed sharp differences in YTP genes expression levels between the early and mature biofilm stages. Not surprisingly, at the mature biofilm stage we observed significant down-regulation of the majority of transporter genes. In particular, low-affinity glucose transporters (*HXT1* and *HXT3)*, oligopeptide (*OPT1,2*), allantoate (*DAL5*), polyamine (*TPO2,4*), amino acid (*PUT4, GAP1, BAT1, VBA1*), iron (*FET4*) transporters as well as ion pumps (*PMA1*) were downregulated.

However about 25% of genes from the analyzed set did not show notable alterations in expression levels between two stages and 10% showed notable up-regulation at the mature biofilm stage. Upregulated genes include high affinity hexose transporters (*HXT6, HXT7, HXT13*), enabling efficient uptake of sugars at low concentrations, *SSU1* sulfite transporter, *SUL2* sulfate transporter, *ENB1* iron transporter, several mitochondrial transporters for carboxylic acids (*MPC1, MPC2, SFC1*). The highest expression level at this stage was detected for *PIC2* gene encoding mitochondrial copper and phosphate carrier.

"Uncharacterized" Genes Exhibiting Abundant Transcription and Significant Up and Down-Regulation

Despite consolidated community efforts in yeast comparative and functional genomics, functions of a significant number of yeast genes still remains unknown. According to recent SGD statistics (May 12, 2019), 1785 genes of *S. cerevisiae* in "Biological Process," 1306 in "Cellular component" and 2562 in "Molecular Function" GO categories are deemed "unknown." This uncertainty may be explained in part by the lack of information about specific conditions when these genes are actually needed. We reasoned that at least some of these genes may have an adaptive role under specific conditions of biological wine aging and biofilm formation.

In the Up4 list of genes highly up-regulated at the mature biofilm stage we found 19 genes within the category "protein of unknown function" (**Supplementary Table S17**). Several genes in this list overlap with the set of genes highly expressed in the mature biofilm. Search through SGD provided limited information concerning phenotypes conferred by null-mutants of these genes – majority fall in the category "competitive fitness – decreased" and "resistance to chemical – decreased."

We therefore manually searched the SPELL database[2] (Hibbs et al., 2007) to identify conditions when these genes were considerably induced. Search terms were limited to various stress conditions, starvation, carbon and nitrogen metabolism that physiologically may resemble the flor yeast biofilm stage (**Supplementary Table S18**).

For the 9 selected up-regulated genes we found 21 studies when these genes were induced in a similar way as in our experiments. The most abundant categories were "stationary phase maintenance" (1 study, 8 genes), heat shock (5 genes, 6 studies), osmotic stress (4 genes, 5 studies), oxidative stress (6 genes, 4 studies), unfolded protein response (3 genes, 3 studies), starvation (4 genes, 3 studies), stress (5 genes, 3 studies). The genes most frequently detected in this search were *TMA10, UIP3, RTC3, RGI1,* and *YKR011C*. Of note, *TMA10, RTC3, RGI1*, along with *EGO4* were also among the top highly expressed genes at the mature biofilm stage. According to SGD description (**Supplementary Table S17**), *TMA10, RTC3, RGI1* are implicated in resistance to different forms of stresses, particularly, DNA replication stress and oxidative stress. The list of "unknown genes" among highly down-regulated is short; it involves four genes that in four studies were down-regulated in response to starvation and different stresses.

Of course, experimental conditions and strains genotypes utilized in our study and in those used for comparison were very different. Recent study concerning species-specific effects on stress induced gene expression show significant role of "biological noise" (Tirosh et al., 2011). Nevertheless, we consider that our comparison provides useful hints about the possible role of "unknown" genes at biofilm stage in flor yeast that can be further verified using various genome editing approaches.

Sulfur Metabolism

Saccharomyces cerevisiae can use a variety of inorganic and organic sulfur sources that are taken up and assimilated through distinct transport and biochemical pathways (Thomas and Surdin-Kerjan, 1997). The major sulfur sources in wine materials and grape juice are sulfate (16–70 mg/l) and sulfite that is added to grape juice for wine making while the content of cysteine and methionine is rather low (<20 mg/l), so the sulfur assimilation pathway (SAP) is triggered during fermentation to support yeast growth (Huang et al., 2017). Biosynthesis of sulfur aminoacids in *S. cerevisiae* occurs through transsulfuration pathway, while in many other yeast species the alternative *O*-acetyl-serine (OAS) pathway also exists (Hébert et al., 2011).

We observed significant up-regulation of the genes of the SAP pathway in the samples derived from the mature biofilm as compared to the early biofilm stage. All three genes involved in first three steps of sulfate reduction to sulfite (Thomas and Surdin-Kerjan, 1997) - the *MET3* gene for ATP sulphurylase, the *MET14* gene for APS kinase, and the *MET16* gene for PAPS reductase were induced 3–4 fold. The *MET5* and *MET10* genes for subunits of sulfite reductase were also up-regulated 2–4 fold.

Coordinate up-regulation was also observed for many genes for initial steps in the cysteine and methionine biosynthesis pathways, mainly for *MET17* for bifunctional cysteine synthase/*O*-acetylhomoserine aminocarboxypropyltransferase responsible for sulfur incorporation into carbon chain, *MET2* for homoserine *O*-acetyltransferase, *CYS3* for cysthatione-gamma lyase. On the contrary, expression levels for genes for enzymes involved in methionine salvage pathway, for production of volatile sulfur compounds, and glutathione biosynthesis were not altered or down-regulated (**Supplementary Table S19**).

A very similar expression pattern for sulfur metabolism genes was observed in the study of transcription responses of laboratory strains to acetaldehyde exposure (Aranda and del Olmo, 2004). Authors showed that this induction is dependent upon transcriptional activators of the SAP and cysteine-methionine biosynthesis pathways. In our study we also observed up-regulation of genes for several relevant transactivators, namely for *MET4* (5-fold), *MET28* (6-fold), *MET32* (35-fold).

Observed induction of sulfur metabolism genes in the two studies may be relevant to protective yeast cell responses against toxic effects of acetaldehyde, for instance, through formation of non-toxic 1-hydroxyethane sulfonate in reaction between acetaldehyde and sulfite (Casalone et al., 1992). Contribution of other sulfur containing aminoacids and glutathione to these detoxifying effects is also plausible. Finally, in this context hydrogen sulfide should be considered not only as biosynthetic intermediate, but also as an important compound for yeast detoxification, population signaling, and life span extension (Hine et al., 2015).

Genes Most Activated or Repressed at the Thin Biofilm Stage

As previously noted, for the most of DEGs, continuous up- or down-regulation was observed in course of flor growth. Nevertheless, 64 and 87 genes had, respectively, a maximum and a minimum of expression level at the intermediate (thin biofilm) stage (**Supplementary Table S7**).

The group of genes most highly expressed at the thin biofilm stage included amino acid (*BAP2*, *BAP3, DIP5, TAP1, TAT1*), iron (*FTR1*, *FET3*) and sulfate (*SUL1*) transporters, and plasma membrane permease *GIT1* mediating uptake of glycerophosphoinositol and glycerophosphocholine as sources of the inositol and phosphate. Up-regulation at this stage was also found for *GDH1* gene encoding glutamate dehydrogenase - the central enzyme in several nitrogen uptake pathways, *ARO10* gene encoding phenylpyruvate decarboxylase – the first enzyme in the Erlich amino acid degradation pathway, and *AAD14* gene for aryl-alcohol dehydrogenase. Up-regulation of these genes probably signaled metabolic shift of flor yeast toward utilization of specific nitrogen and carbon sources, available at this intermediate stage, that are apparently exhausted at the mature biofilm stage. Finally, up-regulation of genes for glutathione biosynthesis (*GSH2*, *GTT2*) and *YHB4* flavohemoglobin may indicate emergence of oxidative stress signal at this stage.

The group of genes down-regulated at the thin biofilm stage was included genes involved in abiotic stress response. In particular, genes involved in trehalose (*NTH1, TPS2, ATH1*) and glycerol (*GPD1, GPP2*) metabolism may mediate resistance to

[2]https://spell.yeastgenome.org/

osmotic and ethanol stresses. Down-regulation of genes coding for some stress-related transcriptional factors (*MIG2, MIG3, MOT3, RSF2, USV1*), DNA damage-responsive protein (*DDR48*), other stress-related proteins (*GRE1*, *GRE3, GAD1*, *PAI3*, *SIP18*) suggested that some stresses are less pronounced at this stage.

Comparison of the lists of genes most strongly up- or down-regulated at the thin biofilm stage indicates that at the intermediate stage yeast cells were not completely limited in readily accessible carbon and nitrogen sources, and environmental conditions at this stage were to some extend less stressful than at the first and the last stages. Indeed, the early stage was characterized by adaptation to osmotic and ethanol stress, and the mature biofilm stage – to high acetaldehyde content, carbon and nitrogen starvation stress. Alterations in the expression of genes involved in amino acid and higher alcohol metabolism at the intermediate stage may influence production of aromatic compounds and contribute to final sensory compositions of wine.

DISCUSSION

Flor yeast strains are the soul of sherry wine formation (Peinado and Mauricio, 2009; Pozo-Bayón and Moreno-Arribas, 2011). Under typical sherry wine-making conditions flor yeast undergo important physiological, morphological and biochemical transitions to adapt to harsh oenological environment. Specific nutrient conditions – very low sugar and high ethanol content, high acetaldehyde concentration induce flor yeast to reprogram their metabolism from fermentative to oxidative one, and to withstand combined action of several stresses, namely nutrient limitation (especially for nitrogen), ethanol stress, oxidative stress, acetaldehyde stress and imbalance of nutritional agents (Alexandre, 2013; Moreno-García et al., 2016). In order to survive flor yeasts developed a biofilm (flor) – a specific multicellular aggregate that is widely considered as an adaptive mechanism ensuring oxygen access and promoting growth on non-fermentable carbon source (Zara et al., 2010).

Thorough characterization and quantification of accompanying transcriptional responses are critical for understanding the molecular mechanisms that govern these changes. To gain insight how gene expression variation contributes to changes in flor yeast physiology and metabolism under conditions of biological wine aging we have used RNA-seq technology to compare gene expression profiles of a flor yeast strain at different stages of biofilm growth. Application of RNA-seq platform enabled us to quantify expression levels of 5320 of 5323 genes annotated in the nuclear genome of flor yeast I-329 strain.

Our analysis showed significant transcriptome alteration with 816 genes up-regulated and 674 down-regulated (more than 2-fold) at the mature biofilm stage as compared to the early biofilm stage, reflecting metabolic and physiological changes in course of biofilm development. From the transcriptomic data the mature biofilm stage seems to resemble the quiescent stage with oxidative metabolism and activation of several stress resistance pathways. Indeed, nutritional conditions at the mature biofilm stage, tight cell–cell adhesion, toxic effects of ethanol and acetaldehyde should suppress cell proliferation, protein translation, and induce DNA damage (García-Ríos and Guillamón, 2019). However, continued expression of many genes required for transcription, translation, respiration, cell wall biogenesis etc suggests that at least some proportion of cells even in mature biofilm is in active, dividing state. In this regard it is necessary to point that flor yeast velum represents a rather heterogeneous multicellular structure composed of different yeast subpopulations thriving in various microenvironments. The difference of oxygen and nutrient availability, ethanol and acetaldehyde concentrations at the air-biofilm and biofilm-liquid interface may induce formation of various cell types that differ in cell metabolism etc. Such variation may lead to ultimate changes in gene expression as shown for yeast subpopulation within colonies grown on solid surfaces (Maršíková et al., 2017). Thus, whole-velum transcriptome data may in fact represent a superposition of transcriptomes of various cell subpopulations, differing in metabolic and physiological microenvironment. Nevertheless, very distinct and profound transcriptome upregulation at the mature biofilm stage was found for many genes, implicated in cell wall biogenesis and resistance to oxidative stress. For cell wall protein genes opposing trends in expression of *FLO11, HSP150, CIS3, PIR1* (upregulated) and *FLO5, FLO8*, *FLO10, DAN4* (downregulated) may reflect significant cell-wall remodeling in the course of flor formation and growth.

Several genes found among top highly expressed and upregulated genes at the mature biofilm stage, as for instance, *EGO4* and *RGI1*, encode proteins with "unknown" or poorly characterized function. Comparative analysis of the expression patterns of selected "unknown" genes with highest expression level using SPELL database indicated their upregulation at various stress conditions suggesting their unexplored adaptive role at the biofilm stage.

It is well known and shown in numerous studies using both microarray and RNA-seq platforms that transcriptional responses of yeast strains to different environmental cues are highly variable depending on the nature of abusing agent, time of exposure, strain genotype etc. (Taymaz-Nikerel et al., 2016; Ibáñez et al., 2017; Mendes et al., 2017; Tondini et al., 2019). It is also necessary to distinguish short and long-term responses and acquired resistance as mechanisms of adaptation (Stanley et al., 2010). The time scale of sampling points in these studies was in the range of hours and days, none had considered time points separated by several weeks. To the best of our knowledge this study is the first attempt to investigate transcriptome state along different stage of the development of the velum during biological aging. Flor yeast biofilms are typical sessile surface associated microbial populations, protected by polymeric extracellular matrix (ECM) (Zara et al., 2009; Costa-Orlandi et al., 2017). Biofilm formation is a gradual process, involving substrate adherence (flotation in the case of flor yeast), yeast cell proliferation over surface, cell-cell cohesion and embedment in ECM (Verstrepen and Klis, 2006). As shown in many studies with yeast and fungal human and plant pathogens, like *Candida albicans*, *Aspergillus fumigatus*, biofilm cells are phenotypically different from free or planktonic cells, are more resistant to environmental stresses and antifungals, that is

a very important factor in their virulence (Fanning and Mitchell, 2012; Costa-Orlandi et al., 2017).

Transcriptome analysis of *C. albicans* and *A. fumigatus*, as well as *S. cerevisiae* during filamentous growth (Verstrepen and Klis, 2006), have revealed major alterations in gene expression patterns between biofilm cells and planktonic cells (García-Sánchez et al., 2004; Verstrepen and Klis, 2006; Gibbons et al., 2012). Despite obvious significant taxonomic differences between flor yeast and these pathogens, we found several common differential gene expression patterns pointing to existence of general mechanisms of transcriptional regulation in the course of biofilm development in these species. First of all this considers upregulation of many cell wall biogenesis genes and adhesins, required both for cell wall and ECM formation. Many of these genes are induced by Ace2 and Swi5 transcription factors, and, similar to *C. albicans*, we observe upregulation of these TF at mature biofilm stage.

Elevated expression of some genes, related to transcription, protein biosynthesis and turnover (ribosomal proteins, proteasomal genes, transcription and translation factors) is another common feature of flor yeasts and *C. albicans* and *A. fumigatus* biofilm cells (Fanning and Mitchell, 2012). This indicates that yeast and fungal biofilm cell are metabolically not dormant. In line with this observation was common upregulation of some amino acid biosynthesis genes, especially for sulfur aminoacids, permeases for poor nitrogen substrates in flor yeast and *C. albicans* biofilm cells (García-Sánchez et al., 2004).

In conclusion, important changes of gene expression of flor yeast strain I-329 at different winemaking stages were discovered as adaptive processes to biofilm formation. The observed differential expression patterns may reflect the physiologically and metabolically stable quiescent phase where different cell subpopulations had already gained resistance to specific nutrient conditions. The identification and functional analysis of biofilm-response genes could shed light on the overall understanding of cell response elicited by velum formation and sherry wine manufacturing conditions, and for the comprehension of relevant regulatory mechanisms.

DATA AVAILABILITY STATEMENT

The datasets generated for this study can be found in the SRR10551665, SRR10551664, SRR10551663, SRR10551662, SRR10551661, SRR10551660, SRR10551659, SRR10551658, SRR10551657.

AUTHOR CONTRIBUTIONS

AM, ME, and NR designed the research project and wrote the manuscript. SK, TT, AB, and AM performed the research. AB, AM, NR, and ME analyzed the data. All authors read and approved the manuscript.

FUNDING

This work was partly supported by Russian Science Foundation (grant 16-16-00109).

ACKNOWLEDGMENTS

This work was performed using the scientific equipment of Core Research Facility 'Bioengineering.'

SUPPLEMENTARY MATERIAL

The Supplementary Material for this article can be found online at: https://www.frontiersin.org/articles/10.3389/fmicb.2020.00538/full#supplementary-material

REFERENCES

Alexandre, H. (2013). Flor yeasts of *Saccharomyces cerevisiae* - their ecology, genetics and metabolism. *Int. J. Food Microbiol.* 167, 269–275. doi: 10.1016/j.ijfoodmicro.2013.08.021

Anders, S., and Huber, W. (2010). Differential expression analysis for sequence count data. *Genome Biol.* 11:R106.

Aranda, A., and del Olmo, M. (2003). Response to acetaldehyde stress in the yeast *Saccharomyces cerevisiae* involves a strain-dependent regulation of several *ALD* genes and is mediated by the general stress response pathway. *Yeast* 20, 747–759. doi: 10.1002/yea.991

Aranda, A., and del Olmo, M. (2004). Exposure of *Saccharomyces cerevisiae* to acetaldehyde induces sulfur amino acid metabolism and polyamine transporter genes, which depend on Met4p and Haa1p transcription factors, respectively. *Appl. Environ. Microbiol.* 70, 1913–1922. doi: 10.1128/aem.70.4.1913-1922.2004

Aranda, A., Querol, A., and del Olmo, M. (2002). Correlation between acetaldehyde and ethanol resistance and expression of *HSP* genes in yeast strains isolated during the biological aging of sherry wines. *Arch. Microbiol.* 177, 304–312. doi: 10.1007/s00203-001-0391-1

Barbosa, C., García-Martínez, J., Pérez-Ortín, J. E., and Mendes-Ferreira, A. (2015). Comparative transcriptomic analysis reveals similarities and dissimilarities in *Saccharomyces cerevisiae* wine strains response to nitrogen availability. *PLoS One* 10:e0122709. doi: 10.1371/journal.pone.0122709

Beltran, G., Novo, M., Leberre, V., Sokol, S., Labourdette, D., Guillamon, J.-M., et al. (2006). Integration of transcriptomic and metabolic analyses for understanding the global responses of low-temperature winemaking fermentations. *FEMS Yeast Res.* 6, 1167–1183. doi: 10.1111/j.1567-1364.2006.00106.x

Berry, D. B., and Gasch, A. P. (2008). Stress-activated genomic expression changes serve a preparative role for impending stress in yeast. *Mol. Biol. Cell* 19, 4580–4587. doi: 10.1091/mbc.e07-07-0680

Boer, V. M., de Winde, J. H., Pronk, J. T., and Piper, M. D. W. (2003). The genome-wide transcriptional responses of *Saccharomyces cerevisiae* grown on glucose in aerobic chemostat cultures limited for carbon, nitrogen, phosphorus, or sulfur. *J. Biol. Chem.* 278, 3265–3274. doi: 10.1074/jbc.m209759200

Brohée, S., Barriot, R., Moreau, Y., and André, B. (2010). YTPdb: a wiki database of yeast membrane transporters. *Biochim. Biophys. Acta Biomembr.* 1798, 1908–1912. doi: 10.1016/j.bbamem.2010.06.008

Brückner, S., Mösch, H.-U., Aa, E., Townsend, J., Adams, R., Nielsen, K., et al. (2012). Choosing the right lifestyle: adhesion and development in

Saccharomyces cerevisiae. *FEMS Microbiol. Rev.* 36, 25–58. doi: 10.1111/j.1574-6976.2011.00275.x

Cao, S. S., and Kaufman, R. J. (2012). Unfolded protein response. *Curr. Biol.* 22, R622–R626.

Carmona-Gutierrez, D., Eisenberg, T., Büttner, S., Meisinger, C., Kroemer, G., and Madeo, F. (2010). Apoptosis in yeast: triggers, pathways, subroutines. *Cell Death Differ.* 17, 763–773. doi: 10.1038/cdd.2009.219

Casalone, E., Colella, C. M., Daly, S., Gallori, E., Moriani, L., and Polsinelli, M. (1992). Mechanism of resistance to sulphite in *Saccharomyces cerevisiae*. *Curr. Genet.* 22, 435–440. doi: 10.1007/bf00326407

Castrejón, F., Codón, A. C., Cubero, B., and Benítez, T. (2002). Acetaldehyde and ethanol are responsible for mitochondrial DNA (mtDNA) restriction fragment length polymorphism (RFLP) in flor yeasts. *Syst. Appl. Microbiol.* 25, 462–467. doi: 10.1078/0723-2020-00127

Causton, H. C., Ren, B., Koh, S. S., Harbison, C. T., Kanin, E., Jennings, E. G., et al. (2001). Remodeling of yeast genome expression in response to environmental changes. *Mol. Biol. Cell* 12, 323–337. doi: 10.1091/mbc.12.2.323

Chandra, J., Kuhn, D. M., Mukherjee, P. K., Hoyer, L. L., McCormick, T., and Ghannoum, M. A. (2001). Biofilm formation by the fungal pathogen *Candida albicans*: development, architecture, and drug resistance. *J. Bacteriol.* 183, 5385–5394. doi: 10.1128/jb.183.18.5385-5394.2001

Coi, A. L., Bigey, F., Mallet, S., Marsit, S., Zara, G., Gladieux, P., et al. (2017). Genomic signatures of adaptation to wine biological ageing conditions in biofilm-forming flor yeasts. *Mol. Ecol.* 26, 2150–2166. doi: 10.1111/mec.14053

Compendium of international methods of wine and must analysis (2018). *International Organization of Vine and Wine*. Available online at: http://www.oiv.int/en/technical-standards-and-documents/methods-of-analysis (accessed March 23, 2020).

Costa-Orlandi, C. B., Sardi, J. C. O., Pitangui, N. S., de Oliveira, H. C., Scorzoni, L., Galeane, M. C., et al. (2017). Fungal biofilms and polymicrobial diseases. *J. Fungi* 3:22.

Eldarov, M. A., Beletsky, A. V., Tanashchuk, T. N., Kishkovskaya, S. A., Ravin, N. V., and Mardanov, A. V. (2018). Whole-genome analysis of three yeast strains used for production of sherry-like wines revealed genetic traits specific to flor yeasts. *Front. Microbiol.* 9:965. doi: 10.3389/fmicb.2018.00965

Espinazo-Romeu, M., Cantoral, J. M., Matallana, E., and Aranda, A. (2008). Btn2p is involved in ethanol tolerance and biofilm formation in flor yeast. *FEMS Yeast Res.* 8, 1127–1136. doi: 10.1111/j.1567-1364.2008.00397.x

Esteve-Zarzoso, B., Peris-Torán, M. J., García-Maiquez, E., Uruburu, F., and Querol, A. (2001). Yeast population dynamics during the fermentation and biological aging of sherry wines. *Appl. Environ. Microbiol.* 67, 2056–2061. doi: 10.1128/aem.67.5.2056-2061.2001

Fanning, S., and Mitchell, A. P. (2012). Fungal biofilms. *PLoS Pathog.* 8:e1002585. doi: 10.1371/journal.ppat.1002585

Fidalgo, M., Barrales, R. R., Ibeas, J. I., and Jimenez, J. (2006). Adaptive evolution by mutations in the *FLO11* gene. *Proc. Natl. Acad. Sci. U.S.A.* 103, 11228–11233. doi: 10.1073/pnas.0601713103

Fierro-Risco, J., Rincón, A. M., Benítez, T., and Codón, A. C. (2013). Overexpression of stress-related genes enhances cell viability and velum formation in Sherry wine yeasts. *Appl. Microbiol. Biotechnol.* 97, 6867–6881. doi: 10.1007/s00253-013-4850-9

Flikweert, M. T., Van Der Zanden, L., Janssen, W. M., Steensma, H. Y., Van Dijken, J. P., and Pronk, J. T. (1996). Pyruvate decarboxylase: an indispensable enzyme for growth of *Saccharomyces cerevisiae* on glucose. *Yeast* 12, 247–257. doi: 10.1002/(sici)1097-0061(19960315)12:3<247::aid-yea911>3.0.co;2-i

Gamero, A., Belloch, C., Ibáñez, C., and Querol, A. (2014). Molecular analysis of the genes involved in aroma synthesis in the species *S. cerevisiae*, *S. kudriavzevii* and *S. bayanus* var. uvarum in winemaking conditions. *PLoS One* 9:e97626. doi: 10.1371/journal.pone.0097626

García-Ríos, E., and Guillamón, J. M. (2019). Mechanisms of yeast adaptation to wine fermentations. *Prog. Mol. Subcell. Biol.* 58, 37–59. doi: 10.1007/978-3-030-13035-0_2

García-Sánchez, S., Aubert, S., Iraqui, I., Janbon, G., Ghigo, J. M., and D'Enfert, C. (2004). *Candida albicans* biofilms: a developmental state associated with specific and stable gene expression patterns. *Eukaryot. Cell* 3, 536–545. doi: 10.1128/ec.3.2.536-545.2004

Gibbons, J. G., Beauvais, A., Beau, R., McGary, K. L., Latgé, J. P., and Rokas, A. (2012). Global transcriptome changes underlying colony growth in the opportunistic human pathogen *Aspergillus fumigatus*. *Eukaryot. Cell* 11, 68–78. doi: 10.1128/ec.05102-11

Grauslund, M., and Rønnow, B. (2000). Carbon source-dependent transcriptional regulation of the mitochondrial glycerol-3-phosphate dehydrogenase gene, *GUT2*, from *Saccharomyces cerevisiae*. *Can. J. Microbiol.* 46, 1096–1100. doi: 10.1139/w00-105

Hébert, A., Casaregola, S., and Beckerich, J. M. (2011). Biodiversity in sulfur metabolism in hemiascomycetous yeasts. *FEMS Yeast Res.* 11, 366–378. doi: 10.1111/j.1567-1364.2011.00725.x

Hibbs, M. A., Hess, D. C., Myers, C. L., Huttenhower, C., Li, K., and Troyanskaya, O. G. (2007). Exploring the functional landscape of gene expression: directed search of large microarray compendia. *Bioinformatics* 23, 2692–2699. doi: 10.1093/bioinformatics/btm403

Hine, C., Harputlugil, E., Zhang, Y., Ruckenstuhl, C., Lee, B. C., Brace, L., et al. (2015). Endogenous hydrogen sulfide production is essential for dietary restriction benefits. *Cell* 160, 132–144. doi: 10.1016/j.cell.2014.11.048

Huang, C. W., Walker, M. E., Fedrizzi, B., Gardner, R. C., and Jiranek, V. (2017). Hydrogen sulfide and its roles in *Saccharomyces cerevisiae* in a winemaking context. *FEMS Yeast Res.* 17:fox058.

Ibáñez, C., Pérez-Torrado, R., Morard, M., Toft, C., Barrio, E., and Querol, A. (2017). RNAseq-based transcriptome comparison of *Saccharomyces cerevisiae* strains isolated from diverse fermentative environments. *Int. J. Food Microbiol.* 257, 262–270. doi: 10.1016/j.ijfoodmicro.2017.07.001

Ji, C. (2012). Mechanisms of alcohol-induced endoplasmic reticulum stress and organ injuries. *Biochem. Res. Int.* 2012:216450.

Jiao, X., Sherman, B. T., Huang, D. W., Stephens, R., Baseler, M. W., Lane, H. C., et al. (2012). DAVID-WS: a stateful web service to facilitate gene/protein list analysis. *Bioinformatics* 28, 1805–1806. doi: 10.1093/bioinformatics/bts251

Jones, R. P. (1990). Roles for replicative deactivation in yeast-ethanol fermentations. *Crit. Rev. Biotechnol.* 10, 205–222. doi: 10.3109/07388559009038208

Juhnke, H., Krems, B., Kötter, P., and Entian, K. D. (1996). Mutants that show increased sensitivity to hydrogen peroxide reveal an important role for the pentose phosphate pathway in protection of yeast against oxidative stress. *Mol. Gen. Genet.* 252, 456–464. doi: 10.1007/bf02173011

Kishkovskaia, S. A., Eldarov, M. A., Dumina, M. V., Tanashchuk, T. N., Ravin, N. V., and Mardanov, A. V. (2017). Flor yeast strains from culture collection: genetic diversity and physiological and biochemical properties. *Appl. Biochem. Microbiol.* 53, 359–367. doi: 10.1134/S0003683817030085

Langmead, B., and Salzberg, S. L. (2012). Fast gapped-read alignment with bowtie 2. *Nat. Methods* 9, 357–359. doi: 10.1038/nmeth.1923

Legras, J.-L., Erny, C., and Charpentier, C. (2014). Population structure and comparative genome hybridization of European flor yeast reveal a unique group of *Saccharomyces cerevisiae* strains with few gene duplications in their genome. *PLoS One* 9:e108089. doi: 10.1371/journal.pone.0108089

Legras, J.-L., Galeote, V., Bigey, F., Camarasa, C., Marsit, S., Nidelet, T., et al. (2018). Adaptation of *S. cerevisiae* to fermented food environments reveals remarkable genome plasticity and the footprints of domestication. *Mol. Biol. Evol.* 35, 1712–1727. doi: 10.1093/molbev/msy066

Legras, J.-L., Moreno-Garcia, J., Zara, S., Zara, G., Garcia-Martinez, T., Mauricio, J. C., et al. (2016). Flor yeast: new perspectives beyond wine aging. *Front. Microbiol.* 7:503. doi: 10.3389/fmicb.2016.00503

Leng, N., Dawson, J. A., Thomson, J. A., Ruotti, V., Rissman, A. I., Smits, B. M., et al. (2013). EBSeq: an empirical bayes hierarchical model for inference in RNA-seq experiments. *Bioinformatics* 29, 1035–1043. doi: 10.1093/bioinformatics/btt087

Leng, N., and Kendziorski, C. (2019). *EBSeq: An R Package for Gene And Isoform Differential Expression Analysis Of RNA-Seq Data*. Available online at: https://bioconductor.org/packages/release/bioc/html/EBSeq.html (accessed March 23, 2020).

Li, B., and Dewey, C. N. (2011). RSEM: accurate transcript quantification from RNA-Seq data with or without a reference genome. *BMC Bioinform.* 12:323. doi: 10.1186/1471-2105-12-323

Luo, W., and Brouwer, C. (2013). Pathview: an R/Bioconductor package for pathway-based data integration and visualization. *Bioinformatics* 29, 1830–1831. doi: 10.1093/bioinformatics/btt285

Marks, V. D., Ho Sui, S. J., Erasmus, D., Van Der Merwe, G. K., Brumm, J., Wasserman, W. W., et al. (2008). Dynamics of the yeast transcriptome during

wine fermentation reveals a novel fermentation stress response. *FEMS Yeast Res.* 8, 35–52. doi: 10.1111/j.1567-1364.2007.00338.x

Maršíková, J., Wilkinson, D., Hlaváèek, O., Gilfillan, G. D., Mizeranschi, A., Hughes, T., et al. (2017). Metabolic differentiation of surface and invasive cells of yeast colony biofilms revealed by gene expression profiling. *BMC Genomics* 18:814. doi: 10.1186/s12864-017-4214-4

Martínez, P., Pérez Rodríguez, L., and Benítez, T. (1997). Evolution of flor yeast population during the biological aging of fino sherry wine. *Am. J. Enol. Vitic.* 48, 160–168.

Measday, V., Moore, L., Retnakaran, R., Lee, J., Donoviel, M., Neiman, A. M., et al. (1997). A family of cyclin-like proteins that interact with the Pho85 cyclin-dependent kinase. *Mol. Cell. Biol.* 17, 1212–1223. doi: 10.1128/mcb.17.3.1212

Mendes, I. I., Sanchez, I., Franco-Duarte, R., Camarasa, C., Schuller, D., Dequin, S., et al. (2017). Integrating transcriptomics and metabolomics for the analysis of the aroma profiles of *Saccharomyces cerevisiae* strains from diverse origins. *BMC Genom.* 18:455. doi: 10.1186/s12864-017-3816-1

Mi, H., Muruganujan, A., Ebert, D., Huang, X., and Thomas, P. D. (2019). PANTHER version 14: more genomes, a new PANTHER GO-slim and improvements in enrichment analysis tools. *Nucleic Acids Res.* 47, D419–D426.

Moreno-García, J., Coi, A. L., Zara, G., García-Martínez, T., Mauricio, J. C., and Budroni, M. (2018a). Study of the role of the covalently linked cell wall protein (Ccw14p) and yeast glycoprotein (Ygp1p) within biofilm formation in a flor yeast strain. *FEMS Yeast Res.* 18:foy005. doi: 10.1093/femsyr/foy005

Moreno-García, J., Garcia-Martinez, T., Millan, M. C., Mauricio, J. C., and Moreno, J. (2015). Proteins involved in wine aroma compounds metabolism by a *Saccharomyces cerevisiae* flor-velum yeast strain grown in two conditions. *Food Microbiol.* 51, 1–9. doi: 10.1016/j.fm.2015.04.005

Moreno-García, J., Mauricio, J. C., Moreno, J., and García-Martínez, T. (2016). Stress responsive proteins of a flor yeast strain during the early stages of biofilm formation. *Process Biochem.* 51, 578–588. doi: 10.1016/j.procbio.2016.02.011

Moreno-García, J., Mauricio, J. C., Moreno, J., and García-Martínez, T. (2017). Differential proteome analysis of a flor yeast strain under biofilm formation. *Int. J. Mol. Sci.* 18:720. doi: 10.3390/ijms18040720

Moreno-García, J., Ogawa, M., Joseph, C. M. L., Mauricio, J. C., Moreno, J., and García-Martínez, T. (2018b). Comparative analysis of intracellular metabolites, proteins and their molecular functions in a flor yeast strain under two enological conditions. *World J. Microbiol. Biotechnol.* 35:6.

Mrsa, V., Ecker, M., Strahl-Bolsinger, S., Nimtz, M., Lehle, L., and Tanner, W. (1999). Deletion of new covalently linked cell wall glycoproteins alters the electrophoretic mobility of phosphorylated wall components of *Saccharomyces cerevisiae*. *J. Bacteriol.* 181, 3076–3086. doi: 10.1128/jb.181.10.3076-3086.1999

Nogae, I., and Johnston, M. (1990). Isolation and characterization of the *ZWF1* gene of *Saccharomyces cerevisiae*, encoding glucose-6-phosphate dehydrogenase. *Gene* 96, 161–169. doi: 10.1016/0378-1119(90)90248-p

Noguchi, C., Grothusen, G., Anandarajan, V., Martínez-Lage García, M., Terlecky, D., Corzo, K., et al. (2017). Genetic controls of DNA damage avoidance in response to acetaldehyde in fission yeast. *Cell Cycle* 16, 45–58. doi: 10.1080/15384101.2016.1237326

Peinado, R. A., and Mauricio, J. C. (2009). "Biologically aged wines," in *Wine Chemistry and Biochemistry*, eds M. V. Moreno-Arribas and M. C. Polo (New York, NY: Springer), doi: 10.1007/978-0-387-74118-5_5

Pozo-Bayón, M. A., and Moreno-Arribas, M. V. (2011). Sherry wines. *Adv. Food Nutr. Res.* 63, 17–40. doi: 10.1016/b978-0-12-384927-4.00002-6

Pronk, J. T., Yde Steensma, H., and Van Dijken, J. P. (1996). Pyruvate metabolism in *Saccharomyces cerevisiae*. *Yeast* 12, 1607–1633.

Roberts, G. G., and Hudson, A. P. (2006). Transcriptome profiling of *Saccharomyces cerevisiae* during a transition from fermentative to glycerol-based respiratory growth reveals extensive metabolic and structural remodeling. *Mol. Genet. Genomics* 276, 170–186. doi: 10.1007/s00438-006-0133-9

Rossignol, T., Dulau, L., Julien, A., and Blondin, B. (2003). Genome-wide monitoring of wine yeast gene expression during alcoholic fermentation. *Yeast* 20, 1369–1385. doi: 10.1002/yea.1046

Rumble, S. M., Lacroute, P., Dalca, A. V., Fiume, M., Sidow, A., and Brudno, M. (2009). SHRiMP: accurate mapping of short color-space reads. *PLoS Comput. Biol.* 5:e1000386. doi: 10.1371/journal.pcbi.1000386

Salvado, Z., Chiva, R., Rodriguez-Vargas, S., Randez-Gil, F., Mas, A., and Guillamon, J. M. (2008). Proteomic evolution of a wine yeast during the first hours of fermentation. *FEMS Yeast Res.* 8, 1137–1146. doi: 10.1111/j.1567-1364.2008.00389.x

Schmitt, M. E., Brown, T. A., and Trumpower, B. L. (1990). A rapid and simple method for preparation of RNA from *Saccharomyces cerevisiae*. *Nucleic Acids Res.* 18, 3091–3192.

Sprague, G. F., and Cronan, J. E. (1977). Isolation and characterization of *Saccharomyces cerevisiae* mutants defective in glycerol catabolism. *J. Bacteriol.* 129, 1335–1342. doi: 10.1128/jb.129.3.1335-1342.1977

Stanley, D., Bandara, A., Fraser, S., Chambers, P. J., and Stanley, G. A. (2010). The ethanol stress response and ethanol tolerance of *Saccharomyces cerevisiae*. *J. Appl. Microbiol.* 109, 13–24.

Supek, F., Bošnjak, M., Škunca, N., and Šmuc, T. (2011). Revigo summarizes and visualizes long lists of gene ontology terms. *PLoS One* 6:e21800. doi: 10.1371/journal.pone.0021800

Taymaz-Nikerel, H., Cankorur-Cetinkaya, A., and Kirdar, B. (2016). Genome-wide transcriptional response of *Saccharomyces cerevisiae* to stress-induced perturbations. *Front. Bioeng. Biotechnol.* 4:17. doi: 10.3389/fbioe.2016.00017

Teixeira, M. C., Monteiro, P. T., Palma, M., Costa, C., Godinho, C. P., Pais, P., et al. (2018). YEASTRACT: an upgraded database for the analysis of transcription regulatory networks in *Saccharomyces cerevisiae*. *Nucleic Acids Res.* 46, D348–D353.

Tenenbaum, D. (2019). *KEGGREST: Client-Side REST Access to KEGG*. Available online at: http://bioconductor.org/packages/release/bioc/html/KEGGREST.html (accessed March 23, 2020).

Thomas, D., and Surdin-Kerjan, Y. (1997). Metabolism of sulfur amino acids in *Saccharomyces cerevisiae*. *Microbiol. Mol. Biol. Rev.* 61, 503–532. doi: 10.1128/.61.4.503-532.1997

Tirosh, I., Wong, K. H., Barkai, N., and Struhl, K. (2011). Extensive divergence of yeast stress responses through transitions between induced and constitutive activation. *Proc. Natl. Acad. Sci. U.S.A.* 108, 16693–16698. doi: 10.1073/pnas.1113718108

Tondini, F., Lang, T., Chen, L., Herderich, M., and Jiranek, V. (2019). Linking gene expression and oenological traits: comparison between *Torulaspora delbrueckii* and *Saccharomyces cerevisiae* strains. *Int. J. Food Microbiol.* 294, 42–49. doi: 10.1016/j.ijfoodmicro.2019.01.014

Tronchoni, J., García-Ríos, E., Guillamón, J. M., Querol, A., and Pérez-Torrado, R. (2017). Transcriptomic analysis of *Saccharomyces cerevisiae* x *Saccharomyces kudriavzevii* hybrids during low temperature winemaking. *F1000Research* 6:679. doi: 10.12688/f1000research.11550.3

Verstrepen, K. J., and Klis, F. M. (2006). Flocculation, adhesion and biofilm formation in yeasts. *Mol. Microbiol.* 60, 5–15. doi: 10.1111/j.1365-2958.2006.05072.x

Walker, M. E., Nguyen, T. D., Liccioli, T., Schmid, F., Kalatzis, N., Sundstrom, J. F., et al. (2014). Genome-wide identification of the Fermentome; genes required for successful and timely completion of wine-like fermentation by *Saccharomyces cerevisiae*. *BMC Genomics* 15:552. doi: 10.1186/1471-2164-15-552

Zara, G., Zara, S., Pinna, C., Marceddu, S., and Budroni, M. (2009). FLO11 gene length and transcriptional level affect biofilm-forming ability of wild flor strains of *Saccharomyces cerevisiae*. *Microbiology* 155(Pt 12), 3838–3846. doi: 10.1099/mic.0.028738-0

Zara, S., Antonio Farris, G., Budroni, M., and Bakalinsky, A. T. (2002). HSP12 is essential for biofilm formation by a Sardinian wine strain of *S. cerevisiae*. *Yeast* 19, 269–276. doi: 10.1002/yea.831

Zara, S., Gross, M. K., Zara, G., Budroni, M., and Bakalinsky, A. T. (2010). Ethanol-independent biofilm formation by a flor wine yeast strain of *Saccharomyces cerevisiae*. *Appl. Environ. Microbiol.* 76, 4089–4091. doi: 10.1128/aem.00111-10

Zhang, H.-M., Yao, S.-J., Peng, L.-F., and Shimizu, K. (2004). Preliminary proteome analysis for *Saccharomyces cerevisiae* under different culturing conditions. *Sheng Wu Gong Cheng Xue Bao* 20, 398–402.

Conflict of Interest: The authors declare that the research was conducted in the absence of any commercial or financial relationships that could be construed as a potential conflict of interest.

frontiers in Microbiology

ORIGINAL RESEARCH
published: 23 April 2020
doi: 10.3389/fmicb.2020.00764

Lachancea fermentati Strains Isolated From Kombucha: Fundamental Insights, and Practical Application in Low Alcohol Beer Brewing

*Konstantin Bellut[1], Kristoffer Krogerus[2] and Elke K. Arendt[1,3]**

[1] School of Food and Nutritional Sciences, University College Cork, Cork, Ireland, [2] VTT Technical Research Centre of Finland Ltd., Espoo, Finland, [3] APC Microbiome Ireland, University College Cork, Cork, Ireland

With a growing interest in non-alcoholic and low alcohol beer (NABLAB), researchers are looking into non-conventional yeasts to harness their special metabolic traits for their production. One of the investigated species is *Lachancea fermentati*, which possesses the uncommon ability to produce significant amounts of lactic acid during alcoholic fermentation, resulting in the accumulation of lactic acid while exhibiting reduced ethanol production. In this study, four *Lachancea fermentati* strains isolated from individual kombucha cultures were investigated. Whole genome sequencing was performed, and the strains were characterized for important brewing characteristics (e.g., sugar utilization) and sensitivities toward stress factors. A screening in wort extract was performed to elucidate strain-dependent differences, followed by fermentation optimization to enhance lactic acid production. Finally, a low alcohol beer was produced at 60 L pilot-scale. The genomes of the kombucha isolates were diverse and could be separated into two phylogenetic groups, which were related to their geographical origin. Compared to a *Saccharomyces cerevisiae* brewers' yeast, the strains' sensitivities to alcohol and acidic conditions were low, while their sensitivities toward osmotic stress were higher. In the screening, lactic acid production showed significant, strain-dependent differences. Fermentation optimization by means of response surface methodology (RSM) revealed an increased lactic acid production at a low pitching rate, high fermentation temperature, and high extract content. It was shown that a high initial glucose concentration led to the highest lactic acid production (max. 18.0 mM). The data indicated that simultaneous lactic acid production and ethanol production occurred as long as glucose was present. When glucose was depleted and/or lactic acid concentrations were high, the production shifted toward the ethanol pathway as the sole pathway. A low alcohol beer (<1.3% ABV) was produced at 60 L pilot-scale by means of stopped fermentation. The beer exhibited a balanced ratio of sweetness from residual sugars and acidity from the lactic acid produced (13.6 mM). However, due to the stopped fermentation, high levels of diacetyl were present, which could necessitate further process intervention to reduce concentrations to acceptable levels.

Keywords: brewing, fermentation, kombucha, *Lachancea fermentati*, lactic acid, NABLAB, response surface methodology, whole genome sequencing

OPEN ACCESS

Edited by:
Francisco A. Cubillos, Universidad de Santiago de Chile, Chile

Reviewed by:
Diego Libkind, CONICET Instituto Andino Patagónico en Tecnologías Biológicas y Geoambientales (IPATEC), Argentina
Diego Bonatto, Federal University of Rio Grande do Sul, Brazil

****Correspondence:***
Elke K. Arendt
e.arendt@ucc.ie

Specialty section:
This article was submitted to Evolutionary and Genomic Microbiology, a section of the journal Frontiers in Microbiology

Received: *20 January 2020*
Accepted: *30 March 2020*
Published: *23 April 2020*

Citation:
Bellut K, Krogerus K and Arendt EK (2020) Lachancea fermentati Strains Isolated From Kombucha: Fundamental Insights, and Practical Application in Low Alcohol Beer Brewing. Front. Microbiol. 11:764. doi: 10.3389/fmicb.2020.00764

INTRODUCTION

Humans have utilized yeasts for the preparation of their foods and beverages long before they even knew of their existence, and beer brewing has been a human activity ever since the Neolithic period (Meussdoerffer, 2009). But it was not until the introduction of brewing with pure culture yeast by Emil Christian Hansen that brewers started to consciously select yeasts for specific purposes (Meussdoerffer, 2009). The species *Saccharomyces cerevisiae* especially, has been harnessed as a trustworthy workhorse in the production of beer, and production volumes have been growing to almost two billion hectoliters in 2018 (Barth-Haas Group, 2019).

However, emerging lifestyle trends, demographics and stricter legislation have led to a slowdown in beer volume growth over the past years, while the non-alcoholic and low alcohol beer (NABLAB) sector has seen a strong and steady growth, which is forecast to continue (Bellut and Arendt, 2019). There are two fundamentally different approaches when it comes to NABLAB production: physical dealcoholization by means of thermal or membrane methods to remove the ethanol after its formation (Müller et al., 2017), and biological methods like stopped fermentation to limit ethanol production in the first place (Brányik et al., 2012).

Another old, biological method for NABLAB production has seen a revival in recent years: the application of non-*Saccharomyces* yeasts (also called non-conventional yeasts) with limited ability to ferment wort sugars, resulting in a low ethanol production. This method was already mentioned in 1929 (Glaubitz and Haehn, 1929), and the proposed species, *Saccharomycodes ludwigii*, has been investigated thoroughly (Narziß et al., 1992; Liu et al., 2011; Mohammadi et al., 2011; Meier-Dörnberg and Hutzler, 2014; Mortazavian et al., 2014; Saerens and Swiegers, 2014; De Francesco et al., 2015, 2018; Jiang et al., 2017; Bellut et al., 2018). However recently, research into other non-*Saccharomyces* species to produce NABLAB has gained momentum (Bellut and Arendt, 2019). Researchers have been looking into isolating yeasts from non-cereal environments, to take advantage of their inability to consume the most abundant wort sugars maltose and maltotriose. Such environments include, for example, grapes and wine (Saerens and Swiegers, 2014; Estela-Escalante et al., 2016), honey (De Francesco et al., 2015), glaciers in Italy and the Antarctica (Thomas-Hall et al., 2010; De Francesco et al., 2018), Japanese miso (Sohrabvandi et al., 2009; Mohammadi et al., 2011) and, more recently, kombucha (Bellut et al., 2018, 2019a).

To date, more than 27 yeast genera have been found in kombucha cultures with up to 25 different species inhabiting a single culture (Jayabalan et al., 2014; Marsh et al., 2014; Reva et al., 2015; Chakravorty et al., 2016). One of the yeast genera associated with kombucha fermentation is the *Lachancea* genus, among which, *Lachancea fermentati* was first recorded by Marsh et al. (2014), and has since been reported to be the most abundant *Lachancea* species in kombucha (Chakravorty et al., 2016). *L. fermentati* has mostly been associated with grape must and kefir (Porter et al., 2019b) but the species was recently proposed as a novel brewing species to create sour beer or low alcohol beer (Osburn et al., 2018; Bellut et al., 2019a). The proposed applications are motivated by the fact that strains of the genus possess the uncommon ability to produce significant amounts of lactic acid during alcoholic fermentation. The production of high amounts of lactic acid by yeasts is an underexplored trait of both the *Lachancea* and *Saccharomyces* genus (Sauer et al., 2010; Jolly et al., 2014; Hranilovic et al., 2017). Lactic acid production is facilitated by the enzyme lactic acid dehydrogenase (LDH), which catalyzes the formation of lactic acid from pyruvate, the product of glycolysis. From a metabolic view-point, this pathway is an alternative, simultaneous means of NADH recycling to NAD^+, with the more common pathway in yeast being via the production of ethanol (Sauer et al., 2010).

Lactic acid production in *Lachancea fermentati* has received little attention, but has been associated with *Lachancea thermotolerans*, where it has been shown to be highly strain-dependent (Porter et al., 2019b). Osburn et al. (2018) proposed the use of lactic acid-producing species like *Lachancea fermentati* to produce single-culture sour beer, making the use of lactic acid bacteria for souring redundant. Bellut et al. (2019a) proposed the use of *Lachancea fermentati* to produce low alcohol beer by stopping fermentation of a diluted wort and exploiting its lactic acid production to counteract residual wort sweetness.

In this study, we investigated four *Lachancea fermentati* strains isolated from four individual kombucha cultures. To better understand the variation in these four strains, whole-genome sequencing of the isolates and the CBS 707 type strain was performed. The strains were characterized for important brewing characteristics like sugar consumption, flocculation behavior, and susceptibility to stress factors like ethanol, low pH and high osmotic pressure. A screening in wort fermentations was performed to show differences in lactic acid production, sugar consumption and the production of volatile fermentation by-products. Further investigation involved an assessment of fermentation conditions and their impact on lactic acid production. Fermentation parameters studied were wort extract, fermentation temperature, and pitching rate, and results were evaluated via response surface methodology (RSM). Alterations of the sugar profile was investigated as another tool to enhance lactic acid production in wort. Finally, a low alcohol beer (<1.3% ABV) was produced by stopped fermentation at 60 L pilot scale and sensory evaluation was conducted with a trained panel.

MATERIALS AND METHODS

Yeast Strains

The *Lachancea fermentati* strains KBI 1.2, KBI 3.2, KBI 5.3, and KBI 12.1 (**Table 1**) were isolated from four individual kombucha cultures according to Bellut et al. (2019a). CBS 707, the *Lachancea fermentati* type strain, was sourced from the CBS collection (Westerdijk Fungal Biodiversity Institute, Utrecht, Netherlands). The brewers' yeast WLP001 (California Ale Yeast) was sourced from White Labs (San Diego, CA, United States).

TABLE 1 | The ploidy and amount of homozygous and heterozygous single nucleotide polymorphisms (SNPs) observed in the *Lachancea fermentati* strains in comparison to the CBS 6772 reference genome.

Strain name	Origin	Measured ploidy	Homozygous SNPs	Heterozygous SNPs	Total SNPs
CBS 6772	Spoiled strawberry soft-drink, South Korea	–	–	–	–
CBS 707	Sediment of peppermint, Unknown	2	20281	838	21119
KBI 1.2	Kombucha, USA (Florida)	2	43937	237929	281866
KBI 3.2	Kombucha, USA (Arizona)	2	44797	235170	279967
KBI 5.3	Kombucha, Australia	1	21245	965	22210
KBI 12.1	Kombucha, USA (Hawaii)	2	45237	205790	251027

Genomics

DNA Content by Flow Cytometry

Flow cytometry was used to estimate the ploidy of the yeast strains essentially as described by Haase and Reed (2002). Cells were grown overnight in YPD medium (1% yeast extract, 2% peptone, 2% glucose), and approximately 1×10^7 cells were washed with 1 mL of 50 mM citrate buffer. Cells were fixed with ice-cold 70% ethanol, and incubated overnight at −20°C. Cells were then washed with 50 mM citrate buffer (pH 7.2), resuspended in 50 mM citrate buffer containing 0.25 mg/mL RNAse A and incubated overnight at 37°C. Proteinase K was then added to a concentration of 1 mg/mL, and cells were incubated for 1 h at 50°C. Cells were then stained with SYTOX Green (2 μM; Life Technologies, United States), and their DNA content was determined using a FACSAria IIu cytometer (Becton Dickinson, United States). DNA contents were estimated by comparing fluorescence intensities. In addition to the *L. fermentati* strains, analysis was also performed on *S. cerevisiae* haploid (CEN.PK113-1A) and diploid (CEN.PK) reference strains. Measurements were performed on duplicate independent yeast cultures, and 100,000 events were collected per sample during flow cytometry.

DNA Extraction and Sequencing

DNA was extracted from pellets using the Sigma GenElute Bacterial Genomic DNA Kit (Sigma-Aldrich, St. Louis MO, United States). After DNA isolation, DNA was quantified using the Qubit High Sensitivity DNA assay (Thermo Fisher Scientific, Waltham, MA, United States) and shotgun metagenomic libraries were prepared using the Nextera XT library preparation kit (Illumina, San Diego, CA, United States) as described by the manufacturer. The final libraries were sequenced on an Illumina NextSeq using a 300 cycle V2 Mid-Output kit as per Illumina guidelines. The raw sequencing reads generated in this study have been submitted to NCBI-SRA under BioProject number PRJNA587400 in the NCBI BioProject database.

Bioinformatics

The 150 bp paired-end reads were quality-analyzed with FastQC (Andrews, 2010) and trimmed and filtered with Trimmomatic (Bolger et al., 2014). Reads were aligned to a reference genome of *L. fermentati* CBS 6772 (NCBI Accession GCA_900074765.1) using SpeedSeq (Chiang et al., 2015). Variant analysis was performed on aligned reads using FreeBayes (Garrison and Marth, 2012). Prior to variant analysis, alignments were filtered to a minimum MAPQ of 50 with SAMtools (Li et al., 2009). The median coverage over 1000 bp windows was calculated with mosdepth (Pedersen and Quinlan, 2018) and visualized in R.

In addition, to test if any of the strains were interspecies hybrids, the trimmed reads were also aligned to a concatenated reference genome consisting of the assembled genomes of the twelve *Lachancea* species available at GRYC[1]. The median coverage over 1000 bp windows was again calculated with mosdepth, and was visualized in R using modified scripts from sppIDer (Langdon et al., 2018).

For phylogenetic analysis, consensus genotypes of the *L. fermentati* strains were called from the identified variants using BCFtools (Li, 2011). A genome assembly of *L.* kluyveri CBS 3082 was retrieved from GRYC[1]. Multiple sequence alignment of the consensus genotypes and genome assemblies was performed with the NASP pipeline (Sahl et al., 2016) using *L. fermentati* CBS 6772 as the reference genome. A matrix of single nucleotide polymorphisms (SNP) in the 7 strains was extracted from the aligned sequences. The SNPs were filtered so that only sites that were present in all 7 strains and with a minor allele frequency greater than 15% (one strain) were retained. The filtered matrix contained 11,517 SNPs at 6,330 sites. A maximum likelihood phylogenetic tree was estimated using IQ-TREE (Nguyen et al., 2015). IQ-TREE was run using the "GTR + ASC" model and 1000 ultrafast bootstrap replicates (Minh et al., 2013). The resulting maximum likelihood tree was visualized in FigTree and rooted with *L. kluyveri* CBS 3082. Haplotype phasing was attempted using WhatsHap (**??**) (Martin et al., 2016), and by dividing haplotypes based on similarity to the reference genome as described by Ortiz-Merino et al. (2018).

Strain Characterization

API Sugar Utilization Test

Substrate utilization test API ID 32C (BioMérieux, Marcy-l'Étoile, France) was used to analyze the biochemical spectrum of all *Lachancea fermentati* strains. Preparation of inoculum and inoculation of the strips was performed according to the manufacturers' instructions. Colonies for the inoculum were grown on YPD agar plates for 48 h at 27°C. After inoculation, API ID 32C strips were incubated for 2 days at 28°C. The samples were evaluated visually by turbidity of the wells, differentiating positive (+), negative (-), and weak (w) growth.

[1]http://gryc.inra.fr

Scanning Electron Microscopy

Yeast cultures for scanning electron microscopy (SEM) were prepared following the protocol for cultured microorganisms by Das Murtey and Ramasamy (2018). Single colonies were taken from YPD agar plate and grown in YPD broth for 24 h at 25°C. One milliliter of sample was centrifuged at 900 *g* for 2 min for pellet formation and resuspended in 5% glutaraldehyde solution prepared in 0.1 M phosphate buffer (pH 7.2) for fixation. After 30 min, the sample was centrifuged, the supernatant was discarded, and the pellet was washed twice in 0.1 M phosphate buffer. Consequently, the pellet was resuspended in 1% osmium tetroxide prepared in 0.1 M phosphate buffer. After 1 h, cells were again washed twice in 0.1 M phosphate buffer. The sample was then dehydrated through ethanol series of 35, 50, 75, 95%, absolute ethanol, and hexamethyldisilazane (HDMS) for 30 min per step (last two ethanol steps twice), centrifuging and discarding the supernatant for each change. Lastly, the second HDMS was discarded and the sample left drying overnight in a desiccator.

The dehydrated yeast sample was mounted onto plain aluminum stubs using carbon double surface adhesive and coated with a 5 nm gold-palladium (80:20) layer using a Gold Sputter Coater (BIO-RAD Polaron Division, SEM coating system, United Kingdom) and observed under a constant accelerating voltage of 5 kV under a JEOL scanning electron microscope type 5510 (JEOL, Tokyo, Japan).

Antifungal Susceptibility Test

Antifungal susceptibility was investigated using an agar-based method where a strip of inert material impregnated with a predefined concentration gradient of a single antifungal agent is used to directly quantify antifungal susceptibility in terms of an MIC (minimal inhibitory concentration) value, which corresponds to the growth inhibition in an elliptical zone. Antifungals tested were Amphotericin B, Fluconazole, Itraconazole, Voriconazole, Caspofungin, and Flucytosine, covering a wide range of antifungal mechanisms of action. Strips and RPMI agar plates were sourced from Liofilchem (Roseto degli Abruzzi, Italy). Yeast cultures were grown on Sabouraud dextrose agar for 48 h at 27°C. Well-isolated colonies were homogenized in sterile saline solution (0.85% NaCl) to obtain a turbidity equivalent to 0.5 McFarland standard. A sterile swab was soaked in the inoculum and used to streak the entire agar surface three times, rotating the plate 60° each time to ensure even distribution of the inoculum. The soaking and streaking procedure was repeated a second time. Strips were carefully applied on dry agar surface and plates were incubated at 35°C. Plates were read after 24, 48, and 72 h following the Etest antifungal reading guide (BioMérieux Antifungal Susceptibility Testing, 2019). The test was carried out in duplicate. If MICs differed between the duplicates, the higher MIC was reported.

POF Test

The phenolic off-flavor test was performed according to Meier-Dörnberg et al. (2017). Yeast strains were spread on yeast and mold agar plates (YM-agar) containing only one of the following precursors: either ferulic acid, cinnamic acid or coumaric acid. After 3 days of incubation at 25°C, plates were evaluated by a trained panel by sniffing to detect any of the following aromas: clove-like (4-vinylguajacol), Styrofoam-like (4-vinylstyrene) and medicinal-like (4-vinylphenol). *Saccharomyces cerevisiae* LeoBavaricus – TUM 68 (Research Center Weihenstephan for Brewing and Food Quality, Freising-Weihenstephan, Germany) was used as a positive control.

Flocculation Test

The flocculation test was performed using a slightly modified Helm's assay (Bendiak et al., 1996; D'Hautcourt and Smart, 1999). Essentially, all cells were washed in EDTA and the sedimentation period was extended to 10 min. Wort was composed of 100 g/L spray-dried malt extract (Spraymalt Light, Muntons plc, Suffolk, United Kingdom) adjusted to 15 IBU (15 mg/mL iso-α-acids; from 30% stock solution; Barth-Haas Group, Nürnberg, Germany).

Stress Tests

Stress tests were performed on microplates through the repeated measurement of absorbance over a time period of 96 h (Multiskan FC, Thermo Fisher Scientific, Waltham, MA, United States).

The substrate for the hop sensitivity test was 75 g/L sterile-filtered wort adjusted to 0, 50, and 100 mg/L iso-α-acids (1 mg/L = 1 International Bitterness Unit, IBU), respectively by using an aliquot of a stock solution of 3% iso-α-acids in 96% (v/v) ethanol (Barth-Haas Group, Nürnberg, Germany).

For testing ethanol sensitivity, the sterile-filtered wort extract was adjusted to 0, 2.5, 5, 7.5, and 10% ABV with an aliquot of 100% (v/v) ethanol.

For testing pH sensitivity by lactic acid, the sterile-filtered wort was adjusted to pH ranges from 5.5 (no addition of acid) to 3.0 in steps of 0.5 with aliquots of 80% lactic acid (corresponding to lactic acid concentrations of 0; 1.7; 3.1; 6.1; 16.3; 48.4 mM).

For testing pH sensitivity by HCl, the sterile-filtered wort was adjusted to pH ranges from 5.5 (no addition of acid) to 1.5 in steps of 0.5 with aliquots of 2 M HCl.

Osmotic stress was tested by adjusting the sterile-filtered wort extract (100 g/L Muntons Spraymalt Light) to sorbitol concentrations of 0, 50, 100, 150, and 200 g/L, respectively.

For inoculation, strains were grown in sterilized wort for 24 h at 25°C under aerobic conditions. The microtiter plate wells were inoculated with a concentration of 10^5 cells/mL. The wells contained 200 μL of the respective wort substrates. Plates were incubated at 25°C and absorbance was measured every 30 min at 600 nm without shaking over a time period of 96 h (Multiskan FC, Thermo Fisher Scientific, Waltham, MA, United States).

Fermentation Trial

Single colonies of the respective strains were taken from YPD agar plates after 72 h growth at 25°C and transferred into a 250 mL sterile Duran glass bottle (Lennox Laboratory Supplies Ltd., Dublin, Ireland) containing 150 mL propagation wort consisting of 75 g/L spray-dried malt and 30 g/L glucose (Gem Pack Foods Ltd., Dublin, Ireland), sterilized at 121°C for 15 min. The bottles were covered with sterile cotton and placed in an incubator with orbital shaker (ES-80 shaker-incubator, Grant

Instruments (Cambridge) Ltd., Shepreth, United Kingdom) and incubated for 48 h at an orbital agitation of 170 rpm at 25°C. Cell count was performed using a Thoma Hemocytometer with a depth of 0.1 mm (Blaubrand, Sigma-Aldrich, St. Louis, MO, United States).

Fermentation wort was prepared by dissolving 100 g/L spray-dried malt extract in 1 L of brewing water and sterilized at 121°C for 15 min followed by filtration through sterile grade 1V Whatman filter (Whatman plc, Maidstone, United Kingdom) to remove hot trub built up during sterilization. Iso-α-acids were added to the wort at a concentration of 15 mg/L (15 IBU).

Fermentation trials were carried out in 250 mL sterile Duran glass bottles, equipped with an air lock. Bottles were filled with 150 mL of wort. Yeast cells for pitching were washed by centrifugation at 900 *g* for 5 min and resuspended in sterile water to ensure no carryover of sugars or acids from the propagation wort into the fermentation wort. Pitching rate was 10^7 cells/mL. Fermentation temperature was 25°C. Fermentation was performed until no change in extract could be measured for two consecutive days.

Lactic Acid Production Optimization of KBI 12.1

Response Surface Methodology (RSM)

To investigate lactic acid production performance by KBI 12.1 at different fermentation parameters, RSM was performed using DesignExpert 9 software (StatEase, Minneapolis, MN, United States). A three factorial, face-centered, central composite design with duplicate factorial points and 6 replications of the center point was chosen. The predictor factors were extract (5, 10, 15°P), temperature (16, 22, 28°C), and pitching rate (5, 32.5, 60×10^6 cells/mL).

Spray-dried malt extract served as substrate. Wort preparation, propagation and inoculation was carried out as outlined in 2.4. Sterilized and filtered wort extract of 15°P was used as the base and diluted with sterile water when necessary. Fermentation volume was 150 mL in 250 mL Duran glass bottles equipped with an air lock. Fermentation was performed until no change in extract could be measured for two consecutive days.

Spiked Glucose Trial

Wort preparation, propagation and inoculation was carried out as outlined in 2.4. The 7°P wort was produced from 75 g wort extract in 1 L of water. The 7°P wort plus 3% glucose was produced from 75 g wort extract and 30 g glucose in 1 L of water. The 10°P wort was produced by dilution of the 15°P wort from 2.5.1 with water. Fermentation volume was 150 mL in 250 mL Duran glass bottles equipped with an air lock. Pitching rate was 5×10^6 cells/mL and fermentation temperature was 25°C. Fermentation was performed until no change in extract could be measured for two consecutive days.

Pilot Brew

Wort for the pilot brew was produced in a 60 L pilot-scale brewing plant consisting of a combined mash-boiling vessel, a lauter tun and whirlpool (FOODING Nahrungsmitteltechnik GmbH, Stuttgart, Germany). Weyermann Pilsner Malt was milled with a two-roller mill ("Derby," Engl Maschinen, Schwebheim, Germany) at a 0.8 mm gap size. Seven kilograms of crushed malt was mashed in with 30 L of brewing water at 50°C. To increase the amount of glucose, 7 g of Amylo 300 (Kerry Group, Tralee, Ireland) were added at the begin of mashing (1 g/kg of malt). The following mashing regime was employed: 20 min at 50°C, 60 min at 65°C and 5 min at 78°C. The mash was pumped into the lauter tun and lautering was performed after a 15 min lauter rest, employing four sparging steps of 5 L hot brewing water each. Boil volume was 50 L at a gravity of 1.038 (9.9°P). At the start of the boil, 15 g of Magnum hop pellets (10.5% iso-α-acids) were added for a calculated IBU content of 6.5. Total boiling time was 45 min. After boiling, gravity was adjusted to 1.034 (8.5°P) with hot brewing water, and hot trub precipitates and hop residue were removed in the whirlpool with a rest of 20 min. Clear wort was pumped through a heat exchanger and filled into 60 L fermentation vessels at a temperature of 25°C.

Yeast was pitched at a pitching rate of 5×10^6 cells/mL. Fermentation temperature was 25 ± 1°C (uncontrolled). Samples were taken every 12 h. After 36 h, 30 L of the young beer were filtered through a plate filter (Seitz K 200; Pall GmbH, Dreieich, Germany) to stop fermentation by removing the yeast, and filled into a 50 L keg. The remaining young beer was left in the fermenter to reach final attenuation. To carbonate the kegged beer, the keg was repeatedly topped up with CO_2 at a pressure of 1 bar at 2°C. Ten days after stopping fermentation, the carbonated beer was filled into 330 mL brown glass bottles with a counter-pressure hand-filler (TOPINCN, Shenzen, China) and capped. Bottles were pasteurized in a pilot retort (APR-95; Surdry, Abadiano, Vizcaya, Spain) with spray water at 65°C for 10 min resulting in approximately 23 pasteurization units (PU). Beer bottles were stored in a dark place at 2°C for further analysis and sensory evaluation.

Sensory

The low alcohol *Lachancea* beer produced at pilot scale (bottled beer) was tasted and judged by a sensory panel of 15 experienced panelists. The panelists were asked to evaluate the intensity of fruitiness in aroma, the sweetness/acidity ratio (0 "too sweet"; 5 "just right"; 10 "too sour") and the general acceptability of the low alcohol beer on a scale from 0, "not acceptable," to 10, "extremely acceptable." Samples were served at a temperature of 12°C.

Analytics

HPLC Analyses

The cell-free supernatant of fermented samples was analyzed using the following methods. Sugars and ethanol were determined by high performance liquid chromatography (HPLC) Agilent 1260 Infinity (Agilent Technologies, Santa Clara, CA, United States) equipped a refractive index detector (RID) and a Sugar-Pak I 10 μm, 6.5 mm × 300 mm column (Waters, Milford, MA, United States) with 50 mg/L Ca-EDTA as mobile phase and a flow rate of 0.5 mL/min at 80°C. Differentiation of maltose and sucrose was achieved with a Nova-Pak 4 μm, 4.6 mm × 250 mm column (Waters, Milford, MA, United States) with acetonitrile/water 78:22 (v/v) as mobile phase and a flow rate

of 1.0 mL/min. Lactic acid was quantified via HPLC (DIONEX UltiMate 3000, Thermo Fisher Scientific, Waltham, MA, United States) with diode array detector (DAD) and a Hi-Plex H 8 μm, 7.7 mm × 300 mm column (Agilent Technologies, Santa Clara, CA, United States) with 5 mM H_2SO_4 as mobile phase and a flow rate of 0.5 mL/min at 60°C. Quantification was achieved by external standards in a calibration range of 0.5–30 mM.

Volatiles Analysis by GC-MS

Analysis of volatiles in the cell-free supernatant of the fermented samples was carried out as follows. Analytes were extracted using liquid-liquid extraction with Methyl-tert-butyl ether directly in the vial. Analysis was performed using a mid-polarity column (Zebron ZB-1701, GC Cap. Column 30 m × 0.25 mm × 0.25 μm; Phenomenex, Torrance, CA, United States) installed in a GC 7890B (Agilent Technologies, Santa Clara, CA, United States) coupled with a quadrupole detector 5977B (Agilent Technologies, Santa Clara, CA, United States). The system was controlled by ChemStation (Agilent Technologies, Santa Clara, CA, United States). The GC-method was set up as described by Pinu and Villas-Boas (2017) with only minor modifications. Samples were analyzed in Selected Ion Monitoring (SIM) mode. Quantifications were performed using external calibration lines.

Free Amino Nitrogen

Free amino nitrogen (FAN) was measured using a ninhydrin-based dying method, where absorbance is measured at 570 nm against a glycine standard (ASBC Method Wort-12 A).

Statistical Analysis

Fermentations and analyses were carried out in triplicate, unless stated otherwise. Statistical analysis was performed using RStudio, Version 1.1.463 with R version 3.5.2 (RStudio Inc., Boston, MA, United States; R Core Team, r-project). One-way ANOVA was used to compare means and Tukey's test with 95% confidence intervals was applied for the pairwise comparison of means. Principal component analysis (PCA) was performed with the R packages FactoMineR and Factoshiny (Le et al., 2008). Values are given as the mean ± standard deviation.

RESULTS

The *Lachancea fermentati* strains investigated in this study were isolated from four individual kombucha cultures. KBI 1.2 and KBI 3.2 originate from the Conterminous United States, while KBI 12.1 originates from Hawaii, and KBI 5.3 originates from a kombucha culture from Australia. They were identified as *Lachancea fermentati* strains via sequencing and comparing the D1/D2 region of the large subunit rDNA to the public NCBI nucleotide database[2] (Bellut et al., 2019a). The country of origin of the strain CBS 707 is unknown. CBS 6772 was isolated from a spoiled strawberry beverage in South Korea (**Table 1**).

[2]https://blast.ncbi.nlm.nih.gov/Blast.cgi

Genomics

To better understand the variation in these four strains, whole-genome sequencing of the four *L. fermentati* kombucha isolates and the CBS707 type strain was performed. These were sequenced with 150 bp paired-end Illumina sequencing to an average coverage ranging from 115× to 139×. Reads were aligned to the reference genome of *L. fermentati* CBS 6772, and single nucleotide polymorphisms (SNPs) were called with FreeBayes. A total of 370,027 variable sites were observed across the five strains compared to the reference genome. Interestingly, a high number of SNPs (>250,000) were observed in the three kombucha isolates originating from the United States (**Table 1**). This corresponds to a nucleotide sequence divergence around 2.4–2.7% in the 10.3 Mbp genome. The majority of these SNPs were heterozygous (>2% heterozygosity), suggesting that not only were these strains non-haploid, but possessed divergent genotypes. Allele frequency peaks at 0, 0.5, and 1, suggested that these strains were diploid (**Figure 1B**). The heterozygosity was considerably higher than what was observed, for example, in any of the recently sequenced 1,011 *S. cerevisiae* strains (Peter et al., 2018) or 14 *Kluyveromyces marxianus* strains (Ortiz-Merino et al., 2018). The kombucha isolate originating from Australia, KBI 5.3, and the CBS707 type strain had around 20,000 SNPs compared to the reference genome. Here, the majority of the SNPs were homozygous, suggesting that the strains were either haploid or homozygous diploids (**Figure 1B**). The average pairwise nucleotide diversity (π) in this limited set of strains was 0.0126, which is comparable to what has been observed for *Kluyveromyces marxianus* (Ortiz-Merino et al., 2018) and slightly higher than for a wild population of *Lachancea quebecensis*. The three heterozygous kombucha isolates also contained several regions where heterozygosity was lost (**Supplementary Figure S1**). Common regions, where loss of heterozygosity (LOH) was observed in all three strains, could be found across chromosome G and on the right arm of chromosome F. In addition, KBI 12.1 had large LOH regions on the left arms of both chromosome F and H.

Flow cytometry was used to confirm the ploidy of the strains. The natural ploidy of *L. fermentati* and other members of the *Lachancea* genus appears to vary, with reports of both haploid and diploid strains (Souciet et al., 2009; Agier et al., 2013; Freel et al., 2014; Banilas et al., 2016; Hranilovic et al., 2017). Here, the three heterozygous kombucha isolates appeared diploid, while KBI 5.3 appeared haploid (**Figure 1A**). Despite the lack of heterozygous SNPs, the CBS707 type strain also appeared diploid. This is in line with what has previously been reported for the strain (Agier et al., 2013). Read coverage also suggested that CBS 707 also harbored an extra third copy of chromosome C, while no aneuploidy was observed in any of the kombucha isolates (**Supplementary Figure S2**). Fluorescence intensities of the *L. fermentati* strains during flow cytometry were slightly lower than those of haploid and diploid *S. cerevisiae* references, as can be expected based on the smaller genome size of *L. fermentati*.

Phylogenetic analysis based on the single nucleotide variants that were observed in the four kombucha isolates and the CBS 707

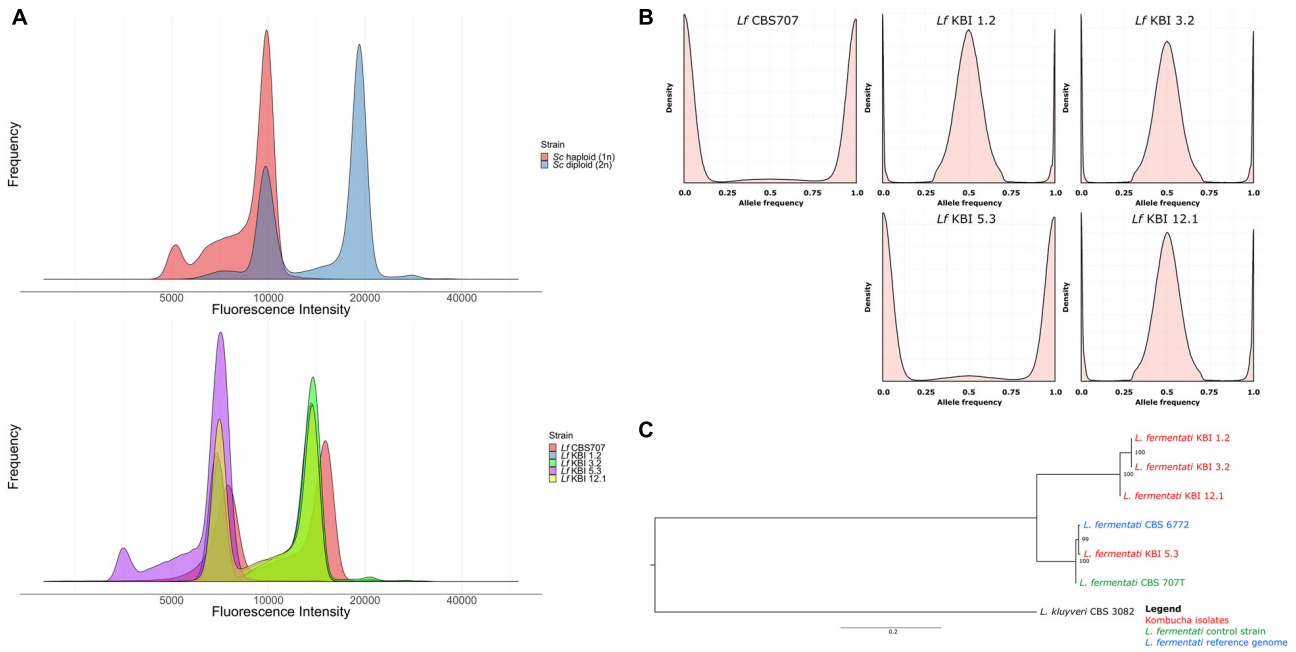

FIGURE 1 | (A) Fluorescence intensity of SYTOX Green-stained haploid and diploid *S. cerevisiae* control strains and the five *L. fermentati* strains during flow cytometry. **(B)** The allele frequency distributions of the single nucleotide variants observed in the five sequenced *L. fermentati* strains. Peaks only at 0 and 1 suggest a single allele at each site, while peaks at 0, 0.5, and 1 suggest two alleles at each site. **(C)** A maximum likelihood phylogenetic tree based on SNPs at 6330 sites in the six *L. fermentati* and one *L. kluyveri* genomes (rooted with *L. kluyveri* as outgroup). Numbers at nodes indicate bootstrap support values. Branch lengths represent the number of substitutions per site.

type strain, separated the three heterozygous kombucha isolates (KBI 1.2, KBI 3.2, and KBI 12.1) into a separate clade from the one containing CBS 707, CBS 6772, and KBI 5.3 (**Figure 1C**). Because of the high heterozygosity, which can skew the results, we attempted to separate the two haplotypes both using variant phasing with WhatsHap and by assigning the haplotypes based on similarity to the reference genome as described by Ortiz-Merino et al. (2018). In both cases, one haplotype could be found together with CBS 707, CBS 6772, and KBI 5.3, while the other haplotype formed a separate clade (**Supplementary Figure S3**). It is therefore likely that the heterozygous kombucha isolates have emerged through breeding between strains from two different *L. fermentati* populations. To ensure that the heterozygous strains were not interspecific hybrids, sequencing reads were also aligned to a concatenated reference genome consisting of the genomes of 12 species in the *Lachancea* genus. Reads aligned almost exclusively to the *L. fermentati* genome, confirming that they were not interspecific hybrids (**Supplementary Figure S4**).

Yeast Characterization

API Sugar Utilization, Flocculation, and POF Test

The API sugar utilization test was performed to investigate intraspecific differences. The results are shown in **Table 2**, alongside the results from the flocculation test and phenolic off-flavor test.

The sugar utilization pattern showed minor differences. The type strain CBS 707 and KBI 5.3 showed no growth with lactic acid as substrate, whereas KBI 1.2, KBI 3.2, and KBI 12.1, exhibited weak growth. However, Kurtzman et al. (2011) reported positive growth for CBS 707. Esculin ferric citrate was positive for KBI 1.2, KBI 3.2, and KBI 12.1 and weak for CBS 707 and KBI 5.3. The color reaction resulting from a positive reaction to esculin ferric citrate is associated with β-glucosidase activity (Pérez et al., 2011). However, cellobiose, a β-1,4-linked sugar, was not metabolized by KBI 5.3 and only weakly by KBI 1.2 and KBI 5.3 despite showing weak or positive reactions to esculin ferric citrate. In a study on *Lachancea fermentati* wine strains, Porter (2017) reported that from 10 tested strains, 80% showed β-glucosidase activity.

According to the modified Helm's assay, CBS 707, KBI 3.2, KBI 5.3, and KBI 12.1 showed low flocculation between 15 and 28%, with no statistically significant difference ($p \leq 0.05$). KBI 1.2 showed, with 88%, the highest flocculation behavior. Flocculation of *Lachancea fermentati* strains has also been reported in other studies and its degree was shown to be strain-dependent (Romano and Suzzi, 1993; Porter, 2017; Porter et al., 2019a). However, yeast flocculation assays like the Helm's assay can deviate from observations on flocculation behavior in practice and can be difficult to reproduce (Stewart, 2018). In a previous study by Bellut et al. (2019a), KBI 12.1 exhibited high flocculation >80%. In fact, from observations during fermentation trials in this study, KBI 12.1 shows a more flocculent behavior than the results of the Helm's assay suggest here, with flocculation more comparable to that of the brewers' yeast WLP001 as previously reported (Bellut et al., 2019a). All strains showed negative POF behavior.

TABLE 2 | API sugar utilization test.

Substrate/Assay	CBS 707	KBI 1.2	KBI 3.2	KBI 5.3	KBI 12.1
Control	–	–	–	–	–
D-Galactose	+	+	+	+	+
Cycloheximide (Actidione)	+	+	+	+	+
D-Saccharose	+	+	+	+	+
Lactic acid	–[1]	w	w	–	w
D-Cellobiose	+	w	w	–	+
D-Raffinose	+	+	+	+	+
D-Maltose	+	+	+	+	+
D-Trehalose	+	+	+	+	+
Potassium 2-Ketogluconate	w	w	w	w	w
Methyl-αD-Glucopyranoside	+	+	+	+	+
D-Mannitol	+	+	+	w	+
D-Sorbitol	+	+	+	+	+
Palatinose	+	+	+	+	+
D-Melezitose	w	+	w	w	+
Potassium gluconate	w	–	w	–	w
D-Glucose	+	+	+	+	+
L-Sorbose	w	+	w	+	+
Esculin ferric citrate	w	+	+	w	+
Flocculation (%)	15 ± 2^a	88 ± 10^b	28 ± 1^a	25 ± 8^a	20 ± 6^a
Definition	Non-flocculent	Very flocculent	Moderately flocculent	Moderately flocculent	Moderately flocculent
Phenolic off-flavor	Negative	Negative	Negative	Negative	Negative

– negative; + positive; w weak. Substrates negative for all strains are not included in the table. Different letters in superscripts indicate a significant difference of the means within a row ($p \leq 0.05$). The full table of substrates is included in ***Supplementary Data Sheet S1****. [1]Deviation from literature which states a positive reaction (Kurtzman et al., 2011).*

Scanning Electron Microscopy (SEM)

To visualize the different yeast strains and to investigate differences in cell morphology, scanning electron microscopy (SEM) was performed. The SEM pictures of the strains can be seen in **Figure 2**.

The SEM confirmed inter- and intraspecific differences in cell morphology that had been suspected from observations under the light microscope. The almost rod-shaped cells of the type strain CBS 707 were longer and thinner than the other *Lachancea fermentati* KBI strains. Bud scars appeared to be mostly located at or near the ends of the rod-shape. The KBI strains seemed to have a rounder shape compared to the type strain. KBI 12.1 appeared to exhibit the highest proportion of oval or spherical shaped cells of the *Lachancea fermentati* strains, while cells of WLP001 showed a substantially more pronounced spherical shape. Regarding cell size, the cells of the brewers' yeast were larger compared to the *Lachancea fermentati* cells. The cell size is related to the total surface area of the cell, which determines import and export rates of nutrients and fermentation products (Michel et al., 2017). The difference in cell size can therefore have a strong effect on fermentation performance and must be considered when choosing pitching rates.

Stress Tests

During fermentation, yeast strains applied in brewing must deal with several stress factors. Iso-α-acid concentrations of 100 and more mg/L are no longer a rarity [e.g., strong India Pale Ales (IPAs)]. Ethanol, another stressor, accumulates during fermentation, especially in high gravity brewing, which by itself involves another stress factor: osmotic stress (here simulated with sorbitol). Sour beers are also gaining popularity and yeasts are required to ferment wort with a low pH and high initial lactic acid concentration (Peyer et al., 2017). Additionally, strains of the *Lachancea* genus can possess the ability to produce significant amounts of lactic acid during alcoholic fermentation. The stress tests were performed to investigate inter- and intraspecific differences. **Table 3** shows the results of the relative growth in wort in microtiter analyses at a snapshot at 48 h after pitching with, and without the stressor in different concentrations.

The concentration of iso-α-acids did not have an influence of the growth of the strains which is in accordance with previous reports on various non-*Saccharomyces* species (Bellut et al., 2018). However, Michel et al. (2016) reported the presence of 90 IBU to affect *Torulaspora delbrueckii* strains, resulting in a slightly prolonged lag phase and slightly decreased slope of the growth curve.

Among the *L. fermentati* strains, the KBI strains exhibited a greater tolerance toward higher ethanol concentrations in the wort compared to CBS 707, which showed a small but significant growth impairment already at 2.5% ABV, manifesting as a 10% decreased relative growth. At 7.5% ABV, CBS 707 showed almost full growth inhibition (5% relative growth remaining) while the KBI strains still showed relative growth between 53 and 71%. At an ABV of 10% in the wort, growth of CBS 707 and KBI 1.2 was fully inhibited, while KBI 3.2, KBI 5.3, and KBI 12.1 still exhibited little growth, at 4–25%, with KBI 3.2 being the most ethanol tolerant strain. In accordance, Porter et al. (2019b) observed full inhibition of a *L. fermentati* strain at 10% ABV during a growth test on agar while it still exhibited growth at 7% ABV. The brewers' yeast WLP001 showed significant inhibition at 5% ABV with 24% decreased relative growth. Full growth inhibition was reached at 10% ABV. Overall, WLP001 showed a greater sensitivity toward ethanol compared to the KBI strains.

During osmotic stress, at the presence of high concentrations of sorbitol, the *Lachancea fermentati* strains showed a greater growth impairment compared to WLP001 with only 26–41% remaining relative growth at 200 g/L sorbitol compared to 70% for WLP001. Intraspecific differences in growth inhibition among the *Lachancea fermentati* were generally low, CBS 707 tentatively showing greater sensitivity.

In the presence of lactic acid, all yeast strains were resilient against concentrations of up to 16.3 mM (pH 3.5). Although statistically significant, growth impairment at lactic acid concentrations between 1.7 and 16.3 mM showed to be very low with a maximum decrease in relative growth by 5%. Only at extreme lactic acid concentrations of 48.4 mM (pH 3), did the *L. fermentati* strains show slight growth impairment of 13–17%, while WLP001 exhibited a growth impairment of 47%.

When the wort pH was adjusted with HCl, the strains showed less sensitivity compared to the pH adjustment with

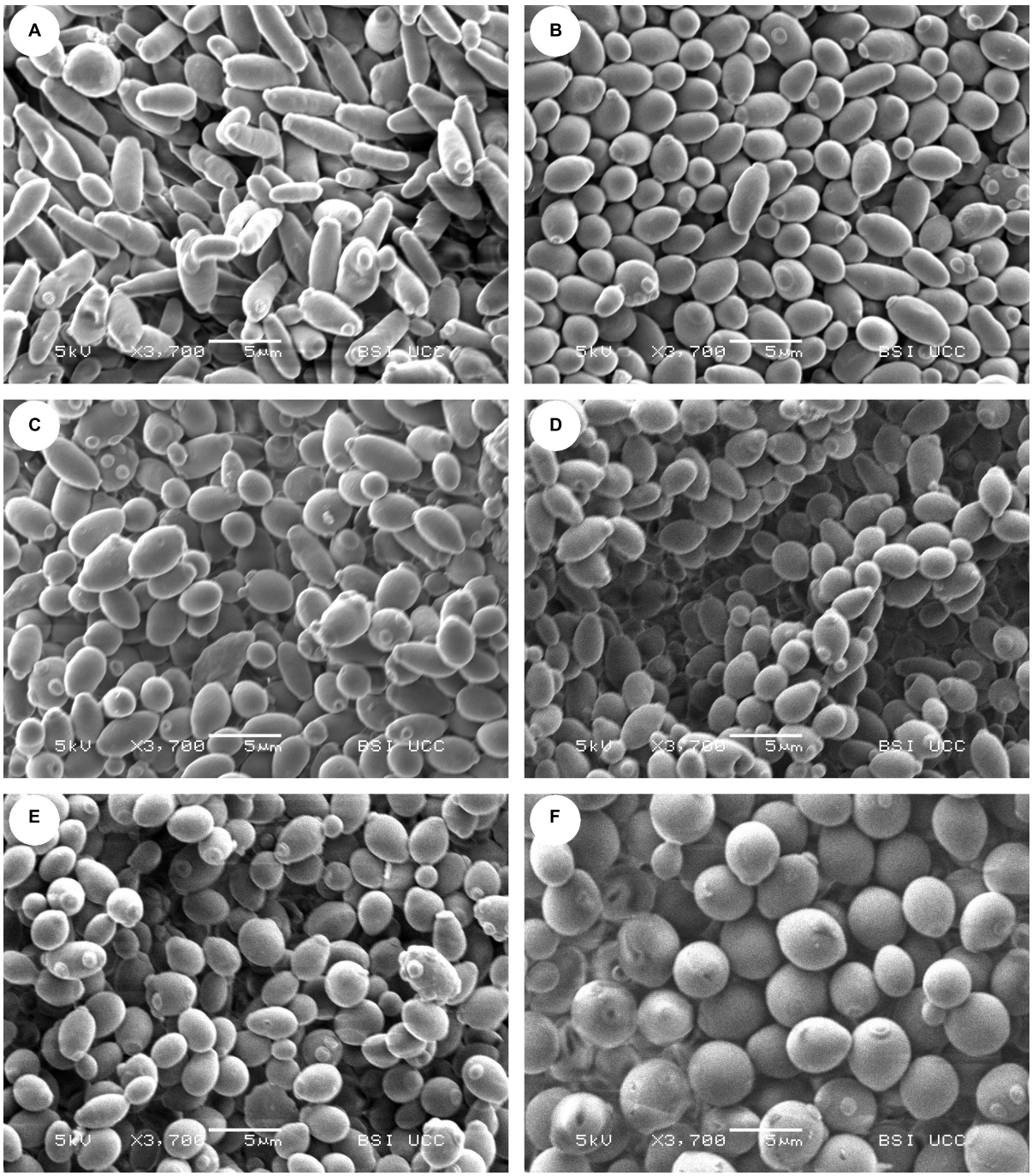

FIGURE 2 | Scanning electron microscopy (SEM) pictures of the yeast strains **(A)** CBS 707, **(B)** KBI 1.2, **(C)** KBI 3.2, **(D)** KBI 5.3, **(E)** KBI 12.1, and **(F)** WLP001 at same magnification of ×3,700. Size of horizontal bar: 5 µm.

lactic acid. For example, at pH 3, WLP001 still exhibited 85% growth compared to 53% at pH 3 when adjusted with lactic acid. However, at pH 2.5 and lower, WLP001 growth was fully inhibited while the *L. fermentati* strains still exhibited relative growth between 72 and 79%. Full growth inhibition of the *L. fermentati* strains was reached at pH 2. Intraspecific differences among the *Lachancea fermentati* strains were small.

Differences in growth impairment by the different acids at same pH can be explained with the chemical property of weak acids. The presence of a weak acid like lactic acid leads to an increased stress for the yeast cell. The lower the extracellular pH, the more lactic acid is present in its protonated form, especially at a pH below the pK_a of the respective acid (lactic acid pK_a: 3.86) and can therefore enter the cell via passive

TABLE 3 | Relative growth in percent in wort after 48 h with and without stressor in different concentrations based on OD_{600} measurements.

Stress factor (Unit)	Concentration	CBS 707	KBI 1.2	KBI 3.2	KBI 5.3	KBI 12.1	WLP001
Hops	0	100	100	100	100	100	100
(IBU)	50	**107**	103	99	100	105	**95**
	100	105	99	99	101	105	98
Ethanol	0	100	100	100	100	100	100
(% ABV)	2.5	**90**	98	97	95	96	95
	5	**77**	87	**87**	**86**	**85**	**76**
	7.5	**5**	**53**	**70**	**66**	**71**	**16**
	10	**0**	**0**	**25**	**8**	**4**	**0**
Sorbitol	0	100	100	100	100	100	100
(g/L)	50	89	89	90	92	**86**	99
	100	**64**	**77**	**78**	**78**	**72**	91
	150	**35**	**52**	**54**	**62**	**46**	83
	200	26	**35**	**32**	**41**	35	**70**
Lactic	5.5	100	100	100	100	100	100
acid (pH)	5	**96**	99	99	99	97	100
	4.5	95	**97**	**97**	**98**	98	101
	4	96	98	98	98	98	104
	3.5	95	97	95	**95**	98	100
	3	**84**	**87**	**83**	**85**	**86**	**53**
HCl	5.5	100	100	100	100	100	100
(pH)	5	101	100	102	101	99	**105**
	4.5	102	101	100	102	100	104
	4	101	102	100	102	98	108
	3.5	98	**98**	**97**	**98**	97	105
	3	**93**	**88**	**87**	**91**	**89**	**85**
	2.5	**71**	**71**	**69**	**79**	**72**	**0**
	2	**1**	**5**	**1**	**1**	**2**	1
	1.5	1	**1**	1	1	1	1

Bold values are significantly different from the previous value within a stress test for the individual strain ($p \leq 0.05$).

diffusion. Inside the cell, at a higher intercellular pH, lactic acid is deprotonated. Consequently, the cell must export the proton as well as the anion, creating an energy-requiring cycle. At high concentrations, this mechanism can lead to the dissipation of the proton motive force, leading to cell death (Colombié et al., 2003; Sauer et al., 2010).

Antifungal Susceptibility

While *Candida* species are the lead cause for fungemia, cases of non-pathogenic species such as *Saccharomyces cerevisiae* acting as opportunistic pathogens in immunocompromised hosts have been reported (Cassone et al., 2003; Hamoud et al., 2011) and one case of fungemia caused by *Lachancea fermentati* in an immunocompromised host has also been recorded (Leuck et al., 2014). Also, given the fact that *Lachancea* species are capable of growth at human body temperature (37°C) (Kurtzman et al., 2011), it is reasonable to investigate potential resistances against antifungal agents. The minimal inhibitory concentration (MIC) of a range of antifungal agents was tested by Etest. The results are shown in **Table 4**. All strains showed to be susceptible to all classes of antifungal agents with only small intra- and interspecific differences.

Fermentation Trials

Fermentation of Wort

Fermentation trials were conducted to investigate strain performances in terms of ethanol and lactic acid production and the concentration of fermentation by-products. Spray-dried wort extract from barley malt served as the substrate for all fermentations. **Table 5** shows the analytical parameters of the fermentation wort including extract, pH, free amino nitrogen (FAN) and sugar concentration.

Analysis of fermented samples

Fermentation was carried out until no change in extract was measurable for two consecutive days. For CBS 707, KBI 1.2, KBI 5.3, and WLP001, final attenuation was reached after 11 days of fermentation at 25°C. KBI 3.2 and KBI 12.1 reached final attenuation after 13 days of fermentation. **Table 6** shows the analytical results of the fermentation trials.

The *L. fermentati* strains reached final attenuations of 70% and lower, owing to their inability to consume maltotriose. KBI 12.1 exhibited, at 55%, the lowest attenuation. Sugar analysis revealed that KBI 12.1 had only used up 76% of maltose while the other strains had depleted it by the end of fermentation. Only WLP001 consumed maltotriose, at 81%, while the *L. fermentati* strains did not consume any maltotriose. At the end of fermentation, slightly higher values for maltotriose than the initial values were detected in some of the worts fermented with the *L. fermentati* strains. Glucose and sucrose were completely consumed by all strains by the end of fermentation. In the wort fermented with CBS 707, a small amount of fructose remained.

Ethanol concentrations correlated with attenuation. The brewers' yeast WLP001 exhibited the highest concentration, at

TABLE 4 | Minimal inhibitory concentration (MIC) of selected antifungal agents after 24 h of incubation.

Antifungal agent	Range	CBS 707	KBI 1.2	KBI 3.2	KBI 5.3	KBI 12.1	WLP001
Amphotericin B	0.002–32	0.032	0.094	0.094	0.125	0.094	1
Caspofungin	0.002–32	1	1.5	1.5	1.5	1.5	0.5
Flucytosine	0.002–32	0.094	0.064	0.125	0.125	0.064	0.023
Fluconazole	0.016–256	12	12	12	12	12	24
Itraconazole	0.002–32	0.5	0.75	1	1	0.75	1
Voriconazole	0.002–32	0.094	0.125	0.125	0.125	0.125	0.125

Values in μg/mL.

TABLE 5 | Analysis of fermentation wort.

Extract	°P	9.40 ± 0.00
pH		4.99 ± 0.01
FAN	mg/L	99 ± 1
Fructose	g/L	1.78 ± 0.02
Glucose	g/L	8.53 ± 0.05
Sucrose	g/L	1.02 ± 0.01
Maltose	g/L	40.64 ± 0.25
Maltotriose	g/L	11.94 ± 0.07

4.4% ABV, followed by four of the *L. fermentati* strains at around 3.7% ABV. KBI 12.1 produced only 3.0% ABV.

Lactic acid concentrations reached 0.94 mM in the sample fermented with WLP001. Li and Liu (2015) reported similar values produced by a lager yeast, at 1.03 mM. The *Lachancea* yeasts exhibited significantly higher final lactic acid values. KBI 12.1 exhibited the highest lactic acid concentration, at 3.47 mM, followed by CBS 707, KBI 3.2, KBI 1.2, and KBI 5.3, at 2.41, 1.82, 1.55, and 1.33 mM, respectively. However, these values were still below the reported flavor threshold of lactic acid in beer of 4.44 mM (400 mg/L) (Siebert, 1999).

FAN consumption by the *L- fermentati* strains was relatively low with 70 or 80% of the initial amount remaining by the end of fermentation. By comparison, WLP001 consumed half of the amount of FAN in the wort. The pattern of a low FAN consumption of non-*Saccharomyces* yeasts compared to brewers' yeasts has been observed in previous studies (Estela-Escalante et al., 2016; Bellut et al., 2018). It has mostly been attributed to a less intensive fermentation due to limited sugar consumption, however, in this study, fermentation and sugar consumption did not differ to an extent that would account for the reduced FAN uptake, suggesting an alternative cause.

When detected, diacetyl values were, at 0.02 mg/L, at or below the flavor threshold of 0.02–0.10 mg/L (Meilgaard, 1975; Saison et al., 2009). Ethyl acetate values were significantly higher in the *L. fermentati* strains compared to WLP001, up to double the concentration. 3-Methylbutyl acetate (isoamyl acetate) concentrations were similar among all strains. 2-Phenylethyl acetate concentrations were significantly higher in KBI 1.2, KBI 3.2, and KBI 12.1 compared to the other strains. CBS 707 produced the highest amount of higher alcohols, at 120 mg/L, and KBI 12.1 produced the lowest amount, at 66 mg/L. **Figure 3** illustrates the relative amounts of volatile fermentation by-products produced by the different yeast strains. WLP001 produced higher amounts of the higher ethyl esters (i.e., ethyl hexanoate, ethyl octanoate, ethyl decanoate) while CBS 707 produced more higher alcohols compared to the other strains. Interestingly, despite the increased lactic acid production by the *Lachancea* strains, ethyl lactate concentrations were higher in the wort fermented with WLP001. None of the volatile fermentation by-products were detected in concentrations above their individual flavor thresholds (**Supplementary Data Sheet S1**).

Lactic Acid Production Optimization With KBI 12.1

While the *L. fermentati* strains produced significantly higher amounts of lactic acid compared to the *S. cerevisiae* control, the values were still below the reported flavor threshold for beer of 4.44 mM (400 mg/L) (Siebert, 1999). Therefore, we applied RSM and conducted a trial in wort extract with spiked glucose to enhance lactic acid production of strain KBI 12.1, which was chosen as the highest lactic acid producer from the screening (**Table 6**).

TABLE 6 | Analysis of fermented worts.

	Attribute	Unit	CBS 707	KBI 1.2	KBI 3.2	KBI 5.3	KBI 12.1	WLP001
	Attenuation		$70\% \pm 0\%^{b}$	$70\% \pm 0\%^{b}$	$68\% \pm 1\%^{b}$	$70\% \pm 0\%^{b}$	$55\% \pm 2\%^{a}$	$85\% \pm 1\%^{c}$
	App. extract	°P	2.83 ± 0.03^{b}	2.83 ± 0.03^{b}	2.99 ± 0.14^{b}	2.79 ± 0.01^{b}	4.27 ± 0.22^{c}	1.38 ± 0.06^{a}
	Real extract	°P	4.14 ± 0.01^{b}	4.17 ± 0.02^{b}	4.27 ± 0.11^{b}	4.12 ± 0.01^{b}	5.31 ± 0.18^{c}	2.94 ± 0.08^{a}
	Ethanol	% ABV	3.73 ± 0.01^{b}	3.73 ± 0.04^{b}	3.63 ± 0.12^{b}	3.76 ± 0.03^{b}	2.96 ± 0.11^{a}	4.42 ± 0.02^{c}
	pH		4.24 ± 0.02^{d}	4.27 ± 0.01^{de}	4.13 ± 0.02^{c}	4.31 ± 0.01^{e}	3.95 ± 0.01^{a}	4.07 ± 0.02^{b}
	Lactic acid	mM	2.41 ± 0.02*e*	1.55 ± 0.03*c*	1.82 ± 0.03*d*	1.33 ± 0.01*b*	3.47 ± 0.12*f*	0.94 ± 0.02*a*
	FAN	mg/L	82 ± 4^{bc}	82 ± 2^{bc}	80 ± 4^{bc}	73 ± 3^{b}	83 ± 1^{c}	52 ± 4^{a}
Sugar	Fructose		$92\% \pm 0\%^{a}$	$100\%^{b}$	$100\%^{b}$	$98\% \pm 4\%^{b}$	$100\%^{b}$	$100\%^{b}$
consumption	Glucose		100%	100%	100%	100%	100%	100%
	Sucrose		100%	100%	100%	100%	100%	100%
	Maltose		$100\%^{b}$	$100\%^{b}$	$98\% \pm 2\%^{b}$	$100\%^{b}$	$76\% \pm 4\%^{a}$	$100\%^{b}$
	Maltotriose		$-4\% \pm 1\%^{a}$	$-8\% \pm 1\%^{a}$	$-5\% \pm 4\%^{a}$	$-10\% \pm 1\%^{a}$	$3\% \pm 1\%^{b}$	$81\% \pm 1\%^{c}$
Fermentation	Diacetyl	mg/L	<LOD	<LOD	0.02 ± 0.02^{a}	<LOD	0.02 ± 0.00^{a}	<LOD
by-products	Ethyl acetate	mg/L	14.35 ± 0.20^{d}	13.72 ± 0.28^{d}	14.01 ± 0.68^{d}	9.06 ± 0.21^{b}	11.70 ± 0.82^{c}	7.06 ± 0.50^{a}
	3-Methylbutyl acetate	mg/L	0.48 ± 0.06^{a}	0.36 ± 0.08^{a}	0.40 ± 0.03^{a}	0.43 ± 0.13^{a}	0.29 ± 0.05^{a}	0.30 ± 0.04^{a}
	2-Phenylethyl acetate	mg/L	0.08 ± 0.01^{a}	0.52 ± 0.03^{c}	0.57 ± 0.02^{c}	0.13 ± 0.02^{a}	0.44 ± 0.04^{b}	0.08 ± 0.02^{a}
	Σ Esters	mg/L	16.14 ± 0.31^{c}	16.02 ± 0.40^{c}	16.10 ± 0.64^{c}	10.84 ± 0.38^{a}	13.61 ± 0.99^{b}	9.52 ± 0.47^{a}
	Σ Alcohols	mg/L	119.98 ± 7.87^{d}	77.83 ± 1.64^{ab}	86.35 ± 4.81^{bc}	81.42 ± 4.72^{bc}	65.61 ± 2.34^{a}	93.39 ± 6.19^{c}

Sugars are given in percent consumption of the initial amount. 100% consumption indicates a concentration below the limit of detection (LOD). Values are shown as means ± standard deviation. Different letters in superscripts indicate a significant difference of the means within a row ($p \leq 0.05$).

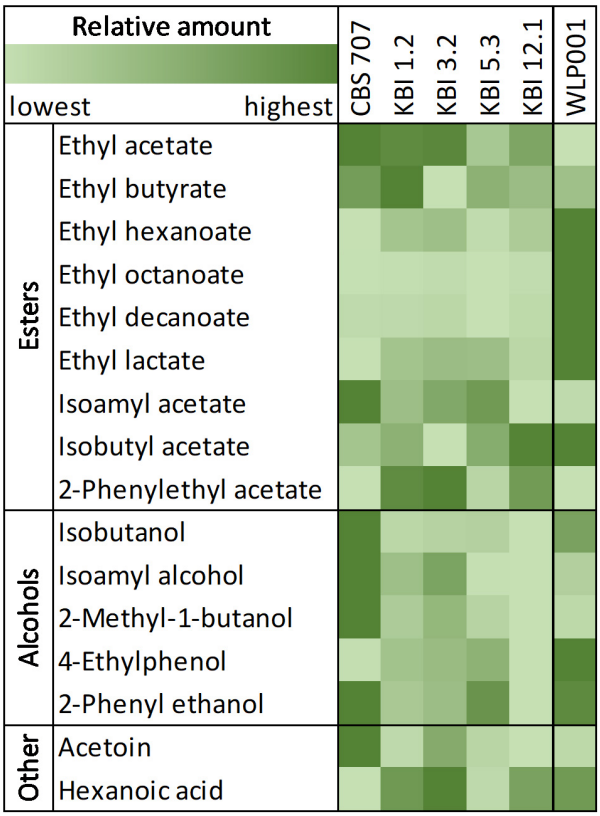

FIGURE 3 | Heatmap of relative amount of volatile compounds in the fermented worts. A full table of relative and quantified compounds can be found in **Supplementary Data Sheet S1**.

Response surface methodology.

Non-*Saccharomyces* yeasts can require a significantly higher pitching rate to show good fermentation performance compared to brewers' yeast due to their typically smaller cell size. A study by Michel et al. (2017) using RSM to optimize fermentation conditions of a *Torulaspora delbrueckii* strain in wort showed that high sensorial desirability of the produced beer was achieved at a high pitching rate of 60 × 10^6 cells/mL. Furthermore, the fermentation temperature can have significant influences on the production of fermentation by-products across yeast genera, e.g., a higher temperature resulting in increased ester production (Verstrepen et al., 2003; Michel et al., 2017; Tyrawa et al., 2019).

To investigate the influences of the fermentation parameters: pitching rate, temperature and starting extract, on the production of lactic acid, RSM was applied. A three factorial, face-centered, central composite design was chosen to investigate the lactic acid production by KBI 12.1 in wort extract in the range of extract content between 5 and 15°P, a pitching rate between 5 and 60 × 10^6 cells/mL, and a fermentation temperature between 16 and 28°C. The detailed experiment design and model statistics are shown in **Supplementary Data Sheet S2**.

Figure 4 shows the response surface as a 3D model of the lactic acid production at 5, 10, and 15°P, as a function of the fermentation temperature and pitching rate.

Increasing extract content enhanced the effect of the temperature and pitching rate parameters. Additionally, a low pitching rate had a very strong positive effect on the lactic acid production. Lactic acid also increased with an increasing fermentation temperature. The highest lactic acid concentration achieved was 11.4 mM at a pitching rate of 5 × 10^6 cells/mL and a fermentation temperature of 28°C. A full table of the results of the response factors can be found in **Supplementary Data Sheet S2**.

Added glucose trial.

To investigate the hypothesis that lactic acid production can be boosted by the presence of higher amounts of glucose at the beginning of fermentation, a trial with a glucose-spiked wort sample was conducted. **Table 7** shows the analytical results of the three worts used in this trial before and after fermentation with KBI 12.1.

The addition of glucose to the 7°P wort led to a significant increase in final lactic acid concentration ($p < 0.01$) of 246%, from 5.2 to 18.0 mM, while the final ethanol content of 2.6% ABV remained unchanged (**Figure 5**). The pH of the glucose spiked wort sample was correspondingly low, at 3.46. On the other hand, increasing the extract content from 7 to 10°P (without the addition of glucose) did not have an influence on the final lactic acid concentration ($p > 0.05$) but resulted in a significantly higher final ethanol content ($p < 0.001$) (**Figure 5**).

The monosaccharides fructose and glucose were depleted by the end of fermentation while maltose was never fully depleted (**Table 7**). Especially the fermented sample with spiked glucose, resulting in high lactic acid production, exhibited high residual maltose concentrations by the end of fermentation which is an indication for a premature inhibition by low pH and/or high lactic acid concentration.

Pilot-Scale Brewing Trial

The results from the lactic acid optimization experiment gave valuable insights for the process development of a scaled-up brewing trial. The RSM results indicated that a low pitching rate and high fermentation temperature are favorable for increased lactic acid production, while the spiked glucose trial indicated that lactic acid production can be boosted by the initial glucose concentration of the wort. Considering these insights, amyloglucosidase was added during the mashing process of wort production to increase the amount of glucose relative to maltose. At the same time, a low pitching rate, at 5 × 10^6 cells/mL, together with a high fermentation temperature (25°C) was chosen to increase lactic acid production on the process side. The aim was to create a low alcohol beer (LAB) by stopping the fermentation prematurely, at a point where the produced lactic acid is in balance with the sweetness of the residual wort sugars. For that reason, samples were taken every 12 h until the fermentation was stopped by filtering out the yeast by means of a plate filter. **Figure 6** illustrates fermentation progress as well as results from volatile fermentation by-products analysis and sensory evaluation of the produced LAB (36 h).

The ethanol concentration of the beer at interruption of fermentation after 36 h had reached 1.26% ABV. The lactic acid

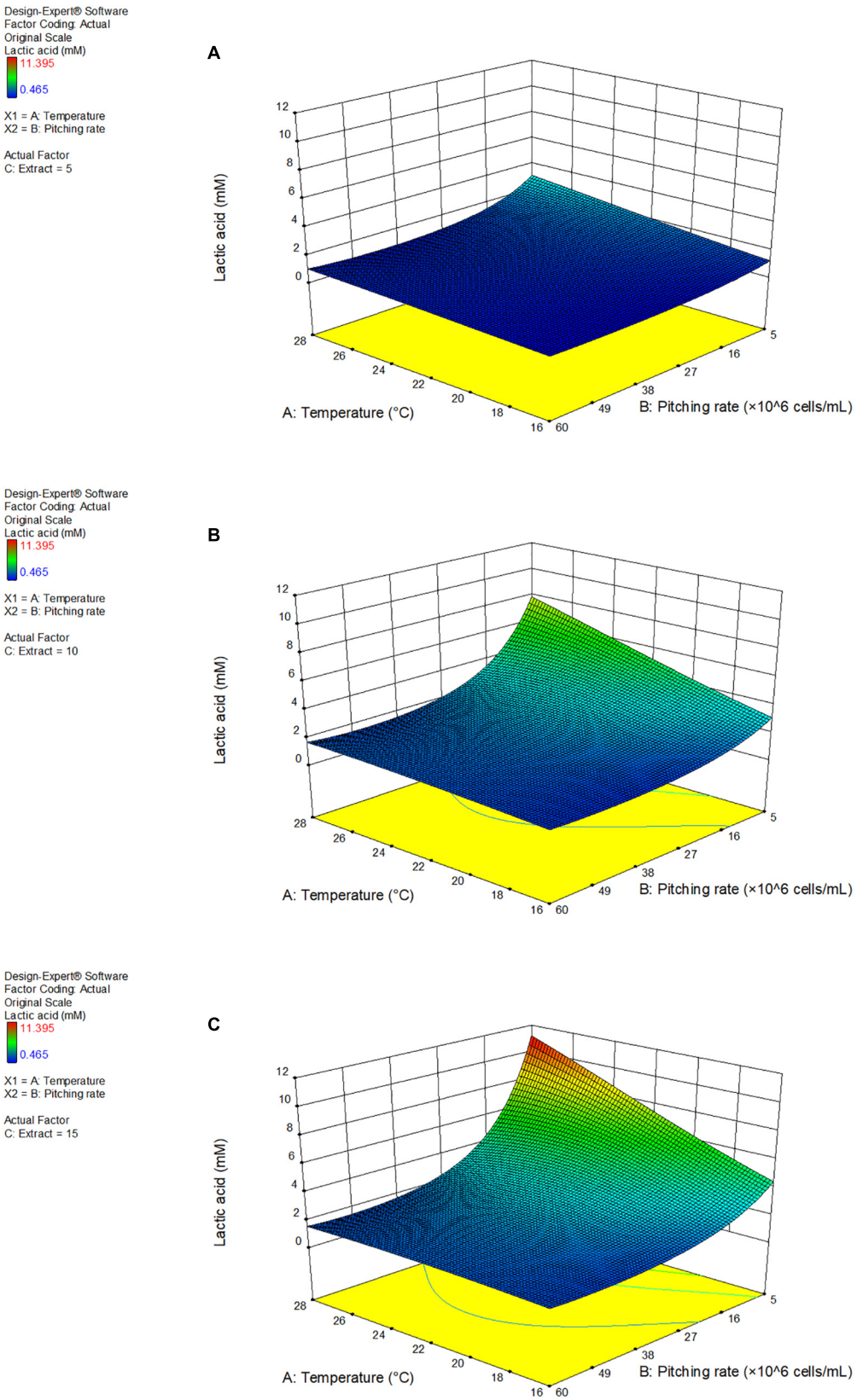

FIGURE 4 | 3D response surface model of response factor lactic acid as a function of fermentation temperature and pitching rate at 5°P **(A)**, 10°P **(B)**, and 15°P **(C)**. Model details and statistics in **Supplementary Data Sheet S2**.

TABLE 7 | Analysis of worts before and after fermentation with KBI 12.1.

Attribute	Unit	7°P		7°P +3% glucose		10°P	
		Wort	Fermented	Wort	Fermented	Wort	Fermented
Attenuation	%	–	65 ± 2^{c}	–	47 ±0*a*	–	60 ±1*b*
App. extract	°P	7.35 ± 0.01	2.57 ± 0.12	9.66 ± 0.02	5.08 ±0.03	9.99 ± 0.01	3.95 ± 0.09
Real extract	°P	7.35 ± 0.01	3.50 ± 0.08	9.66 ± 0.02	5.98 ± 0.02	9.99 ± 0.01	5.15 ± 0.08
Ethanol	% ABV	–	2.61 ± 0.04*a*	–	2.59 ± 0.02*a*	–	3.45 ± 0.03*b*
pH		4.83 ± 0.01	3.81 ± 0.01^{b}	4.88 ± 0.01	3.46 ± 0.09^{a}	4.80 ± 0.01	3.91 ± 0.01^{b}
FAN	mg/L	83 ± 1	n.d.	83 ± 7	n.d.	88 ± 2	n.d.
Lactic acid	mM	–	5.19 ± 0.11*a*	–	18.00 ± 4.64*b*	–	5.10 ± 0.26*a*
Fructose	g/L	1.28 ± 0.01	<LOD	1.56 ± 0.01	<LOD	2.09 ± 0.01	<LOD
Glucose	g/L	6.05 ± 0.01	<LOD	34.59 ± 0.10	<LOD	8.52 ± 0.05	<LOD
Sucrose	g/L	0.78 ± 0.01	<LOD	0.78 ± 0.00	<LOD	1.10 ± 0.01	<LOD
Maltose	g/L	31.06 ± 0.38	2.03 ± 0.77	31.12 ± 0.06	26.49 ± 0.59	43.67 ± 0.25	5.43 ± 0.70
Maltotriose	g/L	9.05 ± 0.11	9.90 ± 0.08	9.03 ± 0.02	8.46 ± 0.13	12.70 ± 0.02	13.56 ± 0.11

Values are given as means ± standard deviation. Different letters in superscripts indicate a significant difference between the fermented samples ($p \leq 0.05$). n.d., not determined.

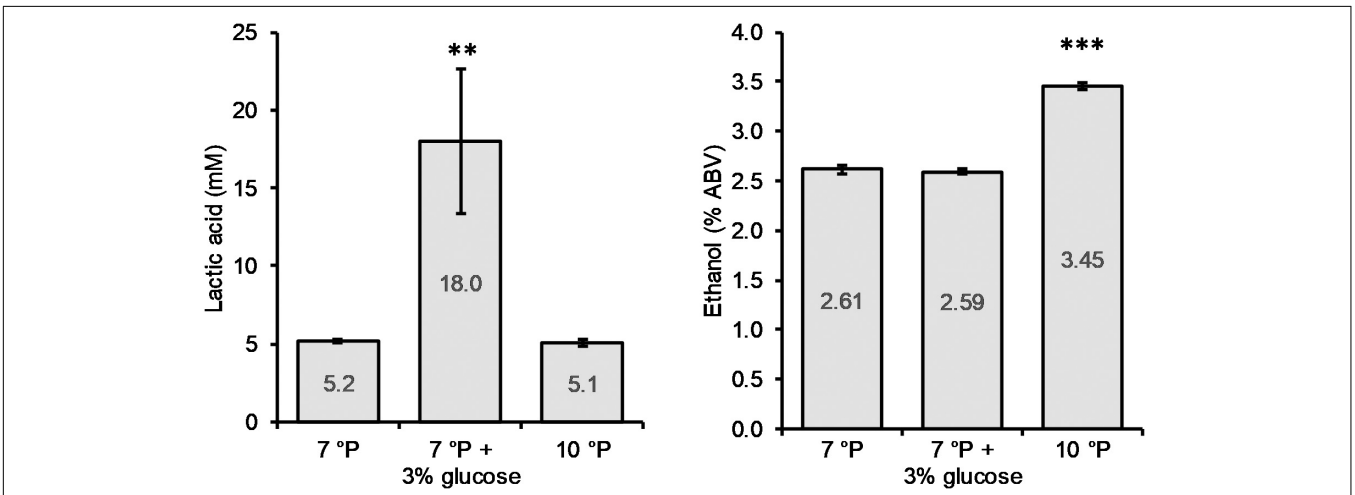

FIGURE 5 | Final lactic acid and ethanol concentrations of 7°P wort extract, 7°P wort extract + 3% glucose, and 10°P wort extract after fermentation with KBI 12.1. $^{**}p \leq 0.01$; $^{***}p \leq 0.001$.

concentration reached 13.6 mM (= 1.23 g/L) at a final pH of 3.56. Final apparent extract of the LAB was 6.23°P. The cell count showed a constant growth in the first 24 h, after which it slowed down to a cell concentration at time of filtration of 43 × 10^6 cells/mL. Glucose was fully depleted after 36 h of fermentation while 0.17 mM (0.24 g/L) of fructose remained. Maltose only saw a small decrease and maltotriose was left untouched. The analysis of the beer that was left in the fermenter to reach final attenuation (216 h) showed only a small further increase in lactic acid to a concentration of 16.1 mM, while doubling in ethanol concentration to a final value of 2.57% ABV. At final attenuation, only about 55% of the maltose was consumed, with maltotriose concentrations unchanged. Analysis of volatile fermentation by-products of the stopped fermentation LAB revealed a low ester concentration of 6.5 mg/L (**Figure 6B**). At 0.27 mg/L, the diacetyl value was as well above its flavor threshold of 0.02–0.10 mg/L (Meilgaard, 1975; Saison et al., 2009). Diacetyl, an unwanted buttery flavor compound, is a fermentation by-product which, at the end of fermentation, is often at concentrations higher than its flavor threshold. In that case, a diacetyl rest is applied to allow yeast to reduce diacetyl to concentrations below the flavor threshold. In this study, the yeast was separated from the young beer before final attenuation was reached, and therefore reduction of the diacetyl concentration was not possible.

The results of the sensory evaluation indicated that a balanced ratio between residual sweetness from maltose and maltotriose and acidity from lactic acid was reached (**Figure 6C**). Fifty percent (interquartile range IQR; 50% of total reported values) of the panelists rated the sweetness/acidity ratio between 4.2 and 6.0 at a scale from 0 to ten, with 0 "too sweet," 5 "just right," and 10 "too sour." Values corresponded to residual sugars of 17.0 mM (12.4 g/L) maltose, 6.2 mM (3.1 g/L) maltotriose, and 0.17 mM (0.24 g/L) fructose and a lactic acid concentration of 13.6 mM (1.23 g/L). The fruitiness was rated medium to high

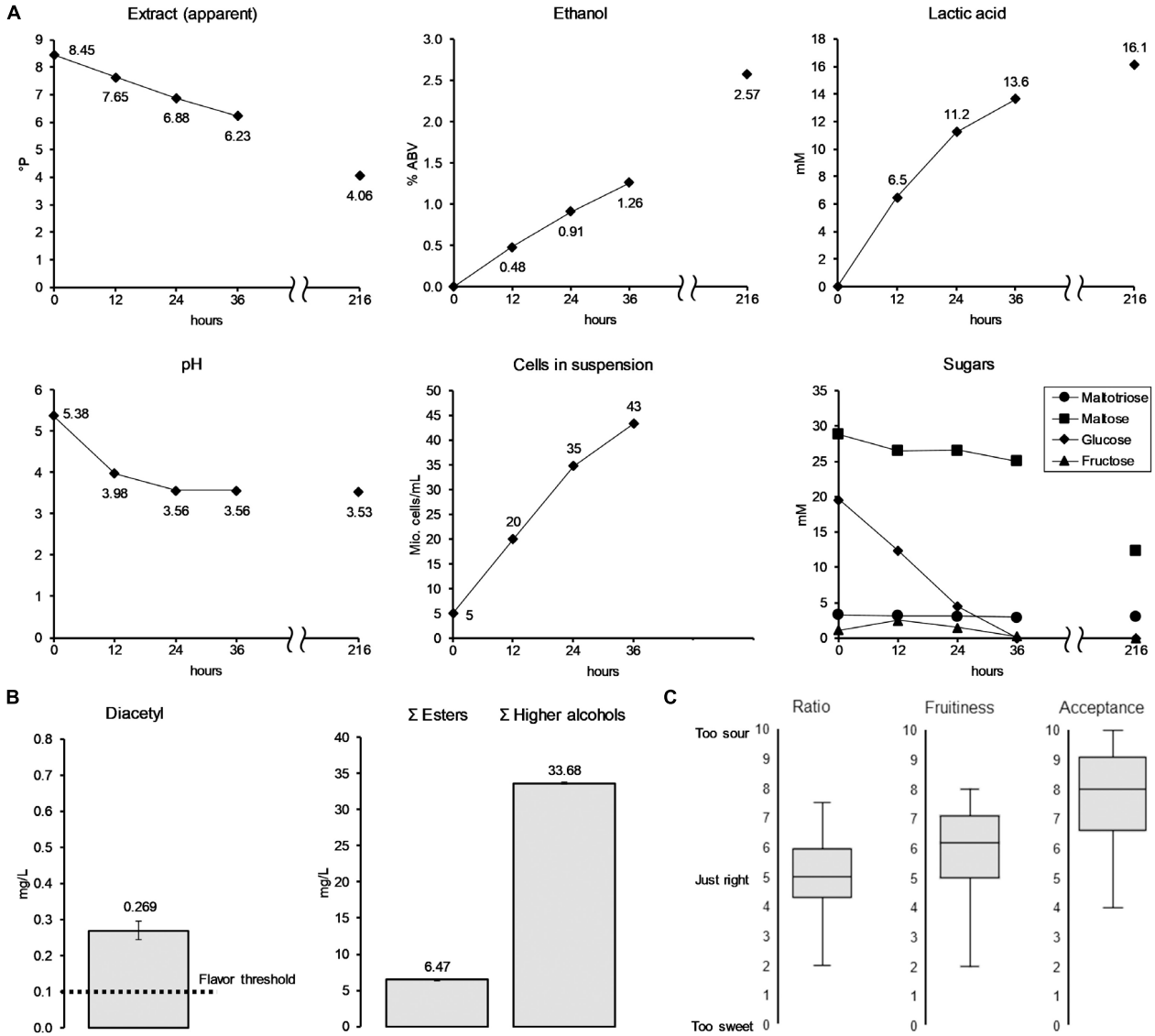

FIGURE 6 | Analyses of pilot-scale (60 L) fermentation **(A)** of low alcoholic beer with KBI 12.1. Fermentation by-products **(B)** and sensory data **(C)** of the low alcoholic beer corresponds to the fermentation data at 36 h (finished low alcohol beer). Values at 216 h show the beer at final attenuation reached without the interuption of fermentation.

with the IQR ranging from 5–7 out of 10. Overall acceptability was rated with an IQR ranging from 6.5–9.0 out of 10.

DISCUSSION

In this study, we investigated four *Lachancea fermentati* strains isolated from kombucha. Genome analysis was performed to gain fundamental insights, to elucidate intraspecific differences due to their origin, and in an attempt to link the strains' genotypes to their phenotype in wort fermentations. The strains were characterized by, e.g., their sugar utilization and stress sensitivities to evaluate their suitability in beer brewing. Screening in wort was performed to investigate intraspecific differences and to determine the best lactic acid producer. Subsequently, the fermentation parameters temperature, pitching rate, and glucose concentration were investigated to enhance lactic acid production. Finally, a low alcohol beer was produced at pilot-scale under optimized conditions.

The results from the genome analysis showed that the four kombucha isolates were diverse and generally separated into two groups, relating to their origin. The diploid isolates KBI 1.2, KBI 3.2, and KBI 12.1 exhibited high heterozygosity, an indication for intraspecific hybrids. Potentially, the isolates share a common ancestor based on patterns in LOH. This hypothesis is supported by the geographically close origin of KBI 1.2 and KBI 3.2, the United States. Due to the remote geographical origin of KBI 12.1 (Hawaii), its close phylogenetic relationship to KBI 1.2 and

KBI 3.2, in contrast to KBI 5.3, calls for the assumption that an exchange of kombucha cultures between the Conterminous United States and Hawaii has taken place at some point. In fact, the exchange of kombucha cultures between kombucha brewers, and kombucha brewer communities has been common practice in the United States (The New York Times, 2010). Unlike the isolates from the United States, KBI 5.3, which originates from Australia, showed a closer phylogenetic relationship to CBS 6772, which originates from South Korea, and CBS 707, whose country of origin is unknown. Unfortunately, to date, very limited sequence data is available for comparison.

Generally, compared to the extensively studied species *Saccharomyces cerevisiae*, the species *L. fermentati* or even the *Lachancea* genus has not been investigated thoroughly. Consequently, only with the initial assumption of a strong degree of homology between the yeast species, assumptions about the *Lachancea fermentati* metabolism can be made.

The greater resistance to low pH conditions of the *Lachancea* strains, compared to the brewers' yeast during the stress test, could tentatively be connected to their tendency to produce significant amounts of lactic acid during alcoholic fermentation. The strains must constantly export lactate and H^+ out of the cell to maintain proton motive force and for this reason may be pre-adapted to high concentrations of H^+-ions. In addition, the acidic kombucha environment has also likely selected for strains with enhanced tolerance to high acid concentrations and low pH values (Chakravorty et al., 2016).

Beside obtaining fundamental insights into the strains' characteristics, we aimed to optimize the lactic acid production by *L. fermentati* during fermentation. The observed values of lactic acid production (between 1.33 and 3.47 mM) in wort extract of the investigated *L. fermentati* strains were low compared to previously reported values. Osburn et al. (2018) reported lactic acid production of 10 mM by a *L. fermentati* strain in a 11.4°P wort at a pitching rate of approximately 5×10^6 cells/mL and 21.7°C. In a previous study with KBI 12.1, Bellut et al. (2019a) reported the production of 14.4 mM of lactic acid in a 6.6°P wort at a pitching rate of 8×10^6 cells/mL and 25°C. However, the aforementioned studies used different fermentation conditions (e.g., pitching rate, temperature) and substrates, which has a significant influence on the lactic acid production, as we have shown in this study. Bellut et al. (2019b) already reported significant differences in lactic acid production by KBI 12.1 in different substrates from cereals, pseudocereals and pulses which could not be traced back to the sugar spectrum or free amino acid spectrum, further underlining the poor state of knowledge regarding factors that modulate lactic acid production in *Lachancea fermentati*.

Whole genome sequencing was performed to connect observations in the phenotype to the genotype of the individual strains. KBI 5.3 carried a mutation (397C > T) in the gene LAFE_0A07888G, resulting in a premature stop codon (Gln133*) (**Supplementary Data Sheet S1**). LAFE_0A07888G is a gene with high similarity to the *JEN1* gene in *S. cerevisiae*. *JEN1* encodes for the monocarboxylate transporter Jen1 that was shown to be a lactic acid exporter (Casal et al., 1999), enhancing lactic acid yield in *S. cerevisiae* strains transformed with bacterial lactic acid dehydrogenases (Branduardi et al., 2006; Pacheco et al., 2012). The nonsense mutation in the *JEN1*-homolog of KBI 5.3 could tentatively have been the reason for the significantly low lactic acid production in comparison to the other *L. fermentati* strains. However, besides Jen1p, at least one other lactic acid transporter exists (Pacheco et al., 2012), which could tentatively explain the remaining, albeit low, lactic acid production. In addition, a single nucleotide deletion (230delT) was also observed in LAFE_0E15192G in the strain KBI 5.3 (**Supplementary Data Sheet S1**). LAFE_0E15192G shows some similarities with *S. cerevisiae* YML054C *CYB2*, a cytochrome b2 (L-lactate cytochrome-c oxidoreductase) component of the mitochondrial intermembrane space which is required for lactate utilization (and repressed by glucose and anaerobic conditions) (Sauer et al., 2010). This frameshift mutation could tentatively explain the inability to grow in lactic acid as the sole substrate in the API test. However, these effects should be tested in future studies by reverse engineering.

The RSM results have shown that in order to boost lactic acid production, a low pitching rate should be used in combination with a high fermentation temperature. Furthermore, in the favored conditions, a higher initial extract led to higher lactic acid concentrations. The fact that the samples with high lactic acid production did not reach final attenuation (**Supplementary Data Sheet S2**) was suggested to be caused by end-product inhibition through the mechanism described in section Stress Tests. Combined with the knowledge that glucose is commonly taken up at the beginning of fermentation before high amounts of maltose, sucrose or maltotriose are consumed (Horák, 2013), it was hypothesized that the increased lactic acid production in the worts with higher extract during the RSM trial was attributed to a higher amount of glucose. The results from the trial with spiked glucose indicated, that lactic acid production by KBI 12.1 can indeed be modulated by the amount of glucose present at the start of fermentation. Within the investigated range of 7–10°P, a higher amount of glucose resulted in increased lactic acid production, but without an increased ethanol production.

The RSM optimization and added glucose trial have shown that lactic acid production by KBI 12.1 is highly dependent on the pitching rate, fermentation temperature and initial glucose concentration. Lactic acid production by the strain KBI 12.1 varied from 0.5 to 18.0 mM based on the fermentation conditions and substrate composition. It was shown that, in order to increase lactic acid production by *Lachancea fermentati* KBI 12.1 in wort, the glucose concentration should be as high as possible, the pitching rate low (5×10^6 cells/mL) and the fermentation temperature high (≥25°C).

The high lactic acid production in samples with a low pitching rate suggests that lactic acid production mostly took place during the growth phase at the beginning of fermentation. In contrast, under the same conditions, but at high pitching rates, little lactic acid was produced. This hypothesis was supported by fermentation data from the scaled-up brewing trial where 84% of total lactic acid was already produced in the first 36 h of fermentation, while the cells in suspension grew from 5 to 43×10^6 cells/mL. However, in the case of the scaled-up

fermentation, the lactic acid production also correlated with the consumption and depletion of glucose.

On a molecular level, the metabolization of pyruvate via lactic acid dehydrogenase is an additional means of NADH recycling, with pyruvate decarboxylase and alcohol dehydrogenase being the more common pathway. NADH is produced during glycolysis, the yeasts' ATP-generating pathway under anaerobic conditions, and has to be recycled to NAD^+ (**Figure 7**). However, while ethanol can leave the cell by passive diffusion, lactic acid has to be actively transported out of the cell at the expense of

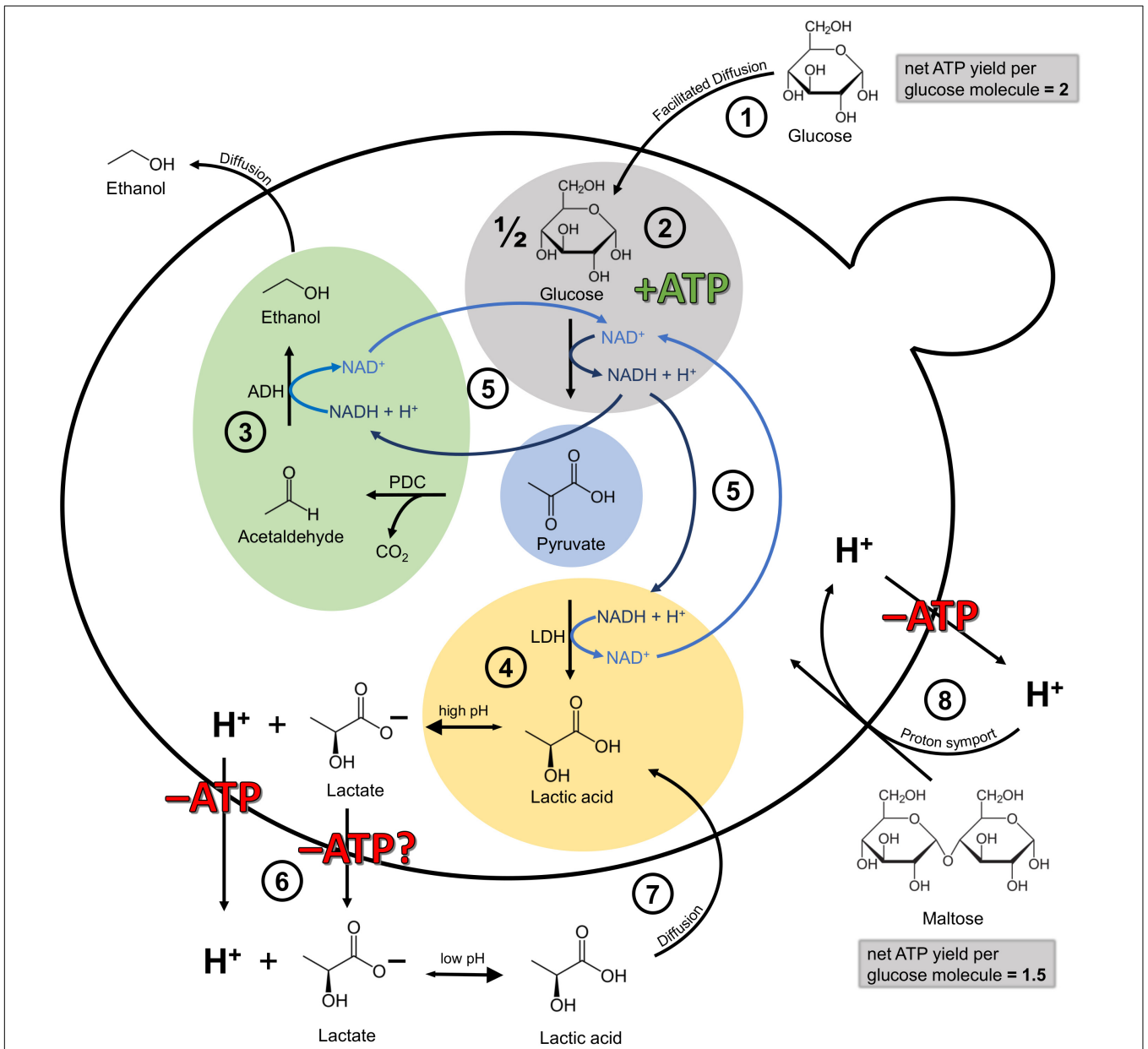

FIGURE 7 | Simplified illustration of the cellular mechanisms involved in lactic acid production and self-inhibition in *Lachancea fermentati* in anaerobic wort fermentations under the assumption of fundamental homology to *Saccharomyces cerevisiae*. Adapted from Sauer et al. (2010) and Bellut et al. (2019a). **(1)** Glucose transport into the cell by facilitated diffusion. The net ATP yield per glucose molecule is 2. **(2)** Glycolysis, yielding one molecule of ATP per molecule pyruvate formed and one molecule of NADH which has to be recycled to NAD^+. **(3)** Ethanol production via pyruvate decarboxylase (PDC) and alcohol dehydrogenase (ADH). The ethanol can leave the cell by passive diffusion. **(4)** Lactic acid production via lactic acid dehydrogenase (LDH). At high intracellular pH, the lactic acid dissociates into lactate and H^+. **(5)** Both, ethanol formation and lactic acid formation are a means to recycle NADH to NAD^+. **(6)** At the very least, the H^+ has to be exported out of the cell at the expense of one molecule of ATP. In the worst case scenario, ATP-dependent mechanisms may be involved in both proton and anion export (Abbott et al., 2009; Mans et al., 2017). **(7)** At low extracellular pH, lactic acid is present in its protonated form and can enter the cell again via passive diffusion, creating an energy-requiring cycle with **6**. **(8)** Maltose transport into the cell is facilitated via proton symport. Consequently, the proton has to be exported out of the cell at the expense of ATP. For that reason, the net ATP yield per glucose molecule from maltose is 1.5 instead of 2.

ATP. This is due to the fact that at high intracellular pH, lactic acid dissociates into lactate and a proton. In order to maintain proton motive force and intracellular pH, this proton has to be exported via the plasma membrane H^+-ATPase, with the expense of one ATP per proton. In the worst case, lactate export is also ATP-dependent, though the exact mechanisms are still unknown (Maris et al., 2004; Abbott et al., 2009; Mans et al., 2017). Abbott et al. (2009) confirmed that the lactic acid export requires energy in the form of ATP, which was shown by a full ATP depletion during anaerobic homolactate fermentation with a *S. cerevisiae* strain. Outside of the cell, at a low extracellular pH, the lactic acid is again present in its protonated form and can thus permeate the cell membrane via passive diffusion, creating an energy-requiring cycle (Sauer et al., 2010). Available evidence suggests therefore that the recycling of NADH via the lactic acid pathway seems to be more expensive for the cell than the ethanol pathway. Why the lactic acid pathway is chosen in the first place, at least at the beginning of fermentation, is still unknown and highlights the need for more research in this area. Presumably, the simultaneous recycling of NADH via the lactic acid and the ethanol pathway, resulting in an accumulation of lactic acid, developed as a strategy to compete with other microbes, comparable to the "make-accumulate-consume" strategy for ethanol in *S. cerevisiae* (Piškur et al., 2006; Pfeiffer and Morley, 2014). In a study on *S. cerevisiae*, Pacheco et al. (2012) found that when glucose is present, the produced lactic acid is exported out of the cell via Jen1 and Ady2, but when glucose (acting as the single carbon source) is depleted, the transporters are also actively involved in lactic acid consumption.

There is a general consensus that all maltose transport systems in *S. cerevisiae* so far characterized mediate the transport into the yeast cells against a concentration gradient in symport with protons. This proton import is balanced by proton export via the plasma membrane H^+-ATPase, at the expense of one ATP per proton. This means, that the uptake of one molecule of maltose comes at the expense of one molecule of ATP (De Kok et al., 2012). Consequently, while glucose enters the cell via facilitated diffusion, maltose has to be actively imported into the cell via proton symport. The consequent export of the proton at the expense of ATP lowers the net ATP yield from maltose to 1.5 ATP per glucose molecule, instead of 2 ATP per molecule of glucose which entered the cell via facilitated diffusion. **Figure 7** illustrates the simplified cellular mechanisms involved in lactic acid production and proton motive force maintenance in *Lachancea fermentati* in anaerobic wort fermentations assuming fundamental homology to *S. cerevisiae*.

The results from this study indicate that at the beginning of fermentation, at relatively high pH, low lactic acid concentration and the presence of glucose, *L. fermentati* KBI 12.1 can afford to simultaneously recycle NADH via the lactic acid pathway. A shift toward the ethanol pathway as the sole means of NADH recycling seemed to occur once glucose was depleted and the proton motive force maintenance became more costly due to a reduced net ATP yield from maltose compared to glucose, combined with an increasing stress caused by increased lactic acid concentrations (**Figure 7**). However, although our results give first indications on the underlying mechanisms for lactic acid production modulation in *L. fermentati* in wort fermentations, more research on ATP utilization and redox balance is necessary to draw conclusions.

It was possible to create a low alcohol beer (1.26% ABV) with KBI 12.1 by interrupting the fermentation after 36 h. The panelists evaluated the ratio of residual sweetness to acidity caused by lactic acid as balanced, giving a good indication for future applications. However, by removing the yeast from the wort prematurely, significant amounts of diacetyl were left in the young beer which can negatively affect the flavor of the beer, limiting the use of this strain for stopped fermentation. The high diacetyl concentration could potentially be tackled post-fermentation with an enzyme treatment by immobilized α-acetolactate decarboxylase (Krogerus and Gibson, 2013). In a previous study, Bellut et al. (2019a) produced a low alcohol beer with KBI 12.1 from a 6.6°P wort. However, the ethanol concentration was, at 2.6% ABV, considerably higher after final attenuation was reached, compared to 1.26% ABV after the interruption of fermentation in this study. Due to the consumption of all fermentable sugars and a high lactic acid production (14.4 mM), the taste of the beer was also characterized as sour. However, diacetyl was below its flavor threshold since the fermentation came to a halt naturally.

CONCLUSION

To conclude, while the exact mechanisms for lactic acid production in *Lachancea fermentati* remain unknown, we have elucidated influencing factors and were able to shine some light on the KBI 12.1 strain's behavior in wort fermentations regarding an enhanced lactic acid production and its consequent induction of a premature fermentation inhibition. We showed that the strain can afford the energy-expensive lactic acid production until a high concentration is reached (here up to 18 mM) only as long as glucose is present in the wort. A low alcohol beer could be produced which had a balanced profile between sweetness from residual sugars and acidity from the produced lactic acid. However, due to the premature cessation of fermentation, diacetyl was present above its flavor threshold. Future application trials should focus on finding the ideal extract value and ideal sugar spectrum of the wort to facilitate high lactic acid concentrations in balance with residual sweetness while still reaching final attenuation. To validate the hypothesis of the influence of the mutated *JEN1*- and *CYB2*-similar genes in KBI 5.3 leading to a reduced lactic acid production, gene knock-out experiments in the strains without the mutation could lead to further insights regarding the modulation of lactic acid production in *Lachancea fermentati*.

DATA AVAILABILITY STATEMENT

The datasets generated for this study can be found in the Illumina reads generated in this study have been submitted to

NCBI-SRA under BioProject number PRJNA587400 in the NCBI BioProject database.

ETHICS STATEMENT

Ethical approval was required for this study in accordance with local guidelines. The sensory trial was carried out in accordance with IFST Guidelines for Ethical and Professional Practices for the Sensory Analysis of Foods and the panel provided written informed consent to take part in the research.

AUTHOR CONTRIBUTIONS

KB performed the fermentation experiments, analyses, and statistics described in this study. KK performed flow cytometry, and bioinformatic analysis of the whole genome sequence data. KB, KK, and EA designed the experiments. KB and KK wrote the manuscript. EA supervised this study. All authors read and approved the final manuscript.

FUNDING

This work was supported by the Baillet Latour Fund within the framework of a scholarship for doctoral students.

ACKNOWLEDGMENTS

We thank Andrea Hoehnel for her assistance regarding HPLC analyses, Jonas Atzler for his help with the scanning electron microscopy, Josh Taylor and the Kerry Group for the kind donation of the enzyme used in this study, and Brian Gibson, David De Schutter, and Luk Daenen for critical reading of the manuscript.

SUPPLEMENTARY MATERIAL

The Supplementary Material for this article can be found online at: https://www.frontiersin.org/articles/10.3389/fmicb.2020.00764/full#supplementary-material

REFERENCES

Abbott, D. A., Van Den Brink, J., Minneboo, I. M. K., Pronk, J. T., and Van Maris, A. J. A. (2009). Anaerobic homolactate fermentation with *Saccharomyces cerevisiae* results in depletion of ATP and impaired metabolic activity. *FEMS Yeast Res.* 9, 349–357. doi: 10.1111/j.1567-1364.2009.00506.x

Agier, N., Romano, O. M., Touzain, F., Lagomarsino, M. C., and Fischer, G. (2013). The spatiotemporal program of replication in the genome of *Lachancea kluyveri*. *Genome Biol. Evol.* 5, 370–388. doi: 10.1093/gbe/evt014

Andrews, S. (2010). *FastQC: A Quality Control Tool for High Throughput Sequence Data*. Available online at: http://www.bioinformatics.babraham.ac.uk/projects/fastqc (accessed December 5, 2019).

Banilas, G., Sgouros, G., and Nisiotou, A. (2016). Development of microsatellite markers for *Lachancea thermotolerans* typing and population structure of wine-associated isolates. *Microbiol. Res.* 193, 1–10. doi: 10.1016/j.micres.2016.08.010

Barth-Haas Group (2019). *The Barth Report Hops 2018/2019. Barth Rep. Hops*. Available online at: https://www.barthhaas.com/fileadmin/user_upload/news/2019-07-23/barthreport20182019en.pdf (accessed November 19, 2019).

Bellut, K., and Arendt, E. K. (2019). Chance and challenge: non-*Saccharomyces* yeasts in nonalcoholic and low alcohol beer brewing: a review. *J. Am. Soc. Brew. Chem.* 77, 77–91. doi: 10.1080/03610470.2019.1569452

Bellut, K., Michel, M., Hutzler, M., Zarnkow, M., Jacob, F., De Schutter, D. P., et al. (2019a). Investigation into the application of *Lachancea fermentati* strain KBI 12.1 in low alcohol beer brewing. *J. Am. Soc. Brew. Chem.* 77, 157–169. doi: 10.1080/03610470.2019.1629227

Bellut, K., Michel, M., Zarnkow, M., Hutzler, M., Jacob, F., Lynch, K. M., et al. (2019b). On the suitability of alternative cereals, pseudocereals and pulses in the production of alcohol-reduced beers by non-conventional yeasts. *Eur. Food Res. Technol.* 245, 2549–2564. doi: 10.1007/s00217-019-03372-3

Bellut, K., Michel, M., Zarnkow, M., Hutzler, M., Jacob, F., De Schutter, D. P., et al. (2018). Application of non-*Saccharomyces* yeasts isolated from kombucha in the production of alcohol-free beer. *Fermentation* 4, 1–13. doi: 10.3390/fermentation4030066

Bendiak, D., Van Der Aar, P., Barbero, F., Benzing, P., Berndt, R., Carrick, K., et al. (1996). Yeast flocculation by absorbance method. *J. Am. Soc. Brew. Chem.* 54, 245–248. doi: 10.1094/asbcj-54-0245

BioMérieux Antifungal Susceptibility Testing (2019). *BioMérieux Antifungal Susceptibility Testing*. Available online at: https://techlib.biomerieux.com/wcm/techlib/techlib/documents/docLink/Package_Insert/35904001-35905000/Package_Insert_-_9305056_-_D_-_en_-_Etest_-_AFST_WW.pdf (accessed August 21, 2019).

Bolger, A. M., Lohse, M., and Usadel, B. (2014). Trimmomatic: A flexible trimmer for Illumina sequence data. *Bioinformatics* 30, 2114–2120. doi: 10.1093/bioinformatics/btu170

Branduardi, P., Sauer, M., De Gioia, L., Zampella, G., Valli, M., Mattanovich, D., et al. (2006). Lactate production yield from engineered yeasts is dependent from the host background, the lactate dehydrogenase source and the lactate export. *Microb. Cell Fact.* 5, 1–12. doi: 10.1186/1475-2859-5-4

Brányik, T., Silva, D. P., Baszczyòski, M., Lehnert, R., Almeida, E., and Silva, J. B. (2012). A review of methods of low alcohol and alcohol-free beer production. *J. Food Eng.* 108, 493–506. doi: 10.1016/j.jfoodeng.2011.09.020

Casal, M., Paiva, S., Andrade, R. P., Gancedo, C., and Leão, C. (1999). The lactate-proton symport of *Saccharomyces cerevisiae* is encoded by JEN1. *J. Bacteriol.* 181, 2620–2623. doi: 10.1128/jb.181.8.2620-2623.1999

Cassone, M., Serra, P., Mondello, F., Girolamo, A., Scafetti, S., Pistella, E., et al. (2003). Outbreak of *Saccharomyces cerevisiae* subtype *boulardii* fungemia in patients neighboring those treated with a probiotic preparation of the organism. *J. Clin. Microbiol.* 41, 5340–5343. doi: 10.1128/JCM.41.11.5340-5343.2003

Chakravorty, S., Bhattacharya, S., Chatzinotas, A., Chakraborty, W., Bhattacharya, D., and Gachhui, R. (2016). Kombucha tea fermentation: microbial and biochemical dynamics. *Int. J. Food Microbiol.* 220, 63–72. doi: 10.1016/j.ijfoodmicro.2015.12.015

Chiang, C., Layer, R. M., Faust, G. G., Lindberg, M. R., Rose, D. B., Garrison, E. P., et al. (2015). SpeedSeq: ultra-fast personal genome analysis and interpretation. *Nat. Methods* 12, 1–5. doi: 10.1038/nmeth.3505

Colombié, S., Dequin, S., and Sablayrolles, J. M. (2003). Control of lactate production by *Saccharomyces cerevisiae* expressing a bacterial LDH gene. *Enzyme Microb. Technol.* 33, 38–46. doi: 10.1016/S0141-0229(03)00082-6

Das Murtey, M., and Ramasamy, P. (2018). Sample preparations for scanning electron microscopy – Life Sciences. *Intech open* 2, 64. doi: 10.5772/32009

De Francesco, G., Sannino, C., Sileoni, V., Marconi, O., Filippucci, S., Tasselli, G., et al. (2018). *Mrakia gelida* in brewing process: An innovative production of low alcohol beer using a psychrophilic yeast strain. *Food Microbiol.* 76, 354–362. doi: 10.1016/j.fm.2018.06.018

De Francesco, G., Turchetti, B., Sileoni, V., Marconi, O., and Perretti, G. (2015). Screening of new strains of *Saccharomycodes ludwigii* and *Zygosaccharomyces rouxii* to produce low-alcohol beer. *J. Inst. Brew.* 121, 113–121. doi: 10.1002/jib.185

De Kok, S., Kozak, B. U., Pronk, J. T., and Van Maris, A. J. A. (2012). Energy coupling in *Saccharomyces cerevisiae*: selected opportunities for metabolic

engineering. *FEMS Yeast Res.* 12, 387–397. doi: 10.1111/j.1567-1364.2012.00799.x

D'Hautcourt, O., and Smart, K. A. (1999). Measurement of brewing yeast flocculation. *J. Am. Soc. Brew. Chem.* 57, 123–128. doi: 10.1094/ASBCJ-57-0129

Estela-Escalante, W. D., Rosales-Mendoza, S., Moscosa-Santillán, M., and González-Ramírez, J. E. (2016). Evaluation of the fermentative potential of *Candida zemplinina* yeasts for craft beer fermentation. *J. Inst. Brew.* 122, 530–535. doi: 10.1002/jib.354

Freel, K. C., Friedrich, A., Hou, J., and Schacherer, J. (2014). Population genomic analysis reveals highly conserved mitochondrial genomes in the yeast species *Lachancea thermotolerans*. *Genome Biol. Evol.* 6, 2586–2594. doi: 10.1093/gbe/evu203

Garrison, E., and Marth, G. (2012). Haplotype-based variant detection from short-read sequencing. *arXiv Prepr [Preprint]*.

Glaubitz, M., and Haehn, H. (1929). *Beer Manufacture. Patent US1898047*.

Haase, S. B., and Reed, S. I. (2002). Improved flow cytometric analysis of the budding yeast cell cycle. *Cell Cycle* 1, 132–136.

Hamoud, S., Keidar, Z., and Hayek, T. (2011). Recurrent *Saccharomyces cerevisiae* fungemia in an otherwise healthy patient. *Isr. Med. Assoc. J.* 13, 575–576.

Horák, J. (2013). Regulations of sugar transporters: insights from yeast. *Curr. Genet.* 59, 1–31. doi: 10.1007/s00294-013-0388-8

Hranilovic, A., Bely, M., Masneuf-Pomarede, I., Jiranek, V., and Albertin, W. (2017). The evolution of *Lachancea thermotolerans* is driven by geographical determination, anthropisation and flux between different ecosystems. *PLoS ONE* 12:e0184652. doi: 10.1371/journal.pone.0184652

Jayabalan, R., Malbaša, R. V., Lonèar, E. S., Vitas, J. S., and Sathishkumar, M. (2014). A review on kombucha tea-microbiology, composition, fermentation, beneficial effects, toxicity, and tea fungus. *Compr. Rev. Food Sci. Food Saf.* 13, 538–550. doi: 10.1111/1541-4337.12073

Jiang, Z., Yang, B., Liu, X., Zhang, S., Shan, J., Liu, J., et al. (2017). A novel approach for the production of a non-alcohol beer (=0.5% abv) by a combination of limited fermentation and vacuum distillation. *J. Inst. Brew.* 123, 533–536. doi: 10.1002/jib.465

Jolly, N. P., Varela, C., and Pretorius, I. S. (2014). Not your ordinary yeast: non-*Saccharomyces* yeasts in wine production uncovered. *FEMS Yeast Res.* 14, 215–237. doi: 10.1111/1567-1364.12111

Krogerus, K., and Gibson, B. R. (2013). 125th anniversary review: diacetyl and its control during brewery fermentation. *J. Inst. Brew.* 119, 86–97. doi: 10.1002/jib.84

Kurtzman, C. P., Fell, J. W., and Boekhout, T. (2011). *The Yeasts, A Taxonomic Study*, 5th Edn, eds C. P. Kurtzman, J. W. Fell, and T. Boekhout. Amsterdam: Elsevier.

Langdon, Q. K., Peris, D., Kyle, B., and Hittinger, C. T. (2018). Sppider: a species identification tool to investigate hybrid genomes with high-throughput sequencing. *Mol. Biol. Evol.* 35, 2835–2849. doi: 10.1093/molbev/msy166

Le, S., Josse, J., and Husson, F. (2008). FactoMineR: An R package for multivariate analysis. 25, 1–18. doi: 10.1016/j.envint.2008.06.007

Leuck, A.-M., Rothenberger, M. K., and Green, J. S. (2014). Fungemia due to *Lachancea fermentati*: a case report. *BMC Infect. Dis.* 14:250. doi: 10.1186/1471-2334-14-250

Li, H. (2011). A statistical framework for SNP calling, mutation discovery, association mapping and population genetical parameter estimation from sequencing data. *Bioinformatics* 27, 2987–2993. doi: 10.1093/bioinformatics/btr509

Li, H., Handsaker, B., Wysoker, A., Fennell, T., Ruan, J., Homer, N., et al. (2009). The sequence alignment/map format and SAMtools. *Bioinformatics* 25, 2078–2079. doi: 10.1093/bioinformatics/btp352

Li, H., and Liu, F. (2015). Changes in organic acids during beer fermentation. *J. Am. Soc. Brew. Chem.* 73, 275–279. doi: 10.1094/ASBCJ-2015-0509-01

Liu, Y., Li, H., and Du, J. (2011). Non-alcoholic beer production by *Saccharomycodes ludwigii*. *CNKI Food Sci.* 32, 186–190.

Mans, R., Hassing, E. J., Wijsman, M., Giezekamp, A., Pronk, J. T., Daran, J. M., et al. (2017). A CRISPR/Cas9-based exploration into the elusive mechanism for lactate export in *Saccharomyces cerevisiae*. *FEMS Yeast Res.* 17, 1–12. doi: 10.1093/femsyr/fox085

Maris, A. J. A., Van, Winkler, A. A., Porro, D., Dijken, J. P., Van, et al. (2004). Homofermentative lactate production cannot sustain anaerobic growth of engineered. *Appl. Environ. Microbiol.* 70, 2898–2905. doi: 10.1128/AEM.70.5.2898

Marsh, A. J., O'Sullivan, O., Hill, C., Ross, R. P., and Cotter, P. D. (2014). Sequence-based analysis of the bacterial and fungal compositions of multiple kombucha (tea fungus) samples. *Food Microbiol.* 38, 171–178. doi: 10.1016/j.fm.2013.09.003

Martin, M., Patterson, M., Garg, S., Fischer, S. O., Pisanti, N., Gunnar, W., et al. (2016). WhatsHap: fast and accurate read-based phasing. *bioRxiv [Preprint]*

Meier-Dörnberg, T., and Hutzler, M. (2014). *Alcohol-Free Wheat Beer with Maltose Negative Yeast Strain Saccharomycodes ludwigii*. Available online at: https://www.researchgate.net/publi.

Meier-Dörnberg, T., Hutzler, M., Michel, M., Methner, F.-J., and Jacob, F. (2017). The importance of a comparative characterization of *Saccharomyces cerevisiae* and *Saccharomyces pastorianus* strains for brewing. *Fermentation* 3, 1–25. doi: 10.3390/fermentation3030041

Meilgaard, M. C. (1975). Flavor chemistry in beer: Part II: Flavor and flavor threshold of 239 aroma volatiles. *Master Brew. Assoc. Am. Tech. Q.* 12, 151–168.

Meussdoerffer, F. G. (2009). "A comprehensive history of beer brewing," in *Handbook of Brewing: Processes, Technology, Markets*, ed. H. M. Eßlinger (Hoboken, NJ: Wiley), 1–42. doi: 10.1002/9783527623488.ch1

Michel, M., Kopecká, J., Meier-Dörnberg, T., Zarnkow, M., Jacob, F., and Hutzler, M. (2016). Screening for new brewing yeasts in the non-*Saccharomyces* sector with *Torulaspora delbrueckii* as model. *Yeast* 33, 129–144. doi: 10.1002/yea.3146

Michel, M., Meier-Dornberg, T., Jacob, F., Schneiderbanger, H., Haselbeck, K., Zarnkow, M., et al. (2017). Optimization of Beer fermentation with a novel brewing strain *Torulaspora delbrueckii* using response surface methodology. *Master Brew. Assoc. Am. Tech. Q* 54, 23–33.

Minh, B. Q., Nguyen, M. A. T., and Von Haeseler, A. (2013). Ultrafast approximation for phylogenetic bootstrap. *Mol. Biol. Evol.* 30, 1188–1195. doi: 10.1093/molbev/mst024

Mohammadi, A., Razavi, S. H., Mousavi, S. M., and Rezaei, K. (2011). A comparison between sugar consumption and ethanol production in wort by immobilized *Saccharomyces cerevisiae*, *Saccharomyces ludwigii* and *Saccharomyces rouxii* on Brewer's Spent Grain. *Braz. J. Microbiol.* 42, 605–615. doi: 10.1590/S1517-83822011000200025

Mortazavian, A. M., Razavi, S. H., Mousavi, S. M., Malganji, S., and Sohrabvandi, S. (2014). The effect of *Saccharomyces* strain and fermentation conditions on quality prameters of non-alcoholic beer. *J. Paramed. Sci.* 5, 21–26.

Müller, M., Bellut, K., Tippmann, J., and Becker, T. (2017). Physical methods for dealcoholization of beverage matrices and their impact on quality attributes. *ChemBioEng Rev.* 4, 310–326. doi: 10.1002/cben.201700010

Narziß, L., Miedaner, H., Kern, E., and Leibhard, M. (1992). Technology and composition of non-alcoholic beers – Processes using arrested fermentation. *Brauwelt Int.* 4, 396–410.

Nguyen, L. T., Schmidt, H. A., Von Haeseler, A., and Minh, B. Q. (2015). IQ-TREE: a fast and effective stochastic algorithm for estimating maximum-likelihood phylogenies. *Mol. Biol. Evol.* 32, 268–274. doi: 10.1093/molbev/msu300

Ortiz-Merino, R. A., Varela, J. A., Coughlan, A. Y., Hoshida, H., da Silveira, W. B., Wilde, C., et al. (2018). Ploidy variation in *Kluyveromyces marxianus* separates dairy and non-dairy isolates. *Front. Genet.* 9:94. doi: 10.3389/fgene.2018.00094

Osburn, K., Amaral, J., Metcalf, S. R., Nickens, D. M., Rogers, C. M., Sausen, C., et al. (2018). Primary souring: a novel bacteria-free method for sour beer production. *Food Microbiol.* 70, 76–84. doi: 10.1016/j.fm.2017.09.007

Pacheco, A., Talaia, G., Sá-Pessoa, J., Bessa, D., Gonçalves, M. J., Moreira, R., et al. (2012). Lactic acid production in *Saccharomyces cerevisiae* is modulated by expression of the monocarboxylate transporters Jen1 and Ady2. *FEMS Yeast Res.* 12, 375–381. doi: 10.1111/j.1567-1364.2012.00790.x

Pedersen, B. S., and Quinlan, A. R. (2018). Mosdepth: Quick coverage calculation for genomes and exomes. *Bioinformatics* 34, 867–868. doi: 10.1093/bioinformatics/btx699

Pérez, G., Fariña, L., Barquet, M., Boido, E., Gaggero, C., Dellacassa, E., et al. (2011). A quick screening method to identify β-glucosidase activity in native wine yeast strains: application of esculin glycerol agar (EGA) medium. *World J. Microbiol. Biotechnol.* 27, 47–55. doi: 10.1007/s11274-010-0425-4

Peter, J., De Chiara, M., Friedrich, A., Yue, J.-X., Pflieger, D., Bergström, A., et al. (2018). Genome evolution across 1,011 *Saccharomyces cerevisiae* isolates. *Nature* 556, 339–344. doi: 10.1038/s41586-018-0030-5

Peyer, L. C., Zarnkow, M., Jacob, F., and De Schutter, D. P. (2017). Sour brewing: impact of *Lactobacillus amylovorus* FST2.11 on technological and quality attributes of acid beers. *J. Am. Soc. Brew. Chem.* 75, 207–216. doi: 10.1094/asbcj-2017-3861-01

Pfeiffer, T., and Morley, A. (2014). An evolutionary perspective on the crabtree effect. *Front. Mol. Biosci.* 1:1–6. doi: 10.3389/fmolb.2014.00017

Pinu, F. R., and Villas-Boas, S. G. (2017). Rapid quantification of major volatile metabolites in fermented food and beverages using gas chromatography-mass spectrometry. *Metabolites* 7, 1–13. doi: 10.3390/metabo7030037

Piškur, J., Rozpedowska, E., Polakova, S., Merico, A., and Compagno, C. (2006). How did *Saccharomyces* evolve to become a good brewer? *Trends Genet.* 22, 183–186. doi: 10.1016/j.tig.2006.02.002

Porter, T. J. (2017). *Biochemical Characterization and Evaluation of the Oenological Attributes of Lachancea* species. Available online at: http://hdl.handle.net/10019.1/102856.

Porter, T. J., Divol, B., and Setati, M. E. (2019a). Investigating the biochemical and fermentation attributes of *Lachancea* species and strains: deciphering the potential contribution to wine chemical composition. *Int. J. Food Microbiol.* 290, 273–287. doi: 10.1016/j.ijfoodmicro.2018.10.025

Porter, T. J., Divol, B., and Setati, M. E. (2019b). *Lachancea* yeast species: Origin, biochemical characteristics and oenological significance. *Food Res. Int.* 119, 378–389. doi: 10.1016/j.foodres.2019.02.003

Reva, O. N., Zaets, I. E., Ovcharenko, L. P., Kukharenko, O. E., Shpylova, S. P., Podolich, O. V., et al. (2015). Metabarcoding of the kombucha microbial community grown in different microenvironments. *AMB Express* 5:124. doi: 10.1186/s13568-015-0124-5

Romano, P., and Suzzi, G. (1993). Potential use for *Zygosaccharomyces* species in winemaking. *J. Wine Res.* 4, 87–94. doi: 10.1080/09571269308717955

Saerens, S., and Swiegers, J. H. (2014). *Production of low-Alcohol or Alcohol-Free Beer with Pichia kluyveri Yeast Strains*. Available online at: https://www.lens.org/lens/patent/155-871-548-073-892.

Sahl, J. W., Lemmer, D., Travis, J., Schupp, J. M., Gillece, J. D., Aziz, M., et al. (2016). NASP: an accurate, rapid method for the identification of SNPs in WGS datasets that supports flexible input and output formats. *Microb. Genomics* 2:e000074. doi: 10.1099/mgen.0.000074

Saison, D., De Schutter, D. P., Uyttenhove, B., Delvaux, F., and Delvaux, F. R. (2009). Contribution of staling compounds to the aged flavour of lager beer by studying their flavour thresholds. *Food Chem.* 114, 1206–1215. doi: 10.1016/j.foodchem.2008.10.078

Sauer, M., Porro, D., Mattanovich, D., and Branduardi, P. (2010). 16 years research on lactic acid production with Yeast–ready for the market? *Biotechnol. Genet. Eng. Rev.* 27, 229–256. doi: 10.1080/02648725.2010.10648152

Siebert, K. J. (1999). Modeling the flavor thresholds of organic acids in beer as a function of their molecular properties. *Food Qual. Prefer.* 10, 129–137. doi: 10.1016/s0950-3293(98)00059-7

Sohrabvandi, S., Razavi, S. H., Mousavi, S. M., Mortazavian, A., and Rezaei, K. (2009). Application of *Saccharomyces rouxii* for the production of non-alcoholic beer. *Food Sci. Biotechnol.* 18, 1132–1137. doi: 10.1080/10942910902818145

Souciet, J. L., Dujon, B., Gaillardin, C., Johnston, M., Baret, P. V., Cliften, P., et al. (2009). Comparative genomics of protoploid *Saccharomycetaceae*. *Genome Res.* 19, 1696–1709. doi: 10.1101/gr.091546.109

Stewart, G. G. (2018). Yeast flocculation—sedimentation and flotation. *Fermentation* 4, 259–308. doi: 10.3390/fermentation4020028

The New York Times (2010). *A Strange Brew May Be a Good Thing*. Available online at: https://www.nytimes.com/2010/03/25/fashion/25Tea.html (accessed November 8, 2019).

Thomas-Hall, S. R., Turchetti, B., Buzzini, P., Branda, E., Boekhout, T., Theelen, B., et al. (2010). Cold-adapted yeasts from Antarctica and the Italian Alps-description of three novel species: *Mrakia robertii* sp. nov., *Mrakia blollopis* sp. nov. and *Mrakiella niccombsii* sp. nov. *Extremophiles* 14, 47–59. doi: 10.1007/s00792-009-0286-7

Tyrawa, C., Preiss, R., Armstrong, M., and van der Merwe, G. (2019). The temperature dependent functionality of *Brettanomyces bruxellensis* strains in wort fermentations. *J. Inst. Brew.* 125, 315–325. doi: 10.1002/jib.565

Verstrepen, K. J., Derdelinckx, G., Dufour, J. P., Winderickx, J., Thevelein, J. M., Pretorius, I. S., et al. (2003). Flavor-active esters: adding fruitiness to beer. *J. Biosci. Bioeng.* 96, 110–118. doi: 10.1016/S1389-1723(03)90112-5

Conflict of Interest: KK was employed by VTT Technical Research Centre of Finland Ltd.

The remaining authors declare that the research was conducted in the absence of any commercial or financial relationships that could be construed as a potential conflict of interest.

The handling editor declared a past co-authorship with one of the authors KK.

frontiers in Genetics

MINI REVIEW
published: 28 April 2020
doi: 10.3389/fgene.2020.00438

Proline Homeostasis in *Saccharomyces cerevisiae*: How Does the Stress-Responsive Transcription Factor Msn2 Play a Role?

Noreen Suliani binti Mat Nanyan[1] *and Hiroshi Takagi*[2]*

[1] School of Industrial Technology, Universiti Sains Malaysia, Gelugor, Malaysia, [2] Division of Biological Science, Graduate School of Science and Technology, Nara Institute of Science and Technology, Ikoma, Japan

Overexpression of *MSN2*, which is the transcription factor gene in response to stress, is well-known to increase the tolerance of the yeast *Saccharomyces cerevisiae* cells to a wide variety of environmental stresses. Recent studies have found that the Msn2 is a feasible potential mediator of proline homeostasis in yeast. This result is based on the finding that overexpression of the *MSN2* gene exacerbates the cytotoxicity of yeast to various amino acid analogs whose uptake is increased by the active amino acid permeases localized on the plasma membrane as a result of a dysfunctional deubiquitination process. Increased understanding of the cellular responses induced by the Msn2-mediated proline incorporation will provide better comprehension of how cells respond to and counteract to different kinds of stimuli and will also contribute to the breeding of industrial yeast strains with increased productivity.

Keywords: *Saccharomyces cerevisiae*, stress-responsive transcription factor, Msn2, proline homeostasis, proline permease, Gnp1, deubiquitinating enzymes, Ubp6

OPEN ACCESS

Edited by:
Amparo Querol, Consejo Superior de Investigaciones Científicas (CSIC), Spain

Reviewed by:
Johan M. Thevelein, KU Leuven, Belgium
Hana Sychrová, Institute of Physiology (ASCR), Czechia

***Correspondence:**
Hiroshi Takagi
hiro@bs.naist.jp

Specialty section:
This article was submitted to Evolutionary and Genomic Microbiology, a section of the journal Frontiers in Genetics

Received: *13 February 2020*
Accepted: *09 April 2020*
Published: *28 April 2020*

Citation:
Mat Nanyan NSb and Takagi H (2020) Proline Homeostasis in Saccharomyces cerevisiae: How Does the Stress-Responsive Transcription Factor Msn2 Play a Role? Front. Genet. 11:438. doi: 10.3389/fgene.2020.00438

INTRODUCTION

Cells of microorganisms are frequently exposed to a variety of stresses in their environment, such as prolonged nutrient starvation, free radicals and toxic molecules, imbalances in osmotic pressure and pH level, and non-optimal growth temperatures (Mager and De Kruijff, 1995; Ruis and Schüller, 1995). To survive in the face of such threatening and detrimental surroundings, eukaryotic cells have evolved a series of defense mechanisms at the transcriptional, protein, as well as metabolic levels (Boy-Marcotte et al., 1998; Toone and Jones, 1998; Estruch, 2000; Gasch et al., 2000; Kandror et al., 2004). External stimuli are perceived and transduced via the signal transduction pathways to cause global remodeling of gene expression, which is governed by transcriptional activators and repressors. In general, cellular stresses severely affect both transcription and translation activities, resulting in the inhibition of *de novo* protein synthesis. Moreover, environmental fluctuations may cause protein-related damages, such as the inhibition of enzyme activities, destabilization of cellular structures, and instability of chemical gradients, which eventually result in cell disruption. Thus, protein quality control and protein homeostasis are essential prerequisites for stress responses. Under harsh stresses, cells also undergo the systematic downregulation of energy-producing and energy-consuming processes in order to enter into a quiescent state, often accompanied

by a dynamic shift in the central metabolic pathways that convert nutrients into energy and biomass. Cells possess tight and precise regulation systems to coordinate all the changes that are interconnected at those different levels.

In recent years, extensive research advances have been made in the field of stress responses using a eukaryotic model organism, the budding yeast *Saccharomyces cerevisiae* (Causton et al., 2001; Gasch, 2003). Earlier studies revealed the importance of the highly conserved stress-responsive transcription factors. Heat-shock factor 1 (Hsf1) was identified as a transcription activator that governs the expression of heat-shock proteins in response to elevated temperature (Sorger, 1990; Smith and Yaffe, 1991). The basic leucine-zipper transcription factor Yap1 is required for the induction of stress-responsive genes under oxidative stress conditions (Harshman et al., 1988; Moye-Rowley et al., 1989). Notably, *S. cerevisiae* cells have also developed species-specific transcription factors, namely Msn2 and Msn4 (Msn2/4) (Estruch and Carlson, 1993; Martínez-Pastor et al., 1996; Görner et al., 1998). Msn2/4 play pivotal roles in stress responses through the activation of hundreds of stress-related genes as a consequence to various stress conditions (Estruch, 2000; Gasch et al., 2000; Hasan et al., 2002; Berry and Gasch, 2008).

S. cerevisiae cells are also equipped with stress response mechanisms at the protein level to ensure protein quality at different subcellular locations, such as the cytosol (Hiraishi et al., 2009; Nillegoda et al., 2010; Theodoraki et al., 2012), endoplasmic reticulum (Brodsky, 2012; Thibault and Ng, 2012; Gardner et al., 2013; Wu et al., 2014), nucleus (Gardner et al., 2005; Rosenbaum and Gardner, 2011), mitochondria (Haynes and Ron, 2010; Baker and Haynes, 2011), and plasma membrane (Zhao et al., 2013; MacGurn, 2014; Shiga et al., 2014). The protein quality control includes all processes that ensure proper protein folding and thus prevent the toxic consequences of protein misfolding (Goldberg, 2003; Turcu et al., 2009). Irreversibly damaged proteins are selectively and effectively removed through proteasomal and/or vacuolar degradation systems, both of which consist of multiple fine-tuned steps including protein ubiquitination and deubiquitination (Finley et al., 2012).

Intracellular metabolism is dynamically changed in response to various stresses in *S. cerevisiae*, as well as in many other organisms. When the nutrient levels (e.g., carbon and nitrogen sources) are reduced, yeast cells reprogram the modes of energy metabolism from fermentation to respiration, a process termed a diauxic shift, in order to maximize the efficiency of energy production (Gray et al., 2004). Simultaneously, cells accumulate storage carbohydrates, such as trehalose and glycogen, which improve their survival rates under stress conditions and extend their life span (Fontana et al., 2010). In addition to carbon metabolites, nitrogen metabolites are consumed and produced in response to external stimuli. Recent studies have reported the significant importance of amino acids not only as building blocks of proteins but also in the control of cellular physiology (Sharma and Dietz, 2006; Takagi, 2008; Zhang et al., 2017). For instance, proline is accumulated and acts as an osmoprotectant in many plant and bacterial cells in response to osmotic stress (Csonka and Hanson, 1991; Kavi Kishor and Sreenivasulu, 2014). Besides that, glutamine plays a substantial role in mammalian cell growth where it facilitates the transport of other amino acids such as leucine into the cells and subsequently activates mTORC1 (Gonzalez and Hall, 2017). Collectively, these multiple regulatory mechanisms at the transcriptional, protein, and metabolic levels constitute a network that protects yeast cells from harmful conditions and allows them to adapt to new environments.

STRESS-INDUCED GENE EXPRESSION VIA TRANSCRIPTION FACTORS MSN2/4

The environmental stress response (ESR) controlled by the yeast-specific transcription factors Msn2 and Msn4 (Msn2/4) includes responses to various stresses, such as oxidative stress, osmotic shock, glucose starvation, high ethanol concentrations, temperature upshift, and freezing stress (Gasch et al., 2000; Izawa et al., 2007; Sadeh et al., 2011, 2012; Sasano et al., 2012a,b); together, these constituent responses of the ESR are required for both acute stress responses and cell survival during prolonged stress (Reiter et al., 2013). Although the Msn2/4 proteins were first reported to be 41% identical to each other and functionally redundant (Estruch and Carlson, 1993), subsequent studies demonstrated that Msn2 and Msn4 individually can induce the expression of different set of genes under certain stress conditions (Gasch, 2003; Watanabe et al., 2007; Berry and Gasch, 2008). Additionally, while the *MSN2* gene is constitutively expressed, transcription of the *MSN4* gene is induced by stress in an Msn2/4-dependent manner (Gasch et al., 2000). Thus, the roles of Msn2/4 are mostly overlapped but can be distinguished in part. Several studies suggest that Msn2 plays a role in transcriptional repression as well. The repression likely occurs via gene expression for transcription repressors or growth inhibitors. Msn2 activates the transcription of the *DOT1* gene, which encodes a repressor of the ribosome biogenesis gene (Elfving et al., 2014). Transcription of the *XBP1* gene, which encodes a repressor of cell-cycle associated genes, is also Msn2-dependent (Miles et al., 2013).

Under non-stress growth conditions, Msn2/4 are phosphorylated by cAMP-dependent protein kinase A (PKA) and reside in the cytoplasm. Once yeast cells are challenged by environmental perturbations, Msn2/4 are rapidly dephosphorylated and translocated into the nucleus (Görner et al., 1998; Beck and Hall, 1999). They then bind to the stress-response element sequence (STRE; AGGGG) in the promoter region of the target genes and subsequently activate the transcription (Boy-Marcotte et al., 1998, 1999; Gasch et al., 2000; Causton et al., 2001). Previous studies identified functional domains of Msn2, which include the C-terminal zinc finger DNA-binding domain (DBD) (Marchler et al., 1993; Martínez-Pastor et al., 1996; Schmitt and McEntee, 1996; Moskvina et al., 1998), the nuclear localization signal (NLS) region (Görner et al., 1998, 2002), the nuclear export signal (NES) region (Görner et al., 1998), and the imperative transcriptional activating domain (TAD) at the N terminus (Boy-Marcotte et al., 2006). In addition to phosphorylation by PKA, multiple upstream pathways are involved in the regulation of Msn2 and/or

Msn4: the target-of-rapamycin (TOR) signaling-dependent cytoplasmic localization (Beck and Hall, 1999), the karyopherin Msn5-dependent nuclear export (Chi et al., 2001; Görner et al., 2002), proteasome-mediated degradation (Durchschlag et al., 2004), the ubiquitin ligase Rsp5-dependent nuclear export of mRNA (Haitani and Takagi, 2008), and the protein kinase Rim15-dependent phosphorylation (Lee et al., 2013).

To understand how Msn2/4 contribute to stress responses, the downstream target genes of Msn2/4 have been comprehensively investigated. First, Msn2/4 directly induce the expression of the genes encoding antioxidant enzymes, such as *CTT1* (for catalase), *SOD1* and *SOD2* (for superoxide dismutases), and *PRX1* and *TSA2* (for thiol peroxidases) (Hasan et al., 2002; Drakulic et al., 2005; Sadeh et al., 2011). Since various kinds of stresses lead to the imbalanced generation of reactive oxygen species (ROS) causing cell death, the elimination of ROS by the antioxidant enzymes is an important stress response. Second, Msn2/4 are essential to the induction of the genes involved in protein quality control, such as the molecular chaperone gene *HSP12*, the sHSP-family genes *HSP26* and *HSP42*, the HSP70-family genes *SSA1* and *SSA4*, and the HSP90-family genes *HSP82* and *HSP104* (Kandror et al., 2004; Eastmond and Nelson, 2006). Under stress conditions, the expression of the polyubiquitin precursor gene *UBI4* is also upregulated to mark proteins for selective degradation via the ubiquitin-proteasome system (Simon et al., 1999). Third, Msn2/4 triggers metabolic reprogramming in response to stress by inducing the expression of the mitochondrial respiratory genes *COX5b*, *COX17*, and *COX20*, the pentose phosphate pathway genes *SOL4*, *GND2*, and *TKL2*, the trehalose synthetic genes *TPS1*, *TPS2*, *TPS3*, and *TSL1*, and the glycogen synthetic genes *GSY1*, *GSY2*, and *GLC3* (Estruch, 2000; Gasch et al., 2000; Causton et al., 2001; Sadeh et al., 2011).

Overexpression of *MSN2* or *MSN4* has been a promising approach for the construction of industrial yeast strains to improve their stress resistance as well as fermentation ability (Cardona et al., 2007; Watanabe et al., 2009; Sasano et al., 2012a,d). For instance, baker's yeast cells are challenged by a variety of baking-associated stresses during dough fermentation, including freeze-thaw, air-drying, and a high sugar content, which trigger the oxidative stress due to the accumulation of intracellular ROS caused by protein misfolding and mitochondrial damage (Kitagaki and Takagi, 2014). Our previous study reported that baker's yeast cells that overexpressed *MSN2* have shown a higher tolerance to freezing stress and enhanced the ability of yeast cells to ferment productively in frozen dough (Sasano et al., 2012a). Furthermore, in second-generation bioethanol production with lignocellulosic biomass, several growth/fermentation inhibitors such as furfural and 5-hydroxymethylfurfural are generated and they are known to produce ROS (Allen et al., 2010). The overexpression of *MSN2* in bioethanol yeast strains that were grown in the presence of furfural upregulates the transcription of antioxidant gene, which in turn increases the cell resistance and leads to recovery of cell growth (Sasano et al., 2012d). Our recent study also showed that the overexpression of *MSN2* shortens the replicative lifespan of yeast cells by reducing the intracellular proline levels (Mukai et al., 2019).

AMINO ACIDS INVOLVED IN STRESS RESPONSE

Among major carbon and nitrogen metabolites, Takagi's laboratory has focused on amino acids as hallmarks and mediators of *S. cerevisiae* stress responses (Takagi et al., 2000; Morita et al., 2002; Matsuura and Takagi, 2005; Kaino et al., 2008; Takagi, 2008; Nishimura et al., 2010). Amino acids essentially serve as a nitrogen source and the building blocks of proteins in yeast. Furthermore, they also contribute to the proliferation and durability of yeast cells following exposure to stresses. For instance, proline and charged amino acids such as arginine and glutamate were suggested to be pivotal for cell resistance in yeast and *Escherichia coli* cells, as these amino acids can inhibit the denaturation of proteins (Takagi et al., 1997; Morita et al., 2002; Shiraki et al., 2002; Chattopadhyay et al., 2004; Golovanov et al., 2004).

In terms of stress-resistance activity, proline is one of the most studied among the 20 naturally occurring amino acids. It has a cryoprotective activity in *S. cerevisiae* cells, as well as in many other kinds of cells (Sleator and Hill, 2001; Maggio et al., 2002; Krishnan et al., 2008; Liang et al., 2013). Although proline synthesis is not induced in response to stress, intracellular proline accumulation via the engineering or modification of the enzymes involved in the proline synthesis and degradation pathway in industrial baker's yeast strains elevates the resistance of freeze-thaw stress, leading to an enhanced fermentation ability in frozen dough (Kaino et al., 2008; Sasano et al., 2012c; Tsolmonbaatar et al., 2016). In addition to the freeze-thaw stress tolerance, proline confers tolerance to high osmolality, desiccation, high concentrations of ethanol, and weak acids (Takagi et al., 2000, 2016; Sasano et al., 2012b). Although the involvement of proline carries considerable importance in general stress responses, the roles played by Msn2/4 that link to the proline homeostasis is poorly understood.

The concerted processes of biosynthesis, degradation, and transport of proline administer the cellular proline homeostasis. Proline, which is incorporated into proteins, is synthesized from glutamate in three enzymatically catalyzed steps. First, the γ-glutamyl kinase Pro1 catalyzes the conversion of glutamate to glutamate-5-phosphate (Brandriss, 1979). Then, the unstable glutamate-5-phosphate is converted to glutamate semialdehyde by the γ-glutamyl phosphate reductase Pro2 (Tomenchok and Brandriss, 1987). Glutamate semialdehyde, then spontaneously cyclizes to form Δ^1-pyrroline-5-carboxylate (P5C), which is converted to proline by the P5C reductase Pro3 (Brandriss and Falvey, 1992). Pro1 is sensitive to proline feedback inhibition, and thus, several known amino acid changes, such as Ile150Thr and Asp154Asn, in Pro1 alleviate feedback inhibition and elevate the level of intracellular proline (Morita et al., 2003; Sekine et al., 2007). At the transcriptional level, only the expression of the *PRO2* gene is under the general amino acid control system (Natarajan et al., 2001), and it is still unknown whether the

proline-synthetic pathway genes are coordinately transcribed by a certain external stimulus. To assimilate proline as a nitrogen source, it is degraded into glutamate via the proline oxidase Put1 and the P5C dehydrogenase Put2, both of which are mitochondrial enzymes (Brandriss, 1979). Loss of the Put1 function contributes to an increase of the intracellular proline content (Takagi et al., 2000). Nitrogen catabolite repression (NCR) transcriptionally represses both the *PUT1* and *PUT2* genes (Hofman-Bang, 1999; Georis et al., 2009), which are positively regulated by the transcription activator Put3 (Ann et al., 1996). NCR prevents the utilization of proline as a nitrogen source when rich nitrogen compounds, such as ammonia and glutamine, are present.

In *S. cerevisiae*, the amino-acid-polyamine-organocation (APC) superfamily consists of 24 permease proteins whose function is to transport amino acids and other amines into the cells (Nelissen et al., 1997; Jack et al., 2000). Four of them, namely Gap1, Put4, Agp1, and Gnp1 are responsible to incorporate proline (Andréasson et al., 2004). Gap1 encodes a high capacity transporter for all naturally occurring amino acids and is regulated by the quality of the nitrogen source present in the growth medium (Grenson et al., 1970; Chen and Kaiser, 2002). Put4 is required for the high-affinity transport of proline and is regulated at the transcriptional level by NCR (Xu et al., 1995; Ter Schure et al., 2000). On the other hand, Agp1 and Gnp1 encode permeases with broad substrate specificity and a high affinity for glutamine, respectively (Zhu et al., 1996; Iraqui et al., 1999). The *AGP1* and *GNP1* genes are induced by the regulation of the Ssy1-Ptr3-Ssy5 amino acid sensor complex (Didion et al., 1998; Iraqui et al., 1999; Forsberg et al., 2001; Ljungdahl, 2009).

Structural analogs of amino acids have been widely used to analyze amino acid homeostasis. L-azetidine-2-carboxylic acid (AZC), a toxic analog for proline, is used in both fundamental and applied researches, as it has been proven to be beneficial to study the cellular metabolism and the production of macromolecules in both prokaryotes and eukaryotes (Bach and Takagi, 2013). AZC is a non-protein amino acid originally found in plants and has a heterocyclic structure with a four-membered nitrogen ring and a carboxylic acid group on one of the ring carbon atoms. The main difference between AZC and proline is that the former has a four-ring member while the latter has a five-ring member. AZC, as well as many other amino acid analogs, is thought to be toxic to cells, because it is carried into the cells through proline permeases, and competes with proline during incorporation into nascent proteins, which consequently causes protein misfolding and cell death (Trotter et al., 2001; Weids and Grant, 2014).

PROSPECTIVE ROLES OF *MSN2* OVEREXPRESSION IN THE CONTROL OF PROLINE HOMEOSTASIS

Our recent study found that overexpression of *MSN2* increased the sensitivity of yeast cells to several toxic amino acid analogs, namely AZC, *o*-fluoro-DL-phenylalanine (OFP), and L-canavanine (Can), which are known to be the analogs of proline, phenylalanine, and arginine, respectively (Mat Nanyan et al., 2019a). This suggests that *MSN2* overexpression negatively controls the growth and survival of yeast cells in media containing those toxic compounds, indicating that overexpression of *MSN2* is involved in the incorporation of amino acids into the cells (Mat Nanyan et al., 2019a). Further investigation showed that the increased AZC sensitivity in *MSN2*-overexpressing (*MSN2*-OE) cells could be due to the increased incorporation of AZC, since higher AZC levels were detected in *MSN2*-OE cells than that observed in wild-type cells (Mat Nanyan et al., 2019a). Not only AZC, but also the overexpression of *MSN2* increased proline levels shortly after the addition of proline into the culture (Mat Nanyan et al., 2019a). Our study also found that quadruple disruption of proline permease genes (*GAP1*, *PUT4*, *AGP1*, and *GNP1*) in *MSN2*-OE cells with the strain CAY29 background conferred higher resistance to AZC (Mat Nanyan et al., 2019a), similar to that observed in wild-type cells with the same quadruple disruption (Andréasson et al., 2004). Moreover, a single disruption of *GNP1* showed the most striking effect among single deletions of the permease genes, where Δ*gnp1* cells showed a higher resistance against AZC, highlighting a predominant role played by Gnp1 in the AZC incorporation as compared to the other three permeases, which suggest that they may have redundant roles (Mat Nanyan et al., 2019a). Consistently, the overexpression or deletion of *GNP1* has no significant effect on the growth of yeast when grown in the media containing OFP or Can because Gnp1 does not incorporate phenylalanine (transported by Gap1, Agp1, and Bap2) or arginine (transported by Can1; Ljungdahl and Daignan-Fornier, 2012). Intriguingly, although the transcription of the typical Msn2-targeted gene *CTT1* was highly upregulated under *MSN2* overexpression, none of the levels of proline permease gene mRNA transcripts were significantly upregulated in *MSN2*-OE cells compared to that of in the wild-type cells, which signifies that *GNP1* or other proline permease genes are not transcriptionally activated by Msn2 (Mat Nanyan et al., 2019a). More importantly, the Gnp1-GFP signal is highly detected in *MSN2*-OE cells, which is largely distributed on the plasma membrane rather than other parts of the cells (Mat Nanyan et al., 2019a). Thus, these results indicate that the endocytic degradation of Gnp1 was defective under *MSN2* overexpression, which highlights the newly discovered network between the ESR which is mediated by Msn2 and proline homeostasis in yeast. It would be intriguing to further examine whether proline permeases and intracellular proline homeostasis under different stress conditions are enhanced via the blocking of endocytosis.

Ubiquitination and deubiquitination are involved in the control of endocytic degradation of amino acid permeases localized on the plasma membrane (Springael and André, 1998; Kimura et al., 2009; Kimura and Tanaka, 2010; Jones et al., 2012; MacGurn, 2014). Since the E3 ubiquitin ligase Rsp5 is responsible for regulating the localization of Gnp1 (Sasaki and Takagi, 2013), *MSN2* overexpression might negatively control the protein ubiquitination mediated by Rsp5. The expression of the kinase gene *NPR1* or other associated inhibitor genes for Rsp5-dependent protein ubiquitination might be induced as a result of *MSN2* overexpression, and could thereby inhibit the endocytosis

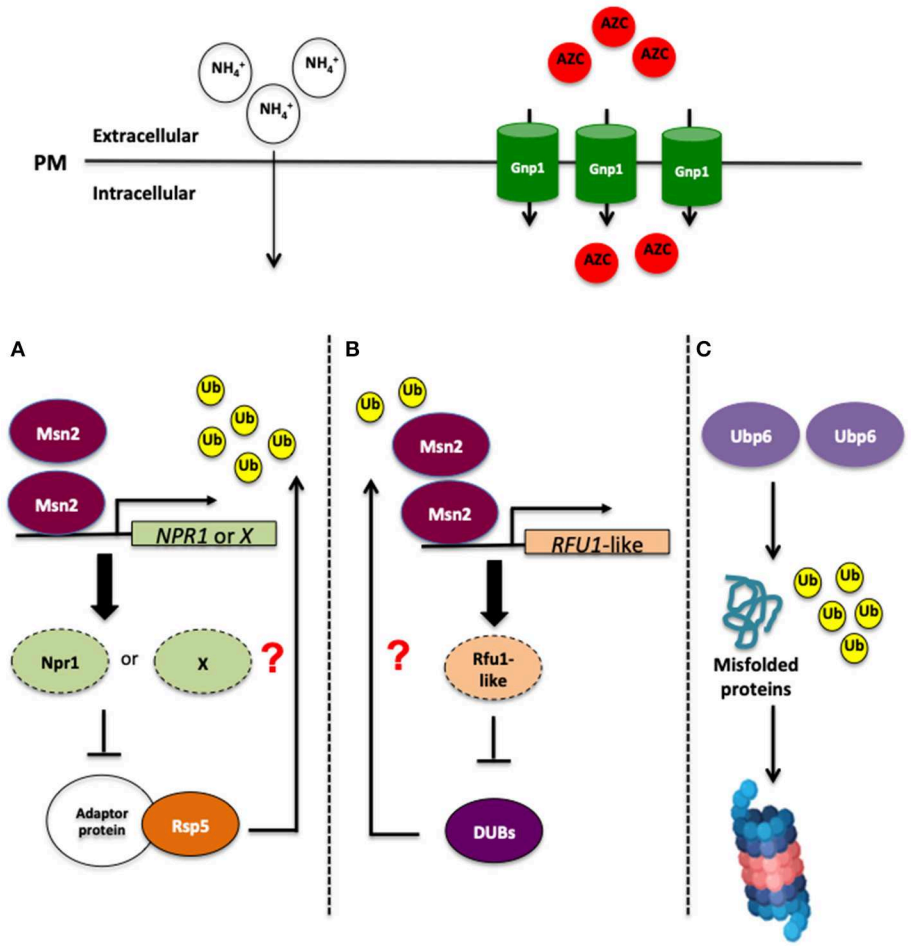

FIGURE 1 | An excess of Msn2 inhibits the endocytic degradation of Gnp1 by unknown mechanisms. There are at least three plausible mechanisms, which could explain this phenomenon. **(A)** Overexpression of *MSN2* might induce the expression of *NPR1* or the associated inhibitor genes for Rsp5-independent protein ubiquitination, therefore Gnp1 could not be ubiquitinated and endocytosed. **(B)** Secondly, a high level of Msn2 may activate the gene expression of DUB repressors such as Rfu1-like protein(s), leading to a reduced or loss function of DUBs. **(C)** In yeast cells overexpressing *UBP6*, an excess of Ubp6 may enhance the ubiquitination and accelerate the degradation of misfolded proteins by unknown mechanisms, for example, the proteasome-mediated mechanism in the *MSN2*-independent manner, leading to the tolerance toward proteotoxic stress caused by intracelullar accumulation of the misfolded proteins.

of Gnp1 (**Figure 1**). Although it is still hard to predict the target of Msn2 that is responsible for the endocytosis of Gnp1, it is crucial to explore and determine the target of many regulators, including the TORC1 pathway, Rsp5, and endocytosis. Interestingly, our recent study demonstrated that yeast cells overexpressing *MSN2* exhibited a higher level of ubiquitinated proteins and a shortage of free ubiquitin content (Mat Nanyan et al., 2019b), similar to what is observed in Δ*ubp6* cells, where the absence of *UBP6* gene encoding one of the yeast deubiquitinating enzymes (DUBs) and is classified into ubiquitin-specific-protease (USP) family caused depletion of free cellular ubiquitin (Chernova et al., 2003; Hanna et al., 2003). These results suggest that the excess level of Msn2 reduces or impairs the activity of DUBs, which could result in the inhibition of endocytosis of Gnp1 (Mat Nanyan et al., 2019b). Further investigations showed that the transcription of *UBP6* and other DUB genes was not significantly changed in *MSN2*-OE cells, indicating that Msn2 does not repress *UBP6* and other DUB genes transcriptionally (Mat Nanyan et al., 2019b). The disruption of *UBP6* in yeast cells makes them more susceptible to the toxicity of translational inhibitors such as cycloheximide and the toxic arginine analog, Can, which are caused by a deficiency of free ubiquitin (Chernova et al., 2003; Hanna et al., 2003). Intriguingly, deletion of *UBP6*, *UBP3* as well as *OTU1* genes aggravates the growth inhibitory effect of toxic amino acid analogs in yeast cells (Mat Nanyan et al., 2019b). In particular, disruption of *UBP6* led to the most remarkable sensitivity

toward AZC, OFP, and Can (Mat Nanyan et al., 2019b). These phenomena were also observed in *MSN2*-OE cells, suggesting that the excess level of Msn2 and Ubp6 deficiency confer a common phenotype of defective resistance against toxic amino acid analogs. The combination of the *MSN2* overexpression and *UBP6* disruption resulted in growth similar to that seen with Δ*ubp6* cells in the presence of low concentrations of AZC (Mat Nanyan et al., 2019b). Moreover, the co-overexpression of *MSN2* and *UBP6* increased the resistance to AZC, OFP, and Can (Mat Nanyan et al., 2019b). Further investigations should be carried out to clarify whether Msn2 and Ubp6 affect AZC resistance via the same mechanism or whether Ubp6 functions independently to counteract the toxicity of amino acid analogs (**Figure 1**). Intriguingly, the Gnp1-GFP signals were elevated in Δ*ubp6* cells and were mostly localized on the plasma membrane, similar to what was observed in *MSN2*-OE cells (Mat Nanyan et al., 2019b). The impaired deubiquitination mediated by an excess of Msn2 might cause the inhibition of the endocytic degradation of proline permeases by unknown mechanisms. We propose here a novel role of Msn2 in the control of intracellular uptake of proline (**Figure 1**). Msn2 is known for its global effect in the control of various regulatory networks in the face of stress conditions such as regulating the antioxidant enzyme genes and molecular chaperones, as well as reprogramming the carbon metabolism. In addition to that, the novel link suggested between Msn2 and proline uptake might further contribute to a deeper comprehension of global stress responses in *S. cerevisiae* in order to withstand various fluctuating growth conditions.

CONCLUSION

In this mini-review, we discuss the current understanding of the stress-responsive transcription factor Msn2 and the stress response in yeast. In particular, the overexpression of *MSN2* has been shown to increase the tolerance of yeast cells for various kinds of stress conditions, such as oxidative and freezing stresses. In addition, we shed light on a potentially important link, namely that the inhibition of endocytic degradation mediated by Msn2 plays an essential role in regulating the proline homeostasis under stress conditions, evidently caused by the loss of function of DUBs. Further investigations will elucidate the profound relationship among Msn2, DUBs, and Gnp1 in the regulation of proline homeostasis, which may serve as a foundation to engineer more robust industrial yeast strains, which might be advantageous in fermentation industries.

AUTHOR CONTRIBUTIONS

NM and HT substantially and intellectually contribute to this work, and reviewed and approved the final version of manuscript.

FUNDING

The study was partially supported by a grant from the Project of the NARO Bio-oriented Technology Research Advancement Institution (Research program on development of innovative technology) to HT under grant number 30017B.

REFERENCES

Allen, S. A., Clark, W., McCaffery, J. M., Cai, Z., Lanctot, A., Slininger, P. J., et al. (2010). Furfural induces reactive oxygen species accumulation and cellular damage in *Saccharomyces cerevisiae*. *Biotechnol. Biofuels.* 3:2. doi: 10.1186/1754-6834-3-2

Andréasson, C., Neve, E. P. A., and Ljungdahl, P. O. (2004). Four permeases import proline and the toxic proline analogue azetidine-2-carboxylate into yeast. *Yeast* 21, 193–199. doi: 10.1002/yea.1052

Ann, S., Etages, G., Fahey, D. A., Reecet, R. J., and Brandriss, M. C. (1996). Functional analysis of the *PUT3* transcriptional activator of the proline utilization pathway in *Saccharomyces cerevisiae*. *Genetics* 142, 1069–1082. doi: 10.1002/zamm.19660460126

Bach, T. M. H., and Takagi, H. (2013). Properties, metabolisms, and applications of L-proline analogues. *Appl. Microbiol. Biotechnol.* 97, 6623–6634. doi: 10.1007/s00253-013-5022-7

Baker, B. M., and Haynes, C. M. (2011). Mitochondrial protein quality control during biogenesis and aging. *Trends Biochem. Sci.* 36, 254–261. doi: 10.1016/j.tibs.2011.01.004

Beck, T., and Hall, M. N. (1999). The TOR signalling pathway controls nuclear localization of nutrient-regulated transcription factors. *Nature* 402, 689–692. doi: 10.1038/45287

Berry, D. B., and Gasch, A. P. (2008). Stress-activated genomic expression changes serve a preparative role for impending stress in yeast. *Mol. Biol. Cell.* 19, 4580–4587. doi: 10.1091/mbc.E07

Boy-Marcotte, E., Garmendia, C., Garreau, H., Lallet, S., Mallet, L., and Jacquet, M. (2006). The transcriptional activation region of Msn2p, in *Saccharomyces cerevisiae*, is regulated by stress but is insensitive to the cAMP signalling pathway. *Mol. Genet. Genomics.* 275, 277–287. doi: 10.1007/s00438-005-0017-4

Boy-Marcotte, E., Lagniel, G., Perrot, M., Bussereau, F., Boudsocq, A., Jacquet, M., et al. (1999). The heat shock response in yeast: Differential regulations and contributions of the Msn2p/Msn4p and Hsf1 regulons. *Mol. Microbiol.* 33, 274–283. doi: 10.1046/j.1365-2958.1999.01467.x

Boy-Marcotte, E., Perrot, M., Bussereau, F., Boucherie, H., and Jacquet, M. (1998). Msn2p and Msn4p control a large number of genes induced at the diauxic transition which are repressed by cyclic AMP in *Saccharomyces cerevisiae*. *J. Bacteriol.* 180, 1044–1052.

Brandriss, M. C. (1979). Isolation and preliminary characterization of *Saccharomyces cerevisiae* proline auxotrophs. *J. Bacteriol.* 138, 816–822.

Brandriss, M. C., and Falvey, D. A. (1992). Proline biosynthesis in *Saccharomyces cerevisiae*: molecular analysis of the *PRO1* gene, which encodes γ-glutamyl kinase. *J. Bacteriol.* 174, 4148–4156. doi: 10.1128/jb.174.12.4148-4156.1992

Brodsky, J. L. (2012). Cleaning up : ER-associated degradation to the rescue. *Cell* 151, 1163–1167. doi: 10.1016/j.cell.2012.11.012

Cardona, F., Carrasco, P., Pérez-Ortín, J. E., Olmo, M. I., and Aranda, A. (2007). A novel approach for the improvement of stress resisitance in wine yeasts. *Int. J. Food Microbiol.* 114, 83–91. doi: 10.1016./j.ijfoodmicro.2006.10.043

Causton, H. C., Ren, B., Koh, S. S., Harbison, C. T., Kanin, E., Jennings, E. G., et al. (2001). Remodeling of yeast genome expression in response to environmental changes. *Mol. Biol. Cell.* 12, 323–337. doi: 10.1091/mbc.12.2.323

Chattopadhyay, M. K., Kern, R., Mistou, M. Y., Dandekar, A. M., Uratsu, S. L., and Richarme, G. (2004). The chemical chaperone proline relieves the thermosensitivity of a *dnaK* deletion mutant at 42°C. *J. Bacteriol.* 186, 8149–8152. doi: 10.1128/JB.186.23.8149-8152.2004

Chen, E. J., and Kaiser, C. A. (2002). Amino acids regulate the intracellular trafficking of the general amino acid permease of *Saccharomyces cerevisiae*. *Proc. Natl. Acad. Sci. U. S. A.* 99, 14837–14842. doi: 10.1073/pnas.232591899

Chernova, T. A., Allen, K. D., Wesoloski, L. M., Shanks, J. R., Chernoff, Y. O., and Wilkinson, K. D. (2003). Pleiotropic effects of Ubp6 loss on drug sensitivities

and yeast prion are due to depletion of the free ubiquitin pool. *J. Biol. Chem.* 278, 52102–52115. doi: 10.1074/jbc.M310283200

Chi, Y., Huddleston, M. J., Zhang, X., Young, R. A., Annan, R. S., Carr, S. A., et al. (2001). Negative regulation of Gcn4 and Msn2 transcription factors by Srb10 cyclin-dependent kinase. *Genes Dev.* 15, 1078–1092. doi: 10.1101/gad.867501

Csonka, L. N., and Hanson, A. D. (1991). Prokaryotic osmoregulation: genetics and physiology. *Ann. Rev. Microbiol.* 45, 569–606. doi: 10.1146/annurev.mi.45.100191.003033

Didion, T., Regenberg, B., Jørgensen, M. U., Kielland-Brandt, M. C., and Andersen, H. A. (1998). The permease homologue Ssy1p controls the expression of amino acid and peptide transporter genes in *Saccharomyces cerevisiae*. *Mol. Microbiol.* 27, 643–650. doi: 10.1046/j.1365-2958.1998.00714.x

Drakulic, T., Temple, M. D., Guido, R., Jarolim, S., Breitenbach, M., Attfield, P. V., et al. (2005). Involvement of oxidative stress response genes in redox homeostasis, the level of reactive oxygen species, and ageing in *Saccharomyces cerevisiae*. *FEMS Yeast Res.* 5, 1215–1228. doi: 10.1016/j.femsyr.2005.06.001

Durchschlag, E., Reiter, W., Ammerer, G., and Schüller, C. (2004). Nuclear localization destabilizes the stress-regulated transcription factor Msn2. *J. Biol. Chem.* 279, 55425–55432. doi: 10.1074/jbc.M407264200

Eastmond, D. L., and Nelson, H. C. M. (2006). Genome-wide analysis reveals new roles for the activation domains of the *Saccharomyces cerevisiae* heat shock transcription factor (Hsf1) during the transient heat shock response. *J. Biol. Chem.* 281, 32909–32921. doi: 10.1074/jbc.M602454200

Elfving, N., Chereji, R. V., Bharatula, V., Bjorklund, S., Morozov, A. V., and Broach, J. R. (2014). A dynamic interplay of nucleosome and Msn2 binding regulates kinetics of gene activation and repression following stress. *Nucleic Acids Res.* 42, 5468–5482. doi: 10.1093/nar/gku176

Estruch, F. (2000). Stress-controlled transcription factors, stress-induced genes and stress tolerance in budding yeast. *FEMS Microbiol. Rev.* 24, 469–486. doi: 10.1111/j.1574-6976.2000.tb00551.x

Estruch, F., and Carlson, M. (1993). Two homologous zinc finger genes identified by multicopy suppression in a SNF1 protein kinase mutant of *Saccharomyces cerevisiae*. *Mol. Cell Biol.* 13, 3872–3881. doi: 10.1128/MCB.13.7.3872

Finley, D., Ulrich, H. D., Sommer, T., and Kaiser, P. (2012). The ubiquitin-proteasome system of *Saccharomyces cerevisiae*. *Genetics* 192, 319–360. doi: 10.1534/genetics.112.140467

Fontana, L., Partridge, L., and Longo, V. D. (2010). Extending healthy life span-from yeast to humans. *Science* 328, 321–326. doi: 10.1126/science.1172539

Forsberg, H., Gilstring, C. F., Zargari, A., Martínez, P., and Ljungdahl, P. O. (2001). The role of the yeast plasma membrane SPS nutrient sensor in the metabolic response to extracellular amino acids. *Mol. Microbiol.* 42, 215–228. doi: 10.1046/j.1365-2958.2001.02627.x

Gardner, B. M., Pincus, D., Gotthardt, K., Gallagher, C. M., and Walter, P. (2013). Endoplasmic reticulum stress sensing in the unfolded protein response. *Cold Spring Harb. Perspect. Biol.* 5:a013169. doi: 10.1101/cshperspect.a013169

Gardner, R. G., Nelson, Z. W., and Gottschling, D. E. (2005). Degradation-mediated protein quality control in the nucleus. *Cell* 120, 803–815. doi: 10.1016/j.cell.2005.01.016

Gasch, A. P. (2003). "The environmental stress response : a common yeast response to diverse environmental stresses," in *Yeast Stress Response,* eds S. Hohmann and W. H. Mager (Berlin: Springer-Verlag), 11–70.

Gasch, A. P., Spellman, P. T., Kao, C. M., Carmel-Harel, O., Eisen, M. B., Storz, G., et al. (2000). Genomic expression programs in the response of yeast cells to environmental changes. *Mol. Biol. Cell.* 11, 4241–4257. doi: 10.1091/mbc.11.12.4241

Georis, I., Feller, A., Tate, J. J., Cooper, T. G., and Dubois, E. (2009). Nitrogen catabolite repression-sensitive transcription as a readout of Tor pathway regulation: the genetic background, reporter gene and GATA factor assayed determine the outcomes. *Genetics* 181, 861–874. doi: 10.1534/genetics.108.099051

Goldberg, A. L. (2003). Protein degradation and protection against misfolded or damaged proteins. *Nature* 426, 895–899. doi: 10.1038/nature02263

Golovanov, A. P., Hautbergue, G. M., Wilson, S. A., and Lian, L. Y. (2004). A simple method for improving protein solubility and long-term stability. *J. Am. Chem. Soc.* 126, 8933–8939. doi: 10.1021/ja049297h

Gonzalez, A., and Hall, M. N. (2017). Nutrient sensing and TOR signaling in yeast and mammals. *EMBO J.* 36, 397–408. doi: 10.15252/embj.201696010

Görner, W., Durchschlag, E., Martinez-Pastor, M. T., Estruch, F., Ammerer, G., Hamilton, B., et al. (1998). Nuclear localization of the C_2H_2 zinc finger protein Msn2p is regulated by stress and protein kinase A activity. *Genes Dev.* 12, 586–597. doi: 10.1101/gad.12.4.586

Görner, W., Durchschlag, E., Wolf, J., Brown, E. L., Ammerer, G., Ruis, H., et al. (2002). Acute glucose starvation activates the nuclear localization signal of a stress-specific yeast transcription factor. *EMBO J.* 21, 135–144. doi: 10.1093/emboj/21.1.135

Gray, J. V., Petsko, G. A., Johnston, G. C., Ringe, D., Singer, R. A., and Werner-Washburne, M. (2004). "Sleeping beauty": quiescence in *Saccharomyces cerevisiae*. *Microbiol. Mol. Biol. Rev.* 68:187206. doi: 10.1128/MMBR.68.2.187

Grenson, M., Hou, C., and Crabeel, M. (1970). Multiplicity of the amino acid permeases in *Saccharomyces cerevisiae* IV. Evidence for a general amino acid permease. *J. Bacteriol.* 103, 770–777.

Haitani, Y., and Takagi, H. (2008). Rsp5 is required for the nuclear export of mRNA of *HSF1* and *MSN2/4* under stress conditions in *Saccharomyces cerevisiae*. *Genes Cells* 13, 105–116. doi: 10.1111/j.1365-2443.2007.01154.x

Hanna, J., Leggett, D. S., and Finley, D. (2003). Ubiquitin depletion as a key mediator of toxicity by translational inhibitors. *Mol. Cell. Biol.* 23, 9251–9261. doi: 10.1128/MCB.23.24.9251

Harshman, K. D., Moye-Rowley, W. S., and Parker, C. S. (1988). Transcriptional activation by the SV40 AP-1 recognition element in yeast is mediated by a factor similar to AP-1 that is distinct from GCN4. *Cell* 53, 321–330. doi: 10.1016/0092-8674(88)90393-5

Hasan, R., Leroy, C., Isnard, A.-D., Labarre, J., Boy-Marcotte, E., and Toledano, M. B. (2002). The control of the yeast H_2O_2 response by the Msn2/4 transcription factors. *Mol. Microbiol.* 45, 233–241. doi: 10.1046/j.1365-2958.2002.03011.x

Haynes, C. M., and Ron, D. (2010). The mitochondrial UPR–protecting organelle protein homeostasis. *J. Cell Sci.* 123, 3849–3855. doi: 10.1242/jcs.075119

Hiraishi, H., Shimada, T., Ohtsu, I., Sato, T., and Takagi, H., (2009). The yeast ubiquitin ligase Rsp5 downregulates the alpha subunit of nascent polypeptide-associated complex Egd2 under stress conditions. *FEBS J.* 276, 5287–5297. doi: 10.1111/j.1742-4658.2009.07226.x

Hofman-Bang, J. (1999). Nitrogen catabolite repression in *Saccharomyces cerevisiae*. *Mol. Biotechnol.* 12, 35–73. doi: 10.1385/MB:12:1:35

Iraqui, L., Vissers, S., Bernard, F., Craene, J. D. E., Boles, E., Urrestarazu, A., et al. (1999). Amino acid signaling in *Saccharomyces cerevisiae* : a permease-like sensor of external amino acids and F-Box protein Grr1p are required for transcriptional induction of the *AGP1* gene, which encodes a broad-specificity amino acid permease. *Mol. Cell. Biol.* 19, 989–1001. doi: 10.1128/MCB.19.2.989

Izawa, S., Ikeda, K., Ohdate, T., and Inoue, Y. (2007). Msn2p/Msn4p-activation is essential for the recovery from freezing stress in yeast. *Biochem. Biophys. Res. Commun.* 352, 750–755. doi: 10.1016/j.bbrc.2006.11.100

Jack, D. L., Paulsen, I. T., and Saier, J. (2000). The amino acid/polyamine/organocation (APC) superfamily of transporters specific for amino acids, polyamines and organocations. *Microbiology* 146, 1797–1814. doi: 10.1099/00221287-146-8-1797

Jones, C. B., Ott, E. M., Keener, J. M., Curtiss, M., Sandrin, V., and Babst, M. (2012). Regulation of membrane protein degradation by starvation-response pathways. *Traffic* 13, 468–482. doi: 10.1111/j.1600-0854.2011.01314.x

Kaino, T., Tateiwa, T., Mizukami-Murata, S., Shima, J., and Takagi, H. (2008). Self-cloning baker's yeasts that accumulate proline enhance freeze tolerance in doughs. *Appl. Environ. Microbiol.* 74, 5845–5849. doi: 10.1128/AEM.00998-08

Kandror, O., Bretschneider, N., Kreydin, E., Cavalieri, D., and Goldberg, A. L. (2004). Yeast adapt to near-freezing temperatures by STRE/Msn2,4-dependent induction of trehalose synthesis and certain molecular chaperones. *Mol. Cell* 13, 771–781. doi: 10.1016/S1097-2765(04)00148-0

Kavi Kishor, P. B., and Sreenivasulu, N. (2014). Is proline accumulation *per se* correlated with stress tolerance or is proline homeostasis a more critical issue? *Plant Cell Environ.* 37, 300–311. doi: 10.1111/pce.12157

Kimura, Y., and Tanaka, K. (2010). Regulatory mechanisms involved in the control of ubiquitin homeostasis. *J. Biochem.* 147, 793–798. doi: 10.1093/jb/mvq044

Kimura, Y., Yashiroda, H., Kudo, T., Koitabashi, S., Murata, S., Kakizuka, A., et al. (2009). An inhibitor of a deubiquitinating enzyme regulates ubiquitin homeostasis. *Cell* 137, 549–559. doi: 10.1016/j.cell.2009.02.028

Kitagaki, H., and Takagi, H. (2014). Mitochondrial metabolism and stress response of yeast: application in fermentation technologies. *J. Biosci. Bioeng.* 117:383–393. doi: 10.1016/j/jbiosc.2013.09.011

Krishnan, N., Dickman, M. B., and Becker, D. F. (2008). Proline modulates the intracellular redox environment and protects mammalian cells against oxidative stress. *Free Radic. Biol. Med.* 44, 671–681. doi: 10.1016/j.freeradbiomed.2007.10.054

Lee, P., Kim, M. S., Paik, S.-M., Choi, S.-H., Cho, B.-R., and Hahn, J.-S. (2013). Rim15-dependent activation of Hsf1 and Msn2/4 transcription factors by direct phosphorylation in *Saccharomyces cerevisiae*. *FEBS Lett.* 587, 3648–3655. doi: 10.1016/j.febslet.2013.10.004

Liang, X., Zhang, L., Natarajan, S. K., and Becker, D. F. (2013). Proline mechanisms of stress survival. *Antioxid. Redox Signal.* 19, 998–1011. doi: 10.1089/ars.2012.5074

Ljungdahl, P. O. (2009). Amino-acid-induced signalling via the SPS-sensing pathway in yeast. *Biochem. Soc. Trans.* 37, 242–247. doi: 10.1042/BST0370242

Ljungdahl, P. O., and Daignan-Fornier, B. (2012). Regulation of amino acid, nucleotide, and phosphate metabolisn in *Saccharomyces cerevisiae*. *Genetics* 190, 885–929. doi: 10.1534/genetics.111.133306

MacGurn, J. A. (2014). Garbage on, garbage off: new insights into plasma membrane protein quality control. *Curr. Opin. Cell Biol.* 29, 92–98. doi: 10.1016/j.ceb.2014.05.001

Mager, W. H., and De Kruijff, A. J. J. (1995). Stress-induced transcriptional activation. *Microbiol. Rev.* 59, 506–531.

Maggio, A., Miyazaki, S., Veronese, P., Fujita, T., Ibeas, J. I., Damsz, B., et al. (2002). Does proline accumulation play an active role in stress-induced growth reduction? *Plant J.* 31, 699–712. doi: 10.1046/j.1365-313X.2002.01389.x

Marchler, G., Schüller, C., Adam, G., and Ruis, H. (1993). A *Saccharomyces cerevisiae* UAS element controlled by protein kinase A activates transcription in response to a variety of stress conditions. *EMBO J.* 12, 1997–2003. doi: 10.1002/jsfa.2740301103

Martínez-Pastor, M. T., Marchler, G., Schüller, C., Marchler-Bauer, A., Ruis, H., and Estruch, F. (1996). The *Saccharomyces cerevisiae* zinc finger proteins Msn2p and Msn4p are required for transcriptional induction through the stress response element (STRE). *EMBO J.* 15, 2227–2235. doi: 10.1002/j.1460-2075.1996.tb00576.x

Mat Nanyan, N. S., Watanabe, D., Sugimoto, Y., and Takagi, H. (2019a). Involvement of the stress-responsive transcription factor gene *MSN2* in the control of amino acid uptake in *Saccharomyces cerevisiae*. *FEMS Yeast Res.* 19:foz052. doi: 10.1093/femsyr/foz052

Mat Nanyan, N. S., Watanabe, D., Sugimoto, Y., and Takagi, H. (2019b). Effect of the deubiquitination enzyme gene *UBP6* on the stress-responsive transcription factor Msn2-mediated control of the amino acid permease Gnp1 in yeast. *J. Biosci. Bioeng.* 129, 423–427. doi: 10.1016/j.jbiosc.2019.10.002

Matsuura, K., and Takagi, H. (2005). Vacuolar functions are involved in stress-protective effect of intracellular proline in *Saccharomyces cerevisiae*. *J. Biosci. Bioeng.* 100, 538–544. doi: 10.1263/jbb.100.538

Miles, S., Li, L., Davison, J., and Breeden, L. L. (2013). Xbp1 directs global repression of budding yeast transcription during the transition to quiescence and is important for the longevity and reversibility of the quiescent state. *PLoS Genet.* 9:e1003854. doi: 10.1371/journal.pgen.1003854

Morita, Y., Nakamori, S., and Takagi, H. (2002). Effect of proline and arginine metabolism on freezing stress of *Saccharomyces cerevisiae*. *J. Biosci. Bioeng.* 94, 390–394. doi: 10.1016/S1389-1723(02)80214-6

Morita, Y., Nakamori, S., and Takagi, H. (2003). L-proline accumulation and freeze tolerance in *Saccharomyces cerevisiae* are caused by a mutation in the *PRO1* gene encoding γ-glutamyl kinase. *Appl. Environ. Microbiol.* 69, 212–219. doi: 10.1128/AEM.69.1.212-219.2003

Moskvina, E., Schüller, C., Maurer, C. T. C., Mager, W. H., and Ruis, H. (1998). A search in the genome of *Saccharomyces cerevisiae* for genes regulated via stress response elements. *Yeast* 14, 1041–1050. doi: 10.1002/(SICI)1097-0061(199808)14:11<1041::AID-YEA296>3.0.CO;2-4

Moye-Rowley, W. S., Harshman, K. D., and Parker, C. S. (1989). Yeast *YAP1* encodes a novel form of the jun family of transcriptional activator proteins. *Genes Dev.* 3, 283–292. doi: 10.1101/gad.3.3.283

Mukai, Y., Kamei, Y., Liu, X., Jiang, S., Sugimoto, Y., Mat Nanyan, N., et al. (2019). Proline metabolism regulates replicative lifespan in the yeast *Saccharomyces cerevisiae*. *Microb. Cell.* 6, 482–490. doi: 10.15698/mic2019.10.694

Natarajan, K., Meyer, M. R., Jackson, B. M., Slade, D., Roberts, C., Hinnebusch, A. G., et al. (2001). Transcriptional profiling shows that Gcn4p is a master regulator of gene expression during amino acid starvation in yeast. *Mol. Cell. Biol.* 21, 4347–4368. doi: 10.1128/MCB.21.13.4347

Nelissen, B., De Wachter, R., and Goffeau, A. (1997). Classification of all putative permeases and other membrane plurispanners of the major facilitator superfamily encoded by the complete genome of *Saccharomyces cerevisiae*. *FEMS Microbiol. Rev.* 21, 113–134. doi: 10.1016/S0168-6445(97)00053-3

Nillegoda, N. B., Theodoraki, M. A., Mandal, A. K., Mayo, K. J., Ren, H. Y., Sultana, R., et al. (2010). Ubr1 and Ubr2 function in a quality control pathway for degradation of unfolded cytosolic proteins. *Mol. Biol. Cell.* 21, 2102–2116. doi: 10.1091/mbc.E10

Nishimura, A., Kotani, T., Sasano, Y., and Takagi, H. (2010). An antioxidative mechanism mediated by the yeast N-acetyltransferase Mpr1: oxidative stress-induced arginine synthesis and its physiological role. *FEMS Yeast Res.* 10, 687–698. doi: 10.1111/j.1567-1364.2010.00650.x

Reiter, W., Klopf, E., De Wever, V., Anrather, D., Petryshyn, A., Roetzer, A., et al. (2013). Yeast protein phosphatase 2A-Cdc55 regulates the transcriptional response to hyperosmolarity stress by regulating Msn2 and Msn4 chromatin recruitment. *Mol. Cell. Biol.* 33, 1057–1072. doi: 10.1128/MCB.00834-12

Rosenbaum, J. C., and Gardner, R. G. (2011). How a disordered ubiquitin ligase maintains order in nuclear protein homeostasis. *Nucleus* 2, 264–270. doi: 10.4161/nucl.2.4.16118

Ruis, H., and Schüller, C. (1995). Stress signaling in yeast. *BioEssays* 17, 959–965. doi: 10.1002/bies.950171109

Sadeh, A., Baran, D., Volokh, M., and Aharoni, A. (2012). Conserved motifs in the Msn2-activating domain are important for Msn2-mediated yeast stress response. *J. Cell Sci.* 125, 3333–3342. doi: 10.1242/jcs.096446

Sadeh, A., Movshovich, N., Volokh, M., Gheber, L., and Aharoni, A. (2011). Fine-tuning of the Msn2/4-mediated yeast stress responses as revealed by systematic deletion of Msn2/4 partners. *Mol. Biol. Cell* 22, 3127–3138. doi: 10.1091/mbc.E10-12-1007

Sasaki, T., and Takagi, H. (2013). Phosphorylation of a conserved Thr357 in yeast Nedd4-like ubiquitin ligase Rsp5 is involved in down-regulation of the general amino acid permease Gap1. *Genes Cells* 18, 459–475. doi: 10.1111/gtc.12049

Sasano, Y., Haitani, Y., Hashida, K., Ohtsu, I., Shima, J., and Takagi, H. (2012a). Overexpression of the transcription activator Msn2 enhances the fermentation ability of industrial baker's yeast in frozen dough. *Biosci. Biotechnol. Biochem.* 76, 624–627. doi: 10.1271/bbb.110959

Sasano, Y., Haitani, Y., Hashida, K., Ohtsu, I., Shima, J., and Takagi, H. (2012b). Simultaneous accumulation of proline and trehalose in industrial baker's yeast enhances fermentation ability in frozen dough. *J. Biosci. Bioeng.* 113, 592–595. doi: 10.1016/j.jbiosc.2011.12.018

Sasano, Y., Haitani, Y., Ohtsu, I., Shima, J., and Takagi, H. (2012c). Proline accumulation in baker's yeast enhances high-sucrose stress tolerance and fermentation ability in sweet dough. *Int. J. Food Microbiol.* 152, 40–43. doi: 10.1016/j.ijfoodmicro.2011.10.004

Sasano, Y., Watanabe, D., Ukibe, K., Inai, T., Ohtsu, I., Shimoi, H., et al. (2012d). Overexpression of the yeast transcription activator Msn2 confers furfural resistance and increases the initial fermentation rate in ethanol production. *J. Biosci. Bioeng.* 113, 451–455. doi: 10.1016/j.jbiosc.2011.11.017

Schmitt, A. P., and McEntee, K. (1996). Msn2p, a zinc finger DNA-binding protein, is the transcriptional activator of the multistress response in *Saccharomyces cerevisiae*. *Biochemistry* 93, 5777–5782. doi: 10.1073/pnas.93.12.5777

Sekine, T., Kawaguchi, A., Hamano, Y., and Takagi, H. (2007). Desensitization of feedback inhibition of the *Saccharomyces cerevisiae* γ-glutamyl kinase enhances proline accumulation and freezing tolerance. *Appl. Environ. Microbiol.* 73, 4011–4019. doi: 10.1128/AEM.00730-07

Sharma, S. S., and Dietz, K. J. (2006). The significance of amino acids and amino acid-derived molecules in plant responses and adaptation to heavy metal stress. *J. Exp. Bot.* 57, 711–726. doi: 10.1093/jxb/erj073

Shiga, T., Yoshida, N., Shimizu, Y., Suzuki, E., Sasaki, T., Watanabe, D., et al. (2014). Quality control of plasma membrane proteins by *Saccharomyces cerevisiae* Nedd4-like ubiquitin ligase Rsp5p under environmental stress conditions. *Eukaryot. Cell* 13, 1191–1199. doi: 10.1128/EC.00104-14

Shiraki, K., Kudou, M., Fujiwara, S., Imanaka, T., and Takagi, M. (2002). Biophysical effect of amino acids on the prevention of protein aggregation. *J. Biochem.* 132, 591–595. doi: 10.1093/oxfordjournals.jbchem.a003261

Simon, J. R., Treger, J. M., and McEntee, K. (1999). Multiple independent regulatory pathways control *UBI4* expression after heat shock in *Saccharomyces cerevisiae*. *Mol. Cell. Biol.* 31, 823–832. doi: 10.1046/j.1365-2958.1999.01220.x

Sleator, R., and Hill, C. (2001). Bacterial osmoadaptation: the role of osmolytes in bacterial stress and virulence. *FEMS Microbiol. Rev.* 25, 49–71. doi: 10.1016/S0168-6445(01)00071-7

Smith, B. J., and Yaffe, M. P. (1991). A mutation in the yeast heat-shock factor gene causes temperature-sensitive defects in both mitochondrial protein import and the cell cycle. *Mol. Cell. Biol.* 11, 2647–2655. doi: 10.1016/0962-8924(91)90074-J

Sorger, P. K. (1990). Yeast heat shock factor contains separable transient and sustained response transcriptional activators. *Cell* 62, 793–805. doi: 10.1016/0092-8674(90)90123-V

Springael, J. Y., and André, B. (1998). Nitrogen-regulated ubiquitination of the Gap1 permease of *Saccharomyces cerevisiae*. *Mol. Biol. Cell.* 9, 1253–1263. doi: 10.1091/mbc.9.6.1253

Takagi, H. (2008). Proline as a stress protectant in yeast: physiological functions, metabolic regulations, and biotechnological applications. *Appl. Microbiol. Biotechnol.* 81, 211–223. doi: 10.1007/s00253-008-1698-5

Takagi, H., Iwamoto, F., and Nakamori, S. (1997). Isolation of freeze-tolerant laboratory strains of *Saccharomyces cerevisiae* from proline-analogue-resistant mutants. *Appl. Microbiol. Biotechnol.* 47, 405–411. doi: 10.1007/s002530050948

Takagi, H., Sakai, K., Morida, K., and Nakamori, S. (2000). Proline accumulation by mutation or disruption of the proline oxidase gene improves resistance to freezing and desiccation stresses in *Saccharomyces cerevisiae*. *FEMS Microbiol. Lett.* 184, 103–108. doi: 10.1111/j.1574-6968.2000.tb08998.x

Takagi, H., Taguchi, J., and Kaino, T. (2016). Proline accumulation protects *Saccharomyces cerevisiae* cells in the stationary phase from ethanol stress by reducing reactive oxygen species levels. *Yeast* 33, 355–363. doi: 10.1002/yea.3154

Ter Schure, E. G., Van Riel, N. A. W., and Verrips, C. T. (2000). The role of ammonia metabolism in nitrogen catabolite repression in *Saccharomyces cerevisiae*. *FEMS Microbiol. Rev.* 24, 67–83. doi: 10.1016/S0168-6445(99)00030-3

Theodoraki, M. A., Nillegoda, N. B., Saini, J., and Caplan, A. J. (2012). A network of ubiquitin ligases is important for the dynamics of misfolded protein aggregates in yeast. *J. Biol. Chem.* 287, 23911–23922. doi: 10.1074/jbc.M112.341164

Thibault, G., and Ng, D. T. W. (2012). The endoplasmic reticulum-associated degradation pathways of budding yeast. *Cold Spring Harb. Perspect. Biol.* 4:a013193. doi: 10.1101/cshperspect.a013193

Tomenchok, D. M., and Brandriss, M. C. (1987). Gene-enzyme relationships in the proline biosynthetic pathway of *Saccharomyces cerevisiae*. *J. Bacteriol.* 169, 5364–5372. doi: 10.1128/jb.169.12.5364-5372.1987

Toone, W. M., and Jones, N. (1998). Stress-activated signalling pathways in yeast. *Genes Cells* 3, 485–498. doi: 10.1046/j.1365-2443.1998.00211.x

Trotter, E. W., Berenfeld, L., Krause, S. A., Petsko, G. A., and Gray, J. V. (2001). Protein misfolding and temperature up-shift cause G1 arrest via a common mechanism dependent on heat shock factor in *Saccharomyces cerevisiae*. *Proc. Natl. Acad. Sci. U. S. A.* 98, 7313–7318. doi: 10.1073./pnas.121172998

Tsolmonbaatar, A., Hashida, K., Sugimoto, Y., Watanabe, D., Furukawa, S., and Takagi, H. (2016). Isolation of baker's yeast mutants with proline accumulation that showed enhanced tolerance to baking-associated stresses. *Int. J. Food Microbiol.* 238: 233–240. doi: 10.1016/j.ijfoodmicro.2016.09.015

Turcu, F. E. R., Ventii, K. H., and Wilkinson, K. D. (2009). Regulation and cellular roles of ubiquitin-specific deubiquitinating enzymes. *Annu. Rev. Biochem.* 78, 363–397. doi: 10.1146/annurev.biochem.78.082307.091526

Watanabe, M., Tamura, K., Magbanua, J. P., Takano, K., Kitamoto, K., Kitagaki, H., et al. (2007). Elevated expression of genes under the control of stress response element (STRE) and Msn2p in an ethanol-tolerance sake yeast Kyokai no. 11. *J. Biosci. Bioeng.* 104, 163–170. doi: 10.1263/jbb.104.163

Watanabe, M., Watanabe, D., Akao, T., and Shimoi, H. (2009). Overexpression of *MSN2* in a sake yeast strain promotes ethanol tolerance and increases ethanol production in sake brewing. *J. Biosci. Bioeng.* 107, 516–518. doi: 10.1016/j.jbiosc.2009.01.006

Weids, A. J., and Grant, C. M. (2014). The yeast peroxiredoxin Tsa1 protects against protein-aggregate-induced oxidative stress. *J. Cell. Sci.* 127, 1327–1335. doi: 10.1242/jcs.144022

Wu, H., Ng, B. S. H., and Thibault, G. (2014). Endoplasmic reticulum stress response in yeast and humans. *Biosci. Rep.* 34, 321–330. doi: 10.1042/BSR20140058

Xu, S., Falvey, D. A., and Brandriss, M. C. (1995). Roles of *URE2* and *GLN3* in the proline utilization pathway in *Saccharomyces cerevisiae*. *Mol. Cell. Biol.* 15, 2321–2330. doi: 10.1128/MCB.15.4.2321

Zhang, J., Pavlova, N. N., and Thompson, C. B. (2017). Cancer cell metabolism: the essential role of the non-essential amino acid, glutamine. *EMBO J.* 36, 1302–1315. doi: 10.15252/embj.201696151

Zhao, Y., MacGurn, J. A., Liu, M., and Emr, S. (2013). The ART-Rsp5 ubiquitin ligase network comprises a plasma membrane quality control system that protects yeast cells from proteotoxic stress. *ELife.* 2, 1–18. doi: 10.7554/eLife.00459

Zhu, X., Garrett, J., Schreve, J., and Michaeli, T. (1996). *GNP1*, the high-affinity glutamine permease of *S. cerevisiae*. *Curr. Genet.* 30, 107–114. doi: 10.1007/s002940050108

Conflict of Interest: The authors declare that the research was conducted in the absence of any commercial or financial relationships that could be construed as a potential conflict of interest.

frontiers in Genetics

ORIGINAL RESEARCH
published: 30 April 2020
doi: 10.3389/fgene.2020.00293

Transcriptional Activity and Protein Levels of Horizontally Acquired Genes in Yeast Reveal Hallmarks of Adaptation to Fermentative Environments

*Joaquín Devia[1,2], Camila Bastías[1,2], Eduardo I. Kessi-Pérez[1], Carlos A. Villarroel[2,3], Matteo De Chiara[4], Francisco A. Cubillos[2,3], Gianni Liti[4], Claudio Martínez[1,5] and Francisco Salinas[1,2,6]**

[1] Centro de Estudios en Ciencia y Tecnología de los Alimentos (CECTA), Universidad de Santiago de Chile (USACH), Santiago, Chile, [2] Millennium Institute for Integrative Biology (iBio), Santiago, Chile, [3] Departamento de Biología, Facultad de Química y Biología, Universidad de Santiago de Chile (USACH), Santiago, Chile, [4] CNRS, INSERM, IRCAN, Université Côte d'Azur, Nice, France, [5] Departamento de Ciencia y Tecnología de los Alimentos, Facultad Tecnológica, Universidad de Santiago de Chile (USACH), Santiago, Chile, [6] Instituto de Bioquímica y Microbiología, Facultad de Ciencias, Universidad Austral de Chile (UACH), Valdivia, Chile

OPEN ACCESS

Edited by:
Feng Gao,
Tianjin University, China

Reviewed by:
Virginie Galeote,
INRA UMR 1083 Unité Mixte de Recherches Sciences Pour l'Enologie, France
Mark A. McCormick,
The University of New Mexico, United States

***Correspondence:**
Francisco Salinas
francisco.salinas@uach.cl

Specialty section:
This article was submitted to Evolutionary and Genomic Microbiology, a section of the journal Frontiers in Genetics

Received: *11 December 2019*
Accepted: *11 March 2020*
Published: *30 April 2020*

Citation:
Devia J, Bastías C, Kessi-Pérez EI, Villarroel CA, De Chiara M, Cubillos FA, Liti G, Martínez C and Salinas F (2020) Transcriptional Activity and Protein Levels of Horizontally Acquired Genes in Yeast Reveal Hallmarks of Adaptation to Fermentative Environments. Front. Genet. 11:293. doi: 10.3389/fgene.2020.00293

In the past decade, the sequencing of large cohorts of *Saccharomyces cerevisiae* strains has revealed a landscape of genomic regions acquired by Horizontal Gene Transfer (HGT). The genes acquired by HGT play important roles in yeast adaptation to the fermentation process, improving nitrogen and carbon source utilization. However, the functional characterization of these genes at the molecular level has been poorly attended. In this work, we carried out a systematic analysis of the promoter activity and protein level of 30 genes contained in three horizontally acquired regions commonly known as regions A, B, and C. In three strains (one for each region), we used the luciferase reporter gene and the *mCherry* fluorescent protein to quantify the transcriptional and translational activity of these genes, respectively. We assayed the strains generated in four different culture conditions; all showed low levels of transcriptional and translational activity across these environments. However, we observed an increase in protein levels under low nitrogen culture conditions, suggesting a possible role of the horizontally acquired genes in the adaptation to nitrogen-limited environments. Furthermore, since the strains carrying the luciferase reporter gene are null mutants for the horizontally acquired genes, we assayed growth parameters (latency time, growth rate, and efficiency) and the fermentation kinetics in this set of deletion strains. The results showed that single deletion of 20 horizontally acquired genes modified the growth parameters, whereas the deletion of five of them altered the maximal CO_2 production rate (Vmax). Interestingly, we observed a correlation between growth parameters and Vmax for an ORF within region A, encoding an ortholog to a thiamine (vitamin B1) transporter whose deletion decreased the growth rate, growth efficiency, and CO_2 production. Altogether, our results provided molecular and phenotypic evidence highlighting the importance of horizontally acquired genes in yeast adaptation to fermentative environments.

Keywords: horizontal gene transfer, yeast, transcriptional activity, protein levels, fermentation

INTRODUCTION

The widespread use of the budding yeast *Saccharomyces cerevisiae* as a eukaryotic model organism led to the sequencing of the genome of this microorganism more than 20 years ago (Goffeau et al., 1996). In addition, a broad range of biotechnological applications has encouraged the genome sequencing of numerous yeast strains associated with different productive activities (Borneman and Pretorius, 2015; Liti, 2015). Currently, the variety of sequenced strains includes isolates from domesticated settings, such as vineyards, breweries, cheese, dairy, and clinical environments as well as wild strains isolated from non-domesticated environments, such as forests, flowers, and tree bark (Liti et al., 2009; Novo et al., 2009; Borneman et al., 2011; Wang et al., 2012; Bergström et al., 2014; Strope et al., 2015; Legras et al., 2018; Peter et al., 2018). In this sense, the "1002 yeast genomes project" is the most comprehensive collection of the genetic variation of yeast, encompassing the genome information of 1011 isolates from diverse geographical origins and ecological niches and describing 26 clades within the yeast population structure (Peter et al., 2018).

The extensive amount of sequencing information accumulated so far has revealed a unique set of genetic features in the yeast genome, which are often related to their adaptation to specific niches (Legras et al., 2018). These genetic hallmarks are frequently absent in the yeast reference genome (lab strain S288C) and, in general, they have been acquired by introgression (probably through mating) from a closely related species or by Horizontal Gene Transfer (HGT) from a more distant species (Morales and Dujon, 2012). In the HGT process, the donor species has a distant phylogenetic relationship with the acceptor species, with both species coexisting in the same ecological niche (Fitzpatrick, 2012). In general terms, the HGT process in eukaryotes is triggered under specific (stressful) environmental conditions, where the acceptor species incorporates the foreign DNA into its genome by an unknown mechanism (Keeling and Palmer, 2008). Currently, detection of HGT is performed by phylogenetic methods to identify genes with a different evolutionary trajectory with respect to the host genes (Roelofs and Van Haastert, 2001; Keeling and Palmer, 2008; Ravenhall et al., 2015).

Multiple HGT events have been described in different yeast species, thus demonstrating the impact of these genomic regions on the adaptation to specific environments (Gojkovic et al., 2004; Novo et al., 2009; Kominek et al., 2019). After the sequencing of the *S. cerevisiae* genome was completed, at least 10 potential cases of HGT from bacteria were identified, including genes related to biotin utilization and pyrimidine biosynthesis (Gojkovic et al., 2004; Hall et al., 2005; Hall and Dietrich, 2007). Recently, the acquisition of an entire operon into the yeast clade *Wickerhamiella/Starmerella* from an ancient bacterium (close to the modern enterobacteriaceae) was described, allowing these yeasts to produce enterobactin and improving their adaptation to the insect gut environment (Kominek et al., 2019). Similarly, in the same clade, the thiamine (vitamin B1) biosynthesis pathway was assembled using genes and operons acquired by HGT from bacteria (Gonçalves and Gonçalves, 2019). This evidence has highlighted the importance of the transcriptional and translational activity of the genes acquired by HGT in the context of the acceptor species, in which the promoter structure, codon usage, and transcription and translation machineries differ at the molecular level between prokaryotes and eukaryotes. Furthermore, even if the two species (donor and acceptor) are eukaryotes, codon usage differences between species may impair the expression of the horizontally acquired genes.

Eukaryote-to-eukaryote HGT events have also been described in yeast, especially under the stressful conditions faced during the fermentation process. Analysis of the genome sequence of the French wine strain EC1118, widely used for Chardonnay wine production, revealed unique genetic features, including three regions not present in the reference genome: region A (38 Kb) carries 12 Open Reading Frames (ORFs), region B (17 Kb) contains 5 ORFs, and region C (65 Kb) harbors 17 ORFs (Novo et al., 2009). Region B was acquired from *Zygosaccharomyces bailii*, a species commonly found in grape must and that coexists with *S. cerevisiae* at the beginning of the fermentation process (Novo et al., 2009). Interestingly, region B replicates through a circular intermediate, explaining the copy number variations observed between yeast strains (Galeote et al., 2011). In a similar way, the subtelomeric regions A and C were acquired from the *Torulaspora* genus, and many species from this genus cohabit with *S. cerevisiae* at the beginning of grape fermentation (Marsit et al., 2015). Several functional genomics efforts have been performed to uncover the cellular and molecular processes in which these horizontally acquired genes play a role. For instance, region C contains the *FSY1* gene, which has been functionally characterized as a fructose transporter, showing the importance of this horizontally acquired gene in the fermentation process since fructose is one of the main sugars present in grape must (Galeote et al., 2010). The region C also includes ORFs related to oligopeptide transport (*FOT* genes), which confer an important adaptive advantage, expanding the sources of nitrogen utilized by wine yeasts during grape must fermentation (Marsit et al., 2015, 2016). Furthermore, region C contains the *XDH1* gene, which encodes for a xylitol dehydrogenase necessary for yeast growth in xylose (Wenger et al., 2010). However, beyond these examples, other genes within these regions have been putatively associated with nitrogen and carbon source transport and metabolism, processes in which they may play important roles in the adaptation of yeast to the fermentation process.

Horizontal gene transfer is not restricted to wine strains of *S. cerevisiae*, as recent sequencing projects have shown that HGT is an extended phenomenon present in yeast isolated from different ecological niches (Legras et al., 2018; Peter et al., 2018). The recent genome sequencing of 82 strains isolated from human-associated environments identified 42 horizontally acquired regions, which are under non-neutral evolution and are important for niche-specific adaptation (Legras et al., 2018). Similarly, several additional horizontally acquired regions were identified by the "1002 yeast genomes project." Here, most of the isolates carry at least one candidate HGT region in the genome (Peter et al., 2018). Current sequencing information has become a powerful resource for functional genomics, allowing researchers to explore the molecular roles of horizontally acquired genes.

However, an important aspect is the molecular detection of the functional activation of these genes, which is of critical importance if the horizontally acquired genes are to participate in yeast adaptation to different environments. So far, there has been a scarce amount of molecular evidence supporting this assumption.

In this work, we used information from the "1002 yeast genomes project" to select three strains carrying the horizontally acquired regions A, B, or C. In these strains, we systematically assayed the transcriptional and translational activity of all the HGT genes, using both the luciferase reporter gene and the *mCherry* fluorescent protein, respectively. These two collections of transformed strains were assayed in four different culture conditions, and while they showed low levels of transcriptional and translational activity across the environments, we observed a general increase in protein levels under nitrogen-limited conditions. Furthermore, we showed that single deletion of several horizontally acquired genes impairs the growth parameters (latency time, growth rate, and efficiency) and fermentation kinetics. Overall, our results provided molecular and phenotypic evidence confirming the substantial role of the horizontally acquired genes in yeast adaptation to the fermentative environment.

MATERIALS AND METHODS

Strains and Culture Conditions

The three strains used in this work (ALL, AHG, and BSS) were part of the "1002 yeast genomes project" (Peter et al., 2018). These strains belong to the Wine/European clade and were isolated from different geographical and ecological origins (**Supplementary Table 1**). These strains were selected based on the information of copy number for each horizontally acquired region (A, B, or C) per haploid genome described by Peter et al. (2018). Specifically, ALL carries a hemizygotic region A in its genome, AHG is haploid and contains region B, whilst BSS harbors region C in hemizygosis (**Supplementary Table 2**). All the strains used and generated in this work are listed in the **Supplementary Table 1**.

The strains were maintained in media YPDA (2% glucose, 2% peptone, 1% yeast extract, and 2% agar) at 30°C. The microcultivation experiments were carried out in 96-well plates with 300 μL of culture medium at 30°C. We used four culture conditions: Synthetic Complete (SC) medium (2% glucose, 0.67% YNB without amino acids and 0.2% complete mix of amino acids); YNB (2% glucose and 0.67% YNB without amino acids); Synthetic Must (SM300) with 300 mg/L of Yeast Assimilable Nitrogen (YAN) (Kessi-Perez et al., 2019a; Molinet et al., 2019); and Synthetic Must (SM60) with 60 mg/L of YAN (Kessi-Perez et al., 2019a; Molinet et al., 2019).

Genomic Information and Bioinformatic Analyses

The genome sequencing information of ALL, AHG, and BSS strains was obtained from the "1002 yeast genomes project" (Peter et al., 2018). The overlapping DNA contigs of regions A, B, and C were assembled using the *de novo* assembler tool from the Geneious 8.1.8 software (Biomatters, New Zealand). The ORFs inside regions A, B, and C were manually annotated using information from the EC1118 genome and the "1002 yeast genomes project" (Novo et al., 2009; Peter et al., 2018). Then, the ORFs were translated and analyzed using blastp from the blast suit of the NCBI[1] and SGD databases[2] for the identification of orthologous genes in the S228c genome (**Table 1**). The Codon Adaptation Index (CAI) was calculated for each ORF within the three horizontally acquired regions using the CAI calculator (Puigbò et al., 2008). This was performed using the codon usage of *S. cerevisiae* as acceptor species and the codon usage of *Z. bailii* (region B) and *T. delbrueckii* (region A and C) as donor species. We used the codon usage information of *T. delbrueckii* because it was the only one available for a yeast of the *Torulaspora* genus in the Codon Usage Database (Nakamura et al., 2000).

The promoter region of each gene inside regions A, B, and C was scanned for transcription factor binding sites, using the YeTFaSCo database (De Boer and Hughes, 2012). We considered as a promoter the 700 bp upstream of the start codon (ATG) of each ORF and used the whole intergenic region if the distance to the ORF upstream was inferior to 700 bp. We retrieved the information for transcription factor binding sites with non-dubious motifs from YeTFaSCo (**Supplementary Table 3**).

Transcriptional Activity Assays

Transcriptional activity was assayed, replacing the target gene with the luciferase reporter, and generating a transcriptional fusion of the promoter region. We replaced the entire coding sequence of the target horizontally acquired genes, from the start codon to the stop codon, using the constructs *Luc-HphMx* or *Luc-NatMx*, which carry the hygromycin (*HphMx*) or nourseothricin (*NatMx*) cassettes as selective markers, respectively (Salinas et al., 2016; Tapia et al., 2018). These genetic constructs encode a destabilized version of the luciferase gene, which contains an ARE sequence for mRNA destabilization and a PEST sequence for proteasome mediated degradation of the protein (Rienzo et al., 2012). The *Luc-HphMx* and *Luc-NatMx* constructs were amplified by PCR using a Phusion flash high-fidelity master mix (Thermo Fisher Scientific, United States) according to the manufacturer's instructions. The primers used in the PCR reactions contain 20 bp for the amplification of the *Luc-HphMx* or *Luc-NatMx* constructs and 50 bp for direct recombination with the target gene (**Supplementary Table 4**). The *Luc-HphMx* PCR products were used to transform the ALL and BSS strains, and the *Luc-NatMx* PCR products were used to transform the AHG strain. Strain transformation was carried out using the standard lithium acetate and heat shock protocol (Gietz and Schiestl, 2007). Transformed strains were selected on YPDA plates supplemented with 100 μg/mL hygromycin or 300 μg/mL nourseothricin, as appropriate. Positive colonies were confirmed by standard colony PCR using GoTaq Green Master Mix (Promega, United States) according to the manufacturer's instructions.

[1] https://blast.ncbi.nlm.nih.gov/Blast.cgi

[2] https://yeastgenome.org/blast-sgd

The luciferase expression assays were carried out in microcultivation experiments using 96-well plates with 300 μL of culture medium at 30°C. SC, YNB, SM300, and SM60 culture medias supplemented with 0.1 mM luciferin were used (Salinas et al., 2016). The experiments were conducted in a Synergy HTX plate reader (BioTek, United States) for the simultaneous measurement of $OD_{600\ nm}$ and luminescence (Lum) every 30 min. The raw luminescence and OD_{600} data

TABLE 1 | Putative functions and orthologous genes for horizontally acquired genes.

Order in the HGT region (annotation name)*	*S. cerevisiae* strain (donor species)	Hypothetical function	EC1118 or S288C ortholog
A1 (0012)	ALL (*Torulaspora sp.*)	Hypothetical protein, putative monoxygenase	No ortholog found
A2 (0023)	ALL (*Torulaspora sp.*)	Enoyl reductase-like, probably dehydrogenase (D-arabinose 1-dehydrogenase)	*YCR102C/YNL134C/YLR460C*
A3 (0034)	ALL (*Torulaspora sp.*)	Sugar (or other) transporter, probably hexose transporter, or plasma membrane high glucose sensor	*RGT2/HXT10/HXT5/STL1/SNF3*
A4 (0045)	ALL (*Torulaspora sp.*)	Aldehyde reductase	*YDR541C/GRE2/ARI1*
A5 (0056)	ALL (*Torulaspora sp.*)	Galactose mutarotase-like, probably UDP-glucose-4-epimerase	*GAL10*
A6 (0078)	ALL (*Torulaspora sp.*)	Fungal transcription factor, probably involved in regulating lysine biosynthesis	*LYS14*
A7 (0089)	ALL (*Torulaspora sp.*)	Arginase	*CAR1*
A8 (0100)	ALL (*Torulaspora sp.*)	Member of the multidrug and toxic compound extrusion (MATE) family, probably Na + -driven multidrug efflux pump	*ERC1/YDR338C*
A9 (0111)	ALL (*Torulaspora sp.*)	Contains a solute binding domain of nucleobase-cation-symport-1 (NCS1) transporter NRT1-like, probably transporter of thiamine or related compound	*THI72/THI7*
A10 (0133)	ALL (*Torulaspora sp.*)	Methyltransferase	*COQ5*
A11 (0144)	ALL (*Torulaspora sp.*)	FAD/FMN-containing dehydrogenase, probably 2-hydroxyglutarate transhydrogenase and minor D-lactate dehydrogenase	*DLD3/DLD2*
A12 (0155)	ALL (*Torulaspora sp.*)	2-Nitropropane dioxygenase or nitronate monooxygenase	*YJR149W*
B24 (0056)	AHG (*Z. bailii*)	Fungal transcription factor	*STB4*
B25 (0012)	AHG (*Z. bailii*)	5-oxoprolinase	*OXP1*
B26 (0023)	AHG (*Z. bailii*)	Member of the Major Facilitator Superfamily (MFS), probably sugar phosphate permease (D-galactonate transporter) or high affinity nicotinic acid plasma membrane permease	*TNA1*
B27 (0034)	AHG (*Z. bailii*)	Flocculation or pseudohypha formation, contains a Flo11 domain	*FLO11*
B28 (0045)	AHG (*Z. bailii*)	Contains a fungal specific transcription factor domain	No ortholog found
C42 (6480)	BSS (*T. microellipsoides*)	Contains a fungal transcription factor domain	*PUT3*
C43 (6491)	BSS (*T. microellipsoides*)	Member of the Major Facilitator Superfamily (MFS), probably allantoate transporter	*SEO1*
C44 (6502)	BSS (*T. microellipsoides*)	Contains a solute binding domain of solute carrier families 5 and 6-like, probably related to amino acid transporter. Oligopeptide transporter.	*FOT1/AVT5/AVT6*
C45 (6524)	BSS (*T. microellipsoides*)	Superoxide dismutase, probably mitochondrial manganese superoxide dismutase	*SOD2*
C46 (6535)	BSS (*T. microellipsoides*)	Ferric reductase with similarity to Fre2p	*FRE7*
C47 (6546)	BSS (*T. microellipsoides*)	Mannitol-1-phosphate/altronate dehydrogenase or mannitol dehydrogenase	*DSF1*
C48 (6557)	BSS (*T. microellipsoides*)	Sugar transporter, probably hexose transporter or transmembrane polyol transporter	*HXT13/HXT17/HXT15/HXT16/GAL2*
C49 (6568)	BSS (*T. microellipsoides*)	Plasma membrane protein, probably ammonium permease	*ATO3*
C50 (6579)	BSS (*T. microellipsoides*)	Galactose mutarotase-like, probably aldose 1-epimerase or UDP-glucose-4-epimerase	*YNR071C/YHR210C/GAL10*
C51 (6612)	BSS (*T. microellipsoides*)	Short-chain dehydrogenase/reductase, probably NADP-dependent mannitol dehydrogenase or peroxisomal 2,4-dienoyl-CoA reductase	*SPS19*
C52 (6623)	BSS (*T. microellipsoides*)	Threonine dehydrogenase or related Zn-dependent dehydrogenase, sorbitol or xylitol dehydrogenase	*XDH1/SOR2/SOR1*
C53 (6634)	BSS (*T. microellipsoides*)	Sugar (or other) transporter, fructose symporter (fructose/H + symporter) or myo-inositol transporter	*FSY1/ITR2/ITR1/CIN10/HXT17/HXT13*
C54 (6645)	BSS (*T. microellipsoides*)	Y' element-encoded DNA helicase	*YRF1-7/YRF1-6/YRF1-1*
C55 (6656)	BSS (*T. microellipsoides*)	Y' element-encoded DNA helicase	*YRF1-7/YRF1-6/YRF1-1*

**ORF order according to the "1002 yeast genomes project" information and annotation name according to the EC1118 strain genome.*

(**Supplementary Figure 1**) of each strain was normalized, dividing the luminescence by the OD_{600} of the cell culture ($Lum/OD_{600\ nm}$). Then, the area under the normalized curves was calculated using the GraphPad Prism 6 software (GraphPad, United States). The total area values were employed as a measurement of the global transcriptional activity for the horizontally acquired genes in a period of 24 h (**Supplementary Figure 2**; Kessi-Perez et al., 2019b). The *TDH3* ORF was replaced by the luciferase reporter gene in the ALL, AHG, and BSS strains and used as a positive control in the luciferase expression experiments. All assays were carried out with three biological replicas.

Protein Level Assays

The protein levels were assayed by replacing the stop codon of the target gene by the gene encoding the *mCherry* fluorescent protein, generating a translational fusion. The stop codon was replaced using the *mCherry-HphMx* or *mCherry-NatMx* constructs, which carry either the hygromycin (*HphMx*) or the nourseothricin (*NatMx*) cassettes as selective markers (Tapia et al., 2018). The *mCherry-HphMx* and *mCherry-NatMx* constructs were amplified by PCR using Phusion flash high-fidelity master mix (Thermo Fisher Scientific, United States) according to the manufacturer's instructions. The primers used in the PCR reactions contain 20 bp for amplification of the *mCherry-HphMx* or *mCherry-NatMx* constructs, and 50 bp for direct recombination with the stop codon of the target genes (**Supplementary Table 4**). The *mCherry-HphMx* PCR products were used to transform the ALL and BSS strains, and the *mCherry-NatMx* PCR products were used to transform the AHG strain. Strain transformation was carried out using the standard lithium acetate and heat shock protocol (Gietz and Schiestl, 2007). Transformed strains were selected on YPDA plates supplemented with 100 μg/mL hygromycin or 300 μg/mL nourseothricin, as appropriate. Positive colonies were confirmed by standard colony PCR using GoTaq Green Master Mix (Promega, United States), according to the manufacturer's instructions. Additionally, stop codon removal in the positive colonies was confirmed by Sanger sequencing of the PCR product (Macrogen Inc., South Korea), which was amplified using primers close to the 3' end of each horizontally acquired gene (**Supplementary Table 4**).

Levels of *mCherry* fluorescent protein were assayed in microcultivation experiments using 96-well plates with 300 μL culture medium (SC, YNB, SM300, and SM60) at 30°C. The experiments were conducted in a Synergy HTX plate reader (BioTek, United States), for the simultaneous measurement of $OD_{600\ nm}$ and fluorescence (Fluo) every 30 min. Fluorescence data were normalized by the OD_{600} data ($Fluo/OD_{600\ nm}$), and the normalized values were corrected by the auto-fluorescence of the wild type strains. Since the *mCherry* fluorescent protein accumulates in the cells over the time course of the experiments, the last time point (24 h) was used to compare the protein levels between horizontally acquired genes. The stop codon of the *TDH3* gene was replaced by the *mCherry* fluorescent protein in strains ALL, AHG, and BSS and used as a positive control in the fluorescence experiments. All assays were performed with three biological replicas.

Growth Curves and Fermentation Experiments

The growth curves of the strains carrying the luciferase reporter gene (deletion strains) were performed in microcultivation experiments using 96-well plates with 300 μL culture medium (SC, YNB, SM300, or SM60) at 30°C. The $OD_{600\ nm}$ of the cell cultures was measured every 30 min using a Synergy HTX plate reader (Biotek, United States). The kinetic parameters were automatically extracted from the growth curves using the Gompertz equation (Zwietering et al., 1990; Yin et al., 2003), which was incorporated as a function in the GraphPad Prism 6 software (GraphPad, United States). The kinetic parameters analyzed for each strain were the latency time (Lag), growth rate (Rate), and growth efficiency (Efficiency) (Warringer and Blomberg, 2003). These phenotypes were normalized, dividing the phenotypes of the strains carrying gene deletions by the phenotypes of their respective wild type strain (ALL, AHG, or BSS), and represented as a heat map using the Heatmapper web server (Babicki et al., 2016). In addition, the phenotypes of each strain were individually compared with respect to the phenotypes of the corresponding wild type version. All experiments were performed with three biological replicas.

The strains carrying the luciferase reporter gene (deletion strains) were also phenotyped by laboratory scale fermentation. These experiments were conducted in 250 mL bottles with 150 mL SM300 medium, using a water bath to control the temperature at 25°C and a magnetic stir plate at 150 rpm to homogenize the cell culture. The fermentations were inoculated with 1×10^6 cells/mL, and progression was monitored every 24 h by CO_2 release, measured as the weight loss during the time course of the experiment. The fermentations were finalized once stable weight loss measurements were recorded (Kessi-Perez et al., 2019a). The CO_2 loss curves were fitted to a sigmoid non-linear regression and the first derivative was calculated to obtain the maximal CO_2 production rate (Vmax) of each strain (Marullo et al., 2006; Molinet et al., 2019). All fermentation experiments were carried out with three biological replicas.

Statistical Analyses

The statistical comparisons for the different data sets were performed using the Student's *t*-test, assuming an unpaired data comparison and a non-parametric distribution of the data using the Mann-Whitney test ($p < 0.05$). All statistical analyses were carried out using GraphPad Prism 6 software (GraphPad, United States).

RESULTS

Genetic Structure and Putative Biological Function of the Horizontally Acquired Regions

For this study, we used information from the "1002 yeast genomes" initiative. As a means to facilitate the posterior genetic analyses and molecular biology manipulations, we selected three strains with a single copy per genome of the horizontally acquired

regions A, B, and C. Thus, we selected the ALL strain for the analysis of region A, the AHG strain for region B, and the BSS strain for region C (**Supplementary Table 2**). Then, we used the genomic information of the EC1118 strain and of the "1002 yeast genomes project" to assemble a full contig, and subsequently annotate the ORFs (> 100 aa) for each region in the selected strains (**Figure 1**). In general, the genetic structure of the three regions was analogous to that observed in the EC1118 strain (Novo et al., 2009).

The putative biological function of the ORFs within each region was extracted from the EC1118 strain genome and the "1002 yeast genomes project" information (**Table 1**). In addition, we translated each ORF *in silico* and performed a blastp alignment against both the NCBI and the fungal SGD databases, allowing us to identify orthologous genes in the reference genome (S288C strain) (**Table 1**). As expected, most of the genes within the three regions have putative functions in the transport and metabolism of carbon and nitrogen sources (**Table 1**). Altogether, the observed genetic structure and hypothetical biological functions for the genes encoded in regions A, B, and C in their respective strains (ALL, AHG, and BSS) do not show differences compared to the regions in the EC1118 strains.

Low Levels of Transcriptional and Translational Activity of the Horizontally Acquired Genes

To assess transcriptional activity and protein levels of each ORF inside regions A, B, and C, we performed a molecular characterization using two different approaches. First, we replaced each ORF with the luciferase reporter gene, generating simultaneously a transcriptional fusion of the promoter region and the deletion of the ORF (**Figure 2**). This procedure was successfully applied to all the ORFs inside regions A, B, and C, except ORF C54, which could not be successfully transformed and was therefore discarded from posterior analyses. Thus, we generated a collection of 30 strains (collection 1), which was assayed for luciferase expression in four different culture conditions (SC, YNB, SM300, and SM60), allowing us to measure the transcriptional activity as the total area under the normalized luminescence curves (**Figure 2**). We observed transcriptional activity for eleven horizontally acquired genes in the different culture conditions evaluated, detecting activity in at least one media for ORFs A5, A6, and A10 for region A; B25 and B26 for region B; and C43, C44, C47, C50, C51, and C52 for region C (**Supplementary Figures 1, 2**). Interestingly, the ORF B25 showed transcriptional activity in the four conditions assayed, whereas ORF B26 was active in SC and fermentative conditions (SM300 and SM60) (**Supplementary Figures 1, 2**). We also observed transcriptional activity for the *FOT1* gene (C44) in YNB, SM300, and SM60 but not in complete medium (SC) (**Supplementary Figures 1, 2**), which is consistent with previous reports that show that *FOT1* is expressed under fermentative conditions (Marsit et al., 2015, 2016). Similarly, we were not able to detect transcriptional activity for the *FSY1* gene (C53) in the assayed culture conditions (**Supplementary Figure 3**), consistent with the described repression of this gene under high levels of glucose (Galeote et al., 2010). Overall, we cannot discard transcriptional activity for the other ORFs present in the analyzed regions, whose promoter regions could have transcriptional activity below the detection level of our destabilized reporter gene. Alternatively, these promoters may have a cryptic behavior or be inactive in the culture conditions assayed. To explore this idea, we scanned the promoter region of each ORF using the YeTFasCo database for yeast transcription factors binding sites, confirming that all ORFs contain multiple and different sites for yeast transcription factor binding in their promoter regions (**Supplementary Table 3**), suggesting that all the ORFs should be transcriptionally active under specific environmental conditions. Interestingly, most of the ORFs (23 out of 31) contain a *GLN3* motif in their promoter regions, suggesting that they play an important role under nitrogen-limited conditions (**Supplementary Table 3**).

Secondly, we further characterized regions A, B, and C by assessing the protein level produced by the ORFs inside these regions. For this, we replaced the stop codon of each ORF with the *mCherry* fluorescent protein, generating a translational fusion (**Figure 2**). This procedure generated a collection of

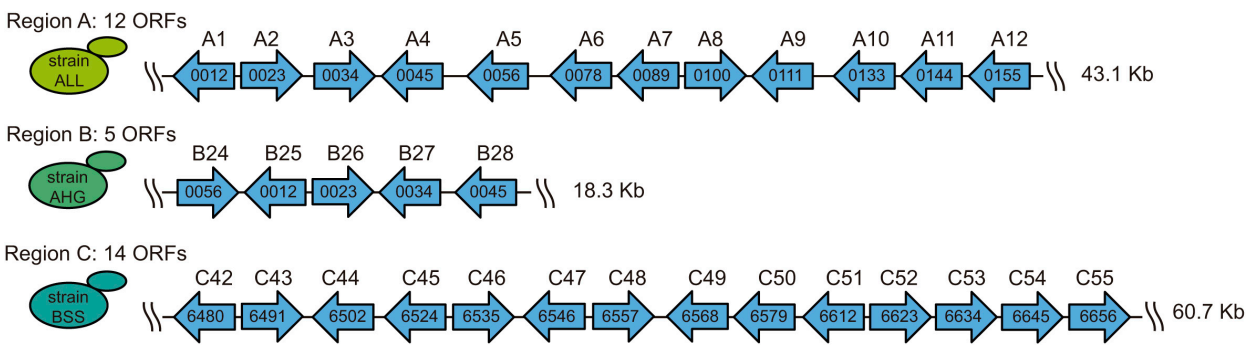

FIGURE 1 | Genetic structure of the horizontally acquired regions. The horizontally acquired regions A, B, and C are present in a single copy per genome in the ALL, AHG, and BSS strains, respectively. The ORFs and their orientation within each region are indicated by arrows. The name inside each ORF corresponds to the annotation according to the genome information of the EC1118 strain. The name above each ORF represents the order in the horizontally acquired region according to the "1002 yeast genomes project" information.

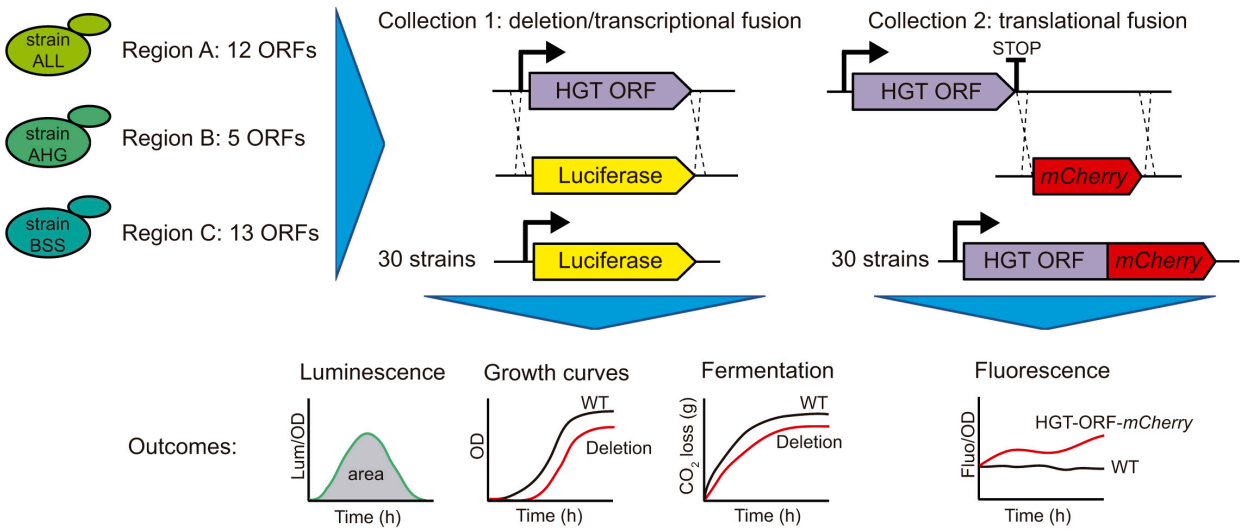

FIGURE 2 | Overview of the molecular characterization of the horizontally acquired regions. In the three selected strains, the ORFs acquired by Horizontal Gene Transfer (HGT) were replaced by the luciferase reporter gene, generating the transcriptional fusion of the promoter region and deletion of the target gene (Collection 1). This collection was assayed for luciferase expression, kinetic parameters using growth curves and fermentation kinetics by laboratory scale fermentations. Similarly, the stop codon of the target genes was replaced by the *mCherry* fluorescent protein, generating a translational fusion (Collection 2). This collection was assayed for *mCherry* fluorescent protein expression.

30 strains (collection 2), which was assayed for *mCherry* fluorescence in the same four different culture conditions (SC, YNB, SM300, and SM60), allowing us to compare the protein levels produced by the horizontally acquired genes (**Figure 2**). We observed detectable levels of *mCherry* protein in at least one of the culture conditions assayed for all the ORFs analyzed (**Supplementary Figure 2**). These results support the idea that all the ORFs present in the horizontally acquired regions are indeed active, even though we were not able to detect their transcriptional activity using a destabilized version of the luciferase reporter gene. Alternatively, the ORFs maybe under cryptic transcription, and we were capable of detecting the *mCherry* fusion proteins due to their accumulation over the time course of the experiment (24 h). However, all ORFs that displayed a luciferase signal also produced the *mCherry* fluorescent protein signal (**Supplementary Figure 2**). Interestingly, the protein levels of six ORFs inside region C (C43, C44, C45, C48, C49, and C53) increased in culture conditions with limited amino acid availability (YNB and SM60) (**Figure 3** and **Supplementary Figure 4**), with the rise being more pronounced in a nitrogen-limited fermentative condition (SM60) (**Figure 3** and **Supplementary Figure 4**). These data confirm the importance of region C for the adaptation of yeast to this environmental condition. Finally, we assessed whether the protein levels measured are influenced by the codon usage differences between the acceptor (*S. cerevisiae*) and donor (*Z. bailii* or *Torulaspora sp.*) species. On calculating the Codon Adaptation Index (CAI) for each ORF of the horizontally acquired regions, we observed a CAI superior to 0.65 for all genes (**Supplementary Figure 5**), confirming that codon usage does not limit protein synthesis. Altogether, our results support the idea that horizontally acquired genes are active in the strains analyzed, showing low levels of transcriptional and translational activity, but with an increase in protein levels under nitrogen-limited conditions for a subset of ORFs from region C.

Deletion of Horizontally Acquired Genes Affects Yeast Growth Parameters and Fermentation Kinetics

Collection 1, whose strains carry the luciferase reporter gene, are also a gene deletion collection for the horizontally acquired genes (**Figure 2**). Therefore, we performed growth curves for these strains, extracting three kinetic parameters (lag time, growth rate, and growth efficiency), and compared these phenotypes to the respective wild type strains (**Figure 4**). We also compared the kinetic parameters across different culture conditions using the normalized phenotypic information (**Figure 4**). In general, we observed that most of the phenotypic differences occur under fermentative conditions (SM300) or nitrogen-limited fermentation conditions (SM60) (**Figure 4**). Importantly, 20 of the 30 strains carrying single ORF deletions showed a statistically significant phenotypic difference compared to the wild type strain in at least one of the culture conditions assayed, with most of the phenotypic differences observed in SM60 medium (**Figure 4**). Interestingly, several gene deletions had the combined effects of increasing the lag time and decreasing the growth rate and growth efficiency with respect to the wild type strain (**Figure 4**). For instance, this finding was observed in ORFs A3 (SM60), A5 (SM60), A7 (SC and SM60), A9 (SM300), C43 (SM60), C44 (SM60), C45 (SM60), and C49 (SM60) (**Figure 4**), suggesting an important contribution of these genes in the maintenance of yeast kinetic parameters in the assayed conditions.

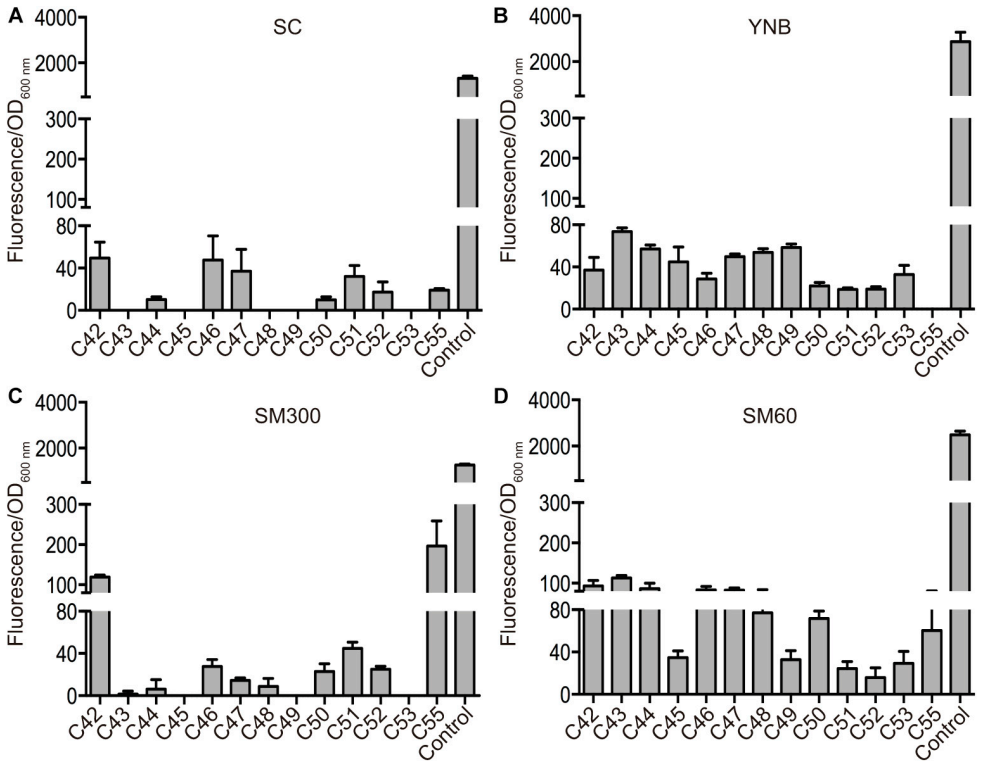

FIGURE 3 | Protein levels of horizontally acquired genes in region C. The protein levels produced by the ORFs inside region C were measured as normalized *mCherry* fluorescence in four culture conditions: SC **(A)**, YNB **(B)**, SM300 **(C)**, and SM60 **(D)**. The translational fusion of the *THD3* gene was used as positive control in all the experiments. The average values of three independent biological replicas (± standard error) are shown.

In order to further investigate the phenotypic effects of our gene deletion collection for horizontally acquired genes over a fermentative phenotype, we performed laboratory scale fermentation in SM300 medium. We monitored the fermentation progress as CO_2 release, measuring the weight loss every 24 h. Then, we fitted the curves to a sigmoid non-linear regression and calculated the first derivative to extract the maximal CO_2 production rate (Vmax) (**Supplementary Figure 6**). This phenotype provided information of when nitrogen is depleted and correlates with the nitrogen demand of the yeast strains (Marullo et al., 2006). The phenotypic information of each strain was compared to the phenotype of the wild type counterpart. Deletion of ORFs A9, C47, C50, and C51 significantly decreased the maximal CO_2 production rate compared to their respective wild type strains (**Figure 5**). The results for ORF A9 correlate well with the phenotypes observed in microcultivation experiments, where a significant reduction in the growth rate and growth efficiency was observed in SM300 (**Figure 4A**). ORF A9 encodes a putative thiamine (vitamin B1) transporter, which is an essential vitamin for amino acid and carbohydrate metabolism during fermentation (Trevelyan and Harrison, 1954). Surprisingly, ORF C42 deletion, encoding a putative transcription factor ortholog to *PUT3,* was the only one that showed a significant increase in the maximal CO_2 production rate compared to the BSS wild type strain (**Figure 5**). Altogether, our results provided strong molecular and phenotypic evidence that highlights the importance of horizontally acquired genes in yeast adaptation to the fermentative environment.

DISCUSSION

The contribution of the HGT process in the configuration of eukaryotic genomes is receiving renewed attention, especially in *S. cerevisiae*, where large-scale sequencing projects have revealed that HGT is a very extensive phenomenon (Legras et al., 2018; Peter et al., 2018). Recently, the molecular incompatibilities between donor and acceptor species have been pointed out, especially in the context of HGT events from bacteria to the yeast clade *Wickerhamiella/Starmerella* (Gonçalves and Gonçalves, 2019; Kominek et al., 2019). The molecular differences between prokaryotes and eukaryotes in the promoter region structure, codon usage, and transcription and translation machineries are barriers to the expression of the horizontally acquired genes (Kominek et al., 2019). If we consider the HGT process in the context of two eukaryotic species (donor and acceptor), the molecular barriers for expression of the horizontally acquired genes should be inferior; however, there is scarce evidence to support this assumption.

We studied the horizontally acquired regions A, B, and C, initially described in the genome of the wine strain EC1118 (Novo et al., 2009), to gain an overview of the molecular processes

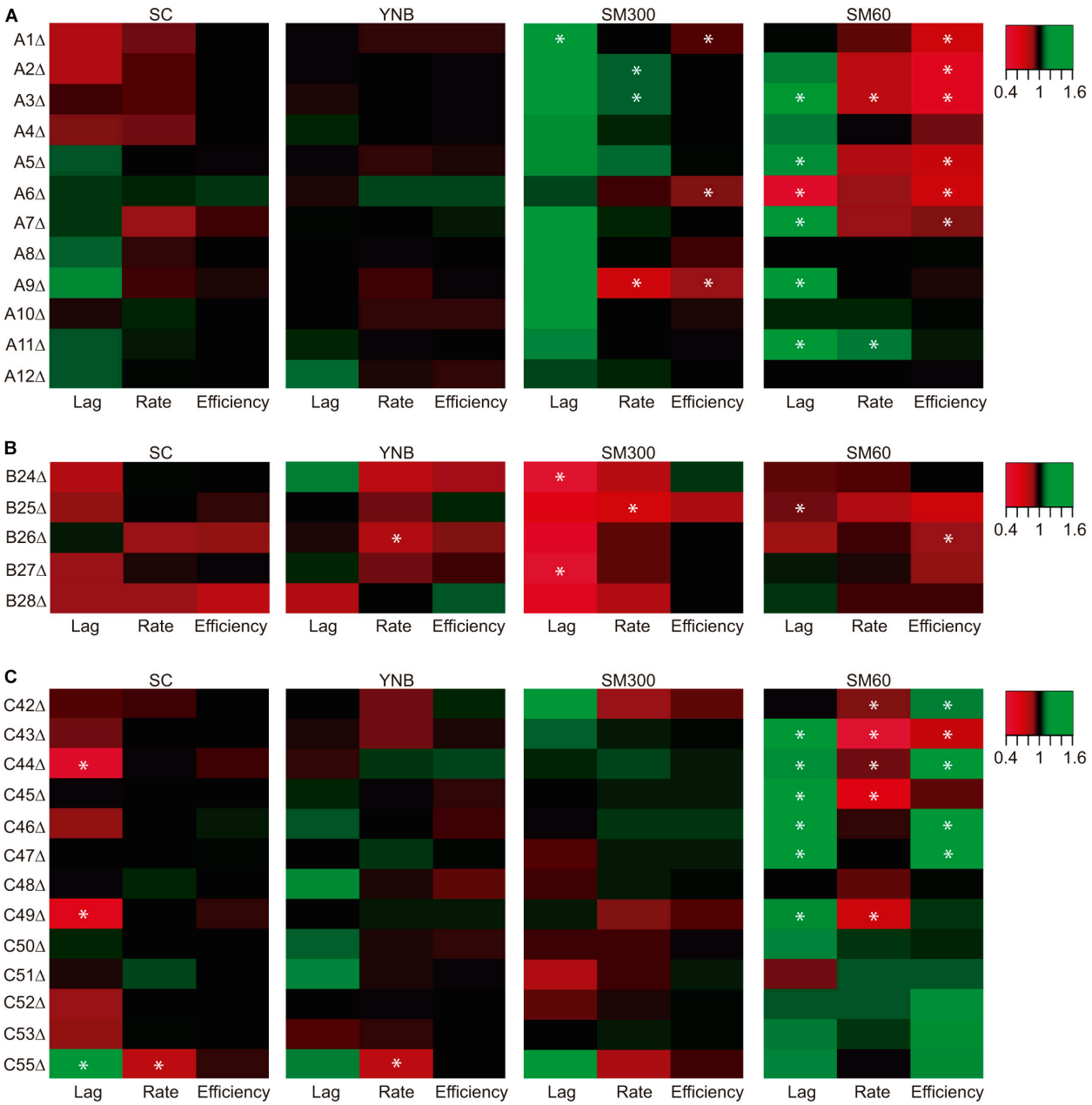

FIGURE 4 | Kinetic parameters for strains carrying deletions in horizontally acquired genes. The strains carrying deletions in different horizontally acquired genes inside region A **(A)**, region B **(B)**, and region C **(C)** were grown in four culture conditions (SC, YNB, SM300, and SM60). The kinetic parameters were extracted from the growth curves for the phenotypic comparison of latency time (Lag), growth rate (Rate) and growth efficiency (Efficiency). The normalized phenotypic values are represented as a heat map where the wild type phenotype has a value equal to 1 in the color scale, and red and green represent lower and higher values of the phenotypes respect to the wild type strain, respectively. Asterisks represent a statistically significant difference between the phenotype of the strain carrying the deletion and its wild type version (*t*-test, $p < 0.05$). The heat map was constructed with the average values of three biological replicas.

underlying the horizontally acquired genes inside those regions and in the genetic context of the acceptor species (*S. cerevisiae*). The genes harbored by these regions have been functionally categorized in the transport and metabolism of nitrogen and carbon sources (Novo et al., 2009). In fact, region C contains the *FOT* genes and the *FSY1* gene, which encode for oligopeptide transporters and a fructose transporter, respectively. These genes make a strong contribution to the fermentative capacities of the EC1118 strain (Galeote et al., 2010; Marsit et al., 2015, 2016). However, other genes contained in region C and genes within regions A and B have received less attention, and their involvement in yeast adaptation is less clear. In our work, three strains were chosen that have genetic backgrounds that facilitate the molecular dissection of the horizontally acquired regions,

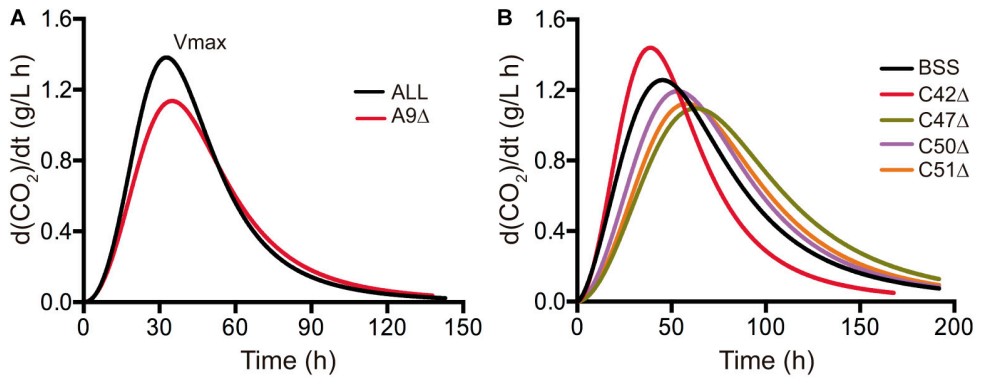

FIGURE 5 | Maximal CO_2 production rate of strains carrying deletions in horizontally acquired genes. Strains carrying single deletions in different horizontally acquired genes and showing statistically significant differences (*t*-test, $p < 0.05$) with respect to the wild type phenotype are shown for region A **(A)** and region C **(B)**. Small scale fermentations in 150 mL of SM300 medium were performed for each strain and CO_2 release was measured as weight loss every 24 h. The CO_2 release curves were fitted to a sigmoid non-linear regression and the first derivative was calculated to obtain the maximal CO_2 production rate (Vmax, peak of the curves). The average values of three biological replicates are shown.

carrying a single copy per genome of these regions, with a similar genetic structure and ORF content to that of the EC1118 strain (Novo et al., 2009). Regions A, B, and C from the selected strains have a similar structure to the regions described in the EC1118 strain (Novo et al., 2009), containing the same number of ORFs inside regions A and B compared to the EC1118 strain (**Figure 1**). In region C, we identified a lower number of ORFs because we did not consider ORFs encoding proteins of less than 100 amino acids. We also examined the putative function of the annotated ORFs in the selected strains using information from the EC1118 strain, the "1002 yeast genomes project" and a blastp search strategy (**Table 1**). In general, we confirmed that the annotated ORFs have possible functions in the transport and metabolism of nitrogen and carbon sources (**Table 1**). Altogether, these results are not unexpected if we consider that selected strains belong to the fermentative Wine/European phylogenetic clade (**Supplementary Table 1**; Peter et al., 2018).

We assessed the transcriptional and translational activity for each ORF within the horizontally acquired regions A, B, and C (**Figure 2**). Using the luciferase reporter gene, we observed low levels of transcriptional activity for 11 of the 30 horizontally acquired genes (**Supplementary Figures 1, 2**). However, the translational reporter (*mCherry*) was consistently detected for all the horizontally acquired genes assayed in at least one culture condition (**Supplementary Figure 2**). These results allowed us to compare the protein levels produced by the horizontally acquired genes in four culture conditions (**Supplementary Figure 2**). Interestingly, multiple ORFs within region C suffered an increase in protein levels under nitrogen-limited fermentation conditions (**Figure 3** and **Supplementary Figure 4**), confirming the importance of this genomic region in yeast adaptation to the fermentation process (Marsit et al., 2015, 2016).

The combined results of the transcriptional and translational reporters thus suggest that horizontally acquired genes are transcribed at low levels, which could not be detected using a destabilized reporter gene such as the luciferase construct used in this study (Rienzo et al., 2012). In a similar way, the promoter regions of the horizontally acquired genes may have a cryptic behavior in the *S. cerevisiae* genetic context, generating unstable transcription or mRNAs of rapid degradation (Wyers et al., 2005; Neil et al., 2009). This hypothesis is also supported by the consistent signal obtained using the *mCherry* fluorescent protein, which is a stable translational reporter that accumulates during the time course of the experiments (Deluna et al., 2010). Importantly, regions A and C are subtelomeric according to the EC1118 strain genome (Novo et al., 2009). Therefore, the ORFs in both these regions could suffer potential subtelomeric repression and be activated only under specific environmental conditions (Ai et al., 2002). A simple and alternative explanation for the low levels of transcriptional activity observed in the horizontally acquired genes is the limited number of environmental conditions used in this work, where only four culture conditions were assayed. Consequently, we cannot discard transcriptional activity for the analyzed ORFs in other culture conditions, especially considering the multiple yeast transcription factor binding sites present in their promoter regions (**Supplementary Table 3**). Furthermore, we also confirmed through the CAI calculation for each ORF that codon usage is not a bias for protein synthesis in the context of *S. cerevisiae* (**Supplementary Figure 5**), observing an average CAI higher than 0.65 for the horizontally acquired genes, which is also higher than the average CAI for the *S. cerevisiae* genome (Ghaemmaghami et al., 2003; Jansen et al., 2003).

We assayed the growth kinetic parameters and the maximal CO_2 production rate in a gene deletion collection of strains (**Figure 2**) and compared these phenotypes to the wild type strains. We found that the single deletion of 20 ORFs produced a significant modification of the kinetic parameters in at least one of the assayed culture conditions, obtaining most of the phenotypic changes in SM60 (**Figure 4**). Importantly, SM60 is a fermentation medium that mimics wine fermentation conditions but contains a limited amount of nitrogen, generating a stressful environment for yeast growth (Kessi-Perez et al., 2019a;

Molinet et al., 2019). In a similar way, the single deletion of five ORFs significantly changed the maximal CO_2 production rate (**Figure 5**). Interestingly, we observed a consistent result between growth parameters and maximal CO_2 production rate for ORF A9 deletion, increasing the lag time and decreasing the growth rate, growth efficiency, and CO_2 production rate (**Figures 4**, **5**). This ORF (A9) encodes for a putative thiamine (vitamin B1) transporter, which is a co-factor for many enzymes that participate in the metabolism of amino acids and carbohydrates (Jurgenson et al., 2009). In the yeast fermentation context, thiamine decreases the level of pyruvate and increases the amount of carboxylase enzymes, generating an increase in the fermentation rate (Trevelyan and Harrison, 1954). This is consistent with our results, where ORF A9 deletion decreased the maximal CO_2 production rate (**Figure 5**).

In conclusion, our results confirm the importance of the deletion approach for yeast functional genomics (Giaever and Nislow, 2014) and provide molecular evidence for the transcriptional and translational activity of the horizontally acquired genes and their importance for niche-specific adaptation, particularly in the fermentative environment. Further complementation of these results with the generation of an overexpression collection of these genes will allow us to uncover novel cellular functions for this important set of genes (Stevenson et al., 2001; Sopko et al., 2006).

DATA AVAILABILITY STATEMENT

The datasets generated for this study are available upon request to the corresponding author.

AUTHOR CONTRIBUTIONS

FS designed the research and wrote the manuscript with insight from all the authors. JD, CB, EK-P, CV, and MD performed the bioinformatics analyses, laboratory experiments, and analyzed the data. FC, GL, CM, and FS supervised the work and provided the reagents and financial support.

FUNDING

This work was supported by CONICYT/FONDEQUIP (grant EQM170052), CONICYT/FONDECYT (grant 11170158), and CONICYT/PCI (grant REDI170239) to FS, Instituto Milenio iBio – Iniciativa Científica Milenio MINECON to FC and FS, CONICYT/FONDECYT (grants 1150522 and 1201104) to CM, Universidad de Santiago de Chile (Grant USA1799-VRIDEI 081998SS-PAP) to EK-P, and CONICYT/FONDECYT (grant 3170404) to CV.

ACKNOWLEDGMENTS

We thank Jennifer Molinet, Walter Tapia, and Claudia Villegas for technical help during this project execution. We also thank Michael Handford (Universidad de Chile) for language support.

SUPPLEMENTARY MATERIAL

The Supplementary Material for this article can be found online at: https://www.frontiersin.org/articles/10.3389/fgene.2020.00293/full#supplementary-material

REFERENCES

Ai, W., Bertram, P. G., Tsang, C. K., Chan, T. F., and Zheng, X. F. (2002). Regulation of subtelomeric silencing during stress response. *Mol. Cell.* 10, 1295–1305. doi: 10.1016/s1097-2765(02)00695-0

Babicki, S., Arndt, D., Marcu, A., Liang, Y., Grant, J. R., Maciejewski, A., et al. (2016). Heatmapper: web-enabled heat mapping for all. *Nucleic Acids Res.* 44, W147–W153. doi: 10.1093/nar/gkw419

Bergström, A., Simpson, J. T., Salinas, F., Barre, B., Parts, L., Zia, A., et al. (2014). A high-definition view of functional genetic variation from natural yeast genomes. *Mol. Biol. Evol.* 31, 872–888. doi: 10.1093/molbev/msu037

Borneman, A. R., Desany, B. A., Riches, D., Affourtit, J. P., Forgan, A. H., Pretorius, I. S., et al. (2011). Whole-genome comparison reveals novel genetic elements that characterize the genome of industrial strains of *Saccharomyces cerevisiae*. *PLoS Genet.* 7:e1001287. doi: 10.1371/journal.pgen.1001287

Borneman, A. R., and Pretorius, I. S. (2015). Genomic insights into the Saccharomyces sensu stricto complex. *Genetics* 199, 281–291. doi: 10.1534/genetics.114.173633

De Boer, C. G., and Hughes, T. R. (2012). YeTFaSCo: a database of evaluated yeast transcription factor sequence specificities. *Nucleic Acids Res.* 40, D169–D179. doi: 10.1093/nar/gkr993

Deluna, A., Springer, M., Kirschner, M. W., and Kishony, R. (2010). Need-based up-regulation of protein levels in response to deletion of their duplicate genes. *PLoS Biol.* 8:e1000347. doi: 10.1371/journal.pbio.1000347

Fitzpatrick, D. A. (2012). Horizontal gene transfer in fungi. *FEMS Microbiol. Lett.* 329, 1–8. doi: 10.1111/j.1574-6968.2011.02465.x

Galeote, V., Bigey, F., Beyne, E., Novo, M., Legras, J. L., Casaregola, S., et al. (2011). Amplification of a Zygosaccharomyces bailii DNA segment in wine yeast genomes by extrachromosomal circular DNA formation. *PLoS One* 6:e17872. doi: 10.1371/journal.pone.0017872

Galeote, V., Novo, M., Salema-Oom, M., Brion, C., Valerio, E., Goncalves, P., et al. (2010). FSY1, a horizontally transferred gene in the Saccharomyces cerevisiae EC1118 wine yeast strain, encodes a high-affinity fructose/H+ symporter. *Microbiology* 156, 3754–3761. doi: 10.1099/mic.0.041673-0

Ghaemmaghami, S., Huh, W. K., Bower, K., Howson, R. W., Belle, A., Dephoure, N., et al. (2003). Global analysis of protein expression in yeast. *Nature* 425, 737–741.

Giaever, G., and Nislow, C. (2014). The yeast deletion collection: a decade of functional genomics. *Genetics* 197, 451–465. doi: 10.1534/genetics.114.161620

Gietz, R. D., and Schiestl, R. H. (2007). High-efficiency yeast transformation using the LiAc/SS carrier DNA/PEG method. *Nat. Protoc.* 2, 31–34. doi: 10.1038/nprot.2007.13

Goffeau, A., Barrell, B. G., Bussey, H., Davis, R. W., Dujon, B., Feldmann, H., et al. (1996). Life with 6000 genes. *Science* 274, 563–547.

Gojkovic, Z., Knecht, W., Zameitat, E., Warneboldt, J., Coutelis, J. B., Pynyaha, Y., et al. (2004). Horizontal gene transfer promoted evolution of the ability to propagate under anaerobic conditions in yeasts. *Mol. Genet. Genomics* 271, 387–393. doi: 10.1007/s00438-004-0995-7

Gonçalves, C., and Gonçalves, P. (2019). Multilayered horizontal operon transfers from bacteria reconstruct a thiamine salvage pathway in yeasts. *Proc. Natl. Acad. Sci. U.S.A.* 116, 22219–22228. doi: 10.1073/pnas.1909844116

Hall, C., Brachat, S., and Dietrich, F. S. (2005). Contribution of horizontal gene transfer to the evolution of Saccharomyces cerevisiae. *Eukaryot. Cell* 4, 1102–1115. doi: 10.1128/ec.4.6.1102-1115.2005

Hall, C., and Dietrich, F. S. (2007). The reacquisition of biotin prototrophy in *Saccharomyces cerevisiae* involved horizontal gene transfer, gene duplication and gene clustering. *Genetics* 177, 2293–2307. doi: 10.1534/genetics.107.074963

Jansen, R., Bussemaker, H. J., and Gerstein, M. (2003). Revisiting the codon adaptation index from a whole-genome perspective: analyzing the relationship between gene expression and codon occurrence in yeast using a variety of models. *Nucleic Acids Res.* 31, 2242–2251. doi: 10.1093/nar/gkg306

Jurgenson, C. T., Begley, T. P., and Ealick, S. E. (2009). The structural and biochemical foundations of thiamin biosynthesis. *Annu. Rev. Biochem.* 78, 569–603. doi: 10.1146/annurev.biochem.78.072407.102340

Keeling, P. J., and Palmer, J. D. (2008). Horizontal gene transfer in eukaryotic evolution. *Nat. Rev. Genet.* 9, 605–618. doi: 10.1038/nrg2386

Kessi-Perez, E. I., Salinas, F., Gonzalez, A., Su, Y., Guillamon, J. M., Hall, M. N., et al. (2019a). KAE1 Allelic variants affect TORC1 activation and fermentation kinetics in *Saccharomyces cerevisiae*. *Front. Microbiol.* 10:1686. doi: 10.3389/fmicb.2019.01686

Kessi-Pérez, E. I., Salinas, F., Molinet, J., González, A., Muñiz, S., Guillamón, J. M., et al. (2019b). Indirect monitoring of TORC1 signalling pathway reveals molecular diversity among different yeast strains. *Yeast* 36, 65–74. doi: 10.1002/yea.3351

Kominek, J., Doering, D. T., Opulente, D. A., Shen, X. X., Zhou, X., Devirgilio, J., et al. (2019). Eukaryotic acquisition of a bacterial operon. *Cell* 176:e1310.

Legras, J. L., Galeote, V., Bigey, F., Camarasa, C., Marsit, S., Nidelet, T., et al. (2018). Adaptation of *S. cerevisiae* to fermented food environments reveals remarkable genome plasticity and the footprints of domestication. *Mol Biol Evol* 35, 1712–1727. doi: 10.1093/molbev/msy066

Liti, G. (2015). The fascinating and secret wild life of the budding yeast *S. cerevisiae*. *eLife* 4:e05835. doi: 10.7554/eLife.05835

Liti, G., Carter, D. M., Moses, A. M., Warringer, J., Parts, L., James, S. A., et al. (2009). Population genomics of domestic and wild yeasts. *Nature* 458, 337–341. doi: 10.1038/nature07743

Marsit, S., Mena, A., Bigey, F., Sauvage, F. X., Couloux, A., Guy, J., et al. (2015). Evolutionary advantage conferred by an eukaryote-to-eukaryote gene transfer event in wine yeasts. *Mol. Biol. Evol.* 32, 1695–1707. doi: 10.1093/molbev/msv057

Marsit, S., Sanchez, I., Galeote, V., and Dequin, S. (2016). Horizontally acquired oligopeptide transporters favour adaptation of *Saccharomyces cerevisiae* wine yeast to oenological environment. *Environ. Microbiol.* 18, 1148–1161. doi: 10.1111/1462-2920.13117

Marullo, P., Bely, M., Masneuf-Pomarede, I., Pons, M., Aigle, M., and Dubourdieu, D. (2006). Breeding strategies for combining fermentative qualities and reducing off-flavor production in a wine yeast model. *FEMS Yeast Res.* 6, 268–279. doi: 10.1111/j.1567-1364.2006.00034.x

Molinet, J., Cubillos, F. A., Salinas, F., Liti, G., and Martinez, C. (2019). Genetic variants of TORC1 signaling pathway affect nitrogen consumption in Saccharomyces cerevisiae during alcoholic fermentation. *PLoS One* 14:e0220515. doi: 10.1371/journal.pone.0220515

Morales, L., and Dujon, B. (2012). Evolutionary role of interspecies hybridization and genetic exchanges in yeasts. *Microbiol. Mol. Biol. Rev.* 76, 721–739. doi: 10.1128/mmbr.00022-12

Nakamura, Y., Gojobori, T., and Ikemura, T. (2000). Codon usage tabulated from international DNA sequence databases: status for the year 2000. *Nucleic Acids Res.* 28, 292. doi: 10.1093/nar/28.1.292

Neil, H., Malabat, C., D'aubenton-Carafa, Y., Xu, Z., Steinmetz, L. M., and Jacquier, A. (2009). Widespread bidirectional promoters are the major source of cryptic transcripts in yeast. *Nature* 457, 1038–1042. doi: 10.1038/nature07747

Novo, M., Bigey, F., Beyne, E., Galeote, V., Gavory, F., Mallet, S., et al. (2009). Eukaryote-to-eukaryote gene transfer events revealed by the genome sequence of the wine yeast *Saccharomyces cerevisiae* EC1118. *Proc. Natl. Acad. Sci. U.S.A.* 106, 16333–16338. doi: 10.1073/pnas.0904673106

Peter, J., De Chiara, M., Friedrich, A., Yue, J. X., Pflieger, D., Bergstrom, A., et al. (2018). Genome evolution across 1,011 Saccharomyces cerevisiae isolates. *Nature* 556, 339–344. doi: 10.1038/s41586-018-0030-5

Puigbò, P., Bravo, I. G., and Garcia-Vallve, S. (2008). CAIcal: a combined set of tools to assess codon usage adaptation. *Biol. Direct.* 3:38. doi: 10.1186/1745-6150-3-38

Ravenhall, M., Skunca, N., Lassalle, F., and Dessimoz, C. (2015). Inferring horizontal gene transfer. *PLoS Comput. Biol.* 11:e1004095. doi: 10.1371/journal.pcbi.1004095

Rienzo, A., Pascual-Ahuir, A., and Proft, M. (2012). The use of a real-time luciferase assay to quantify gene expression dynamics in the living yeast cell. *Yeast* 29, 219–231. doi: 10.1002/yea.2905

Roelofs, J., and Van Haastert, P. J. (2001). Genes lost during evolution. *Nature* 411, 1013–1014. doi: 10.1038/35082627

Salinas, F., De Boer, C. G., Abarca, V., Garcia, V., Cuevas, M., Araos, S., et al. (2016). Natural variation in non-coding regions underlying phenotypic diversity in budding yeast. *Sci. Rep.* 6:21849. doi: 10.1038/srep21849

Sopko, R., Huang, D., Preston, N., Chua, G., Papp, B., Kafadar, K., et al. (2006). Mapping pathways and phenotypes by systematic gene overexpression. *Mol. Cell.* 21, 319–330. doi: 10.1016/j.molcel.2005.12.011

Stevenson, L. F., Kennedy, B. K., and Harlow, E. (2001). A large-scale overexpression screen in Saccharomyces cerevisiae identifies previously uncharacterized cell cycle genes. *Proc. Natl. Acad. Sci. U.S.A.* 98, 3946–3951. doi: 10.1073/pnas.051013498

Strope, P. K., Skelly, D. A., Kozmin, S. G., Mahadevan, G., Stone, E. A., Magwene, P. M., et al. (2015). The 100-genomes strains, an *S. cerevisiae* resource that illuminates its natural phenotypic and genotypic variation and emergence as an opportunistic pathogen. *Genome Res.* 25, 762–774. doi: 10.1101/gr.185538.114

Tapia, S. M., Cuevas, M., Abarca, V., Delgado, V., Rojas, V., Garcia, V., et al. (2018). GPD1 and ADH3 natural variants underlie glycerol yield differences in wine fermentation. *Front. Microbiol.* 9:1460. doi: 10.3389/fmicb.2018.01460

Trevelyan, W. E., and Harrison, J. S. (1954). Studies on yeast metabolism. IV. The effect of thiamine on yeast fermentation. *Biochem. J.* 57, 561–566. doi: 10.1042/bj0570561

Wang, Q. M., Liu, W. Q., Liti, G., Wang, S. A., and Bai, F. Y. (2012). Surprisingly diverged populations of Saccharomyces cerevisiae in natural environments remote from human activity. *Mol. Ecol.* 21, 5404–5417. doi: 10.1111/j.1365-294x.2012.05732.x

Warringer, J., and Blomberg, A. (2003). Automated screening in environmental arrays allows analysis of quantitative phenotypic profiles in *Saccharomyces cerevisiae*. *Yeast* 20, 53–67. doi: 10.1002/yea.931

Wenger, J. W., Schwartz, K., and Sherlock, G. (2010). Bulk segregant analysis by high-throughput sequencing reveals a novel xylose utilization gene from *Saccharomyces cerevisiae*. *PLoS Genet.* 6:e1000942. doi: 10.1371/journal.pgen.1000942

Wyers, F., Rougemaille, M., Badis, G., Rousselle, J. C., Dufour, M. E., Boulay, J., et al. (2005). Cryptic pol II transcripts are degraded by a nuclear quality control pathway involving a new poly(A) polymerase. *Cell* 121, 725–737. doi: 10.1016/j.cell.2005.04.030

Yin, X., Goudriaan, J., Lantinga, E. A., Vos, J., and Spiertz, H. J. (2003). A flexible sigmoid function of determinate growth. *Ann. Bot.* 91, 361–371. doi: 10.1093/aob/mcg029

Zwietering, M. H., Jongenburger, I., Rombouts, F. M., and Van'T Riet, K. (1990). Modeling of the bacterial growth curve. *Appl. Environ. Microbiol.* 56, 1875–1881.

Conflict of Interest: The authors declare that the research was conducted in the absence of any commercial or financial relationships that could be construed as a potential conflict of interest.

frontiers in Genetics

ORIGINAL RESEARCH
published: 25 May 2020
doi: 10.3389/fgene.2020.00519

GTR1 Affects Nitrogen Consumption and TORC1 Activity in *Saccharomyces cerevisiae* Under Fermentation Conditions

*Jennifer Molinet[1], Francisco Salinas[2,3,4], José Manuel Guillamón[5] and Claudio Martínez[1,3]**

[1] Departamento de Ciencia y Tecnología de los Alimentos, Universidad de Santiago de Chile (USACH), Santiago, Chile, [2] Millennium Institute for Integrative Biology (iBio), Santiago, Chile, [3] Centro de Estudios en Ciencia y Tecnología de Alimentos (CECTA), Universidad de Santiago de Chile (USACH), Santiago, Chile, [4] Instituto de Bioquímica y Microbiología, Facultad de Ciencias, Universidad Austral de Chile, Valdivia, Chile, [5] Departamento de Biotecnología de los Alimentos, Instituto de Agroquímica y Tecnología de los Alimentos (CSIC), Valencia, Spain

OPEN ACCESS

Edited by:
Cecile Fairhead, Université Paris-Sud, France

Reviewed by:
Peter William Piper, University of Sheffield, United Kingdom
Alexander DeLuna, Centro de Investigación y Estudios Avanzados, Instituto Politécnico Nacional de México (CINVESTAV), Mexico

***Correspondence:**
Claudio Martínez
claudio.martinez@usach.cl

Specialty section:
This article was submitted to Evolutionary and Genomic Microbiology, a section of the journal Frontiers in Genetics

Received: *19 December 2019*
Accepted: *28 April 2020*
Published: *25 May 2020*

Citation:
Molinet J, Salinas F, Guillamón JM and Martínez C (2020) GTR1 Affects Nitrogen Consumption and TORC1 Activity in Saccharomyces cerevisiae Under Fermentation Conditions. Front. Genet. 11:519. doi: 10.3389/fgene.2020.00519

The TORC1 pathway coordinates cell growth in response to nitrogen availability present in the medium, regulating genes related to nitrogen transport and metabolism. Therefore, the adaptation of *Saccharomyces cerevisiae* to changes in nitrogen availability implies variations in the activity of this signaling pathway. In this sense, variations in nitrogen detection and signaling pathway are one of the main causes of differences in nitrogen assimilation during alcoholic fermentation. Previously, we demonstrated that allelic variants in the *GTR1* gene underlying differences in ammonium and amino acids consumption between Wine/European (WE) and West African (WA) strains impact the expression of nitrogen transporters. The *GTR1* gene encodes a GTPase that participates in the EGO complex responsible for TORC1 activation in response to amino acids availability. In this work, we assessed the role of the *GTR1* gene on nitrogen consumption under fermentation conditions, using a high sugar concentration medium with nitrogen limitation and in the context of the WE and WA genetic backgrounds. The *gtr1*Δ mutant presented a reduced TORC1 activity and increased expression levels of nitrogen transporters, which in turn favored ammonium consumption, but decreased amino acid assimilation. Furthermore, to identify the SNPs responsible for differences in nitrogen consumption during alcoholic fermentation, we studied the polymorphisms present in the *GTR1* gene. We carried out swapping experiments for the promoter and coding regions of *GTR1* between the WE and WA strains. We observed that polymorphisms in the coding region of the WA *GTR1* gene are relevant for TORC1 activity. Altogether, our results highlight the role of the *GTR1* gene on nitrogen consumption in *S. cerevisiae* under fermentation conditions.

Keywords: *Saccharomyces cerevisiae*, wine fermentation, *GTR1* gene, TORC1 pathway, allelic diversity

INTRODUCTION

Nitrogen is one of the most important nutrients present in grape must affecting various outcomes of alcoholic fermentation (Tesnière et al., 2015). The main microorganism responsible for this process is *Saccharomyces cerevisiae* (Pretorius, 2000), which responds to changes in nitrogen availability by adjusting its metabolism to new environmental conditions. The adaptation of *S. cerevisiae* strains to nitrogen availability involves changes in signaling pathway and gene expression (Rossignol et al., 2003; Brice et al., 2014b, 2018; Tesnière et al., 2015). However, the responses of *S. cerevisiae* to changes in nitrogen availability have been poorly studied under conditions that mimic industrial fermentation, where yeast has to face a stressful environment with high concentration of sugar (20% of glucose and fructose) and ethanol, low pH (pH 3.0–4.0), anaerobiosis (low O_2) and limited availability of nitrogen (Pretorius, 2000; Kessi-Pérez et al., 2020).

Grape musts contain a wide variety of nitrogen sources, however, yeast have a hierarchical preference for their consumption (Magasanik and Kaiser, 2002) favoring ammonium and amino acids (Bell and Henschke, 2005). In this sense, yeasts coordinate their protein synthesis and growth rate according to the quantity and quality of available nitrogen (Broach, 2012). Under fermentation conditions using a culture medium that mimics industrial fermentation, yeasts initially consume nitrogen sources whose permeases are regulated by the Ssy1-Ptr3-Ssy5 system (SPS), followed by nitrogen sources whose transporters are regulated by the Nitrogen Catabolite Repression (NCR) system (Crépin et al., 2012). Once the nitrogen sources are assimilated, most are incorporated into the Nitrogen Central Metabolism, transformed into glutamate or glutamine, and stored as amino acid pools in the cytoplasm, while positively charged amino acids such as arginine are stored in the vacuole (Crépin et al., 2014, 2017; Gutiérrez et al., 2016). The intracellular pools are used when the extracellular nitrogen is depleted, incorporating them in *de novo* amino acid synthesis or directly into proteins to initiate cell growth (Gutiérrez et al., 2016; Crépin et al., 2017). However, *S. cerevisiae* strains present different nitrogen consumption profiles (Contreras et al., 2012; Gutiérrez et al., 2012; Brice et al., 2014b, 2018; Jara et al., 2014; Cubillos et al., 2017), where variations in nitrogen metabolism and signaling are largely responsible for these phenotypic differences (Brice et al., 2014a; Cubillos et al., 2017; Molinet et al., 2019).

Recently, we demonstrated that a large diversity exists within the TORC1 pathway and allelic variants from this pathway significantly impact nitrogen metabolism, influencing the nitrogen consumption differences between strains representative of four clean lineages described in *S. cerevisiae* (Wine/European WE, West African WA, North American NA, and Sake SA) (Molinet et al., 2019). Furthermore, during alcoholic fermentation, TORC1 plays a key role in controlling the expression of genes related to nitrogen utilization (Rossignol et al., 2003), and on the fermentative capacity in nitrogen starved cells (Brice et al., 2014a). Similarly, Kessi-Pérez et al. (2019b) demonstrated a large phenotypic variation in TORC1 activity between the same four strains, with the greatest TORC1 activity observed in the SA strain and the lowest in the WE strain. Interestingly, the SA strain has a preference for amino acids consumption, while the WE strain presents a preference for ammonium (Cubillos et al., 2017). Thus, variations in the TORC1 activity imply differential activation of the downstream pathways such as NCR and SPS systems, which ultimately affect nitrogen consumption.

The TORC1 pathway coordinates cell growth in response to nutrient availability (De Virgilio and Loewith, 2006; Broach, 2012; Conrad et al., 2014; Zhang et al., 2018), predominantly detecting the quantity and quality of available nitrogen sources (Broach, 2012). TOCR1 activity is inhibited under nitrogen depletion conditions, whereas its activity increases upon nitrogen upshift. Its main downstream targets are the protein kinase Sch9p and the Tap42-PP2A complex, positively regulating ribosomal biogenesis and translation, and inhibiting the stress response (Conrad et al., 2014). TORC1 is regulated by the EGO complex (EGOC) composed of four proteins: Ego1p, Ego3p, Grt1p, and Gtr2p. This complex regulates TORC1 interacting physically with its subunits. Gtr1p and Gtr2p are Ras-family GTPases. When Gtr1p binds to GTP and Gtr2p to GDP it forms a heterodimeric complex resulting in the activation of TORC1 by EGOC (Hatakeyama and De Virgilio, 2016). Therefore, the localization of EGOC in the vacuole outer membrane, next to TORC1, allows the detection of amino acid levels and regulates TORC1 activity. Hence, this signal may involve mobilization of amino acids from their stores in the intracellular pools or vacuole (Broach, 2012).

The TORC1 pathway activity has been poorly studied under fermentation conditions, with the majority of studies done at the transcriptional level (Rossignol et al., 2003; Brice et al., 2014b; Walker et al., 2014; Tesnière et al., 2015). Previously, we identified seven genes of the TORC1 pathway (*GTR1, SAP185, SIT4, EAP1, NPR1, EAP1,* and *TOR2*) whose allelic diversity affects nitrogen consumption during alcoholic fermentation. We observed that *GTR1* allelic variants affect the consumption of amino acids and ammonium, where the Wine/European allele (WE) of this gene presented a preference for ammonium consumption, whereas the West African allele (WA) showed a preference for amino acids, similarly to that reported by Cubillos et al. (2017). Furthermore, the presence of the WE allele resulted in a higher expression level of ammonium permeases (*MEP1, MEP2* and *MEP3*) in line with higher ammonium consumption (Molinet et al., 2019). Therefore, considering that the regulation of TORC1 activity could be relevant to nitrogen consumption, we decided to further study the role of the *GTR1* gene on this phenotype.

In this work, we assessed the role of the *GTR1* gene on nitrogen consumption under fermentation conditions, using a media with high sugar concentration and nitrogen limitation, in the WE and WA genetic backgrounds. We evaluated nitrogen consumption in the *gtr1*Δ mutant and in different strains with swapped regulatory and coding regions for *GTR1*. The results showed a reduced TORC1 activation and higher expression levels of

nitrogen transporters in the *gtr1*Δ mutant, favoring ammonium consumption but decreasing amino acid assimilation. Finally, a SNP in the coding region of the *GTR1* gene is relevant for TORC1 activity in the WA strain. Altogether, our results indicate that *GTR1* regulates nitrogen consumption under fermentation conditions in *S. cerevisiae*.

MATERIALS AND METHODS

Strains and Culture Media

The haploid strains used in this work correspond to DBVPG6765 (WE, Wine/European, *Mat* α, *ho::HygMX, ura3::KanMX*) and DBVPG6044 (WA, West African, *Mat* α, *ho::HygMX, ura3::KanMX*), previously described by Cubillos et al. (2009). All the strains were maintained on YPD solid media (1% yeast extract, 2% peptone, 2% glucose, 2% agar).

Synthetic must (SM) used in fermentations has been previously described (Bely et al., 1990; Rossignol et al., 2003; Martínez et al., 2014) and contains a mixture of sugar (125 g L^{-1} of glucose and 125 g L^{-1} of fructose), mineral salts (750 mg L^{-1} KH_2PO_4, 500 mg L^{-1} K_2SO_4, 250 mg L^{-1} $MgSO_4{\cdot}7H_2O$, 155 mg L^{-1} $CaCl_2{\cdot}2H_2O$, 200 mg L^{-1} NaCl, 4 mg L^{-1} $MnSO_4{\cdot}H_2O$, 4 mg L^{-1} $ZnSO_4{\cdot}7H_2O$, 1 mg L^{-1} $CUSO_4{\cdot}5H_2O$, 1 mg L^{-1} KI, 0.4 mg L^{-1} $CoCl_2{\cdot}6H_2O$, 1 mg L^{-1} H_3BO_3 and 1 mg L^{-1} $NaMoO_4{\cdot}2H_2O$), vitamins (20 mg L^{-1} myo-inositol, 2 mg L^{-1} nicotinic acid, 1.5 mg L^{-1} calcium panthothenate, 0.25 mg L^{-1} thiamine HCl, 0.25 mg L^{-1} pyridoxine HCl and 0.003 mg L^{-1} biotin) and anaerobic factors (15 mg L^{-1} ergosterol, 5 mg L^{-1} sodium oleate) in Tween 80/ethanol solution (50/50 v/v). SM medium was adjusted to pH 3.3 with HCl and filtered. The final concentration of yeast assimilable nitrogen was 300 mg L^{-1} to SM300 and 140 mg L^{-1} to SM140 medium. The nitrogen concentration in SM300 corresponded to 120 mgN L^{-1} of ammonium and 180 mgN L^{-1} of amino acids mixture (612.6 mg L^{-1} L-proline, 503.5 mg L^{-1} L-glutamine, 503.5 mg L^{-1} L-arginine monohydrochloride, 179.3 mg L^{-1} L-tryptophan, 145.3 mg L^{-1} L-alanine, 120.4 mg L^{-1} L-glutamic acid, 78.5 mg L^{-1} L-serine, 75.92 mg L^{-1} L-threonine, 48.4 mg L^{-1} L-leucine, 44.5 mg L^{-1} L-aspartic acid, 44.5 mg L^{-1} L-valine, 37.9 mg L^{-1} L-phenylalanine, 32–7 mg L^{-1} L-isoleucine, 50.0 mg L^{-1} L-histidine monohydrochloride monohydrate, 31.4 mg L^{-1} L-methionine, 18.3 mg L^{-1} L-tyrosine, 18.3 mg L^{-1} L-glycine, 17.0 mg L^{-1} L-lysine monohydrochloride, and 13.1 mg L^{-1} L-cysteine). SM140-ammonium medium corresponds to synthetic must previously described, but with a final concentration of 140 mgN L^{-1} of ammonium. In the same way, SM140-amino acids medium presented a final concentration of 140 mgN L^{-1} of amino acids mixture (612.6 mg L^{-1} L-proline, 503.5 mg L^{-1} L-glutamine, 503.5 mg L^{-1} L-arginine monohydrochloride, 179.3 mg L^{-1} L-tryptophan, 145.3 mg L^{-1} L-alanine, 120.4 mg L^{-1} L-glutamic acid, 78.5 mg L^{-1} L-serine, 75.92 mg L^{-1} L-threonine, 48.4 mg L^{-1} L-leucine, 44.5 mg L^{-1} L-aspartic acid, 44.5 mg L^{-1} L-valine, 37.9 mg L^{-1} L-phenylalanine, 32–7 mg L^{-1} L-isoleucine, 50.0 mg L^{-1} L-histidine monohydrochloride monohydrate, 31.4 mg L^{-1} L-methionine, 18.3 mg L^{-1} L-tyrosine, 18.3 mg L^{-1} L-glycine, 17.0 mg L^{-1} L-lysine monohydrochloride, and 13.1 mg L^{-1} L-cysteine).

Generation of Null Mutants and Strains by Allele Swapping

The null mutants were previously described (Kessi-Pérez et al., 2019b; Molinet et al., 2019). The strains with the swapping promoter and coding regions of *GTR1* were obtained by *in vivo* assembly recombinational cloning (Oldenburg et al., 1997; Salinas et al., 2016). Briefly, the constructs containing the promoter, ORF and hygromycin cassette (hphMx) were designed *in silico* considering the same transcriptional orientation to avoid convergent transcription using the Geneious software 8.1.8 (Biomatters, New Zealand). Then, the promoter, ORF and hphMX were PCR amplified using Phusion High-Fidelity DNA polymerase (Thermo Fisher Scientific, United States). The yeast strain BY4741 (*MATa, his3*Δ*1, leu2*Δ*0, LYS2, met15*Δ*0, ura3*Δ*0*) was transformed using PCR products with 50–70 bp of overlap between them, and the linear plasmid pRS426. The circular plasmids were then recovered from the yeast and transferred to an *E. coli* DH5α strain. Plasmids from three positive colonies for each construct were purified and sequenced using the standard Sanger sequencing service (Macrogen, South Korea). The sequences were analyzed using the SGRP (Saccharomyces Genome Resequencing Project) BLAST[1] server and MUSCLE[2]. The complete constructs were PCR amplified using Phusion High-Fidelity DNA polymerase (Thermo Fisher Scientific, United States), using primers with 70 bp of homology with the target locus (**Supplementary Table S1**), and used to transform the WE and WA strains. Five different colonies for each construct were confirmed by standard yeast colony PCR.

Fermentation in Synthetic Must

Fermentations in synthetic must (SM300) (Bely et al., 1990; Rossignol et al., 2003) were carried out in nine biological replicates as previously described (Cubillos et al., 2017; Molinet et al., 2019). The pre-cultures were grown in SM300 for 24 h at 25°C without agitation. Then, 12 mL of SM300 were inoculated with 1×10^6 cells mL^{-1} and incubated at 25°C for 20 days without agitation. Fermentations were monitored weighing the tubes daily and determining weight loss over time. The kinetic parameters (the maximal CO_2 production rate V_{max}, V_{50}/V_{max} ratio and efficiency) (Marullo et al., 2006) were calculated from the CO_2 loss curves previously fitted with a sigmoid non-linear regression (Martinez et al., 2013).

Determination of Nitrogen Consumption

Nitrogen consumption was determined in three independent biological replicates as previously described (Cubillos et al., 2017; Molinet et al., 2019). Briefly, supernatants from fermentations were collected by centrifugation at 9000xg for 10 min and the concentration of ammonium and the 19 amino acids present in the must were determined by derivatization with diethyl

[1]http://www.moseslab.csb.utoronto.ca/sgrp/

[2]http://www.ebi.ac.uk/Tools/msa/muscle/

ethoxymethylenemalonate (DEEMM) (Gómez-Alonso et al., 2007). Subsequently, they were separated by HPLC using a Bio-Rad HPX-87H column in a Shimadzu Prominence HPLC equipment (Shimadzu, United States) (Nissen et al., 1997). This analysis was carried out on the sixth day of fermentation where most of the nitrogen consumption differences can be observed (Martinez et al., 2013; Jara et al., 2014). The uptake of each nitrogen source was estimated as the difference between the initial and final concentration before and after fermentation, respectively (Jara et al., 2014; Cubillos et al., 2017).

Determination of Growth Variables

Growth variables were determined from micro-cultivation experiments in SM300, SM140- ammonium, and SM140-amino acids media at 30°C for 48 h. The pre-cultures were grown in synthetic must medium at 30°C for 24 h and used to inoculate a 96-well plate with a final volume of 200 μL at an initial $OD_{600\ nm}$ of 0.1. The growth curves were monitored by measuring the $OD_{600\ nm}$ every 20 min in a Tecan Sunrise absorbance microplate reader (Tecan Group Ltd., Switzerland). The experiments were all carried out in three biological replicates. Lag phase, growth efficiency ($\Delta\ OD_{600\ nm}$) and the maximum specific growth rate (μ_{max}) were determined as previously described (Warringer and Blomberg, 2003; Ibstedt et al., 2015). For this, the parameters were calculated following curve fitting (OD values were transformed to ln) utilizing the Gompertz function (Zwietering et al., 1990) using the R software version 3.3.2.

RNA Extraction and qPCR Assay

Gene expression analysis was performed by qPCR from fermentations in SM300 medium as previously described (Molinet et al., 2019). Briefly, cells at 6 h of fermentation were collected by centrifugation and treated with 10 units of Zymolyase (Seikagaku Corporation, Japan) for 30 min at 37°C. RNA was extracted using the E.Z.N.A Total RNA Kit I (OMEGA) according to manufacturers' instructions. Then, genomic DNA traces were removed by treating samples with DNase I (Promega) and total RNA was recovered using the GeneJET RNA Cleanup and Concentration Micro Kit (Thermo Fisher Scientific). Concentrations of the purified RNA were determined with a UV-Vis spectrophotometer EPOCH equipment (BioTeK Instruments Inc., United States) and verified on 1.5% agarose gels. The RNA extractions were performed in two biological replicates.

cDNA was synthesized using one unit of M-MLV Reverse transcriptase (Promega), 0.4 μg of Oligo $(dT)_{15}$ primer and 0.8 μg of RNA in a final volume of 25 μL according to manufacturers' instructions. cDNA samples obtained were quantified using a UV-Vis spectrophotometer EPOCH equipment (BioTeK Instruments Inc., United States). The qPCR reactions were carried out using HOT FIREPol EvaGreen qPCR Mix Plus (Solis BioDyne) in a final volume of 20 μL, containing 0.25 μM of each primer and 1 μL of the cDNA previously synthesized. The qPCR reactions were carried out in three technical replicates per biological replicate using a Step One Plus Real-Time PCR System (Applied Biosystems, United States) under the following conditions: 95°C for 15 min and 40 cycles at 95°C for 15 s and 55°C for 15 s. The genes and primers used are listed in **Supplementary Table S1**. The mathematical method described by Pfaffl (2001) was used to quantify the relative expression of each gene. Expression levels were normalized with three housekeeping genes *ACT1*, *UBC6* and *RPN2* (Teste et al., 2009) according to Vandesompele et al. (2002). The ΔCt were analyzed using the nonparametric Mood test (Yuan et al., 2006).

TORC1 Pathway Activation in Micro-Culture Conditions

The TORC1 pathway activation was monitored using an indirect method described by Kessi-Pérez et al. (2019b), employing the expression of the *RPL26A* gene as an indirect readout for the activity status of TORC1. For this, we swapped the *RPL26A* ORF with the *Luc-URA3* reporter construct and measured the luminescence produced by yeast cells in micro-culture conditions. The strains carrying the *Luc-URA3* reporter construct were generated as described by Kessi-Pérez et al. (2019b). The pre-cultures were grown in synthetic must medium at 30°C for 24 h and used to inoculate a 96-well plate with a final volume of 300 μL supplemented with luciferin (1 mM) at an initial $OD_{600\ nm}$ of 0.1 and growth at 30°C. Luminescence was measured up to 24 h using 30 min intervals at 30°C in a Synergy HTX plate reader (BioTek, United States). All the experiments were performed in three biological replicates. From the luminescence curves three parameters were extracted: maximum luminescence (Max), maximum luminescence time (Time) and area under the curve of luminescence (AUC) (Kessi-Pérez et al., 2019a,b).

Statistical Analysis

An analysis of variance (ANOVA) was used to compare the enological and kinetic parameters. The experimental mean values were statistically analyzed using Student's *t*-test. The parameters associated with luminescence curves were compared using a non-parametric Kruskal–Wallis test. A *p*-value less than 0.05 ($p < 0.05$) was considered statistically significant.

RESULTS

Deletion of the *GTR1* Gene Affects Nitrogen Consumption and Expression of Nitrogen Transporters Under Fermentation Conditions

Previously, we have demonstrated that a large allelic diversity exits within the TORC1 pathway and these allelic variants significantly impact nitrogen consumption. In this sense, *GTR1* allelic variants affect the consumption of amino acids and ammonium, where the Wine/European allele (WE) of this gene presented a preference for ammonium consumption, whereas the West African allele (WA) showed a preference for amino acids (Molinet et al., 2019). In this context, we assessed the role of the *GTR1* gene on nitrogen consumption under fermentation conditions, in a media with a high concentration of sugar and nitrogen as a limiting nutrient (SM300), in the WE and WA genetic backgrounds. Initially, we studied the phenotypic effects of *GTR1* deletion (*gtr1*Δ) in both strains. The deletion of the

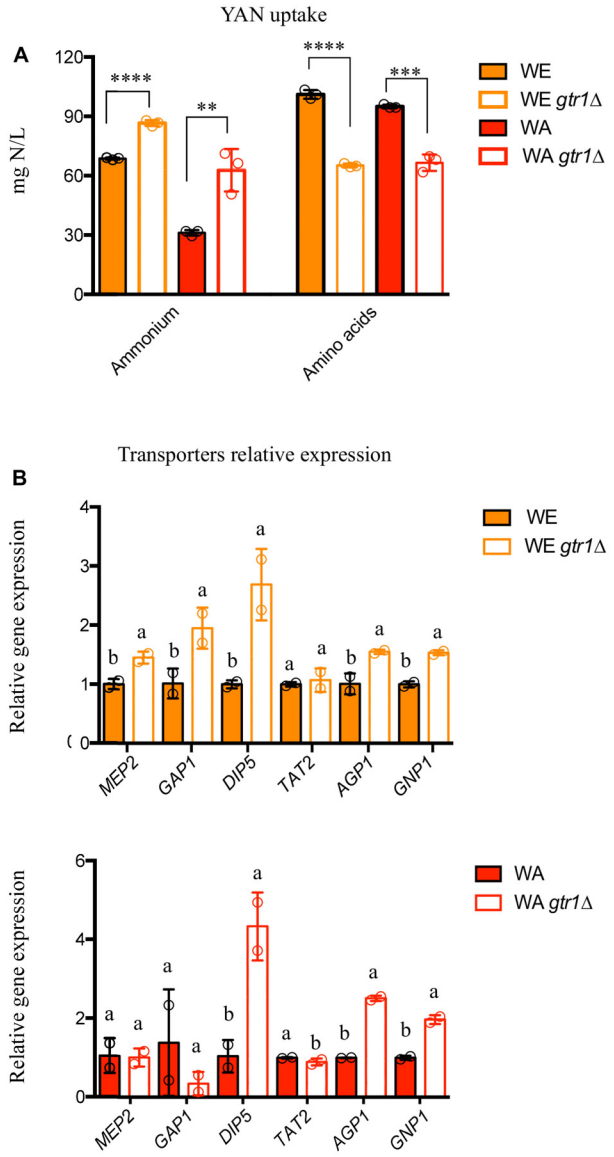

FIGURE 1 | Fermentation performance of the *GTR1* null mutants in SM300 medium. **(A)** Nitrogen consumption for null mutants and wild type strains. Plotted values correspond to the average of three biological replicates (dots), with their standard error represented by bars (mean ± SE). The asterisks represent different levels of significance between the phenotypes of null mutants and wild type strains (*t*-test; $^{**}p < 0.01$, $^{***}p < 0.001$, and $^{****}p < 0.0001$). **(B)** Relative gene expression at 6 h of fermentation for nitrogen transporters in the WE (top panel) and WA (bottom panel) genetic backgrounds. Expression levels were normalized using three housekeeping genes. Plotted values correspond to the average of two biological replicates (dots), with their standard error represented by bars (mean ± SE). Different letters represent significant statistical difference between the null mutants and wild type strains (Mood test with $p < 0.05$). WE: Wine/European; WA: West African.

GTR1 gene only increased the fermentative capacity by 22% in the WE genetic background, when compared to the wild type strain (**Supplementary Figures S1, S2**). However, both null mutants presented higher ammonium consumption, with a 21 and 50% difference between the null mutant strains and the respective wild type (WE and WA) strains (**Figure 1A**). In addition, *gtr1*Δ strains showed a lower overall amino acid consumption, with 35 and 30% differences between the null mutant strains and the respective wild type (WE and WA) strains (**Figure 1A**). The amino acids with statistically significant differences were aspartic acid, serine, glutamine, glycine, arginine, threonine, alanine, tyrosine, valine, isoleucine, leucine, and lysine (**Supplementary Tables S3, S4**). Despite this, null mutants improved the kinetic parameters resulting in a lower lag time and a higher efficiency than the wild type strains in micro-cultivation experiments in SM300 synthetic must (**Supplementary Figure S3**). In conclusion, the *GTR1* gene regulates nitrogen consumption under fermentation conditions affecting both the fermentative capacity and growth efficiency.

We then evaluated the relative gene expression of different nitrogen transporters (*MEP2*, *GAP1*, *DIP5*, *TAT2*, *AGP1*, and *GNP1*) regulated by TORC1 in the same set of strains (**Figure 1B**). Although, the WA strain presented higher expression levels of transporters than the WE strain (**Supplementary Figure S4**), this does not correlate with nitrogen consumption, since the WE strain takes up 55% more ammonium and 6% more amino acids than the WA strain (**Figure 1A**). Likewise, the deletion of *GTR1* in the WE genetic background presented higher expression levels in all the genes evaluated, except *TAT2* (**Figure 1B**). Similarly, the *gtr1*Δ strain showed higher gene expression of *DIP5*, *AGP1*, and *GNP1* in the WA genetic background (**Figure 1B**). Thus, the absence of the *GTR1* gene positively regulates the expression of nitrogen transporters.

GTR1 Deletion Decrease TORC1 Activation Under Fermentation Conditions

With the aim of evaluating the effect of *GTR1* deletion on TORC1 activity, we employed the expression of the *RPL26A* gene as an indirect readout for the activity status of TORC1. An active TORC1 leads to a transcriptional up-regulation of the *RPL26A* gene, whereas inactivation of TORC1 suppresses the transcription of *RPL26A* (Kessi-Pérez et al., 2019b). In this sense, we used the same strategy described by Kessi-Pérez et al. (2019b) and monitored the luminescence in strains containing the *Luc-URA3* reporter construct controlled by the *RPL26A* promoter in microculture conditions and in SM300 medium (**Figure 2**). In this condition, the behavior of the strains was similar to the one observed in nitrogen upshift experiments with two peaks of luciferase expression, one before 4 h and a second peak between 4 and 12 h (Kessi-Pérez et al., 2019b). However, in nitrogen upshift experiments, the WA strain presented a higher maximum luciferase expression than the WE strain, but in SM300 the WE strain had a greater maximum peak of expression (**Figure 2**), indicative of a possible higher TORC1 activation in the WE strain compared to the WA strain. Thus, the TORC1 activity under fermentation conditions (SM300) is different to that observed in laboratory media with a single nitrogen source. We should

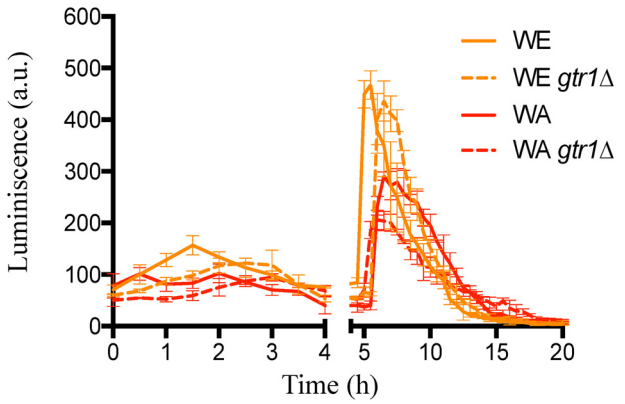

FIGURE 2 | Indirect TORC1 activity in *GTR1* null mutants. Indirect monitoring of TORC1 activity was evaluated as luciferase expression controlled by *RPL26A* promoter under micro-culture conditions in SM300 medium until 20 h. Plotted values correspond to the average of three biological replicates, with their standard error represented by bars (mean ± SE). WE: Wine/European; WA: West African.

keep in mind that SM300 was made up of a complex mixture of ammonium and 19 amino acids that yeasts consume in sequential order of preference (Crépin et al., 2012).

Deletion of *GTR1* did not abolish the luminescence signal, which imply EGOC independent activation of the TORC1 pathway (Stracka et al., 2014). However, the results showed an effect in the TORC1 activity, where a lower peak of luminescence and a delay in the maximum luminescence were observed in the deletion strains compared to their wild type versions (**Figure 2** and red values in **Supplementary Table S2**). In consequence, the differences observed in nitrogen consumption and expression of transporters between the null mutants (*gtr1*Δ) and their wild type strains could be the result of differences in the times and intensity of TORC1 activation. Altogether, these results confirmed the role of the *GTR1* gene on TORC1 activation in *S. cerevisiae* under fermentation conditions.

SNPs Present in the *GTR1* Gene Affect Its Expression Levels During Alcoholic Fermentation

Previously, we determined that allelic diversity in the *GTR1* gene underlies nitrogen consumption differences between WE and WA strains (Molinet et al., 2019). This gene has three SNPs in the ORF of the WE and WA strains, two synonymous (C345T and A714G) in the WE strain and one non-synonymous (R113S) in the WA strain (**Figure 3A**). According to the SIFT prediction, although the non-synonymous mutation would be tolerated for protein function (Molinet et al., 2019), it may nevertheless cause an impact since this SNP is localized in the GTPase domain of the protein. With regards to the regulatory region, there are two SNPs in the region encompassing 600 bp upstream of the ATG codon: A-8C and A-321G present in the WA strain (**Figure 3A**). Considering that phenotypic differences between strains may be explained by polymorphisms in coding and/or non-coding regions (Thompson and Cubillos, 2017), we decided to determine the causal polymorphisms responsible for these phenotypic differences by an allele swapping strategy in the parental strains. We swapped the ORF, the regulatory region or both regions in the parental backgrounds (**Figure 3B**). We first determined the *GTR1* expression in all the modified strains at 6 h of fermentation (**Figure 4**). The WA strain showed a higher *GTR1* expression level compared to the WE strain due to a combination of cis and trans factors (**Figure 4**). These results point out that *GTR1* expression levels do not correlate with the TORC1 activation observed in the wild type strains (**Figure 2**), where WA strain showed lower TORC1 activation, suggesting an EGOC independent activation of TORC1 in the WE strain.

In the WE genetic background, we observed a higher *GTR1* expression level in the modified strains than in the WE wild type strain, with a greater effect for the polymorphisms inside the ORF region than the regulatory region of WA origin (**Figure 4A**). However, *GTR1* expression levels in the modified strains did not reach the level of the WA strain, highlighting the importance of trans factors and genetic interactions. On the other hand, in the WA genetic background, we observed differences in the expression levels only in the strain with both regions of WE origin, lower than the WA strain but higher than the WE strain (**Figure 4B**). These results indicate that not only the polymorphisms in the regulatory regions are important for *GTR1* gene expression, but also the polymorphisms in the coding region. As a result, SNPs present in the *GTR1* ORF of the WA strain affect *GTR1* expression in the WE genetic background, whereas the synergistic contribution of *GTR1* SNPs present in the ORF and regulatory region of the WE strain have a mild effect on *GTR1* expression in the WA genetic background.

GTR1 Coding Region From the WA Strain Modify TORC1 Activation in the WE Genetic Background

In order to evaluate the effect of polymorphisms present in the *GTR1* gene on TORC1 activity, we evaluated the TORC1 activation in the modified strains using the same indirect method previously assayed. In general, we observed a time delay in the maximum peak of luminescence in the modified WE strains which was similar to the WA strain, however, the intensity of the maximum peaks of luminescence were similar to the WE wild type strain (**Figure 5A**, blue values in **Supplementary Table S2**). During the first 4 h of growth, the WE strains with the promoter or both (promoter and ORF) regions of WA origin presented a delay in the maximum expression peak time with respect to the WE wild type strain (**Figure 5A**). In addition, the WE strain with the ORF of WA origin presented an intermediate phenotype between the WE and WA strains (**Figure 5A**), showing a delay in the time of the second peak, which correlates with the *GTR1* expression levels observed for this strain. Sequence analysis of 55 different strains of *S. cerevisiae* showed that the *GTR1* non-synonymous SNP is present only in strains from WA origin (**Supplementary Figure S5**), suggesting that this variant could be subject to selection in the palm wine ecological niche. Thus,

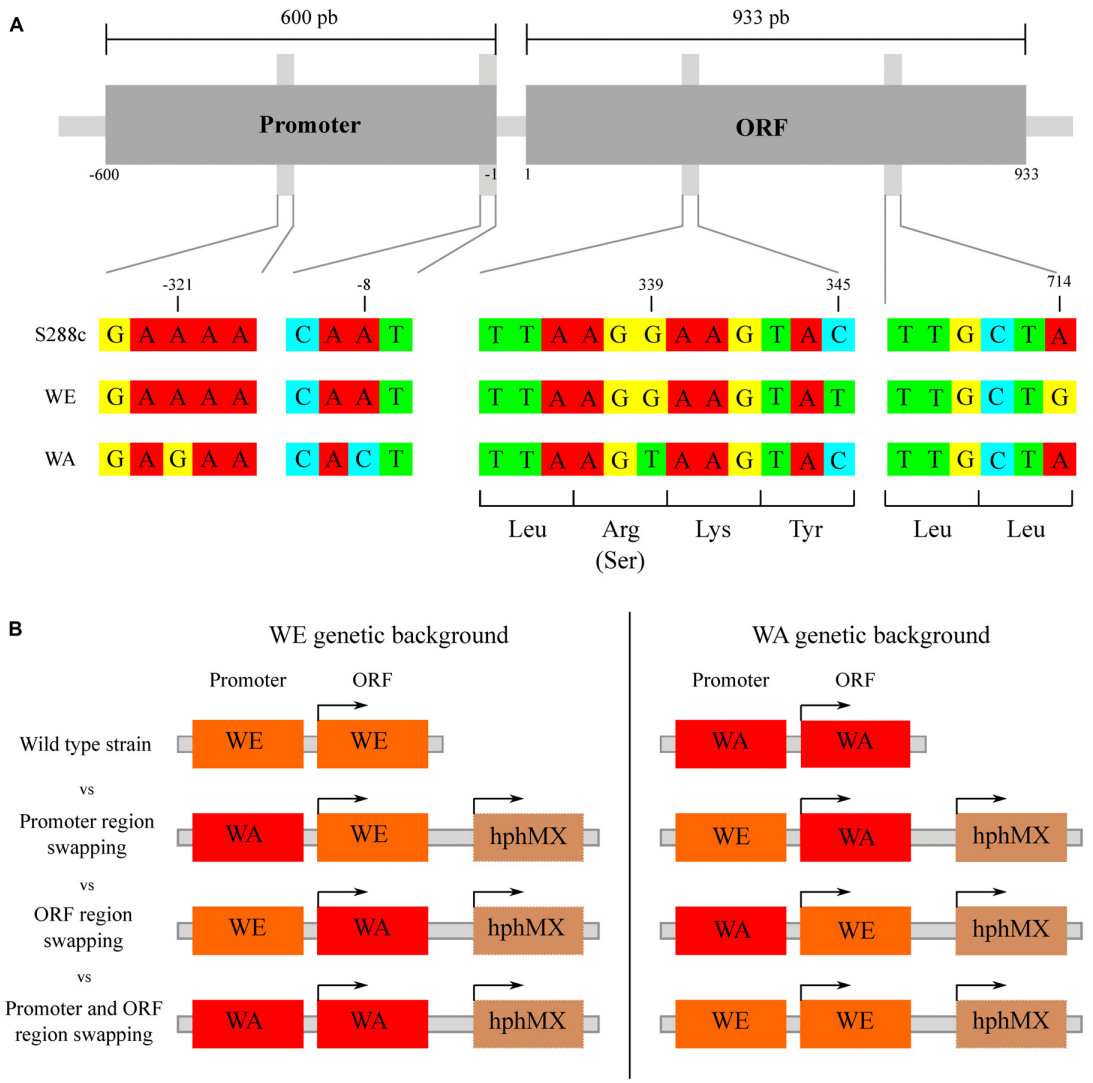

FIGURE 3 | Nucleotide sequence variation for *GTR1* gene. **(A)** Alignment of the promoter and coding regions of the *GTR1* gene. The nucleotide sequence of S288c (reference), WE and WA strains were downloaded from the SGRP BLAST server of the University of Toronto (http://www.moseslab.csb.utoronto.ca/sgrp/) and aligned using MUSCLE (http://www.ebi.ac.uk/Tools/msa/muscle/). **(B)** Scheme of the swap strategy for promoter region, ORF region or both regions. Each promoter and/or ORF was swapped in the opposite genetic background, generating three different combinations. The strain background is shown as an orange (WE) or red (WA) rectangle.

this polymorphism has a greater probability of affecting the phenotype in strains of other ecological origins or phylogenetic clades. Finally, we did not observe differences in the TORC1 activity of the WA strain with the promoter region, coding sequence or both swapped regions of the *GTR1* gene coming from the WE strain (**Figure 5B**), indicative of a strong trans-regulation and genetic interaction in the WA strain.

GTR1 Coding Region From the WA Strain Impairs the Fermentative Performance in the WE Genetic Background

We then determined the effect of the *GTR1* SNPs on the fermentative kinetics and nitrogen consumption (**Figure 6**). In the WE genetic background, the phenotype of the strain with the WA *GTR1* ORF was intermediate between the two wild type strains (**Figures 6A,B**). We observed the same intermediary behavior in the growth kinetics in SM300 and SM140 with only ammonium or amino acids as a nitrogen source (**Figure 7A** and **Table 1**). In SM300 medium, we observed differences in the maximum specific growth rate and efficiency (**Table 1**), with intermediary values for the WE strain with the WA *GTR1* ORF, which correlates with the fermentative phenotype. These results highlight the importance of the SNPs in the coding region of *GTR1* for its biological function. Furthermore, considering our previous results in reciprocal hemizygote assays, the hemizygous strain with the WA allele had a preference for amino acid consumption, while the hemizygous strain with WE allele had

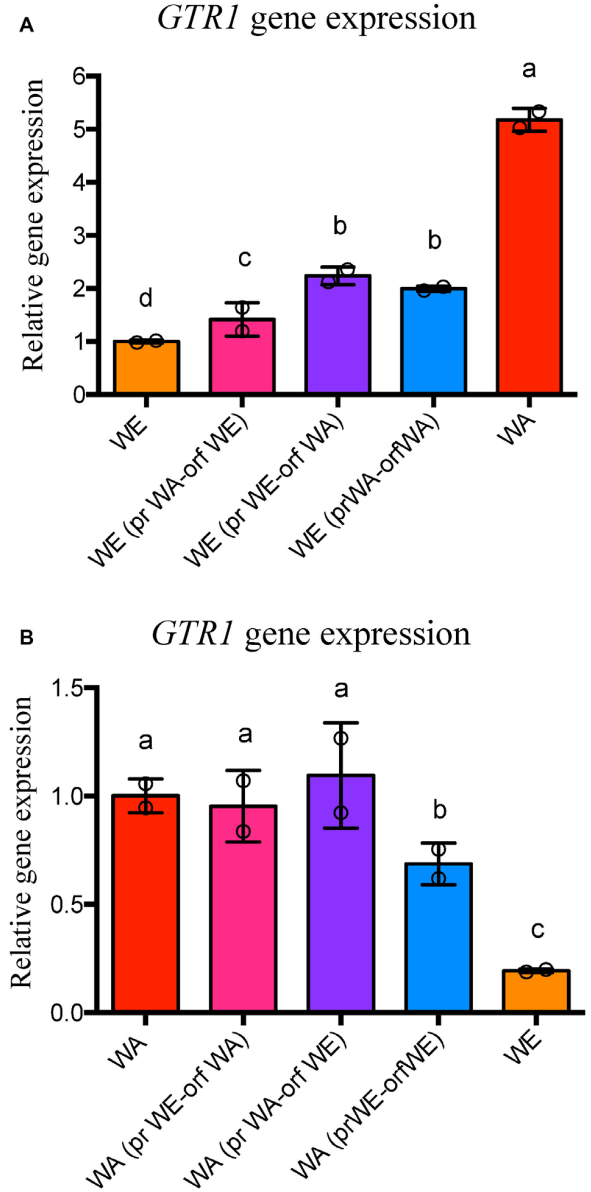

FIGURE 4 | *GTR1* gene expression in strains with swapped regions. **(A)** Relative gene expression at 6 h of fermentation for the *GTR1* gene in the WE strains with swapped regions of *GTR1* coming from the WA strains. Expression levels are relative to the WE strain. **(B)** Relative gene expression at 6 h of fermentation for the *GTR1* gene in the WA strains with swapped regions of *GTR1* coming from the WE strains. Expression levels are relative to the WA strain. In both panels, expression levels were normalized using three housekeeping genes. Plotted values correspond to the average of two biological replicates (dots), with their standard error represented by bars (mean ± SE). Different letters represent significant statistical differences between the strains constructed and wild type strains (Mood test with $p < 0.05$). WE: Wine/European; WA, West African; pr, Promoter; orf, Open Reading Frame (ORF).

a preference for ammonium consumption (Molinet et al., 2019), we decided to evaluate the growth kinetics in media containing only ammonium or amino acids as nitrogen sources (**Figure 7** and **Table 1**). Results showed that the WE strain with a preference for ammonium consumption showed a higher maximum specific growth rate and a lower lag time in comparison to the WA strain in SM140-ammonium medium (**Table 1**). However, the WA strain showed higher growth efficiency in all the assayed culture conditions (**Figure 7A**). Interestingly, the WE strain with the WA ORF presented the same efficiency as the WA strain in SM140-ammonium (**Figure 7A**). On the contrary, in SM140-amino acids medium, the WE strain with the WA ORF presented the same efficiency as the WE strain (**Figure 7A**), but an intermediary value of maximum specific growth rate between WE and WA strains (**Table 1**). In addition, the previously described preference for amino acids consumption in the hemizygous strain with WA allele (Molinet et al., 2019) was confirmed by the higher efficiency and lower lag time for the WA strain in comparison to the WE strain in SM140-amino acids medium (**Table 1**). In summary, the strain with the WA ORF of the *GTR1* gene in the WE genetic background presented intermediary phenotypes between the wild type strains, confirming the effect of the coding region polymorphisms in the phenotypes evaluated.

We did not observe statistically significant differences in ammonium and amino acids consumption between the wild type and WE strain with the WA *GTR1* ORF (**Figure 6C**), but these strains showed an intermediate phenotype for alanine consumption (**Figure 6D**). This phenotypic difference is important considering the preference for ammonium consumption observed in the WE strain. Furthermore, when both regions of WA origin were present, we observed a higher consumption of alanine, valine, isoleucine, leucine and lysine in comparison to the WE wild type strain (**Supplementary Table S3**). Therefore, the effect of the *GTR1* polymorphisms on nitrogen consumption depends on genetic interactions, which is characteristic of complex traits (Nieduszynski and Liti, 2011; Swinnen et al., 2012).

Finally, in the WA genetic background, we observed a 21% difference in ammonium consumption between the strain with the WE *GTR1* ORF and its wild type strain (**Supplementary Table S4**). The modified strain presented a higher ammonium consumption, which correlates with the consumption of the WE wild type strain. We also evaluated the growth kinetics in SM300, SM140ammonium, and SM140-amino acids media (**Figure 7B** and **Table 1**), observing an intermediate efficiency between the two wild type strains in SM140-amino acids medium (**Figure 7B**). Altogether, these results highlight the importance of the SNPs in the *GTR1* coding region on the fermentative phenotype of *S. cerevisiae* and on its preference for the nitrogen source.

DISCUSSION

Studies in *S. cerevisiae* under fermentation conditions have shown that differences in nitrogen requirements between strains originate from variations in nitrogen sensing and signaling pathways (Brice et al., 2014b; Cubillos et al., 2017; Molinet et al., 2019). Previously, we identified and confirmed that allelic variants within the TORC1 pathway significantly impact nitrogen metabolism, influencing nitrogen consumption

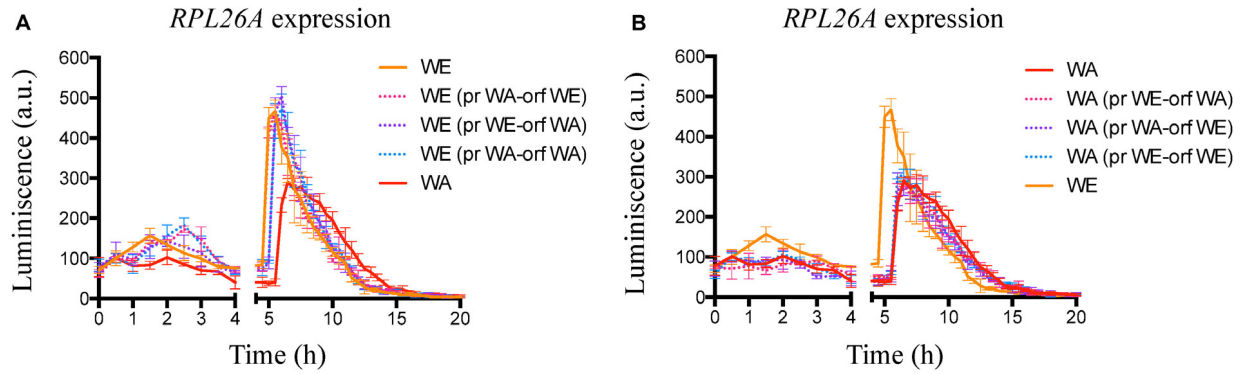

FIGURE 5 | Indirect TORC1 activity in strains with *GTR1* swapped regions. **(A)** Indirect monitoring of TORC1 activity in the WE strains with swapped regions of *GTR1* coming from the WA strain, using micro culture conditions until 20 h. **(B)** Indirect monitoring of TORC1 activity in the WA strains with swapped regions of *GTR1* coming from the WE strain, using micro culture conditions until 20 h. Plotted values correspond to the average of three biological replicates, with their standard error represented by bars (mean ± SE). WE, Wine/European; WA, West African; pr, Promoter; orf: Open Reading Frame (ORF).

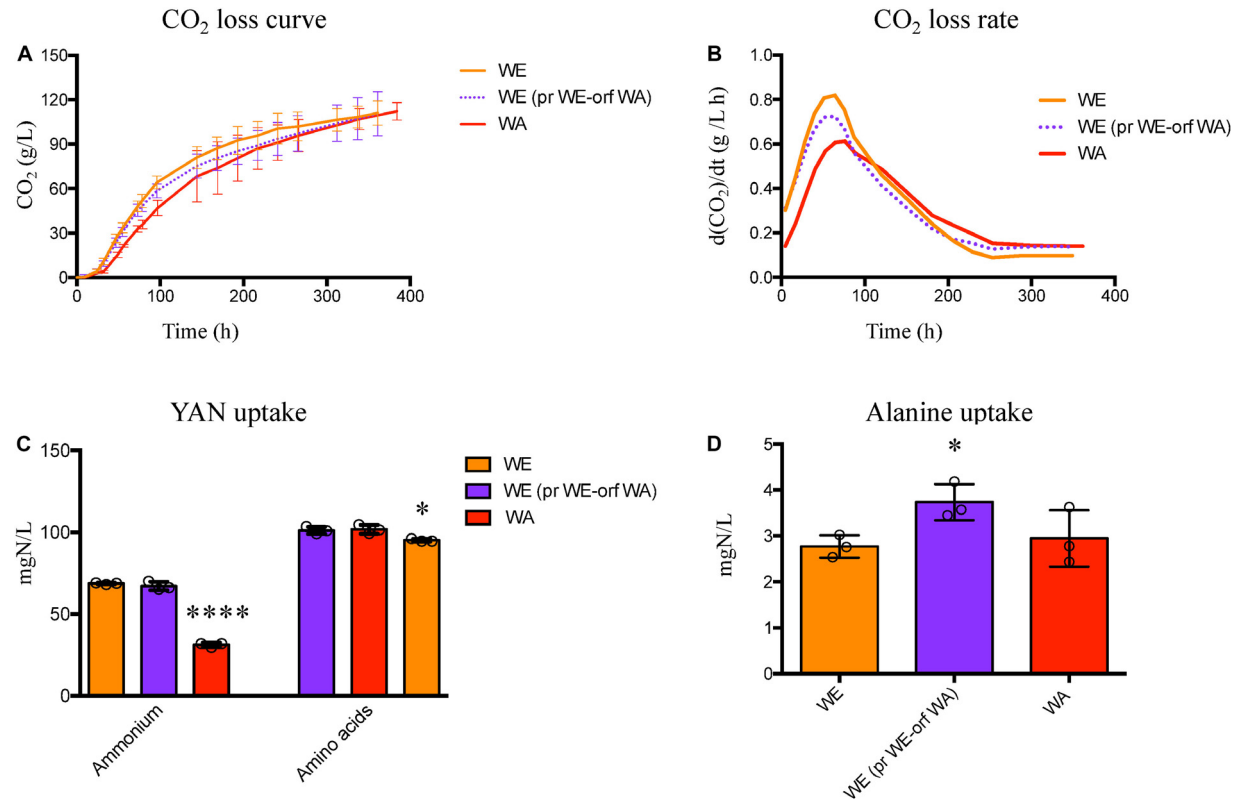

FIGURE 6 | Fermentation performance for the WE strain with *GTR1* allele swapping. **(A)** Fermentative performance was evaluated by CO_2 loss over the time and the kinetic parameters were extracted from the curves. **(B)** Maximum CO_2 loss rate was determined by calculating the first derivate of the CO_2 loss curve. **(C)** Ammonium and amino acids consumption for the WE strain with *GTR1* ORF swapping and the wild type parental strains. **(D)** Alanine consumption for the WE strain with *GTR1* ORF swapping and the wild type parental strains. Plotted values correspond to the average of three biological replicates (dots), with their standard error represented by bars (mean ± SE). The asterisks represent different levels of significance between the phenotypes of strains constructed and wild type strains (*t*-test; $*p < 0.05$ and $****p < 0.0001$). WE, Wine/European; WA, West African; pr, Promoter; orf: Open Reading Frame (ORF).

differences between strains representative of four clean lineages described in *S. cerevisiae* (Wine/European WE, West African WA, North American NA, and Sake SA). In particular, allelic variants of the *GTR1* gene affect the consumption of ammonium and amino acids. The WE allele of this gene presented a preference for ammonium consumption, while the WA allele had a preference for amino acids consumption (Molinet et al., 2019). In consequence, considering that regulation of TORC1 activity

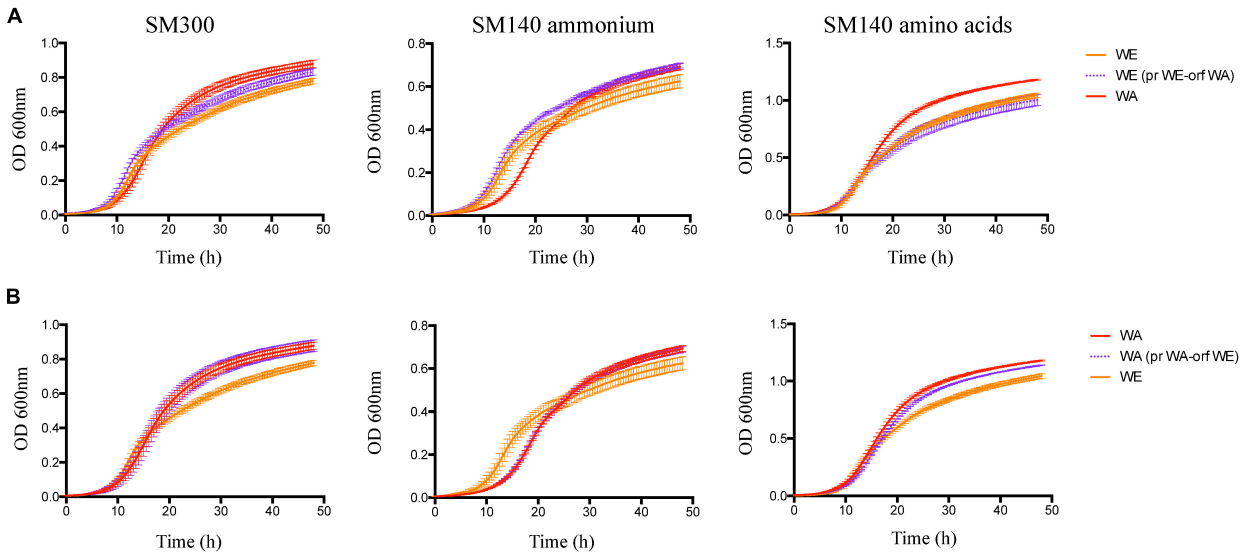

FIGURE 7 | Growth performance for the WE and WA strains with *GTR1* allele swapping. **(A)** Growth curves for the strains with *GTR1* ORF swapping in WE genetic background, and WA genetic background **(B)**. Plotted values correspond to the average of three biological replicates, with their standard error represented by bars (mean ± SE). WE, Wine/European; WA, West African; pr, Promoter; orf, Open Reading Frame (ORF).

could be relevant to nitrogen consumption, we decided to further study the role of the *GTR1* gene on this phenotype in two different genetic backgrounds, providing evidence of the participation of this gene in nitrogen consumption and identifying relevant SNPs that affect TORC1 activation under fermentation conditions.

Null mutants of the *GTR1* gene took up more ammonium and less amino acid than the wild type strains in both genetic backgrounds. Furthermore, expression levels of the nitrogen transporters were higher in these null mutants (**Figure 1**). We did not observe correlation between amino acids consumption and expression levels of their respective transporters, possibly because gene expression and nitrogen consumption were measured at one single point during alcoholic fermentation. Thus, we cannot discard differences in gene expression throughout the fermentation process, where a hierarchical amino acids consumption was previously described (Crépin et al., 2012; Gutiérrez et al., 2016). Therefore, it would be relevant to study the kinetics of nitrogen consumption together with nitrogen transporters expression through the time course of fermentation.

Gtr1p participates in the EGO (Broach, 2012) and Gse complexes (Gao and Kaiser, 2006). The Gse complex regulates the Gap1p (general amino acid permease) intracellular sorting from late endosome to plasmatic membrane and Gap1p recycling is blocked in GSE mutants (Gao and Kaiser, 2006; MacDonald and Piper, 2017). Thus, in this complex, the *GTR1* deletion could be affecting amino acid consumption due to a decrease of Gap1p in the plasmatic membrane.

The EGO complex regulates TORC1 activity in response to nitrogen availability (Zhang et al., 2018). The addition of any amino acid to nitrogen-depleted cells was found to result in rapid but transient EGO-dependent TORC1 activation. However, longer TORC1 activation was only observed upon addition of a nitrogen source sustaining optimal growth, for example glutamine or ammonium, and in an EGO complex independent manner (Stracka et al., 2014). Thus, deletion of *GTR1* could transiently inactivate TORC1, activating the expression of genes regulated by NCR, such as ammonium permeases (*MEP1*, *MEP2,* and *MEP3*), and increasing ammonium consumption. This ammonium consumption could then activate TORC1 independently of the EGO complex, favoring the expression of some amino acid permeases (*AGP1, GNP1,* and *DIP5*). Thus, the deletion of *GTR1* affects cellular growth, where higher ammonium consumption increases growth efficiency and decreases lag time.

In this regard, we indirectly evaluated TORC1 activation using the expression of the *RPL26A* gene as readout for TORC1 activation (Kessi-Pérez et al., 2019b). This method was previously validated in four different strains representative of clean lineages described in *S. cerevisiae* (WE and WA background inclusive) and compared with traditional methods based on immunoblot of Sch9p and Rps6 phosphorylation, exposing strains a proline-to-glutamine upshift, where the maximum luminescence and the area under the curve obtained from graphics of absolute luminescence versus time resemble the results obtained by immunoblot of Sch9p and Rps6p (Kessi-Pérez et al., 2019a,b). Interestingly, the wild type strains showed the same behavior in nitrogen upshift experiments and in synthetic must (SM300), which simulates fermentation conditions. However, in nitrogen upshift experiments, the WA strain presented a higher maximum luciferase expression compared to the WE strain, but in SM300 the WE strain had a greater maximum peak of expression (**Figure 2**), indicating a possible higher TORC1 activation in SM300 in the WE strain. This behavior coincides with other phenotypes controlled by TORC1 activation such as chronological life span, where under fermentation conditions the role of Sir2p, Hst2p, Gcn5p, and Atg7 was the opposite to

TABLE 1 | Kinetic parameters for strains with *GTR1* allele swapping in SM300, SM140-ammonium and SM140-amino acids culture conditions.

Strain	SM300			SM140-ammonium			SM140-amino acids		
	Lag (h)	μ_{max} (h^{-1})	Efficiency (ΔOD)	Lag (h)	μ_{max} (h^{-1})	Efficiency (ΔOD)	Lag (h)	μ_{max} (h^{-1})	Efficiency (ΔOD)
WE	2.26 ± 0.388	0.371 ± 0.008	0.772 ± 0.016	1.32 ± 0.183	0.319 ± 0.011	0.619 ± 0.029	2.74 ± 0.141	0.421 ± 0.374	1.040 ± 0.021
WE (prWA)	2.13 ± 0.496	0.380 ± 0.008	0.758 ± 0.054	1.35 ± 0.169	0.324 ± 0.006	0.651 ± 0.025	3.76 ± 0.679	0.374 ± 1.040	0.977 ± 0.013*
WE (orfWA)	2.03 ± 0.120	0.351 ± 0.009*	0.823 ± 0.020*	1.43 ± 0.327	0.310 ± 0.008	0.690 ± 0.012*	2.53 ± 0.070	0.387 ± 0.010*	0.997 ± 0.049
WE (pr-orfWA)	2.04 ± 0.276	0.362 ± 0.017	0.758 ± 0.073	1.79 ± 0.252	0.308 ± 0.012	0.669 ± 0.025	3.00 ± 1.031	0.409 ± 0.008	1.077 ± 0.046
WA	1.85 ± 0.098	0.323 ± 0.005	0.871 ± 0.020	2.52 ± 0.154	0.260 ± 0.002	0.687 ± 0.014	2.36 ± 0.133	0.351 ± 0.006	1.172 ± 0.005
WA (prWE)	1.69 ± 0.429	0.341 ± 0.009*	0.927 ± 0.021*	2.30 ± 0.229	0.254 ± 0.007	0.670 ± 0.052	2.60 ± 0.405	0.338 ± 0.007	1.149 ± 0.013*
WA (orf WE)	2.07 ± 0.294	0.325 ± 0.005	0.872 ± 0.031	2.06 ± 0.141	0.269 ± 0.004*	0.684 ± 0.014*	2.65 ± 0.188	0.328 ± 0.009*	1.131 ± 0.005***
WA (pr-orfWE)	1.95 ± 0.148	0.313 ± 0.003*	0.907 ± 0.022	2.48 ± 0.142	0.245 ± 0.001***	0.685 ± 0.025	2.82 ± 0.121*	0.330 ± 0.011*	1.170 ± 0.010

*Values correspond to mean and SE of three biological replicates. Asterisks indicate significant differences between phenotypes of strains constructed and wild type strains (t-test, *p < 0.05 and ***p < 0.001). WE, Wine/European; WA, West African; orf, Open Reading Frame; pr: promoter.*

standard laboratory aging conditions (Orozco et al., 2012; Picazo et al., 2015). These results highlight the importance of evaluating TORC1 activity under fermentation conditions since its activity is dependent on the environment.

The *GTR1* deletion modify TORC1 activity with a lower peak of luminescence and maximum luminescence times higher than the wild type strains (**Figure 2** and **Supplementary Table S2**). Thus, the differences observed in nitrogen consumption and expression of transporters between the *GTR1* null mutants and their wild type strains could be the consequence of difference in time and intensity in TORC1 activation. It has been reported that the inability of the Sake strain Kyokai n°7 (K7) to sporulate under nitrogen starvation conditions is due to a reduced TORC1 activity (Nakazawa et al., 2016). Consequently, a diminished TORC1 activity may have an impact on multiple phenotypes. Similarly, our results indicate a possible relationship between a diminished TORC1 activity and higher expression levels of nitrogen transporters, favoring ammonium consumption, but decreasing amino acid assimilation.

Since we previously described allelic variants of the *GTR1* gene that explain nitrogen consumption differences (Molinet et al., 2019), we sought to identify the SNPs responsible for these differences through an allele swapping approach in the parental strains. We swapped the ORF, the regulatory region or both regions in the parental backgrounds (**Figure 3B**). Initially, we determined *GTR1* expression in all the modified strains at 6 h of fermentation (**Figure 4**). Surprisingly, the WA strain presented a higher expression level compared to the WE strain, despite a lower TORC1 activity in this strain (**Figure 2**). Therefore, these results suggest that *GTR1* levels in the cell could affect TORC1 activity. It is important to mention that we did not evaluate the effect of hphMX on the phenotypes studied, thus we cannot discard cis effect and genetic interactions on the *GTR1* expression. However, the constructs were designed using the same orientation for the promoter, ORF and hphMX cassette, avoiding potential problems of convergent transcription and RNA polymerases collision (Pannunzio and Lieber, 2016).

In the case of the WE genetic background, we observed a higher impact in the studied phenotypes in the strain with the WA *GTR1* ORF. This strain presented higher expression levels of the *GTR1* gene compared to the wild type strain (**Figure 4**). In addition, it presented an intermediate TORC1 activity between the WE and WA strains (**Figure 5**). The WE strain with both regions (promoter and ORF) from WA origin presented a similar phenotype to the WE strain with only the ORF from WA origin during the second peak of luminescence, emphasizing the importance of the SNP present in the coding region of the GTR1 gene on the WE genetic background (**Figure 5**). Importantly, this non-synonymous SNP, R113S, is present only in strains from West African origin (**Supplementary Figure S5**), suggesting that this variant could be subject to selection in the palm wine ecological niche. However, we compared a very low number of sequences to validate this assumption and further analysis are necessary, including a higher number of strains used for palm wine fermentation. The R113S SNP is localized in the GTPase domain of the protein, where the GTP and GDP-bound conformations of Gtr1p are crucial for TORC1

activation and inactivation (Gong et al., 2011). Finally, the WE strain with the WA ORF of *GTR1* presented an intermediate fermentation and growth kinetic phenotypes with respect to the wild type strains in SM300 (**Figures 6A,B**, **7A**). This confirms the effect of the polymorphisms in the *GTR1* coding region on the phenotypes evaluated.

In the case of the WA genetic background, we observed moderate effects on the studied phenotypes showing a greater *GTR1* expression compared to WE strain (**Figure 4**). Furthermore, the WA strain with the *GTR1* ORF and regulatory region coming from WE origin showed a slight but significant decrease in *GTR1* expression compared to the wild type WA strain (**Figure 4**). These results indicate the importance of the *GTR1* polymorphisms in the coding region on its own gene expression. Studies in different organisms have determined that the effect of synonymous SNPs in codon usage impact on nucleic acid stability, protein levels, protein structure and functions, even many human diseases have been associated to synonymous SNPs (Bali and Bebok, 2015).

Interestingly, we did not observe differences in the *RPL26A* expression profiles in the WA genetic background, indicative of strong trans-regulation and genetic interactions in the WA strain. Similar results were previously obtained studying the natural variation of the *GPD1* gene. Promoter swapping experiments between the evaluated strains showed different *GPD1* expression levels and times; however, no phenotypic differences were observed (glycerol yield) between wild type and modified strains (Tapia et al., 2018). Therefore, our results highlight how important the SNPs in the coding region of *GTR1* are to the fermentative phenotype of *S. cerevisiae*.

CONCLUSION

In conclusion, we attempted to understand the role of the *GTR1* gene on nitrogen uptake during alcoholic fermentation in *S. cerevisiae*. In this regard, we observed in the *gtr1*Δ mutants a diminish TORC1 activity, an increase in expression levels of nitrogen transporters and ammonium consumption, but a decrease in the assimilation of amino acids. Furthermore, the non-synonymous polymorphism (R113S) present in the *GTR1* gene of the WA strain is relevant for TORC1 activity in the context of the WE strain. However, we were unable to identify mild phenotypic differences due to genetic interactions, suggesting further experiments are required to assess the phosphorylation levels of the proximal TORC1 targets or the GTPase activity of Gtr1p.

DATA AVAILABILITY STATEMENT

All datasets generated for this study are included in the article/**Supplementary Material**.

AUTHOR CONTRIBUTIONS

JM performed lab experiments and analyzed the experimental data. JM and FS prepared the manuscript. All authors designed and funded the research, discussed the results, read, and approved the final manuscript.

FUNDING

This work was supported by the Comisión Nacional de Investigación Científica y Tecnológica (CONICYT) Programa Formación de Capital Humano Avanzado (PCHA) Doctorado Nacional (Grant No. 2014-21140935 to JM), Fondo Nacional de Desarrollo Científico y Tecnológico (FONDECYT) (Grant No. 1150522 to CM and Grant No. 11170158 to FS) and Programa de Cooperación Internacional (CONICYT/PCI) (Grant No. REDI170239 to FS and CM); by the Instituto Milenio iBio – Iniciativa Científica Milenio MINECON to FS; and by the Spanish Government through "Ministerio de Ciencia, Innovación y Universidades" (MICINN) and "Fondo Europeo de Desarrollo Regional" (FEDER) (Grant No. PCIN-2015-143; European Project ERA-IB "YeastTempTation" to JG).

ACKNOWLEDGMENTS

We thank Eduardo Kessi-Pérez for his constructive comments on this work and Ying Su for her technical help.

SUPPLEMENTARY MATERIAL

The Supplementary Material for this article can be found online at: https://www.frontiersin.org/articles/10.3389/fgene.2020.00519/full#supplementary-material

REFERENCES

Bali, V., and Bebok, Z. (2015). Decoding mechanisms by which silent codon changes influence protein biogenesis and function. *Int. J. Biochem. Cell Biol.* 64, 58–74. doi: 10.1016/j.biocel.2015.03.011

Bell, S.-J., and Henschke, P. A. (2005). Implications of nitrogen nutrition for grapes, fermentation and wine. *Aust. J. Grape Wine Res.* 11, 242–295. doi: 10.1111/j.1755-0238.2005.tb00028.x

Bely, M., Sablayrolles, J.-M., and Barre, P. (1990). Automatic detection of assimilable nitrogen deficiencies during alcoholic fermentation in oenological conditions. *J. Ferment. Bioeng.* 70, 246–252. doi: 10.1016/0922-338X(90)90057-4

Brice, C., Cubillos, F. A., Dequin, S., Camarasa, C., and Martínez, C. (2018). Adaptability of the *Saccharomyces cerevisiae* yeasts to wine fermentation conditions relies on their strong ability to consume nitrogen. *PLoS One* 13:e0192383. doi: 10.1371/journal.pone.0192383

Brice, C., Sanchez, I., Bigey, F., Legras, J., and Blondin, B. (2014a). A genetic approach of wine yeast fermentation capacity in nitrogen-starvation reveals the key role of nitrogen signaling. *BMC Genomics* 15:495. doi: 10.1186/1471-2164-15-495

Brice, C., Sanchez, I., Tesnière, C., and Blondin, B. (2014b). Assessing the mechanisms responsible for differences between nitrogen requirements of *Saccharomyces cerevisiae* wine yeasts in alcoholic fermentation. *Appl. Environ. Microbiol.* 80, 1330–1339. doi: 10.1128/AEM.03856-13

Broach, J. R. (2012). Nutritional control of growth and development in yeast. *Genetics* 192, 73–105. doi: 10.1534/genetics.111.135731

Conrad, M., Schothorst, J., Kankipati, H. N., Van Zeebroeck, G., Rubio-Texeira, M., and Thevelein, J. M. (2014). Nutrient sensing and signaling in the yeast *Saccharomyces cerevisiae*. *FEMS Microbiol. Rev.* 38, 254–299. doi: 10.1111/1574-6976.12065

Contreras, A., García, V., Salinas, F., Urzúa, U., Ganga, M. A., and Martínez, C. (2012). Identification of genes related to nitrogen uptake in wine strains of *Saccharomyces cerevisiae*. *World J. Microbiol. Biotechnol.* 28, 1107–1113. doi: 10.1007/s11274-011-0911-3

Crépin, L., Nidelet, T., Sanchez, I., Dequin, S., and Camarasa, C. (2012). Sequential use of nitrogen compounds by *Saccharomyces cerevisiae* during wine fermentation: a model based on kinetic and regulation characteristics of Nitrogen permeases. *Appl. Environ. Microbiol.* 78, 8102–8111. doi: 10.1128/AEM.02294-12

Crépin, L., Sanchez, I., Nidelet, T., Dequin, S., and Camarasa, C. (2014). Efficient ammonium uptake and mobilization of vacuolar arginine by *Saccharomyces cerevisiae* wine strains during wine fermentation. *Microb. Cell Fact.* 13:109. doi: 10.1186/s12934-014-0109-0

Crépin, L., Truong, N. M., Bloem, A., Sanchez, I., Dequin, S., and Camarasa, C. (2017). Management of multiple nitrogen sources during wine fermentation by *Saccharomyces cerevisiae*. *Appl. Environ. Microbiol.* 83:AEM.02617-16. doi: 10.1128/AEM.02617-16

Cubillos, F., Brice, C., Molinet, J., Tisné, S., Abarca, V., Tapia, S., et al. (2017). Identification of Nitrogen consumption genetic variants in yeast through QTL mapping and bulk segregant RNA-Seq analyses. *G3* 7, 1693–1705. doi: 10.1534/g3.117.042127

Cubillos, F. A., Louis, E. J., and Liti, G. (2009). Generation of a large set of genetically tractable haploid and diploid *Saccharomyces* strains. *FEMS Yeast Res.* 9, 1217–1225. doi: 10.1111/j.1567-1364.2009.00583.x

De Virgilio, C., and Loewith, R. (2006). Cell growth control: little eukaryotes make big contributions. *Oncogene* 25, 6392–6415. doi: 10.1038/sj.onc.1209884

Gao, M., and Kaiser, C. A. (2006). A conserved GTPase-containing complex is required for intracellular sorting of the general amino-acid permease in yeast. *Nat. Cell Biol.* 8, 657–667. doi: 10.1038/ncb1419

Gómez-Alonso, S., Hermosín-Gutiérrez, I., and García-Romero, E. (2007). Simultaneous HPLC analysis of biogenic amines, amino acids, and ammonium ion as aminoenone derivatives in wine and beer samples. *J. Agric. Food Chem.* 55, 608–613. doi: 10.1021/jf062820m

Gong, R., Li, L., Liu, Y., Wang, P., Yang, H., Wang, L., et al. (2011). Crystal structure of the Gtr1p-Gtr2p complex reveals new insights into the amino acid-induced TORC1 activation. *Genes Dev.* 25, 1668–1673. doi: 10.1101/gad.16968011

Gutiérrez, A., Chiva, R., Sancho, M., Beltran, G., Arroyo-López, F. N., and Guillamon, J. M. (2012). Nitrogen requirements of commercial wine yeast strains during fermentation of a synthetic grape must. *Food Microbiol.* 31, 25–32. doi: 10.1016/j.fm.2012.02.012

Gutiérrez, A., Sancho, M., Beltran, G., Guillamon, J. M., and Warringer, J. (2016). Replenishment and mobilization of intracellular nitrogen pools decouples wine yeast nitrogen uptake from growth. *Appl. Microbiol. Biotechnol.* 100, 3255–3265. doi: 10.1007/s00253-015-7273-y

Hatakeyama, R., and De Virgilio, C. (2016). Unsolved mysteries of Rag GTPase signaling in yeast. *Small GTPases* 7, 239–246. doi: 10.1080/21541248.2016.1211070

Ibstedt, S., Stenberg, S., Bagés, S., Gjuvsland, A. B., Salinas, F., Kourtchenko, O., et al. (2015). Concerted Evolution of Life Stage Performances Signals Recent Selection on Yeast Nitrogen Use. *Mol. Biol. Evol.* 32, 153–161. doi: 10.1093/molbev/msu285

Jara, M., Cubillos, F. A., García, V., Salinas, F., Aguilera, O., Liti, G., et al. (2014). Mapping genetic variants underlying differences in the central nitrogen metabolism in fermenter yeasts. *PLoS One* 9:e86533. doi: 10.1371/journal.pone.0086533

Kessi-Pérez, E. I., Molinet, J., and Martínez, C. (2020). Disentangling the genetic bases of *Saccharomyces cerevisiae* nitrogen consumption and adaptation to low nitrogen environments in wine fermentation. *Biol. Res.* 53, 1–10. doi: 10.1186/s40659-019-0270-3

Kessi-Pérez, E. I., Salinas, F., González, A., Su, Y., Guillamón, J. M., Hall, M. N., et al. (2019a). KAE1 allelic variants affect TORC1 activation and fermentation kinetics in *Saccharomyces cerevisiae*. *Front. Microbiol.* 10:1686. doi: 10.3389/fmicb.2019.01686

Kessi-Pérez, E. I., Salinas, F., Molinet, J., González, A., Muñiz, S., Guillamón, J. M., et al. (2019b). Indirect monitoring of TORC1 signalling pathway reveals molecular diversity among different yeast strains. *Yeast* 36, 65–74. doi: 10.1002/yea.3351

MacDonald, C., and Piper, R. C. (2017). Genetic dissection of early endosomal recycling highlights a TORC1-independent role for Rag GTPases. *J. Cell Biol.* 216, 3275–3290. doi: 10.1083/jcb.201702177

Magasanik, B., and Kaiser, C. A. (2002). Nitrogen regulation in *Saccharomyces cerevisiae*. *Gene* 290, 1–18. doi: 10.1016/S0378-1119(02)00558-9

Martínez, C., Contreras, A., Aguilera, O., Ganga, A., and García, V. (2014). The ICY1 gene from *Saccharomyces cerevisiae* affects nitrogen consumption during alcoholic fermentation. *Electron. J. Biotechnol.* 17, 150–155. doi: 10.1016/j.ejbt.2014.04.006

Martinez, C., García, V., González, D., Jara, M., Aguilera, M., and Ganga, M. A. (2013). Gene expression of specific enological traits in wine fermentation. *Electron. J. Biotechnol.* 16, 4–11. doi: 10.2225/vol16-issue4-fulltext-8

Marullo, P., Bely, M., Masneuf-Pomarède, I., Pons, M., Aigle, M., and Dubourdieu, D. (2006). Breeding strategies for combining fermentative qualities and reducing off-flavor production in a wine yeast model. *FEMS Yeast Res.* 6, 268–279. doi: 10.1111/j.1567-1364.2006.00034.x

Molinet, J., Cubillos, F. A., Salinas, F., Liti, G., and Martínez, C. (2019). Genetic variants of TORC1 signaling pathway affect nitrogen consumption in *Saccharomyces cerevisiae* during alcoholic fermentation. *PLoS One* 14:e0220515. doi: 10.1371/journal.pone.0220515

Nakazawa, N., Sato, A., and Hosaka, M. (2016). TORC1 activity is partially reduced under nitrogen starvation conditions in sake yeast Kyokai no. 7. *Saccharomyces cerevisiae*. *J. Biosci. Bioeng.* 121, 247–252. doi: 10.1016/j.jbiosc.2015.07.002

Nieduszynski, C. A., and Liti, G. (2011). From sequence to function: Insights from natural variation in budding yeasts. *Biochim. Biophys. Acta* 1810, 959–966. doi: 10.1016/j.bbagen.2011.02.004

Nissen, T. L., Schulze, U., Nielsen, J., and Villadsen, J. (1997). Flux distributions in anaerobic, glucose-limited continuous cultures of *Saccharomyces cerevisiae*. *Microbiology* 143, 203–218. doi: 10.1099/00221287-143-1-203

Oldenburg, K. R., Vo, K. T., Michaelis, S., and Paddon, C. (1997). Recombination-mediated PCR-directed plasmid construction in vivo in yeast. *Nucleic Acids Res.* 25, 451–452. doi: 10.1093/nar/25.2.451

Orozco, H., Matallana, E., and Aranda, A. (2012). Wine yeast sirtuins and Gcn5p control aging and metabolism in a natural growth medium. *Mech. Ageing Dev.* 133, 348–358. doi: 10.1016/j.mad.2012.03.013

Pannunzio, N. R., and Lieber, M. R. (2016). Dissecting the roles of divergent and convergent transcription in chromosome instability. *Cell Rep.* 14, 1025–1031. doi: 10.1016/j.celrep.2015.12.098

Pfaffl, M. W. (2001). A new mathematical model for relative quantification in real-time RT-PCR. *Nucleic Acids Res.* 29:e45. doi: 10.1093/nar/29.9.e45

Picazo, C., Orozco, H., Matallana, E., and Aranda, A. (2015). Interplay among Gcn5, Sch9 and mitochondria during chronological aging of wine yeast is dependent on growth conditions. *PLoS One* 10:e0117267. doi: 10.1371/journal.pone.0117267

Pretorius, I. S. (2000). Tailoring wine yeast for the new millennium: novel approaches to the ancient art of winemaking. *Yeast* 16, 675–729. doi: 10.1002/1097-0061(20000615)16:8<675::AID-YEA585<3.0.CO;2-B

Rossignol, T., Dulau, L., Julien, A., and Blondin, B. (2003). Genome-wide monitoring of wine yeast gene expression during alcoholic fermentation. *Yeast* 20, 1369–1385. doi: 10.1002/yea.1046

Salinas, F., de Boer, C. G., Abarca, V., García, V., Cuevas, M., Araos, S., et al. (2016). Natural variation in non-coding regions underlying phenotypic diversity in budding yeast. *Sci. Rep.* 6:21849. doi: 10.1038/srep21849

Stracka, D., Jozefczuk, S., Rudroff, F., Sauer, U., and Hall, M. N. (2014). Nitrogen Source Activates TOR (Target of Rapamycin) Complex 1 via Glutamine and Independently of Gtr/Rag Proteins. *J. Biol. Chem.* 289, 25010–25020. doi: 10.1074/jbc.M114.574335

Swinnen, S., Thevelein, J. M., and Nevoigt, E. (2012). Genetic mapping of quantitative phenotypic traits in *Saccharomyces cerevisiae*. *FEMS Yeast Res.* 12, 215–227. doi: 10.1111/j.1567-1364.2011.00777.x

Tapia, S. M., Cuevas, M., Abarca, V., Delgado, V., Rojas, V., García, V., et al. (2018). GPD1 and ADH3 natural variants underlie glycerol yield differences in wine fermentation. *Front. Microbiol.* 9:1460. doi: 10.3389/fmicb.2018.01460

Tesnière, C., Brice, C., and Blondin, B. (2015). Responses of *Saccharomyces cerevisiae* to nitrogen starvation in wine alcoholic fermentation. *Appl. Microbiol. Biotechnol.* 99, 7025–7034. doi: 10.1007/s00253-015-6810-z

Teste, M.-A., Duquenne, M., François, J. M., and Parrou, J.-L. (2009). Validation of reference genes for quantitative expression analysis by real-time RT-PCR in Saccharomyces cerevisiae. *BMC Mol. Biol.* 10:99. doi: 10.1186/1471-2199-10-99

Thompson, D. A., and Cubillos, F. A. (2017). Natural gene expression variation studies in yeast. *Yeast* 34, 3–17. doi: 10.1002/yea.3210

Vandesompele, J., De Preter, K., Pattyn, F., Poppe, B., Van Roy, N., De Paepe, A., et al. (2002). Accurate normalization of real-time quantitative RT-PCR data by geometric averaging of multiple internal control genes. *Genome Biol.* 3:0034. doi: 10.1186/gb-2002-3-7-research0034

Walker, M. E., Nguyen, T. D., Liccioli, T., Schmid, F., Kalatzis, N., Sundstrom, J. F., et al. (2014). Genome-wide identification of the Fermentome; genes required for successful and timely completion of wine-like fermentation by *Saccharomyces cerevisiae*. *BMC Genomics* 15:552. doi: 10.1186/1471-2164-15-552

Warringer, J., and Blomberg, A. (2003). Automated screening in environmental arrays allows analysis of quantitative phenotypic profiles in *Saccharomyces cerevisiae*. *Yeast* 20, 53–67. doi: 10.1002/yea.931

Yuan, J., Reed, A., Chen, F., and Stewart, C. N. (2006). Statistical analysis of real-time PCR data. *BMC Bioinformatics* 7:85. doi: 10.1186/1471-2105-7-85

Zhang, W., Du, G., Zhou, J., and Chen, J. (2018). Regulation of sensing, transportation, and catabolism of nitrogen sources in *Saccharomyces cerevisiae*. *Microbiol. Mol. Biol. Rev.* 82:e0040-17. doi: 10.1128/MMBR.00040-17

Zwietering, M. H., Jongenburger, I. L., Rombouts, F. M., and Van Riet, K. (1990). Modeling of the bacterial growth curve. *Appl. Environ. Microbiol.* 56, 1875–1881.

Conflict of Interest: The authors declare that the research was conducted in the absence of any commercial or financial relationships that could be construed as a potential conflict of interest.

frontiers in Genetics

ORIGINAL RESEARCH
published: 03 June 2020
doi: 10.3389/fgene.2020.00518

Improving Industrially Relevant Phenotypic Traits by Engineering Chromosome Copy Number in *Saccharomyces pastorianus*

Arthur R. Gorter de Vries†‡, Ewout Knibbe†, Roderick van Roosmalen, Marcel van den Broek, Pilar de la Torre Cortés, Stephanie F. O'Herne, Pascal A. Vijverberg, Anissa el Masoudi, Nick Brouwers, Jack T. Pronk‡ and Jean-Marc G. Daran‡*

Department of Biotechnology, Delft University of Technology, Delft, Netherlands

The lager-brewing yeast *Saccharomyces pastorianus* is a hybrid between *S. cerevisiae* and *S. eubayanus* with an exceptional degree of aneuploidy. While chromosome copy number variation (CCNV) is present in many industrial *Saccharomyces* strains and has been linked to various industrially-relevant traits, its impact on the brewing performance of *S. pastorianus* remains elusive. Here we attempt to delete single copies of chromosomes which are relevant for the production of off-flavor compound diacetyl by centromere silencing. However, the engineered strains display CNV of multiple non-targeted chromosomes. We attribute this unintended CCNV to inherent instability and to a mutagenic effect of electroporation and of centromere-silencing. Regardless, the resulting strains displayed large phenotypic diversity. By growing centromere-silenced cells in repeated sequential batches in medium containing 10% ethanol, mutants with increased ethanol tolerance were obtained. By using CCNV mutagenesis by exposure to the mitotic inhibitor MBC, selection in the same set-up yielded even more tolerant mutants that would not classify as genetically modified organisms. These results show that CCNV of alloaneuploid *S. pastorianus* genomes is highly unstable, and that CCNV mutagenesis can generate broad diversity. Coupled to effective selection or screening, CCNV mutagenesis presents a potent tool for strain improvement.

Keywords: *Saccharomyces pastorianus*, chromosome missegregation, chromosome copy number stability, strain engineering, lager beer brewing

OPEN ACCESS

Edited by:
Francisco A. Cubillos, Universidad de Santiago de Chile, Chile

Reviewed by:
Kristoffer Krogerus, VTT Technical Research Centre of Finland Ltd, Finland
Jing Li, Sun Yat-sen University Cancer Center (SYSUCC), China

***Correspondence:**
Jean-Marc G. Daran
j.g.daran@tudelft.nl

† These authors have contributed equally to this work

‡ORCID:
Arthur R. Gorter de Vries
orcid.org/0000-0002-0841-6583
Jack T. Pronk
orcid.org/0000-0002-5617-4611
Jean-Marc G. Daran
orcid.org/0000-0003-3136-8193

Specialty section:
This article was submitted to Evolutionary and Genomic Microbiology, a section of the journal Frontiers in Genetics

Received: *12 March 2020*
Accepted: *28 April 2020*
Published: *03 June 2020*

Citation:
Gorter de Vies AR, Knibbe E, van Roosmalen R, van den Broek M, de la Torre Cortés P, O'Herne SF, Vijverberg PA, el Masoudi A, Brouwers N, Pronk JT and Daran J-MG (2020) Improving Industrially Relevant Phenotypic Traits by Engineering Chromosome Copy Number in Saccharomyces pastorianus. Front. Genet. 11:518. doi: 10.3389/fgene.2020.00518

INTRODUCTION

The lager brewing yeast *Saccharomyces pastorianus* is an interspecific hybrid of *Saccharomyces cerevisiae* and the cold-tolerant *Saccharomyces eubayanus* (Libkind et al., 2011; Salazar et al., 2019). Chromosomes from both parental species are present in the genome of *S. pastorianus* in varying number of copies, making the genome alloploid and aneuploid (Dunn and Sherlock, 2008). Quantitative measurement based on a combination of sequencing data and flow cytometry based DNA quantification estimated the chromosome copy number ranging from 49 to 79 chromosomes in *S. pastorianus*, a quantification that contributed to distinguish two groups based on copy number of chromosomes from each parental species. Although all *S. pastorianus* strains have

an approximately diploid *S. eubayanus* subgenome, Group 1 strains (Saaz) have a, generally incomplete, haploid *S. cerevisiae* subgenome, while Group 2 strains (Frohberg) have a diploid or higher *S. cerevisiae* subgenome (Nakao et al., 2009; van den Broek et al., 2015; Okuno et al., 2016). Reflecting these differences in genome composition, Group 1 strains are more cold-tolerant whereas Group 2 strains exhibit more efficient maltotriose consumption, traits associated with *S. eubayanus* and *S. cerevisiae*, respectively (Gibson et al., 2013; Brouwers et al., 2019a,b). Chromosome recombinations at the *ZUO1*, *MAT*, *HSP82*, and *XRN1*/*KEM1* loci which were found in all *S. pastorianus* isolates suggest that they evolved from a single hybrid ancestor, and that the extensive CCNV of *S. pastorianus* strains emerged during its domestication (Hewitt et al., 2014; Walther et al., 2014; van den Broek et al., 2015; Okuno et al., 2016; Gorter de Vries et al., 2019b). Moreover, there are large copy number differences between the genomes of *S. pastorianus* strains, even among supposedly clonal isolates, suggesting high genomic plasticity and chromosome copy number instability (Bolat et al., 2008; van den Broek et al., 2015).

Chromosomal copy number variation (CCNV) in yeast is generally caused by chromosome missegregation during mitosis. Normally, chromosome segregation during anaphase is ensured by attachment of the microtubule spindle to the kinetochore. Despite numerous control mechanisms (checkpoints) for correct kinetochore attachment, cells can proceed to anaphase while chromosomes are incorrectly attached, leading to gain and loss of a chromosome copy in the resulting daughter cells (Musacchio and Salmon, 2007). The rate at which chromosome missegregation occurs is increased in polyploid and aneuploid genomes, resulting in increased chromosomal copy number instability (Sheltzer et al., 2011; Storchova, 2014). Changes in chromosome copy number are generally reflected by altered expression levels of genes on the affected chromosome and the correspondingly altered protein levels can cause significant phenotypic effects (Pavelka et al., 2010; Dephoure et al., 2014). In accordance with the greater phenotypic impact of copy number than SNPs in *Saccharomyces* strains (Peter et al., 2018), CCNV can be beneficial under specific selective conditions due to the effect of single or multiple affected genes (Gorter de Vries et al., 2017). Indeed, spontaneous chromosome gain and loss are common in *Saccharomyces* yeast strains derived from mutation accumulation experiments, laboratory evolution studies and industrial settings (Zhu et al., 2014; Hose et al., 2015; Gorter de Vries et al., 2017, 2019c). In an evolutionary context aneuploidy and CCNV appear to have a role in creating large phenotypic diversity in a population and thereby allowing large phenotypic leaps (Chen et al., 2012). However, when introducing CCNV in euploid strains, aneuploidy causes deleterious effects such as increased genome instability, low sporulation efficiency, reduced growth rate, increased nutrient uptake rates, and reduced replicative life span, which are jointly referred to as the aneuploidy-associated stress response (AASR). AASR was attributed to an imbalance of gene expression, specifically of protein complexes, and to overloading of the protein degradation pathways (Torres et al., 2011; Santaguida and Amon, 2015b). Due to the combination of beneficial and detrimental effects of CCNV, aneuploidy can be a transient adaptation to stress which is subsequently replaced by mutations with less side effects after continued evolution (Yona et al., 2012). However, in many wild and industrial yeasts, no direct detrimental effects from aneuploidy are reported and the typical AASR is not observed (Hose et al., 2015), indicating that cells can adapt to minimize the negative impact of aneuploidy while still benefiting from the phenotypic diversity generated by CCNV.

The CCNV in lager brewing yeast *S. pastorianus* affects more chromosomes than the few chromosomes typically observed after laboratory evolution or in natural isolates (Brickwedde et al., 2017). As the current CCNV in *S. pastorianus* strains emerged under the selective pressure of the lager brewing environment and is apparently stably maintained, it likely contributes to its performance in this environment. Indeed, CCNV correlates with industrially-relevant traits such as flocculation and diacetyl production in otherwise nearly isogenic *S. pastorianus* strains (van den Broek et al., 2015). However, to determine if CCNV is causal for flocculation and diacetyl production, a method to engineer CCNV in *S. pastorianus* is required to generate a library of isogenic strains which differ only in CCNV. In *S. cerevisiae* strains, targeted gain or loss of a single chromosome copy can be achieved by introducing an inducible promotor and a counter-selectable marker gene immediately adjacently to a centromere through homologous recombination (Hill and Bloom, 1987). Strong promoter expression disrupts centromere function, increasing the frequency of missegregation of sister chromatids and leading to daughter cells which either a lost or a duplicated chromosome (Panzeri et al., 1984). Cells that lost or duplicated the chromosome can be selected based on selection or counter-selection of an inserted marker. Such conditional centromeres have been used to construct diploid *S. cerevisiae* strains hemizygous or disomic for various chromosomes (Reid et al., 2008; Anders et al., 2009).

In this study, conditional centromeres were introduced and induced in *S. pastorianus* Group 2 strain CBS 1483 in order to create isogenic *S. pastorianus* strains differing only by their CCNV. Brewing relevant phenotypes of the resulting strains were characterized to investigate the effect of CCNV in the complex aneuploid genome of *S. pastorianus*. In addition, CCNV stability of CBS 1483 during growth and during genetic manipulation was evaluated. Finally the potential of inducing CCNV using centromere-silencing or chemical mutagenesis to generate phenotypic diversity was investigated by selecting for strains with increased ethanol tolerance.

MATERIALS AND METHODS

Yeast Strains and Media

The *Saccharomyces* strains used in this study are indicated in **Table 1**. *S. pastorianus* strain CBS 1483 was obtained from the Westerdijk Fungal Biodiversity Institute.[1] Yeast strains and *E. coli* strains containing plasmids were stored at −80°C in 30% glycerol (vol/vol). For preparation of stock cultures and

[1] http://www.westerdijkinstitute.nl/

TABLE 1 | *Saccharomyces pastorianus* strains used in this study.

Strain Name	Host strain	Description or intended mutation	Sequenced genotype	References
CBS 1483	–	Group 2 strain	wildtype	(van den Broek et al., 2015; Brickwedde et al., 2017)
IMI350	CBS 1483	*SeCEN6::amdS-GAL1p*	Not sequenced	This study
IMS349	CBS 1483	SeCHRVI^{-1}	SeCHRVI^{-1}	This study
IMI351	IMI350	SeCHRVI^{-1}	*Sc*CHRV^{-1} *Sc*CHRX-*Se*CHRX^{+1} *Se*CHRVI^{-1} *Se*CHRX-*Sc*CHRX^{-1}	This study
IMI352	CBS 1483	*ScCEN9*::*amdS-GAL1*p	Not sequenced	This study
IMI353	IMI352	*Sc*CHRIX^{-1}	*Sc*CHRXV-XI^{-1}	This study
IMI359	CBS 1483	*Sc*CEN10:: *amdS-GAL1*p	Not sequenced	This study
IMI360	CBS 1483	*Sc*CEN12:: *amdS-GAL1*p	Not sequenced	This study
IMI361	CBS 1483	*Sc*CEN14:: *amdS-GAL1*p	*Sc*CEN14:: *amdS-GAL1*p *Sc*CHRII^{-1} *Sc*CHRVIII^{-1} SeCHRVII-ScCHRVII^{-1}	This study
IMI363	CBS 1483	*Se*CEN3:: *amdS-GAL1*p	Not sequenced	This study
IMI366	CBS 1483	*Se*CEN8:: *amdS-GAL1*p	Not sequenced	This study
IMI367	CBS 1483	*Se*CEN10:: *amdS-GAL1*p	Not sequenced	This study
IMI368	CBS 1483	*Se*CEN12:: *amdS-GAL1*p	Not sequenced	This study
IMI369	CBS 1483	*Se*CEN14:: *amdS-GAL1*p	Not sequenced	This study
IMI373	IMI359	*Sc*CHRX-*Se*CHRX^{-1}	*Sc*CHRX-*Se*CHRX^{-1} *Se*CHRIX	This study
IMI374	IMI360	*Sc*CHRXII^{-1}	*Sc*CHRII *Sc*CHRVIII^{-1} *Sc*CHRXII^{-1} *Se*CHRIX^{-1}	This study
IMI375	IMI361	*Sc*CHRXIV^{-1}	*Sc*CHRII^{-1} *Sc*CHRV^{-1} *Sc*CHRVIII^{-3} *Sc*CHRXIII^{-1} *Sc*CHRXIV^{-1} *Se*CHRI^{-1} *Se*CHRIII-*Sc*CHRIII^{-1} SeCHRVII-ScCHRVII^{-1} SeCHRVIII-XV^{+1}	This study
IMI377	IMI363	*Se*CHRIII^{-1}	*Sc*CHRI^{1} *Sc*CHRVIII^{-1} *Se*CHRIX^{-1}	This study
IMI380	IMI366	*Se*CHRVIII^{-1}	*Sc*CHRV^{-1} *Sc*CHRVIII^{-2} SeCHRIX^{+2}	This study
IMI381	IMI367	*Se*CHRX^{-1}	*Sc*CHRIV^{+1} *Sc*CHRVIII^{-1} *Sc*CHRIX^{+1} *Sc*CHRXI^{-1} *Sc*CHRXII^{-1} *Se*CHRII-IV$^{-1(D)}$ *Se*CHRX-*Sc*CHRX^{-1} *Se*CHRXI^{+1}	This study
IMI382	IMI368	*Se*CHRXII^{-1}	*Sc*CHRIV^{-1} *Sc*CHRV^{-1} *Sc*CHRVIII^{-1} *Sc*CHRX-*Se*CHRX^{-1} *Se*CHRVI^{-1} *Se*CHRXII^{-1} *Se*CHRXV-VIII$^{-1(D)}$	This study
IMI383	IMI369	*Se*CHRXIV^{-1}	*Sc*CHRX-*Se*CHRX^{-1} *Se*CHRIX^{-1}	This study
IMS0687	CBS 1483	MBC mutagenesis reactor MBC1	*Sc*CHRI^{-1} *Sc*CHRV^{-1} *Sc*CHRXIII^{-1} *Se*CHRIX^{+1} *Se*CHRX-ScCHRX^{-1} *Se*CHRXIV^{-1} *Se*CRXV-VIII^{-1}	This study
IMS0688	CBS 1483	MBC mutagenesis reactor MBC1	Not sequenced	This study
IMS0689	CBS 1483	MBC mutagenesis reactor MBC1	Not sequenced	This study
IMS0690	CBS 1483	MBC mutagenesis reactor MBC1	Not sequenced	This study
IMS0691	CBS 1483	MBC mutagenesis reactor MBC1	Not sequenced	This study
IMS0692	CBS 1483	MBC mutagenesis reactor MBC1	Not sequenced	This study
IMS0693	CBS 1483	MBC mutagenesis reactor MBC1	Not sequenced	This study
IMS0694	CBS 1483	MBC mutagenesis reactor MBC1	Not sequenced	This study
IMS0695	CBS 1483	MBC mutagenesis reactor MBC1	Not sequenced	This study
IMS0696	CBS 1483	MBC mutagenesis reactor MBC1	Not sequenced	This study
IMS0697	CBS 1483	MBC mutagenesis reactor MBC1	Not sequenced	This study
IMS0698	CBS 1483	MBC mutagenesis reactor MBC1	Not sequenced	This study
IMS0699	CBS 1483	MBC mutagenesis reactor MBC1	Not sequenced	This study
IMS0700	CBS 1483	MBC mutagenesis reactor MBC1	Not sequenced	This study
IMS0701	CBS 1483	MBC mutagenesis reactor MBC1	Not sequenced	This study
IMS0702	CBS 1483	MBC mutagenesis reactor MBC1	Not sequenced	This study
IMS0703	CBS 1483	MBC mutagenesis reactor MBC1	*Sc*CHRI^{-1} *Sc*CHRV^{-1} *Sc*CHRVIII^{-1} *Sc*CHRXIII^{-1} *Se*CHRIX^{-1} *Se*CHRXIV^{-1} *Se*CRXV-VIII^{-1}	This study
IMS0704	CBS 1483	MBC mutagenesis reactor MBC1	Not sequenced	This study
IMS0705	CBS 1483	Electroporated	*Sc*CHRVIII^{-1} *Se*CHRVI^{+1} *Se*CHRX-ScCHRX^{-1}	This study
IMS0706	CBS 1483	Electroporated	*Sc*CHRI^{-1} *Sc*CHRVIII^{-1} *Se*CHRIX^{-1}	This study
IMS0707	CBS 1483	Electroporated	Not sequenced	This study
IMS0708	CBS 1483	Electroporated	*Sc*CHRI^{-1} *Se*CHRX-*Sc*CHRX^{-1} *Se*CHRXVI^{-1}	This study
IMS0709	CBS 1483	Electroporated	*Sc*CHRI^{-1} *Sc*CHRVIII^{-1} SeCHRIX^{-1}	This study
IMS0710	CBS 1483	Restreaked untransformed	ploidy unchanged	This study

(Continued)

TABLE 1 | Continued

Strain Name	Host strain	Description or intended mutation	Sequenced genotype	References
IMS0711	CBS 1483	Restreaked untransformed	*Se*CHRVII-*Sc*CHRVII^{+1}	This study
IMS0712	CBS 1483	Restreaked untransformed	*Se*CHRX-ScCHRX^{-1}	This study
IMS0713	CBS 1483	Restreaked untransformed	Not sequenced	This study
IMS0714	CBS 1483	Restreaked untransformed	*Sc*CHRIX^{-1}	This study
IMS0715	CBS 1483	MBC mutagenesis reactor MBC2	Not sequenced	This study
IMS0716	CBS 1483	MBC mutagenesis reactor MBC2	*Sc*CHRI^{-1} *Sc*CHRV^{-1} *Sc*CHRVII^{+1} ScCHRVIII^{-2} *Sc*CHRXV-XI^{-1} *Se*CHRVII-ScCHRVII^{-1} *Se*CHRXIV^{-1} *Se*CRXV-VIII^{-1}	This study
IMS0717	CBS 1483	MBC mutagenesis reactor MBC2	Not sequenced	This study
IMS0718	CBS 1483	MBC mutagenesis reactor MBC2	Not sequenced	This study
IMS0719	CBS 1483	MBC mutagenesis reactor MBC2	Not sequenced	This study
IMS0720	CBS 1483	MBC mutagenesis reactor MBC2	Not sequenced	This study
IMX1875	IMI361	Galactose induction mutagenesis reactor GAL1	Not sequenced	This study
IMX1876	IMI361	Galactose induction mutagenesis reactor GAL1	Not sequenced	This study
IMX1877	IMI361	Galactose induction mutagenesis reactor GAL1	Not sequenced	This study
IMX1878	IMI361	Galactose induction mutagenesis reactor GAL1	Not sequenced	This study
IMX1879	IMI361	Galactose induction mutagenesis reactor GAL1	Not sequenced	This study
IMX1880	IMI361	Galactose induction mutagenesis reactor GAL1	Not sequenced	This study
IMX1881	IMI361	Galactose induction mutagenesis reactor GAL1	Not sequenced	This study
IMX1882	IMI361	Galactose induction mutagenesis reactor GAL1	Not sequenced	This study
IMX1883	IMI361	Galactose induction mutagenesis reactor GAL1	Not sequenced	This study
IMX1884	IMI361	Galactose induction mutagenesis reactor GAL1	Not sequenced	This study
IMX1885	IMI361	Galactose induction mutagenesis reactor GAL1	Not sequenced	This study
IMX1886	IMI361	Galactose induction mutagenesis reactor GAL1	Not sequenced	This study
IMX1887	IMI361	Galactose induction mutagenesis reactor GAL1	Not sequenced	This study
IMX1888	IMI361	Galactose induction mutagenesis reactor GAL1	Not sequenced	This study
IMX1889	IMI361	Galactose induction mutagenesis reactor GAL1	Not sequenced	This study
IMX1890	IMI361	Galactose induction mutagenesis reactor GAL2	Not sequenced	This study
IMX1891	IMI361	Galactose induction mutagenesis reactor GAL2	Not sequenced	This study
IMX1892	IMI361	Galactose induction mutagenesis reactor GAL2	Not sequenced	This study
IMX1893	IMI361	Galactose induction mutagenesis reactor GAL2	Not sequenced	This study

For each strain, the strain from which it was derived is indicated, and the genotype is indicated for strains which were sequenced.

inocula of bioreactors, yeast strains were routinely propagated in shake flasks containing 100 mL YPD (10 g/L yeast extract, 20 g/L yeast peptone and 20 g/L glucose) at 30°C and 200 RPM in an Brunswick Innova43/43R shaker (Eppendorf Nederland B.V., Nijmegen, Netherlands). For cultivation on solid media, YPD medium was supplemented with 20 g/L Bacto agar (Becton Dickinson, Breda, Netherlands) and incubation was done at 30°C. Synthetic medium (SM), containing 3 g/L KH_2PO_4, 0.5 g/L $MgSO_4.7H_2O$, 5 g/L $(NH_4)_2SO_4$, 1 mL/L of a trace element solution and 1 mL/L of a vitamin solution, was prepared as previously described (Bruinenberg et al., 1983; Verduyn et al., 1992). For growth in the presence of ethanol, absolute ethanol (Sigma Aldrich, St. Louis, MO, United States) was added in varying concentration to YPD or SMD (20 with g/L glucose) with a correspondingly decreased volume of water to avoid dilution of medium components. Selection for the *amdS* marker was performed on SM-AC: SM with 0.6 g/L acetamide and 6.6 g/L K_2SO_4 instead of $(NH_4)_2SO_4$ as nitrogen source (Solis-Escalante et al., 2013). Induction of the *GAL1* promoter ($GAL1_p$) was performed on YPGal medium (10 g/L yeast extract, 20 g/L yeast peptone and 20 g/L galactose) or on SMGal-AC medium: SM-AC medium with 20 g/L galactose instead of glucose. For counter selection of the *amdS* marker, strains were first grown on YPD and then on SMD-FAC: SMD supplemented with 2.3 g/L fluoroacetamide (Solis-Escalante et al., 2013). Industrial wort was provided by HEINEKEN Supply Chain B.V. (Zoeterwoude, Netherlands), and contained 14.4 g/L glucose, 2.3 g/L fructose, 85.9 g/L maltose, 26.8 g/L maltotriose, and 269 mg/L free amino nitrogen (Brickwedde et al., 2017). The wort was supplemented with 1.5 mg/L Zn^{2+} by addition of $ZnSO_4.7H_2O$, then autoclaved for 30 min at 121°C and, prior to use, filtered through Nalgene 0.2 μm SFCA bottle-top filters (ThermoFisher Scientific, Waltham, MA, United States). For experiments performed with diluted wort, two volumes of sterile demineralized water were added per volume of wort. To prevent excessive foaming during the aeration phase of the bioreactor experiments, (un)diluted wort was supplemented with 0.2 mL/L of sterile Pluronic PE 6100 antifoam (Sigma-Aldrich).

Analytical Methods and Statistics

Optical density at 660 nm was measured with a Libra S11 spectophotometer (Biochrom, Cambridge, United Kingdom).

HPLC analysis of sugar and metabolite concentrations was performed with an Agilent Infinity 1260 chromatography system (Agilent Technologies, Santa Clara, CA, United States) with an Aminex HPX-87 column (Bio-Rad, Lunteren, Netherlands) at 65°C, eluted with 5 mM H_2SO_4 (Diderich et al., 2018). Vicinal diketone concentrations (diacetyl and 2,3 pentanedione) were measured using static headspace gas chromatography in a 7890A Agilent GC (Agilent) with an electron capture detector on a CP-Sil 8 CB capillary column, prior to injection 450 µl of supernatant was mixed with 50 µl of 1 mg/L 2,3 hexanedione which acts as an internal standard, and samples were pre-heated for 30 min to 65°C (Brickwedde et al., 2017). Injection was performed with a CTC Combi Pal headspace autoinjector (CTC analytics AG, Zwingen, Switzerland). Significance of data was assessed by an unpaired two-tailed Student's *t*-test with a 95% confidence interval.

Genomic DNA Extraction, Whole Genome Sequencing and Analysis

Yeast cultures were inoculated from frozen stocks into 500 mL shake flasks containing 100 mL liquid YPD medium and incubated at 12°C on an orbital shaker set at 200 rpm until the strains reached stationary phase with an OD_{660} between 12 and 20. Genomic DNA was isolated using the Qiagen 100/G kit (Qiagen, Hilden, Germany) according to the manufacturer's instructions and quantified using a Qubit® Fluorometer 2.0 (ThermoFisher Scientific, Waltham, MA, United States). Genomic DNA of CBS 1483, IMI349, IMI351, IMI353, IMS0687, IMS703, IMS705, IMS706, IMS708-IMS714, IMS716 was sequenced at Novogene Bioinformatics Technology Co., Ltd (Yuen Long, Hong Kong) on a HiSeq2500 sequencer (Illumina, San Diego, CA, United States) with 150 bp paired-end reads using PCR-free library preparation (Brickwedde et al., 2018). Genomic DNA of IMI363, IMI373, IMI374, IMI375, IMI377, IMI370, IMI381, IMI382, IMI383 was sequenced in house on a MiSeq sequencer (Illumina) with 300 bp paired-end reads using PCR-free library preparation.

More than 3 Gb of data per strain representing a minimum of 50-fold coverage of the aneuploid genome of the *S. pastorianus* were generated. Sequence reads of each strain were mapped onto *S. pastorianus* CBS 1483 sequence [genome PRJNA522669, (Salazar et al., 2019)] using the Burrows–Wheeler Alignment tool (BWA) and further processed using SAMtools (Li and Durbin, 2009, 2010). Single-nucleotide variations and indels were determined using Pilon (Walker et al., 2014) based on the BWA.bam output file. The Pilon results file.vcf was visualized using the Integrative Genomics Viewer IGV4. All Illumina sequencing data are available at NCBI[2] under the bioproject accession number PRJNA522669 and PRJNA612191. Prediction of chromosome copy number was performed using Magnolya, as previously described in Nijkamp et al. (2012).

The variant calling files (vcf) for strains IMS0687, IMS0703, and IMS0716 are available at the 4TU Centre for data research[3] under the Digital Object Identifier doi: 10.4121/uuid:e5bc2cfe-d726-44a1-bc0a-d3a06653694b.

Plasmids Construction

All plasmids were propagated in *E. coli* DH5α (**Table 2**). Primers were ordered at Sigma Aldrich (**Supplementary Table S1**). pART001 was constructed using the NEBuilder® HiFi DNA Assembly method with the backbone of pUG-amdSYM, amplified using primers 8624 & 8556, and the *GAL1* promoter of pAG426GAL (pAG426GAL Addgene plasmid # 14155; http://n2t.net/addgene:14155) (Alberti et al., 2007) that was amplified using primers 8623 & 8436. Genomic DNA of CBS 1483 was extracted with the YeaStarTM Genomic DNA kit (Zymo Research, Irvine, CA, United States) according to Protocol I supplied by the manufacturer. For each targeted centromere, 1000 bp just downstream of the centromere and 1000 bp including the centromere were PCR amplified from genomic DNA of CBS 1483, using primer overhangs for plasmid construction using the NEBuilder® HiFi DNA Assembly method. Homologous sequences were amplified using primers pairs 9857 & 9858 and 9859 & 9860 for *Sc*CEN8, primers pairs 8443 & 8444 and 8557 & 8510 for *Sc*CEN9, primers pairs 10088 & 10089 and 9863 & 9864 for *Sc*CEN10, primers pairs 9865 & 9866 and 9867 & 9868 for *Sc*CEN12, primers pairs 9869 & 9870 and 9871 & 9872 for *Sc*CEN14, primers pairs 9873 & 9874 and 9875 & 9876 for *Se*CEN3, primers pairs 8451 & 8452 and 8453 & 8454 for *Se*CEN6, primers pairs 9877 & 9878 and 9879 & 9880 for *Se*CEN8, primers pairs 9881 & 9882 and 10090 & 10091 for *Se*CEN10, primers pairs 9885 & 9886 and 9887 & 9888 for *Se*CEN12, primers pairs 9889 & 9890 and 9891 & 9892 for *Se*CEN14 and primers pairs 11044 & 11045 and 11046 & 11047 for *Se*CEN15/8. The *amdS-GAL1*$_p$ construct was amplified from pART001 using primers 8439 and 8440 and the plasmid backbone was amplified from pART001 using primers 8442 and 8441. Plasmids pART002-pART012 were constructed using the NEBuilder® HiFi DNA Assembly method with the amplified backbone, the amplified

TABLE 2 | Plasmids used in this study.

Plamid	Relevant genotype	References
pUG-amdSYM	*amdS*	Solis-Escalante et al., 2013
pAG426GAL	*bla*, 2µ, *URA3, GAL1*$_p$	Alberti et al., 2007
pART001	*bla*, 2µ, *amdS-GAL1*$_p$	This study
pART002	*bla*, 2µ, *ScCEN8-amdS-GAL1*$_p$*-Sc*CEN8	This study
pART003	*bla* 2µ, *ScCEN9-amdS-GAL1*$_p$ *-Sc*CEN9	This study
pART004	*bla*, 2µ, *ScCEN10-amdS- GAL1*$_p$	This study
pART005	*bla*, 2µ, *ScCEN12-amdS-GAL1*$_p$ *-Sc*CEN12	This study
pART006	*bla*, 2µ, *ScCEN14-amdS-GAL1*$_p$ *-Sc*CEN14	This study
pART007	*bla*, 2µ, *SeCEN3-amdS-GAL1*$_p$ *Se*CEN3	This study
pART008	*bla*, 2µ, *SeCEN6-amdS-GAL1*$_p$ *-Se*CEN6	This study
pART009	*bla*, 2µ, *SeCEN8-amdS-GAL1*$_p$ *-Se*CEN8	This study
pART010	*bla*, 2µ, *SeCEN10-amdS-GAL1*$_p$ *-Se*CEN10	This study
pART011	*bla*, 2µ, *SeCEN12-amdS-GAL1*$_p$ *-Se*CEN12	This study
pART012	*bla*, 2µ, *SeCEN14-amdS-GAL1*$_p$ *-Se*CEN14	This study

[2]https://www.ncbi.nlm.nih.gov/

[3]https://data.4tu.nl/

*amdS-GAL1*p construct and of the two homology arms for the targeted centromere (**Figure 1A**).

Strain Construction

The *amdS-GAL1*$_p$ integration cassettes targeting different centromeres were amplified from pART002 using primers 9857 and 9860, from pART003 using primers 8443 and 8510, from pART004 using primers 10088 and 9864, from pART005 using primers 9865 and 9868, from pART006 using primers 9869 and 9872, from pART007 using primers 9873 and 9876, from pART008 using primers 8451 and 8454, from pART009 using primers 9877 and 9880, from pART010 using primers 9881 and 10091, from pART011 using primers 9885 and 9888 and from pART012 using primers 9889 and 9893 (**Figure 1B**). Yeast transformation was done by electroporation as previously described (Thompson et al., 1998). A frozen stock of CBS 1483 was used to inoculate a 500 mL shake-flask containing 100 mL YPD. Upon exponential growth, the pre-culture was used to inoculate a fresh 500 mL shake-flask containing 100 mL YPD at a density of 5×10^6 cells/mL, that was incubated at 20°C and 200 rpm until a density of 10^8 cells/mL was reached. 50 mL of culture was re-suspended twice in 25 mL of ice-cold demi-water, re-suspended once in 2 mL 1 M ice-cold sorbitol, re-suspended once in 2 mL ice-cold 100 mM Lithium acetate with 10 mM dithiothreitol, re-suspended once in 2 mL ice-cold sorbitol and once in 250 µL ice-cold sorbitol. 50 µL of competent cells and up to 5 µL DNA were then electroporated in an ice-cold 0.2 cm cuvette with a pulse at 1.5 kV. Transformed cells were incubated in 0.5 mL YPD during 1 h, after which they were re-suspended in 100 µL of sterile demi-water and plated on selective medium. Strains were re-streaked from the transformation plates twice prior to storage of single colony isolates. Strain IMI350 (*Sc*CEN6:*amdS-GAL1*$_p$) was constructed by transforming CBS 1483 with 1 µg of insertion cassette amplified from pART008 (**Figure 1B**), and streaking on SM-Ac plates. Similarly, IMI353 was made using pART003, IMI359

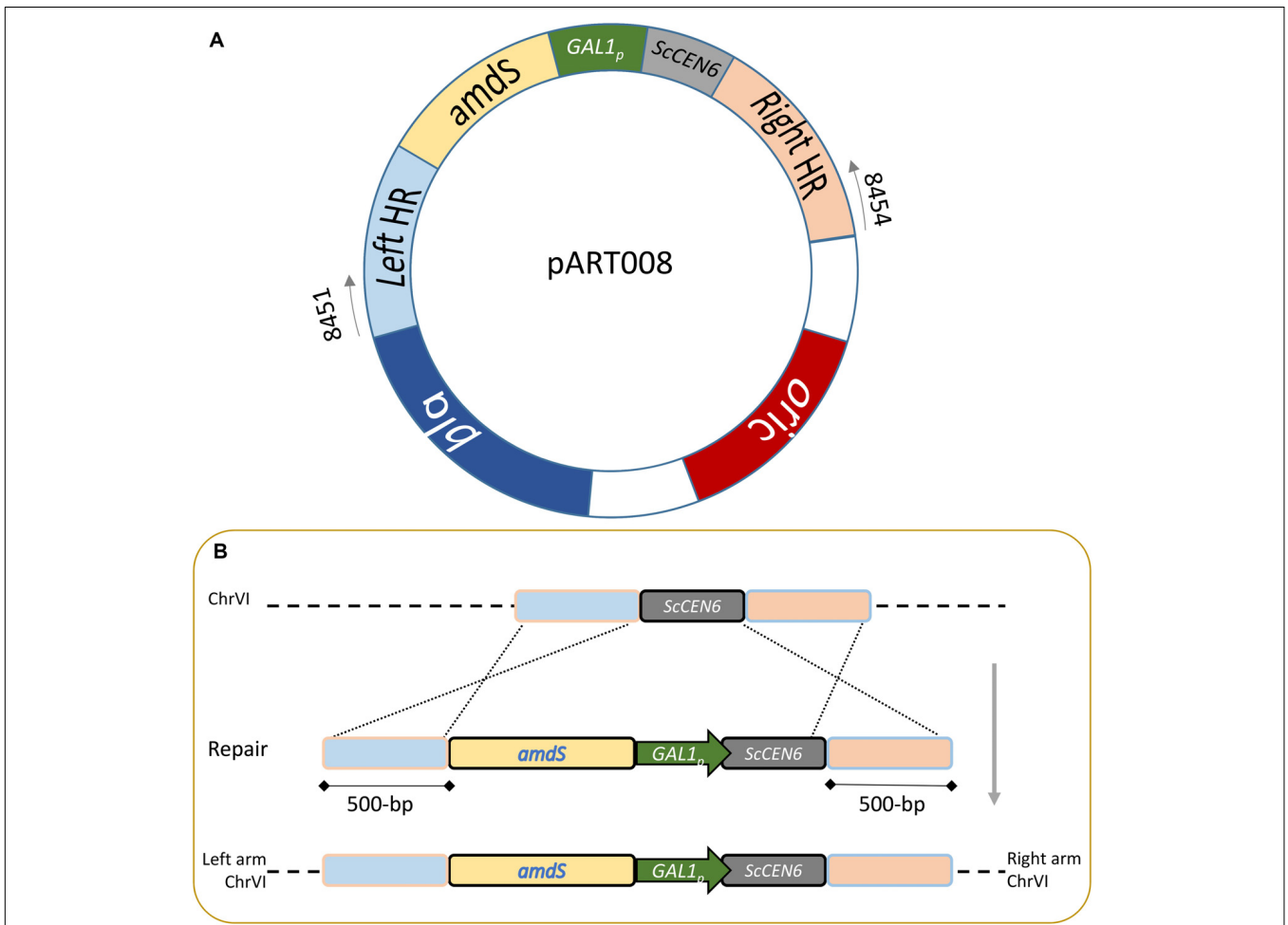

FIGURE 1 | Centromere silencing strain construction. **(A)** The plasmid pART series illustrated by pART008 is designed to introduce the amdS selection marker and the constitutive strong promoter *GAL1* (*GAL1*$_p$) upstream a centromere (*Sc*CEN6 in the case of pART008). In addition pART plasmids contain an E. coli replication origin from pBR322 and the bla gene conferring resistance to β-lactam antibiotics. **(B)** Integration of the centromere silencing construct at the *Sc*CEN6 locus in *S. pastorianus* CBS 1483. Schematic representation of the integration of *amdS* selection marker and the *GAL1* promoter containing linear fragment amplified with primers 8451 and 8454. The integration is directed by homology regions of ∼500 bp to complete the double cross over integration.

was made using pART004, IMI360 was made using pART005, IMI361 was made using pART006, IMI363 was made using pART007, IMI366 was made using pART009, IMI367 was made using pART010, IMI368 was made using pART011, IMI369 was made using pART012. Strain IMI351 (*Sc*CHRV^{-1} *Sc*CHRX-*Se*CHRX^{+1} *Se*CHRVI^{-1} *Se*CHRX-*Sc*CHRX^{-1}) was constructed by incubating strain IMI350 (*Se*CEN6:amdS-*GAL1*$_p$) on YPGal medium and streaking on SMD-FAc plates. Similarly, IMI353 was constructed from IMI352, IMI373 from IMI359, IMI374 from IMI360, IMI375 from IMI361, IMI377 from IMI363, IMI380 from IMI366, IMI381 from IMI367, IMI382 from IMI368, and IMI383 from IMI369.

Characterisation of Growth in Wort

Growth was characterized in triplicate in 100 mL serum bottles containing 100 mL of filtered undiluted industrial wort, supplemented with 1.6 mL/L of Pluronic PE 6100 antifoam (BASF, Ludwigshafen, Germany). Bottles were inoculated to an OD_{660} of 0.2 from pre-cultures grown for 2 days at 20°C in aerated 50 mL Greiner tubes on YPD, and incubated at 12°C at 200 RPM. Growth was monitored by OD_{660} and extracellular metabolites were measured by HPLC and GC analysis.

Evaluation of the Mutagenic Effect on CBS 1483 of Electroporation and of Restreaking

To evaluate if electroporation could be responsible for the extensive chromosome CNV observed in strains in which chromosome copy removal was attempted, CBS 1483 was electroporated as described above without adding any DNA and streaked on YPD instead of selective medium. After restreaking twice on YPD, single colony isolates were made and named IMS0705-IMS0709 and sent for whole genome sequencing.

To evaluate if inherent instability of CBS 1483 could be responsible for the extensive chromosome CNV observed in strains in which chromosome copy removal was attempted, CBS 1483 was cultured on liquid YPD and streaked three times on YPD plates: a frozen stock of CBS 1483 was used to inoculate a 500 mL shake-flask containing 100 mL YPD. Upon exponential growth, the pre-culture was used to inoculate a fresh 500 mL shake-flask containing 100 mL YPD at a density of 5 x 10^6 cells/mL, that was incubated at 20°C and 200 rpm until a density of 10^8 cells/mL was reached. Medium was streaked on YPD and re-streaked twice to obtain single colony isolates, named IMS0710-IMS0714, that were sent for whole genome sequencing.

Galactose-Promoter-Mediated Induction of Chromosome Missegregation and Selection of Ethanol Tolerant Mutants

Strain IMI361 (*Sc*CEN14::*amdS-GAL1*$_p$) was grown overnight in 100 mL SMGAL in a 500 mL shake flask to induce chromosome missegregation and then transferred in SMD-FAC culture inoculated at an OD_{660} of 0.2 and incubated for 3 days at 20°C and 200 rpm. The mutagenized culture had an OD_{660} of 9.25 and 5 mL was used to inoculate two duplicate repeated batch fermentations in Multifors 2 Mini Fermenters (INFORS HT, Velp, Netherlands). Each batch was performed in 100 mL of SMD with 10% v/v ethanol, supplemented with 10 mg/L ergosterol, 420 mg/L Tween 80 and 0.9 mL/L antifoam C (Sigma Aldrich). The fermenters were kept at 20°C, stirred at 500 rpm, sparged with 50 mL/min N_2 and the pH was maintained at 7 by automated addition of 2 M KOH. The CO_2 composition in the offgas was analyzed using a BCP-CO_2 gas analyser (Bluesens, Herten, Germany) and when the CO_2 concentration dropped to less than 10% of its maximum during the batch, the fermenter was emptied leaving approximately 6 mL to inoculate the next batch, and fresh medium was added up to a total volume of 100 mL. The fermentation was monitored using IRIS software (version 6, Infors AG, Bottmingen, Switzerland) and samples of approximately 5 mL were taken at regular intervals to monitor viability using the FACS and to analyze metabolite concentrations by HPLC. At the end of the third batch, single colony isolates were obtained using FACS and restreaking, yielding strains IMX1875-IMX1890 for reactor GAL1 and strains IMX1891-IMX1894 for reactor GAL2.

Chemical Induction of Chromosome Missegregation and Selection of Ethanol Tolerant Mutants

Saccharomyces pastorianus CBS 1483 was grown overnight in 100 mL YPD in a 500 mL shake flask, and transferred to 100 mL SMG containing 10 μg/mL of the mitotic inhibitor MBC (methyl benzimidazole-2-yl carbamate, Sigma Aldrich). After 2 days at 20°C and 250 rpm, approximately 2 mL of culture with an OD_{660} of 4.12 was used to inoculate two duplicate repeated batch fermentations in Multifors 2 Mini Fermenters (INFORS HT, Velp, Netherlands). Each batch was performed in 100 mL of SMG with 10% v/v ethanol, supplemented with 10 mg/L ergosterol, 420 mg/L Tween 80 and 0.9 mL/L antifoam C (Sigma Aldrich). The fermenters were kept at 20°C, stirred at 500 rpm, sparged with 50 mL/min N_2 and the pH was maintained at 7 by automated addition of 2M KOH. The CO_2 composition in the offgas was analyzed using a BCP-CO_2 gas analyser (Bluesens, Herten, Germany) and when the CO_2 concentration dropped to less than 10% of its maximum during the batch, the fermenter was emptied leaving approximately 6 mL to inoculate the next batch, and fresh medium was added up to a total volume of 100 mL. The fermentations were performed as described in the previous paragraph. At the end of the third batch, single colony isolates were obtained using FACS and re-streaking, yielding strains IMS687-IMS704 for reactor MBC1 and strains IMS715-IMS720 for reactor MBC2.

FACS Analysis and Sorting

Cultures for FACS analysis and sorting were diluted in sterile Isoton II and vortexed thoroughly to disrupt cell aggregates. For cell sorting, 50 mM EDTA was added to disrupt cell aggregates formed by flocculation. The cultures were analyzed on a BD FACSAriaTM II SORP Cell Sorter (BD Biosciences, Franklin Lakes, NJ, United States) equipped with 355, 445, 488, 561, and 640 nm lasers and a 70 μm nozzle, and FACSFlowTM sheath fluid (BD Biosciences). Correct cytometer performance was evaluated

prior to each experiment by running a Cytometer Setup and Tracking cycle using a CS&T bead kit (BD Biosciences) for calibration. Drop delay for sorting was determined by running an Auto Drop Delay cycle using Accudrop Beads (BD Biosciences). Morphology of the cells was analyzed by plotting forward scatter (FSC) against side scatter (SSC). Prior to sorting, at least 10^5 events were analyzed. Sorting regions ("gates") were set on these plots to determine the types of cells to be sorted. Gated single cells were sorted in 96-well microtiter plates containing YPD using a "single cell" sorting mask (0/32/16), and the plates were incubated at RT for 2 days. FACS data were analyzed using FlowJo® software (version 3.05230, FlowJo, LLC, Ashland, OR, United States) (Gorter de Vries et al., 2019a).

Determination of the Fraction of Growing Cells

After FACS sorting, the fraction of growing cells was determined by counting the number of wells in which growth was observed. For populations with low viabilities, up to 1000 cells were sorted per well and Poisson statistics were used to estimate the fraction of growing cells (Dube et al., 2008). The fraction of growing cells was calculated from (P), the fraction of wells containing a colony, (W) the total number of wells and (n), the total number of cells sorted into the wells (Eq. 1).

$$\text{Fraction of growing cells} = \frac{\ln(1 - \mathrm{P}) \bullet \mathrm{W}}{n} \quad (1)$$

Screening of Galactose-Promoter Mutagenized Isolates With Increased Ethanol Tolerance

Isolates IMX1875-IMX1890 from reactor GAL1 and isolates IMX1891-IMX1894 from reactor GAL2 were screened for increased ethanol tolerance by evaluating growth on SMG with 10% ethanol v/v in airlock-capped bottles. Precultures of the isolates, of unmutagenized CBS 1483 and of unmutagenized IMI361 were grown at 20°C and 200 rpm in 500 ml shake flasks containing 100 mL SMG for 5 days. After washing of the precultured cells in demineralized water, airlock-capped 100 mL cylindrical bottles containing 100 mL SMG with 10% ethanol v/v were inoculated to an OD_{660} of 1. The bottles were incubated at 20°C and 200 rpm during 8 days and regularly sampled through the septum using a needle to measure OD_{660} and extracellular metabolite concentrations.

Screening of MBC-Mutagenized Isolates With Increased Ethanol Tolerance

Isolates IMS0687-IMS0704 from reactor MBC1 and isolates IMS0715-IMS0720 from reactor MBC2 were screened for increased ethanol tolerance by evaluating growth on SMG with 10% ethanol v/v. Precultures of the isolates and unmutagenized CBS 1483 were grown at 20°C and 200 rpm in 100 mL SMG in 500 mL shake flasks for 7 days. 500 mL shake flasks containing 100 mL SMG with 10% ethanol v/v were inoculated from these precultures at an OD_{660} of 0.5 and incubated at 20°C and 200 rpm during 142 h. The OD_{660} and extracellular metabolite concentrations were measure at regular intervals to monitor growth.

Characterisation of Ethanol Tolerance Under Micro-Aerobic Conditions

The ethanol tolerance of galactose-promotor-mutagenized isolates IMX1882, IMX1886, IMX1891, and IMX1893, and of MBC-mutagenized isolates IMS0687, IMS0698, IMS0699, IMS0703, and IMS0716 was characterized under micro-aerobic conditions, by evaluating growth in SMG with 10% ethanol in airlock-capped bottles. Precultures of the isolates, of unmutagenized CBS 1483 and of unmutagenized IMI361 were grown at 20°C and 200 rpm in 500 ml shake flasks containing 100 mL SMG for 5 days. As isolate IMS0699 did not grow to as sufficient OD_{660}, it was discarded for the rest of the experiment. After washing of the precultured cells in demineralized water, triplicate airlock-capped 250 mL cylindrical bottles containing 100 mL SMG with 10% ethanol v/v supplemented with 10 mg/L ergosterol and 420 mg/L Tween 80 were inoculated to an OD_{660} of 1. The bottles were incubated at 20°C and 200 rpm during 4 days and regularly sampled through the septum using a needle to measure OD_{660} and extracellular metabolite concentrations.

RESULTS

Engineering Chromosome Copy Number in *S. pastorianus* Type Strain CBS 1483

In order to assess the phenotypic impact of chromosome CNV in an alloaneuploid *S. pastorianus* genome, we attempted to delete copies of individual chromosomes in strain CBS 1483 (Bolat et al., 2013; Brickwedde et al., 2017). Due to the hypothesized role of their CCNV in the production of off-flavor diacetyl, chromosomes harboring genes of the valine biosynthesis pathway were targeted (van den Broek et al., 2015): chromosomes *Se*CHRIII (*SeILV6*), *Se*CHRVI (negative control), *Se*CHRVIII (*SeBAT1*), *Se*CHRX (*SeILV3* and *SeBAT2*), *Se*CHRXII (*SeILV5*), *Se*CHRXIV (*SeILV2*), *Sc*CHRVIII (*ScBAT1*), *Sc*CHRIX (negative control), *Sc*CHRX (*ScILV3* and *ScBAT2*), *Sc*CHRXII (*ScILV5*), and *Sc*CHRXIV (*ScILV2*) (**Figure 2A**). In *S. cerevisiae*, cloning of the *GAL1* promoter and *URA3* marker adjacent to a centromere sequence enabled targeted loss or gain of specific chromosomes (Reid et al., 2008; Anders et al., 2009). In contrast to *URA3* that needs to be used in an auxotrophic host, the *amdS* marker can be selected for by growth with acetamide as sole nitrogen source and similarly, to *URA3* can be counter-selected for by growth in the presence of fluoroacetamide, but in any strains including prototrophs (Solis-Escalante et al., 2013). Therefore, plasmid pART001 containing a centromere-silencing cassette with the *amdS* marker upstream of $GAL1_p$ was constructed. In order to insert this cassette in targeted chromosomes, 1000 bp of genetic material was amplified from both sides of each targeted integration site, immediately downstream of the centromere of targeted chromosomes (**Figure 1**). The amplified homology arms were inserted into pART001 at the flanks of the *amdS*-$GAL1_p$ cassette, resulting in plasmids pART002 to pART012. CBS 1483 was then transformed with PCR-amplified insertion cassettes from pART002 to pART012 and successful transformants were selected on SMD-AC medium. After verification of correct insertion by PCR-amplification of the

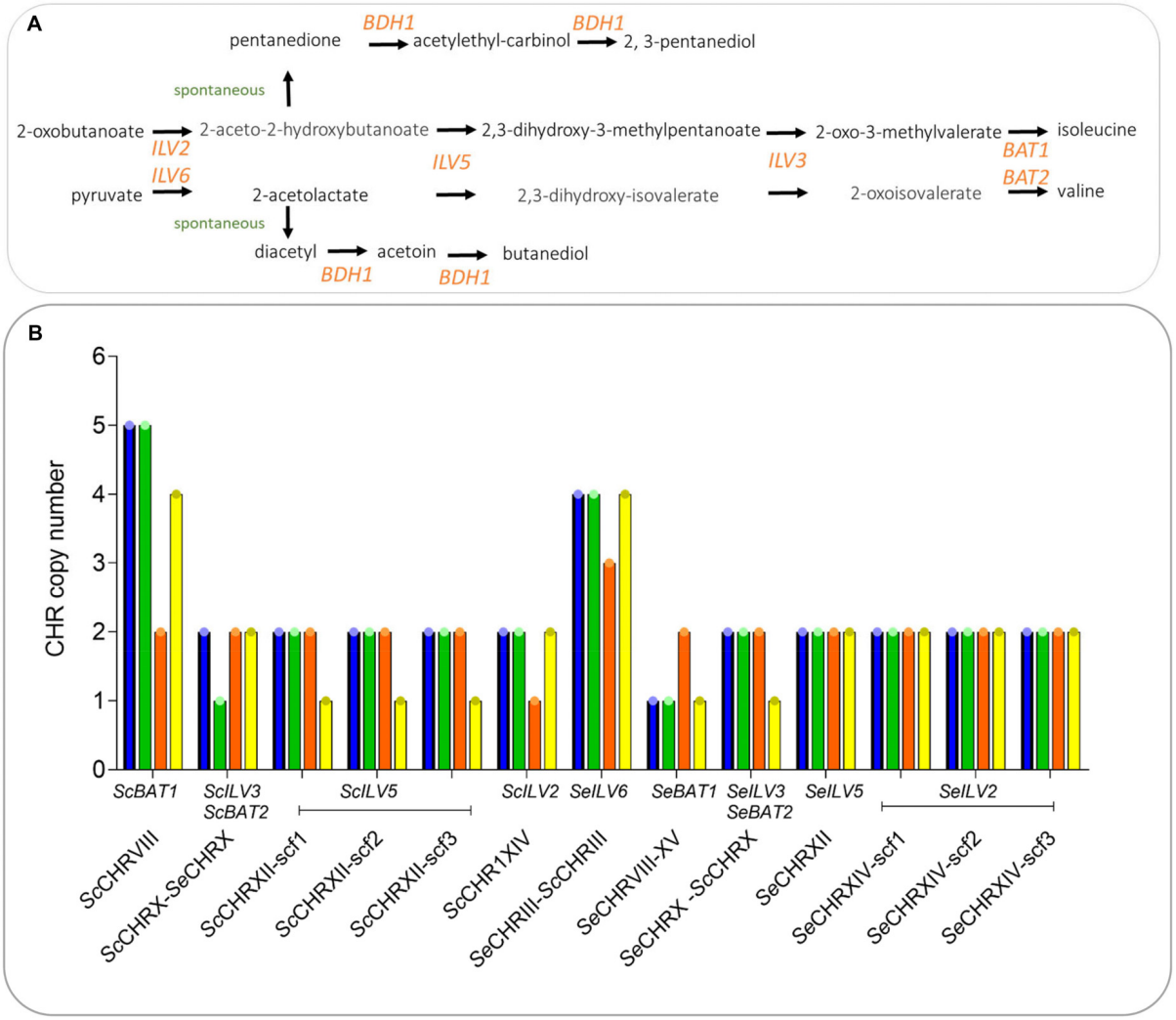

FIGURE 2 | Vicinal diketones formation in *S. pastorianus*. **(A)** Schematic illustration of the diacetyl, pentanedione and branched chain amino acid biosynthesis pathways. **(B)** Valine, isoleucine, pentanedione and diacetyl biosynthetic pathways and chromosome copy number of the genes involved in the metabolic routes in strains CBS 1384 (blue bar), IMI373 (ScCHRX-SeCHRX^{-1} SeCHRIX^{-1}) (green bar) that was targeted for loss of ScCHRX, IMI375 (*Sc*CHRII^{-1} *Sc*CHRV^{-1} *Sc*CHRVIII^{-3} *Sc*CHRXIII^{-1} ScCHRXIV^{-1} SeCHRI^{-1} *Se*CHRIII-*Sc*CHRIII^{-1} *Se*CHRVII-*Sc*CHRVII^{-1} *Se*CHRVIII-XV^{+1}) (orange bar) that was targeted for loss of ScCHRXIV and IMI381 (*Sc*CHRIV^{+1} *Sc*CHRVIII^{-1} *Sc*CHRIX^{+1} *Sc*CHRXI^{-1} *Sc*CHRXII^{-1} *Se*CHRX-*Se*CHRX^{-1} *Se*CHRII-IV^{-1} *Se*CHRXI^{+1}) (yellow bar) that was targeted for the loss of SeCHRX. The chromosome copy number was predicted using Magnolya (Nijkamp et al., 2012).

targeted *CEN* locus, single colony isolates were stocked as IMI349 and IMI350 (*Se*CEN6), IMI352 (*Sc*CEN9), IMI359 (*Sc*CEN10) IMI360 (*Sc*CEN12), IMI361 (*Sc*CEN14), IMI363 (*Se*CEN3), IMI366 (*Se*CEN8), IMI367 (*Se*CEN10), IMI368 (*Se*CEN12), and IMI369 (*Se*CEN14) (**Table 1**). The strains harboring *amdS-GAL1*$_p$ centromere silencing cassettes were then grown on YPGal medium, to induce centromere silencing and therefore chromosome missegregation by growth on galactose. Single colony isolates were purified and stocked as IMI349 and IMI351 (*Se*CHRVI), IMI353 (*Sc*CHRIX), IMI373 (*Sc*CHRX), IMI374 (*Sc*CHRXII), IMI375 (*Sc*CHRXIV), IMI377 (*Se*CHRIII), IMI380 (*Se*CHRVIII), IMI381 (*Se*CHRX), IMI382 (*Se*CHRXII), and IMI383 (*Se*CHRXIV) (**Table 1**). These isolates were whole genome sequenced, along with the parental strain CBS 1483. Chromosome copy number was determined by analyzing sequencing coverage (Nijkamp et al., 2012). Single chromosome copies were successfully deleted when targeting *Sc*CHRVI, *Sc*CHRX-*Se*CHRX, *Sc*CHRXII, *Sc*CHRXIV, *Se*CHRX-*Sc*CHRX and *Se*CHRXII but not when targeting *Se*CHRIII-*Sc*CHRIII, *Se*CHRVIII-XV and *Se*CHRXIV indicating successful removal of the targeted chromosome in 71% of the constructed strains (**Table 1**). However, coverage analysis also revealed alterations of the copy number of non-targeted chromosomes in all but one [IMI349 (*Se*CHRVI)] of the tested isolates. The magnitude of the CCNV varied from 1 to 10 chromosomes (**Figure 3**). The most extreme case was illustrated by the isolate IMI375 that had lost 11 chromosome copies and gained one, that resulted in a CCNV of ten chromosomes. To investigate if galactose-induced

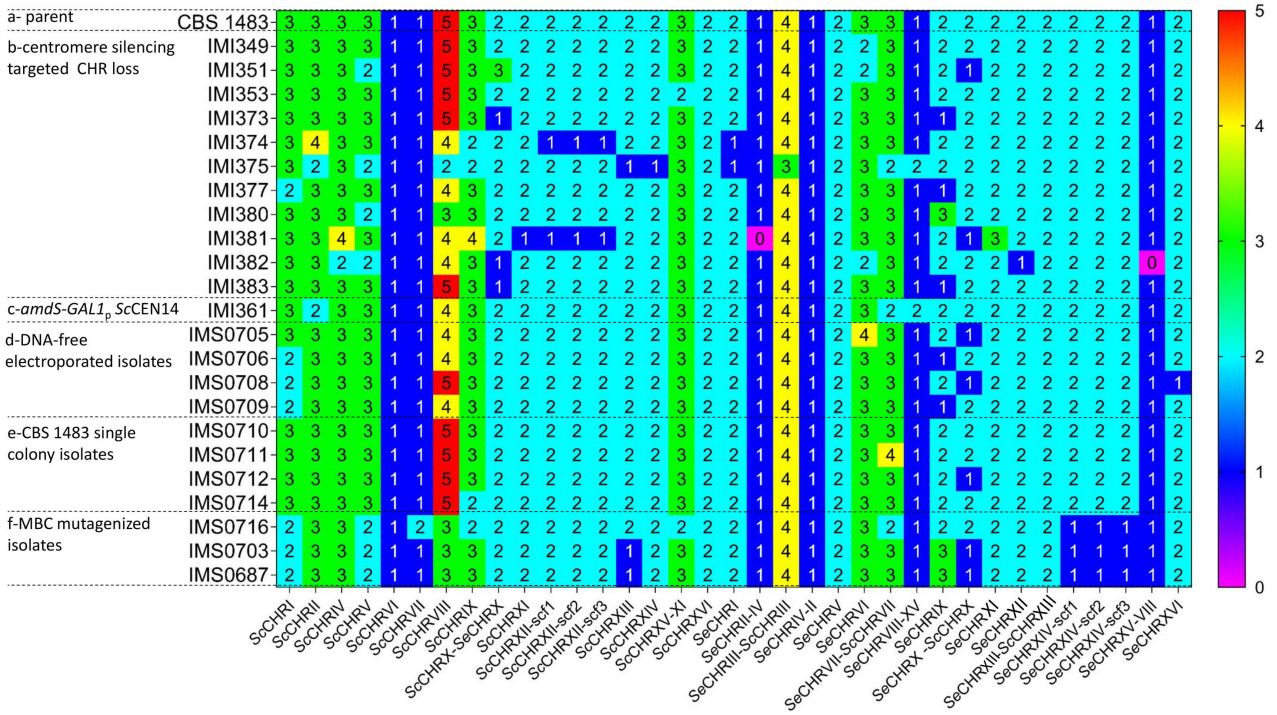

FIGURE 3 | Chromosome copy number in various *S. pastorianus* strains. **(a)** Chromosome copy number of the parental *S. pastorianus* strain CBS 1483. **(b)** Chromosome copy number of strains obtained after centromere silencing of *Se*CEN6 (in IMI350), *Sc*CEN9 (in IMI352), *Sc*CEN10 (in IMI359), *Sc*CEN12 (in IMI360), *Sc*CEN14 (in IMI361), *Se*CEN3 (in IMI363), *Se*CEN8 (in IMI366), *Se*CEN10 (in IMI367), *Se*CEN12 (in IMI368) and *Se*CEN14 (in IMI369). **(c)** Chromosome copy number of a strain engineered for targeted loss of ScCEN14 before centromere silencing induction. **(d)** Chromosome copy number of strains after electroporation without DNA. **(e)** Chromosome copy number of single isolates of the *S. pastorianus* strain CBS 1483. **(f)** Chromosome copy number of isolates obtained of treatment with methyl benzimidazole 2 yl carbamate (MBC). Chromosome copy number was predicted using Magnolya (Nijkamp et al., 2012).

centromere silencing was responsible for the untargeted CCNV, non-induced intermediate strain IMI361 (*Sc*CEN14::*amdS-GAL1*$_p$) was sequenced as well. IMI361 displayed an increased copy number of *Se*CHRVIII-XV and decreased copy number of *Sc*CHRVIII and chimeric *Se*CHRVII-*Sc*CHRVII (+1 or −1 copy each) relative to untransformed CBS 1483, indicating that the insertion of the *amdS-GAL1*$_p$ cassette itself may already cause CCNV. However, the IMI361-derived strain IMI375 (Δ*Sc*CEN14), displayed additional CCNV. Expectedly IMI375 harbored one copy less of the targeted *Sc*CHRXIV (−1, this will be denoted as *Sc*CHRXIV^{-1} throughout the manuscript), it also showed decreased copy number for six additional chromosomes (*Sc*CHRV^{-1} *Sc*CHRVIII^{-2} *Sc*CHRIX^{-1} *Sc*CHRXIII^{-1} *Se*CHRI^{-1} *Se*CHRIII-*Sc*CHRIII^{-1}) relative to IMI361, indicating that induction the *amdS-GAL1*$_p$ cassette also contributed to the modification of genotype (**Figure 3**).

Genetic Instability of CBS 1483 and Mutagenic Effect of Electroporation

The observation that CCNV occurred when inserting the *amdS-GAL1*$_p$ cassette could be the result of an inherent instability of CBS 1483 or more generally alloaneuploid *S. pastorianus* strains, to a mutagenic effect of the general transformation procedure or to a specific effect of insertion of *amdS-GAL1*$_p$. To investigate the stability of CBS 1483, a frozen aliquot was grown in YPD medium for two generations as this would be done for a transformation, then the culture was streaked on a YPD plate and five randomly selected single colony isolates were re-streaked on two successive YPD plates to simulate isolation procedure. The resulting strains were stocked as IMS0710-IMS0714. In parallel, cells from the same YPD culture were prepared for transformation and electroporated in absence of DNA. The resulting strains were plated on YPD and five randomly picked single colony isolates were re-streaked on two successive YPD plates. The resulting strains were stocked as IMS0705-IMS0709. Eight of these isolates IMS0705-IMS0706, IMS0708-IMS709, and IMS0710-IMS0712, IMS0714 were sequenced and chromosome copy number was determined by analyzing sequencing coverage and comparing the copy numbers to those of CBS 1483. Non-electroporated cell lines IMS0710-IMS0712, IMS0714 already exhibited moderate CCNV, out the four sequenced isolates three showed gain or loss of a single chromosome. The cell line IMS0711 gained one copy of chimeric *Se*CHRVII-*Sc*CHRVII, while IMS0712 and IMS0714 has lost one copy of *Se*CHRX-ScCHRX and *Sc*CHRIX, respectively. The fourth sequenced isolate IMS0710 showed a chromosome complement identical to that of CBS 1483 (Salazar et al., 2019). Overall, the non-electroporated single cell lines have an average of 76.8 ± 0.8 chromosomes which represent an average loss of 0.2 chromosome relative to CBS 1483 whose

genome comprise 77 chromosomes (**Figure 3**). Upon DNA-free electroporation, karyotype of single cell lines IMS0705-IMS0706, IMS0708-IMS709 was more significantly affected as more chromosomes displayed CCNV. With the exception of the *Se*CHRVI in IMS0705 that showed an increase from three to four copies, all other CCNV involved loss of a single copy. Some chromosomes were affected in several strains, the copy number of *Sc*CRHVIII and *Sc*CHRI was decreased in three isolates (IMS0705, IMS0706, and IMS0709). The chromosome number of *Se*CHRX-*Sc*CHRX was decreased in two of the sequenced cell lines (IMS0705 and IMS0708). Thus on average electroporated single cell lines had 74.5 ± 1.0 chromosomes which represent an average loss of 2.5 chromosome relative to CBS 1483. These results indicated that the chromosome copy number of CBS 1483 is inherently unstable under cultivation conditions, and that the procedure of electroporation significantly exacerbates copy number alterations ($^{\text{Student } t-\text{test}}p_{\text{value}}$ = 1.1E-2). It should be noted that the strains in which copy number alterations were attempted showed even higher CCNV, with an average of 73.4 ± 3.8 chromosomes (**Figure 3**).

Mutants With Altered Chromosome Copy Number Display Diverse Phenotypes

The presence of untargeted chromosome copy number alterations prevented the initially-intended investigation of the effect of specific copy number changes on diacetyl production. However, it resulted in a set of isogenic strains with extensive CCNV. Since CCNV can result in altered phenotypes of potential interest for industrial application (Gorter de Vries et al., 2017), we characterized three isolates by growing them in industrial wort under micro-aerobic conditions. IMI373 (*Se*CHRX-*Sc*CHRX^{-1} *Se*CHRIX^{-1}), IMI375 (*Sc*CHRII^{-1} *Sc*CHRV^{-1} *Sc*CHRVIII^{-3} *Sc*CHRIX^{1} *Sc*CHRXIII^{-1} *Sc*CHRXIV^{-1} *Se*CHRI^{-1} *Se*CHRIII-*Sc*CHRIII^{-1} *Se*CHRVII-*Sc*CHRVII^{-1} SeCHRVIII-XV^{+1}) and IMI381 (*Sc*CHRIV^{+1} *Sc*CHRVIII^{-1} *Sc*CHRIX^{+1} *Sc*CHRXI^{-1} *Sc*CHRXII^{-1} *Se*CHRII-IV$^{-1(D)}$ *Se*CHRX-*Sc*CHRX^{-1} *Se*CHRXI^{+1}) were characterized by monitoring their growth rates, sugar consumption profiles and diacetyl production (**Figure 4**). The average growth rates of IMI373, IMI375 and IMI381 were 0.031, 0.040, and 0.033 1/h, respectively, representing an up to 38% decrease relative to the growth rate of 0.050 1/h of CBS 1483. In addition, IMI373 and IMI375 did not flocculate as strongly as CBS 1483: the OD_{660} decreased by 90 and 95% relative to its maximal value after 200 h of fermentation for CBS 1483 and IMI381, respectively, while it only decreased by 20% for IMI373 and did not decrease at all for IMI375 (**Figure 4**). While sugar consumption profiles cannot be compared directly due to the differences in growth rates, IMI373 and IMI381 clearly did not consume all di- and tri-glucosides (**Figure 4**), a trait that was not correlated with the flocculation phenotype of the strain. In accordance with the hypothesized effect of copy number differences of chromosomes harboring genes of the valine synthesis pathway (van den Broek et al., 2015), IMI373 and IMI381 displayed altered diacetyl production profiles. While the concentration of diacetyl did not exceed 400 μg/l for CBS 1483 and IMI375, concentrations of about 4 and 10 mg/L were reached for IMI381 and IMI373, respectively. Moreover, while diacetyl concentrations decreased to 300 μg/L for IMI381, they remained above 5 mg/L for IMI373 (**Figure 4**). In both cases these levels were above the diacetyl sensory threshold that is fixed at 150 μg/L in lager fermented products (Krogerus and Gibson, 2013). Although pentanedione does not contribute to off-flavor formation, the production-re-consumption profiles correlated with those of diacetyl (**Figure 4**). The IMI373 and IMI381 phenotypes were characterized by significant diacetyl accumulation (**Figure 4**) could be associated with a decreased flux through the branched chain amino acid pathway and be linked to the loss of single *Sc*CHRX-*Se*CHRX and dual *Sc*CHRXII and *Se*CHRX-*Sc*CHRX, respectively (**Figure 2B**). These chromosomes carries genes *ILV5* (CHRXII) and *ILV3* (CHRX) that act downstream 2-acetolactate, precursor of diacetyl. Overall, these results indicated a strong phenotypic impact of chromosome copy number alterations, notably affecting the industrially-relevant traits of flocculation, sugar utilization and diacetyl production.

Centromere Silencing as a Strain Engineering Tool

The impact of centromere-silencing on CCNV, might thus be used as a mutagenesis instrument that could result in new phenotypes of industrial interest. Recent trends for high gravity beer brewing result in inhibition due to increasing ethanol concentrations (Puligundla et al., 2011). Therefore, the methods of centromere silencing-induced CCNV was evaluated to improve ethanol tolerance of *S. pastorianus* CBS 1483. To this end, IMI361 (*amdS-GAL1*$_{\text{p}}$ cassette in *Sc*CHRXIV) was grown on YPGal medium to induce centromere silencing. The mutagenized population was inoculated in duplicate bioreactors (GAL1 and GAL2) containing SMD medium with 10% ethanol v/v supplemented with anaerobic growth factors. Growth was monitored by measuring the off-gas CO_2 concentration and the medium was replenished when growth was completed, this was perpetuated over four sequential batches. Due to sparging with N_2 gas, the concentration of ethanol decreased steadily during the batches until growth could occur. The viability dropped below 40% in all batches, indicating a strong inhibitory selective effect of ethanol. During the fourth batch, samples were taken and single cell lines named IMX1875-IMX1889 were isolated from reactor GAL1 and IMX1890-IMX1893 from reactor GAL2.

The ethanol tolerance of CBS 1483, IMI361 and IMX1875-IMX1893 was evaluated by growing them in airlock-capped bottles containing 100 mL SMD with 10% ethanol v/v at 20°C for 9 days. Growth was monitored by measuring the OD_{660}. CBS 1483 and IMI361 reached final OD_{660} values of 3.78 and 2.68. While fourteen of the isolates reached a higher OD_{660} than IMI361, only four mutants reached a higher OD_{660} than CBS 1483. The four single cell lines IMX1878, IMX1891, IMX1886, IMX1893 displayed a biomass yield at least 22 and 72% higher that of CBS 1483 and IMI361, respectively, and the isolate IMX1893 reached the highest OD values that were 50 and 110% higher that of CBS 1483 and IMI361, respectively. Based on their improved growth capacity under ethanol stress the mutants cell lines IMX1882, IMX1886, IMX1891 and IMX1893 were selected for further characterization. Together with CBS 1483 and IMI361,

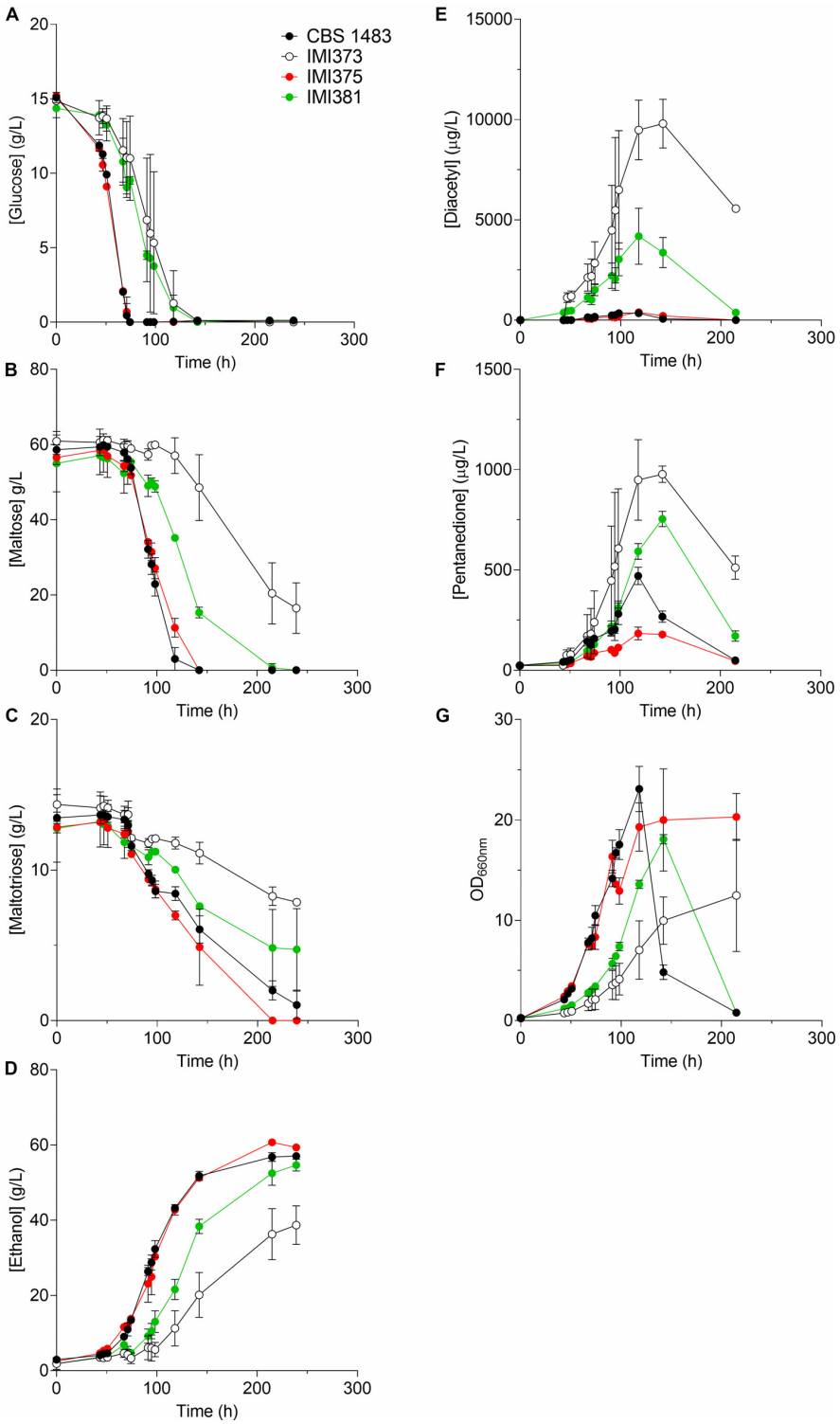

FIGURE 4 | Characterisation of CBS 1483, and IMI373, IMI375 and IMI381 under brewing conditions. The *S. pastorianus* strains CBS 1483 (black circle), IMI373 (ScCHRX-SeCHRX^{-1} SeCHRIX^{-1}) (white circle), IMI375 (*Sc*CHRII^{-1} *Sc*CHRV^{-1} *Sc*CHRVIII^{-3} *Sc*CHRXIII^{-1} ScCHRXIV^{-1} SeCHRI^{-1} *Se*CHRIII-*Sc*CHRIII^{-1} *Se*CHRVII-*Sc*CHRVII^{-1} *Se*CHRVIII-XV^{+1}) (red circle) and IMI381 (*Sc*CHRIV^{+1} *Sc*CHRVIII^{-1} *Sc*CHRIX^{+1} *Sc*CHRXI^{-1} *Sc*CHRXII^{-1} *Se*CHRX-*Se*CHRX^{-1} *Se*CHRII-IV^{-1} *Se*CHRXI^{+1}) (green circle) were grown in air-capped 100 ml serum bottles in undiluted industrial wort at 12 °C. Average and standard deviation from duplicates (IMI373 and IMI375) or triplicates (IMI381 and CBS 1483) are shown. **(A)** displays glucose, **(B)** maltose, **(C)** maltotriose, **(D)** ethanol determined by liquid chromatography; **(E)** diacetyl, **(F)** pentanedione concentrations produced in industrial wort measured using static headspace gas chromatography and **(G)** optical density measured at 660 nm (OD_{660} is directly related with biomass concentration in suspension).

the four mutants were grown in triplicate in bottles as described above during 9 days, and samples were taken at regular intervals to measure the OD_{660} and extracellular metabolites. While the growth rates of mutant strains did not significantly exceed that of CBS 1483 (**Figure 5**), the OD_{660} of IMX1891 and IMX1893 was significantly higher than that of CBS 1483 throughout the whole culture (**Figure 5**). Correspondingly, glucose consumption was faster in IMX1891 and IMX1893 than in CBS 1483, and IMX1893 depleted all glucose after 216 h, while 1.5 g/L glucose was still left for CBS 1483 (**Figure 5**). These results indicate a moderate improvement of growth in the presence of ethanol for some of the obtained mutants.

Chemical Induction of Chromosome Missegregation as a Strain Engineering Tool

Strains obtained by centromere-silencing displayed large CCNV and industrially-relevant phenotypic diversity. While mutagenesis using centromere-silencing and selection for ethanol tolerant mutants resulted mostly in mutants with inferior growth in the presence of ethanol, some isolates consistently outperformed their parental strain. While centromere-silencing may have potential as a mutagenesis method, its reliance on genome editing to introduce centromere-silencing cassettes makes the resulting strains genetically modified organisms. Chromosome missegregation can also be achieved by exposure to chemicals, such as the mitotic inhibitor methyl benzimidazole 2 yl carbamate (MBC) (Wood, 1982). Exposure to MBC has been successfully used as a mutagenesis method to obtain a bioethanol-producing *Saccharomyces cerevisiae* strain with improved fermentative capacity under high-gravity conditions, enhanced viability after drying, and higher final ethanol titers (Zheng et al., 2013, 2014; Zhang et al., 2015). Therefore, we mutagenized strain CBS 1483 by growing it in SMD medium containing 10 μg/mL MBC and selected ethanol-tolerant mutants by growth during four consecutive batches in duplicate reactors (MBC1 and MBC2) containing SMD medium with 10% ethanol (v/v) supplemented with anaerobic growth factors. During the fourth batch, samples were taken and strains IMS0687-IMS0704 were isolated from reactor MBC1 and strains IMS715-IMS720 from reactor MBC2.

The ethanol tolerance of CBS 1483, IMS0687-IMS0704 and IMS0715-IMS0720 was evaluated in batch cultures in shake flasks containing 100 mL SMD with 10% ethanol (v/v) at 20°C during 7 days. Growth was monitored by measuring the OD_{660} and extracellular metabolite concentrations. The strains IMS0687, IMS0698, IMS0703, and IMS0716 that reached the higher OD_{660} were selected and grown along the parental strain CBS 1483 in triplicate in bottles with SMD 10% ethanol as described above for 10 days. Samples were taken at regular intervals to measure the OD_{660} and extracellular metabolites. The exponential growth rates of IMS0687, IMS0703 and IMS0716 were similar to that of CBS 1483, and the growth rate of IMS0698 was significantly lower (**Figure 6**). However, after about 60 h the growth of CBS 1483 slowed down (**Figure 6**), but still reached OD_{660} of 3.2 after 212 h. In contrast IMS0687, IMS0703, and IMS0716 reached 3.2

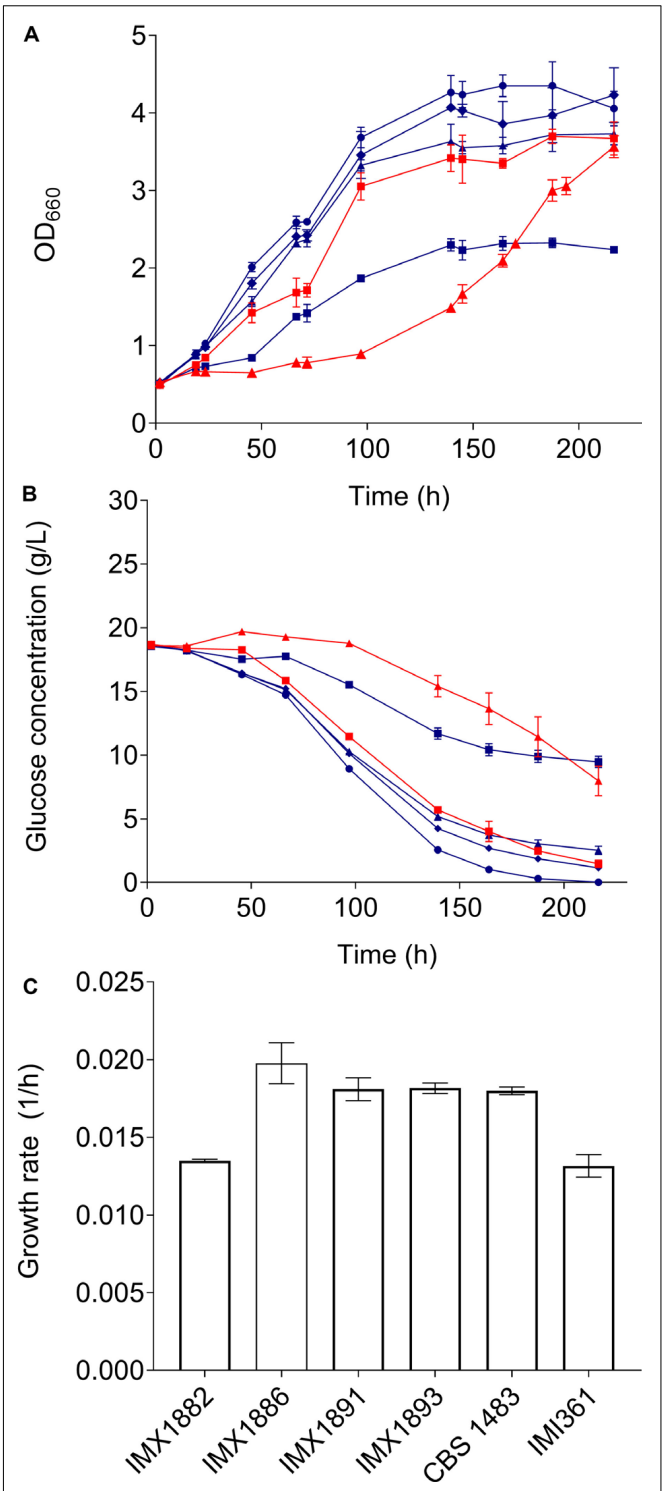

FIGURE 5 | Characterisation of mutants obtained by centromere-silencing mutagenesis in medium containing 10% ethanol. Strains IMX1882 (blue squares), IMX1886 (blue triangles), IMX1891 (blue diamonds), IMX1893 (blue circles), CBS 1483 (red squares) and IMI361 (red triangles) were grown in triplicate in micro-aerobic bottle fermentations on SMD medium containing 10% ethanol at 20°C during 9 days. During the experiment OD_{660} **(A)** and extracellular glucose concentrations **(B)** were monitored. The growth rates were calculated from at least 6 measurements with an R^2 superior to 0.95 **(C)**.

after less than 90 h. Moreover, the final OD_{660} of the mutant strains was between 15 and 33% higher than that of CBS 1483. Correspondingly, IMS0687, IMS0703, and IMS0716 consumed all glucose within 111 h and IMS0698 within 164 h. In the same period the parental strain CBS 1483 only consumed 88% of available sugar (**Figure 6**). These results indicate that these mutants have acquired more robust growth and sugar utilization in the presence of 10% ethanol.

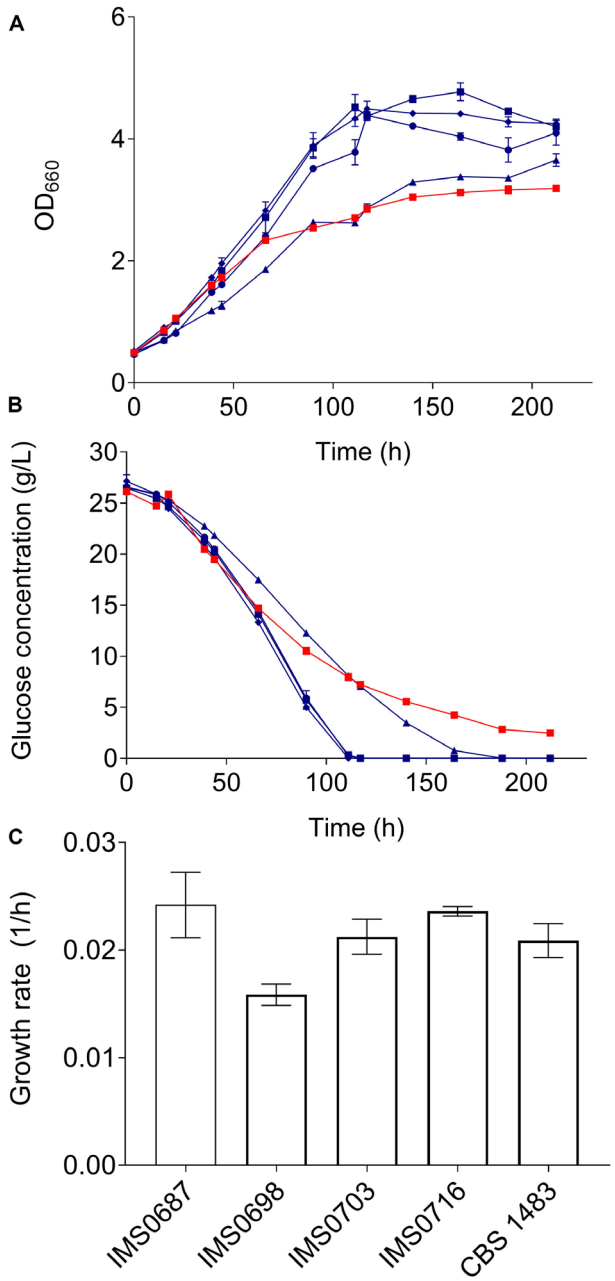

FIGURE 6 | Characterisation of mutants obtained by MBC mutagenesis in medium containing 10% ethanol. Strains IMS0687 (blue squares), IMS0698 (blue triangles), IMS0703 (blue diamonds), IMS0716 (blue circles) and CBS 1483 (red squares) were grown in triplicate in micro-aerobic bottle fermentations on SMG medium containing 10% ethanol at 20°C during 9 days. During the experiment OD_{660} **(A)** and extracellular glucose concentrations **(B)** were monitored. The growth rates were calculated from at least 6 measurements with an R^2 superior to 0.95 **(C)**.

To evaluate the impact of MBC on the genome composition of improved mutants IMS0687, IMS0703, and IMS0716, these isolates were subsequently sequenced and chromosome copy number was determined by analyzing sequencing coverage (Nijkamp et al., 2012). The changes in genome composition were significantly larger than what had been previously observed for isolates obtained through centromere silencing ($^{\text{student } t-\text{test}}p_{\text{value}}$ = 2.0E-4). On average, MBC treated mutants exhibiting ethanol tolerance have lost and gained 10.7 ± 1.2 chromosomes resulting in genomes composed of 68.7 ± 0.6 chromosomes. Although the set of sequenced mutants was small, the strains IMS0687, IMS0703, and IMS0716 displayed unique genome composition. However they all showed systematic CCNV for $ScCHRI^{-1}$, $ScCHRV^{-1}$, $ScCHRVIII^{-1}$, and $SeCHRXIV^{-1}$.

Chromosome copy number variation might not be the only genetic determinant underlying the ethanol tolerance, single nucleotide variations (SNV) and genetic reduction involving loss of heterozygosity might be as critical. However, current assembly algorithms reduce genome assemblies to consensus sequences. Information about sequence variation between different chromosome haplotypes is not captured by consensus assemblies (Salazar et al., 2019). In spite the awareness of this pitfall, analysis of sequence variation of IMS0687, IMS0703, and IMS0716 relative to the CBS 1483 consensus sequence was performed (**Figure 3**). While IMS0716 harbored variations in 24 genes, about 2.5-fold more genes were affected in strains IMS0687 and IMS0703. Out of the 59 and 60 genes identified carrying mutations in IMS0687 and IMS0703, respectively, 52 were shared by the two strains. A close inspection of these SNV revealed that 33 genes (64%) were located on *Sc*CHRXIII (**Figure 7**). The two mutant strains were monosomic for *Sc*CHRXIII conversely to the parental CBS 1483 that was disomic and this SNV enrichment on ScCHRXIII therefore reflected an heterozygosity of the two chromosomal copies in CBS 1483 and likely not occurrence of de novo mutations. This shows that in addition to impact on gene dosage, CCNV through loss of heterozygosity might also play an important role in the expression of alleles (likely recessive) necessary to improve ethanol tolerance phenotype.

DISCUSSION

Saccharomyces pastorianus is an interspecific hybrid of *S. cerevisiae* and *S. eubayanus* (Nakao et al., 2009; Libkind et al., 2011) that has been domesticated in Europe since the late Middle Ages (Meussdoerffer, 2009) and that accounts for 89% of brewed beer worldwide. Both Saaz and Frohberg type lager brewing yeast are characterized by an alloaneuploid genome. The present study demonstrated that these yeasts are intrinsically genetically instable and that this property could be harnessed to speed up strain improvement programs. While this notion was generally well accepted, we quantified the impact of this instability on the chromosome complement of the Frohberg

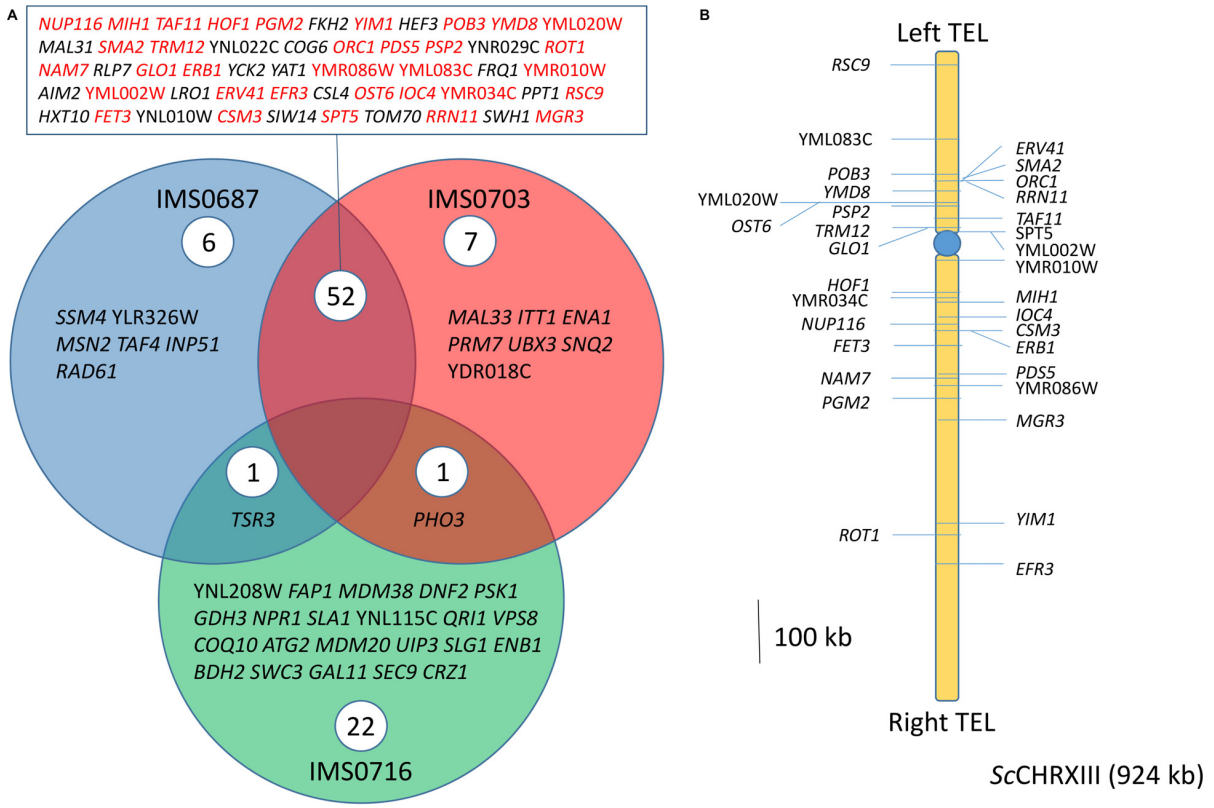

FIGURE 7 | SNV on monosomic ScCHRXIII after MCB treatment predominantly originate from Loss of heterozygosity. **(A)** Venn Diagram of Single Nucleotide Variations (SNV) found in coding sequences relative to the parental strain CBS 1483 identified in *S. pastorianus* strains IMS0687 (blue), IMS0703 (red) and IMS0716 (green) obtained after MBC treatment. Genes found in IMS0687-IMS0703 intersection and denoted in red were located on *Sc*CHRXIII whose copy number decreased from two to one copy. **(B)** Schematic representation of the SNV derived from LOH on ScCHRXIII of IMS0687 and IMS0703 MBC treated mutants.

S. pastorianus strain CBS 1483. It appeared that even on a limited set of tested isolates (#4) chromosomal copy number alterations were noticeable (**Figure 3**). Although limited to a single chromosome variation, this showed that over a small number of transfers new karyotypes can emerged. Next to replicative aging, such genetic drift might contribute to the deterioration of brewing properties of lager yeast after re-pitching, an industrial practice that consists in harvesting of the yeast biomass upon completion of fermentation and its reuse in subsequent fermentations (Jenkins et al., 2003). While decreased brewing performance was often associated to the strong selection pressure encountered by yeast in brewing environment (high ethanol and CO_2, nutrient limitation and low temperature) (Gibson et al., 2007; Kalayu, 2019), our data showed that other factors such as natural genetic instability and physical treatment (e.g., electroporation) may strongly contribute to changes in karyotype. Poor genetic stability is a highly undesired trait at industrial brewing scale, since lager beer properties (e.g., flavor profiles, attenuation) are strictly standardized and contribute to the specific organoleptic signature of one beverage and of the strain that is associated to it.

This study confirmed that isolated variants from a strain population with CCNV exhibited distinct brewing related phenotypes as variation in flocculation, diacetyl reduction, sugar consumption rate and attenuation (Bolat et al., 2008; van den Broek et al., 2015). Therefore, methodologies to manipulate chromosome copy number represent a valuable strategy for lager yeast strain improvement (Gorter de Vries et al., 2017). Targeted engineering of chromosome copy number using centromere silencing was successfully applied to induce CCNV. But in contrast to previous examples in *S. cerevisiae* (Reid et al., 2008), this method unexpectedly yielded extensive off-targeting (**Figure 3**), which precluded the use of this approach to eliminate a single chromosome copy and therefore assess the impact of CCNV of an individual chromosome. Moreover, the requirement to introduce the centromere destabilizing construct further precludes the application of this method for the development of new brewing yeast primarily caused by producers' concerns about consumer acceptance of beer brewed by genetically modified yeasts (Ishii and Araki, 2016, 2017). Conversely, chemical mutagenesis using methyl benzimidazole 2 yl carbamate (MBC) (Wood, 1982) is, considered as non-GMO method to induce CCNV in *S. pastorianus* and therefore applicable to develop new brewing yeasts.

Accurate measurement of chromosome copy numbers after centromere silencing and MBC treatment generated a

unique data set to explore CCNV distribution across mutants quantitatively. Interestingly, loss of chromosomes was more frequent than gain in strains induced for chromosome loss (**Figures 3**, **8**). Theoretically, random chromosome missegregation should cause chromosome loss in the daughter cell and gain in the mother cell or vice versa, leading to equal rates of loss and gain. A higher loss frequency could indicate that chromosome gain is more detrimental than loss, leading to strong selection for cells that have randomly lost rather than gained a chromosome (Santaguida and Amon, 2015b). This is however, contrasting with observation in diploid *S. cerevisiae*, in which chromosome gain (2N to 3N) was more frequent than chromosome loss (2N to 1N), possibly because gain would cause a lower relative change in copy number and thus a lower gene expression impact (Zhu et al., 2014). Chromosome missegregation might also be associated with increased DNA damage and consequently increase chromosome loss after incorporation in a micronucleus as observed in mammalian cells (Santaguida and Amon, 2015a).

Our analysis also revealed that CCNV frequency was different for each chromosome. The loss of *Sc*CHRVIII was significantly more frequent than that of any other ($^{\text{Fischer exact test}}p_{\text{value}}$ = 4.2E-2) (**Figure 8**). Chromosome stability has also been shown to be dependent on the centromere sequence, as the rate of plasmids loss carrying a CEN14 was lower than for plasmids carrying CEN3 which indicates that the frequency of chromosome loss might be associated also the nature of the centromeric region and not only dependent on the genes present on this chromosome. While chromosome stability has also been linked to chromosome size (Kumaran et al., 2013), our data did not corroborate this observation.

The two mutagenesis approaches successfully yielded mutants with improved ethanol tolerance phenotypes. While deep next generation sequencing allows a precise deciphering of the

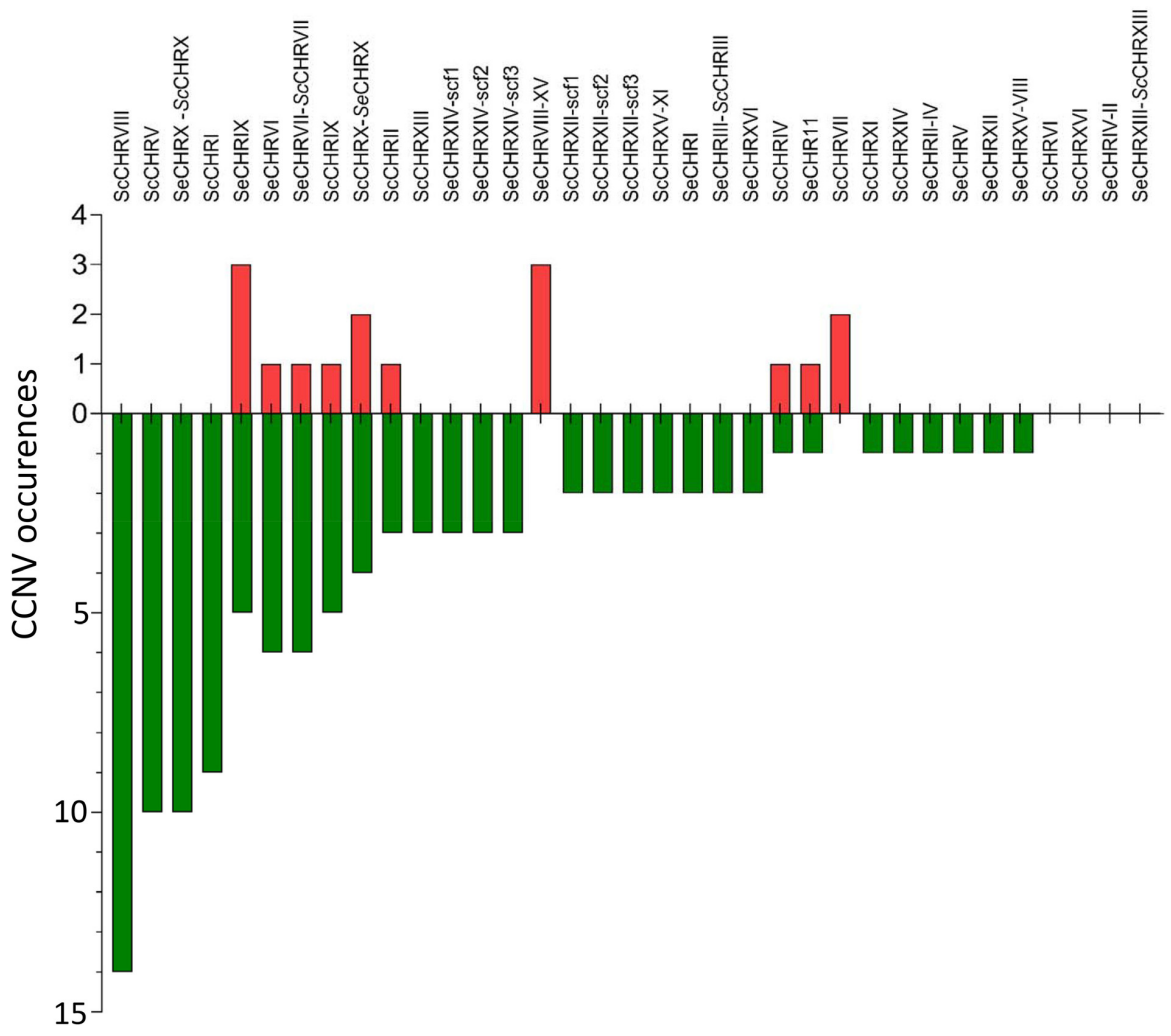

FIGURE 8 | Bar plot of chromosome copy number changes observed in strains generated in this study. Chromosomes were not lost equally in the sequenced strains, untargeted chromosome alterations have been summed over all the analyzed strains for each chromosome and shown in order of observed copy number changes. Instances of loss are shown in green and gain in red.

chromosomal copy number, the link between this information and the phenotype remains difficult to establish (**Figures 2–4**). Mechanisms involving ploidy changes as diploidization or aneuploidy have already been implicated in adaptation of *S. cerevisiae* to high ethanol concentration (Voordeckers et al., 2015; Krogerus et al., 2018; Morard et al., 2019). In a broader context these genetic alterations are more frequently reported (Yona et al., 2012; Bracher et al., 2017; Brickwedde et al., 2017; Harari et al., 2018a,b; Mangado et al., 2018), and changes in full, partial or segmental ploidy, have been shown to contribute effectively to reformatting transcriptome and therefore provide a fast and flexible adaptation to less optimal conditions.

Our study did not completely disentangle the exact contribution of the intrinsic genome instability of the *S. pastorianus* strain and of the mutagenic treatments to obtaining ethanol tolerant variants. Deeper insight could have been gained by submitting the untreated parental strain to the selection procedure experienced by the mutagenized populations. However, based on previous adaptive laboratory evolution strategies to improve ethanol tolerance, generation of tolerant mutants required several hundreds of generations (Voordeckers et al., 2015; Lopandic et al., 2016; Krogerus et al., 2018), contrasting with the reduced number (ca. 25) of generations applied in our study. Further, quantification of CCNV caused by mutagenic treatments showed a significant higher chromosome loss/gain following mutagenesis that would advocate for a key role of the centromere silencing method and MCB treatment in creating a pool of genetic diversity necessary to accelerate the evolution process and the generation of potentially useful variants.

Next to their potential for strain improvement, these methods enabled generation of chromosomal haplotypes by reduction of genomic complexity to chromosome monosomy. The loss of one of the two copies of *Sc*CHRXIII in strain IMS0687 and IMS0703 revealed SNV relative to the parental reference genome that were not acquired de novo but instead resulted from the loss of one of the chromosome copy identifying heterozygous position but also enabling their physical linkage. This illustrates how consensus genome sequence can hide information. In CBS 1483, these two copies were not identical; the lost copy was the one captured in the consensus assembly while the second chromosome variant was revealed by LOH (**Figure 7**). While heterozygosity at a specific position can be derived from sequencing coverage, allocation of adjacent variants to either chromosome copy (phasing) remains challenging. Sequencing of multiple variants obtained after MBC treatment might be complementary to regular genome sequencing program of polyploid and aneuploid strains to unravel chromosome haplotypes.

In conclusion, despite intrinsic genome instability, exacerbation of this trait is a suitable approach to generate extensive genetic diversity that when coupled to effective selection and screening represents a potent method for strain improvement.

DATA AVAILABILITY STATEMENT

The datasets generated for this study can be found in the NCBI (https://www.ncbi.nlm.nih.gov/) under the bioproject accession numbers: PRJNA522669 and PRJNA612191. Variant calling files were made publicly available at the 4TU Centre for data research (https://data.4tu.nl/) under the Digital Object Identifier (doi): 10.4121/uuid:e5bc2cfe-d726-44a1-bc0a-d3a06653694.

AUTHOR CONTRIBUTIONS

AG, EK, RR, and AM performed the molecular biology work. AG, SO'H, and PV performed the mutagenesis and selection experiments. EK, SO'H, and PV performed the growth characterization. PT performed inhouse next generation sequencing. AG, EK, and MB performed the bioinformatics analysis. AG, JP, and J-MD conceptualized and supervised the study. NB provided critical feedback throughout the study. AG, EK, and J-MD wrote the manuscript. All authors read and approved the final manuscript.

FUNDING

This work was supported by the BE-Basic R&D Program (http://www.be-basic.org/), which was granted an FES subsidy from the Dutch Ministry of Economic Affairs, Agriculture and Innovation (EL&I).

ACKNOWLEDGMENTS

We thank Dr. Niels Kuijpers (Heineken Supply Chain B.V.), Dr. Jan-Maarten Geertman (Heineken Supply Chain B.V.), for their support and for critically reading the manuscript.

SUPPLEMENTARY MATERIAL

The Supplementary Material for this article can be found online at: https://www.frontiersin.org/articles/10.3389/fgene.2020.00518/full#supplementary-material

REFERENCES

Alberti, S., Gitler, A. D., and Lindquist, S. (2007). A suite of Gateway cloning vectors for high-throughput genetic analysis in *Saccharomyces cerevisiae*. *Yeast* 24, 913–919. doi: 10.1002/yea.1502

Anders, K. R., Kudrna, J. R., Keller, K. E., Kinghorn, B., Miller, E. M., Pauw, D., et al. (2009). A strategy for constructing aneuploid yeast strains by transient nondisjunction of a target chromosome. *BMC Genet.* 10:36. doi: 10.1186/1471-2156-10-36

Bolat, I., Romagnoli, G., Zhu, F., Pronk, J. T., and Daran, J. M. (2013). Functional analysis and transcriptional regulation of two orthologs of ARO10, encoding broad-substrate-specificity 2-oxo-acid decarboxylases, in the brewing yeast *Saccharomyces pastorianus* CBS 1483. *FEMS Yeast Res.* 13, 505–517. doi: 10.1111/1567-1364.12051

Bolat, I., Walsh, M. C., and Turtoi, M. (2008). Isolation and characterization of two lager yeast strains from the WS34/70 population. *Roum. Biotechnol. Lett.* 13, 62–73.

Bracher, J. M., de Hulster, E., Koster, C. C., van den Broek, M., Daran, J. G., van Maris, A. J. A., et al. (2017). Laboratory evolution of a biotin-requiring *Saccharomyces cerevisiae* strain for full biotin prototrophy and identification of causal mutations. *Appl. Environ. Microbiol.* 83:e00892-17. doi: 10.1128/AEM.00892-17

Brickwedde, A., Brouwers, N., van den Broek, M., Gallego Murillo, J. S., Fraiture, J. L., Pronk, J. T., et al. (2018). Structural, physiological and regulatory analysis of maltose transporter genes in *Saccharomyces eubayanus* CBS 12357(T). *Front. Microbiol.* 9:1786. doi: 10.3389/fmicb.2018.01786

Brickwedde, A., van den Broek, M., Geertman, J. A., Magalhaes, F., Kuijpers, N. G. A., Gibson, B., et al. (2017). Evolutionary engineering in chemostat cultures for improved maltotriose fermentation kinetics in *Saccharomyces pastorianus* lager brewing yeast. *Front. Microbiol.* 8:1690. doi: 10.3389/fmicb.2017.01690

Brouwers, N., Brickwedde, A., Gorter de Vries, A. R., van den Broek, M., Weening, S. M., van den Eijnden, L., et al. (2019a). Himalayan *Saccharomyces eubayanus* genome sequences reveal genetic markers explaining heterotic maltotriose consumption by *Saccharomyces pastorianus* hybrids. *Appl. Environ. Microbiol.* 85:e01516-19. doi: 10.1128/AEM.01516-19

Brouwers, N., Gorter de Vries, A. R., van den Broek, M., Weening, S. M., Elink Schuurman, T. D., Kuijpers, N. G. A., et al. (2019b). In vivo recombination of *Saccharomyces eubayanus* maltose-transporter genes yields a chimeric transporter that enables maltotriose fermentation. *PLoS Genet.* 15:e1007853. doi: 10.1371/journal.pgen.1007853

Bruinenberg, P. M., van Dijken, J. P., and Scheffers, W. A. (1983). An enzymic analysis of NADPH production and consumption in *Candida utilis*. *J. Gen. Microbiol.* 129, 965–971. doi: 10.1099/00221287-129-4-965

Chen, G., Rubinstein, B., and Li, R. (2012). Whole chromosome aneuploidy: big mutations drive adaptation by phenotypic leap. *Bioessays* 34, 893–900. doi: 10.1002/bies.201200069

Dephoure, N., Hwang, S., O'Sullivan, C., Dodgson, S. E., Gygi, S. P., Amon, A., et al. (2014). Quantitative proteomic analysis reveals posttranslational responses to aneuploidy in yeast. *eLife* 3:e03023. doi: 10.7554/eLife.03023

Diderich, J. A., Weening, S. M., van den Broek, M., Pronk, J. T., and Daran, J. G. (2018). Selection of Pof(-) *Saccharomyces eubayanus* variants for the construction of *S. cerevisiae* x *S. eubayanus* hybrids with reduced 4-vinyl Guaiacol formation. *Front. Microbiol.* 9:1640. doi: 10.3389/fmicb.2018.01640

Dube, S., Qin, J., and Ramakrishnan, R. (2008). Mathematical analysis of copy number variation in a DNA sample using digital PCR on a nanofluidic device. *PLoS One* 3:e2876. doi: 10.1371/journal.pone.0002876

Dunn, B., and Sherlock, G. (2008). Reconstruction of the genome origins and evolution of the hybrid lager yeast *Saccharomyces pastorianus*. *Genome Res.* 18, 1610–1623. doi: 10.1101/gr.076075.108

Gibson, B. R., Lawrence, S. J., Leclaire, J. P., Powell, C. D., and Smart, K. A. (2007). Yeast responses to stresses associated with industrial brewery handling. *FEMS Microbiol. Rev.* 31, 535–569. doi: 10.1111/j.1574-6976.2007.00076.x

Gibson, B. R., Storgards, E., Krogerus, K., and Vidgren, V. (2013). Comparative physiology and fermentation performance of Saaz and Frohberg lager yeast strains and the parental species *Saccharomyces eubayanus*. *Yeast* 30, 255–266. doi: 10.1002/yea.2960

Gorter de Vries, A. R., Koster, C. C., Weening, S. M., Luttik, M. A. H., Kuijpers, N. G. A., Geertman, J. A., et al. (2019a). Phenotype-independent isolation of interspecies saccharomyces hybrids by dual-dye fluorescent staining and fluorescence-activated cell sorting. *Front. Microbiol.* 10:871. doi: 10.3389/fmicb.2019.00871

Gorter de Vries, A. R., Pronk, J. T., and Daran, J. G. (2019b). Lager-brewing yeasts in the era of modern genetics. *FEMS Yeast Res.* 19:foz063. doi: 10.1093/femsyr/foz063

Gorter de Vries, A. R., Pronk, J. T., and Daran, J. G. (2017). Industrial relevance of chromosomal copy number variation in Saccharomyces yeasts. *Appl. Environ. Microbiol.* 83:e03206-16. doi: 10.1128/AEM.03206-16

Gorter de Vries, A. R., Voskamp, M. A., van Aalst, A. C. A., Kristensen, L. H., Jansen, L., van den Broek, M., et al. (2019c). Laboratory evolution of a *Saccharomyces cerevisiae* x *S. eubayanus* hybrid under simulated lager-brewing conditions. *Front. Genet.* 10:242. doi: 10.3389/fgene.2019.00242

Harari, Y., Ram, Y., and Kupiec, M. (2018a). Frequent ploidy changes in growing yeast cultures. *Curr. Genet.* 64, 1001–1004. doi: 10.1007/s00294-018-0823-y

Harari, Y., Ram, Y., Rappoport, N., Hadany, L., and Kupiec, M. (2018b). Spontaneous changes in Ploidy are common in yeast. *Curr. Biol.* 28, 825–835.e4. doi: 10.1016/j.cub.2018.01.062

Hewitt, S. K., Donaldson, I. J., Lovell, S. C., and Delneri, D. (2014). Sequencing and characterisation of rearrangements in three *S. pastorianus* strains reveals the presence of chimeric genes and gives evidence of breakpoint reuse. *PLoS One* 9:e92203. doi: 10.1371/journal.pone.0092203

Hill, A., and Bloom, K. (1987). Genetic manipulation of centromere function. *Mol. Cell Biol.* 7, 2397–2405. doi: 10.1128/mcb.7.7.2397

Hose, J., Yong, C. M., Sardi, M., Wang, Z., Newton, M. A., and Gasch, A. P. (2015). Dosage compensation can buffer copy-number variation in wild yeast. *eLife* 4:e05462. doi: 10.7554/eLife.05462

Ishii, T., and Araki, M. (2016). Consumer acceptance of food crops developed by genome editing. *Plant Cell Rep.* 35, 1507–1518. doi: 10.1007/s00299-016-1974-2

Ishii, T., and Araki, M. (2017). A future scenario of the global regulatory landscape regarding genome-edited crops. *GM Crops Food* 8, 44–56. doi: 10.1080/21645698.2016.1261787

Jenkins, C. L., Kennedy, A. I., Hodgson, J. A., Thurston, P., and Smart, K. A. (2003). Impact of serial repitching on lager brewing yeast quality. *J. Am. Soc. Brew. Chem.* 61, 1–9. doi: 10.1094/ASBCJ-61-0001

Kalayu, G. (2019). Serial re-pitching: its effect on yeast physiology, fermentation performance, and product quality. *Ann. Microbiol.* 69, 787–796. doi: 10.1007/s13213-019-01493-4

Krogerus, K., and Gibson, B. (2013). 125th anniversary review: diacetyl and its control during brewery fermentation. *J. Inst. Brew.* 119, 86–97. doi: 10.1002/jib.84

Krogerus, K., Holmstrom, S., and Gibson, B. (2018). Enhanced Wort fermentation with *de novo* lager hybrids adapted to high-ethanol environments. *Appl. Environ. Microbiol.* 84:e02302-17. doi: 10.1128/AEM.02302-17

Kumaran, R., Yang, S. Y., and Leu, J. Y. (2013). Characterization of chromosome stability in diploid, polyploid and hybrid yeast cells. *PLoS One* 8:e68094. doi: 10.1371/journal.pone.0068094

Li, H., and Durbin, R. (2009). Fast and accurate short read alignment with Burrows-Wheeler transform. *Bioinformatics* 25, 1754–1760. doi: 10.1093/bioinformatics/btp324

Li, H., and Durbin, R. (2010). Fast and accurate long-read alignment with Burrows-Wheeler transform. *Bioinformatics* 26, 589–595. doi: 10.1093/bioinformatics/btp698

Libkind, D., Hittinger, C. T., Valerio, E., Goncalves, C., Dover, J., Johnston, M., et al. (2011). Microbe domestication and the identification of the wild genetic stock of lager-brewing yeast. *Proc. Natl. Acad. Sci. U.S.A.* 108, 14539–14544. doi: 10.1073/pnas.1105430108

Lopandic, K., Pfliegler, W. P., Tiefenbrunner, W., Gangl, H., Sipiczki, M., and Sterflinger, K. (2016). Genotypic and phenotypic evolution of yeast interspecies hybrids during high-sugar fermentation. *Appl. Microbiol. Biotechnol.* 100, 6331–6343. doi: 10.1007/s00253-016-7481-0

Mangado, A., Morales, P., Gonzalez, R., and Tronchoni, J. (2018). Evolution of a yeast with industrial background under winemaking conditions leads to Diploidization and Chromosomal copy number variation. *Front. Microbiol.* 9:1816. doi: 10.3389/fmicb.2018.01816

Meussdoerffer, F. G. (2009). "A comprehensive history of beer brewing," in *Handbook of Brewing*, ed. H. M. Eßlinger, (Weinheim: Wiley-VCH). doi: 10.1002/9783527623488

Morard, M., Macias, L. G., Adam, A. C., Lairon-Peris, M., Perez-Torrado, R., Toft, C., et al. (2019). Aneuploidy and ethanol tolerance in *Saccharomyces cerevisiae*. *Front. Genet.* 10:82. doi: 10.3389/fgene.2019.00082

Musacchio, A., and Salmon, E. D. (2007). The spindle-assembly checkpoint in space and time. *Nat. Rev. Mol. Cell Biol.* 8, 379–393. doi: 10.1038/nrm2163

Nakao, Y., Kanamori, T., Itoh, T., Kodama, Y., Rainieri, S., Nakamura, N., et al. (2009). Genome sequence of the lager brewing yeast, an interspecies hybrid. *DNA Res.* 16, 115–129. doi: 10.1093/dnares/dsp003

Nijkamp, J. F., van den Broek, M. A., Geertman, J. M., Reinders, M. J., Daran, J. M., and de Ridder, D. (2012). De novo detection of copy number variation by co-assembly. *Bioinformatics* 28, 3195–3202. doi: 10.1093/bioinformatics/bts601

Okuno, M., Kajitani, R., Ryusui, R., Morimoto, H., Kodama, Y., and Itoh, T. (2016). Next-generation sequencing analysis of lager brewing yeast strains reveals the evolutionary history of interspecies hybridization. *DNA Res.* 23, 67–80. doi: 10.1093/dnares/dsv037

Panzeri, L., Groth-Clausen, I., Shepard, J., Stotz, A., and Philippsen, P. (1984). "Centromeric DNA in yeast," in *Chromosomes Today*, Vol. 8, eds M. D. Bennett, A. Gropp, and U. Wolf, (Dordrecht: Springer).

Pavelka, N., Rancati, G., Zhu, J., Bradford, W. D., Saraf, A., Florens, L., et al. (2010). Aneuploidy confers quantitative proteome changes and phenotypic variation in budding yeast. *Nature* 468, 321–325. doi: 10.1038/nature09529

Peter, J., De Chiara, M., Friedrich, A., Yue, J. X., Pflieger, D., Bergstrom, A., et al. (2018). Genome evolution across 1,011 *Saccharomyces cerevisiae* isolates. *Nature* 556, 339–344. doi: 10.1038/s41586-018-0030-5

Puligundla, P., Smogrovicova, D., Obulam, V. S., and Ko, S. (2011). Very high gravity (VHG) ethanolic brewing and fermentation: a research update. *J. Ind. Microbiol. Biotechnol.* 38, 1133–1144. doi: 10.1007/s10295-011-0999-3

Reid, R. J. D., Sunjevaric, I., Voth, W. P., Ciccone, S., Du, W., Olsen, A. E., et al. (2008). Chromosome-scale genetic mapping using a set of 16 conditionally stable *Saccharomyces cerevisiae* chromosomes. *Genetics* 180, 1799–1808. doi: 10.1534/genetics.108.087999

Salazar, A. N., Gorter de Vries, A. R., van den Broek, M., Brouwers, N., de la Torre Cortes, P., Kuijpers, N. G. A., et al. (2019). Chromosome level assembly and comparative genome analysis confirm lager-brewing yeasts originated from a single hybridization. *BMC Genomics* 20:916. doi: 10.1186/s12864-019-6263-3

Santaguida, S., and Amon, A. (2015a). Aneuploidy triggers a TFEB-mediated lysosomal stress response. *Autophagy* 11, 2383–2384. doi: 10.1080/15548627.2015.1110670

Santaguida, S., and Amon, A. (2015b). Short- and long-term effects of chromosome mis-segregation and aneuploidy. *Nat. Rev. Mol. Cell Biol.* 16, 473–485. doi: 10.1038/nrm4025

Sheltzer, J. M., Blank, H. M., Pfau, S. J., Tange, Y., George, B. M., Humpton, T. J., et al. (2011). Aneuploidy drives genomic instability in yeast. *Science* 333, 1026–1030. doi: 10.1126/science.1206412

Solis-Escalante, D., Kuijpers, N. G., Bongaerts, N., Bolat, I., Bosman, L., Pronk, J. T., et al. (2013). amdSYM, a new dominant recyclable marker cassette for *Saccharomyces cerevisiae*. *FEMS Yeast Res.* 13, 126–139. doi: 10.1111/1567-1364.12024

Storchova, Z. (2014). Ploidy changes and genome stability in yeast. *Yeast* 31, 421–430. doi: 10.1002/yea.3037

Thompson, J. R., Register, E., Curotto, J., Kurtz, M., and Kelly, R. (1998). An improved protocol for the preparation of yeast cells for transformation by electroporation. *Yeast* 14, 565–571. doi: 10.1002/(SICI)1097-0061(19980430)14:6<565::AID-YEA251>3.0.CO;2-B

Torres, E., Williams, B., Tang, Y.-C., and Amon, A. (2011). Thoughts on Aneuploidy. *Cold Spring Harb. Symp. Quant. Biol.* 75, 445–451. doi: 10.1101/sqb.2010.75.025

van den Broek, M., Bolat, I., Nijkamp, J. F., Ramos, E., Luttik, M. A., Koopman, F., et al. (2015). Chromosomal copy number variation in *Saccharomyces pastorianus* is evidence for extensive genome dynamics in industrial lager brewing strains. *Appl. Environ. Microbiol.* 81, 6253–6267. doi: 10.1128/AEM.01263-15

Verduyn, C., Postma, E., Scheffers, W. A., and Van Dijken, J. P. (1992). Effect of benzoic acid on metabolic fluxes in yeasts: a continuous-culture study on the regulation of respiration and alcoholic fermentation. *Yeast* 8, 501–517. doi: 10.1002/yea.320080703

Voordeckers, K., Kominek, J., Das, A., Espinosa-Cantu, A., De Maeyer, D., Arslan, A., et al. (2015). Adaptation to high ethanol reveals complex evolutionary pathways. *PLoS Genet.* 11:e1005635. doi: 10.1371/journal.pgen.1005635

Walker, B. J., Abeel, T., Shea, T., Priest, M., Abouelliel, A., Sakthikumar, S., et al. (2014). Pilon: an integrated tool for comprehensive microbial variant detection and genome assembly improvement. *PLoS One* 9:e112963. doi: 10.1371/journal.pone.0112963

Walther, A., Hesselbart, A., and Wendland, J. (2014). Genome sequence of Saccharomyces carlsbergensis, the world's first pure culture lager yeast. *G3* 4, 783–793. doi: 10.1534/g3.113.010090

Wood, J. S. (1982). Genetic effects of methyl benzimidazole-2-yl-carbamate on *Saccharomyces cerevisiae*. *Mol. Cell. Biol.* 2, 1064–1079. doi: 10.1128/MCB.2.9.1064

Yona, A. H., Manor, Y. S., Herbst, R. H., Romano, G. H., Mitchell, A., Kupiec, M., et al. (2012). Chromosomal duplication is a transient evolutionary solution to stress. *Proc. Natl. Acad. Sci. U.S.A.* 109, 21010–21015. doi: 10.1073/pnas.1211150109

Zhang, K., Tong, M., Gao, K., Di, Y., Wang, P., Zhang, C., et al. (2015). Genomic reconstruction to improve bioethanol and ergosterol production of industrial yeast *Saccharomyces cerevisiae*. *J. Ind. Microbiol. Biotechnol.* 42, 207–218. doi: 10.1007/s10295-014-1556-7

Zheng, D., Zhang, K., Gao, K., Liu, Z., Zhang, X., Li, O., et al. (2013). Construction of novel *Saccharomyces cerevisiae* strains for bioethanol active dry yeast (ADY) production. *PLoS One* 8:e85022. doi: 10.1371/journal.pone.0085022

Zheng, D. Q., Chen, J., Zhang, K., Gao, K. H., Li, O., Wang, P. M., et al. (2014). Genomic structural variations contribute to trait improvement during whole-genome shuffling of yeast. *Appl. Microbiol. Biotechnol.* 98, 3059–3070. doi: 10.1007/s00253-013-5423-7

Zhu, Y. O., Siegal, M. L., Hall, D. W., and Petrov, D. A. (2014). Precise estimates of mutation rate and spectrum in yeast. *Proc. Natl. Acad. Sci. U.S.A.* 111, E2310–E2318. doi: 10.1073/pnas.1323011111

Conflict of Interest: The authors declare that the research was conducted in the absence of any commercial or financial relationships that could be construed as a potential conflict of interest.

frontiers in Genetics

REVIEW
published: 10 June 2020
doi: 10.3389/fgene.2020.00602

Diversity of Oligopeptide Transport in Yeast and Its Impact on Adaptation to Winemaking Conditions

*Carmen Becerra-Rodríguez[1], Souhir Marsit[2] and Virginie Galeote[1]**

[1] SPO, INRAE, Université de Montpellier, Montpellier SupAgro, Montpellier, France, [2] Institut de Biologie Intégrative et des Systèmes, Regroupement Québécois de Recherche sur la Fonction, l'Ingénierie et les Applications des Protéines, (PROTEO), Département de Biologie, Université Laval, Québec City, QC, Canada

Nitrogen is an essential nutrient for yeasts and its relative abundance is an important modulator of fermentation kinetics. The main sources of nitrogen in food are ammonium and free amino acids, however, secondary sources such as oligopeptides are also important contributors to the nitrogen supply. In yeast, oligopeptide uptake is driven by different families of proton–coupled transporters whose specificity depends on peptide length. Proton-dependent Oligopeptide Transporters (POT) are specific to di- and tri-peptides, whereas the Oligopeptide Transport (OPT) family members import tetra- and pentapeptides. Recently, the novel family of Fungal Oligopeptide Transporters (FOT) has been identified in *Saccharomyces cerevisiae* wine strains as a result of a horizontal gene transfer from *Torulaspora microellipsoides*. In natural grape must fermentations with *S. cerevisiae*, Fots have a broader range of oligopeptide utilization in comparison with non-Fot strains, leading to higher biomass production and better fermentation efficiency. In this review we present the current knowledge on the diversity of oligopeptide transporters in yeast, also discussing how the consumption of oligopeptides provides an adaptive advantage to yeasts within the wine environment.

Keywords: oligopeptides, peptide transport, yeast, wine fermentation, *Saccharomyces cerevisiae*, Fungal Oligopeptide Transporters, adaptation

OPEN ACCESS

Edited by:
Roberto Pérez-Torrado, Consejo Superior de Investigaciones Científicas (CSIC), Spain

Reviewed by:
Florian F. Bauer, Stellenbosch University, South Africa
Ignacio Belda, Complutense University of Madrid, Spain

****Correspondence:***
Virginie Galeote
virginie.galeote@inrae.fr

Specialty section:
This article was submitted to Evolutionary and Genomic Microbiology, a section of the journal Frontiers in Genetics

Received: *31 March 2020*
Accepted: *18 May 2020*
Published: *10 June 2020*

Citation:
Becerra-Rodríguez C, Marsit S and Galeote V (2020) Diversity of Oligopeptide Transport in Yeast and Its Impact on Adaptation to Winemaking Conditions. Front. Genet. 11:602. doi: 10.3389/fgene.2020.00602

INTRODUCTION

Yeasts are unicellular, eukaryotic organisms that are commonly found in food environments, where they normally consume sugars to produce energy in anaerobic conditions. This process is known as fermentation, a reaction by which carbohydrates and other organic molecules are catabolized to release energy in the absence of oxygen, using an organic molecule as the final electron acceptor. Alcoholic fermentation, i.e., the transformation of monomeric sugars into ethanol and carbon dioxide, is the predominant form of fermentation in yeast. Several foods and beverages such as bread, sake, beer or wine are the result of such alcoholic fermentation performed by yeasts and other microorganisms.

As any other known form of life, yeasts require nitrogen for building some essential macromolecules, i.e., proteins and nucleic acids. This makes nitrogen one of the main nutrients and therefore a key modulator in yeast life cycle. In a winemaking context, nitrogen availability controls yeast growth rate and fermentation kinetics, nitrogen deficiency being the first cause of slow and incomplete fermentations (Alexandre and Charpentier, 1998; Bisson, 1999; Bell and Henschke, 2005). Indeed, nitrogen supplementation during fermentation effectively

prevents sluggish or stuck fermentations (Blateyron and Sablayrolles, 2001). Nitrogen availability also affects the formation of volatile compounds during fermentation, which are largely responsible for shaping wine aroma profiles and thus are an important enological trait (Hazelwood et al., 2008). Ammonium and free amino acids are the primary nitrogen sources for yeast, as main constituents of total assimilable nitrogen in grape must (Henschke and Jiranek, 1993). However, there are other molecules, such as oligopeptides, polypeptides, proteins, amides, biogenic amines and even nucleic acids that constitute secondary and diverse sources of nitrogen (Ough et al., 1991).

Oligopeptides, also simply termed peptides, consist in short sequences of a few amino acids covalently joined by peptide bonds (Nelson and Cox, 2013). In nature, they mainly result from proteolytic processes. Analysis of the nitrogen sources in soils established that oligopeptides correspond to the peptide fraction with a molecular weight < 1 kDa, which is equivalent to peptides with 2–9 amino acid residues (Farrell et al., 2011). Oligopeptide composition in foods and beverages is highly diverse, since it depends on the industrial and/or domestic processing that these products usually undergo during manufacturing (Clapperton, 1971; Henschke and Jiranek, 1993; Takahashi et al., 2012; D'Souza et al., 2018). In grape must, peptide composition is also conditioned by the grape variety, terroir or vintage, among other environmental factors (Moreno-Arribas et al., 1996). However, some amino acids have been found as predominant in the peptide fractions of different samples. Previous studies on Chardonnay grape must from Coursan (France, 2012) showed that glutamate and glutamine were the most abundant amino acids in the oligopeptide fraction, followed by glycine, asparagine and aspartate (Marsit et al., 2015); a similar composition was found in the peptide fractions of Koshu wines, beers, or soy (Yokotsuka et al., 1975; Dale and Young, 1989; Kitagawa et al., 2008). Nevertheless, analyses of oligopeptide composition in grape musts and other foods and beverages are still scarce.

In the same way as bacteria, plants, mammals and other fungi, yeasts can uptake oligopeptides from the environment for use as nitrogen and carbon sources. In grape must, the oligopeptide fraction constitutes 17% of total nitrogen and 10% of the nitrogen assimilated by yeast (Yokotsuka and Fukui, 2002; Marsit et al., 2015). In beer, 30–50% of wort peptides are utilized during fermentation as nutrients and precursors of the cell wall, although growth rate is lower when oligopeptides are the sole source of nitrogen (Clapperton, 1971; Ingledew and Patterson, 1999; Mo et al., 2013). Furthermore, Mo et al. (2013) showed that only peptide fractions below 5 kDa (corresponding to peptides with up to 45 amino acid residues approximatively) were assimilated by yeast during beer fermentation, with a particularly fast decrease in peptides below 1 kDa. Extracellular protease activity is highly regulated, allowing yeasts to degrade the polypeptides from wort into assimilable oligopeptides (Lekkas et al., 2009). While the uptake of some amino acids may be strictly inhibited or repressed, yeasts can indirectly acquire those amino acids through the consumption of oligopeptides and their subsequent hydrolysis (Kevvai et al., 2016; Marsit et al., 2016). In wine fermentation, oligopeptides assimilation can lead to the release of some amino acids that are then consumed after depletion of the other nitrogen sources (Marsit et al., 2016). Furthermore, experiments on synthetic media containing ammonia and free amino acids supplemented with yeast hydrolysate have shown that nitrogen provided by peptides eventually constitutes 40% of the yeast protein fraction during alcoholic fermentation, which highlights the important anabolic role of oligopeptides versus other nitrogen sources such as ammonium, which only contributes 20% of this fraction (Kevvai et al., 2016).

Besides being a nutrient source, some oligopeptides have other important, specific functions within living organisms and environments. Glutathione (γ-L-Glutamyl-L-cysteinylglycine) is a tripeptide whose antioxidant functions in the cell have been extensively described. In wine fermentation, glutathione from grape musts mitigates the oxidative stress caused by copper and prevents browning reactions by blocking the oxidation of brown pigment precursors (Rigaud et al., 1991; Zimdars et al., 2019). Small peptides found in foods are taste determinants of umami, along with glutamate and ribonucleotides (Zhang et al., 2017). Other peptides are produced by bacteria, fungi, plants and animals as antimicrobial agents, and thus some of them have been commercially used as antibiotics and bioactive compounds in food (Rai and Jeyaram, 2015; Yang and Yousef, 2018). In addition, some of the described antifungal peptides have other reported activities within cells, such as antioxidants, protease and ion channel inhibitors or surface-immobilized peptides (Wang et al., 2016; see The Antimicrobial Peptide Database)[1]. In yeast, killer toxins constitute a widespread phenotype of peptides that are produced to penetrate and kill cells through interaction with membrane-associated complex carbohydrates, usually targeting spoilage and pathogenic microorganisms in fermentative environments (Mannazzu et al., 2019). More precisely, it has been described how some *Saccharomyces cerevisiae* strains secrete peptides to inhibit the growth of non-*Saccharomyces* yeasts during fermentation, enabling competitors exclusion and broader access to nutrients (Albergaria et al., 2010; Branco et al., 2017).

Despite the importance that oligopeptides seem to have in yeast performance during fermentation, their role has been long underestimated, which explains the insufficient number of studies dedicated to this issue. Here we provide a state-of-the-art review about oligopeptide transport in yeast, focusing on the impact of peptide uptake during wine fermentation and the role of oligopeptide transporters in the adaptation of *S. cerevisiae* to wine environments.

FAMILIES OF OLIGOPEPTIDE TRANSPORTERS IN YEAST

Oligopeptide transport is a mechanism that has been retained throughout evolution, as demonstrated by its presence in bacteria, fungi, plants and mammals. It consists in the energy-dependent uptake of small peptides across the biological membrane into the cell. It works as an independent process from amino acid transport, with high stereoselectivity for α-peptide bonds and amino acid residues in L-form in all transport systems

[1] http://aps.unmc.edu/AP/main.php

(Steiner et al., 1995). In bacteria, peptide transport is mainly carried out by the ATP-binding cassette (ABC) superfamily, with Dpp and Opp as the best-known systems (Higgins and Gibson, 1986; Manson et al., 1986; Hiles et al., 1987). ABC transporters are characterized by two transmembrane domains and two nucleotide-binding domains that enable peptide import through the hydrolysis of two ATP molecules (reviewed by Rees et al., 2009). Although the ABC superfamily is widespread among eukaryotes, some of its members have evolved into functionalities different from nutrient uptake. For example, ABC transporters in entomopathogenic fungi mediate host-pathogen interactions, working as metabolite efflux pumps (Baral, 2017). In *S. cerevisiae*, ABC transporters are involved in peptide pheromone secretion, regulation of mitochondrial function, vacuolar detoxification, pleiotropic drug resistance and stress adaptation (Jungwirth and Kuchler, 2006). In fungi, peptide uptake is generally energized by the symport with protons, depending thus on proton-coupled transporters. It is noteworthy that peptide transport is not an essential mechanism, since mutation-induced inactivation of transport systems has been proved not to be lethal (Perry et al., 1994). Nevertheless, the development of multiple transport systems (as illustrated in **Table 1**) among fungi and yeasts illustrates the importance of oligopeptide transport to cope with different nitrogen sources for survival.

Proton-Dependent Oligopeptide Transport Family

Paulsen and Skurray (1994) first designated the Proton-dependent Oligopeptide Transport (POT) family after finding sequence similarity between different non-ABC-type, proton-dependent transporters, such as PepT1 and PepT2 in mammals, *Arabidopsis thaliana* nitrate transporter Ckl1, DtpT oligopeptide transporter in *Lactococcus lactis* or the *S. cerevisiae* peptide transporter Ptr2. They predicted a shared topological domain consisting in 12 putative α-helical transmembrane segments, with two specific conserved motifs that had not been found in any other protein at that time. However, Steiner et al. (1995) considered that the designation POT was inappropriate, since not all the transporters in the denominated POT family had been proved to be proton-dependent or to mediate oligopeptide transport. They therefore proposed the use of the term Peptide Transport family (PTR) to refer to a group of non-ABC-type, proton-dependent oligopeptide transporters with a high similarity at protein sequence level and multiple conserved motifs for phosphorylation and glycosylation. Currently, the PTR or POT denominations are indiscriminately used in literature referring to the proton-dependent oligopeptide transporters family with specificity for di- and tri-peptides. POT have been identified in both eukaryotes and prokaryotes, with the exception of archaea. A possible explanation for this exception is the absence of peptides in the extreme environments usually inhabited by archaea (Newstead, 2017). The POT family has been grouped as a member of the Major Facilitator Superfamily (MFS) in the Transporter Classification Database (TCDB,[2] reference for POT: TC# 2.A.17).

[2]http://www.tcdb.org

In *S. cerevisiae*, the PTR system consists of three interdependent genes: *PTR2* encodes the integral membrane transporter Ptr2, the best-known member of the PTR family with isoforms also found in *Candida albicans* (Basrai et al., 1992) and *A. thaliana* (Steiner et al., 1994). *PTR1* and *PTR3* work as regulatory elements: *PTR1* is essential for the expression of *PTR2* and consequently for transporter functionality; on the other hand, *PTR3* is involved in the induction of peptide transport in presence of poor sources of nitrogen, although its activity is not crucial for di- and tripeptide transport by Ptr2 (Barnes et al., 1998). Despite its broadly multi-specific substrate preferences, Ptr2 from *S. cerevisiae* has a higher affinity for di- and tri-peptides containing aromatic, branched or basic amino acids (Phe, Trp, Tyr, Ile, Leu, Val, Arg, Lys, and His) and a lower affinity for negatively charged amino acids (Asp and Glu), glycine and proline (Ito et al., 2013). Additionally, members of the POT family in plants have acquired the ability to transport other nitrogen sources, such as the nitrate permease AtCHL1 in *A. thaliana* (Steiner et al., 1995; Williams and Miller, 2001; Léran et al., 2014).

Oligopeptide Transporters

All ATP-binding cassette and PTR have been found to transport only di- and tri-peptides (Becker and Naider, 1980; Ganapathy and Leibach, 1991; Payne and Smith, 1994). However, Lubkowitz et al. (1997) identified a new oligopeptide transporter in *C. albicans* able to uptake peptides with four or five amino acid residues with high affinity. This new transporter was independent of the di- and tripeptide transport systems, as shown by substrate competition experiments using radiolabeled peptides. The lack of sequence homology of this new transporter with the PTR or ABC transporters demonstrated that it belonged to a novel family of oligopeptide transporters, receiving the name of Opt1 from Oligo Peptide Transporter (OPT; TC# 2.A.67). In the following years, sequence homology analyses enabled the identification of new isoforms of the OPT family in *Schizosaccharomyces pombe* (Lubkowitz et al., 1998), Opt1 and Opt2 in *S. cerevisiae* (Hauser et al., 2000) and up to four new functional members in *C. albicans* (Opt2-3-4-5). Moreover, OPT transporters were also identified in prokaryotes and plants (Hauser et al., 2001; Gomolplitinant and Saier, 2011). Studies with the Opt1 isoform in *S. cerevisiae* showed that the OPT system also works with the proton-motive force (Hauser et al., 2001; Osawa et al., 2006). The deduced protein sequence of Opt1 in *C. albicans* revealed a membrane-associated, hydrophobic protein with 12 putative transmembrane domains (Wiles et al., 2006b). However, later studies revealed that OPT transporters actually contained 16 transmembrane domains originated from sequential duplication events of a 2-transmembrane domain precursor element (Gomolplitinant and Saier, 2011).

Although OPT are often defined as tetra- and pentapeptide transporters, some isoforms in *C. albicans* are able to uptake peptides of up to eight amino acid residues (Reuß and Morschhäuser, 2006). Opt1 can also transport glutathione, with higher affinity for the reduced form, as well as the pentapeptides known as enkephalins (Bourbouloux et al., 2000; Hauser et al., 2000; Zulkifli et al., 2016). The other OPT member

TABLE 1 | List of oligopeptide transport systems.

Family of peptide transporters	Organisms	Energy source for transport	Examples	Species	Substrates
ABC	Bacteria	ATP hydrolysis	Dpp, Opp	*Escherichia coli Salmonella typhimurium Streptococcus pneumoniae*	Dipeptides, Oligopeptides
POT/PTR	Bacteria, fungi, mammals, plants	Proton-coupled symport	Ptr2	*S. cerevisiae C. albicans A. thaliana*	Di- and tripeptides
			DtpT	*L. lactis*	
			PepT	*S. oneidensis S. thermophilus*	
			PepT1, PepT2	*Homo sapiens*	Di- and tripeptides, β-lactam antibiotics, antiviral and anticancer drugs
OPT	Bacteria, fungi, mammals, plants	Proton-coupled symport	Opt1	*S. cerevisiae C. albicans S. pombe*	Tetra- and pentapeptides, glutathione, enkephalins
			Opt2	*S. cerevisiae C. albicans*	Tetrapeptides
			Opt3, Opt4, Opt5, Opt6, Opt7, Opt8	*C. albicans*	Up to eight amino acid residues
			Ys1	*A. thaliana Zea mays*	Peptides and metal-NA complexes
FOT	Fungi	Proton-coupled symport	Fot1*, Fot2*	*S. cerevisiae* wine strains	Di- and tripeptides, glutathione
			Fot3*		Non-characterized
			FotX, FotY, Fot2tomi	*T. microellipsoides*	Non-characterized
Dal5	Yeast	Cation/proton-coupled symport		*S. cerevisiae*	Allantoate, ureidosuccinate, dipeptides
Asp3	Yeast	Unknown		*S. cerevisiae** *W. anomalus*	Dipeptides with asparagine in the C-terminal
Gap1	Yeast	Unknown		*S. cerevisiae*	γ-glutamyl dipeptides

**Originated from a HGT phenomenon. The table includes some examples of the families of transporters that have shown oligopeptide transport activity.*

in *S. cerevisiae*, Opt2, shares 31% identity with Opt1, and can transport tetrapeptides. Opt2 participates in the fusion of small vesicles into a larger vacuole, which plays an important role in drug detoxification processes (Aouida et al., 2009). Additionally, Opt2 is involved in the regulation of Opt1 expression (Hauser et al., 2001). The third putative member *OPT3* (also referred to as *YGL114w*) has only been identified through a low sequence homology, with no evidence of any encoded and expressed protein in yeast (Hauser et al., 2001; Wiles et al., 2006b). Regarding substrate specificity, there is still a lack of information related to the composition of the oligopeptides preferred by OPT transporters. However, it is known that OPT have a broad range of distinct substrates with peptide-length specificity (Osawa et al., 2006; Reuß and Morschhäuser, 2006).

Fungal Oligopeptide Transporters

Using a complementary DNA expression library from an environmental sample of soil eukaryotes, Damon et al. (2011) identified six putative genes for di- and tripeptide transporters that were not homologous to Ptr2. The predicted protein structure determined 11 transmembrane domains and a N-terminal cytosolic tail. These six sequences shared high sequence identity, with homologous sequences found in other fungal species. When phylogenetic analyses were performed, the six putative transporter genes grouped with 15 other fungal sequences that belonged to 10 species from the Ascomycota and Basidiomycota phyla. Although none of these 15 sequences had been previously characterized, many of them had already been annotated as putative amino acid transporters. Due to the specificity of this new group to the fungi kingdom, they proposed the denomination Fungal Oligopeptide Transporters (FOT). Additionally, experiments in *Xenopus* oocytes demonstrated that the proton symport was the driving force of FOT peptide transport (Damon et al., 2011).

The phylogenetic analysis performed by Damon et al. (2011) identified two members of the *FOT* gene family in *S. cerevisiae* wine strain EC1118. The tandem *FOT1-2* genes in EC1118 had been previously annotated as permeases for neutral amino acids by Novo et al. (2009), who sequenced the strain's genome. Marsit et al. (2015) reported that *FOT* genes were only present in *S. cerevisiae* wine strains as a result of a horizontal gene transfer (HGT) from the species *Torulaspora microellipsoides*. Sequence analysis enabled the identification of *FOT2* from EC1118 as an isoform of *FOT2_tomi* in *T. microellipsoides*, since they share the same sequence (**Table 2A**). Conversely, *FOT1* from EC1118 or *FOT3* from the wine strain K1 were the result of gene conversions between the two tandem genes *FOTX* and *FOT2_tomi* in *T. microellipsoides* (Marsit et al., 2015). In any

case, all the identified FOT members share a high sequence homology at gene and protein level (**Table 2B**), with *FOTY* from *T. microellipsoides* as the most divergent.

Currently, only few studies have been performed on FOT members in *S. cerevisiae*, with scarce information regarding those members in the non-*Saccharomyces* species. In 59A, a haploid derivative strain of EC1118, FOT transporters have shown a wide specificity for di- and tripeptides, particularly those containing glutamate (Damon et al., 2011; Marsit et al., 2015). The comparison of peptide consumption between strains with Fot1-2 and fot1-2 deleted mutants showed that the wild type could consume up to 118 dipeptides and 8 tripeptides, whereas the fot1-2 mutant could only consume 28 di-peptides and 4 tri-peptides (Damon et al., 2011). In addition, FOT-containing yeasts also consumed more glutathione (Marsit et al., 2015).

Some members of the FOT family may have evolved into different peptide substrate specificities, acquiring potentially specialized functions, however, this possibility still remains unexplored. Furthermore, FOT have only been characterized for di/tripeptide transport, whereas it is still not known whether they are also able to import tetra-, penta- or even deca-peptides.

Other Permeases With Peptide Transport Activity

Other permeases with another main function in yeast have also shown peptide transporter activity. Dal5 is an allantoate/ureidosuccinate permease that is able to import dipeptides into the cytoplasm in *S. cerevisiae*. As a member of the allantoate permease family (TC# 2.A.1.14), it belongs to the anion:cation symporter subfamily from the MFS, although it is not known whether Dal5 works in symport with protons or another cation (Nelissen et al., 1997; Hellborg et al., 2008). Even though its affinity for allantoate, ureidosuccinate and allantoin is higher than that for peptides, Dal5 constitutes the predominant dipeptide transporter in some *S. cerevisiae* strains, such as the wild-type strain W303 (Cai et al., 2007). Contrary to Ptr2, Dal5 preferably transports non-N-end rule dipeptides, i.e., peptides without basic (Arg, His, Lys) or bulky hydrophobic (Ile, Leu, Phe, Trp, or Tyr) amino acid residues at the N terminus, which highlights the complementary activities of the different di- and tripeptide transporters (Cai et al., 2007). It has also been suggested that the amino acid permease asparaginase II Asp3p can transport dipeptides with asparagine in the C-terminal by an as-yet-unidentified mechanism (Homann et al., 2005). Interestingly, the presence of the *ASP3* locus in *S. cerevisiae* seems to be due to a horizontal gene transfer phenomenon from the wine yeast *Wickerhamomyces anomalus* (League et al., 2012). However, *ASP3* locus is not homogeneous among *S. cerevisiae* strains; for example, a functional *ASP3* gene is absent from wine strain EC1118, vineyard isolate Y55 or different clinical isolates (Lashkari et al., 1997; Homann et al., 2005; Novo et al., 2009). Additionally, it has been reported that general amino acid permease Gap1 is responsible for the consumption of γ-glutamyl

TABLE 2 | Fungal Oligopeptide Transporters share a high sequence identity at gene and protein level.

(A)

	FOTY	*FOT2*	*FOT2_TOMI*	*FOT1*	*FOT3*	*FOTX*	Accession number
FOTY	100	90.07	90.07	90.17	90.48	90.11	TOMI0S02e18250g
FOT2	90.07	100	100	95.25	94.22	93.01	EC1118_1O4_6513p
FOT2_TOMI	90.07	100	100	95.25	94.22	93.01	TOMI0S04e13212g
FOT1	90.17	95.25	95.25	100	96.11	97.54	EC1118_1O4_6502g
FOT3	90.48	94.22	94.22	96.11	100	98.34	GCA_900099285
FOTX	90.11	93.01	93.01	97.54	98.34	100	TOMI0S04e13190g

(B)

	FotY	Fot2	Fot2_Tomi	Fot1	Fot3	FotX	
FotY	100	91.72	91.72	91.35	92.21	91.87	TOMI0S02e18250g1_1
Fot2	91.72	100	100	96.21	94.84	94.66	CAY86673.1
Fot2_Tomi	91.72	100	100	96.21	94.84	94.66	TOMI0S04e13212g1_1
Fot1	91.35	96.21	96.21	100	97.26	98.11	CAY86672.1
Fot3	92.21	94.84	94.84	97.26	100	98.8	GCA_900099285
FotX	91.87	94.66	94.66	98.11	98.8	100	TOMI0S04e13190g1_1

*Percentage identity matrices were built by multiple-alignments with the six FOT genes **(A)** and protein sequences **(B)** from S. cerevisiae (in green) and T. microellipsoides (in purple) using Clustal Omega (Sievers et al., 2011). The guide trees to the right show the distance between the sequences based on the pairwise scores. FOT1 and FOT2 protein and gene accession numbers correspond to the NCBI database; FOTX, FOTY and FOT2_TOMI accession numbers correspond to the Genome Resources for Yeast Chromosomes (GRYC) database; FOT3 sequence can be found in the genome assembly for S. cerevisiae strain K1-28-2B deposited at the European Nucleotide Archive (ENA).*

dipeptides when they were the sole nitrogen sources in the medium, with no apparent implication of Ptr2, Dal5 or Opt1-2 (Rubio-Texeira et al., 2012).

REGULATION OF OLIGOPEPTIDE TRANSPORT

Peptide transport in yeast cells greatly depends on the transport system and environmental factors, specially the presence of other nitrogen sources such as ammonium or amino acids (**Figure 1**). Nitrogen sources regulate peptide transport both at transcriptional level and by modulating the activity and degradation of enzymes and transporters. Ammonium and amino acids such as glutamate, glutamine or arginine are considered as rich nitrogen sources because they support a fast cell growth. However, the consideration as preferred nitrogen source also derives from the capacity of not de-repressing the uptake of alternative nitrogen sources held by the nitrogen catabolite repression (NCR) pathways (Cooper, 1982, 2002; Cooper and Sumrada, 1983; Basrai et al., 1992; Magasanik and Kaiser, 2002; Boer et al., 2007; Crépin et al., 2012). In *S. cerevisiae*, this repression by NCR affects *PTR2*, *DAL5*, and *OPT1-2*. In conditions of nitrogen starvation or presence of poor nitrogen sources such as allantoin or proline, the expression of *PTR2*, *OPT1-2*, and even *ASP3* is triggered (Bon et al., 1997; Lubkowitz et al., 1998; Magasanik and Kaiser, 2002). Although permease Dal5 is expressed constitutively for allantoate transport, it is also affected by NCR in the same way as Ptr2 and OPT transporters (Rai et al., 1987). For Ptr2, even micromolar concentrations of the non-preferred amino acids overcome NCR-mediated repression by ammonium, acting as inducers of peptide assimilation (Island et al., 1987; Perry et al., 1994). Expression of *OPT1* is also de-repressed by most non-preferred amino acids, particularly by leucine and tryptophan, however, *OPT1* is specifically induced in sulfur starvation conditions (Basrai et al., 1992; Wiles et al., 2006a). Therefore, methionine and cysteine do not belong to the group of amino acids inducers of *OPT1*. On the other hand, the expression of *OPT2* seems not to be affected by amino acid concentrations in the same way as *OPT1* or *PTR2* (Wiles et al., 2006a).

Another regulatory element of peptide transport is the amino acid sensor complex Ssy1p-Ptr3p-Ssy5p (SPS). Due to its sensor activity, SPS regulates the expression of several amino acid permeases depending on the presence of the corresponding substrate in the medium (Forsberg and Ljungdahl, 2001). In the same way, SPS is involved in the amino acid-driven regulation of Ptr2 and Opt1 expression and it has been demonstrated that the presence of *SSY1* and *PTR3* is required for the induction of both *PTR2* and *OPT1* (Didion et al., 1998; Wiles et al., 2006a).

Additionally, the import of dipeptides with basic and bulky amino acids in the N-terminal position (N-end rule dipeptides) upregulates the *PTR2* expression. This group of dipeptides bind to Ubr1p and activate the degradation of Cup9p, a transcriptional repressor of *PTR2* (Byrd et al., 1998; Turner et al., 2000; Hauser et al., 2001; Du et al., 2002). This *PTR2* upregulation mechanism initiates a positive feedback loop for the preferential uptake of N-end rule peptides by Ptr2 (Homann et al., 2005). Cup9p also represses the expression of *OPT2*, although it is unknown whether the N-end rule dipeptides have the same inducing effect as for *PTR2*. On the other hand, *OPT1* seems not to be affected by Cup9p. Contrary to the effect on *PTR2* or *OPT2*, Cup9p upregulates the expression of *DAL5* (Wiles et al., 2006a; Cai et al., 2007).

Fungal Oligopeptide Transporters expression has not been thoroughly studied yet. However, it has been shown that wine strains containing Fot1 and Fot2 initially consume small peptides from grape must before using some amino acids, such as histidine, alanine or glutamine, indicating that oligopeptides are a preferred source of nitrogen during the early stages of fermentation. This suggests that *FOT* genes may be expressed in *S. cerevisiae* wine strains from the beginning of fermentation (Marsit et al., 2016). However, analyzing the expression of *FOT* genes with different nitrogen supply in the medium would be helpful to better define the physiological role of these transporters throughout wine fermentation.

The divergent but complementary regulation in the expression of the peptide transport systems allows yeast to adapt to various environmental conditions and nutrient availabilities. However, Homann et al. (2005) suggested that oligopeptide transport seems to be subject to conflicting evolutionary pressures. The peptide transport machinery not only transports peptides serving as nutrients, but also antimicrobial peptides, which makes them a source of vulnerability for the cell. This assumption is based on the reported import of nikkomycin by di- and tripeptide transporters in pathogenic *C. albicans*, which initiated the development of peptide-analog antifungal drugs (McCarthy et al., 1985; St Georgiev, 2000). This idea is therefore only formulated from a clinical context perspective; theorizing about oligopeptide transporters as a source of vulnerability for yeasts would require further investigation of the hypothetic impact of antifungal peptides import by POT, OPT, FOT or the other permeases on yeast adaptation to natural, fermentative environments.

ROLE OF OLIGOPEPTIDE CONSUMPTION IN THE ADAPTATION OF *S. CEREVISIAE* TO THE WINE ENVIRONMENT

Wine fermentation conditions constitute a harsh and stressful environment, exerting a great selective pressure on yeasts present in grape must. Actually, there are several sources of stress in grape must: the osmotic pressure caused by the high concentrations of sugar, high acidity, presence of sulfites or oxidative stress. Other sources of stress emerge as a consequence of the progress of fermentation, such as nutrient depletion and ethanol production. Indeed, nitrogen content is a limiting factor for yeast growth: after the latency phase, yeasts grow exponentially until reaching a maximum population and fermentation rate, consuming most nitrogen sources; at the stationary phase, undergoing nutrient starvation, yeasts stop growing and consume sugars through fermentation, which progressively increases ethanol

level, another stress factor. Therefore, in addition to its nutrient-linked properties, nitrogen sources and availability can also qualitatively affect various outcomes of alcoholic fermentation (Agenbach, 1977; Cramer et al., 2002).

Saccharomyces cerevisiae is the yeast species best adapted to the winemaking environment, maintaining over 90% viability during the stationary phase until complete sugar supply depletion (Marsit and Dequin, 2015). Different molecular mechanisms have been shown to contribute to yeast adaptation to wine environments. Among them are gene copy number variations, chromosomal rearrangements, hybridization, introgression or horizontal gene transfer (Bidenne et al., 1992; Goto-Yamamoto et al., 1998; Rachidi et al., 1999; Pérez-Ortín et al., 2002; Dunn et al., 2005, 2012; Belloch et al., 2009; Novo et al., 2009; Stambuk et al., 2009; Esberg et al., 2011; Libkind et al., 2011; League et al., 2012; Morales and Dujon, 2012; Zimmer et al., 2014; Marsit et al., 2015, 2017; Legras et al., 2018).

Novo et al. (2009) sequenced the genome of *S. cerevisiae* wine strain EC1118 to investigate the molecular mechanisms that participate in the adaptation of wine yeasts to their environment. Sequence comparisons with other *S. cerevisiae* genomes revealed three genomic regions, A, B, and C, that had been acquired by HGT. Regions B and C had been shown to originate from two distantly related yeast species also found in wine, *Zygosaccharomyces bailii* and *T. microellipsoides*, respectively (Novo et al., 2009; Marsit et al., 2015). The three regions contained 39 putative genes coding for proteins involved in carbon and nitrogen metabolism, with *FOT* genes in region C among them. Region C was widespread among *S. cerevisiae* wine strains, albeit showing different rearrangements and/or gene losses. However, the two tandem genes *FOT1-2* encoding peptide transporters were strongly conserved in all the wine strains carrying region C. Some of the strains only conserved one copy of these genes, evolving into a new isoform of the *FOT* family with a high degree of homology, *FOT3* (**Tables 2A,B**). This result supported the idea that FOT transporters could confer an adaptive advantage within the wine environment (Marsit et al., 2015). To demonstrate this hypothesis, Marsit et al. (2015) evaluated wine strain 59A containing *FOT1-2* and the corresponding fot1-2-deleted mutant in fermentation experiments. Natural grape must was used because of its diverse sources of nitrogen that include oligopeptides, enabling the assessment of the strains into the complex matrix usually colonized by wine strains. Although the wild-type strain 59A showed lower fermentation and growth rates during the first hours of fermentation, mutants for fot1-2 eventually had a

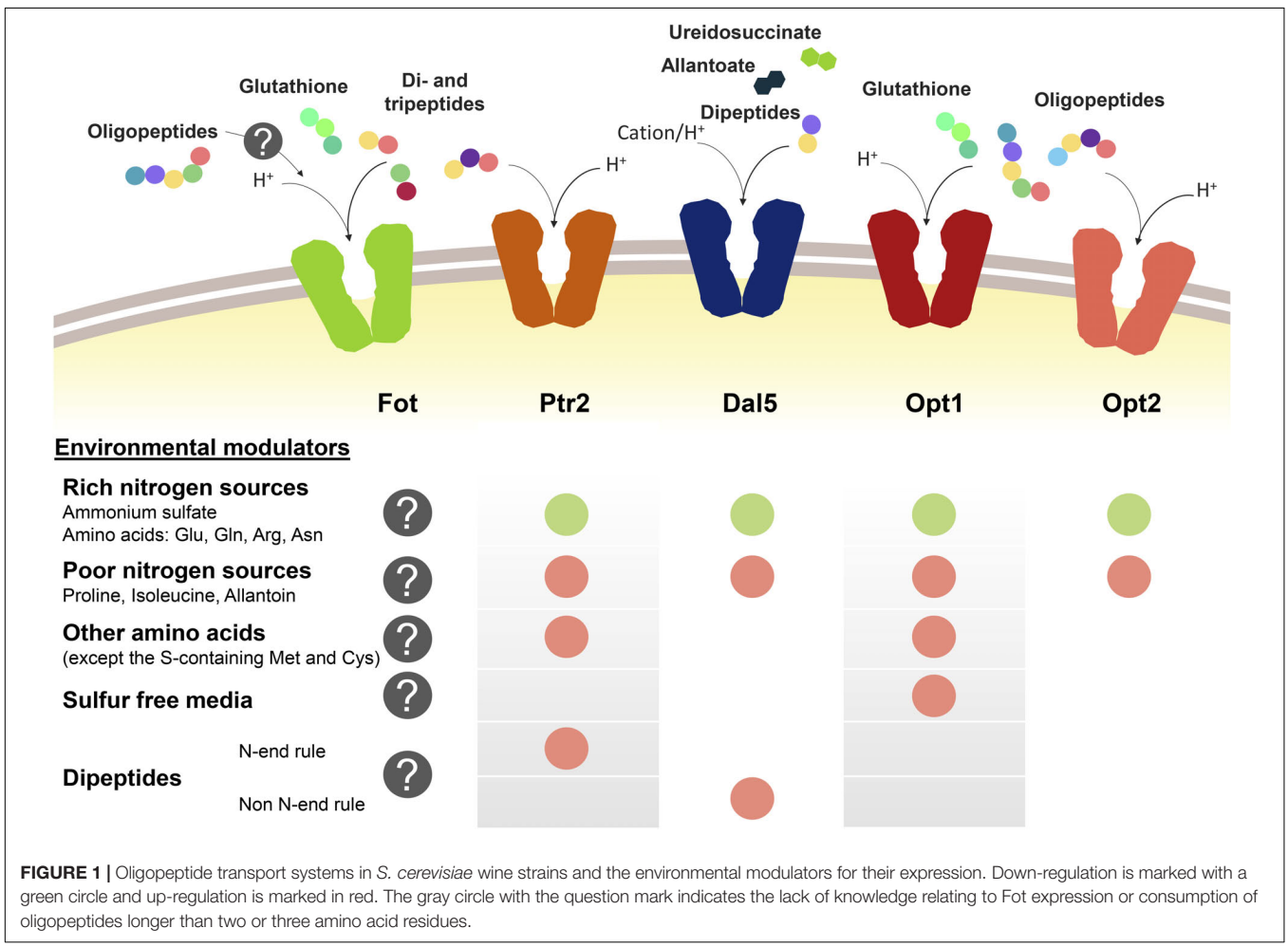

FIGURE 1 | Oligopeptide transport systems in *S. cerevisiae* wine strains and the environmental modulators for their expression. Down-regulation is marked with a green circle and up-regulation is marked in red. The gray circle with the question mark indicates the lack of knowledge relating to Fot expression or consumption of oligopeptides longer than two or three amino acid residues.

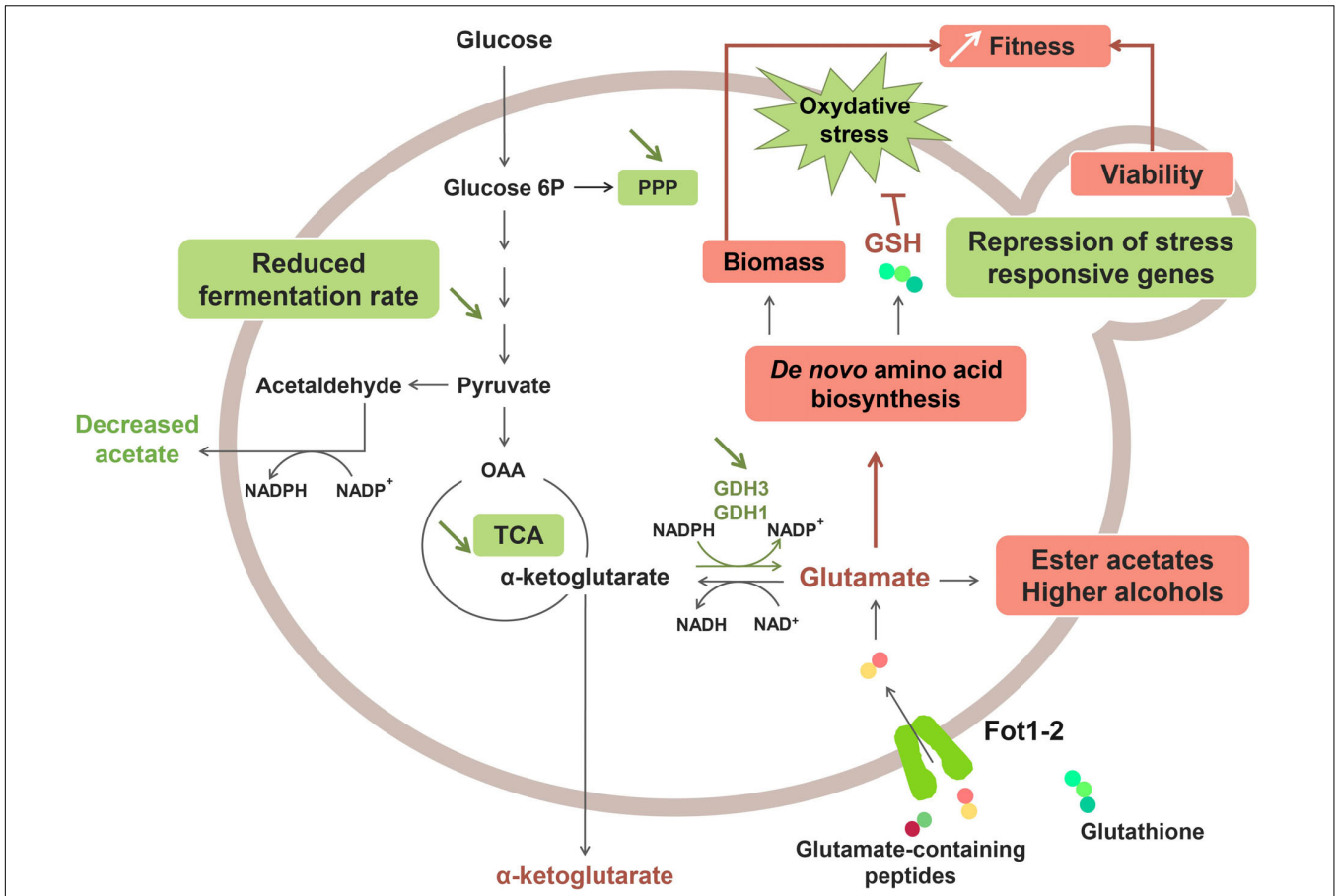

FIGURE 2 | Effect of Fot1-2-mediated peptide uptake on the metabolism of 59A in oenological conditions. Molecules with higher production and upregulated pathways are marked in red, whereas downregulation and lower production are marked in green.

12% lower biomass and a higher mortality rate than 59A, leading to residual fructose at the end of fermentation, an indicator of incomplete fermentation (Marsit et al., 2015). Since Fot1 and Fot2 are responsible for a wider range of oligopeptide transport (Damon et al., 2011), the assumption was that the greater consumption of oligopeptides by FOT not only increased biomass but also improved cell viability and fermentation performance in *S. cerevisiae*. Additionally, competition experiments between the wild-type and fot1-2 mutants on natural grape must revealed the competitive advantage of the wild-type over the mutant, demonstrating the beneficial role of Fot1-2 transporters in the adaptation of *S. cerevisiae* to the wine environment (Marsit et al., 2015).

A recent study revealed that the greater consumption of glutathione and glutamate-rich peptides by Fot1-2 entailed a remodeling of the central carbon and nitrogen metabolism pathways (Marsit et al., 2016; **Figure 2**). Transcriptomic analyses showed that several genes involved in glutamate production (*GDH1* and *GDH3*), glycolysis, the tricarboxylic acid (TCA) cycle and the pentose-phosphate pathway (PPP) were downregulated in strain 59A (Marsit et al., 2016). The assumption is that the reverse conversion of α-ketoglutarate into glutamate is repressed due to high cell concentrations in glutamate originating from the consumption of glutamate/glutamine-rich oligopeptides. Consequently, α-ketoglutarate levels increase, leading to the repression of the upstream catabolic pathways, that is, TCA and glycolysis. Likewise, the downregulation of genes involved in the glycolytic pathway would explain the lower fermentation rate that was previously observed for 59A in comparison with the fot1-2 deleted strain. Furthermore, the $NADP^+$/NADPH balance of the cell was also affected by the repression of α-ketoglutarate conversion into glutamate, resulting in a lower consumption of NADPH. NADPH accumulation agrees with the lower levels of acetate observed for 59A, since acetate production is an important source of NADPH. Additionally, the higher availability of glutamate derived from peptides acts as a nitrogen signal in the cell, inducing genes involved in the *de novo* biosynthesis of amino acids and glutathione. Higher concentrations of glutathione and NADPH have a positive impact on the protection against oxidative stress, which correlates with the repression observed for genes involved in the oxidative stress response (Marsit et al., 2016). Therefore, the assumption is that FOT contribute to the better response of 59A against oxidative stress, which is in accordance with its better survival at the

end of fermentation when compared with fot1-2 deleted strains (Marsit et al., 2015). Furthermore, an accumulation of α-keto acids as a result of higher nitrogen availability was observed, leading to the increased production of ester acetates and fusel alcohols (Hazelwood et al., 2008; Rollero et al., 2015; Marsit et al., 2016) that are volatile molecules responsible for fruity and floral aromas in wine. Although high concentrations of fusel alcohols can have a detrimental effect on wine aroma, the increased levels of these molecules in wines fermented with 59A remained below 300 mg/L; at this concentration, it has been reported that fusel alcohols add a desirable level of complexity to wine aroma (Rapp and Versini, 1991; reviewed by Swiegers et al., 2005). These results, along with the decrease in acetate production, imply an improvement on the aroma profile of wines that is developed during fermentation. Consequently, a greater consumption of oligopeptides from grape must led by FOT constitutes a desirable oenological trait in yeasts. While that improvement of fermentation kinetics associated to biomass formation and cell survival is probably the main selection pressure permitting wine yeast strains adaptation, these potentially beneficial organoleptic properties, together with the reported positive impact on fermentation efficiency and cell viability, suggest a possible influence of domestication in Fot acquisition by *S. cerevisiae* wine strains. Humans, in their eagerness to obtain aromatically attractive wines and enhance the fermentation process, may have indirectly chosen those yeast inocula with strains containing Fot, i.e., strains able to consume more peptides from grape musts.

Currently FOT are the only oligopeptide transporters whose impact in the winemaking context has been evaluated. In other ecological niches, such as nectar, a recent study on the role of nitrogen as a competitive resource has shown that nitrogen scavenging genes, including oligopeptide transporters, drive priority effects on the microbial communities (Dhami et al., 2016). For *C. albicans*, PTR and OPT transporters have been shown to play a crucial role in nutrient acquisition, contributing to the success of the species as a commensal or pathogenic organism in mammalian hosts (Dunkel et al., 2013). In addition to the strong evidences provided for FOT supporting the crucial role of oligopeptide consumption, these results open new prospects for studying in more depth the other families of peptide transporters during wine fermentation.

CONCLUSION AND PROSPECTS

Oligopeptides present in natural ecosystems constitute a non-negligible nitrogen source for yeasts. Despite the substantial advances recently made on the important role of oligopeptides during winemaking, many pending questions remain to be thoroughly investigated. First, it would be necessary to improve the existing methodologies dedicated to the quantification and qualitative analysis of peptide fractions within foods and beverages. Despite some previous work on this issue (Yokotsuka et al., 1975; Dale and Young, 1989; Monteiro et al., 2001; Moreno-Arribas et al., 2002; De Person et al., 2004; Takahashi et al., 2012), there is currently no standardized, thorough yet less laborious protocols that could be adapted to any sample with complex protein fractions. With a better knowledge of oligopeptide composition in grape musts, it would be easier to mimic oligopeptide matrices in the synthetic media normally used in a laboratory, allowing the development of new research subjects. For example, the influence of nitrogen availability on gene expression has been thoroughly studied in winemaking conditions, although none of these studies ever considered oligopeptides as potential modulators of gene expression (reviewed by Gobert et al., 2019). Oligopeptides have also been omitted from other studies concerning the ability of *S. cerevisiae* and non-*Saccharomyces* species to consume different nitrogen sources during winemaking fermentation (Crépin et al., 2012; Cubillos et al., 2017; Gobert et al., 2017; Seguinot et al., 2018; Su et al., 2020), or the effect of different nitrogen conditions in the adaptation of *S. cerevisiae* to wine environment (Ibstedt et al., 2015; Brice et al., 2018). This lack of information, contrasted with previous results on the adaptive advantage conferred by a greater consumption of oligopeptides due to FOT (Marsit et al., 2015, 2016), suggest a very promising field of study. Furthermore, analysis of peptide matrices would contribute to the characterization of oligopeptide transporters' substrate specificities. A better characterization of transporters' oligopeptide preferences in yeast definitely is a matter of interest not only for fermentation technologies, but also in distinct fields such as nutrition or drug design (Nielsen and Brodin, 2003; Ito et al., 2013). Finally, studying FOT expression is still required to refine the description of the peptide transport regulation already provided by the analysis of Ptr2, Opt1, Opt2, and Dal5. Understanding the physiological role of the novel FOT family in wine-related yeasts would help elucidate peptide catabolism and its interactions with other metabolic pathways, unraveling potential new functions of peptides within yeast life cycle and its relation to wine environment.

AUTHOR CONTRIBUTIONS

CB-R and VG drafted the manuscript. CB-R wrote the manuscript. All authors created the tables and figures, read and approved the final manuscript. SM and VG provided the writing guidance and revised the manuscript.

FUNDING

This project has received funding from the European Union's Horizon 2020 Research and Innovation Program under the Marie Skłodowska-Curie Grant Agreement No. 764927. SM was supported by the Fonds de recherche du Québec – Santé (FRQS) (#270686) post-doctoral fellowship.

ACKNOWLEDGMENTS

We thank Jean-Luc Legras for his helpful remarks on the manuscript.

REFERENCES

Agenbach, W. A. (1977). "A study of must nitrogen content in relation to incomplete fermentations, yeast production and fermentation activity," in *Proceedings South African Society of Enology and Viticulture* (Cape Town: Stellenbosh, S. A), 66–87.

Albergaria, H., Francisco, D., Gori, K., Arneborg, N., and Gírio, F. (2010). *Saccharomyces cerevisiae* CCMI 885 secretes peptides that inhibit the growth of some non-*Saccharomyces* wine-related strains. *Appl. Microbiol. Biotechnol.* 86, 965–972. doi: 10.1007/s00253-009-2409-6

Alexandre, H., and Charpentier, C. (1998). Biochemical aspects of stuck and sluggish fermentation in grape must. *J. Ind. Microbiol. Biotechnol.* 20, 20–27. doi: 10.1038/sj.jim.2900442

Aouida, M., Khodami-Pour, A., and Ramotar, D. (2009). Novel role for the *Saccharomyces cerevisiae* oligopeptide transporter Opt2 in drug detoxification. *Biochem. Cell Biol.* 87, 653–661. doi: 10.1139/O09-045

Baral, B. (2017). Evolutionary trajectories of entomopathogenic fungi ABC transporters. *Adv. Genet.* 98, 117–154. doi: 10.1016/bs.adgen.2017.07.002

Barnes, D., Lai, W., Breslav, M., Naider, F., and Becker, J. M. (1998). PTR3, a novel gene mediating amino acid-inducible regulation of peptide transport in Saccharomyces cerevisiae. *Mol. Microbiol.* 29, 297–310. doi: 10.1046/j.1365-2958.1998.00931.x

Basrai, M. A., Zhang, H. L., Miller, D., Naider, F., and Becker, J. M. (1992). Toxicity of oxalysine and oxalysine-containing peptides against Candida albicans: regulation of peptide transport by amino acids. *J. Gen. Microbiol.* 138, 2353–2362. doi: 10.1099/00221287-138-11-2353

Becker, J. M., and Naider, F. (1980). "Transport and utilization of peptides by yeast," in *Microorganisms and Nitrogen Sources*, ed. J. W. Payne (New York: John Wiley & Sons, Inc), 257–279.

Bell, S. J., and Henschke, P. A. (2005). Implications of nitrogen nutrition for grapes, fermentation and wine. *Aust. J. Grape Wine Res.* 11, 242–295. doi: 10.1111/j.1755-0238.2005.tb00028.x

Belloch, C., Pérez-Torrado, R., González, S. S., Pérez-Ortín, J. E., García-Martínez, J., Querol, A., et al. (2009). Chimeric genomes of natural hybrids of *Saccharomyces cerevisiae* and *Saccharomyces kudriavzevii*. *Appl. Environ. Microbiol.* 75, 2534–2544. doi: 10.1128/AEM.02282-08

Bidenne, C., Blondin, B., Dequin, S., and Vezinhet, F. (1992). Analysis of the chromosomal DNA polymorphism of wine strains of Saccharomyces cerevisiae. *Curr. Genet.* 22, 1–7. doi: 10.1007/BF00351734

Bisson, L. F. (1999). Stuck and sluggish fermentations. *Am. J. Enol. Vitic.* 50, 107–119. doi: 10.1046/j.1365-2672.1998.00380.x

Blateyron, L., and Sablayrolles, J. M. (2001). Stuck and slow fermentations in enology: statistical study of causes and effectiveness of combined additions of oxygen and diammonium phosphate. *J. Biosci. Bioeng.* 91, 184–189. doi: 10.1263/jbb.91.184

Boer, V. M., Tai, S. L., Vuralhan, Z., Arifin, Y., Walsh, M. C., Piper, M. D. W., et al. (2007). Transcriptional responses of Saccharomyces cerevisiae to preferred and nonpreferred nitrogen sources in glucose-limited chemostat cultures. *FEMS Yeast Res.* 7, 604–620. doi: 10.1111/j.1567-1364.2007.00220.x

Bon, E. P. S., Carvajal, E. M., Stanbrough, M., Rowen, D., and Magasanik, B. (1997). Asparaginase II of *Saccharomyces cerevisiae: GLN3/URE2* regulation of a periplasmic enzyme. *Appl. Biochem. Biotechnol.* 63–65, 203–212. doi: 10.1007/BF02920425

Bourbouloux, A., Shahi, P., Chakladar, A., Delrot, S., and Bachhawat, A. K. (2000). Hgt1p, a high affinity glutathione transporter from the yeast *Saccharomyces cerevisiae*. *J. Biol. Chem.* 275, 13259–13265. doi: 10.1074/jbc.275.18.13259

Branco, P., Francisco, D., Monteiro, M., Almeida, M. G., Caldeira, J., Arneborg, N., et al. (2017). Antimicrobial properties and death-inducing mechanisms of saccharomycin, a biocide secreted by *Saccharomyces cerevisiae*. *Appl. Microbiol. Biotechnol.* 101, 159–171. doi: 10.1007/s00253-016-7755-6

Brice, C., Cubillos, F. A., Dequin, S., Camarasa, C., and Martínez, C. (2018). Adaptability of the Saccharomyces cerevisiae yeasts to wine fermentation conditions relies on their strong ability to consume nitrogen. *PLoS One* 13:e0192383. doi: 10.1371/journal.pone.0192383

Byrd, C., Turner, G. C., and Varshavsky, A. (1998). The N-end rule pathway controls the import of peptides through degradation of a transcriptional repressor. *EMBO J.* 17, 269–277. doi: 10.1093/emboj/17.1.269

Cai, H., Hauser, M., Naider, F., and Becker, J. M. (2007). Differential regulation and substrate preferences in two peptide transporters of *Saccharomyces cerevisiae*. *Eukaryot. Cell* 6, 1805–1813. doi: 10.1128/EC.00257-06

Clapperton, J. F. (1971). Simple peptides of wort and beer. *J. Inst. Brew.* 77, 177–180. doi: 10.1002/j.2050-0416.1971.tb03371.x

Cooper, T. G. (1982). "Nitrogen metabolism in *Saccharomyces cerevisiae*," in *The Molecular Biology of the Yeast Saccharomyces*, eds J. N. Strathern, E. W. Jones, and J. R. Broach (Cold Spring Harbor: NY: Cold Spring Harbor Monograph Archive), 39–99. doi: 10.1101/0.39-99

Cooper, T. G. (2002). Transmitting the signal of excess nitrogen in *Saccharomyces cerevisiae* from the Tor proteins to the GATA factors: connecting the dots. *FEMS Microbiol. Rev.* 26, 223–238. doi: 10.1111/j.1574-6976.2002.tb00612.x

Cooper, T. G., and Sumrada, R. A. (1983). What is the function of nitrogen catabolite repression in *Saccharomyces cerevisiae*? *J. Bacteriol.* 155, 623–627. doi: 10.1128/jb.155.2.623-627.1983

Cramer, A. C., Vlassides, S., and Block, D. E. (2002). Kinetic model for nitrogen-limited wine fermentations. *Biotechnol. Bioeng.* 77, 49–60. doi: 10.1002/bit.10133

Crépin, L., Nidelet, T., Sanchez, I., Dequin, S., and Camarasa, C. (2012). Sequential use of nitrogen compounds by saccharomyces cerevisiae during wine fermentation: a model based on kinetic and regulation characteristics of nitrogen permeases. *Appl. Environ. Microbiol.* 78, 8102–8111. doi: 10.1128/AEM.02294-12

Cubillos, F. A., Brice, C., Molinet, J., Tisné, S., Abarca, V., Tapia, S. M., et al. (2017). Identification of nitrogen consumption genetic variants in yeast through QTL mapping and bulk segregant RNA-Seq analyses. *G3* 7, 1693–1705. doi: 10.1534/g3.117.042127

Dale, C. J., and Young, T. W. (1989). Fractionation of small peptides from beer. *J. Inst. Brew.* 95, 35–41. doi: 10.1002/j.2050-0416.1989.tb04608.x

Damon, C., Vallon, L., Zimmermann, S., Haider, M. Z., Galeote, V., Dequin, S., et al. (2011). A novel fungal family of oligopeptide transporters identified by functional metatranscriptomics of soil eukaryotes. *ISME J.* 5, 1871–1880. doi: 10.1038/ismej.2011.67

De Person, M., Sevestre, A., Chaimbault, P., Perrot, L., Duchiron, F., and Elfakir, C. (2004). Characterization of low-molecular weight peptides in champagne wine by liquid chromatography/tandem mass spectrometry. *Anal. Chim. Acta* 520, 149–158. doi: 10.1016/j.aca.2004.03.094

Dhami, M. K., Hartwig, T., and Fukami, T. (2016). Genetic basis of priority effects: insights from nectar yeast. *Proc. R. Soc. B Biol. Sci.* 283:20161455. doi: 10.1098/rspb.2016.1455

Didion, T., Regenberg, B., Jørgensen, M. U., Kielland-Brandt, M. C., and Andersen, H. A. (1998). The permease homologue Ssy1p controls the expression of amino acid and peptide transporter genes in *Saccharomyces cerevisiae*. *Mol. Microbiol.* 27, 643–650. doi: 10.1046/j.1365-2958.1998.00714.x

D'Souza, R. N., Grimbs, A., Grimbs, S., Behrends, B., Corno, M., Ullrich, M. S., et al. (2018). Degradation of cocoa proteins into oligopeptides during spontaneous fermentation of cocoa beans. *Food Res. Int.* 109, 506–516. doi: 10.1016/j.foodres.2018.04.068

Du, F., Navarro-Garcia, F., Xia, Z., Tasaki, T., and Varshavsky, A. (2002). Pairs of dipeptides synergistically activate the binding of substrate by ubiquitin ligase through dissociation of its autoinhibitory domain. *Proc. Natl. Acad. Sci. U.S.A.* 99, 14110–14115. doi: 10.1073/pnas.172527399

Dunkel, N., Hertlein, T., Franz, R., Reuß, O., Sasse, C., Schäfer, T., et al. (2013). Roles of different peptide transporters in nutrient acquisition in Candida albicans. *Eukaryot. Cell* 12, 520–528. doi: 10.1128/EC.00008-13

Dunn, B., Levine, R. P., and Sherlock, G. (2005). Microarray karyotyping of commercial wine yeast strains reveals shared, as well as unique, genomic signatures. *BMC Genomics* 6:53. doi: 10.1186/1471-2164-6-53

Dunn, B., Richter, C., Kvitek, D. J., Pugh, T., and Sherlock, G. (2012). Analysis of the *Saccharomyces cerevisiae* pan-genome reveals a pool of copy number variants distributed in diverse yeast strains from differing industrial environments. *Genome Res.* 22, 908–924. doi: 10.1101/gr.130310.111

Esberg, A., Muller, L. A. H., and McCusker, J. H. (2011). Genomic structure of and genome-wide recombination in the *Saccharomyces cerevisiae* S288C progenitor isolate EM93. *PLoS One* 6:e25211. doi: 10.1371/journal.pone.0025211

Farrell, M., Hill, P. W., Farrar, J., Bardgett, R. D., and Jones, D. L. (2011). Seasonal variation in soluble soil carbon and nitrogen across a grassland productivity gradient. *Soil Biol. Biochem.* 43, 835–844. doi: 10.1016/j.soilbio.2010.12.022

Forsberg, H., and Ljungdahl, P. O. (2001). Genetic and biochemical analysis of the yeast plasma membrane Ssy1p-Ptr3p-Ssy5p sensor of extracellular amino acids. *Mol. Cell. Biol.* 21, 814–826. doi: 10.1128/mcb.21.3.814-826.2001

Ganapathy, V., and Leibach, F. H. (1991). Proton-coupled solute transport in the animal cell plasma membrane. *Curr. Opin. Cell Biol.* 3, 695–701. doi: 10.1016/0955-0674(91)90043-X

Gobert, A., Tourdot-Maréchal, R., Morge, C., Sparrow, C., Liu, Y., Quintanilla-Casas, B., et al. (2017). Non-*Saccharomyces* yeasts nitrogen source preferences: impact on sequential fermentation and wine volatile compounds profile. *Front. Microbiol.* 8:2175. doi: 10.3389/fmicb.2017.02175

Gobert, A., Tourdot-Maréchal, R., Sparrow, C., Morge, C., and Alexandre, H. (2019). Influence of nitrogen status in wine alcoholic fermentation. *Food Microbiol.* 83, 71–85. doi: 10.1016/j.fm.2019.04.008

Gomolplitinant, K. M., and Saier, M. H. (2011). Evolution of the Oligopeptide Transporter Family. *J. Membr. Biol.* 240, 89–110. doi: 10.1007/s00232-011-9347-9

Goto-Yamamoto, N., Kitano, K., Shiki, K., Yoshida, Y., Suzuki, T., Iwata, T., et al. (1998). SSU1-R, a sulfite resistance gene of wine yeast, is an allele of SSU1 with a different upstream sequence. *J. Ferment. Bioeng.* 86, 427–433. doi: 10.1016/S0922-338X(98)80146-3

Hauser, M., Donhardt, A. M., Barnes, D., Naider, F., and Becker, J. M. (2000). Enkephalins are transported by a novel eukaryotic peptide uptake system. *J. Biol. Chem.* 275, 3037–3041. doi: 10.1074/jbc.275.5.3037

Hauser, M., Narita, V., Donhardt, A. M., Naider, F., and Becker, J. M. (2001). Multiplicity and regulation of genes encoding peptide transporters in *Saccharomyces cerevisiae*. *Mol. Membr. Biol.* 18, 105–112. doi: 10.1080/09687680010029374

Hazelwood, L. A., Daran, J. M., Van Maris, A. J. A., Pronk, J. T., and Dickinson, J. R. (2008). The Ehrlich pathway for fusel alcohol production: a century of research on *Saccharomyces cerevisiae* metabolism. *Appl. Environ. Microbiol.* 74, 2259–2266. doi: 10.1128/AEM.02625-07

Hellborg, L., Woolfit, M., Arthursson-Hellborg, M., and Piškur, J. (2008). Complex evolution of the DAL5 transporter family. *BMC Genomics* 9:164. doi: 10.1186/1471-2164-9-164

Henschke, P. A., and Jiranek, V. (1993). "Yeasts-metabolism of nitrogen compounds," in *Wine Microbiology and Biotechnology*, ed. G. H. Fleet (Reading: Harwood Academic Publishers), 77–164.

Higgins, C. F., and Gibson, M. M. (1986). Peptide transport in bacteria. *Methods Enzymol.* 125, 365–377. doi: 10.1016/S0076-6879(86)25031-4

Hiles, I. D., Gallagher, M. P., Jamieson, D. J., and Higgins, C. F. (1987). Molecular characterization of the oligopeptide permease of *Salmonella* typhimurium. *J. Mol. Biol.* 195, 125–142. doi: 10.1016/0022-2836(87)90332-9

Homann, O. R., Cai, H., Becker, J. M., and Lindquist, S. L. (2005). Harnessing natural diversity to probe metabolic pathways. *PLoS Genet.* 1:e80. doi: 10.1371/journal.pgen.0010080

Ibstedt, S., Stenberg, S., Bagés, S., Gjuvsland, A. B., Salinas, F., Kourtchenko, O., et al. (2015). Concerted evolution of life stage performances signals recent selection on yeast nitrogen use. *Mol. Biol. Evol.* 32, 153–161. doi: 10.1093/molbev/msu285

Ingledew, W. M., and Patterson, C. A. (1999). Effect of nitrogen source and concentration on the uptake of peptides by a lager yeast in continuous culture. *J. Am. Soc. Brew. Chem.* 57, 9–17. doi: 10.1094/asbcj-57-0009

Island, M. D., Naider, F., and Becker, J. M. (1987). Regulation of dipeptide transport in *Saccharomyces cerevisiae* by micromolar amino acid concentrations. *J. Bacteriol.* 169, 2132–2136. doi: 10.1128/jb.169.5.2132-2136.1987

Ito, K., Hikida, A., Kawai, S., Lan, V. T. T., Motoyama, T., Kitagawa, S., et al. (2013). Analysing the substrate multispecificity of a proton-coupled oligopeptide transporter using a dipeptide library. *Nat. Commun.* 4, 1–10. doi: 10.1038/ncomms3502

Jungwirth, H., and Kuchler, K. (2006). Yeast ABC transporters – a tale of sex, stress, drugs and aging. *FEBS Lett.* 580, 1131–1138. doi: 10.1016/j.febslet.2005.12.050

Kevvai, K., Kütt, M. L., Nisamedtinov, I., and Paalme, T. (2016). Simultaneous utilization of ammonia, free amino acids and peptides during fermentative growth of *Saccharomyces cerevisiae*. *J. Inst. Brew.* 122, 110–115. doi: 10.1002/jib.298

Kitagawa, S., Mukai, N., Furukawa, Y., Adachi, K., Mizuno, A., and Iefuji, H. (2008). Effect of soy peptide on brewing beer. *J. Biosci. Bioeng.* 105, 360–366. doi: 10.1263/jbb.105.360

Lashkari, D. A., Derisi, J. L., Mccusker, J. H., Namath, A. F., Gentile, C., Hwang, S. Y., et al. (1997). Yeast microarrays for genome wide parallel genetic and gene expression analysis. *Proc. Natl. Acad. Sci. U.S.A.* 94, 13057–13062. doi: 10.1073/pnas.94.24.13057

League, G. P., Slot, J. C., and Rokas, A. (2012). The ASP3 locus in *Saccharomyces cerevisiae* originated by horizontal gene transfer from Wickerhamomyces. *FEMS Yeast Res.* 12, 859–863. doi: 10.1111/j.1567-1364.2012.00828.x

Legras, J.-L., Galeote, V., Bigey, F., Camarasa, C., Marsit, S., Nidelet, T., et al. (2018). Adaptation of *S. cerevisiae* to fermented food environments reveals remarkable genome plasticity and the footprints of domestication. *Mol. Biol. Evol.* 35, 1712–1727. doi: 10.1093/molbev/msy066

Lekkas, C., Hill, A. E., Taidi, B., Hodgson, J., and Stewart, G. G. (2009). The role of small wort peptides in brewing fermentations. *J. Inst. Brew.* 115, 134–139. doi: 10.1002/j.2050-0416.2009.tb00358.x

Léran, S., Varala, K., Boyer, J. C., Chiurazzi, M., Crawford, N., Daniel-Vedele, F., et al. (2014). A unified nomenclature of nitrate transporter 1/peptide transporter family members in plants. *Trends Plant Sci.* 19, 5–9. doi: 10.1016/j.tplants.2013.08.008

Libkind, D., Hittinger, C. T., Valeˆrio, E., Gonçalves, C., Dover, J., Johnston, M., et al. (2011). Microbe domestication and the identification of the wild genetic stock of lager-brewing yeast. *Proc. Natl. Acad. Sci. U.S.A.* 108, 14539–14544. doi: 10.1073/pnas.1105430108

Lubkowitz, M. A., Barnes, D., Breslav, M., Burchfield, A., Naider, F., and Becker, J. M. (1998). Schizosaccharomyces pombe isp4 encodes a transporter representing a novel family of oligopeptide transporters. *Mol. Microbiol.* 28, 729–741. doi: 10.1046/j.1365-2958.1998.00827.x

Lubkowitz, M. A., Hauser, L., Breslav, M., Naider, F., and Becker, J. M. (1997). An oligopeptide transport gene from Candida albicans. *Microbiology* 143, 387–396. doi: 10.1099/00221287-143-2-387

Magasanik, B., and Kaiser, C. A. (2002). Nitrogen regulation in *Saccharomyces cerevisiae*. *Gene* 290, 1–18. doi: 10.1016/S0378-1119(02)00558-9

Mannazzu, I., Domizio, P., Carboni, G., Zara, S., Zara, G., Comitini, F., et al. (2019). Yeast killer toxins: from ecological significance to application. *Crit. Rev. Biotechnol.* 39, 603–617. doi: 10.1080/07388551.2019.1601679

Manson, M. D., Blank, V., Brade, G., and Higgins, C. F. (1986). Peptide chemotaxis in *E. coli* involves the Tap signal transducer and the dipeptide permease. *Nature* 321, 253–256. doi: 10.1038/321253a0

Marsit, S., and Dequin, S. (2015). Diversity and adaptive evolution of *Saccharomyces* wine yeast: a review. *FEMS Yeast Res.* 15:fov067. doi: 10.1093/femsyr/fov067

Marsit, S., Leducq, J. B., Durand, É, Marchant, A., Filteau, M., and Landry, C. R. (2017). Evolutionary biology through the lens of budding yeast comparative genomics. *Nat. Rev. Genet.* 18, 581–598. doi: 10.1038/nrg.2017.49

Marsit, S., Mena, A., Bigey, F., Sauvage, F. X., Couloux, A., Guy, J., et al. (2015). Evolutionary advantage conferred by an eukaryote-to-eukaryote gene transfer event in wine yeasts. *Mol. Biol. Evol.* 32, 1695–1707. doi: 10.1093/molbev/msv057

Marsit, S., Sanchez, I., Galeote, V., and Dequin, S. (2016). Horizontally acquired oligopeptide transporters favour adaptation of *Saccharomyces cerevisiae* wine yeast to oenological environment. *Environ. Microbiol.* 18, 1148–1161. doi: 10.1111/1462-2920.13117

McCarthy, P. J., Troke, P. F., and Gull, K. (1985). Mechanism of action of nikkomycin and the peptide transport system of Candida albicans. *J. Gen. Microbiol.* 131, 775–780. doi: 10.1099/00221287-131-4-775

Mo, F., Zhao, H., Lei, H., and Zhao, M. (2013). Effects of nitrogen composition on fermentation performance of brewer's yeast and the absorption of peptides with different molecular weights. *Appl. Biochem. Biotechnol.* 171, 1339–1350. doi: 10.1007/s12010-013-0434-5

Monteiro, S., Piçarra-Pereira, M. A., Mesquita, P. R., Loureiro, V. B., Teixeira, A., and Ferreira, R. B. (2001). The wide diversity of structurally similar wine proteins. *J. Agric. Food Chem.* 49, 3999–4010. doi: 10.1021/jf0013914

Morales, L., and Dujon, B. (2012). Evolutionary role of interspecies hybridization and genetic exchanges in yeasts. *Microbiol. Mol. Biol. Rev.* 76, 721–739. doi: 10.1128/mmbr.00022-12

Moreno-Arribas, M. V., Pueyo, E., and Polo, M. C. (2002). Analytical methods for the characterization of proteins and peptides in wines. *Anal. Chim. Acta* 2002, 63–75. doi: 10.1016/S0003-2670(01)01531-8

Moreno-Arribas, V., Pueyo, E., and Polo, M. C. (1996). Peptides in musts and wines. changes during the manufacture of cavas (Sparkling Wines). *J. Agric. Food Chem.* 44, 3783–3788. doi: 10.1021/jf960307a

Nelissen, B., De Wachter, R., and Goffeau, A. (1997). Classification of all putative permeases and other membrane plurispanners of the major facilitator superfamily encoded by the complete genome of Saccharomyces cerevisiae. *FEMS Microbiol. Rev.* 21, 113–134. doi: 10.1016/S0168-6445(97)00053-3

Nelson, D. L., and Cox, M. M. (2013). *Lehninger Principles of Biochemistry*, 6th Edn. New York: W. H. Freeman.

Newstead, S. (2017). Recent advances in understanding proton coupled peptide transport via the POT family. *Curr. Opin. Struct. Biol.* 45, 17–24. doi: 10.1016/j.sbi.2016.10.018

Nielsen, C., and Brodin, B. (2003). Di / tri-peptide transporters as drug delivery targets: regulation of transport under physiological and patho-physiological conditions. *Curr. Drug Targets* 4, 373–388. doi: 10.2174/1389450033491028

Novo, M., Bigey, F., Beyne, E., Galeote, V., Gavory, F., Mallet, S., et al. (2009). Eukaryote-to-eukaryote gene transfer events revealed by the genome sequence of the wine yeast Saccharomyces cerevisiae EC1118. *Proc. Natl. Acad. Sci. U.S.A.* 106, 16333–16338. doi: 10.1073/pnas.0904673106

Osawa, H., Stacey, G., and Gassmann, W. (2006). ScOPT1 and AtOPT4 function as proton-coupled oligopeptide transporters with broad but distinct substrate specificities. *Biochem. J.* 393, 267–275. doi: 10.1042/bj20050920

Ough, C. S., Huang, Z., An, D., and Stevens, D. (1991). Amino acid uptake by four commercial yeasts at two different temperatures of growth and fermentation: effects on urea excretion and reabsorption. *Am. J. Enol. Vitic.* 42, 26–40.

Paulsen, I. T., and Skurray, R. A. (1994). The POT family of transport proteins. *Trends Biochem. Sci.* 19:404. doi: 10.1016/0968-0004(94)90087-6

Payne, J. W., and Smith, M. W. (1994). Peptide transport by micro-organisms. *Adv. Microb. Physiol.* 36, 1–80. doi: 10.1016/s0065-2911(08)60176-9

Pérez-Ortín, J. E., Querol, A., Puig, S., and Barrio, E. (2002). Molecular characterization of a chromosomal rearrangement involved in the adaptie evolution of yeast strains. *Genome Res.* 12, 1533–1539. doi: 10.1101/gr.436602

Perry, J. R., Basrai, M. A., Steiner, H. −Y., Naider, F., and Becker, J. M. (1994). Isolation and characterization of a *Saccharomyces cerevisiae* peptide transport gene. *Mol. Cell. Biol.* 14, 104–115. doi: 10.1128/mcb.14.1.104

Rachidi, N., Barre, P., and Blondin, B. (1999). Multiple Ty-mediated chromosomal translocations lead to karyotype changes in a wine strain of Saccharomyces cerevisiae. *Mol. Gen. Genet.* 261, 841–850. doi: 10.1007/s004380050028

Rai, A., and Jeyaram, K. (2015). "Health benefits of functional proteins in fermented foods," in *Health Benefits of Fermented Foods and Beverages*, ed. J. Tamang (Boca Raton, FL: CRC Press), 457–476. doi: 10.13140/RG.2.1.2335.6963

Rai, R., Genbauffe, F., Lea, H. Z., and Cooper, T. G. (1987). Transcriptional regulation of the DAL5 gene in *Saccharomyces cerevisiae*. *J. Bacteriol.* 169, 3521–3524. doi: 10.1128/jb.169.8.3521-3524.1987

Rapp, A., and Versini, G. (1991). "Influence of nitrogen compounds in grapes on aroma compounds in wine," in *Proceedings of the International Symposium on Nitrogen in Grapes and Wine*, Seattle, USA (Davis, CA: American Society of Enology and Viticulture), 156–164.

Rees, D. C., Johnson, E., and Lewinson, O. (2009). ABC transporters: the power to change. *Nat. Rev. Mol. Cell Biol.* 10, 218–227. doi: 10.1038/nrm2646

Reuß, O., and Morschhäuser, J. (2006). A family of oligopeptide transporters is required for growth of Candida albicans on proteins. *Mol. Microbiol.* 60, 795–812. doi: 10.1111/j.1365-2958.2006.05136.x

Rigaud, J., Cheynier, V., Souquet, J. −M., and Moutounet, M. (1991). Influence of must composition on phenolic oxidation kinetics. *J. Sci. Food Agric.* 57, 55–63. doi: 10.1002/jsfa.2740570107

Rollero, S., Bloem, A., Camarasa, C., Sanchez, I., Ortiz-Julien, A., Sablayrolles, J. M., et al. (2015). Combined effects of nutrients and temperature on the production of fermentative aromas by *Saccharomyces cerevisiae* during wine fermentation. *Appl. Microbiol. Biotechnol.* 99, 2291–2304. doi: 10.1007/s00253-014-6210-9

Rubio-Texeira, M., Van Zeebroeck, G., and Thevelein, J. M. (2012). Peptides induce persistent signaling from endosomes by a nutrient transceptor. *Nat. Chem. Biol.* 8, 400–408. doi: 10.1038/nchembio.910

Seguinot, P., Rollero, S., Sanchez, I., Sablayrolles, J. M., Ortiz-Julien, A., Camarasa, C., et al. (2018). Impact of the timing and the nature of nitrogen additions on the production kinetics of fermentative aromas by *Saccharomyces cerevisiae* during winemaking fermentation in synthetic media. *Food Microbiol.* 76, 29–39. doi: 10.1016/j.fm.2018.04.005

Sievers, F., Wilm, A., Dineen, D., Gibson, T. J., Karplus, K., Li, W., et al. (2011). Fast, scalable generation of high-quality protein multiple sequence alignments using Clustal Omega. *Mol. Syst. Biol.* 7:539. doi: 10.1038/msb.2011.75

St Georgiev, V. (2000). Membrane transporters and antifungal drug resistance. *Curr. Drug Targets* 1, 261–284. doi: 10.2174/1389450003349209

Stambuk, B. U., Dunn, B., Alves, S. L., Duval, E. H., and Sherlock, G. (2009). Industrial fuel ethanol yeasts contain adaptive copy number changes in genes involved in vitamin B1 and B6 biosynthesis. *Genome Res.* 19, 2271–2278. doi: 10.1101/gr.094276.109

Steiner, H. Y., Naider, F., and Becker, J. M. (1995). The PTR family: a new group of peptide transporters. *Mol. Microbiol.* 16, 825–834. doi: 10.1111/j.1365-2958.1995.tb02310.x

Steiner, H. Y., Song, W., Zhang, L., Naider, F., Becker, J. M., and Stacey, G. (1994). An *Arabidopsis peptide* transporter is a member of a new class of membrane transport proteins. *Plant Cell* 6, 1289–1299. doi: 10.1105/tpc.6.9.1289

Su, Y., Seguinot, P., Sanchez, I., Ortiz-Julien, A., Heras, J. M., Querol, A., et al. (2020). Nitrogen sources preferences of non-*Saccharomyces* yeasts to sustain growth and fermentation under winemaking conditions. *Food Microbiol.* 85:103287. doi: 10.1016/j.fm.2019.103287

Swiegers, J. H., Bartowsky, E. J., Henschke, P. A., and Pretorius, I. S. (2005). Yeast and bacterial modulation of wine aroma and flavour. *Aust. J. Grape Wine Res.* 11, 139–173. doi: 10.1111/j.1755-0238.2005.tb00285.x

Takahashi, K., Tokuoka, M., Kohno, H., Sawamura, N., Myoken, Y., and Mizuno, A. (2012). Comprehensive analysis of dipeptides in alcoholic beverages by tag-based separation and determination using liquid chromatography/electrospray ionization tandem mass spectrometry and quadrupole-time-of-flight mass spectrometry. *J. Chromatogr. A* 1242, 17–25. doi: 10.1016/j.chroma.2012.03.076

Turner, G. C., Du, F., and Varshavsky, A. (2000). Peptides accelerate their uptake by activating a ubiquitin-dependent proteolytic pathway. *Nature* 405, 579–583. doi: 10.1038/35014629

Wang, G., Li, X., and Wang, Z. (2016). APD3: the antimicrobial peptide database as a tool for research and education. *Nucleic Acids Res.* 44, D1087–D1093. doi: 10.1093/nar/gkv1278

Wiles, A. M., Cai, H., Naider, F., and Becker, J. M. (2006a). Nutrient regulation of oligopeptide transport in *Saccharomyces cerevisiae*. *Microbiology* 152, 3133–3145. doi: 10.1099/mic.0.29055-0

Wiles, A. M., Naider, F., and Becker, J. M. (2006b). Transmembrane domain prediction and consensus sequence identification of the oligopeptide transport family. *Res. Microbiol.* 157, 395–406. doi: 10.1016/j.resmic.2005.10.004

Williams, L., and Miller, A. (2001). Transporters responsible for the uptake and partitioning of nitrogenous solutes. *Annu. Rev. Plant Physiol. Plant Mol. Biol.* 52, 659–688. doi: 10.1146/annurev.arplant.52.1.659

Yang, X., and Yousef, A. E. (2018). Antimicrobial peptides produced by *Brevibacillus* spp.: structure, classification and bioactivity: a mini review. *World J. Microbiol. Biotechnol.* 34:57. doi: 10.1007/s11274-018-2437-4

Yokotsuka, K., and Fukui, M. (2002). Changes in nitrogen compounds in berries of six grape cultivars during ripening over two years. *Am. J. Enol. Vitic.* 53, 69–77.

Yokotsuka, K., Umehara, Y., Aihara, T., and Kushida, T. (1975). Isolation and structural anlysis of peptides in Koshu white wine. *Ferment. Technol.* 53, 620–625.

Zhang, Y., Venkitasamy, C., Pan, Z., Liu, W., and Zhao, L. (2017). Novel umami ingredients: umami peptides and their taste. *J. Food Sci.* 82, 16–23. doi: 10.1111/1750-3841.13576

Zimdars, S., Schrage, L., Sommer, S., Schieber, A., and Weber, F. (2019). Influence of glutathione on yeast fermentation efficiency under copper

stress. *J. Agric. Food Chem.* 67, 10913–10920. doi: 10.1021/acs.jafc.9b03519

Zimmer, A., Durand, C., Loira, N., Durrens, P., Sherman, D. J., and Marullo, P. (2014). QTL dissection of lag phase in wine fermentation reveals a new translocation responsible for Saccharomyces cerevisiae adaptation to sulfite. *PLoS One* 9:e86298. doi: 10.1371/journal.pone.0086298

Zulkifli, M., Yadav, S., Thakur, A., Singla, S., Sharma, M., and Bachhawat, A. K. (2016). Substrate specificity and mapping of residues critical for transport in the high-affinity glutathione transporter Hgt1p. *Biochem. J.* 473, 2369–2382. doi: 10.1042/BCJ20160231

Conflict of Interest: The authors declare that the research was conducted in the absence of any commercial or financial relationships that could be construed as a potential conflict of interest.

frontiers in Microbiology

ORIGINAL RESEARCH
published: 29 June 2020
doi: 10.3389/fmicb.2020.01331

SSU1 Checkup, a Rapid Tool for Detecting Chromosomal Rearrangements Related to the *SSU1* Promoter in *Saccharomyces cerevisiae*: An Ecological and Technological Study on Wine Yeast

Philippe Marullo[1,2†], Olivier Claisse[1†], Maria Laura Raymond Eder[3†], Marine Börlin[1], Nadine Feghali[4,5], Margaux Bernard[1,2], Jean-Luc Legras[6], Warren Albertin[1], Alberto Luis Rosa[3] and Isabelle Masneuf-Pomarede[1,7]*

[1] University of Bordeaux, INRAE, ENSCBP Bordeaux-INP, UR Oenology, EA-4577, USC-1366, ISVV, Villenave-d'Ornon, France, [2] Biolaffort, Bordeaux, France, [3] Laboratorio de Genética y Biología Molecular, IRNASUS-CONICET, Bioquímica de Alimentos II, Facultad de Ciencias Químicas, Universidad Católica de Córdoba, Córdoba, Argentina, [4] Faculty of Agriculture and Veterinary Medicine, Lebanese University, Beirut, Lebanon, [5] Department of Agricultural Science, University of Sassari, Sassari, Italy, [6] SPO, INRA, Montpellier SupAgro, University of Montpellier, Montpellier, France, [7] Bordeaux Sciences Agro, Gradignan, France

Chromosomal rearrangements (CR) such as translocations, duplications and inversions play a decisive role in the adaptation of microorganisms to specific environments. In enological *Saccharomyces cerevisiae* strains, CR involving the promoter region of the gene *SSU1* lead to a higher sulfite tolerance by enhancing the SO_2 efflux. To date, three different *SSU1* associated CR events have been described, including translocations XV-t-XVI and VIII-t-XVI and inversion inv-XVI. In the present study, we developed a multiplex PCR method (*SSU1* checkup) that allows a rapid characterization of these three chromosomal configurations in a single experiment. Nearly 600 *S. cerevisiae* strains collected from fermented grape juice were genotyped by microsatellite markers. We demonstrated that alleles of the *SSU1* promoter are differently distributed according to the wine environment (cellar versus vineyard) and the nature of the grape juice. Moreover, rearranged *SSU1* promoters are significantly enriched among commercial starters. In addition, the analysis of nearly isogenic strains collected in wine related environments demonstrated that the inheritance of these CR shapes the genetic diversity of clonal populations. Finally, the link between the nature of *SSU1* promoter and the tolerance to sulfite was statistically validated in natural grape juice containing various SO_2 concentrations. The *SSU1* checkup is therefore a convenient new tool for addressing population genetics questions and for selecting yeast strains by using molecular markers.

Keywords: sulfite resistance, domestication, translocation, multiplex PCR, marker assisted selection

OPEN ACCESS

Edited by:
Roberto Pérez-Torrado, Consejo Superior de Investigaciones Científicas (CSIC), Spain

Reviewed by:
Vasileios Englezos, University of Turin, Italy
Chris Putnam, University of California, San Diego, United States

***Correspondence:**
Philippe Marullo
philippe.marullo@u-bordeaux.fr

†These authors share first authorship

Specialty section:
This article was submitted to Evolutionary and Genomic Microbiology, a section of the journal Frontiers in Microbiology

Received: *12 February 2020*
Accepted: *25 May 2020*
Published: *29 June 2020*

Citation:
Marullo P, Claisse O, Raymond Eder ML, Börlin M, Feghali N, Bernard M, Legras J-L, Albertin W, Rosa AL and Masneuf-Pomarede I (2020) SSU1 Checkup, a Rapid Tool for Detecting Chromosomal Rearrangements Related to the SSU1 Promoter in Saccharomyces cerevisiae: An Ecological and Technological Study on Wine Yeast. Front. Microbiol. 11:1331. doi: 10.3389/fmicb.2020.01331

INTRODUCTION

Microorganisms develop various strategies for being better adapted to various environments. Among them, the yeast *Saccharomyces cerevisiae* is a noteworthy example of a microorganism whose evolution led to specialized genetic groups associated with different human-related environments (Sicard and Legras, 2011; Borneman and Pretorius, 2014; Marsit and Dequin, 2015). In a winemaking context, this species has been exposed to stressful conditions (high alcohol content, high osmotic pressure, low pH, etc.) for millennia, potentially resulting in adaptive differentiation.

In wine production, sulfite addition is widely used since the middle age as a preservative because of its antimicrobial, antioxidant, and antioxydasic activities. Produced by dissolution of sulfur dioxide (SO_2), sulfite inhibits key glycolytic enzymes like *Tdh* and *Adh* proteins, binds carbonyl compounds such as pyruvate and acetaldehyde (Hinze and Holzer, 1986) affects transporter activity by binding membrane proteins (Divol et al., 2012) and down-regulates the expression of many central metabolism genes (Park and Hwang, 2008). Therefore, sulfite tolerance has been unconsciously selected by wine making practices and constitutes a desired trait in *Saccharomyces* wine yeast strains. Cellular mechanisms of sulfite tolerance have been extensively reviewed in *S. cerevisiae* (Divol et al., 2012; García-Ríos and Guillamón, 2019). They include the overproduction of acetaldehyde (Cheraiti et al., 2010) the regulation of sulfite reduction systems and more generally of the sulfur metabolic pathway (Divol et al., 2012). Moreover, sulfite tolerance mostly depends on the pumping of SO_2 through the plasma membrane. This sulfite efflux involves the sulfite pump Ssu1p which is encoded by the *SSU1* gene. This gene shows a high level of polymorphism (Aa et al., 2006) and deleterious mutations in its coding sequence cause SO_2 susceptibility (Avram and Bakalinsky, 1997; Park and Bakalinsky, 2000).

The expression level of *SSU1* has a direct consequence on sulfite tolerance and has been widely studied (Pérez-Ortín et al., 2002; Nardi et al., 2010; Engle and Fay, 2012; Zimmer et al., 2014; García-Ríos et al., 2019). Interestingly, the *SSU1* promoter sequence is involved in three Chromosomal Rearrangements (CR) (i.e., XV-t-XVI, VIII-t-XVI, and inv-XVI) that increase its expression leading to a more efficient sulfite pumping over (Pérez-Ortín et al., 2002; Zimmer et al., 2014; García-Ríos et al., 2019). These three independent CR events constitute a hallmark on parallel evolutionary routes driven by human selection. In the VIII-t-XVI translocation, the native promoter of *SSU1* is replaced by tandem repeated sequences of the *ECM34* promoter from chromosome VIII (Pérez-Ortín et al., 2002). In the XV-t-XVI translocation, the upstream region of *SSU1* is placed head to tail with the *ADH1* promoter from chromosome XV (Zimmer et al., 2014). The inversion of chromosome XVI (inv-XVI) involves the *SSU1* and *GCR1* regulatory regions, increasing the expression of *SSU1* (García-Ríos et al., 2019).

To date, the distribution of translocation (XV-t-XVI and VIII-t-XVI) and inversion (inv-XVI) events of the *SSU1* gene have been investigated for a small number of strains (Pérez-Ortín et al., 2002; Zimmer et al., 2014; García-Ríos et al., 2019). Here, we set up a multiplex method (*SSU1 checkup*) based on labeled primers with different fluorochromes, to identify in a single assay the three types of *SSU1* associated CR (VIII-t-XVI, XV-t-XVI, and inv-XVI) as well as the wild type forms of these chromosomes (VIII-wt, XV-wt, and XVI-wt). The *SSU1* was applied to nearly 600 yeast strains, including natural isolates and commercial starters, and provides new insights on the allele frequency of rearranged *SSU1* promoters. In addition, by using microsatellite genotyping, the genetic relationships between strains of the collection were established allowing the study of CR occurrence in nearly isogenic clones. Finally, for a subset of strains, the phenotypic impact of different CR was evaluated by measuring their parameters of growth in grape juice containing different concentrations of SO_2.

MATERIALS AND METHODS

Origin of Samples

A total of 628 *S. cerevisiae* isolates were collected from grapes and fermented must (white, red, and sweet) originating from five different countries (France, Lebanon, Argentina, Spain, and Italy), two different *Vitis* species (mostly *V. vinifera* and to a lesser extent *V. labrusca*) and nine different varieties. Two different procedures were used for strain isolation depending on the environment considered: vineyard or cellar. For vineyard isolates, around 2 kg of healthy and mostly undamaged grapes were collected a few days before the harvest in the vineyard, crushed in sterile conditions and macerated for 2 h with 50 mg/L of SO_2. The juice was fermented at 21°C in small glass-reactors (500 mL). For cellar isolates, yeast colonies were obtained from spontaneous fermentation vats containing sulfited grape juices according to local enological practices (ranging from 20 to 50 mg/L of sulfur dioxide) except for sweet wines for which no sulfur dioxide was added. For both sampling procedures, fermentations were allowed to proceed until 2/3 of the must sugars were consumed and fermented juices were plated onto YPD plates (yeast extract, 1% w/v; peptone, 1% w/v; glucose, 2% w/v; agar 2% w/v) with 100 μg/mL of chloramphenicol and 150 μg/mL of biphenyl to delay bacterial and mold growth. Around 30 colonies per sample were randomly chosen and after sub-cloning on YPD plates, each yeast colony was stored in 30% (v/v) glycerol at −80°C. Additionally, a collection of 103 industrial *S. cerevisiae* starters was constituted by streaking on YPD plates a small aliquot of Active Dry Yeast obtained from different commercial suppliers.

Microsatellite Analysis

Strains were genotyped using fifteen polymorphic microsatellite loci (C3, C4, C5, C6, C8, C9, C11, SCAAT1, SCAAT2, SCAAT3, SCAAT5, SCAAT6, SCYOR267C, YKL172W, YPL009C) developed for estimating the genetic relationships among *S. cerevisiae* strains (Legras et al., 2007). Most of the strains were previously genotyped in our lab (Börlin et al., 2016;

Raymond et al., 2018; Peltier et al., 2018a; Borlin, 2015) and the additional 82 strains were genotyped in this work using identical experimental conditions. Briefly, two multiplex PCRs were carried out in a final volume of 12.5 μL containing 6.25 μL of the Qiagen Multiplex PCR master mix (Qiagen, France), 1 μL of DNA template, and 1.94 μL of each mix, using the conditions previously reported (Peltier et al., 2018b). Both reactions were run using an initial denaturation step at 95°C for 5 min, followed by 35 cycles of 95°C for 30 s, 57°C for 2 min, 72°C for 1 min, and a final extension step at 60°C for 30 min. The size of PCR products was determined by the MWG company (Ebersberg, Germany), using 0.2 μL of 600 LIZ GeneScan (Applied Biosystems, France) as a standard marker, and chromatograms were analyzed with the GeneMarker (V2.4.0, Demo) program. Only strains that amplified at least 12 of 15 loci were kept. On the 735 strains collected, 586 met this criterion and were used in this study (listed on **Supplementary Table S1**). The microsatellite data set was analyzed by means of the *poppr* R package using the Bruvo's distance matrix. Strains showing a strong similarity were identified by applying a cut of value of 0.15 to the Bruvo's genetic distance matrix. In this way, 194 very closely related strains were identified and considered as "clones." This cut off value was defined in order to restore the normality of the distribution (**Supplementary Figure S1**). The assignment of clustering methods was achieved by using the *find.clusters* function (*adegenet* package). The selection of the optimal groups was computed by the Ward's clustering method using the Bayesian Information Criterion (BIC) as statistical criterion (Avramova et al., 2018).

The SSU1 Checkup Method

In order to experimentally detect in a single multiplex PCR test all the CR involving the gene *SSU1*, labeled primers were designed using a specific dye per chromosome position as follows: 6-FAM (Chr8: VIII-14558), ATTO550 (Chr15: XV-160994), HEX (Chr16: XVI-373707), and ATTO565 (Chr16: XVI-412453) (**Table 1**). All the primers (**Table 1** and **Supplementary Table S2**) were synthesized by Eurofins genomics (Ebersberg, Germany). A multiplex PCR was carried out in a final volume of 20 μL using 100 nM of each primer, 1 μL of template DNA and the Qiagen PCR multiplex PCR kit (Qiagen, France) on a T100TM Thermal cycler (Bio-Rad, France). The following PCR program allows the amplification of all the expected fragments from the rearranged and the wild type VIII, XV and XVI chromosomes: initial denaturation at 95°C for 15 min, followed by 35 cycles of 94°C for 30 s, 55°C for 90 s, 72°C for 90 s, ending with a hold at 60°C for 30 min. DNA templates for PCR were extracted in 96-well microplates using the previously described LiAc-SDS protocol (Chernova et al., 2018). Before analysis, PCR products were diluted 60 times in ddH_2O and 1 μL of this solution was mixed with 0.2 μL of the internal size standard GenScan^{TM} 1200 LIZ (Applied Biosystems, France) and 9.8 μL of highly deionized Hi-DiTM formamide (Applied Biosystems, France). Samples were analyzed by Eurofins genomics (Ebersberg, Germany) on an ABI-3710 Genetic Analyzer. Each peak was identified according to the color and size and attributed to the alleles (**Figure 1**). Each allele was also sequenced by amplifying both strands with non-labeled primers. The sequences were released on GenBank with the following accession numbers: ID MT028493-MT028507.

SO_2 Tolerance Assessment

To assess SO_2 tolerance, a subset of 34 strains (**Supplementary Table S3**) was cultivated in white grape juice (Sauvignon blanc from the Bordeaux area, France). This must had a total SO_2 concentration of 14 mg/L and was spiked with 0, 25, 50, and 75 mg/L of total SO_2. Cultures were achieved in 96-well plates (U flat well, Greiner, France) filled with 200 μL of grape juice sterilized by a nitrate-cellulose membrane filtration (Millipore, France). Yeasts were pre-cultivated in YPD media (yeast extract, 1% w/v; peptone, 1% w/v; glucose, 2% w/v) for 16 h at 28°C and inoculated into the grape juice to a final concentration of 1×10^6 cells/mL. Growth was monitored by OD_{600} measurements for 96 h at 28°C using a microplate spectrophotometer (Synergy HT Multi-Mode Reader, BioTek Instruments, Inc., United States). Culture plates were shaken every 25 min for 30 s prior to the OD_{600} measurements. The well position on the microplate was randomized and six replicates were done for each strain*media condition. Data from the microplate reader were transformed with the polynomial curve $y = -0.0018*x3+0.1464*x2+0.7757*x+0.0386$ to correct the non-linearity of the optical recording at higher cell densities as previously reported (Martí-Raga et al., 2016). Growth kinetic data were fitted using the *Richards* flexible inflection point model implemented by the *fit growthmodel* function, R package *growthrates*. This model allows the estimation of the maximal growth rate (μmax). A second parameter, *Lag Time,* was manually computed from raw data by considering the time necessary to reach twice the OD_{600} of the inoculum. A linear model was applied for estimating effects of the SO_2 concentration and type of chromosome XVI and their possible interactions:

$$(1)\ \text{Lm1: } Y_{ik} = m + ChrXVI_{\ i} + SO_{2\ k} + (ChrXVI{:}SO_2)_{\ ik} + E_{\ ijk}$$

Where Y are the values of the trait (μmax and *Lag Time)*, for *j ChrXVI* configurations $(i = 1to6)$, and *k* SO_2 $(k = 1to\ 4)$ concentrations, *m* was the overall mean and E_{ijk} the residual error. Homoscedasticity of the ANOVA was tested by *LeveneTest* function (*car* package) while the normal distribution of models' residuals was estimated by visual inspection (*qq plot*).

RESULTS AND DISCUSSION

Assessment of the Genetic Diversity of Starters and Natural Isolates Populations of *S. cerevisiae*

In this study, we analyzed a large dataset of 586 isolates that were genotyped using 15 microsatellite loci. This collection includes 103 industrial starters and 483 indigenous isolates from different origins (sampling mode, red or white grape must, country). Since many natural isolates were sampled in the same juice, some of them could have originated from clonal expansion and be

TABLE 1 | Primers used for the *SSU1* checkup method and the strains used as positive controls.

Chromosome	Strain	Primer F			Primer R			Size[a]	Position[b]
		Name	Sequence	Dye	Name	Sequence	Dye		
VIII	SB	1189	ATGGCAGCTTCTAAGTTGTGG	FAM	1190	GTTTATGTTTGGTTTGGGGG	na	604	VIII-14558
	GN							667	to VIII-15162
XV	SB	1191	AAAGAAGTTGCATGCGCCTA	ATTO550	1192	ACCTGAGTGCATTTGCAACA	na	702	XV-160994
	F10							702	to XV-161695
XVI	SB	1193	TGTCAAGTTGAGACAAACCGA	na	1194	GGGGAAAGCTGTAATTTGTGT	Hex	991	XVI-372717 to XVI-373707
VIII-t-XVI	F10	1189	ATGGCAGCTTCTAAGTTGTGG	FAM	1194	GGGGAAAGCTGTAATTTGTGT	Hex	555	VIII-14558 to XVI-373707
XV-t-XVI	GN	1191	AAAGAAGTTGCATGCGCCTA	ATTO550	1194	GGGGAAAGCTGTAATTTGTGT	Hex	496	XV-160994 to XVI-373707
inv-XVI	P5	1196	TGCATAAGCAGGCAACTCCT	ATTO565	1194	GGGGAAAGCTGTAATTTGTGT	Hex	781	XVI-373707-412453

[a]*PCR product lengths in base pairs;* [b]*position in the chromosome for reference strain S288c; na: not applicable.*

very similar from a genetic point of view. A filtering procedure was applied for keeping only one representative genotype of each clonal population by removing all but one strain having a Bruvo's genetic distance lower than 0.15 (**Supplementary Figure S1**). By this procedure, many natural isolates closely related to industrial starters were identified (**Supplementary Figure S2**) demonstrating the wide dissemination of commercial yeasts in vineyard and winery environments as previously reported (Valero et al., 2005; Borlin, 2015). In addition, 21 isogenic strains were found among commercial starters. This filtering procedure defined three subpopulations: "starters = 82," "natural isolates = 310," and "closely related clones = 194" (**Supplementary Table S1**). The genetic relationships for each strain within the *starters* and *natural isolates* subpopulations were then analyzed by a principal component analysis ($k = 6$). The constitution of genetic groups based on microsatellites inheritance was carried out by using a k-mean based algorithm (see section "Materials and Methods").

This genetic analysis clustered the 82 commercial strains in three groups with a group C clearly separated from the other two (**Supplementary Figure S3**) and corresponding to "Champenoise" strains, a particular wine yeast group previously described (Legras et al., 2007; Novo et al., 2009; Borneman et al., 2016). Its detection validated our clustering analysis based on the use of k-mean clustering. The structure of the 310 *natural isolates* collected was also investigated and six subgroups were defined. **Figure 2A** shows the first two dimensions of the PCA; axis one clearly identified a group of isolates from Argentina, while axis 2 broadly discriminated the five other groups. The assignment of subgroups on neighbor-joining tree (unrooted) illustrates that isolates are mostly clustered according to their geographical origins (**Figure 2B**). Some groups are specific to sampling zones such as group 3 ($n = 16$) and group 6 ($n = 84$) that only contain strains sampled in Argentina and Lebanon, respectively. In contrast, group 2 ($n = 177$) encompassed isolates from different geographic origins (Italy, Spain, France, and Lebanon) (**Supplementary Table S4**). Although not perfectly discriminating, this first analysis filtered the redundancy of our collection and provided a clear overview of the genetic diversity of non-redundant strains.

Development of the SSU1 Checkup, a Simple Method for Genotyping SSU1 Chromosomal Rearrangements in *S. cerevisiae*

To date, translocation events (i.e., XV-t-XVI and VIII-t-XVI) have been detected by classical PCR experiments narrowing the chromosomal break points identified by two original works (Pérez-Ortín et al., 2002; Zimmer et al., 2014). Recently, an additional chromosomal rearrangement involving the gene *SSU1* (inv-XVI) was also described (García-Ríos et al., 2019). Because these classical PCR amplifications are scarcely adapted to screen multiple genotypes in large populations, a multiplexed method (*SSU1* checkup) was set up aiming to identify, in a single PCR reaction, these three types of chromosomal rearrangements (VIII-t-XVI, XV-t-XVI, and inv-XVI) as well as the wild type alleles of the corresponding chromosomes (VIII-wt, XV-wt, and XVI-wt). Since primers are labeled with different fluorochromes they allow the identification of the different allelic combinations. Primers used for amplifying the wild type chromosomes (VIII-wt, XV-wt, and XVI-wt) were labeled with a single fluorophore (FAM, ATTO 550, Hex), providing blue, yellow, and green peaks, respectively (**Figure 1A**). With this set of primers, the amplifications of the rearranged *SSU1* promoter regions result to be labeled with two fluorophores, allowing the easy identification of the recombined forms (**Figure 1B**). The allele sizes amplified range between 388 and 991 bp and were analyzed by following the fluorescence of PCR products with an ABI sequencer (**Figure 1C**). In preliminary studies, we used reference strains SB (XVI-wt), GN (XV-t-XVI), F10 (VIII-t-XVI), and P5 (inv-XVI), to design and validate primers. Primers position, as well as the length of the DNA fragments amplified for the reference strains, are summarized in **Table 1**. The sequences of all the alleles identified were submitted to GenBank (ID 2310529). The strain P5 is a commercial starter able to sporulate (data not

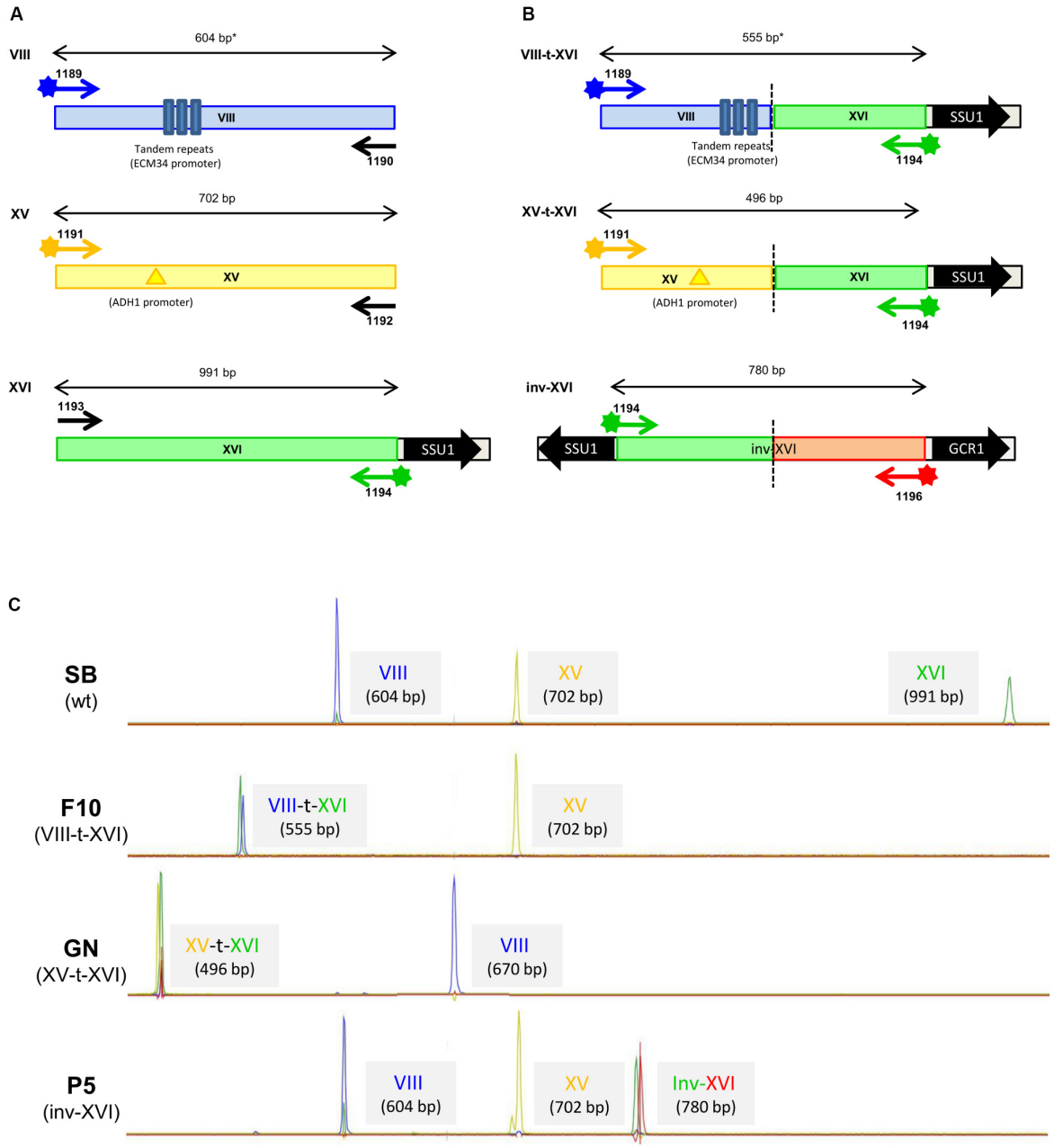

FIGURE 1 | (A) Position of labeled primers for on the non-rearranged chromosomes VIII, XV, and XVI. The position of the promoter regions ECM34 and ADH1 were represented by a multiple blue bar and a yellow triangle, respectively. The gene SSU1 is represented by a black arrow. The tandem repeats on chromosome VIII (indicated by an *) generates multiple type of amplicons. Labeled primers are represented by a star and the colors blue, yellow, and green represent the specific dye used :FAM, ATO550, and HEX. **(B)** Rearranged chromosome XVI investigated in this study (VIII-t-XVI, XV-t-XVI, and inv-XVI). The relative position of the gene SSU1 and the modified promoter regions (ECM34, ADH1, and GCR1) are indicated. The hatched line represents the chromosomal break point in rearranged strains F10 (VIII-t-XVI), GN (XV-t-XVI), and P5 (inv-XVI), respectively. The red star represents the primer specific to the inv-XVI chromosome labeled with the fluorochrome ATO 565. **(C)** Chromatograms of multiplexed PCR reactions for the reference strains. The wt and rearranged XVI chromosomes were detected by co migration of fragment of different size labeled with specific dyes. For Chromosome VIII different sizes were obtained according to the strain due to the differential number of tandem repeats in ECM34 promoter.

shown) and would be therefore diploid. The ploidy level of strains SB, GN, and F10 has been previously determined by several genetic analyses (Albertin et al., 2009). These strains are fully homozygous diploids (2n) and were obtained by the sporulation of the commercial starters Actiflore BO213, Zymaflore VL1 and Zymaflore F10, Laffort, France) as previously reported (Marullo et al., 2006, 2009). Their associated chromatograms showed the different types of alleles reported in this study (**Figure 1C**). In

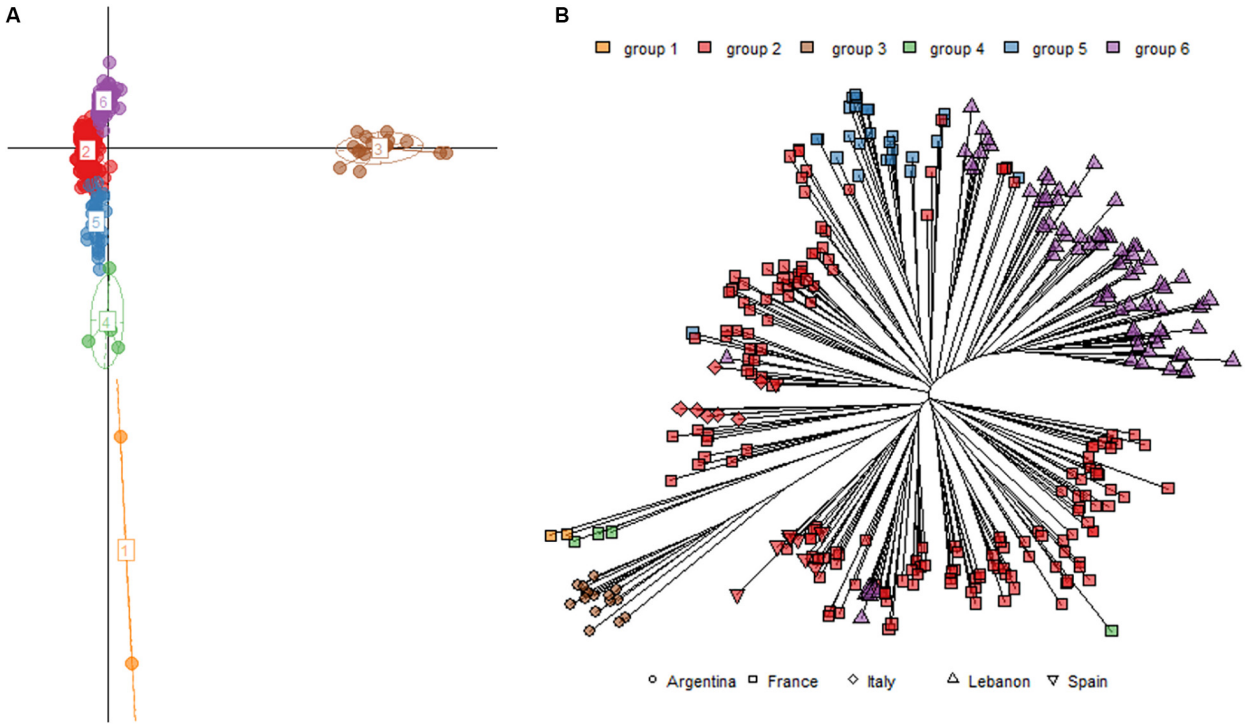

FIGURE 2 | (A) Principal component analysis of 310 natural isolates discriminated by 15 polymorphic loci. The six groups represented (1 to 6) were inferred by k-mean clustering. The **(B)** represents the position of the strains according to the inferred groups and the country origin of their sampling.

order to simplify the chromatographic patterns, the detection of reciprocal translocation events (XVI-t-XV and XVI-t-VIII) was not included in the *SSU1* checkup. However, the strains GN and F10 harbor reciprocal translocations that have been verified by PCR using the primers given in **Supplementary Table S2**.

The *SSU1* checkup was used for tracking the two translocation events (VIII-t-XVI and XV-t-XVI) as well as the chromosomal inversion (inv-XVI) in a large collection of strains (n = 586). In the VIII-t-XVI translocation, the native promoter of *SSU1* is replaced by DNA sequences of the *ECM34* promoter (located on chromosome VIII) (Pérez-Ortín et al., 2002). Alleles for this CR (i.e., VIII-t-XVI^{388}, VIII-t-XVI^{478}, VIII-t-XVI^{555}, and VIII-t-XVI^{631} bp) result from the alternative number of units of tandem repeated motifs (76 bp and/or 47 bp) localized in the promoter region of the gene *ECM34* (**Supplementary Figure S4**). In the XV-t-XVI translocation, the upstream region of *SSU1* is placed head to tail with the *ADH1* promoter (located on chromosome XV) (Zimmer et al., 2014) and a single allele has been recognized (XV-t-XV^{496}). Finally, the chromosomal rearrangement (inv-XVI) has been recently reported by García-Ríos et al. (2019) and consist in a chromosome XVI inversion generating a new *SSU1* promoter placed head to tail with the *GCR1* promoter. This event was detected in only 19 natural isolates and showed a single allele of 781 bp (inv-XVI^{781}). Surprisingly, twenty strains definitively failed to amplify any fragment even when performing single PCR reactions using alternative primers (**Supplementary Table S2**). This interesting result suggests that these strains could harbor another still uncharacterized chromosomal rearrangement flanking the *SSU1* gene. Such possible new CR should be tracked by chromosome walking PCR starting from *SSU1* gene or by de novo assembly of whole genome sequences.

Landscape of the Different SSU1-Promoter Alleles in Natural and Selected Populations

The *SSU1* checkup method allows the detection of four types of chromosome XVI structures in a single PCR reaction. However, this method is not quantitative, and it is not possible to know the number of copies of each haplotype. Since all the fragments amplified by the primer 1194 (Hex) are physically linked to the chromosome XVI's centromere (*CEN16*), they belong to chromosome XVI during the cell division process. Therefore, native and rearranged chromosome XVI alleles can be merged in order to have an integrated overview of the chromosome XVI inheritance. This allows following the inheritance of the different promoter versions of the *SSU1* gene.

The different alleles of chromosome XVI were counted among the 392 non-redundant *S. cerevisiae* strains analyzed. As a first approximation, we considered that all the strains analyzed are diploids. This assumption is based on the fact that 87% the *S. cerevisiae* strains are diploid and that polyploids/aneuploid strains are mostly observed in ale beer and sake strains (Peter et al., 2018). In contrast, wine yeast strains are generally euploids and diploids likely due to their homothallic character

(Mortimer et al., 1994). In our population, 65% of the population genotyped proved to be heterozygous (and therefore diploid) for at least two microsatellite loci (**Supplementary Table S1**) which is consistent with previous population genetic observations for wine *S. cerevisiae* strains (Legras et al., 2007). Assuming this hypothesis, when a strain showed a single chromosome XVI allele we assigned two identical genotypes as done for routine microsatellite analysis (Legras et al., 2007). In this way, strains showing more than two distinct alleles for chromosome XVI were considered to have an extra copy of this chromosome. For example, the strain Zymaflore VL2 inherited the alleles XVI-wt^{991}, VIII-t-XVI^{555}, and XV-t-XVI^{496} (**Supplementary Table S1**) and was considered as aneuploid for the chromosome XVI (three CEN16 centromeres instead of two).

The allele frequencies computed are given in **Table 2**; the occurrence of each allele between *natural isolates* and *starters* populations was compared by a Chi^2 test. Among the 392 non-redundant *S. cerevisiae* strains analyzed, the most frequent alleles found were VIII-t-XVI^{555} (0.41) and XVI-wt^{991} (0.34). However, their allelic frequencies are not evenly distributed. Indeed, the *starters* group (n = 82) is significantly enriched in alleles VIII-t-XVI^{388} and XV-t-XVI^{496} compared to the *natural isolates* group (n = 310); in contrast, *natural isolates* mostly harbor the VIII-t-XVI^{555} allele.

Since chromosomal rearrangements lead to more active *SSU1* genes, these alleles are supposed to be mostly dominant (Clowers et al., 2015; Peltier et al., 2018a). Therefore, for having a more accurate understanding of the functional impact of chromosome XVI forms, the percentage of homozygous strains for the different alleles is also given in **Table 2**. The homozygosity level of VIII-t-XVI alleles is much higher among *natural isolates* (49.1 vs. 13.8%) than among *starters*. Interestingly, for these two subgroups of strains, we do not find a significant discrepancy for the overall homozygosity level of the 15 microsatellite markers analyzed (23 vs. 23% for *natural isolates* and *starters*, respectively). However, the microsatellite marker C6 localized on the chromosome XVI at less than 100 kb of the *SSU1* gene, shows a similar homozygous level discrepancy than the VIII-t-XVI alleles (35 vs. 17%, for natural and industrial strains, respectively). In the same way, although allele frequencies of XVI-wt^{991} are quite similar between the two populations, homozygous strains are more frequent in the *natural isolates* group (25.4 vs. 8.8%, corrected Chi^2 test, $p = 1.10^{-4}$). Consequently, from a functional point of view, only seven industrial strains lacked any rearranged *SSU1* allele (*ECM34-SSU1*, *ADH1-SSU1*, or *GCR1-SSU1*). Furthermore, an overall difference of heterozygosity was not observed for the 15 microsatellite markers but was significative for the marker C6 (42.1 vs. 11.4% for natural and industrial strains, respectively). Altogether, these observations suggest that the different ratio of homozygosity observed between *starters* and *natural isolates* in the region of *SSU1* could be due to a local loss of heterozygosity that remains unexplained.

Out of the 21 possible biallelic combinations of the seven chromosome XVI alleles, 18 biallelic combinations were found among the 586 strains typed using the *SSU1* checkup. The percentage of strains carrying at least one type of CR is shown in **Figure 3**. Industrial strains are significantly enriched in translocations VIII-t-XVI and XV-t-XVI compared to natural isolates. In contrast, the inv-XVI allele was rarer and never found in industrial strains (the reference strain P5 was not included here). Interestingly, two industrial starters (3%) carry both translocated chromosomes. In addition, 11 starters (13%) have an extra copy of chromosome XVI (aneuploidy), a fraction much higher than for the *natural isolates* group (1 out of 310). It has been suggested that an extra-copy number of chromosome XVI would confer a gain of fitness during fermentation (Brion et al., 2013). As shown in **Table 2**, seven industrial strains are homozygous for the XVI-wt allele (8.5% of the population). These starters are usually recommended for red grape juice winemaking or Cognac distillation, where the SO_2 pressure is lower than in white wine production.

Linking Chromosomal Rearrangement Events of Chromosome XVI and Yeast Ecology

Wine-related natural isolates allow the study of broad ecological factors influencing the chromosomal configurations of *SSU1's* promoter. It has been shown that *SSU1* related translocations in wine yeast isolates are advantageous for growth in sulfited grape juice and contribute to a fitness gain respect to oak yeast strains (Clowers et al., 2015). Furthermore, previous studies revealed that variations in the promoter region of *SSU1* gene in wine yeasts enhance the *SSU1* gene expression during fermentation, and have a remarkable effect on the SO_2 resistance levels (Pérez-Ortín et al., 2002; Zimmer et al., 2014; García-Ríos and Guillamón, 2019). The subpopulation of 310 unique strains characterized in this work were split according to the sampling procedure applied: *cellar* (n = 205) vs. *vineyard* (n = 105) isolates (**Supplementary Table S1**). *Cellar* strains were isolated from spontaneously fermented vats in various wine estates, from sulfited grape musts according to the recommended practices of the area of origin. *Vineyard* strains were isolated from grapes manually harvested, crushed, and fermented in sterile laboratory conditions (see section "Materials and Methods").

The occurrence percentage of the 18 allelic combinations found in both groups is shown in **Figure 4A**. The proportion of genotypes (555:555 and 991:555) is significantly higher in the *cellar* group while *vineyard* isolates are slightly enriched in 781:781 genotypes (p-value < 0.1, corrected Chi^2 test). Moreover, strains having inherited at least one rearranged chromosome XVI are significantly more frequent in the *cellar* group (**Figure 4A**). The occurrence percentage observed here could reflect that among wine-related yeast isolates, *cellar* strains undergo a stronger selective pressure than *vineyard* strains likely due to winemaking operations.

The impact of the nature of the grape juice from which strains were isolated was also tested. For this study, we focused our investigation only on *cellar* populations (n = 205) that have been subjected to *in situ* enological treatments. Indeed, according to the enological practices and doses, grape juices are

TABLE 2 | Allele frequency and percentage of homozygosity of different chromosome XVI forms within starters and natural isolates populations.

Chromosome XVI alleles	Allele frequencies				% of Homozygous strains			
	Total samples *n* = 392	Natural isolates *n* = 310	Starters *n* = 82	Chi² test (*p*-value)	Total samples *n* = 392	Natural isolates *n* = 310	Starters *n* = 82	Chi² test (*p*-value)
VIII-t-XVI^{388}	0.093	0.021	0.369	$<2.2.10^{-16}$	3.8	2.1	10.0	$1.9.10^{-2}$
VIII-t-XVI^{478}	0.027	0.034	0.000	nr	2.2	2.8	0.0	nr
VIII-t-XVI^{555}	0.411	0.464	0.206	$5.5.10^{-8}$	34.6	43.2	3.8	$3.1\ 10^{-4}$
VIII-t-XVI^{631}	0.008	0.010	0.000	nr	0.8	1.0	0.0	nr
VIII-t-XVI (*all alleles*)	0.539	0.529	0.575	0.18	41.4	49.1	13.8	$6.7.10^{-8}$
XV-t-XVI^{496}	0.041	0.026	0.100	$8.4.10^{-3}$	1.4	0.6	3.6	nr
inv-XVI^{781}	0.042	0.053	0.000	nr	4.4	5.6	0.0	nr
XVI-wt^{991}	0.337	0.322	0.394	0.21	21.8	25.4	8.5	$3.1\ 10^{-4}$

nr: not relevant.

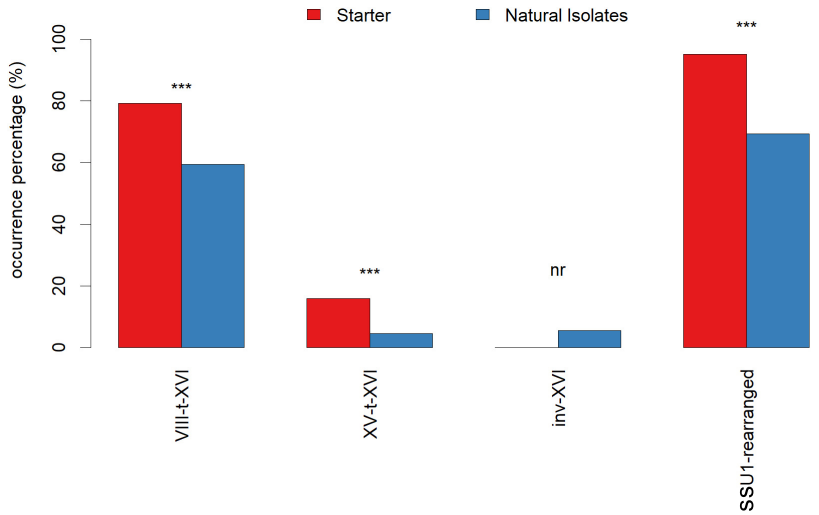

FIGURE 3 | Starters are enriched in rearranged chromosome XVI forms respect to natural isolates. The frequency (%) of "Starter" (red) and "Natural" (blue) isolates carrying at least one Chromosomal Rearrangement (CR) is represented. Significant differences are marked with ***.

not equally sulfited. This is consistent with the recommendations of International Organization of the Vine and Wine (OIV) that regulates the limits for total SO_2 in wines (150 mg/L for red wines and 200 mg/L for white wines and rosés) (OIV, 2019). Strains were split in three groups depending on the type of grape juice matrix: *sweet* (n = 67), *white* (n = 95) and *red* (n = 43). As shown in **Figure 4B**, strains isolated from *white juice* are enriched in the VIII-t-XVI rearrangements and a few of them are homozygous for the XVI-wt^{991} allele. In contrast, strains isolated from *sweet* grape juices are strongly enriched in the native chromosome form. For this group, the occurrence percentage of XVI-wt is 0.55, which is twice as much as the overall percentage of cellar population (0.26). These results are consistent with the traditional enological practices used in the Bordeaux area, where the addition of sulfite in the musts is routinely used for dry white wine fermentation, but mostly avoided in the beginning of sweet wine fermentation to limit SO_2 binding phenomena. This suggests that the selection of CR is strongly influenced by the winemaking practices used in cellars.

Analysis of *SSU1* Allelic Variability in Closely Related Populations

The impact of translocations in the phenotypic adaptation of yeast has been widely investigated by using genetically engineered strains (Tosato and Bruschi, 2015; Fleiss et al., 2019). However, the survey of chromosomal rearrangements in clonal populations is much less described. The *SSU1* checkup method provides an indirect opportunity to analyze this CR variability. In this section, the pool of 194 closely related clones was used in order to identify nearly isogenic groups of strains. In order to minimize the genetic distance inside a group, only strains showing less than two VNTR (Variable Number of Tandem Repeat) or LOH (Loss of Heterozygosity) were grouped together. By this way, 16 nearly genetic groups were identified encompassing 125 strains

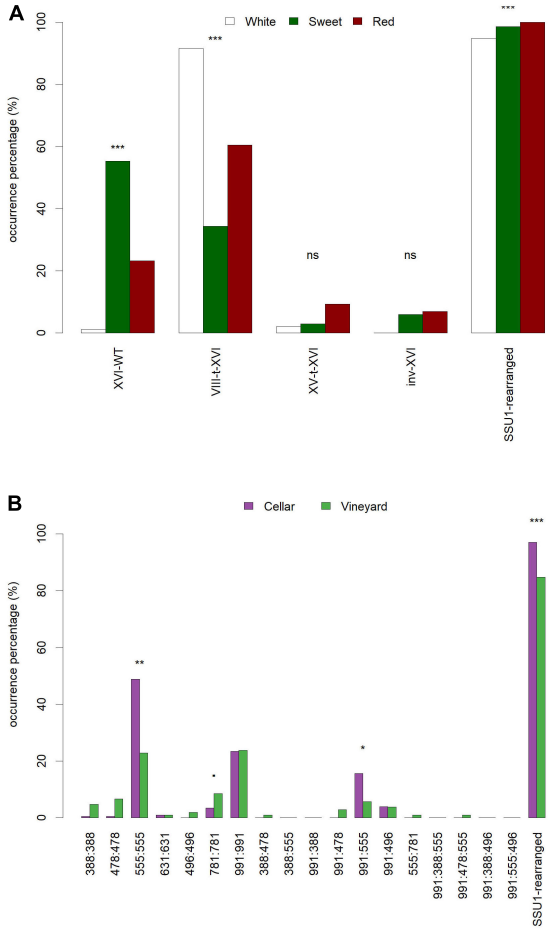

FIGURE 4 | Grape juice matrixes and sampling methods impact the occurrence of SSU1 alleles. **(A)** Occurrence frequency (%) of 18 biallelic combinations of the seven chromosome XVI alleles. **(B)** Occurrence frequency (%) of rearranged chromosome XVI forms and chromosome XVI-wt form based on the type of grape juice matrix (sweet, white and red). *** significance level <0.001; ** significance level <0.05; * significance level <0.1, corrected Chi^2 test; ns: not significant.

(**Supplementary Table S5**). Group sizes ranged between 3 and 22 individuals, with a Bruvo's genetic distance between the strains of each group always lower than 0.106. In most of the cases, strains belonging to the same group were isolated from the same vat/cellar/area samples; however, in groups 6, 11, and 15 strong similarities were found between strains from white and red samples. This is consistent with the fact that isogenic strains can be isolated from different grape juices/cellars as previously demonstrated (Borlin, 2015; Franco-Duarte et al., 2015). The relative distance between each group was illustrated by a Principal Component Analysis (**Figure 5A**).

Considering that each isogenic group is derived from a common clonal population, we analyzed the heterogeneity fraction in each group for three types of loci: microsatellites, chromosome VIII and chromosome XVI. For each group, the most frequent genotype was used as a reference (**Supplementary Table S5**). For microsatellite loci, few VNTR and LOH variations were detected among individuals. Within the 15 microsatellite markers, the average heterogeneity fraction was 2.4 and 2.1%, for VNTR and LOH, respectively (**Table 3**). In the same way, the heterogeneity fraction for chromosomes VIII and XVI were computed. Interestingly, a noteworthy variability was found for 10 out the 16 groups. For chromosome VIII, LOH events were observed only in groups 4 and 14 while tandem repeat shifts of the *ECM34* promoter (VNTR) impacted in four groups. The overall allelic variability for the chromosome VIII locus was 4.5%, which is slightly higher than the average variability observed for neutral markers (microsatellites) (**Table 3**).

The inheritance of chromosome XVI is more complex to analyze due to the combined influences of VNTR, LOH and the different CR (**Figure 5B**). These changes were observed in 7 out the 16 groups, being their overall frequency 2.9, 1.3, and 7.7%, respectively. These allelic changes were mostly found within strains isolated at the same place and showing the same microsatellite pattern. For VNTR, four isogenic groups showed allelic variations in the VIII-t-XVI translocation. These variations were due to a different number of tandem repeats on the *ECM34* promoter; their frequencies were similar to those observed for chromosome VIII (2.9 vs. 3.7%). LOH variations were observed for two groups (i.e., 3 and 11). For instance, the main genotype observed in the group 11 was 555:555 (12 out 16 strains) but two strains (*3bibi6_26* and *3bebi3_13*) have the genotype 991:555. This difference suggested that the strains that have inherited the XVI-wt^{991} form might have resulted from a hybridization event; alternatively the strain group homozygous for the translocation VIII-t-XVI^{555} could have been the result of meiotic segregation (Mortimer et al., 1994). Interestingly, the C6 microsatellite (localized on chromosome XVI) did not have the same inheritance in the strains *3bibi6_26* and *3bebi3_13*. Also, in the same group 11, the strains CLA2016 1 and 2 isolated from Chardonnay (white grape juice) showed a longer VIII-t-XVI allele (617:617) but shared exactly the same microsatellite pattern than the 12 strains isolated from Merlot vats. This supports the idea that alternative numbers of tandem repetitions in the *ECM34* promoter can be found in clonal populations. More surprisingly, different CR were also observed within isogenic groups. This is the case of strains 13AQGUICUV1 (555:555) and 14AQGUICUV1 (991:496) isolated from the same area in sweet wines. The first strain is homozygous with a VIII-t-XVI form while the second strain is heterozygous with both XVI-wt and XV-t-XVI forms. These two clones could have resulted from the meiotic segregation of an aneuploid strain carrying the three chromosome XVI alleles (VIII-t-XVI^{555}, XVI-wt^{991} and XV-t-XVI^{496}). One more time, the microsatellite C6 has not the same inheritance between these two strains supporting this hypothesis. A similar case of heterogeneity was also observed for strains 2duSPO9 (555:555) and 3mabi1_10 (991:496) that belong to group 6. Interestingly, the strain 2duSPO9 (555:555) was isolated from a Sauvignon blanc juice while all the other strains of this group were isolated from red grape juice (**Supplementary Table S5**). This is consistent with the fact that the translocation VIII-t-XVI^{555} was more frequently found in samples isolated from white grape juice (**Figure 4B**). All these findings were verified by simple PCR reactions,

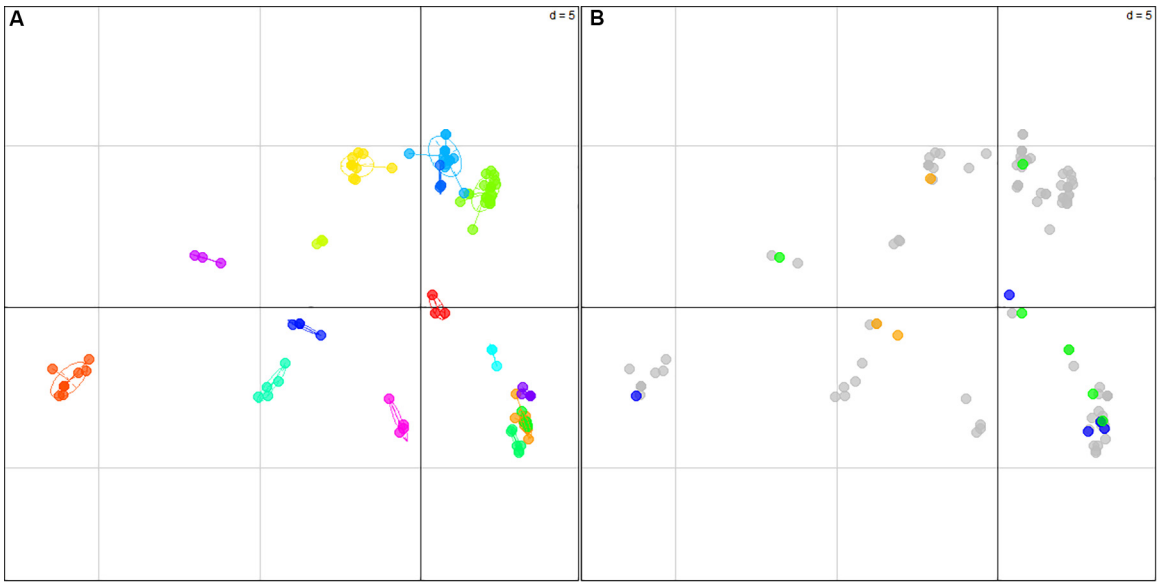

FIGURE 5 | Alleles of chromosome XVI show a rapid evolution in isogenic populations. **(A)** Principal Component Analysis of 125 closely related clones (nearly isogenic) discriminated by 15 polymorphic loci. The sixteen groups were inferred manually by considering as isogenic the strains having an identical genotype for at least 13 microsatellite loci. The projection of each strain according to the 16 groups represents 14.3% of the total inertia. The Bruvo's genetic distance within each group is always lower than 0.105. **(B)** represents the same projection, but strains were colored according to the type of change occurring on chromosome XVI. Gray dots represent the major allelic form found in each subgroup while orange, blue, and green dots represent LOH, VNTR, and CR, respectively.

TABLE 3 | Heterogeneity fraction of VNTR, LOH and CR in isogenic populations.

Group	Number of strains	Average Bruvo's distance[a]	Microsatellites		Chromosome VIII		Chromosome XVI		
			VNTR[b]	LOH[b]	VNTR[b]	LOH[b]	VNTR[b]	LOH[b]	CR[b]
1	5	0.09	2.7	6.7	0	0	0	0	0
2	3	0.04	0	0	0	0	0	0	0
3	12	0.03	1.7	1.7	0	0	0	8.3	0
4	6	0.006	2.2	0	16.7	50	0	0	0
5	6	0.105	7.8	0	0	0	16.7	0	0
6	15	0.05	3.1	2.2	6.7	0	0	0	6.7
7	4	0.07	1.7	6.7	0	0	0	0	0
8	3	0.05	0	2.2	0	0	0	0	0
9	3	0.02	0	2.2	0	0	0	0	33.3
10	22	0.06	1.5	5.5	0	0	0	0	0
11	16	0.014	2.5	0	0	0	12.5	12.5	0
12	10	0.037	2.7	0	0	0	0	0	0
13	4	0.044	5	0	25	0	0	0	50
14	3	0.023	0	2.2	0	33.3	33.3	0	33.3
15	4	0.055	6.7	1.7	0	0	0	0	0
16	9	0.07	1.5	3	11.1	0	11.1	0	0
TOTAL	125	0.05	2.4	2.1	3.7	5.2	2.9	1.3	7.7

[a]Average genetic distance computed from the genetic distance matrix between all the strains of the group. [b]The average heterogeneity fraction was expressed in percentage of change per locus (15 loci for microsatellites and one locus for chromosomes VIII and XVI). VNTR: Variable Number of Tandem Repeat, LOH: Loss Of Heterozygosity, CR: Chromosomal Rearrangement.

after additional DNA extractions. Although the number of events observed is not sufficient for providing robust data, our results illustrate an important heterogeneous fraction among *SSU1* alleles in clonal populations that would likely be due to meiotic recombination events. These microevolutionary changes between an industrial strain and its descendants selected after persistence in nature were previously reported using inter-*delta* markers (Franco-Duarte et al., 2015). In the case of the *SSU1* promoter, these allelic changes would play a significant role in the adaptative responses to different environments

especially due to the use or not of SO_2 in the early stages of vinification.

Impact of Chromosomal Rearrangements on Yeast Fitness Parameters in Sulfited Grape Juice

Finally, we compared groups of unrelated strains harboring six different promoter regions of the gene *SSU1*. Five representative yeast strains of each group were selected by choosing strains with contrasted microsatellite inheritance and sampling origins. Indeed, strains belonging to each group showed an average Bruvo's genetic distance higher than 0.50. These genetic distances were similar to those observed for the total population (**Supplementary Figure S5**). Therefore, the strains selected could be considered as genetically unrelated. To simplify the interpretation of the data, the strains selected are homozygous for the six promoter regions. Growth kinetics of these strains in filtered Sauvignon blanc grape juice spiked with different SO_2 concentrations were analyzed by OD_{600} measurements. Since some strains did not reach an OD_{600} plateau after 96 h, only μmax (maximal growth rate) and *Lag Time* (Lag phase time) parameters were analyzed. An overview of the kinetics for the reference strains GN, SB, P5 and Fx10 is given in **Supplementary Figure S6**. The effect of SO_2 concentration and type of chromosome XVI were estimated by a two-way ANOVA (model Lm1, see section "Materials and Methods"). The variance explained by factors is given in **Table 4**. As expected, SO_2 addition to the grape juice significantly impacted the μmax and the *Lag Time* parameters explaining 14.8 and 18.4% of total variance, respectively. This confirms the selective pressure imposed by increasing SO_2 concentrations, which delayed the beginning of exponential growth and reduced the maximum growth rates of *S. cerevisiae* strains. In addition, the type of chromosome XVI significantly impacted these two parameters (**Table 4**) contributing in higher proportion to the total variance observed (23.5% for *Lag Time* and 17.0% for μmax). Finally, a significant interaction was detected between SO_2 concentration and the type of chromosome XVI type for the *Lag Time* parameter ($p < 1.10^{-6}$).

The specific impact of the form of the *SSU1* promoter is illustrated in **Figure 6**. Since five unrelated strains were tested in each group, the impact of the different *SSU1* promoters is partially decoupled to the strain effect. As expected, "*non-rearranged*

TABLE 4 | Analysis of variance of SO_2 and SSU1 promoter forms for lag time and μmax.

Trait	SO_2		Chr XVI		SO_2:Chr XVI interactions		Residual	Levene test (*p*-value)
	Effect	*p*-value[a]	Effect	*p*-value[a]	Effect	*p*-value		
Lag time	18.4	$<2.2\ 10^{-16}$	23.5	$<2.2\ 10^{-16}$	7.0	$1.1\ 10^{-5}$	50.7	0.06
μ max	14.8	$1.8\ 10^{-11}$	17.0	$6.9\ 10^{-10}$	2.5	0.12	65.6	0.002

[a]*ANOVA p-value.*

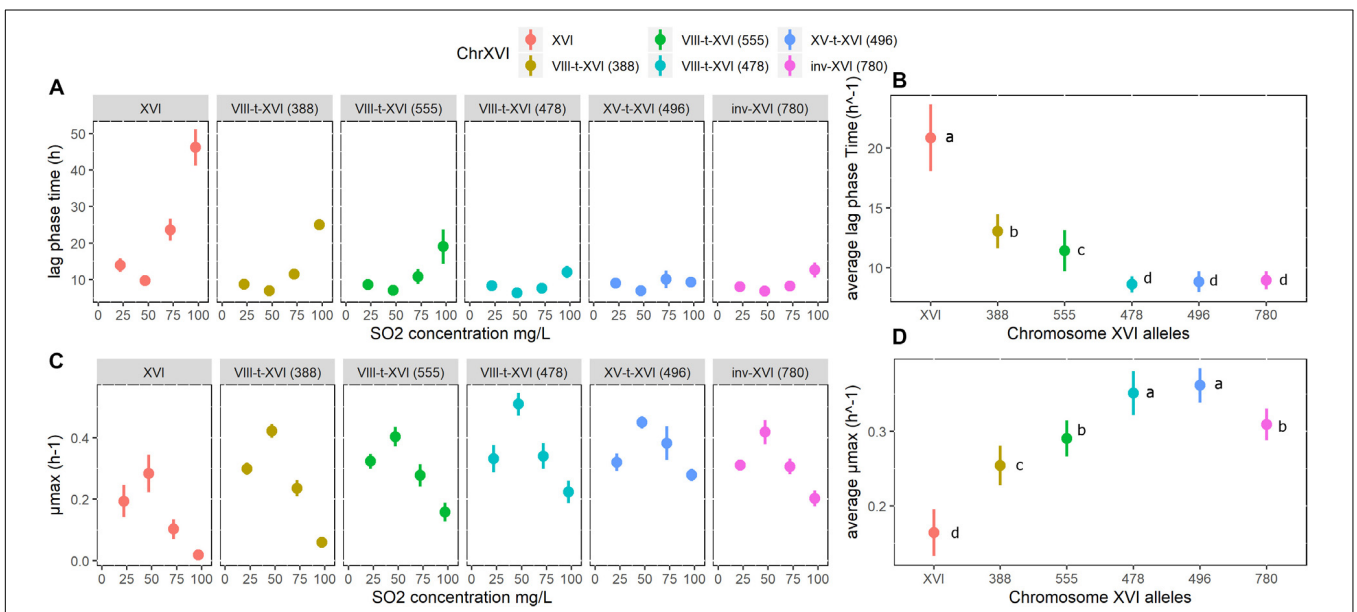

FIGURE 6 | Phenotypic impact of six SSU1 promoter alleles. **(A)** Mean of the Lag Times (in hours) of the 5 strains tested at different SO_2 concentrations, for each of the chromosome XVI alleles. **(B)** Mean of the Lag Times (in hours) of the 5 strains tested at all SO_2 concentrations, for each of the chromosome XVI alleles. **(C)** Mean of the μmax of the 5 strains tested at different SO_2 concentrations, for each of the chromosome XVI alleles. **(D)** Mean of the μmax of the 5 strains tested at all SO_2 concentrations, for each of the chromosome XVI alleles.

strains" (i.e., XVI-wt/XVI-wt) present the highest *Lag Time* and the lowest μmax at high SO_2 concentrations. The translocation XV-t-XVI and the inversion (inv-XVI) appear to be very efficient to cope with higher SO_2 concentrations. Indeed, strains carrying these alleles were poorly affected by the addition of 75 mg/L of SO_2. These findings are consistent with the elevated *SSU1* expression levels reported for these two chromosomal rearrangements (Zimmer et al., 2014; García-Ríos and Guillamón, 2019). For the VIII-t-XVI translocations, only three allelic forms (VIII-t-XVI^{388}, VIII-t-XVI^{478}, VIII-t-XVI^{555}) were tested. The fourth allele (VIII-t-XVI^{631}) was found in only three strains, two of them being clearly isogenic. The allele VIII-t-XVI^{478} was the most efficient in reducing the *Lag Time* and preserving the μmax. The other two alleles (VIII-t-XVI^{388} and VIII-t-XVI^{555}) resulted in the least favorable rearrangements for sulfite tolerance (**Figure 6**).

Differences in the length of the VIII-t-XVI translocation alleles mainly result from the variable number of 76 bp tandem repeat units (Goto-Yamamoto et al., 1998). The number of tandem repeats (76 and 47 bp) for the VIII-t-XVI translocation was verified by DNA sequencing and results are summarized in **Supplementary Figure S4**. Alleles VIII-t-XVI^{388}, VIII-t-XVI^{478}, and VIII-t-XVI^{555} show two, three, and four 76 bp tandem repeats plus one additional 47 bp tandem repeat, respectively. Since the allele VIII-t-XVI^{478} out competed the other two forms (**Figure 6**), we can conclude that the number of tandem repeats and the SO_2 tolerance are not fully correlated, as previously reported (Yuasa et al., 2004). Therefore, undetermined natural allelic variations in the *SSU1* coding sequence, in flanking regions, or in other genomic loci are possibly also involved in this trait.

By comparing for the first time the effect of six configurations of the *SSU1* promoter on yeast fitness we pave the way for screening sulfite tolerance of strains in a simple genetic test. The alleles XV-t-XVI, inv-XVI and VIII-t-XVI^{478} confer an efficient adaptation for growing in grape juices with high concentrations of SO_2. In addition, we illustrate that for the translocation VIII-t-XVI, the sulfite resistance (maximal growth rate and lag phase) is not perfectly related to the number of 76 bp tandem repeats. Indeed, from a technological point of view, the allele VIII-t-XVI^{478} would be the most efficient form to tolerate high sulfite concentrations in natural grape juice.

CONCLUSION

In yeast, CR are thought to play a role in adaptation and species evolution and might have physiological consequences (Tosato and Bruschi, 2015). The setup of a *SSU1* checkup provides a rapid molecular tool for obtaining a complete overview of three CR involving the promoter region of *SSU1*. This molecular diagnostic was helpful to address some questions related to the impact of domestication of wine yeast and to progress in the identification of physio-ecological parameters that reshape the genome organization in natural isolates. From an ecological point of view, the *SSU1* checkup could be in the future a key molecular tool for addressing different questions in relation to the use of sulfites in wine. Indeed, in the recent years, the consumer-driven push for decreasing the levels of SO_2 in the wine industry and the low-sulfite wine market are increasing and could modify the allelic frequency of *SSU1* promoter alleles. From a more applied point of view, we established a link between quantitative phenotypes and the inheritance of CR in genetically unrelated groups paving the way for yeast selection programs mediated by molecular markers.

DATA AVAILABILITY STATEMENT

The datasets generated for this study can be found in the GenBank (ID 2310529).

AUTHOR CONTRIBUTIONS

PM, OC, and IM-P designed the experiment. MR, OC, MBö, NF, MBe, and AR did the experiment. PM, OC, and MR wrote the manuscript. MBö, WA, J-LL, PM, OC, and MR analyzed the data. PM, AR, and IM-P got the grants. All authors contributed to the article and approved the submitted version.

FUNDING

PM recieved funds from the Biolaffort Company and form the Region Aquitaine Grant SESAM for delevopping Marker Assisted Selection. This work was supported by PICT-2014-3113 from Fondo para la Investigación Científica y Tecnológica (FONCyT) (Argentina) and SUV2015 (Universidad Católica de Córdoba) to AR. MR held a fellowship from the National Research Council of Argentina (CONICET). AR is a Career Research Investigator from CONICET. The funder bodies were not involved in the study design, collection, analysis, interpretation of data, the writing of this article or the decision to submit it for publication.

ACKNOWLEDGMENTS

The authors would like to thank José Manuel Guillamon (Spanish National Research Council) for providing the P5 strain.

SUPPLEMENTARY MATERIAL

The Supplementary Material for this article can be found online at: https://www.frontiersin.org/articles/10.3389/fmicb.2020.01331/full#supplementary-material

FIGURE S1 | Bruvo's distance distribution and cut off threshold used for removing very similar strains.

FIGURE S2 | Natural isolates closely related to industrial starters.

FIGURE S3 | (A) Principal Component analysis of 82 commercial starters discriminated by 15 polymorphic loci. The three groups represented (A to C) were inferred by k-mean clustering. The **(B)** represents the position of the strains according to the inferred groups.

FIGURE S4 | Schematic representation of a VIII allele of S. cerevisiae. The figure shows the location of the 76 bp Tandem Repeats and the 47 bp Tandem Repeats, as well as the translocation point (TP) and the upstream (5′ region; from the end of the forward primer to the beginning of the 76 bp tandem repeats) and downstream (3′region; from the end of the 47 bp tandem repeats to the translocation point) flanking regions. The hybridization position for the primers forward (F; p1189) and reverse (R; either p1190 or p1194), are indicated.

FIGURE S5 | Genetic distance between individuals sharing six SSU1 promoter types, only the strains homozygous for these alleles were considered. The color blue and red indicate the distribution of pair wise Bruvo's genetic distance for the total set of strains and the subset of five strains selected.

FIGURE S6 | Growth curves of reference strains in different grape juice containing different SO_2 concentrations expressed in mg/L. The data presented are the average of two independent replicates for the strain Fx10 (red), GN (green), P5 (cyan), and SB (purple). Standard error was figured out by the shaded area.

TABLE S1 | List of the 586 strains analyzed in this work.

TABLE S2 | Additional primers used.

TABLE S3 | List of the 30 strains phenotyped.

TABLE S4 | Contingency table of natural isolates origin according to the microsatellite groups.

TABLE S5 | List of the 16 isogenic subgroups identified encompassing 125 strains.

REFERENCES

Aa, E., Townsend, J. P., Adams, R. I., Nielsen, K. M., and Taylor, J. W. (2006). Population structure and gene evolution in *Saccharomyces cerevisiae*. *FEMS Yeast Res.* 6, 702–715. doi: 10.1111/j.1567-1364.2006.00059.x

Albertin, W., Marullo, P., Aigle, M., Bourgais, A., Bely, M., Dillmann, C., et al. (2009). Evidence for autotetraploidy associated with reproductive isolation in *Saccharomyces cerevisiae*: Towards a new domesticated species. *J. Evol. Biol.* 22, 2157–2170. doi: 10.1111/j.1420-9101.2009.01828.x

Avram, D., and Bakalinsky, A. T. (1997). SSU1 encodes a plasma membrane protein with a central role in a network of proteins conferring sulfite tolerance in *Saccharomyces cerevisiae*. *J. Bacteriol.* 179, 5971–5974. doi: 10.1128/jb.179.18.5971-5974.1997

Avramova, M., Cibrario, A., Peltier, E., Coton, M., Coton, E., Schacherer, J., et al. (2018). *Brettanomyces bruxellensis* population survey reveals a diploid-triploid complex structured according to substrate of isolation and geographical distribution. *Sci. Rep.* 8:4136. doi: 10.1038/s41598-018-22580-7

Borlin, M. (2015). *Diversity and Population Structure of Yeast Saccharomyces cerevisiae at the Scale of the Vineyard of Bordeaux?: Impact of Different Factors on Diversity*. Available online at: https://tel.archives-ouvertes.fr/tel-01293834 (accessed December 2015).

Börlin, M., Venet, P., Claisse, O., Salin, F., Legras, J.-L., and Masneuf-Pomarede, I. (2016). Cellar-associated *Saccharomyces cerevisiae* population structure revealed high-level diversity and perennial persistence at sauternes wine estates. *Appl. Environ. Microbiol.* 82, 2909–2918. doi: 10.1128/AEM.03627-15

Borneman, A. R., Forgan, A. H., Kolouchova, R., Fraser, J. A., and Schmidt, S. A. (2016). Whole genome comparison reveals high levels of inbreeding and strain redundancy across the spectrum of commercial wine strains of *Saccharomyces cerevisiae*. *G3* 6, 957–971. doi: 10.1534/g3.115.025692

Borneman, A. R., and Pretorius, I. S. (2014). Genomic insights into the Saccharomyces sensu stricto complex. *Genetics* 199, 281–291. doi: 10.1534/genetics.114.173633

Brion, C., Ambroset, C., Sanchez, I., Legras, J.-L., and Blondin, B. (2013). Differential adaptation to multi-stressed conditions of wine fermentation revealed by variations in yeast regulatory networks. *BMC Genomics* 14:681. doi: 10.1186/1471-2164-14-681

Cheraiti, N., Guezenec, S., and Salmon, J.-M. (2010). Very early acetaldehyde production by industrial *Saccharomyces cerevisiae* strains: a new intrinsic character. *Appl. Microbiol. Biotechnol.* 86, 693–700. doi: 10.1007/s00253-009-2337-5

Chernova, M., Albertin, W., Durrens, P., Guichoux, E., Sherman, D. J., Masneuf-Pomarede, I., et al. (2018). Many interspecific chromosomal introgressions are highly prevalent in Holarctic *Saccharomyces uvarum* strains found in human-related fermentations. *Yeast* 35, 141–156. doi: 10.1002/yea.3248

Clowers, K. J., Heilberger, J., Piotrowski, J. S., Will, J. L., and Gascha, P. (2015). Ecological and genetic barriers differentiate natural populations of *Saccharomyces cerevisiae*. *Mol. Biol. Evol.* 32, 2317–2327. doi: 10.1093/molbev/msv112

Divol, B., Du Toit, M., and Duckitt, E. (2012). Surviving in the presence of sulphur dioxide: Strategies developed by wine yeasts. *Appl. Microbiol. Biotechnol.* 95, 601–613. doi: 10.1007/s00253-012-4186-x

Engle, E. K., and Fay, J. C. (2012). Divergence of the yeast transcription factor FZF1 affects sulfite resistance. *PLoS Genet.* 8:e2763. doi: 10.1371/journal.pgen.1002763

Fleiss, A., O'Donnell, S., Fournier, T., Lu, W., Agier, N., Delmas, S., et al. (2019). Reshuffling yeast chromosomes with CRISPR/Cas9. *PLoS Genet.* 15:e1008332. doi: 10.1371/journal.pgen.1008332

Franco-Duarte, R., Bigey, F., Carreto, L., Mendes, I., Dequin, S., Santos, M. A., et al. (2015). Intrastrain genomic and phenotypic variability of the commercial *Saccharomyces cerevisiae* strain Zymaflore VL1 reveals microevolutionary adaptation to vineyard environments. *FEMS Yeast Res.* 15:fov063. doi: 10.1093/femsyr/fov063

García-Ríos, E., and Guillamón, J. M. (2019). Sulfur dioxide resistance in *Saccharomyces cerevisiae*: beyond SSU1. *Microb. Cell* 6, 527–530. doi: 10.15698/mic2019.12.699

García-Ríos, E., Nuévalos, M., Barrio, E., Puig, S., and Guillamón, J. M. (2019). A new chromosomal rearrangement improves the adaptation of wine yeasts to sulfite. *Environ. Microbiol.* 21, 1771–1781. doi: 10.1111/1462-2920.14586

Goto-Yamamoto, N., Kitano, K., Shiki, K., Yoshida, Y., Suzuki, T., Iwata, T., et al. (1998). SSU1-R, a sulfite resistance gene of wine yeast, is an allele of SSU1 with a different upstream sequence. *J. Ferment. Bioeng.* 86, 427–433. doi: 10.1016/S0922-338X(98)80146-3

Hinze, H., and Holzer, H. (1986). Analysis of the energy metabolism after incubation of *Saccharomyces cerevisiae* with sulfite or nitrite. *Arch. Microbiol.* 145, 27–31. doi: 10.1007/BF00413023

Legras, J.-L. L., Merdinoglu, D., Cornuet, J.-M. M., and Karst, F. (2007). Bread, beer and wine: *Saccharomyces cerevisiae* diversity reflects human history. *Mol. Ecol.* 16, 2091–2102. doi: 10.1111/j.1365-294X.2007.03266.x

Marsit, S., and Dequin, S. (2015). Diversity and adaptive evolution of Saccharomyces wine yeast: a review. *FEMS Yeast Res.* 15:fov067. doi: 10.1093/femsyr/fov067

Martí-Raga, M., Marullo, P., Beltran, G., Mas, A., Marti-Raga, M., Marullo, P., et al. (2016). Nitrogen modulation of yeast fitness and viability during sparkling wine production. *Food Microbiol.* 54, 106–114. doi: 10.1016/j.fm.2015.10.009

Marullo, P., Bely, M., Masneuf-Pomarède, I., Pons, M., Aigle, M., Dubourdieu, D., et al. (2006). Breeding strategies for combining fermentative qualities and reducing off-flavor production in a wine yeast model. *FEMS Yeast Res.* 6, 268–279. doi: 10.1111/j.1567-1364.2006.00034.x

Marullo, P., Mansour, C., Dufour, M., Albertin, W., Sicard, D., Bely, M., et al. (2009). Genetic improvement of thermo-tolerance in wine *Saccharomyces cerevisiae* strains by a backcross approach. *FEMS Yeast Res.* 9, 1148–1160. doi: 10.1111/j.1567-1364.2009.00550.x

Mortimer, R. K., Romano, P., Suzzi, G., and Polsinellif, M. (1994). Genome renewal: a new phenomenon revealed from a genetic study of 43 Strains of *Saccharomyces cerevisiae* derived from natural fermentation of grape musts. *YEAST* 10, 1543–1552. doi: 10.1002/yea.320101203

Nardi, T., Corich, V., Giacomini, A., and Blondin, B. (2010). A sulphite-inducible form of the sulphite efflux gene SSU1 in a *Saccharomyces cerevisiae* wine yeast. *Microbiology* 156, 1686–1696. doi: 10.1099/mic.0.036723-0

Novo, M., Bigey, F., Beyne, E., Galeote, V., Gavory, F., Mallet, S., et al. (2009). Eukaryote-to-eukaryote gene transfer events revealed by the genome sequence of the wine yeast *Saccharomyces cerevisiae* EC1118. *Proc. Natl. Acad. Sci. U.S.A.* 106, 16333–16338. doi: 10.1073/pnas.0904673106

OIV (2019). *Compendium of International Methods of Analysis of Wine and Musts*. Paris: OIV.

Park, H., and Bakalinsky, A. T. (2000). SSU1 mediates sulphite efflux in *Saccharomyces cerevisiae*. *Yeast* 16, 881–888. doi: 10.1002/1097-0061(200007)16:10<881::AID-YEA576<3.0.CO;2-3

Park, H., and Hwang, Y. S. (2008). Genome-wide transcriptional responses to sulfite in *Saccharomyces cerevisiae*. *J. Microbiol.* 46, 542–548. doi: 10.1007/s12275-008-0053-y

Peltier, E., Sharma, V., Marti Raga, M., Roncoroni, M., Bernard, M., Jiranek, V., et al. (2018a). Genetic basis of genetic x environment interaction in an enological context. *BMC Genomics*, 19:772.

Peltier, E., Sharma, V., Raga, M. M., Roncoroni, M., Bernard, M., Yves, G., et al. (2018b). Dissection of the molecular bases of genotype x environment interactions: a study of phenotypic plasticity of *Saccharomyces cerevisiae* in grape juices. *BMC Genomics* 19:772. doi: 10.1186/s12864-018-5145-4

Pérez-Ortín, J. E., Querol, A., Puig, S., and Barrio, E. (2002). Molecular characterization of a chromosomal rearrangement involved in the adaptive evolution of yeast strains. *Genome Res.* 12, 1533–1539. doi: 10.1101/gr.436602

Peter, J., De Chiara, M., Friedrich, A., Yue, J.-X., Pflieger, D., Bergström, A., et al. (2018). Genome evolution across 1,011 *Saccharomyces cerevisiae* isolates. *Nature* 556, 339–344. doi: 10.1038/s41586-018-0030-5

Raymond, E. M. L., Conti, F., and Rosa, A. L. (2018). Differences between indigenous yeast populations in spontaneously fermenting musts from *V. vinifera* L. and *V. labrusca* L. Grapes harvested in the same geographic location. *Front. Microbiol.* 9:1320. doi: 10.3389/fmicb.2018.01320

Sicard, D., and Legras, J. L. (2011). Bread, beer and wine: Yeast domestication in the Saccharomyces sensu stricto complex. *Comptes Rendus Biol.* 334, 229–236. doi: 10.1016/j.crvi.2010.12.016

Tosato, V., and Bruschi, C. V. (2015). Per aspera ad astra: When harmful chromosomal translocations become a plus value in genetic evolution. lessons from *Saccharomyces cerevisiae*. *Microb. Cell* 2, 363–375. doi: 10.15698/mic2015.10.230

Valero, E., Schuller, D., Cambon, B., Casal, M., and Dequin, S. (2005). Dissemination and survival of commercial wine yeast in the vineyard: A large-scale, three-years study. *FEMS Yeast Res.* 5, 959–969. doi: 10.1016/j.femsyr.2005.04.007

Yuasa, N., Nakagawa, Y., Hayakawa, M., and Iimura, Y. (2004). Distribution of the sulfite resistance gene SSU1-R and the variation in its promoter region in wine yeasts. *J. Biosci. Bioeng.* 98, 394–397. doi: 10.1263/jbb.98.394

Zimmer, A., Durand, C., Loira, N., Durrens, P., Sherman, D. J., and Marullo, P. (2014). QTL dissection of lag phase in wine fermentation reveals a new translocation responsible for *Saccharomyces cerevisiae* adaptation to sulfite. *PLoS One* 9:e86298. doi: 10.1371/journal.pone.0086298

Conflict of Interest: MB and PM are employed by the Biolaffort company.

The remaining authors declare that the research was conducted in the absence of any commercial or financial relationships that could be construed as a potential conflict of interest.

frontiers in Genetics

MINI REVIEW
published: 27 August 2020
doi: 10.3389/fgene.2020.00916

Genomic Adaptation of *Saccharomyces* Species to Industrial Environments

Konstantina Giannakou[1,2], *Mark Cotterrell*[2] *and Daniela Delneri*[1]*

[1] *Manchester Institute of Biotechnology, Faculty of Biology, Medicine and Health, The University of Manchester, Manchester, United Kingdom,* [2] *Cloudwater Brew Co., Manchester, United Kingdom*

The budding yeast has been extensively studied for its physiological performance in fermentative environments and, due to its remarkable plasticity, is used in numerous industrial applications like in brewing, baking and wine fermentations. Furthermore, thanks to its small and relatively simple eukaryotic genome, the molecular mechanisms behind its evolution and domestication are more easily explored. Considerable work has been directed into examining the industrial adaptation processes that shaped the genotypes of species and hybrids belonging to the *Saccharomyces* group, specifically in relation to beverage fermentation performances. A variety of genetic mechanisms are responsible for the yeast response to stress conditions, such as genome duplication, chromosomal re-arrangements, hybridization and horizontal gene transfer, and these genetic alterations are also contributing to the diversity in the *Saccharomyces* industrial strains. Here, we review the recent genetic and evolutionary studies exploring domestication and biodiversity of yeast strains.

Keywords: fermentation, *Saccharomyces*, adaptation, diversity, evolution

OPEN ACCESS

Edited by:
Francisco A. Cubillos, University of Santiago, Chile

Reviewed by:
Alexander DeLuna, Instituto Politécnico Nacional de México (CINVESTAV), Mexico
Marti Aldea, Instituto de Biología Molecular de Barcelona (IBMB), Spain

***Correspondence:**
Daniela Delneri
d.delneri@manchester.ac.uk

Specialty section:
This article was submitted to Evolutionary and Genomic Microbiology, a section of the journal Frontiers in Genetics

Received: *30 April 2020*
Accepted: *23 July 2020*
Published: *27 August 2020*

Citation:
Giannakou K, Cotterrell M and Delneri D (2020) Genomic Adaptation of Saccharomyces Species to Industrial Environments. Front. Genet. 11:916. doi: 10.3389/fgene.2020.00916

YEAST EVOLUTION IN INDUSTRIAL SETTINGS

Beer brewing and winemaking have been rapidly changing over the years involving the development of several fermentation protocols and the use of starter cultures. In the past, these processes were mainly occurring naturally. For example, grape juice and fresh hoppy wort were exposed to open air microorganisms to spontaneously ferment wine and beer.

While this natural process still find application in some beers (traditional lambic style, Spitaels et al., 2014) and specific type of wines (Walker, 2014; Chen et al., 2020), commercial products now largely employ the usage of starter cultures. The first pure yeast starter was created and used in beer production back in 1880s by E. C. Hansen from the Carlsberg laboratory in Denmark. In 1890s, also the first inoculation of a grape must with a yeast starter was performed. These practices became more common and *Saccharomyces cerevisiae* starters are primarily being used in wine and beer fermentations, to facilitate the consistency of fermented beverages resulting in products with stable characteristics, aromas and flavors as well as ensuring rapid fermentation times (Valero et al., 2007).

Yeast species belonging to the *Saccharomyces* genus have been extensively used in fermentation, and throughout the years the ability to ferment has evolved from the exposure to stressful conditions (Gallone et al., 2016). *Saccharomyces* "make-accumulate-tolerate-consume" strategy enables fast growth during anaerobic conditions, maximizes ethanol and flavor metabolites production together with preventing growth of antagonistic microbes by creating a hostile

environment for them to survive (Piškur et al., 2006; Goold et al., 2017). During wine and beer fermentation yeasts are exposed to numerous stresses such as high osmotic pressure, oxidative stress, temperature shifts, low oxygen availability, CO_2 accumulation, nutrient restraint and high ethanol concentration (Legras et al., 2018). Typically, *Saccharomyces spp.* expresses its fermentative ability either in mixture of high sugar environments such as brewing wort and grape juice or even in hydrolyzed lactose in fermented milk. As a result of this environmental variation, yeast strains diversified extensively in industrial settings and became adapted to the production of specific beverages (**Table 1**).

The extent of these adaptations can be easily detected in *S. cerevisiae* and *S. pastorianus*, the workhorses of beer fermentation, that have shown wide phenotypic variation to different beer fermentation conditions. These species have evolved so that their unique complexity and diversity can generate different beer related products. Some characteristics of industrial isolates are high consumption rate of complex sugars like maltose and maltotriose, enhanced tolerance to hyperosmotic stress, high ethanol production and simultaneous repression of undesired metabolites such as beer off-flavors (Gibson et al., 2013; Steensels et al., 2014; Hill, 2015; Gallone et al., 2018). Normally, brewing strains are able to ferment adequately a 12–14 P wort and produce 5–6% ethanol (v/v). However, some yeasts are suitable for "high gravity" brewing (i.e., high amount of total sugars diluted in water) as they are able to utilize the elevated sugar content and tolerate the higher ethanol concentrations. In high gravity brewing, highly concentrated wort is fermented to beer and then diluted to the desired ethanol concentration. It is a sustainable approach for increasing brewery yields, reduce production costs, and produce a variety of different products with higher or lower alcohol levels (Pátková et al., 2000; Piddocke et al., 2009; Caspeta et al., 2019). Wort gravity also affects the final beer flavor and the formation of volatiles and thus not all yeast strains are suitable for this fermentation (Piddocke et al., 2009; Lei et al., 2012). Industrial isolates from different sources have phenotypes associated with adaptation to that specific source. For example, rapid maltose utilization and fermentation is found in baker's yeast (Bell et al., 2001) and higher ethanol production rates in sake and wine yeast (Uebayashi et al., 2018), however, the same ability varies significantly in non-industrial yeast strains.

MECHANISMS TO INDUCE GENETIC VARIATION IN INDUSTRIAL STRAINS

The environmental discontinuity has facilitated genetic diversification and phenotypic plasticity of yeast strains. Molecular patterns of domestication have now been explored in industrial yeasts, and significant variation have been shown among *Saccharomyces* beer, wine, sake and cider strains. *S. cerevisiae* brewing strains have shown remarkable population differentiation and are polyphyletic deriving from different geographical beer clades such as German, Belgian, and British ale. On the contrary wine, sake, and bread yeast have not shown much phenotypic diversity and are monophyletic (Almeida et al., 2015; Gonçalves et al., 2016). Population genomic studies of hundreds of *Saccharomyces* yeast strains reveal a remarkable level of variation in recombination rates and patterns even across very closely related lineages which can potentially translate in different phenotypic characteristics (Liti et al., 2009; Schacherer et al., 2009; Almeida et al., 2015). Advances in sequencing technologies have helped identification of yeast's genetic traits underpinning different phenotypes from a plethora of environments (Sniegowski, 1999; Cromie et al., 2013; David et al., 2014). For instance, High- Throughput Sequencing approaches facilitated the understanding of the grape microbiome in different environmental conditions. In grapes and berries the identified microbiome included species belonging to the family of *Dothioraceae*, *Pleosporaceae*, *Saccharomycodaceae*, *Enterobacteriales*, *Pseudomonadales*, *Bacillales,* and *Rhodospirillales* and differences in field origin were examined for its relevance to wine fermentation and production of flavor metabolites in Cannonau wine from Sardinia (Mezzasalma et al., 2017). Sequencing of polyploidy beer strains revealed a common genetic ancestry with wine strains from European and Asian lineages. Polyploidization facilitated the gain or loss of genetic variation related with brewing characteristics and also indicates the usage of co-cultures has been employed in fermented beverages (Fay et al., 2019).

Several mechanisms that accelerate evolution in environmental challenges and stressful conditions have been studied. Yeast adapt to new environments via smaller and/or larger genetic changes (Peter et al., 2018). Small variations can be caused from single nucleotide and frame shift mutations, insertions or deletions, which will end up creating alterations in the structure/function of the encoding protein or alterations in the gene expression. Larger changes include structural variation such as chromosomal rearrangements (duplications, translocations, and inversions), segmental duplication and gene copy number variation. Genetic variations can also be driven from interspecific hybridization with introgression and horizontal gene transfer events. This enables the generation of novel characteristics to the genome that it could not occur with other nucleotide arrangements.

COPY NUMBER VARIATIONS AND RE-ARRANGEMENTS

Recent whole genome sequencing and large-scale phenotyping data for 157 *S. cerevisiae* industrial brewing strains revealed that these yeasts are genetically and phenotypically separated from their wild ancestors through complex domestication events in the man-made environments (Gallone et al., 2016). The analysis shows that industrial strains can tolerance various stresses, have better performance and lack sexual reproduction. Insertions and deletions of small or large fragments were detected in most of the strains analyzed with the size of the fragment varying from a few base pairs to complete chromosomes. Deletion patterns and copy number variations commonly found in beer strains are connected with the high aneuploidy or polyploidy characteristic of brewing strains. It was also observed that all the industrial strains even from different beer clades show clear marks of domestication and

TABLE 1 | *Saccharomyces* spp. in production of alcoholic beverages.

Environment	Microorganism	Product	Stresses induced	References	Favorable characteristic
Brewing	*S. pastorianus*	Lager style beers	Cold fermentation temperature (7–10°C), maltose utilization, oxygen depletion	Hill, 2015	Clean "non-fruity" taste
Brewing	*S. cerevisiae*	Ale style beer	Maltose utilization, oxygen depletion	Hill, 2015	Fruity and aromatic taste
Brewing	*S. cerevisiae var. diastaticus*	German wheat beers	Starch utilization	Meier-Dörnberg et al., 2018	Phenolic flavor
Winemaking	*S. bayanus*	Chardonnay wines	High sugar content, high alcohol tolerance	Eglinton et al., 2000; Kelly et al., 2018	Application in cool climate vineyards
Winemaking	*Flor yeast*	Spanish sherry wines	O_2 presence, alcohol as the main carbon source	Jackson, 2014	Acetaldehyde
Winemaking	*S. cerevisiae S. bayanus*	Champagne	High ethanol tolerance	Martínez-Rodríguez et al., 2001	Foaming
Cider	*S. bayanus*	Ice-cider	Hyperosmotic stress, low pH, 15°C fermentation	Pando Bedriñana et al., 2017	Minimum residual sugars, 10% (v/v) final alcohol content
Sake	*S. cerevisiae*	Sake	High sugar content, high ethanol content	Katou et al., 2009	Isoamyl acetate, ethyl caproate
Distilling	*S. cerevisiae*	Whisky	40°C fermentation, high alcohol content	Walker et al., 2012	Dry finish, flavor consistency
Distilling	*S. cerevisiae*	Tequila	High fructose and ethanol content	Aldrete-Tapia et al., 2018	Reduced fermentation times

adaptation to industrial niches. This is consistent with the fact that the brewing industry is following common practices distinct from the wineries. In fact, wine yeast differs from the brewing ones, because of the seasonality of the wine production, the nutritional fluctuations and their sexual cycles. This can explain the population diversity (both in population size and in genome variety) of beer yeasts compared to wine yeasts. Chromosomal re-arrangements play an important role in the phenotypic variation of yeast strains both in the laboratory environment (Colson et al., 2004; Naseeb et al., 2016, 2017a) and in nature, where karyotypic instability is found in wild strains and can affect their performance when transferred to industrial settings (Carro et al., 2003; Dujon, 2010; Peter et al., 2018).

Genome re-arrangements and copy number variations results also in extensive alterations of the gene expression network (Naseeb et al., 2016) and it is not only limited to the function of a specific duplicated gene. Any fitness improvement is resulting from both environmental and genomic conditions and multiple changes in the transcriptome (Guan et al., 2007; Hakes et al., 2007; Naseeb et al., 2017a). Furthermore, differences have been identified in the copy number of genes involved in the metabolism of fermentable sugars such as maltose and maltotriose. Copy number variations are often reported as an adaptation mechanism to environmental changes (**Figure 1A**; Magadum et al., 2013). The maltose metabolism consists of 3 gene families: *MALT*, *MALS,* and *MALR* which comprise maltose transporters, maltases and regulator proteins, respectively (Brown et al., 2010). Fluctuations in chromosomal location and copy number of the involved *MAL* genes are present in many industrial strains. Typically, beer strains contain six or more copies of the *MAL3* locus (Gonçalves et al., 2016). Some German yeast strains were found to contain 15 copies of the *MAL31* gene while wine *Saccharomyces* strains contains only three copies (Gonçalves et al., 2016). Uptake and breakdown of maltose, the main carbon source in beer fermentation but not in grape/must, has been of great importance for the survival and performance of brewing yeast strains. This remarkable genetic alteration in maltose uptake is giving a great selection of brewing candidates that are able of fast utilization of this sugar. van der Broek and co-workers examined chromosomal number variation in *S. pastorianus* and its link with the phenotype. They analyzed three *S. pastorianus* W34/70 isolates that produced different diacetyl concentrations during beer fermentation. Diacetyl, a vicinal diketone, with butter flavor is considered an undesirable metabolite occurring through yeast valine metabolism during beer fermentation (Kusunoki and Ogata, 2012). Analysis of the DNA sequence of the valine biosynthetic genes (*ILV2, ILV6, ILV5,* and *ILV3*) in the three isolates did not reveal any single nucleotide polymorphism, however, copy number variation in the chromosomes carrying those genes was identified. This resulted in one isolate containing extra copies of the *ILV5* and *ILV3* genes, that responsible for the downstream catalysis of a-acetolactate the precursor of diacetyl. Thus, this strain was a low-diacetyl producing isolate of W34/70 (van den Broek et al., 2015).

In wine yeast, studies have shown significant adaptation motifs to sulfite compounds. Sulfite contained chemicals are used extensively as preservatives in wineries. A way that yeast can tolerate the excess levels of sulfite is by increasing the regulation of the sulfite uptake and efflux through the *SSU1*

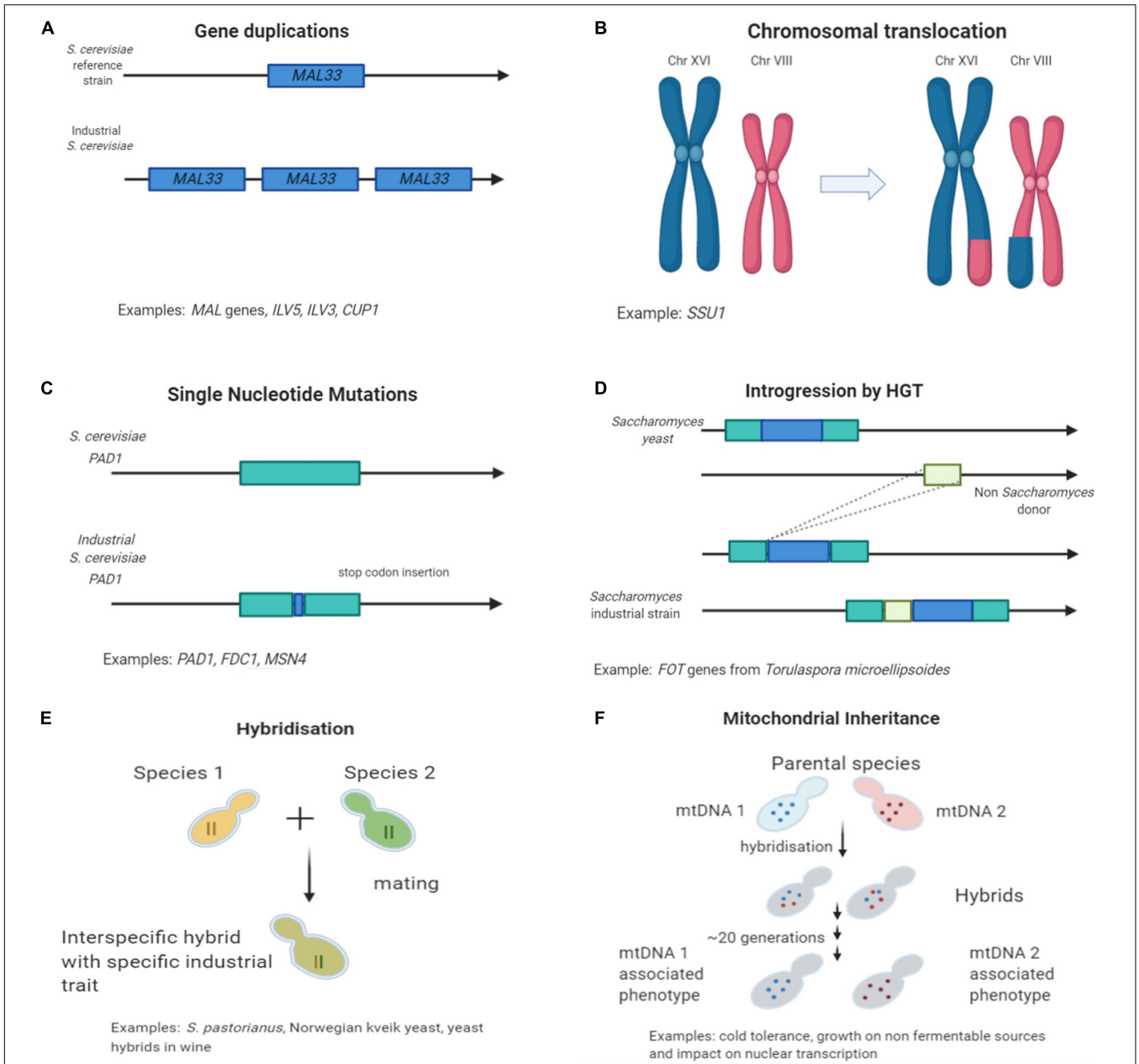

FIGURE 1 | Mechanisms of genetic variation found in industrial *Saccharomyces* strains in fermentative environments. **(A)** Gene duplication and copy number variation; **(B)** Chromosomal re-arrangements; **(C)** Single nucleotide polymorphism causing loss of function; **(D)** Horizontal gene transfer events; **(E)** Interspecific hybridization; and **(F)** Mitochondrial inheritance.

plasma membrane pump encoded gene (Pérez-Ortín et al., 2002). An increase in expression of *SSU1* was observed in wine yeast strains compared to laboratory strains. Studies about the mechanism of sulfite resistance, identified a chromosomal translocation (**Figure 1B**) and non-homologous recombination of the *SSU1* gene promoter (Pérez-Ortín et al., 2002). Moreover, a chromosomal inversion between XVI and VIII connected with the *SSU1* regulatory region also result in overexpression of *SSU1* and thus in sulfite resistance to commercial wine strains (García-Ríos et al., 2019b).

Another adaptation in wine yeast has been triggered by the copper-based pesticides used in wineries. The *CUP1* gene, responsible for copper binding and mediating resistance to high concentrations, was found in a higher copy number in wine strains associated with higher resistance to $CuSO_4$ compared with natural isolates (Almeida et al., 2015). Liu et al. (2015) identified a promoter variant of *CUP1* gene with increased expression suggesting that this benefit is involved in an adapting mechanism of the strains into a stressful condition. Interestingly, in organic vineyards where the usage of pesticides is strictly limited, a lower

number of different yeast strains has been detected, as other wild micro-organisms naturally resistant to copper such as *Aureobasidium pullulans* and *Starmerella bacillaris* dominate (Grangeteau et al., 2017).

SINGLE NUCLEOTIDE POLYMORPHISMS

Yeast domestication studies for beer and wine using sequencing technologies have unravel traits and performance improvements in different populations. In beer, an example illustrating well the process of trait improvement through selection and domestication, is the loss of function of genes related with ferulic acid decarboxylation. 4-vinylguaiacol is a phenolic compound with a distinct clove-like aroma. The decarboxylation of ferulic acid to 4-vinylguaiacol is occurring through yeast metabolism under the regulation of genes *PAD1* (phenylacrylic acid decarboxylase) and *FDC1* (ferulic acid decarboxylase) (Gallone et al., 2016; Gonçalves et al., 2016). The production of 4-vinylguaiacol during beer fermentation is considered a phenolic off-flavor (POF), and the strains are described as POF+. The clove-like aroma is considered characteristic only in some specific style of beers, such as Belgian and German wheat beers, but even for those a low threshold of POF would be desirable (Scholtes et al., 2014). Yeasts used for the production of alcoholic beverages produce an amount of undesired metabolites characterized as off-flavors and ideally that accumulation should be limited. The biological role of *PAD1* and *FDC1* is to help detoxifying phenylacrylic acids from the cell walls of plants (Mukai et al., 2014), which explains why wild yeast express those genes in order to survive and proliferate in natural habitats. Genomic studies revealed that in many industrial brewing strains the genes appear to be inactive and have acquired a frameshift mutation or a premature stop codon in the *PAD1* gene sequence (**Figure 1C**; Mukai et al., 2014; Chen et al., 2015). Interestingly, these type of mutations are not present in strains used in German like wheat beers. Such data show that different strains acquired different disruptive mutations, related to the presence of varied adaptive strategies in response to human selection against production of the POF+ character (Gallone et al., 2016).

Adaptation mechanisms due to different stressful conditions are also found yeast used in sake fermentation. These strains belong to the *Saccharomyces cerevisiae Kyokai* no. 7 group (K7). In sake brewing, the final ethanol content reaches almost 20%. Therefore, sake yeast genome has evolved to produce and accumulate high ethanol concentrations. The *Kyokai* strains express high fermentation rates. Both rapid fermentation and high ethanol production has been linked with environmental stress responses (Zhao and Bai, 2009). Studies in K7 yeast revealed a loss of function mutation in the genes *MSN4*, and *MSN2* that are responsible for transcription factors regulation during different types of stresses. Interestingly, the K7 group acquired a dysfunctional *MSN4* genes and results in high initial fermentation rate despite its lower stress tolerance compared to reference laboratory strains (Urbanczyk et al., 2011; Watanabe et al., 2011). The variant Km67 strain, belonging to the K7 sake group, has also been recently studied for its distinct characteristic of stress tolerance among the group. This strain has been used extensively and repeatedly as a starter culture for sake fermentation and surprisingly it doesn't acquire the same loss-of-function mutation in stress response related genes and also confers unique sensory characteristics and high production of ethanol as the rest of the *Kyokai* group. This suggests that other underlying genomic adaptations have contributed to the phenotype and performance of Km67 and the strain represents a genetically distinguished isolate within the group (Takao et al., 2018). The same strain was also recently reported for high folate production compared to other strains in the K7 group but the mechanisms underlying this accumulation are yet to be determined (Shibata et al., 2019).

HORIZONTAL GENE TRANSFER

Horizontal gene transfer (HGT), including introgression of DNA fragments from one species to another, is a known mechanism to generate variation in prokaryotes and eukaryotes (Keeling and Palmer, 2008). In yeast, HGT has been proposed as a mechanism of genetic adaptation to a particular niche (Hall et al., 2005). For example, a wine yeast *S. cerevisiae* strain gained 2 *FOT* genes –responsible for encoding oligopeptide transporters- from *Torulaspora microellipsoides* by several HGT and re-arrangement events (**Figure 1D**). Gaining these genes conferred *Saccharomyces* a competitive advantage during wine fermentation as the strain could utilize more nitrogen sources and oligopeptides, enabling its cell viability and proliferation. As mentioned before, grape juice is often a nitrogen-limited environment thus the wine yeast are challenged from the availability (Marsit et al., 2015). In another study, in the wine strain *S. cerevisiae* EC1118, a unique gene has been identified contributing to glucose and fructose metabolism and adaptation to low nitrogen conditions. The genes were acquired from non *S. cerevisiae* donors mostly closely related to *Zygosaccharomyces rouxii* a wild species commonly found in wineries (Novo et al., 2009). HGT is a mechanism of acquisition of new genetic material between different species, not yet fully explored in eukaryotes, and further future studies will help understanding the causes, the likelihood and the environmental background of this genetic exchange.

HYBRIDIZATION

Another mechanism, that has facilitated the evolution of industrial species, is the generation of interspecific hybrids (**Figure 1E**). The novel resulting combinations of genes (Nakao et al., 2009; Hewitt et al., 2014) and proteins (Piatkowska et al., 2013)is contributing to unique characteristics and advantages for the progenies compared to the parental strains. These unique phenotypes enable survival and proliferation in a new environment with a better performance over the parental species.

Interspecific hybridization has been extensively studied in the *Saccharomyces*. The lager yeast *S. pastorianus*, is a hybrid between

S. cerevisiae and S. eubayanus and it is the most widely known and used in the beer industry. The history of *S. pastorianus* can be tied to lager beer brewing during the winter months requiring a cooler fermentation temperature. A hybridization between *S. cerevisiae,* a great fermenter strain, and *S. eubayanus*, a cryotolerant isolate, created a new yeast suitable for adapting and performing in the new demanding of the beer making (Martini and Martini, 1987; Nakao et al., 2009; Hewitt et al., 2014; Monerawela and Bond, 2018). Several other hybrids have been isolated from industrial applications such as, hybrids of *S. cerevisiae* and *S. kudriavzevii* in beer, cider and wine (Masneuf et al., 1998; González et al., 2008) and hybrids of *S. cerevisiae* and *S. uvarum* (Le Jeune et al., 2007). The molecular drivers and biochemical pathways important for the cryotolerance trait in *S. kudriavzevii* has been recently unveiled, showing that temperature-induced redox imbalances could be compensated by either increased glycerol accumulation or production of cytosolic acetaldehyde (Paget et al., 2014).

Recently, a *S. cerevisiae* × *S. uvarum* unique hybrid was isolated from the Norwegian kveik farmhouse yeast (Krogerus et al., 2018b). Sequencing and phenotypic investigation on the strain showed that, this hybrid has been generated in brewing conditions and results in desirable characteristics such as tolerance to a wide temperature range, tolerance to high ethanol and good production of ester-flavor compounds.

Hybridization events have also been reported in wine strains. Garcia-Rios and co-workers constructed a non-GMO *S. cerevisiae* x *S. uvarum* hybrid to improve the wine fermentation properties of the parental *S. cerevisiae* strain. They performed growth and fermentation tests in a variety of different temperatures and media to evaluate the cryotolerance character of the hybrid. It is know that wine fermentations in colder temperatures improve the character, quality and fruit-flavor of wine (Molina et al., 2007). The hybrids generated were evaluated and compared to their parental strains in competition experiments to generate phenotypic maps and identify the different recombination events from the expressed phenotypes (García-Ríos et al., 2019a). Wine hybrids were constructed in order to generate strains able to survive and proliferate in low nitrogen levels commonly found in grapes (Su et al., 2019). Nitrogen is essential for yeast metabolism and fermentation ability as it is also responsible for the accumulation of aroma-related compounds (Rollero et al., 2018). Occurrence of natural interspecific triploid hybrids is also found in fermentative environments: *S. cerevisiae* × *S. cerevisiae* × *S. kudriavzevii* hybrids have been isolated from wineries providing a growth advantage in cold temperatures and high production of volatile thiols (Borneman et al., 2012). Triploid and tetraploid hybrids are also common in beer, with *S. pastorianus* forming two groups based on its DNA content. Saaz (Group 1) lager yeast are allotriploid strains with fermentation phenotypic characteristic close to the *S. eubayanus* parent while the Frohberg strains are allotetraploid with a similar fermentation performance to the *S. cerevisiae* parent (Walther et al., 2014). Hybrids generation among the *Saccharomyces* species have therefore resulted in a variety of phenotypes with great industrial fermentative potential (Bellon et al., 2011). Stress responses associated with wine and beer fermentation seem to have influenced the spontaneous generation of natural hybrids with different physiological traits.

MITOCHONDRIAL INHERITANCE

Another important factor related to the occurrence of specific characteristics in industrial strains is the inheritance of mitochondrial DNA (mtDNA). During hybridization, different hybrids can inherit the mitochondria from either one or the other parental species (**Figure 1F**).

Compared to the nuclear genomes, the mtDNA in *Saccharomyces cerevisiae* is more diverted and highly assorted. Structural rearrangements are rare in mtDNA resulting in few cases of DNA loss (De Chiara et al., 2020), however, mitochondrial recombination is common and can lead to phenotypic differentiation if enough divergence is present in the parental species (Leducq et al., 2017). Recent studies showed a strong influence on the different parental mtDNA in *S. pastorianus* strains related with adaptation to cold temperatures (Baker et al., 2019; Hewitt et al., 2020). Yeast mitochondria contribute to evolutionary divergence of cold tolerant strains (Li et al., 2019) and the type of mtDNA inherited in the hybrids affects both the cellular fitness in different nutritional conditions (Albertin et al., 2013; Hewitt et al., 2020), and the nuclear transcription in the hybrid (Hewitt et al., 2020).

FUTURE PERSPECTIVES ON INDUSTRIAL STRAIN IMPROVEMENT

The strong impact of molecular techniques and sequencing technologies have shed a light into evolutionary insights of industrial *Saccharomyces* species. Yeast domestication in man-made environments have been driven due to different stimuli that can include temperature and nutrient stresses, microbial competition, and ethanol and CO_2 toxicity. Evidence of yeast adaptation in the fermentative environments show that an incredible variety of mechanisms, such as gene duplication events, chromosomal rearrangement, hybridization, HGT, and type of mitochondria inherited, contribute to re-shape the yeast genome for better survival traits.

Such acquired knowledge on yeast biology and evolution can now enable researchers to work on strain improvement and generate candidates that will facilitate the food and beverages industry. This include approaches such as selection of isolates with desirable characteristics, usage of non-conventional yeast and generation of hybrids.

Adaptive laboratory evolution experiments have introduced specific mutations in relevant traits or aneuploidy in domesticated yeast (Gorter De Vries et al., 2019), improved fermentation performance in polyploid strains and hybrids (Voordeckers et al., 2015; Krogerus et al., 2018a) and osmotic stress response resulted in shorter fermentation times (Ekberg et al., 2013). Laboratory adaptive evolution can lead to identification and observation of important fermentation characteristics as well as the ability to design and perform future experiments that will lead to yeast strain with desired industrial properties (Iattici et al., 2020).

Evolutionary selection is still the methodology of choice for yeast strain improvement and it's usually preferred to classical

breeding techniques. Breeding can generate progeny with desired phenotypic traits but is much more challenging because of yeast aneuploidy and poor sporulation efficiencies (Codon et al., 1995). The phenotypic characterization and evaluation of new strains improved via breeding can help the selection superior segregants that could be implemented in food and beverages industry (Sanchez et al., 2012; Figueiredo et al., 2017).

Interspecific hybrid sterility is a drawback in the generation of offspring with different combination of desirable traits. Several works have tried to overcome sterility through allotetraploidization. Through this method we are able to obtain fertile diploid spores, from an allotetraploid, allowing a recombination of traits between the different species (Greig et al., 2002; Sebastiani et al., 2002). The construction of complex *de novo* interspecific hybrids strains can result in phenotypic traits that weaken or strengthen under meiotic recombination and increase the diversity of the existing industrial candidates (Krogerus et al., 2017; Peris et al., 2020).

The fermentative potential of *Saccharomyces* species has not yet fully explored. *S. kudriavzevii* and *S. uvarum* are cold tolerant strains that have been isolated from fermentative environments. *S. mikatae*, *S. paradoxus*, *S. jurei*, yeast that possess traits such as cold tolerance and maltose utilization could be further exploited through interspecific hybridization (Fleet, 2006; Salvadó et al., 2011; Naseeb et al., 2017b, 2018). Hybrid strains can also address the need of aromatic novelty in fermented beverages (Nikulin et al., 2018).

Furthermore, applying population genomic studies will facilitate exploring the biodiversity of non-conventional yeast such as *Brettanomyces bruxellensis*, *Torulaspora delbrueckii*. These species, commonly found in wine and beer fermentations and characterized as spoilage yeast, have increasingly gained scientific and biotechnological interest (Avramova et al., 2018; Zhang et al., 2018). The occurrence and industrial potential of non-*Saccharomyces* yeast should further be considered as it will diversify the industrial strains suitable for generation of novel food products (Basso et al., 2016). In addition, the usage of mixed starter cultures of *Saccharomyces* and non-*Saccharomyces* strains can guide new product development with distinct flavors and performance characteristics. The exo-metabolites resulting from co-culturing strains during fermentation can influence yeast-yeast interactions and ultimately alter the population structure due to different competitive pressure (Ye et al., 2014).

Although there is now clear evidence for patterns of evolution and adaptation of *Saccharomyces* strains in the fermentative environments, not much is yet known on the survival of wild strains in natural habitats. Adaptation trajectories and mutations arising from extreme environmental conditions are still yet to be explored in wild yeast isolates (Aouizerat et al., 2019). Further exploration on the effect of harsh conditions and climate fluctuations on different yeast strains and species will broaden the understanding on how to maintain their biodiversity and on the importance of yeast-environment interactions.

AUTHOR CONTRIBUTIONS

KG performed the literature search with the inputs of DD and MC. KG and DD wrote the manuscript with the input of MC. All authors contributed to the article and approved the submitted version.

FUNDING

This work was supported by H2020-MSCA-ITN-2017 (764364). KG was supported by Innovate-UK grant between the University of Manchester and Cloudwater Brew.

ACKNOWLEDGMENTS

We thank Federico Visinoni and Javier Pinto Aguirre for helpful comments and suggestions on the manuscript.

REFERENCES

Albertin, W., da Silva, T., Rigoulet, M., Salin, B., Masneuf-Pomarede, I., de Vienne, D., et al. (2013). The mitochondrial genome impacts respiration but not fermentation in interspecific *Saccharomyces* hybrids. *PLoS One* 8:e75121. doi: 10.1371/journal.pone.0075121

Aldrete-Tapia, J. A., Miranda-Castilleja, D. E., Arvizu-Medrano, S. M., and Hernández-Iturriaga, M. (2018). Selection of yeast strains for tequila fermentation based on growth dynamics in combined fructose and ethanol media. *J. Food Sci.* 83, 419–423. doi: 10.1111/1750-3841.14031

Almeida, P., Barbosa, R., Zalar, P., Imanishi, Y., Shimizu, K., Turchetti, B., et al. (2015). A population genomics insight into the Mediterranean origins of wine yeast domestication. *Mol. Ecol.* 24, 5412–5427. doi: 10.1111/mec.13341

Aouizerat, T., Gelman, D., Szitenberg, A., Gutman, I., Glazer, S., Reich, E., et al. (2019). Eukaryotic adaptation to years-long starvation resembles that of bacteria. *iScience* 19, 545–558. doi: 10.1016/j.isci.2019.08.002

Avramova, M., Cibrario, A., Peltier, E., Coton, M., Coton, E., Schacherer, J., et al. (2018). *Brettanomyces bruxellensis* population survey reveals a diploid-triploid complex structured according to substrate of isolation and geographical distribution. *Sci. Rep.* 8:4136. doi: 10.1038/s41598-018-22580-7

Baker, E. C. P., Peris, D., Moriarty, R. V., Li, X. C., Fay, J. C., and Hittinger, C. T. (2019). Mitochondrial DNA and temperature tolerance in lager yeasts. *Sci. Adv.* 5:eaav1869. doi: 10.1126/sciadv.aav1869

Basso, R. F., Alcarde, A. R., and Portugal, C. B. (2016). Could non-*Saccharomyces* yeasts contribute on innovative brewing fermentations? *Food Res. Int.* 86, 112–120. doi: 10.1016/j.foodres.2016.06.002

Bell, P. J. L., Higgins, V. J., and Attfield, P. V. (2001). Comparison of fermentative capacities of industrial baking and wild-type yeasts of the species *Saccharomyces cerevisiae* in different sugar media. *Lett. Appl. Microbiol.* 32, 224–229. doi: 10.1046/j.1472-765X.2001.00894.x

Bellon, J. R., Eglinton, J. M., Siebert, T. E., Pollnitz, A. P., Rose, L., De Barros Lopes, M., et al. (2011). Newly generated interspecific wine yeast hybrids introduce flavour and aroma diversity to wines. *Appl. Microbiol. Biotechnol.* 91, 603–612. doi: 10.1007/s00253-011-3294-3

Borneman, A. R., Desany, B. A., Riches, D., Affourtit, J. P., Forgan, A. H., Pretorius, I. S., et al. (2012). The genome sequence of the wine yeast VIN7 reveals an allotriploid hybrid genome with *Saccharomyces cerevisiae* and *Saccharomyces kudriavzevii* origins. *FEMS Yeast Res.* 12, 88–96. doi: 10.1111/j.1567-1364.2011.00773.x

Brown, C. A., Murray, A. W., and Verstrepen, K. J. (2010). Rapid expansion and functional divergence of subtelomeric gene families

in yeasts. *Curr. Biol.* 20, 895–903. doi: 10.1016/j.cub.2010.04.027

Carro, D., Bartra, E., and Piña, B. (2003). Karyotype rearrangements in a wine yeast strain by rad52-dependent and rad52-independent mechanisms. *Appl. Environ. Microbiol.* 69, 2161–2165. doi: 10.1128/AEM.69.4.2161-2165.2003

Caspeta, L., Coronel, J., Montes de Oca, A., Abarca, E., González, L., and Martínez, A. (2019). Engineering high−gravity fermentations for ethanol production at elevated temperature with *Saccharomyces cerevisiae*. *Biotechnol. Bioeng.* 116, 2587–2597. doi: 10.1002/bit.27103

Chen, P., Dong, J., Yin, H., Bao, X., Chen, L., He, Y., et al. (2015). Single nucleotide polymorphisms and transcription analysis of genes involved in ferulic acid decarboxylation among different beer yeasts. *J. Inst. Brew.* 121, 481–489. doi: 10.1002/jib.249

Chen, Y., Zhang, W., Yi, H., Wang, B., Xiao, J., Zhou, X., et al. (2020). Microbial community composition and its role in volatile compound formation during the spontaneous fermentation of ice wine made from Vidal grapes. *Proc. Biochem.* 92, 365–377. doi: 10.1016/j.procbio.2020.01.027

Codon, A. C., Gasent-Ramirez, J. M., and Benitez, T. (1995). Factors which affect the frequency of sporulation and tetrad formation in *Saccharomyces cerevisiae* baker's yeasts. *Appl. Environ. Microbiol.* 61, 630–638. doi: 10.1128/aem.61.2.630-638.1995

Colson, I., Delneri, D., and Oliver, S. G. (2004). Effects of reciprocal chromosomal translocations on the fitness of *Saccharomyces cerevisiae*. *EMBO Rep.* 5, 392–398. doi: 10.1038/sj.embor.7400123

Cromie, G. A., Hyma, K. E., Ludlow, C. L., Garmendia-Torres, C., Gilbert, T. L., May, P., et al. (2013). Genomic sequence diversity and population structure of *Saccharomyces cerevisiae* assessed by RAD-seq. *G3* 3, 2163–2171. doi: 10.1534/g3.113.007492

David, V., Terrat, S., Herzine, K., Claisse, O., Rousseaux, S., Tourdot-Maréchal, R., et al. (2014). High-throughput sequencing of amplicons for monitoring yeast biodiversity in must and during alcoholic fermentation. *J. Ind. Microbiol. Biotechnol.* 41, 811–821. doi: 10.1007/s10295-014-1427-2

De Chiara, M., Friedrich, A., Barré, B., Breitenbach, M., Schacherer, J., and Liti, G. (2020). Discordant evolution of mitochondrial and nuclear yeast genomes at population level. *BMC Biol.* 18:49. doi: 10.1186/s12915-020-00786-4

Dujon, B. (2010). *Yeast Evolutionary Genomics*. Berlin: Nature Publishing Group, doi: 10.1038/nrg2811

Eglinton, J. M., McWilliam, S. J., Fogarty, M. W., Francis, I. L., Kwiatkowski, M. J., Hoj, P. B., et al. (2000). The effect of *Saccharomyces bayanus*-mediated fermentation on the chemical composition and aroma profile of Chardonnay wine. *Aust. J. Grape Wine Res.* 6, 190–196. doi: 10.1111/j.1755-0238.2000.tb00178.x

Ekberg, J., Rautio, J., Mattinen, L., Vidgren, V., Londesborough, J., and Gibson, B. R. (2013). Adaptive evolution of the lager brewing yeast *Saccharomyces pastorianus* for improved growth under hyperosmotic conditions and its influence on fermentation performance. *FEMS Yeast Res.* 13, 335–349. doi: 10.1111/1567-1364.12038

Fay, J. C., Liu, P., Ong, G. T., Dunham, M. J., Cromie, G. A., Jeffery, E. W., et al. (2019). A polyploid admixed origin of beer yeasts derived from European and Asian wine populations. *PLoS Biol.* 17:e3000147. doi: 10.1371/journal.pbio.3000147

Figueiredo, B. I. C., Saraiva, M. A. F., de Souza Pimenta, P. P., de Souza Testasicca, M. C., Sampaio, G. M. S., da Cunha, A. C., et al. (2017). New lager brewery strains obtained by crossing techniques using cachaça (Brazilian spirit) yeasts. *Appl. Environ. Microbiol.* 83:e01582-17. doi: 10.1128/AEM.01582-17

Fleet, G. H. (2006). "*Saccharomyces* and related genera," in *Food Spoilage Microorganisms*, ed. C. W. de Blackburn (Amsterdam: Elsevier), 306–335. doi: 10.1533/9781845691417.3.306

Gallone, B., Mertens, S., Gordon, J. L., Maere, S., Verstrepen, K. J., and Steensels, J. (2018). Origins, evolution, domestication and diversity of *Saccharomyces* beer yeasts. *Curr. Opin. Biotechnol.* 49, 148–155. doi: 10.1016/j.copbio.2017.08.005

Gallone, B., Steensels, J., Prahl, T., Soriaga, L., Saels, V., Herrera-Malaver, B., et al. (2016). Domestication and divergence of *Saccharomyces cerevisiae* beer yeasts. *Cell* 166, 1397–1410.e16. doi: 10.1016/j.cell.2016.08.020

García-Ríos, E., Guillén, A., De La Cerda, R., Pérez-Través, L., Querol, A., and Guillamón, J. M. (2019a). Improving the cryotolerance of wine yeast by interspecific hybridization in the genus *Saccharomyces*. *Front. Microbiol.* 10:3232. doi: 10.3389/fmicb.2018.03232

García-Ríos, E., Nuévalos, M., Barrio, E., Puig, S., and Guillamón, J. M. (2019b). A new chromosomal rearrangement improves the adaptation of wine yeasts to sulfite. *Environ. Microbiol.* 21, 1771–1781. doi: 10.1111/1462-2920.14586

Gibson, B. R., Storgårds, E., Krogerus, K., and Vidgren, V. (2013). Comparative physiology and fermentation performance of Saaz and Frohberg lager yeast strains and the parental species *Saccharomyces eubayanus*. *Yeast* 30, 255–266. doi: 10.1002/yea.2960

Gonçalves, M., Pontes, A., Almeida, P., Barbosa, R., Serra, M., Libkind, D., et al. (2016). Distinct domestication trajectories in top-fermenting beer yeasts and wine yeasts. *Curr. Biol.* 26, 2750–2761. doi: 10.1016/j.cub.2016.08.040

González, S. S., Barrio, E., and Querol, A. (2008). Molecular characterization of new natural hybrids of *Saccharomyces cerevisiae* and *S. kudriavzevii* in brewing. *Appl. Environ. Microbiol.* 74, 2314–2320. doi: 10.1128/AEM.01867-07

Goold, H. D., Kroukamp, H., Williams, T. C., Paulsen, I. T., Varela, C., and Pretorius, I. S. (2017). Yeast's balancing act between ethanol and glycerol production in low-alcohol wines. *Microb. Biotechnol.* 10, 264–278. doi: 10.1111/1751-7915.12488

Gorter De Vries, A. R., Voskamp, M. A., Van Aalst, A. C. A., Kristensen, L. H., Jansen, L., Van Den Broek, M., et al. (2019). Laboratory evolution of a *Saccharomyces cerevisiae* × *Saccharomyces eubayanus* hybrid under simulated lager-brewing conditions. *Front. Genet.* 10:242. doi: 10.3389/fgene.2019.00242

Grangeteau, C., David, V., Hervé, A., Guilloux-Benatier, M., and Rousseaux, S. (2017). The sensitivity of yeasts and yeasts-like fungi to copper and sulfur could explain lower yeast biodiversity in organic vineyards. *FEMS Yeast Res.* 17:fox092. doi: 10.1093/femsyr/fox092

Greig, D., Borts, R. H., Louis, E. J., and Travisano, M. (2002). Epistasis and hybrid sterility in *Saccharomyces*. *Proc. R. Soc. Lond. Ser. B Biol. Sci.* 269, 1167–1171. doi: 10.1098/rspb.2002.1989

Guan, Y., Dunham, M. J., and Troyanskaya, O. G. (2007). Functional analysis of gene duplications in *Saccharomyces cerevisiae*. *Genetics* 175, 933–943. doi: 10.1534/genetics.106.064329

Hakes, L., Pinney, J. W., Lovell, S. C., Oliver, S. G., and Robertson, D. L. (2007). All duplicates are not equal: the difference between small-scale and genome duplication. *Genome Biol.* 8:R209. doi: 10.1186/gb-2007-8-10-r209

Hall, C., Brachat, S., and Dietrich, F. S. (2005). Contribution of horizontal gene transfer to the evolution of *Saccharomyces cerevisiae*. *Eukaryotic Cell* 4, 1102–1115. doi: 10.1128/EC.4.6.1102-1115.2005

Hewitt, S. K., Donaldson, I. J., Lovell, S. C., and Delneri, D. (2014). Sequencing and characterisation of rearrangements in three *S. pastorianus* strains reveals the presence of chimeric genes and gives evidence of breakpoint reuse. *PLoS One* 9:e0092203. doi: 10.1371/journal.pone.0092203

Hewitt, S. K., Duangrattanalert, K., Burgis, T., Zeef, L. A. H., Naseeb, S., and Delneri, D. (2020). Plasticity of mitochondrial DNA inheritance and its impact on nuclear gene transcription in yeast hybrids. *Microorganisms* 8:494. doi: 10.3390/microorganisms8040494

Hill, A. E. (2015). "Introduction to brewing microbiology," in *Brewing Microbiology: Managing Microbes, Ensuring Quality and Valorising Waste*, ed. A. Hill (Cambridge: Woodhead Publishing), xxvii–xxix. doi: 10.1016/B978-1-78242-331-7.02001-3

Iattici, F., Catallo, M., and Solieri, L. (2020). Designing new yeasts for craft brewing: when natural biodiversity meets biotechnology. *Beverages* 6:3. doi: 10.3390/beverages6010003

Jackson, R. S. (2014). "Specific and distinctive wine styles," in *Wine Science*, ed. R. Jackson (Amsterdam: Elsevier), 677–759. doi: 10.1016/b978-0-12-381468-5.00009-9

Katou, T., Namise, M., Kitagaki, H., Akao, T., and Shimoi, H. (2009). QTL mapping of sake brewing characteristics of yeast. *J. Biosci. Bioeng.* 107, 383–393. doi: 10.1016/j.jbiosc.2008.12.014

Keeling, P. J., and Palmer, J. D. (2008). Horizontal gene transfer in eukaryotic evolution. *Nat. Rev. Genet.* 9, 605–618. doi: 10.1038/nrg2386

Kelly, J., Yang, F., Dowling, L., Nurgel, C., Beh, A., Di Profio, F., et al. (2018). Characterization of *Saccharomyces bayanus* CN1 for fermenting partially dehydrated grapes grown in cool climate winemaking regions. *Fermentation* 4, 1–13. doi: 10.3390/fermentation4030077

Krogerus, K., Holmström, S., and Gibson, B. (2018a). Enhanced wort fermentation with de novo lager hybrids adapted to high-ethanol environments. *Appl. Environ. Microbiol.* 84:e02302-17. doi: 10.1128/AEM.02302-17

Krogerus, K., Preiss, R., and Gibson, B. (2018b). A unique *Saccharomyces cerevisiae* × *Saccharomyces uvarum* hybrid isolated from norwegian farmhouse beer: characterization and reconstruction. *Front. Microbiol.* 9:2253. doi: 10.3389/fmicb.2018.02253

Krogerus, K., Seppänen-Laakso, T., Castillo, S., and Gibson, B. (2017). Inheritance of brewing-relevant phenotypes in constructed *Saccharomyces cerevisiae*×*Saccharomyces eubayanus* hybrids. *Microb. Cell Fact.* 16, 1–22. doi: 10.1186/s12934-017-0679-8

Kusunoki, K., and Ogata, T. (2012). Construction of self-cloning bottom-fermenting yeast with low vicinal diketone production by the homo-integration of *ILV5*. *Yeast* 29, 435–442. doi: 10.1002/yea.2922

Le Jeune, C., Lollier, M., Demuyter, C., Erny, C., Legras, J.-L., Aigle, M., et al. (2007). Characterization of natural hybrids of *Saccharomyces cerevisiae* and *Saccharomyces bayanus* var. *uvarum*. *FEMS Yeast Res.* 7, 540–549. doi: 10.1111/j.1567-1364.2007.00207.x

Leducq, J. B., Henault, M., Charron, G., Nielly-Thibault, L., Terrat, Y., Fiumera, H. L., et al. (2017). Mitochondrial recombination and introgression during speciation by hybridization. *Mol. Biol. Evol.* 34, 1947–1959. doi: 10.1093/molbev/msx139

Legras, J. L., Galeote, V., Bigey, F., Camarasa, C., Marsit, S., Nidelet, T., et al. (2018). Adaptation of *S. cerevisiae* to fermented food environments reveals remarkable genome plasticity and the footprints of domestication. *Mol. Biol. Evol.* 35, 1712–1727. doi: 10.1093/molbev/msy066

Lei, H., Zhao, H., Yu, Z., and Zhao, M. (2012). Effects of wort gravity and nitrogen level on fermentation performance of brewer's yeast and the formation of flavor volatiles. *Appl. Biochem. Biotechnol.* 166, 1562–1574. doi: 10.1007/s12010-012-9560-8

Li, X. C., Peris, D., Hittinger, C. T., Sia, E. A., and Fay, J. C. (2019). Mitochondria-encoded genes contribute to evolution of heat and cold tolerance in yeast. *Sci. Adv.* 5:eaav1848. doi: 10.1126/sciadv.aav1848

Liti, G., Carter, D. M., Moses, A. M., Warringer, J., Parts, L., James, S. A., et al. (2009). Population genomics of domestic and wild yeasts. *Nature* 458, 337–341. doi: 10.1038/nature07743

Liu, J., Martin-Yken, H., Bigey, F., Dequin, S., François, J. M., and Capp, J. P. (2015). Natural yeast promoter variants reveal epistasis in the generation of transcriptional-mediated noise and its potential benefit in stressful conditions. *Genome Biol. Evol.* 7, 969–984. doi: 10.1093/gbe/evv047

Magadum, S., Banerjee, U., Murugan, P., Gangapur, D., and Ravikesavan, R. (2013). Gene duplication as a major force in evolution. *J. Genet.* 92, 155–161. doi: 10.1007/s12041-013-0212-8

Marsit, S., Mena, A., Bigey, F., Sauvage, F.-X., Couloux, A., Guy, J., et al. (2015). Evolutionary advantage conferred by an eukaryote-to-eukaryote gene transfer event in wine yeasts. *Mol. Biol. Evol.* 32, 1695–1707. doi: 10.1093/molbev/msv057

Martínez-Rodríguez, A., Carrascosa, A. V., Barcenilla, J. M., Angeles Pozo-Bayón, M., and Carmen Polo, M. (2001). Autolytic capacity and foam analysis as additional criteria for the selection of yeast strains for sparkling wine production. *Food Microbiol.* 18, 183–191. doi: 10.1006/fmic.2000.0390

Martini, A. V., and Martini, A. (1987). Three newly delimited species of *Saccharomyces sensu stricto*. *Antonie Leeuwenhoek* 53, 77–84. doi: 10.1007/bf00419503

Masneuf, I., Hansen, J., Groth, C., Piskur, J., and Dubourdieu, D. (1998). New hybrids between *Saccharomyces sensu stricto* yeast species found among wine and cider production strains. *Appl. Environ. Microbiol.* 64, 3887–3892. doi: 10.1128/aem.64.10.3887-3892.1998

Meier-Dörnberg, T., Kory, O. I, Jacob, F., Michel, M., and Hutzler, M. (2018). *Saccharomyces cerevisiae* variety *diastaticus* friend or foe?—spoilage potential and brewing ability of different *Saccharomyces cerevisiae* variety *diastaticus* yeast isolates by genetic, phenotypic and physiological characterizati. *FEMS Yeast Res.* 18:foy023. doi: 10.1093/femsyr/foy023

Mezzasalma, V., Sandionigi, A., Bruni, I., Bruno, A., Lovicu, G., Casiraghi, M., et al. (2017). Grape microbiome as a reliable and persistent signature of field origin and environmental conditions in Cannonau wine production. *PLoS One* 12:e0184615. doi: 10.1371/journal.pone.0184615

Molina, A. M., Swiegers, J. H., Varela, C., Pretorius, I. S., and Agosin, E. (2007). Influence of wine fermentation temperature on the synthesis of yeast-derived volatile aroma compounds. *Appl. Microbiol. Biotechnol.* 77, 675–687. doi: 10.1007/s00253-007-1194-3

Monerawela, C., and Bond, U. (2018). The hybrid genomes of *Saccharomyces pastorianus*?: a current perspective. *Yeast* 35, 39–50. doi: 10.1002/yea.3250

Mukai, N., Masaki, K., Fujii, T., and Iefuji, H. (2014). Single nucleotide polymorphisms of *PAD1* and *FDC1* show a positive relationship with ferulic acid decarboxylation ability among industrial yeasts used in alcoholic beverage production. *J. Biosci. Bioeng.* 118, 50–55. doi: 10.1016/j.jbiosc.2013.12.017

Nakao, Y., Kanamori, T., Itoh, T., Kodama, Y., Rainieri, S., Nakamura, N., et al. (2009). Genome sequence of the lager brewing yeast, an interspecies hybrid. *DNA Res.* 16, 115–129. doi: 10.1093/dnares/dsp003

Naseeb, S., Alsammar, H., Burgis, T., Donaldson, I., Knyazev, N., Knight, C., et al. (2018). Whole genome sequencing, de novo assembly and phenotypic profiling for the new budding yeast species *Saccharomyces jurei*. *G3* 8, 2967–2977. doi: 10.1534/g3.118.200476

Naseeb, S., Ames, R. M., Delneri, D., and Lovell, S. C. (2017a). Rapid functional and evolutionary changes follow gene duplication in yeast. *Proc. R. Soc. B Biol. Sci.* 284:20171393. doi: 10.1098/rspb.2017.1393

Naseeb, S., Carter, Z., Minnis, D., Donaldson, I., Zeef, L., and Delneri, D. (2016). Widespread impact of chromosomal inversions on gene expression uncovers robustness via phenotypic buffering. *Mol. Biol. Evol.* 33, 1679–1696. doi: 10.1093/molbev/msw045

Naseeb, S., James, S. A., Alsammar, H., Michaels, C. J., Gini, B., Nueno-Palop, C., et al. (2017b). Saccharomyces jurei sp. Nov., isolation and genetic identification of a novel yeast species from *Quercus robur*. *Int. J. Syst. Evol. Microbiol.* 67, 2046–2052. doi: 10.1099/ijsem.0.002013

Nikulin, J., Krogerus, K., and Gibson, B. (2018). Alternative *Saccharomyces* interspecies hybrid combinations and their potential for low-temperature wort fermentation. *Yeast* 35, 113–127. doi: 10.1002/yea.3246

Novo, M., Bigey, F., Beyne, E., Galeote, V., Gavory, F., Mallet, S., et al. (2009). Eukaryote-to-eukaryote gene transfer events revealed by the genome sequence of the wine yeast *Saccharomyces cerevisiae EC1118*. *Proc. Natl. Acad. Sci. U.S.A.* 106, 16333–16338. doi: 10.1073/pnas.0904673106

Paget, C. M., Schwartz, J. M., and Delneri, D. (2014). Environmental systems biology of cold-tolerant phenotype in *Saccharomyces* species adapted to grow at different temperatures. *Mol. Ecol.* 23, 5241–5257. doi: 10.1111/mec.12930

Pando Bedriñana, R., Mangas Alonso, J. J., and Suárez Valles, B. (2017). Evaluation of autochthonous *Saccharomyces bayanus* strains under stress conditions for making ice ciders. *Food Sci. Technol.* 81, 217–225. doi: 10.1016/j.lwt.2017.03.055

Pátková, J., Šmogrovičová, D., Dömény, Z., and Bafrncová, P. (2000). Very high gravity wort fermentation by immobilised yeast. *Biotechnol. Lett.* 22, 1173–1177. doi: 10.1023/A:1005689313775

Pérez-Ortín, J. E., Querol, A., Puig, S., and Barrio, E. (2002). Molecular characterization of a chromosomal rearrangement involved in the adaptive evolution of yeast strains. *Genome Res.* 12, 1533–1539. doi: 10.1101/gr.436602

Peris, D., Alexander, W. G., Fisher, K. J., Moriarty, R. V., Basuino, M. G., Ubbelohde, E. J., et al. (2020). Synthetic hybrids of six yeast species. *Nat. Commun.* 11:2085. doi: 10.1038/s41467-020-15559-4

Peter, J., De Chiara, M., Friedrich, A., Yue, J. X., Pflieger, D., Bergström, A., et al. (2018). Genome evolution across 1,011 *Saccharomyces cerevisiae* isolates. *Nature* 556, 339–344. doi: 10.1038/s41586-018-0030-5

Piatkowska, E. M., Naseeb, S., Knight, D., and Delneri, D. (2013). Chimeric protein complexes in hybrid species generate novel phenotypes. *PLoS Genet.* 9:e1003836. doi: 10.1371/journal.pgen.1003836

Piddocke, M. P., Kreisz, S., Heldt-Hansen, H. P., Nielsen, K. F., and Olsson, L. (2009). Physiological characterization of brewer's yeast in high-gravity beer fermentations with glucose or maltose syrups as adjuncts. *Appl. Microbiol. Biotechnol.* 84, 453–464. doi: 10.1007/s00253-009-1930-y

Piškur, J., Rozpedowska, E., Polakova, S., Merico, A., and Compagno, C. (2006). How did *Saccharomyces* evolve to become a good brewer? *Trends Genet.* 22, 183–186. doi: 10.1016/j.tig.2006.02.002

Rollero, S., Bloem, A., Ortiz-Julien, A., Camarasa, C., and Divol, B. (2018). Fermentation performances and aroma production of non-conventional wine yeasts are influenced by nitrogen preferences. *FEMS Yeast Res.* 18:foy055. doi: 10.1093/femsyr/foy055

Salvadó, Z., Arroyo-López, F. N., Guillamón, J. M., Salazar, G., Querol, A., and Barrio, E. (2011). Temperature adaptation Markedly determines evolution within the genus *Saccharomyces*. *Appl. Environ. Microbiol.* 77, 2292–2302. doi: 10.1128/AEM.01861-10

Sanchez, R. G., Solodovnikova, N., and Wendland, J. (2012). Breeding of lager yeast with *Saccharomyces cerevisiae* improves stress resistance and fermentation performance. *Yeast* 29, 343–355. doi: 10.1002/yea.2914

Schacherer, J., Shapiro, J. A., Ruderfer, D. M., and Kruglyak, L. (2009). Comprehensive polymorphism survey elucidates population structure of *Saccharomyces cerevisiae*. *Nature* 458, 342–345. doi: 10.1038/nature07670

Scholtes, C., Nizet, S., and Collin, S. (2014). Guaiacol and 4-Methylphenol as specific markers of torrefied malts. fate of volatile phenols in special beers through aging. *J. Agric. Food Chem.* 62, 9522–9528. doi: 10.1021/jf5015654

Sebastiani, F., Barberio, C., Casalone, E., Cavalieri, D., and Polsinelli, M. (2002). Crosses between *Saccharomyces cerevisiae* and *Saccharomyces bayanus* generate fertile hybrids. *Res. Microbiol.* 153, 53–58. doi: 10.1016/S0923-2508(01)01286-4

Shibata, Y., Yamada, T., Morimoto, T., Fujii, T., Akao, T., Goshima, T., et al. (2019). Mechanism of high folate accumulation in a sake yeast other than *Kyokai* yeasts. *J. Biosci. Bioeng.* 129, 1–5. doi: 10.1016/j.jbiosc.2019.07.008

Sniegowski, P. (1999). Evolution: the genomics of adaptation in yeast. *Curr. Biol.* 9, 897–898. doi: 10.1016/s0960-9822(00)80078-0

Spitaels, F., Wieme, A. D., Janssens, M., Aerts, M., Daniel, H.-M., Van Landschoot, A., et al. (2014). The microbial diversity of traditional spontaneously fermented lambic beer. *PLoS One* 9:e95384. doi: 10.1371/journal.pone.0095384

Steensels, J., Meersman, E., Snoek, T., Saels, V., and Verstrepen, K. J. (2014). Large-scale selection and breeding to generate industrial yeasts with superior aroma production. *Appl. Environ. Microbiol.* 80, 6965–6975. doi: 10.1128/AEM.02235-14

Su, Y., Gamero, A., Rodríguez, M. E., Lopes, C. A., Querol, A., and Guillamón, J. M. (2019). Interspecific hybridisation among diverse *Saccharomyces* species: a combined biotechnological solution for low-temperature and nitrogen-limited wine fermentations. *Int. J. Food Microbiol.* 310:108331. doi: 10.1016/j.ijfoodmicro.2019.108331

Takao, Y., Takahashi, T., Yamada, T., Goshima, T., Isogai, A., Sueno, K., et al. (2018). Characteristic features of the unique house sake yeast strain *Saccharomyces cerevisiae Km67* used for industrial sake brewing. *J. Biosci. Bioeng.* 126, 617–623. doi: 10.1016/j.jbiosc.2018.05.008

Uebayashi, K., Shimizu, H., and Matsuda, F. (2018). Comparative analysis of fermentation and enzyme expression profiles among industrial *Saccharomyces cerevisiae* strains. *Appl. Microbiol. Biotechnol.* 102, 7071–7081. doi: 10.1007/s00253-018-9128-9

Urbanczyk, H., Noguchi, C., Wu, H., Watanabe, D., Akao, T., Takagi, H., et al. (2011). Sake yeast strains have difficulty in entering a quiescent state after cell growth cessation. *J. Biosci. Bioeng.* 112, 44–48. doi: 10.1016/j.jbiosc.2011.03.001

Valero, E., Cambon, B., Schuller, D., Casal, M., and Dequin, S. (2007). Biodiversity of *Saccharomyces* yeast strains from grape berries of wine-producing areas using starter commercial yeasts. *FEMS Yeast Res.* 7, 317–329. doi: 10.1111/j.1567-1364.2006.00161.x

van den Broek, M., Bolat, I., Nijkamp, J. F., Ramos, E., Luttik, M. A. H., Koopman, F., et al. (2015). Chromosomal copy number variation in *Saccharomyces pastorianus* is evidence for extensive genome dynamics in industrial lager brewing strains. *Appl. Environ. Microbiol.* 81, 6253–6267. doi: 10.1128/AEM.01263-15

Voordeckers, K., Kominek, J., Das, A., Espinosa-Cantú, A., De Maeyer, D., Arslan, A., et al. (2015). Adaptation to high ethanol reveals complex evolutionary pathways. *PLoS Genet.* 11:e1005635. doi: 10.1371/journal.pgen.1005635

Walker, G., Brosnan, J., Bringhurst, T., and Jack, F. (2012). Chapter 16 Selecting new distilling yeasts for improved fermentation and for sustainability. *Yeast* 1–11.

Walker, G. M. (2014). "Wines: microbiology of winemaking," in *Encyclopedia of Food Microbiology: Second Edition*, Vol. 3, eds C. Batt and C. A. Batt (New York, NY: Academic Press), 787–792. doi: 10.1016/B978-0-12-384730-0.00356-6

Walther, A., Hesselbart, A., and Wendland, J. (2014). Genome sequence of *Saccharomyces carlsbergensis*, the world's first pure culture lager yeast. *G3* 4, 783–793. doi: 10.1534/g3.113.010090

Watanabe, D., Wu, H., Noguchi, C., Zhou, Y., Akao, T., and Shimoi, H. (2011). Enhancement of the initial rate of ethanol fermentation due to dysfunction of yeast stress response components Msn2p and/or Msn4p. *Appl. Environ. Microbiol.* 77, 934–941. doi: 10.1128/AEM.01869-10

Ye, M., Yue, T., and Yuan, Y. (2014). Effects of sequential mixed cultures of *Wickerhamomyces anomalus* and *Saccharomyces cerevisiae* on apple cider fermentation. *FEMS Yeast Res.* 14, 873–882. doi: 10.1111/1567-1364.12175

Zhang, B.-Q., Luan, Y., Duan, C.-Q., and Yan, G.-L. (2018). Use of *Torulaspora delbrueckii* Co-fermentation with two *Saccharomyces cerevisiae* strains with different aromatic characteristic to improve the diversity of red wine aroma profile. *Front. Microbiol.* 9:606. doi: 10.3389/fmicb.2018.00606

Zhao, X. Q., and Bai, F. W. (2009). Mechanisms of yeast stress tolerance and its manipulation for efficient fuel ethanol production. *J. Biotechnol.* 144, 23–30. doi: 10.1016/j.jbiotec.2009.05.001

Conflict of Interest: MC was employed by the company Cloudwater Brew Co.

The remaining authors declare that the research was conducted in the absence of any commercial or financial relationships that could be construed as a potential conflict of interest.

frontiers in Genetics

ORIGINAL RESEARCH
published: 31 August 2020
doi: 10.3389/fgene.2020.00908

Characterization of Sub-Regional Variation in *Saccharomyces* Populations and Grape Phenolic Composition in Pinot Noir Vineyards of a Canadian Wine Region

Elaine Cheng[1†], Jonathan T. Martiniuk[1†], Jonah Hamilton[1], Garrett McCarthy[1,2], Simone Diego Castellarin[1] and Vivien Measday[1]*

[1] Wine Research Centre, Faculty of Land and Food Systems, The University of British Columbia, Vancouver, BC, Canada, [2] Department of Biology, The University of British Columbia, Kelowna, BC, Canada

OPEN ACCESS

Edited by:
Amparo Querol, Consejo Superior de Investigaciones Científicas (CSIC), Spain

Reviewed by:
Braulio Esteve-Zarzoso, Rovira i Virgili University, Spain
Patrizia Romano, University of Basilicata, Italy

***Correspondence:**
Vivien Measday
vmeasday@mail.ubc.ca

† These authors have contributed equally to this work

Specialty section:
This article was submitted to Evolutionary and Genomic Microbiology, a section of the journal Frontiers in Genetics

Received: *08 April 2020*
Accepted: *22 July 2020*
Published: *31 August 2020*

Citation:
Cheng E, Martiniuk JT, Hamilton J, McCarthy G, Castellarin SD and Measday V (2020) Characterization of Sub-Regional Variation in Saccharomyces Populations and Grape Phenolic Composition in Pinot Noir Vineyards of a Canadian Wine Region. Front. Genet. 11:908. doi: 10.3389/fgene.2020.00908

Wine is a product of grape juice fermentation by yeast. *Terroir* is a term that encompasses all environmental factors and interactions at a specific geographical site, resulting in the development of regional-specific microbial strains and grape metabolites. In this study we determine the distribution of vineyard-associated wine yeast strains and characterize the flavonoid profile of Pinot Noir grapes among 3 sub-regions in the Okanagan Valley (OV), a major wine region in British Columbia, Canada. Pinot Noir grape samples were collected from 13 vineyards among 3 sub-regions of the OV, namely Kelowna (KE), Naramata-Penticton (NP) and Oliver-Osoyoos (OO), within a week prior to the winery harvesting date in 2016 and 2017. A total of 156 spontaneous Pinot Noir fermentations were conducted and vineyard-associated *Saccharomyces* strains were isolated from fermentations that reached two-thirds sugar depletion. Using microsatellite genotyping, we identified 103 *Saccharomyces cerevisiae* strains and 9 *Saccharomyces uvarum* strains. We also identified *Saccharomyces paradoxus* in one vineyard using ITS sequencing. We developed a microsatellite database of 160 commercial *S. cerevisiae* strains to determine the identity of the isolated strains and we include the database herein. Commercial strains were widely distributed across the three sub-regions. Forty-two of our 103 *S. cerevisiae* strains were equivalent or highly similar to commercial strains whereas the remaining 61 were considered as 'unknown' strains. Two *S. uvarum* strains were previously isolated in other OV studies and none matched the *S. uvarum* commercial strain BMV58. *S. cerevisiae* population structure was driven by sub-region, although *S. cerevisiae* populations did not differ significantly across vintages. *S. uvarum* and *S. paradoxus* were only identified in the 2017 vintage, demonstrating dynamic wine yeast populations between vintages. We found that the flavonoid profile of Pinot Noir grapes from the same 13 vineyards was also affected by sub-regional *terroir*. The anthocyanin content was lower and the proportion of methoxylated anthocyanins and

flavonols was higher in Pinot Noir grapes from OO, the warmer sub-region as compared to KE, the cooler sub-region. Our study demonstrates that both yeast populations and metabolites associated with the Pinot Noir variety have sub-regional variation within a viticultural area.

Keywords: anthocyanin, fermentation, flavonol, flavonoid, *Saccharomyces cerevisiae*, *Saccharomyces uvarum*, *Vitis vinifera* L., wine

INTRODUCTION

The characteristics of a wine region are believed to influence the sensory profiles of wines made in these regions, a concept referred to as *terroir* (van Leeuwen and Seguin, 2006). These characteristics include abiotic factors such as climate, topography and topology as well as biotic factors such as soil, fruit and vineyard microbiota. While regional abiotic factors have a more obvious impact on the differentiation of wine characteristics, the regional composition and structure of microbial communities has been correlated with differences in wine chemical and sensory profiles (Knight et al., 2015; Bokulich et al., 2016). In particular, the composition of wine grape phenolic compounds, which are important for red wine quality, can be influenced by *terroir*. Anthocyanins determine the color of the red grape and wine (Gould and Lister, 2005). Tannins confer astringency and bitter sensorial notes to grapes and wines, and provide texture to red wines (Flamini and Traldi, 2010). Flavonols influence wine quality by forming non-covalent interactions with anthocyanin molecules. The interaction of flavonols with anthocyanins results in color intensity enhancement of grape skins (Pollastri and Tattini, 2011; Trouillas et al., 2016). Abiotic factors such as light, temperature, and water availability strongly affect grape phenolic compounds (Castellarin et al., 2007; Mori et al., 2007; Cohen et al., 2008; Matus et al., 2009; Savoi et al., 2017). Arguably, the soil and the above abiotic factors, are the major components of the *terroir* that affect the phenolic composition of the grapes and wines (van Leeuwen, 2010; Willwerth et al., 2010; Ferndandez-Marin et al., 2013; Artem et al., 2016; Del-Castillo-Alonso et al., 2016).

The Okanagan Valley (OV) is a major wine region of Canada. The narrow valley spans from the United States border with Washington State to approximately 250 km north and is marked by several lakes. The OV climate is considered cool and arid (Senese et al., 2012). Given its great latitudinal range, the OV has many microclimates and diverse soil types, lending itself to the production of premium wines made from many grape cultivars (Bowen et al., 2005). While the majority of red wine grapes are grown in the Oliver-Osoyoos (OO) area at the south end of the valley (containing Canada's only semi-desert), Pinot Noir is commonly grown in all areas of OV. However, more acres of Pinot Noir are planted in the Naramata-Penticton (NP, central) and more northern Kelowna (KE) sub-regions. Pinot Noir is an early ripening vine and therefore cool climate regions provide ideal viticulture sites to prevent pre-maturation of grapes that may cause loss of acidy and aroma. Little information exists on the microbial populations in OV vineyards and the variation of phenolic accumulation in grape berries. Knowledge of the regional variation in Pinot Noir flavonoid grape composition (anthocyanins, tannins, flavonols) will constitute baseline information for investigating the impact of OV *terroir* on Pinot Noir wine quality.

Saccharomyces species are essential in winemaking both for their roles in alcoholic fermentation and for their influence on wine organoleptic profiles through the production or release of volatile compounds (Fleet, 2003; Styger et al., 2011; Cordente et al., 2012). *Saccharomyces cerevisiae* is by far most common in wine fermentations, while *S. uvarum* may also occur in mixed populations with *S. cerevisiae* or as the dominant yeast in white wine fermentations (Demuyter et al., 2004; Tosi et al., 2009; Masneuf-Pomarede et al., 2010). There are two strategies of wine fermentation: inoculated and spontaneous. Inoculated fermentation is initiated by the addition of an industrial *Saccharomyces* strain to grape must; by our estimation, over 150 industrial *S. cerevisiae* strains and one *S. uvarum* strain are available for winemaking purposes. The use of industrial starter cultures, of which a diverse array of strains is available, is popular amongst winemakers due to the reliability of a rapid fermentation that completes in a timely manner. Spontaneous fermentation, in contrast, is carried out by yeasts present on grape and winery surfaces that include various fermentative species from several yeast genera. Spontaneous fermentations may be initiated by a variety of weakly fermentative yeast species but by the end of fermentation are typically dominated by one or often multiple strains of *S. cerevisiae* and/or *S. uvarum* (Pretorius, 2000; Varela and Borneman, 2017). Wines made by spontaneous fermentation may have more complex sensory profiles than those fermented by single strain inocula due to the diverse metabolic activity of multiple yeast species and strains (Jolly et al., 2014).

Saccharomyces cerevisiae wine strains across global wine regions have demonstrated close genetic relatedness; they cannot be satisfactorily differentiated by geographical origin but are distinct from strains in other ecological niches (Legras et al., 2007; Liti et al., 2009; Schacherer et al., 2009; Almeida et al., 2015; Peter et al., 2018). Nevertheless, *S. cerevisiae* population structure has been identified on a smaller scale across various wine regions in France, Portugal, New Zealand and Italy spanning tens to hundreds of kilometers (Gayevskiy and Goddard, 2012; Schuller et al., 2012; Knight and Goddard, 2015; Borlin et al., 2016; Rantsiou et al., 2017). A factor confounding analysis of regional *S. cerevisiae* population structure is the dissemination of commercial wine strains into the winery and surrounding environment. Commercial *S. cerevisiae* strains may be highly abundant or dominate spontaneous fermentations in wineries using commercial strains (Beltran et al., 2002; Hall et al., 2011; Tello et al., 2011; Scholl et al., 2016). However, indigenous strains can dominate spontaneous fermentations and outcompete commercial strains when co-inoculated (Tello et al., 2011;

Capece et al., 2019). In large-scale surveys of *S. cerevisiae* populations in vineyards and wineries across multiple wine regions, commercial strains were found to represent a very low proportion of the total yeast population (Gayevskiy and Goddard, 2012; Schuller et al., 2012; Knight and Goddard, 2015). However, widespread dissemination of commercial strains was detected across three Italian wine regions (Viel et al., 2017). The presence of commercial yeast strains was also found to be a driver of population structure in a small-scale vineyard and winery (Martiniuk et al., 2016). In all cases, identification of commercial wine isolates is dependent on access to a database containing the genetic strain profile of each commercial strain.

In contrast to *S. cerevisiae*, less information exists on the population structure and genetic diversity of *S. uvarum*. Sequence analysis of 54 *S. uvarum* strains revealed three clades including a holoarctic clade comprised of natural isolates and wine-making strains from North America, Europe and the Far East (Almeida et al., 2014). Microsatellite analysis of a larger group of *S. uvarum* strains consisting mostly of European wine and cider isolates did not reveal a strong association between genetic relatedness and region of origin (Masneuf-Pomarede et al., 2016). Another clear difference between *S. cerevisiae* and *S. uvarum* winery and vineyard isolates is that a much higher percentage of *S. uvarum* wine strains are homozygous, suggesting that the species is in-bred (Zhang et al., 2015; Masneuf-Pomarede et al., 2016). However, two recent studies identified a highly diverse heterogenous population of *S. uvarum* in spontaneous Chardonnay fermentations from an OV winery in two separate vintages (Morgan et al., 2019; McCarthy et al., Unpublished). A subset of the OV *S. uvarum* strains are genetically distinct from global *S. uvarum* strains and have a higher degree of heterozygosity based on microsatellite analyses (Morgan et al., 2019).

Herein, we elucidate the regional population structure of vineyard-associated *Saccharomyces* strains among three winemaking sub-regions of the Okanagan Valley (KE, NP, and OO) over two vintages (2016–2017), and compile a database of over 150 commercial *S. cerevisiae* strains to profile commercial yeast dissemination across the region. We also denote the different flavonol and anthocyanin profiles and seed tannin levels of Pinot Noir grapes between the three sub-regions in the 2017 vintage. Our work is the first study looking at the regional-specificity of Pinot Noir grapes in the OV, British Columbia, Canada.

MATERIALS AND METHODS

Experimental Design

In autumn 2016 and 2017, we aseptically harvested healthy grape clusters from 13 Pinot Noir vineyards from the OV within a week prior to the winery harvesting date (**Figure 1**). The vineyards spanned a 100 km distance from north to south and included three OV sub-regions – KE in the north, NP in the center, and OO in the south. In total, 4 KE, 5 NP and 4 OO Pinot Noir vineyards were sampled. Weather data were retrieved from three weather stations, namely "Oliver STP," "Penticton A," and "Kelowna UBCO" (Government of Canada, 2020). Growing degree days (GDD) were calculated as base 10°C degree-days from 1st April to 31 October 2017 and cumulative precipitations for the same period was identified (Amerine and Winkler, 1944).

Grape Sampling and Processing

A ∼0.25 hectare area of each Pinot Noir vineyard was selected for sampling with outer vineyard rows and the first 6 m of each row excluded. Each area was sub-divided into thirty-two 18 m sections of two rows; six sections were randomly selected for sampling. Each sample consisted of 30 grape clusters aseptically harvested within each section. All samples were transported directly to the lab on ice and processed within 24 h of harvest. Each sample was manually crushed for 15 min; 500 mL of juice (excluding skins and seeds) was transferred from each sample to a sterile airlock-sealed vessel and fermented aseptically, for a total of 78 fermentations (six per vineyard) for each vintage. Fermentations were conducted at 25°C and sampled at two-thirds sugar depletion (as determined by weight loss). Fermentations that did not reach two-thirds sugar depletion within 40 days were excluded from further analysis.

In 2017, 4 of the 6 sections selected for yeast isolation in each vineyard were randomly selected for grape composition analyses. Forty berries per section were randomly picked by hand for total soluble solids (TSS) analyses. Another 40 berries per replicate were randomly harvested with scissors for flavonoid analysis by cutting off the berry at the pedicel level to avoid any damage that could create oxidation to the berry. The grape samples were taken to the laboratory on dry ice, where they were stored in a −80°C freezer until processing.

Saccharomyces Isolation and DNA Extraction

At two-thirds sugar depletion, fermentation samples were serially diluted in 0.1% peptone and plated in duplicate on yeast extract-peptone-dextrose (YPD) agar plates containing 0.015% biphenyl and 0.01% chloramphenicol to inhibit mold and bacterial growth, respectively (Singleton and Sainsbury, 1987; Luck and Jager, 1997). For each fermentation sampled, up to 48 *Saccharomyces* colonies were isolated when possible from a plate containing 30–300 colonies. Suspected *Saccharomyces* colonies were confirmed by plating on Wallerstein nutrient agar, which differentiates *Saccharomyces* and non-*Saccharomyces* yeasts based on colony color, and cross-verified by negative growth on lysine agar (Heard and Fleet, 1986; Pallman et al., 2001). All isolates were arrayed in 96-well plates and frozen at −80°C. Yeast DNA was extracted as previously described and diluted to 25 μg/μl in sterile 10 mM Tris pH 8.0 (Martiniuk et al., 2016).

Differentiation of *S. cerevisiae* and *S. uvarum* Isolates

Saccharomyces cerevisiae and *S. uvarum* were differentiated based on polymorphism at the *MET2* locus using restriction fragment

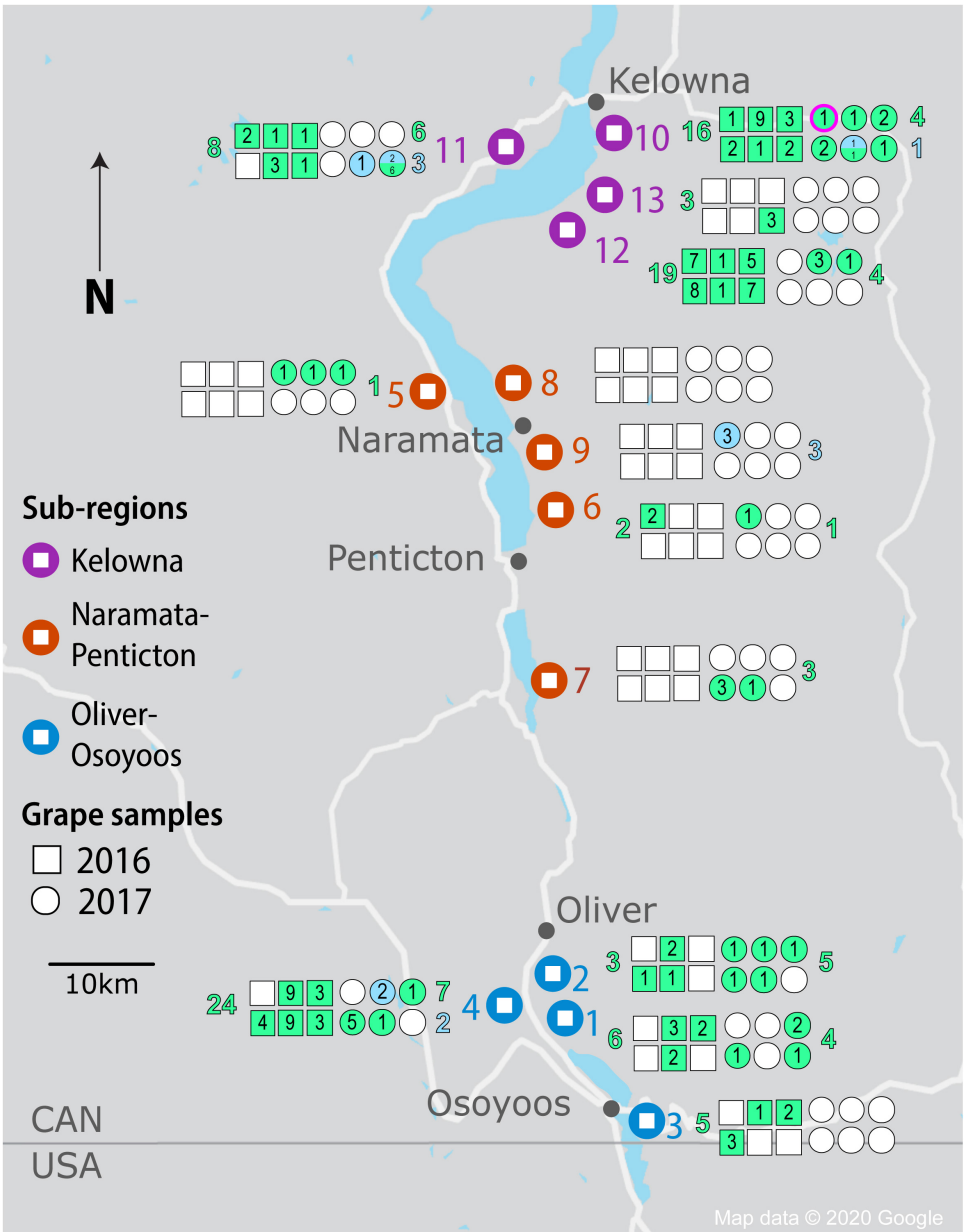

FIGURE 1 | Isolation of *Saccharomyces* yeasts by sample, vineyard, sub-region and vintage from the OV wine region. Vineyard locations are denoted by large markers and colored by region (KE-purple, NP-orange, and OO-blue). Squares and circles represent each of 6 spontaneous fermentations conducted for each vineyard in 2016 and 2017, respectively. Shaded squares and circles indicate fermentations that reached two-thirds sugar depletion; green shading indicates *Saccharomyces cerevisiae* strains while blue shading indicates *Saccharomyces uvarum* strains. The number of strains isolated from a spontaneous fermentation is noted within each square or circle. The number of *S. cerevisiae* and *S. uvarum* strains isolated in total from each vineyard are listed in green and blue, respectively (to the left of the vineyard for 2016 fermentations and to the right of the vineyard for 2017 fermentations). The circle outlined in fuschia for vineyard #10 denotes the fermentation from which *S. paradoxus* was isolated.

length polymorphism (RFLP)-polymerase chain reaction (PCR) (Masneuf et al., 1996). The diluted DNA (1 µl) was added into 19 µl of *MET2* PCR master mix [20% 5× dNTPs, 10% 10× BioBasic Taq Buffer, 10% MgSO4 (20 mM), 0.6% *MET2* forward primer (100 µM), 0.6% *MET2* reverse primer (100 µM), 0.5% BioBasic Taq Polymerase]. Amplification was performed under the following conditions: initial denaturation step of 5 min at 94°C, 35 cycles of 30 s at 94°C, 45 s at 50°C and 1 min at 72°C, and a final elongation step of 10 min at 72°C. The PCR products were digested separately by *EcoRI* and *PstI* at 37°C for 30 min, then analyzed by electrophoresis on a 1.2% agarose gel. *EcoRI* digests only the *MET2* gene of *S. cerevisiae* whereas *PstI* digests only the *MET2* gene of *S. uvarum*.

Identification of *Saccharomyces paradoxus*

For DNA from isolates with *MET2* that could not be digested with *EcoRI* or *Pst1*, internal transcribed spacer (ITS)-PCR was performed to identify the species. The diluted DNA (1 μl) was added into 19 μl of PCR master mix [20% 5× dNTPs, 20% 5× Phusion HF buffer, 0.5% ITS1 primer (100 μM), 0.5% ITS4 primer (100 μM), 1% Phusion Taq Polymerase] (Op, De Beeck et al., 2014). ITS amplification was performed under the following conditions: initial denaturation step of 2 min at 98°C, 35 cycles of 10 s at 98°C, 30 s at 62°C, 30 s at 72°C, and a final elongation step of 10 min at 72°C. The ITS PCR products were cleaned by the E.Z.N.A Cycle Pure Kit and sent to Genewiz for Sanger sequencing. The sequencing data were analyzed by BLAST to identify the species.

Commercial *S. cerevisiae* Collection Compilation

One hundred and sixty commercial *S. cerevisiae* strains were generously donated or purchased from various companies and wineries and from the lab of Dr. Daniel M. Durall, University of British Columbia, Canada. Strains received on slants were streaked for single colonies on YPD agar, while active dry yeasts were rehydrated for 10 min in water and streaked for single colonies on YPD agar. Certain commercial strains were sourced from multiple locations; in cases where genotypes from the same strain differed between sources, all MLGs were included in the database (**Supplementary Table S1**).

Microsatellite Analysis

Isolated and commercial *S. cerevisiae* strains were genotyped using ten short tandem repeat (STR) loci selected from previous studies (**Supplementary Table S2**) (Legras et al., 2005; Richards et al., 2009). These loci were amplified according to (Martiniuk et al., 2016). For *S. uvarum*, we selected eleven STR loci that were previously identified (Zhang et al., 2015; Masneuf-Pomarede et al., 2016) (**Supplementary Table S3**). Each STR amplification reaction contained 5 μl of Qiagen Multiplex PCR Master Mix, 4 μl of primer mix, and 1 μl of diluted DNA. Primer sequences for *S. cerevisiae* and *S. uvarum* microsatellite amplification are provided in **Supplementary Tables S4, S5**, respectively. The PCR was carried out with an initial denaturation step of 5 min at 97°C; 34 cycles of 30 s at 95°C, 60 s at 54°C, and 120 s at 72°C; and a final elongation step of 10 min at 72°C. Microsatellite amplicons were analyzed at the UBC Sequencing and Bioinformatics Consortium on an AB3730 DNA Analyzer. GeneMapper software was used to generate a multi-locus genotype (MLG) for each amplicon profile. Each unique MLG was considered as an individual strain.

Saccharomyces Population Data Analysis

Saccharomyces MLG counts and genetic distance calculations were performed in R v.3.5.3 using the poppr package v.2.6.0 (Kamvar et al., 2014; Kamvar et al., 2015). *S. cerevisiae* isolate MLGs were compared against our *S. cerevisiae* commercial strain collection using a custom R script based on the genetic relatedness measure Bruvo Distance (BD) (Bruvo et al., 2004). Isolate MLGs $\leq$ 0.25 BD from the closest commercial strain relative were classified as commercial strains whereas the remainder were classified as unknown. *S. uvarum* isolate MLGs were compared against a database of 20 *S. uvarum* strains previously isolated from around the world, 10 *S. uvarum* strains previously isolated in OV wineries and 1 *S. uvarum* commercial strain, BMV 58 (**Supplementary Table S6**). Venn diagrams were created in Jvenn to visualize the number of strains isolated in each sub-region and each vintage (Bardou et al., 2014). Analysis of molecular variance (AMOVA) was performed in poppr and Bayesian clustering of MLGs in InStruct (Gao et al., 2007). Subpopulation membership in InStruct was determined using the admixture model with a burn-in of 50,000 iterations, 200,000 iterations per chain with 5 chains per cluster, or *K*, from $K = 3$ to $K = 20$. The Instruct analysis was narrowed to $K = 7$ through 12 with 5 chains of 1,000,000 iterations per K and a burn-in of 100,000. The optimal K or number of sub-populations was determined using the Deviance Information Criterion method (Gao et al., 2011). The InStruct output was aligned in CLUMPP using the LargeKGreedy algorithm (Jakobsson and Rosenberg, 2007) and visualized in DISTRUCT (Rosenberg, 2004). The correlation between InStruct inferred population structure and sub-regions or sub-populations of interest was evaluated in ObStruct (Gayevskiy et al., 2014). Phylogenetic networks were produced in SplitsTree 4.14.6 using the Neighbor-Net algorithm (Bryant and Moulton, 2004; Huson and Bryant, 2006).

Grape Compositional Analysis

The berries collected for TSS analysis were weighed and squeezed, and the juice was analyzed with a digital refractometer (Sper Scientific 300017). For flavonoid analysis, the pedicels were removed from the berry samples before the weight was taken. The berries were carefully dissected by a scalpel to separate the skin and seed materials. Skins and seeds were weighed and kept frozen in liquid nitrogen before being ground into a fine powder using mortars and pestles. The fine powder samples of skins and seeds were stored in a −80°C freezer prior to flavonoid analyses.

Anthocyanin and flavonol extractions were completed as described (Downey and Rochfort, 2008). The extraction was performed twice on the skin fine powder (0.180 g samples with 1.8 g solvent in each extraction), then the solution was filtered by a 3-mL Luer-Lok Tip syringe coupled with a 0.22 mm × 13 mm PVDF filter, and diluted 10-fold with the extraction solvent. Diluted extracts were injected into an Agilent 1100 Series LC/DAD/MSD Trap XCT Plus System equipped with an Agilent ZORBAX SB-C18 Column (1.8 μm, 4.6 × 50 mm). The mobile phases were composed of a solvent A (water with 2% formic acid) and a solvent B (acetonitrile with 2% formic acid). The binary solvent gradient for the liquid chromatographic separation was achieved as followed: 0 min, 5% solvent B; 6 min, 20% solvent B; 9 min, 80% solvent B; 10 min, 90% solvent B; 11 min, 5% solvent B. The analysis was run at a flow rate of 1.20 mL/min at a constant temperature of 67°C. Anthocyanins were examined at 520 nm. Flavonols were examined by the mass spectrometer because co-elution occurred at 353 nm.

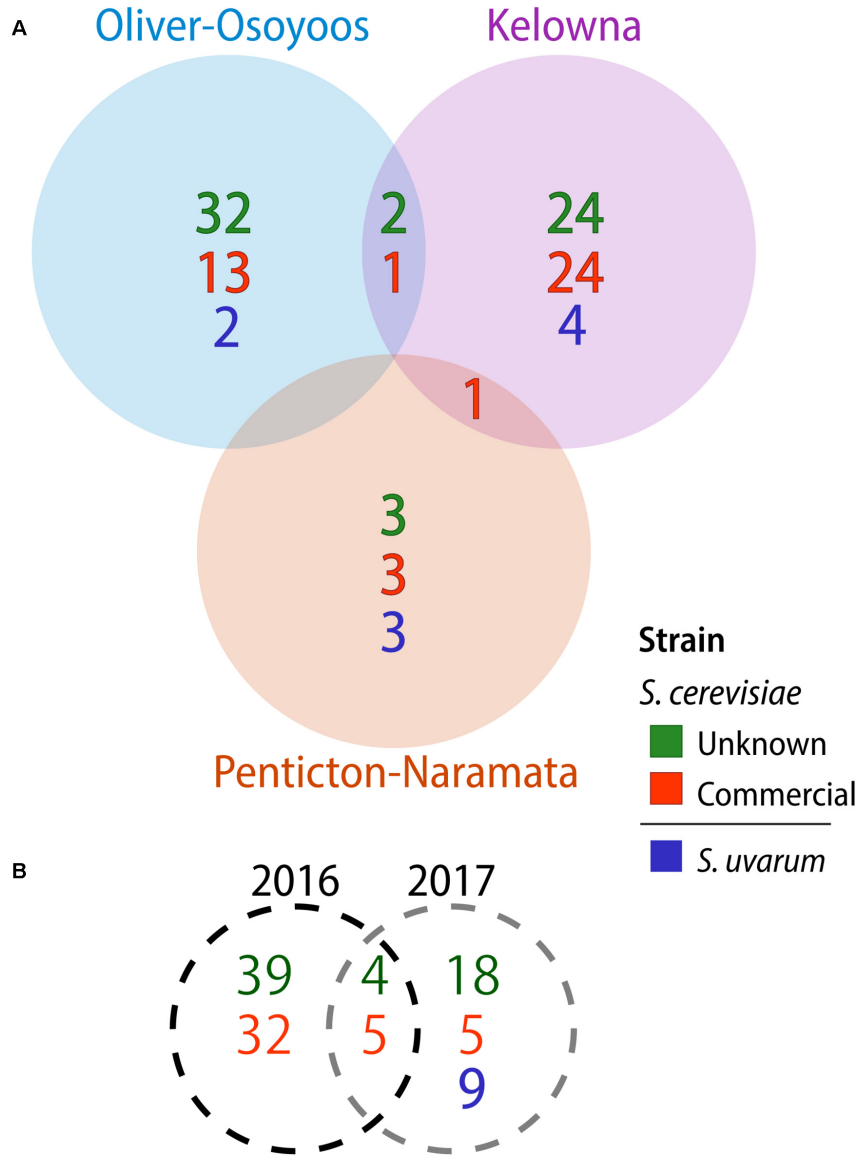

FIGURE 2 | *Saccharomyces cerevisiae* and *S. uvarum* strains isolated by **(A)** OV sub-region and **(B)** vintage. Commercial *S. cerevisiae* strains are in red, unknown strains in green, while *S. uvarum* strains are blue.

Compound identification was conducted by (i) comparing their retention times with those of authentic standards (3-*O*-glucosides of cyanidin, peonidin, delphinidin, petunidin, and malvidin, (ii) matching the mass spectra of identified peaks with anthocyanin and flavonol compounds retrieved from published papers, and (iii) comparing their elution order (Mazza et al., 1999; Garcia-Beneytez et al., 2003; Castillo-Munoz et al., 2007; Downey and Rochfort, 2008). Anthocyanin and flavonol concentrations were reported in malvidin 3-glucoside and quercetin-3-glucoside equivalents, respectively, and expressed as μg/berry and μg/g of berry fresh weight.

For the extraction of skin and seed tannins, 0.18 g of berry skins or seeds were added to 1.8 mL of acetone/water solution (70/30) and shaken gently for 24 h. The sample was centrifuged (10 min at 14,000 *g*), then 1 mL of supernatant was removed into a new 2 mL-micro tube, and the acetone was evaporated via 1 h of speed vacuum. The residual aqueous extract was adjusted to 1 mL with deionised water. After this, tannins were measured by the protein precipitation assay (Harbertson et al., 2002). Skin and seed tannins were expressed as mg/berry and mg/g of berry fresh weight. Measurement of tannins was carried out in duplicate from each sample, and the two values obtained were averaged.

The general berry and flavonoid data are presented as mean ± standard error and analyzed by an ANOVA test where the effect of the sub-regions (n = 3) on the various parameters was assessed with vineyards (n = 13) considered as nested factors within sub-regions. Different letters indicate significant

TABLE 1 | AMOVA of *S. cerevisiae* MLGs isolated in this study by vintage and sub-region, with and without commercial MLGs.

		w/C MLGs			*w/o C MLGs*		
Factor	**Hierarchical level**	**Variation (%)**	**Φ**	***P***	**Variation (%)**	**Φ**	***P***
Vintage	Between vintages	−1.44	−0.01	0.6415	0.51	0.01	0.2563
	Vineyards within vintages	16.71	0.16	<0.0001	21.75	0.22	<0.0001
	Within vineyards	51.35	0.61	<0.0001	59.28	0.76	<0.0001
	Within samples	33.38	0.67	<0.0001	18.46	0.81	<0.0001
Sub-region	Between sub-regions	5.44	0.05	0.0278	10.40	0.10	0.0295
	Vineyards within sub-regions	8.82	0.09	<0.0001	7.94	0.09	0.0008
	Within vineyards	53.44	0.62	<0.0001	63.58	0.78	<0.0001
	Within samples	32.28	0.68	<0.0001	18.08	0.82	<0.0001

Significance was determined from 9999 permutations. PN strains were excluded from this analysis due to small sample size. w/C MLGs, with commercial strains isolated from this study; w/o C MLGs, without commercial strains.

differences ($p < 0.05$) between sub-regions according to a Tukey's HSD test. Statistical analyses were performed using JMP 14 (Statistical Discovery™ from SAS Institute Inc.).

RESULTS

Isolation of *Saccharomyces* Strains From Pinot Noir Spontaneous Fermentations in Three OV Sub-Regions

We chose to isolate *Saccharomyces* from Pinot Noir spontaneous fermentations once two-thirds of the sugar was depleted to identify strains that were vigorous during active fermentation. Of the 78 spontaneous fermentations conducted in each vintage, 33 (42%) in 2016 and 29 (37%) in 2017 reached two-thirds sugar depletion (**Figure 1** and **Supplementary Table S7**). The number of fermentations reaching two-thirds sugar depletion varied substantially among sub-regions and between vintages. Even though NP had the fewest spontaneous fermentations reaching two-thirds sugar depletion among the three sub-regions in both vintages, NP had many more successful fermentations in 2017 than 2016 (7 out of 30 compared to 1 out of 30, respectively). In contrast, both OO and KE had fewer successful fermentations in the 2017 vintage than 2016 vintage (**Figure 1** and **Supplementary Table S7**). In 2016, OO had 14 out of 24 fermentations reach two-thirds sugar depletion (58%) compared to 12 out of 24 (50%) in 2017. Likewise, KE had 18 out of 24 (75%) fermentations reach two-thirds sugar depletion in 2016 compared to 10 out of 24 (42%) in 2017. In both vintages, the exact same vineyards and where possible, the same locations within the vineyard were sampled.

A total of 1,544 *Saccharomyces* colonies were isolated in 2016 compared to 1,368 in 2017. Only *S. cerevisiae* was isolated in 2016. In contrast, in 2017 three *Saccharomyces* species were identified: 1,176 isolates of *S. cerevisiae*, 164 of *S. uvarum* and 28 of *Saccharomyces paradoxus*. Both *S. cerevisiae* and *S. uvarum* were identified in all three OV sub-regions, while *S. paradoxus* was only isolated from KE vineyard #10 (**Figure 1**). We used microsatellite analysis of 10 *S. cerevisiae* STR loci and 11 *S. uvarum* STR loci to genotype our *Saccharomyces* isolates whereas no genotyping was conducted on *S. paradoxus*. A total of 103 *S. cerevisiae* MLGs and 9 *S. uvarum* MLGs were identified in this study (**Supplementary Tables S8, S9**, respectively). Each MLG is considered to be an individual strain and will be referred to as 'strain' or "MLG" from now on. The distribution of strains across vintages, sub-regions, vineyards and between replicate spontaneous fermentations was highly heterogeneous (**Figure 1**). As few as one and as many as nine *Saccharomyces* strains were isolated from a single spontaneous fermentation that reached two-thirds sugar depletion. We compared our isolated *S. cerevisiae* strains against a database that we generated of 160 commercial *S. cerevisiae* strains used for wine (150 strains), beer (8 strains) and spirit (2 strains) production (**Supplementary Table S1**). Of the 160 commercial strains profiled in this study, only 125 MLGs were generated, indicating a high degree of redundancy between commercially available strains. Out of the 103 vineyard isolate strains, 42 were the equivalent to, or highly similar to, commercial strain isolates (≤0.25 BD from closest commercial strain relative) whereas 61 strains were different from commercial strains and will henceforth be referred to as 'unknown' strains. A comparison of the *S. cerevisiae* strains isolated across vintages and OV sub-regions revealed that very few strains were isolated from both vintages or multiple sub-regions (**Figure 2**). Three *S. cerevisiae* strains were shared between OO and KE, one between NP and KE and none between OO and NP (**Figure 2A**). Only 9 *S. cerevisiae* strains were identified in both 2016 and 2017 whereas 71 strains were identified solely in the 2016 vintage and 23 strains solely in the 2017 vintage (**Figure 2B**). While a greater number of unknown *S. cerevisiae* strains than commercial were isolated in each vintage, fewer unknown strains (4) than commercial strains (5) were shared between vintages (**Figure 2B**). Across sub-regions in both vintages, 24 unknown strains were isolated only from KE, 32 only from OO and 3 only from NP (**Figure 2A**). OO had the highest proportion of unknown strains (68%).

None of the 9 *S. uvarum* MLGs identified in this study were shared between sub-regions (**Figure 2**). There were 4 *S. uvarum* strains isolated from KE, 3 from NP, and 2 from OO (**Figure 2A**).

None of the 9 *S. uvarum* MLGs were equivalent to the commercial *S. uvarum* commercial strain, BMV58 (Lallemand). However, 2 of our *S. uvarum* strains had been isolated in previous OV studies [(Morgan et al., 2019; McCarthy et al., Unpublished) and unpublished data from this group].

Saccharomyces Population Structure

Saccharomyces cerevisiae

We conducted hierarchical AMOVAs on *S. cerevisiae* MLGs to elucidate strain population structure across vintages and between sub-regions, both with and without commercial MLGs included. Separate AMOVAs were conducted using vintage and sub-region as factors, and NP strains were excluded from this analysis due to small sample size (**Table 1**). In both analyses, within-vineyard strain populations were most variable. While very few strains were shared between vintages, AMOVA identified no significant difference between 2016 and 2017 strain populations whether or not commercial strains were included (−1.44%, $p = 0.6415$; 0.51, $p = 0.2563$), indicating that the populations in each vintage were genetically similar. In contrast, significant variation was found between KE and OO sub-regional populations with commercial strains included (5.44%, $p = 0.0278$). Notably, the variation nearly doubled when commercial strains were removed from the analysis (10.40%, $p < 0.0295$), indicating stronger spatial population structure of unknown strains. We further evaluated *S. cerevisiae* strain population structure using InStruct, a clustering software optimized for inbred or clonal populations like *S. cerevisiae* that assigns individuals in a population to a given number of statistically determined subpopulations (Gao et al., 2007, 2011). Instruct analysis identified 10 subpopulations in the *S. cerevisiae* MLG dataset (K1–K10) and ancestry profiles for each MLG by sub-region were visualized using Distruct (**Figure 3**). Profiles containing >80% of a particular color indicate MLGs belonging to a single subpopulation, while profiles consisting of multiple colors indicate admixed or interbred MLGs. Subpopulations K1, K5, and K6 correspond to *S. cerevisiae* commercial MLGs DV10, Vt3.001/CY3079, and RC212/D254, respectively, while other commercial strains are represented by admixture of two or more subpopulations (**Figure 3**). For example, LalBM45 in KE has a membership coefficient of ∼0.2 in each of K2, K4, and K10 (**Figure 3**). Two subpopulations, K8 and K9, are not associated with any commercial strains; these are most prevalent in the OO populations (**Figure 3**). InStruct inferred *S. cerevisiae* population structure is significantly correlated with sub-region ($R^2 = 0.13$, $p < 0.0001$) as determined by ObStruct, with OO populations contributing most to sub-region as a driver of this structure (**Supplementary Table S10**). Interestingly, subpopulation K9 is also a strong driver of population structure ($R^2 = 0.06$ when K9 is removed), which agrees with the increased differentiation between sub-regions when commercial strains were removed (**Table 1**).

A phylogenetic network was constructed using a BD matrix to visualize the genetic relationships between unknown and commercial *S. cerevisiae* strains (**Figure 4**). While some of the strains classified as unknown appear related to commercial strains, two sub-regional clusters of unknown *S. cerevisiae* strains from OO (blue circle) and KE (purple circle) were identified. Thus, most of the unknown strains isolated from OO and KE were more genetically related to strains isolated from the same sub-region as compared to strains between sub-regions or other commercial strains (**Figure 4**). Additionally, many of these strains have >60% membership in the two InStruct subpopulations not associated with commercial MLGs (K8, K9, **Figure 3**). It should be noted that some *S. cerevisiae* strains isolated from KE were closely genetically associated with strains in the OO cluster (e.g., OK221 and OK222). In addition, OK128 and OK140 were isolated in both KE and OO (**Figure 4**). Unexpectedly, we found that two unknown *S. cerevisiae* strains isolated from NP (OK11 and OK12) were genetically closely associated with beer strains (**Figure 4**).

Saccharomyces uvarum

Only 9 MLGs were identified from all 164 *S. uvarum* isolates so AMOVA could not be performed on the *S. uvarum* dataset due to the low number of strains isolated. We compared our *S. uvarum* MLGs to 31 *S. uvarum* strains previously isolated from locations in British Columbia (OV wineries, Hornby Island) and other regions worldwide and displayed the data using a phylogenetic network (**Figure 5** and **Supplementary Table S6**). One *S. uvarum* MLG from OO (SuOK08) was identical to a strain isolated from a previously unpublished OV study that we conducted with Pinot Gris grapes and named OV13-11. Another *S. uvarum* MLG from KE (SuOK03) was identical to a strain isolated from OV spontaneous Chardonnay fermentations and named MLG13 (McCarthy et al., Unpublished). One KE *S. uvarum* genotype, SuOK04, is closely related to PYCC 6860, a strain previously isolated from an oak tree on Hornby Island in British Columbia (Almeida et al., 2014). Two OO *S. uvarum* strains (SuOK08 and SuOK09) and three NP *S. uvarum* strains (SuOK05, SuOK06, and SuOK07) are more closely related to each other than between their respective sub-regions. By contrast, *S. uvarum* strains isolated from KE (SuOK01, SuOK2, and SuOK04) are distantly related to each other. For example, SuOK01 is more closely related to two *S. uvarum* strains isolated from New Zealand (A1 and A9) (Zhang et al., 2015).

Flavonoid Composition of Pinot Noir Grape Berries From OV Sub-Regions

In the 2017 vintage, in addition to performing 6 spontaneous fermentations from each of 13 OV vineyards, we also sampled the Pinot Noir berries from each vineyard to determine how grape berry weight and metabolites may differ in the 3 OV sub-regions. In particular, we focused on the three major flavonoid classes: anthocyanins, flavonols, and tannins. We observed that the berry weight as well as the number of seeds per berry were affected by the sub-region (**Supplementary Table S11**). The average berry weight and seed number were higher in NP than OO and KE. The other parameters analyzed – skin weight, seed weight, skin to berry ratio, seed to berry ratio, and TSS – did not vary among the three OV sub-regions. Importantly, the TSS were not significantly different among all three sub-regions, ensuring that we could accurately compare the flavonoid composition in the Pinot Noir berries.

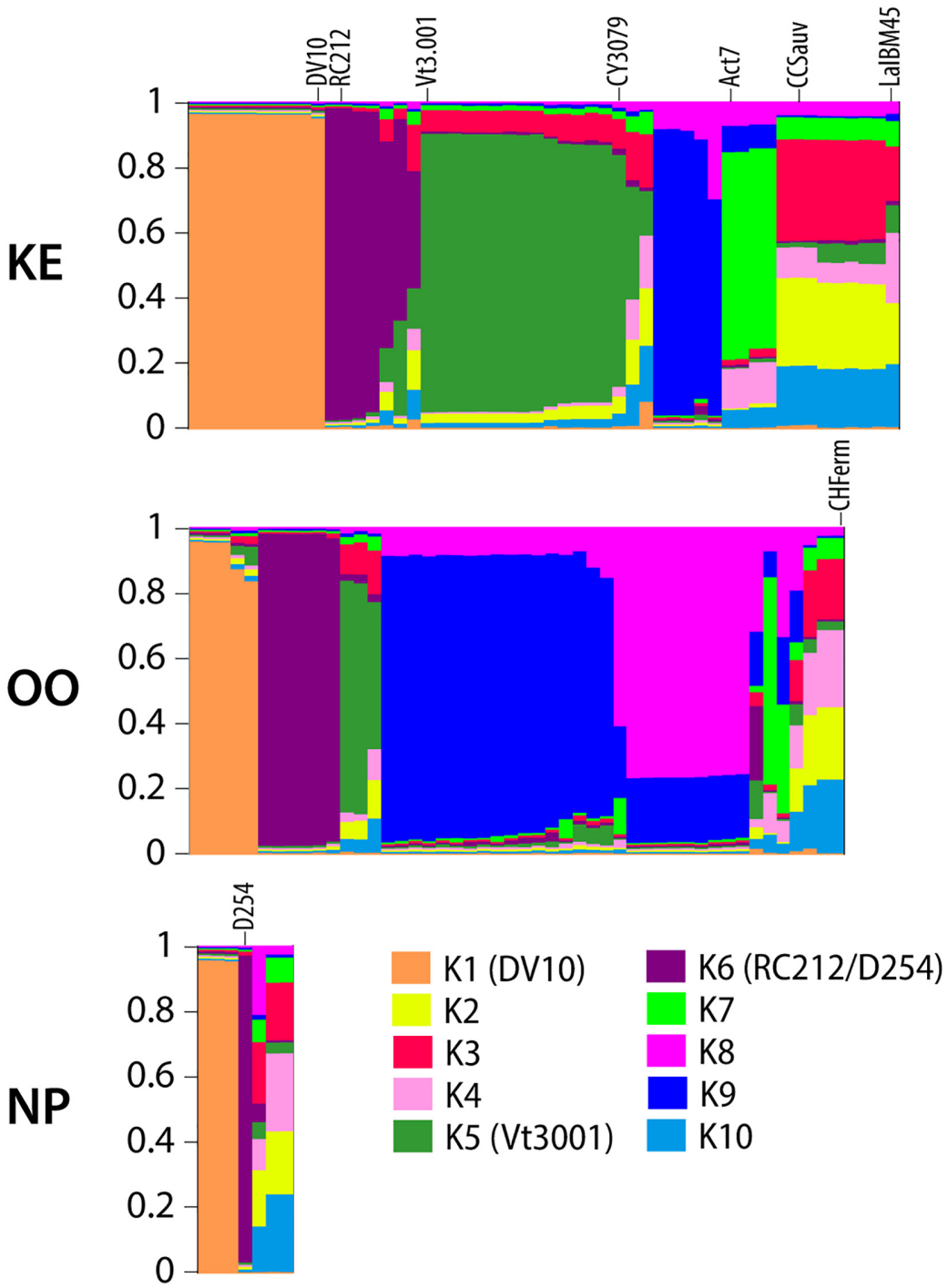

FIGURE 3 | DISTRUCT plots of inferred ancestry profiles of *S. cerevisiae* strains isolated from KE, OO, and NP sub-regions. Each column represents an ancestry profile for an individual MLG. Each color corresponds to one of ten inferred subpopulations as noted in the legend. The proportion of each color in a column represents the proportion (membership coefficient) of the MLG's ancestry profile assigned to that subpopulation as measured on the *y*-axis of each plot. Selected commercial isolate MLG ancestry profiles are labeled on the plot, and subpopulations containing commercial MLGs with membership coefficients >80% are labeled in the legend with the strain name in parentheses.

Five anthocyanins were identified and quantified in all the Pinot Noir grape samples collected; the monoglucosides of delphinidin (D-3-G), cyanidin (C-3-G), petunidin (Pt-3-G), peonidin (Pn-3-G), and malvidin (M-3-G) (**Figure 6A**). M-3-G was the most abundant anthocyanin while C-3-G was the least abundant anthocyanin. The content (expressed as μg/berry) of

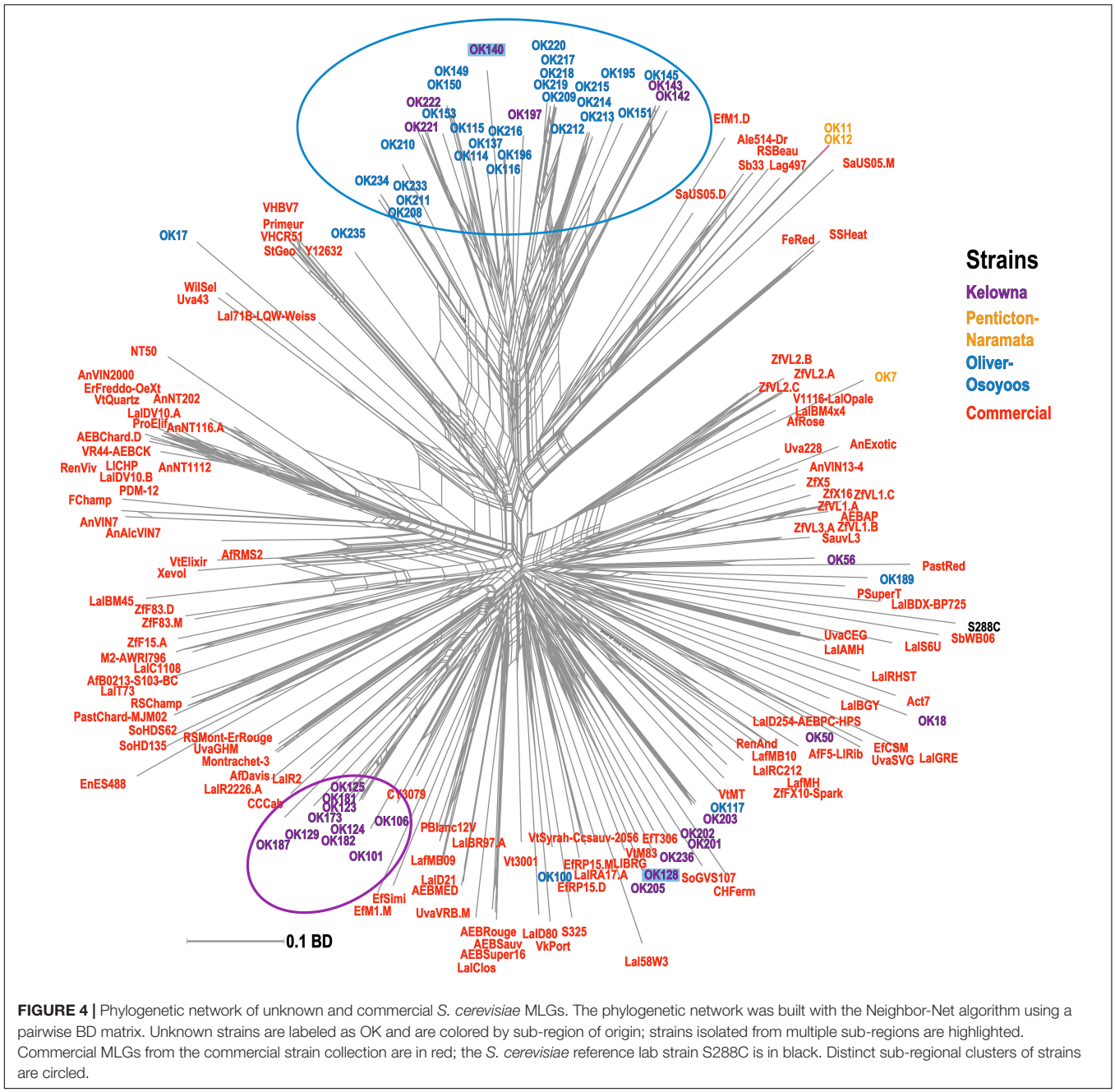

FIGURE 4 | Phylogenetic network of unknown and commercial *S. cerevisiae* MLGs. The phylogenetic network was built with the Neighbor-Net algorithm using a pairwise BD matrix. Unknown strains are labeled as OK and are colored by sub-region of origin; strains isolated from multiple sub-regions are highlighted. Commercial MLGs from the commercial strain collection are in red; the *S. cerevisiae* reference lab strain S288C is in black. Distinct sub-regional clusters of strains are circled.

all anthocyanins except M-3-G was higher in KE than OO. NP had intermediate levels of all anthocyanins except M-3-G which was higher in NP than OO. The content of total anthocyanins was higher in KE and NP than OO. The concentrations (expressed as μg/g berry) of D-3-G, C-3-G and Pt-3-G were greater in KE than OO berries, while Pn-3-G and M-3-G concentrations were not affected by the sub-region (**Supplementary Figure S1**). The concentration of total anthocyanins was higher in KE than OO (**Supplementary Figure S1A**).

Nine flavonols were identified in Pinot Noir grapes collected from the three OV sub-regions (**Figure 6B**). These compounds were the glucosides of myricetin (My-3-Glu), quercetin (Qu-3-Glu), laricitrin (La-3-Glu), kaempferol (Ka-3-Glu), isorhamnetin (Is-3-Glu), and syringetin (Sy-3-Glu), the galactosides of myricetin (My-3-Gal) and quercetin (Qu-3-Gal), and the glucuronide of quercetin (Qu-3-Gld). Qu-3-Glu was the most abundant flavonol compound in the Pinot Noir berries while La-3-Glu and Sy-3-Glu were the least abundant flavonols identified (**Figure 6B**). The content (expressed as μg/berry) of all quercetin conjugates was higher in KE than OO berries. Qu-3-Glu was also higher in KE than NP berries while Qu-3-Gld was as high in NP as KE berries. The content of myricetin conjugates was also higher in KE than OO berries (**Figure 6B**). My-3-Gal

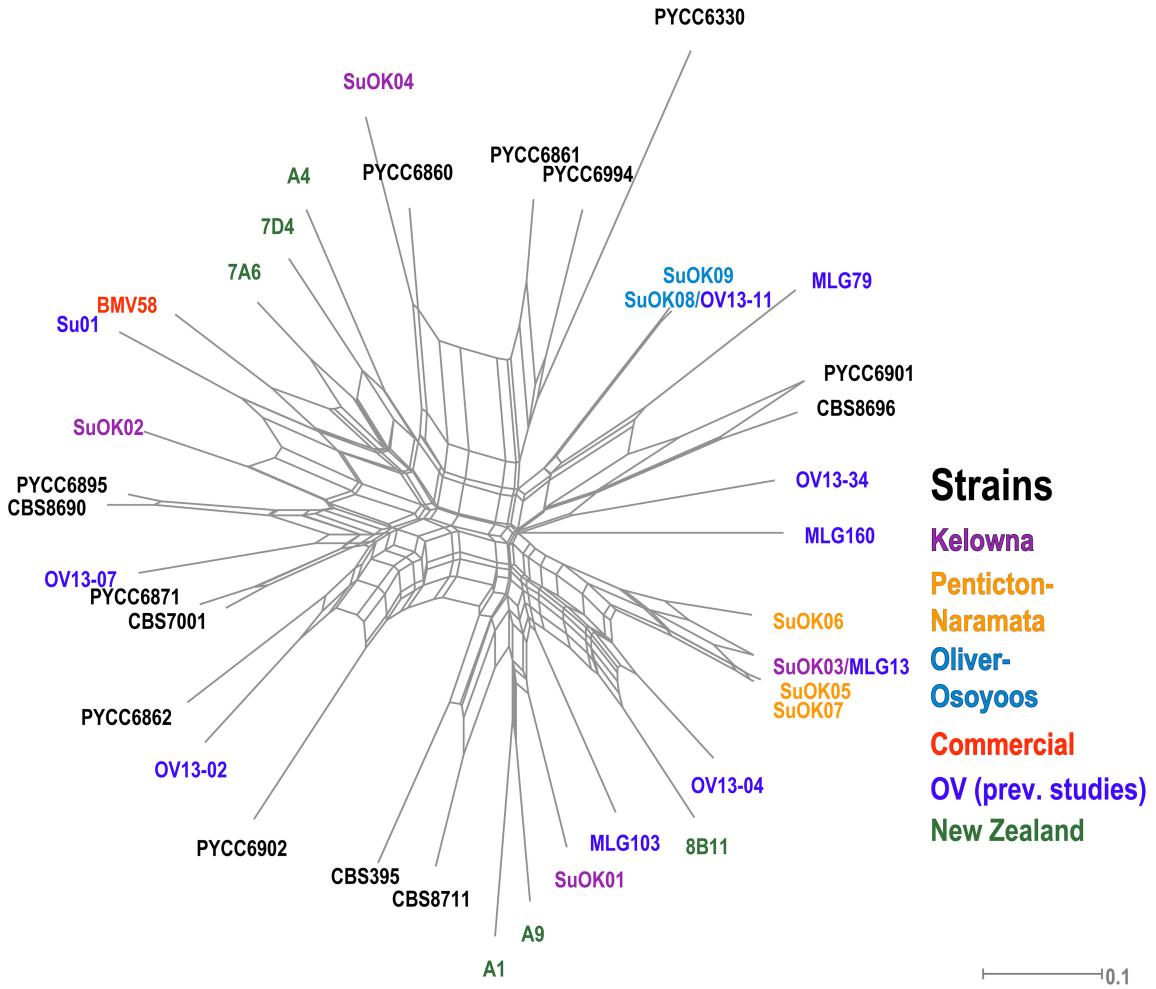

FIGURE 5 | Phylogenetic network of *S. uvarum* strains. The phylogenetic relationship was established by the Neighbor-Net algorithm based on BD. Newly discovered strains are labeled as "SuOK" and colored according to the region of isolation. SuOK08 and SuOK03 are indicated with strains isolated from the OV in previous studies (OV13-11 and MLG13, respectively, **Supplementary Table S6**). Green strains were isolated from a study in New Zealand (Zhang et al., 2015), the commercial *S. uvarum* strain BMV58 is indicated in red and black colored strains are from CBS and PYCC databases (**Supplementary Table S6**).

content was intermediate in NP berries whereas My-3-Glu content was as high in NP as KE berries. Similar results were observed when the flavonols were reported as a concentration (expressed as μg/g berry). The concentration of most flavonols were higher in KE than OO and NP generally had intermediate levels (**Supplementary Figure S1B**). The content of total flavonols was higher in KE and NP than OO berries (**Figure 6B**) and the concentration was higher in KE than OO berries, while NP berries had intermediate levels (**Supplementary Figure S1B**).

Unlike the anthocyanin and flavonol data, the skin tannin content and concentration of Pinot Noir grapes did not vary among the three OV sub-regions (**Figure 6C** and **Supplementary Figure S1C**). However, the seed tannin content (expressed as mg/berry) and concentration (expressed as mg/g berry) were the highest in NP berries and the lowest in OO berries, and at intermediate levels in KE berries (**Figure 6C** and **Supplementary Figure S1C**).

The profile of the relative abundance of each anthocyanin was plotted as a percentage of the total amount of anthocyanins in the Pinot Noir grape samples from each sub-region (**Figure 7A**). The major anthocyanin was M-3-G in all three sub-regions, however, the relative abundance of M-3-G was higher in OO (55.79 ± 2.36%) than KE (49.89 ± 1.13%) berries. In contrast, the relative abundances of both D-3-G and Pt-3-G were higher in KE than OO berries. We also grouped the anthocyanins into di-substituted, which refers to two substituted sites (e.g., hydroxylation and methoxylation) at the B-ring (Cy-3-G and Pn-3-G), and tri-substituted, which refers to three substituted sites at the B-ring (D-3-G, Pt-3-G, and M-3-G), groups (Bakowska-Barczak, 2005). We found that the relative abundance of di-substituted and tri-substituted anthocyanins did not change among OV sub-regions (**Figure 7A**). We also considered the level of methoxylation at the B-ring of the anthocyanins. Interestingly, we found that the relative abundance of methoxylated anthocyanins (Pt-3-G,

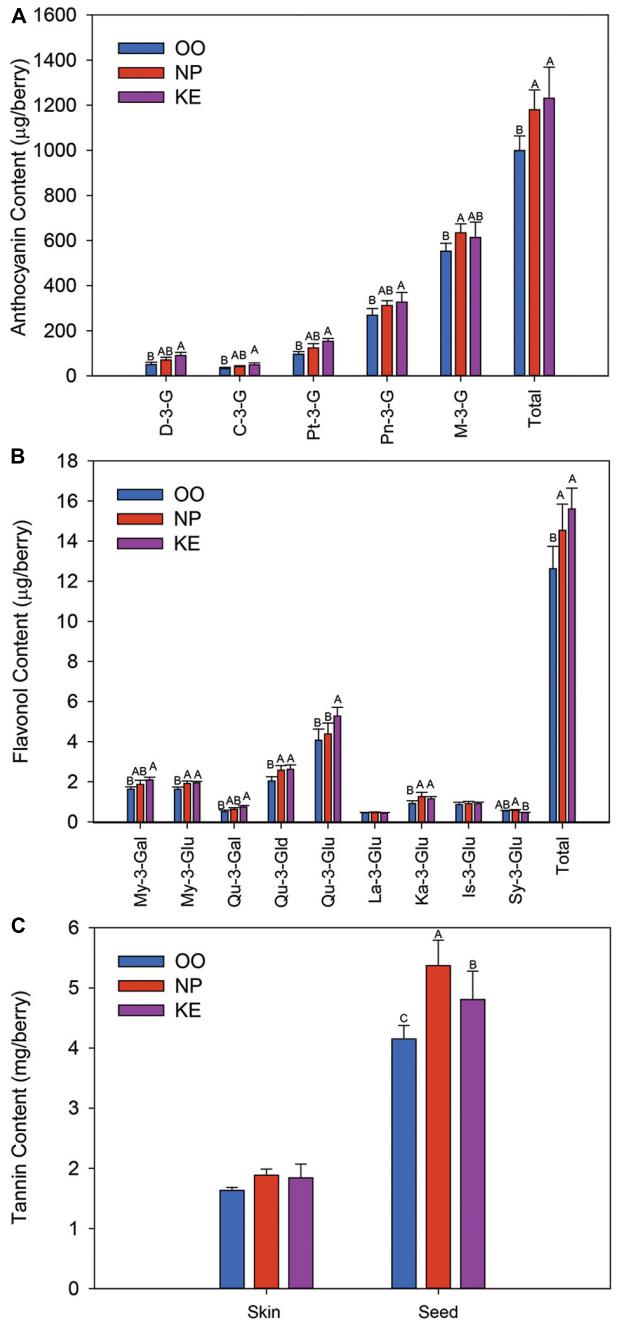

FIGURE 6 | Anthocyanin **(A)**, flavonol **(B)**, and tannin **(C)** content (amount per berry) of Pinot Noir grapes from three sub-regions of the OV (OO, blue; NP, red; and KE, purple). D-3-G, delphinidin-3-glucoside; C-3-G, cyanidin-3-glucoside; Pt-3-G, petunidin-3-glucoside; Pn-3-G, peonidin-3-glucoside; M-3-G, malvidin-3-glucoside for anthocyanins **(A)**; and My-3-Gal, myricetin-3-galactoside; My-3-Glu, myricetin-3-glucoside; Qu-3-Gal, quercetin-3-galactoside; Qu-3-Gld, quercetin-3-glucuronide; Qu-3-Glu, quercetin-3-glucoside; La-3-Glu, laricitrin-3-glucoside; Ka-3-Glu, kaempferol-3-glucoside; Is-3-Glu, isorahamnetin-3-glucoside; Sy-3-Glu, syringetin-3-glucoside for flavonols **(B)**. Error bars indicate the standard error within each sub-region. An ANOVA was performed to test the effect of the sub-regions with vineyards considered as nested factors within sub-regions. Different letters indicate significant differences ($p < 0.05$) between sub-regions according to a Tukey's HSD test.

Pn-3-G, and M-3-G) was higher in OO and NP than KE berries (**Figure 7A**).

The six aglycones of flavonols, detected in the various glycoside forms, were myricetin, quercetin, laricitrin, kaempferol, isorhamnetin, and syringetin and their relative abundances were plotted as a percentage of total flavonols per OV sub-region (**Figure 7B**). Quercetin was the most abundant flavonol with a higher relative abundance in KE (54.68 ± 0.91) than NP (50.51 ± 1.58%), and OO (49.40 ± 2.43%) berries. The relative abundance of laricitrin was higher in OO than KE berries whereas syringetin was higher in OO and NP than KE berries. As with the anthocyanins, we compared groups of mono-, di-, and tri-substituted flavonols across the OV sub-regions. We found that the relative abundance of mono-substituted flavonols (kaempferol) was higher in NP than OO berries, di-substituted flavonols (isorhamnetin and quercetin) was higher in KE than NP and OO berries, and tri-substituted flavonols (myricetin, laricitrin, and syringetin) was higher in OO and NP than KE berries (**Figure 7B**). Similar to what we discovered for anthocyanins, the relative abundance of methoxylated flavonols (laricitrin, isorhamnetin, and syringetin) was higher in OO and NP than KE Pinot Noir berries (**Figure 7B**).

DISCUSSION

In this study we surveyed 100 km of a wine region in British Columbia, Canada for yeast populations and flavonoids associated with Pinot Noir berries. We sampled from 13 vineyards which were grouped into the northern (KE), central (NP), and southernmost (OO) sub-regions of the OV. We performed spontaneous fermentations using grapes sampled from 13 vineyards for two consecutive vintages for a total of 156 spontaneous fermentations. Fewer than 50% of the grape must samples achieved two-thirds sugar depletion within 40 days of fermentation, with little consistency between vintages (**Supplementary Table S7**). In part, this may be due to our method of grape sampling, where grapes were taken from six discrete vineyard sections, and also due to the relatively low abundance (0.1%) of *S. cerevisiae* in the fungal microflora of a grape berry (Mortimer and Polsinelli, 1999; Tofalo et al., 2013). Our results reflect those in previous studies where unpredictability is associated with spontaneous fermentation, including a dynamic vineyard yeast population between vintages and geographical locations (Schuller et al., 2012; Knight and Goddard, 2015; Rantsiou et al., 2017).

The number of fermentations reaching two-thirds sugar depletion from NP in both vintages (8) was markedly lower than KE (28) and OO (26) (**Supplementary Table S7**). The fewer wine yeasts isolated from NP may be explained by various factors including the proximity to winery facilities, wind and weather patterns. Two NP vineyards (#5 and #8) are situated over 1km from the nearest known winery, while two others (#6 and #9) are located at least 100 m uphill of wineries, against prevailing wind conditions (**Figure 1**). NP also has the highest cumulative precipitation and lowest cumulative GDD among the 3 OV sub-regions in both vintages (Government of Canada, 2020).

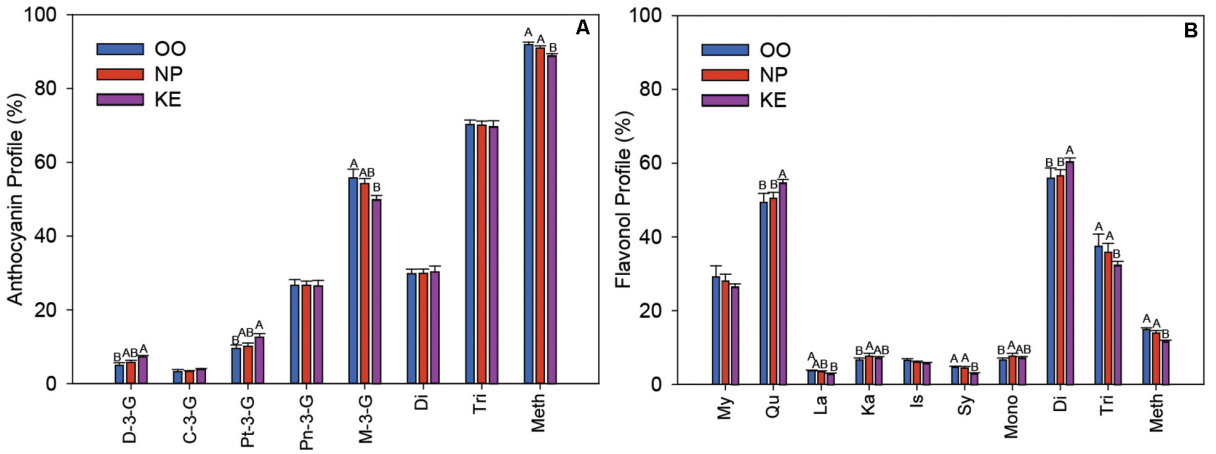

FIGURE 7 | Relative abundance of individual anthocyanins and anthocyanin fractions **(A)** and individual flavonols and flavonol fractions **(B)** in the three sub-regions of the OV (OO, blue; NP, red; and KE, purple). C, cyanidin; Pn, peonidin; D, delphinidin; Pt, petunidin; M, malvidin; Di, di-substituted; Tri, tri-substituted; Meth, methoxylated for anthocyanins **(A)**; and My, myricetin; Qu, quercetin; La, laricitrin; Ka, kaempferol; Is, isorhamnetin; Sy, syringetin; Mono, mono-substituted; Di, di-substituted; Tri, tri-substituted; Meth, methoxylated for flavonols **(B)**. Error bars indicate standard error within each sub-region. An ANOVA was performed to test the effect of the sub-regions with vineyards considered as nested factors within sub-regions. Different letters indicate significant differences ($p < 0.05$) between sub-regions according to a Tukey's HSD test.

Rain and cool temperatures may discourage the development of *S. cerevisiae* on fruit as well as the presence of other biological vectors (birds and insects) that are involved in the dispersal of wine yeasts (Goddard and Greig, 2015). While very few strains were shared between sub-regions, the most distant sub-regions (OO and KE) had the most strains in common (**Figure 2A**). Although NP is situated between KE and OO, these two latter sub-regions are much larger in size than NP and may have greater trafficking of equipment and personnel between them. OO is better suited to grow later ripening red grape cultivars due to its warmer climate, and many KE wineries may source grapes from or farm vineyards in this sub-region.

The isolation of either *S. cerevisiae*, *S. uvarum*, or both species from each vineyard and each vintage had no clear pattern except that *S. uvarum* was only isolated in the 2017 vintage (**Figure 1**). This result may correspond to the dynamic composition of vineyard-associated microbiota, which varies between vintages due to a variety of factors (Bokulich et al., 2014). In 2017, the number of *S. cerevisiae* isolates was over sevenfold higher than for *S. uvarum* (1,176 vs. 164 isolates, **Supplementary Table S7**). *S. uvarum* has lower ethanol and temperature tolerance that may result in a stuck fermentation at 24°C (Masneuf-Pomarede et al., 2010). Furthermore, due to its crytolerant traits, *S. uvarum* has typically been identified in white wine fermentations at lower temperatures (∼15°C) (Demuyter et al., 2004; Masneuf-Pomarede et al., 2010; Lopez-Malo et al., 2013; Knight and Goddard, 2015). Therefore, it was surprising to isolate *S. uvarum* from a Pinot Noir spontaneous fermentation carried out at ambient temperature (25°C) that may not favor the growth of *S. uvarum.* Moreover, although *S. uvarum* can out-compete *S. cerevisiae* in mixed culture fermentations with *S. cerevisiae* at 12°C, *S. uvarum* was isolated as a minority species in fermentations at 25°C in this study, which is expected as *S. cerevisiae* has a better fermentative competitiveness and ethanol tolerance at 25°C (Alonso-Del-Real et al., 2017; Su et al., 2019; Morgan et al., 2020). *S. paradoxus* was only identified from one KE vineyard in a single fermentation that also contained *S. cerevisiae* (**Figure 1**). We isolated 28 colonies of *S. paradoxus* but did not carry out strain genotyping, therefore the number of strains is unknown (**Supplementary Table S7**). Although *S. paradoxus* is typically more likely to be isolated from wild environments, multiple studies have identified *S. paradoxus* in vineyards and spontaneous fermentations (Redzepovic et al., 2002; Valero et al., 2007; Hyma and Fay, 2013; Sipiczki, 2016; Vaudano et al., 2019).

As found in other wine regions, *S. cerevisiae* populations differed among the three sub-regions sampled (Gayevskiy and Goddard, 2012; Schuller et al., 2012; Knight and Goddard, 2015). Among the 103 identified *S. cerevisiae* strains, there were only 4 strains identified in more than one sub-region and no strains identified in all three sub-regions (**Figure 2**). AMOVA results further indicate that *S. cerevisiae* populations are genetically dissimilar between OO and KE sub-regions, which suggests that geography is a driver of population structure within the OV wine region (**Table 1**). Variation was higher amongst vineyards within the same sub-region and vintage, rather than sub-regions themselves, highlighting the high heterogeneity of *S. cerevisiae* distribution between and within vineyards (**Table 1**). Viticulture practices among the vineyards sampled in this study were variable, with several vineyards employing organic practices. Viticulture management techniques can influence the fungal biota on fruit, which may in turn impact the diversity of *S. cerevisiae* strains in the vineyard environment (Setati et al., 2012; Morrison-Whittle et al., 2017). Our study also systematically profiled *S. cerevisiae* populations in the same sections of the same vineyards over 2 years,

enabling a direct comparison of populations between vintages. Interestingly, while very few MLGs were isolated from both vintages, no significant difference was found between 2016 and 2017 *S. cerevisiae* populations (**Table 1**). It is reasonable to expect that yeast populations may remain similar over multiple years, as *S. cerevisiae* can reside in soil and in environments proximate to vineyards, which act as reservoirs for the yeast during winter (Knight and Goddard, 2016; Sipiczki, 2016; Gonzalez et al., 2020).

Even though the grapes we sampled never entered a winery, we still identified a relatively high proportion of commercial MLGs (40.7%) in the dataset (**Figure 2**). Our previous work in three closely situated OV vineyards also found commercial yeast dissemination into the vineyards and a wider regional survey in Italy similarly found a high number of commercial *S. cerevisiae* strains in vineyards across multiple sub-regions (Martiniuk et al., 2016; Viel et al., 2017). The occurrence of commercial yeast genotypes within the different sub-regions has a weakening effect on the differentiation of sub-regional yeast populations as observed in AMOVA results, which is consistent with a previous study (Viel et al., 2017). It is very likely that many of the commercial *S. cerevisiae* strains identified in this study originated from the wineries that source grapes from the vineyards we sampled. These strains could be introduced into the vineyard if the winery facility is in close proximity (Valero et al., 2005). Using composted winery waste (e.g., pomace and lees) as fertilizer may also introduce cellar yeast into the vineyard. While we do not have composting data for all participating vineyards, at least three vineyards (#1, #7, and #8) composted winery waste in one or both years of this study, however, commercial strains were only isolated from one of these vineyards. It is also possible that other biological vectors such as insects, birds or human activity may have transported these and other strains shared between sub-regions (Goddard et al., 2010; Francesca et al., 2012). Curiously, we also identified 2 unknown strains isolated from NP (OK11 and OK12) that are related to commercial beer yeast strains (**Figure 4**). OK11 and OK12 may have originated from a brewery located within NP and were introduced by human or other vectors into the vineyard.

InStruct results indicate that there were two clusters of *S. cerevisiae* strains (K8 and K9) that appear unassociated with commercial strains isolated from the various vineyards (**Figure 3**). The phylogenetic network of unknown and commercial strains compiled for this study further indicates that there are sub-populations of *S. cerevisiae* strains that are genetically distinct from commercial strains (**Figure 4**). There is an intimate genetic association between global *S. cerevisiae* wine strains and *S. cerevisiae* wine strain populations in Europe, which implies that European wine strains migrated around the globe and became separate sub-populations (Borneman et al., 2016; Gayevskiy et al., 2016; Peter et al., 2018). Further studies characterizing the genomic similarity between unknown OV strains and European wine strains using whole genome sequencing will be necessary to understand the origin of *S. cerevisiae* strains identified in OV.

None of the 9 identified *S. uvarum* genotypes were isolated from multiple sub-regions. This may indicate that *S. uvarum* genotypes were exclusively associated to a sub-region, although because fermentation conditions were not optimized for *S. uvarum* enrichment, it is difficult to conclude this. The majority of the *S. uvarum* genotypes appear closely related to strains previously isolated from the OV, with the exception of SuOK4, which is closely related to PYCC6860 (**Figure 5**). Interestingly, PYCC6860 was previously isolated from an oak tree on Hornby Island off the coast of Vancouver, British Columbia which is ∼600 km away from the OV (Almeida et al., 2014). The ancestry of *S. uvarum* strains SuOK01 and SuOK02, which appear more distantly related to the reference *S. uvarum* strains, are unknown. *S. uvarum* strains associated with European wine fermentation have prevalent and extensive introgressions from *Saccharomyces eubayanus* whereas strains isolated from the environment, such as PYCC6860, do not (Almeida et al., 2014). Two of our *S. uvarum* strains (SuOK03 and SuOK08) were identical to strains (MLG13 and OV13-11, respectively) that were isolated from industrial spontaneous fermentations conducted in the OV in previous vintages [(McCarthy et al., Unpublished) and unpublished data from this group]. The discovery of these previously isolated *S. uvarum* strains in KE and OO suggests that these strains may be prevalent in OV vineyards, or that they were introduced from the winery via a biological vector.

In the 2017 vintage, we combined our yeast population study with a metabolite analysis of Pinot Noir berries from the same 13 vineyards. Berries collected from all three OV sub-regions contained similar amounts of TSS indicating that grape samples were generally collected at similar developmental stages and ripeness among sub-regions (**Supplementary Table S11**). Therefore, we can exclude ripening effects as a factor influencing our results. Pinot Noir berry weight and seed number were both higher in the NP sub-region than OO and KE which is probably related to higher number of seeds per berry, which was also higher in NP than OO and KE (**Supplementary Table S11**) (Keller, 2010).

Pinot Noir grapes sampled from OO had lower anthocyanin content than NP and KE (**Figure 6A**). Changes in anthocyanin accumulation are likely associated with sub-regional differences in anthocyanin biosynthesis and/or degradation rather than to variation in berry size (Mori et al., 2007). Smaller berry size often results in a higher skin:berry ratio and can promote the concentration of anthocyanins and other skin phenolics (Roby et al., 2004; Wong et al., 2016). However, in this study we observed no differences in skin:berry ratio among sub-regions (**Supplementary Table S11**). In general, anthocyanin biosynthesis is affected by biotic and abiotic factors [reviewed in Teixeira et al. (2013)]. Temperature is known to strongly affect anthocyanin accumulation in grapes (Spayd et al., 2002; Yamane et al., 2006; Mori et al., 2007; Nicholas et al., 2011). At moderate growing temperatures (i.e., 20–25°C) anthocyanin accumulation is promoted, while at relatively high temperatures (30–35°C) anthocyanin accumulation is reduced, possibly because of a lower biosynthesis and/or higher rate of degradation (Yamane et al., 2006; Mori et al., 2007; Artem et al., 2016). Therefore, the temperature differences in the OV sub-regions may have contributed to the observed differences in anthocyanins (**Figure 6A**). Among these 3 sub-regions, active heat summation was highest in OO, with 1,513 GDD, followed by KE, with

1,263 GDD, and lowest in NP, with 1,157 GDD. Furthermore, the number of days with the maximum temperature reaching 35°C was greater in OO (12 days) than KE (7 days) and NP (2 days). Consistent with the previous studies reported above, the lowest levels of anthocyanins were observed in the warmest region (OO).

Aside from temperature, water availability is another factor affecting anthocyanin accumulation because water deficit generally promotes anthocyanin accumulation (Matthews and Anderson, 1989; Castellarin et al., 2007; Savoi et al., 2017). The OV sub-regions had also different cumulative precipitation from April 01 to October 31, 2017. The highest was recorded in NP (198 mm), followed by OO (140 mm), and the lowest in KE (121 mm). Moreover, OO soils are characterized by a lower water holding capacity than NP and KE soils (British Columbia Wine Institute, 2020). However, all the sampled vineyards were irrigated in order to avoid water deficit events. Therefore, we speculate that precipitation and water availability in general had no effect or a limited effect in determining the anthocyanin differences observed among the OV sub-regions.

Similar to the concentration of anthocyanins, flavonol levels varied among the three OV sub-regions (**Figure 6B**). Previous studies have demonstrated that temperature variation and water availability have little or inconsistent effects on flavonol accumulation (Price et al., 1995; Spayd et al., 2002; Downey et al., 2004; Azuma et al., 2012). However, a recent study from our group indicates that, as for anthocyanins, high temperatures (i.e., 30–35°C) impair flavonol accumulation in the berry which is consistent with our observations here that the lowest level of flavonols is in OO, the warmest region (Yan et al., 2020). Studies have shown that sunlight intensity, and particularly the intensity of UV light, positively correlates with flavonol levels in grapes (Price et al., 1995; Spayd et al., 2002; Azuma et al., 2012; Martinez-Luscher et al., 2014a,b; Del-Castillo-Alonso et al., 2016). In this study, radiation levels were not available and a correlation analysis could not be performed.

Seed tannin, but not skin tannin content was affected by the sub-region and the seed tannin data was consistent with the number of seeds per berry (**Figure 6C** and **Supplementary Table S11**). OO had both a lower seed number per berry and lower seed tannin content than NP. This is consistent with previous results indicating that seed tannin content varies with the seed number (Harbertson et al., 2002). Previous studies on the association of grape tannin content with *terroir* have yielded inconsistent results (Ferndandez-Marin et al., 2013; Artem et al., 2016). The effect of environmental factors such as temperature and water availability on tannins still remains unclear as contrasting results have been reported among studies indicating that the grape variety, as well as the interaction among various environmental factors affect tannin content (Cohen et al., 2008; Nicholas et al., 2011; Zarrouk et al., 2012; Genebra et al., 2014; Kyraleou et al., 2017). Based on our study, high temperature (see GDD for OO above) is likely to reduce seed tannin accumulation in Pinot Noir, while a low temperature (see GDD for NP above) is likely to enhance seed tannin accumulation.

Although the proportion of several anthocyanins and flavonols were significantly different in OV sub-regions, there was little consistency among the various compounds. The major anthocyanin accumulated in Pinot Noir berries, M-3-G, was proportionally higher in OO than KE berries and yet, KE and NP berries had the highest total anthocyanin levels (**Figures 6A**, **7A**). Anthocyanins with a higher number of methoxylated groups present in the B-ring, such as M-3-G, are more stable (Yang et al., 2018). Grape berries grown at high temperature (30–35°C) normally have a higher relative abundance of methoxylated anthocyanins and flavonols in grape skins (Mori et al., 2007; Zhu et al., 2017; Yan et al., 2020). The higher proportion of methoxylated anthocyanins in OO than KE berries could be linked to the higher temperatures in OO compared to KE (**Figure 7A**, see GDD for these two regions above). Higher temperatures may favor the synthesis of the more stable methoxylated anthocyanins or, alternatively, may favor the degradation of the non-methoxylated anthocyanins, which in either scenario would cause a relative increase of the methoxylated fraction.

The relative abundance of mono-, di-, tri-substituted flavonols varied by sub-region. We found that the coolest region, KE, had an increase in di-substituted but a decrease in tri-substituted flavonols when compared to OO and NP (**Figure 7B**). Our data is consistent with our recent study of Merlot berries that demonstrated similar effects of di- versus tri-substituted flavonols when low temperatures were compared to high temperatures (Yan et al., 2020). Moreover, Pastore et al. (2017) reported a higher proportion of di-substituted flavonols with increased light exposure of berries. The changes observed in our study are probably driven by the increase in the quercetin conjugates observed in KE berries (**Figure 6B**). Quercetin, a di-substituted flavonol, is the major flavonol produced in Pinot Noir berries and its variable levels in the OV sub-regions might be the major determinant of the shifts in flavonol profile.

At present, we do not have sufficient data to determine if there is any correlation between the *Saccharomyces* strains isolated from OV sub-regions and the flavonoid profiles presented here. It has been shown that grape cultivars may drive *S. cerevisiae* population structure, suggesting there may be adaptation or preference of yeasts to certain grape cultivars (Schuller et al., 2012). *S. cerevisiae* strains have variable effects on final phenolic composition in red wines, which indicates the potential for interaction between regional yeast populations and grape phenolic profiles that is reflected in the finished wine (Carew et al., 2013). Further research is required to determine how regional-specific wine yeast strains and the flavonoid profile of Pinot Noir grapes affect the quality of wine production in the OV.

DATA AVAILABILITY STATEMENT

All datasets generated for this study are included in the article/**Supplementary Material**.

AUTHOR CONTRIBUTIONS

EC collected samples, performed and analyzed *Saccharomyces* microsatellite and polyphenolic data for the 2017 vintage, and contributed to the writing of the manuscript. JM collected samples, designed experiments, performed *Saccharomyces* microsatellite and population analysis for 2016 and 2017 vintages, and contributed to the writing of the manuscript. JH monitored and sampled fermentations and performed commercial *S. cerevisiae* microsatellite analyses. GM collected samples, monitored and sampled fermentations, and performed *Saccharomyces* microsatellite analyses. SC collected samples, analyzed polyphenolic data, and contributed to writing of the manuscript. VM analyzed *Saccharomyces* population data and wrote the manuscript. All authors contributed to the article and approved the submitted version.

FUNDING

This research was supported by a BC Wine Grape Council grant to VM and SC, a MITACS, Inc. Accelerate Project to VM and SC (IT10479), and Natural Sciences and Engineering Research Council of Canada (NSERC) grants to VM (RGPIN-2016-04261) and SC (RGPIN-2015-04760). JM was supported by NSERC-CGS-M, NSERC-CREATE (UBC ECOSCOPE), and American Wine Society Education Fund scholarships. EC was supported by a Mary and David Macaree Fellowship, a Leonard S. Klinck Memorial Fellowship, and an American Society for Enology and Viticulture Traditional Scholarship.

ACKNOWLEDGMENTS

We would like to acknowledge the owners of the 13 vineyards who participated in this study and allowed us to access their vineyards. We would like to thank Lina Madilao at the UBC Wine Research Centre Mass Spectrometry facility for running the grape samples for the anthocyanin and flavonol profiles. We gratefully acknowledge Lallemand and Cellar-Tek for providing us with some of the commercial strains included in this study. We would also like to acknowledge the Durall Lab at UBC-Okanagan for their contribution of commercial *S. cerevisiae* strains to our collection and sharing *S. uvarum* strains prior to publication. Finally, we would like to thank Soon Lee and Richard Gardner at The University of Auckland for contribution of New Zealand *S. uvarum* wine strains.

SUPPLEMENTARY MATERIAL

The Supplementary Material for this article can be found online at: https://www.frontiersin.org/articles/10.3389/fgene.2020.00908/full#supplementary-material

REFERENCES

Almeida, P., Barbosa, R., Zalar, P., Imanishi, Y., Shimizu, K., Turchetti, B., et al. (2015). A population genomics insight into the Mediterranean origins of wine yeast domestication. *Mol. Ecol.* 24, 5412–5427. doi: 10.1111/mec.13341

Almeida, P., Gonçalves, C., Teixeira, S., and Libkind, D. (2014). A Gondwanan imprint on global diversity and domestication of wine and cider yeast *Saccharomyces uvarum*. *Nat. Commun.* 5:4044. doi: 10.1038/ncomms5044

Alonso-Del-Real, J., Lairon-Peris, M., Barrio, E., and Querol, A. (2017). Effect of temperature on the prevalence of saccharomyces non cerevisiae species against a *S. cerevisiae* wine strain in wine fermentation: competition, physiological fitness, and influence in final wine composition. *Front. Microbiol.* 8:150. doi: 10.3389/fmicb.2017.00150

Amerine, M. A., and Winkler, A. J. (1944). Composition and quality of musts and wines of california grapes. *Hilgardia* 15, 493–675. doi: 10.3733/hilg.v15n06p493

Artem, V., Antoce, A. O., Ranca, A., Nechita, A., Enache, L., and Postolache, E. (2016). The Influence of Terroir on Phenolic Composition of Red Grapes. *Bull. Univers. Agric. Sci. Vet. Med. (UASVM) Hortic.* 73, 109–115.

Azuma, A., Yakushiji, H., Koshita, Y., and Kobayashi, S. (2012). Flavonoid biosynthesis-related genes in grape skin are differentially regulated by temperature and light conditions. *Planta* 236, 1067–1080. doi: 10.1007/s00425-012-1650-x

Bakowska-Barczak, A. (2005). Acylated anthocyanins as stable, natural food colorants – A review. *Pol. J. Food Nutr. Sci.* 14, 107–115.

Bardou, P., Mariette, J., Escudie, F., Djemiel, C., and Klopp, C. (2014). jvenn: an interactive Venn diagram viewer. *BMC Bioinf.* 15:293. doi: 10.1186/1471-2105-15-293

Beltran, G., Torija, M. J., Novo, M., Ferrer, N., Poblet, M., Guillamn, J. M., et al. (2002). Analysis of yeast populations during alcoholic fermentation: a six year follow-up study. *Systemat. Appl. Microbiol.* 25, 287–293. doi: 10.1078/0723-2020-00097

Bokulich, N. A., Collins, T. S., Masarweh, C., Allen, G., Heymann, H., Ebeler, S. E., et al. (2016). Associations among wine grape microbiome, metabolome, and fermentation behavior suggest microbial contribution to regional wine characteristics. *mBio*. 7:e00631-16.

Bokulich, N. A., Thorngate, J. H., Richardson, P. M., and Mills, D. A. (2014). Microbial biogeography of wine grapes is conditioned by cultivar, vintage, and climate. *Proc. Natl. Acad. Sci. U.S.A.* 111, E139–E148. doi: 10.1073/pnas.1317377110

Borlin, M., Venet, P., Claisse, O., Salin, F., Legras, J. L., and Masneuf-Pomarede, I. (2016). Cellar-associated *Saccharomyces cerevisiae* population structure revealed high-level diversity and perennial persistence at sauternes wine estates. *Appl. Environ. Microbiol.* 82, 2909–2918. doi: 10.1128/aem.03627-15

Borneman, A. R., Forgan, A. H., Kolouchova, R., Fraser, J. A., and Schmidt, S. A. (2016). Whole genome comparison reveals high levels of inbreeding and strain redundancy across the spectrum of commercial wine strains of *Saccharomyces cerevisiae*. *G3-Genes Genomes Genetics* 6, 957–971. doi: 10.1534/g3.115.025692

Bowen, P. A., Bogdanoff, C. P., Estergaard, B. F., Marsh, S. G., Usher, K. B., Smith, C. A. S., et al. (2005). Geology and wine 10: use of geographic information system technology to assess viticulture performance in the okanagan and similkameen valleys, British Columbia. *Geoscience Canada* 32, 161–176.

British Columbia Wine Institute (2020). *Discovery BC Wine Country*. Available: https://winebc.com/discover-bc-wine-country/ (accessed July 27, 2018). doi: 10.1111/mec.12155

Bruvo, R., Michiels, N. K., D'Souza, T. G., and Schulenburg, H. (2004). A simple method for the calculation of microsatellite genotype distances irrespective of ploidy level. *Mol. Ecol.* 13, 2101–2106. doi: 10.1111/j.1365-294X.2004.02209.x

Bryant, D., and Moulton, V. (2004). Neighbor-net: an agglomerative method for the construction of phylogenetic networks. *Mol. Biol. Evol.* 21, 255–265. doi: 10.1093/molbev/msh018

Capece, A., Pietrafesa, R., Siesto, G., Romaniello, R., Condelli, N., and Romano, P. (2019). Selected indigenous *Saccharomyces cerevisiae* strains as profitable strategy to preserve typical traits of primitivo wine. *Fermentation* 5, 1–17.

Carew, A. L., Smith, P., Close, D. C., Curtin, C., and Dambergs, R. G. (2013). Yeast effects on pinot noir wine phenolics, color, and tannin composition. *J. Agric. Food Chem.* 61, 9892–9898. doi: 10.1021/jf4018806

Castellarin, S. D., Matthews, M. A., Di Gaspero, G., and Gambetta, G. A. (2007). Water deficits accelerate ripening and induce changes in gene expression regulating flavonoid biosynthesis in grape berries. *Planta* 227, 101–112. doi: 10.1007/s00425-007-0598-8

Castillo-Munoz, N., Gomez-Alonso, S., Garcia-Romero, E., and Hermosin-Gutierrez, I. (2007). Flavonol profiles of *Vitis vinifera* red grapes and their single-cultivar wines. *J. Agric. Food Chem.* 55, 992–1002. doi: 10.1021/jf062800k

Cohen, S. D., Tarara, J. M., and Kennedy, J. A. (2008). Assessing the impact of temperature on grape phenolic metabolism. *Anal. Chim. Acta* 621, 57–67. doi: 10.1016/j.aca.2007.11.029

Cordente, A. G., Curtin, C. D., Varela, C., and Pretorius, I. S. (2012). Flavour-active wine yeasts. *Appl. Microbiol. Biotechnol.* 96, 601–618. doi: 10.1007/s00253-012-4370-z

Del-Castillo-Alonso, M. A., Castagna, A., Csepregi, K., Hideg, E., Jakab, G., Jansen, M. A., et al. (2016). Environmental factors correlated with the metabolite profile of *Vitis vinifera* cv, pinot noir berry skins along a european latitudinal gradient. *J. Agric. Food Chem.* 64, 8722–8734. doi: 10.1021/acs.jafc.6b03272

Demuyter, C., Lollier, M., Legras, J. L., and Le Jeune, C. (2004). Predominance of *Saccharomyces uvarum* during spontaneous alcoholic fermentation, for three consecutive years, in an Alsatian winery. *J. Appl. Microbiol.* 97, 1140–1148. doi: 10.1111/j.1365-2672.2004.02394.x

Downey, M. O., Harvey, J. S., and Robinson, S. P. (2004). The effect of bunch shading on berry development and flavonoid accumulation in shiraz grapes. *Austr. J. Grape Wine Res.* 10, 55–73. doi: 10.1111/j.1755-0238.2004.tb00008.x

Downey, M. O., and Rochfort, S. (2008). Simultaneous separation by reversed-phase high-performance liquid chromatography and mass spectral identification of anthocyanins and flavonols in Shiraz grape skin. *J. Chromatogr. A* 1201, 43–47. doi: 10.1016/j.chroma.2008.06.002

Ferndandez-Marin, M. I., Guerrero, R. F., Garcia-Parrilla, M. C., Puertas, B., Ramirez, P., and Cantos-Villar, E. (2013). Terroir and variety: two key factors for obtaining stilbene-enriched grapes. *J. Food Compos. Anal.* 31, 191–198. doi: 10.1016/j.jfca.2013.05.009

Flamini, R., and Traldi, P. (2010). "Grape and wine polyphenols," in *Mass Spectrometry in Grape and Wine Chemistry*, eds D. M. Desiderio and N. M. Nibbering (Hoboken, NJ: John Wiley & Sons, Inc), 163–225. doi: 10.1002/9780470552926.ch6

Fleet, G. H. (2003). Yeast interactions and wine flavour. *Int. J. Food Microbiol.* 86, 11–22. doi: 10.1016/s0168-1605(03)00245-9

Francesca, N., Canale, D. E., Settanni, L., and Moschetti, G. (2012). Dissemination of wine-related yeasts by migratory birds. *Environ. Microbiol. Rep.* 4, 105–112. doi: 10.1111/j.1758-2229.2011.00310.x

Gao, H., Bryc, K., and Bustamante, C. D. (2011). On identifying the optimal number of population clusters via the deviance information criterion. *PLoS ONE* 6:e21014. doi: 10.1371/journal.pone.0021014

Gao, H., Williamson, S., and Bustamante, C. D. (2007). A Markov chain Monte Carlo approach for joint inference of population structure and inbreeding rates from multilocus genotype data. *Genetics* 176, 1635–1651. doi: 10.1534/genetics.107.072371

Garcia-Beneytez, E., Cabello, F., and Revilla, E. (2003). Analysis of grape and wine anthocyanins by HPLC-MS. *J. Agric. Food Chem.* 51, 5622–5629. doi: 10.1021/jf0302207

Gayevskiy, V., and Goddard, M. R. (2012). Geographic delineations of yeast communities and populations associated with vines and wines in New Zealand. *ISME J.* 6, 1281—-1290. doi: 10.1038/ismej.2011.195

Gayevskiy, V., Klaere, S., Knight, S., and Goddard, M. R. (2014). ObStruct: a method to objectively analyse factors driving population structure using Bayesian ancestry profiles. *PLoS One* 9:e85196. doi: 10.1371/journal.pone.0085196

Gayevskiy, V., Lee, S., and Goddard, M. R. (2016). European derived *Saccharomyces cerevisiae* colonisation of New Zealand vineyards aided by humans. *FEMS Yeast Res.* 16:fow091. doi: 10.1093/femsyr/fow091

Genebra, T., Santos, R. R., Francisco, R., Pinto-Marijuan, M., Brossa, R., Serra, A. T., et al. (2014). Proanthocyanidin accumulation and biosynthesis are modulated by the irrigation regime in tempranillo seeds. *Int. J. Mol. Sci.* 15, 11862–11877. doi: 10.3390/ijms150711862

Goddard, M. R., Anfang, N., Tang, R. Y., Gardner, R. C., and Jun, C. (2010). A distinct population of *Saccharomyces cerevisiae* in New Zealand: evidence for local dispersal by insects and human-aided global dispersal in oak barrels. *Environ. Microbiol.* 12, 63–73. doi: 10.1111/j.1462-2920.2009.02035.x

Goddard, M. R., and Greig, D. (2015). *Saccharomyces cerevisiae*: a nomadic yeast with no niche? *FEMS Yeast Res.* 15:fov009.

Gonzalez, M. L., Sturm, M. E., Lerena, M. C., Rojo, M. C., Chimeno, S. V., Combina, M., et al. (2020). Persistence and reservoirs of *Saccharomyces cerevisiae* biodiversity in different vineyard niches. *Food Microbiol.* 86:103328. doi: 10.1016/j.fm.2019.103328

Gould, K. S., and Lister, C. (2005). "Flavonoid function in plants," in *Flavonoids: Chemistry, Biochemistry and Applications*, eds O. M. Anderson and K. R. Markham (Boca Raton, FL: CRC Press), 397–442.

Government of Canada (2020). *Past Weather and Climate: Historical Data [Online]*. Available online at: https://climate.weather.gc.ca/historical_data/search_historic_data_e.html (accessed March 21, 2019).

Hall, B., Durall, D. M., and Stanley, G. (2011). Population dynamics of *Saccharomyces cerevisiae* during spontaneous fermentation at a British Columbia winery. *Am. J. Enol. Viticult.* 62, 66–72. doi: 10.5344/ajev.2010.10054

Harbertson, J. F., Kennedy, J. A., and Adams, D. O. (2002). Tannin in skins and seeds of cabernet sauvignon, syrah, and pinot noir berries during ripening. *Am. J. Enol. Viticul.* 53, 54–59.

Heard, G. M., and Fleet, G. H. (1986). Evaluation of selective media for enumeration of yeasts during wine fermentation. *J. Appl. Bacteriol.* 60, 477–481. doi: 10.1111/j.1365-2672.1986.tb01086.x

Huson, D. H., and Bryant, D. (2006). Application of phylogenetic networks in evolutionary studies. *Mol. Biol. Evol.* 23, 254–267. doi: 10.1093/molbev/msj030

Hyma, K. E., and Fay, J. C. (2013). Mixing of vineyard and oak-tree ecotypes of *Saccharomyces cerevisiae* in North American vineyards. *Mol. Ecol.* 22, 2917–2930. doi: 10.1111/mec.12155

Jakobsson, M., and Rosenberg, N. A. (2007). CLUMPP: a cluster matching and permutation program for dealing with label switching and multimodality in analysis of population structure. *Bioinformatics* 23, 1801–1806. doi: 10.1093/bioinformatics/btm233

Jolly, N. P., Varela, C., and Pretorius, I. S. (2014). Not your ordinary yeast: non-saccharomyces yeasts in wine production uncovered. *FEMS Yeast Res.* 14, 215–237. doi: 10.1111/1567-1364.12111

Kamvar, Z. N., Brooks, J. C., and Grunwald, N. J. (2015). Novel R tools for analysis of genome-wide population genetic data with emphasis on clonality. *Front. Genet.* 6:208. doi: 10.3389/fgene.2015.00208

Kamvar, Z. N., Tabima, J. F., and Grunwald, N. J. (2014). Poppr: an R package for genetic analysis of populations with clonal, partially clonal, and/or sexual reproduction. *PeerJ* 2:e281. doi: 10.7717/peerj.281

Keller, M. (2010). *The Science of Grapevines Anatomy and Physiology*, 1st Edn. Cambridge: Academic Press.

Knight, S., and Goddard, M. R. (2015). Quantifying separation and similarity in a *Saccharomyces cerevisiae* metapopulation. *ISME J* 9, 361–370. doi: 10.1038/ismej.2014.132

Knight, S., Klaere, S., Fedrizzi, B., and Goddard, M. R. (2015). Regional microbial signatures positively correlate with differential wine phenotypes: evidence for a microbial aspect to terroir. *Sci. Rep.* 5:14233. doi: 10.1038/srep14233

Knight, S. J., and Goddard, M. R. (2016). Sporulation in soil as an overwinter survival strategy in *Saccharomyces cerevisiae*. *FEMS Yeast Res.* 16:fov102. doi: 10.1093/femsyr/fov102

Kyraleou, M., Kallithraka, S., Theodorou, N., Teissedre, P. L., Kotseridis, Y., and Koundouras, S. (2017). Changes in tannin composition of syrah grape skins and seeds during fruit ripening under contrasting water conditions. *Molecules* 22:1453. doi: 10.3390/molecules22091453

Legras, J. L., Merdinoglu, D., Cornuet, J. M., and Karst, F. (2007). Bread, beer and wine: *Saccharomyces cerevisiae* diversity reflects human history. *Mol. Ecol.* 16, 2091–2102. doi: 10.1111/j.1365-294X.2007.03266.x

Legras, J. L., Ruh, O., Merdinoglu, D., and Karst, F. (2005). Selection of hypervariable microsatellite loci for the characterization of *Saccharomyces cerevisiae* strains. *Int. J. Food Microbiol.* 102, 73–83. doi: 10.1016/j.ijfoodmicro.2004.12.007

Liti, G., Carter, D. M., Moses, A. M., Warringer, J., Parts, L., James, S. A., et al. (2009). Population genomics of domestic and wild yeasts. *Nature* 458, 337–341. doi: 10.1038/nature07743

Lopez-Malo, M., Querol, A., and Guillamon, J. M. (2013). Metabolomic comparison of *Saccharomyces cerevisiae* and the cryotolerant species S. *bayanus*

var. uvarum and *S. kudriavzevii* during wine fermentation at low temperature. *PLoS ONE* 8:e60135. doi: 10.1371/journal.pone.0060135

Luck, E., and Jager, M. (1997). *Biphenyl. In Antimicrobial food additives: characteristics, uses, effects*. Berlin, Germany: Springer-Verlag.

Martinez-Luscher, J., Sanchez-Diaz, M., Delrot, S., Aguirreolea, J., Pascual, I., and Gomes, E. (2014a). Ultraviolet-B radiation and water deficit interact to alter flavonol and anthocyanin profiles in grapevine berries through transcriptomic regulation. *Plant Cell Physiol.* 55, 1925–1936. doi: 10.1093/pcp/pcu121

Martinez-Luscher, J., Torres, N., Hilbert, G., Richard, T., Sanchez-Diaz, M., Delrot, S., et al. (2014b). Ultraviolet-B radiation modifies the quantitative and qualitative profile of flavonoids and amino acids in grape berries. *Phytochemistry* 102, 106–114. doi: 10.1016/j.phytochem.2014.03.014

Martiniuk, J. T., Pacheco, B., Russell, G., Tong, S., Backstrom, I., and Measday, V. (2016). Impact of commercial strain use on *Saccharomyces cerevisiae* population structure and dynamics in pinot noir vineyards and spontaneous fermentations of a canadian winery. *PLoS ONE* 11:e0160259. doi: 10.1371/journal.pone.0160259

Masneuf, I., Aigle, M., and Dubourdieu, D. (1996). Development of a polymerase chain reaction/restriction fragment length polymorphism method for *Saccharomyces cerevisiae* and *Saccharomyces bayanus* identification in enology. *FEMS Microbiol. Lett.* 138, 239–244. doi: 10.1111/j.1574-6968.1996.tb08164.x

Masneuf-Pomarede, I., Bely, M., Marullo, P., Lonvaud-Funel, A., and Dubourdieu, D. (2010). Reassessment of phenotypic traits for *Saccharomyces bayanus* var. uvarum wine yeast strains. *Int. J. Food Microbiol.* 139, 79–86. doi: 10.1016/j.ijfoodmicro.2010.01.038

Masneuf-Pomarede, I., Salin, F., Börlin, M., Coton, E., Coton, M., Jeune, C. L., et al. (2016). Microsatellite analysis of *Saccharomyces uvarum* diversity. *FEMS Yeast Res.* 16:fow002.

Matthews, M. A., and Anderson, M. M. (1989). Reproductive development in grape (*Vitis vinifera* L.): responses to seasonal water deficits. *Am. J. Enol. Viticult.* 40, 52–60.

Matus, J. T., Loyola, R., Vega, A., Pena-Neira, A., Bordeu, E., Arce-Johnson, P., et al. (2009). Post-veraison sunlight exposure induces MYB-mediated transcriptional regulation of anthocyanin and flavonol synthesis in berry skins of *Vitis vinifera*. *J. Exp. Bot.* 60, 853–867. doi: 10.1093/jxb/ern336

Mazza, G., Fukumoto, L., Delaquis, P., Girard, B., and Ewert, B. (1999). Anthocyanins, phenolics, and color of cabernet franc, merlot, and pinot noir wines from british columbia. *J. Agric. Food Chem.* 47, 4009–4017. doi: 10.1021/jf990449f

Morgan, S. C., Haggerty, J. J., Jiranek, V., and Durall, D. M. (2020). Competition between *Saccharomyces cerevisiae* and *Saccharomyes uvarum* in controlled chardonnay wine fermentations . *Am. J. Enol. Viticult.* 71, 198–207. doi: 10.5344/ajev.2020.19072

Morgan, S. C., McCarthy, G. C., Watters, B. S., Tantikachornkiat, M., Zigg, I., Cliff, M. A., et al. (2019). Effect of sulfite addition and pied de cuve inoculation on the microbial communities and sensory profiles of *Chardonnay wines*: dominance of indigenous *Saccharomyces uvarum* at a commercial winery. *FEMS Yeast Res* 19:foz049. doi: 10.1093/femsyr/foz049

Mori, K., Goto-Yamamoto, N., Kitayama, M., and Hashizume, K. (2007). Loss of anthocyanins in red-wine grape under high temperature. *J. Exp. Bot.* 58, 1935–1945. doi: 10.1093/jxb/erm055

Morrison-Whittle, P., Lee, S. A., and Goddard, M. R. (2017). Fungal communities are differentially affected by conventional and biodynamic agricultural management approaches in vineyard ecosystems. *Agricult. Ecosyst. Environ.* 246, 306–313. doi: 10.1016/j.agee.2017.05.022

Mortimer, R., and Polsinelli, M. (1999). On the origins of wine yeast. *Res. Microbiol.* 150, 199–204. doi: 10.1016/s0923-2508(99)80036-9

Nicholas, K. A., Matthews, M. A., Lobell, D. B., Willits, N. H., and Field, C. B. (2011). Effect of vineyard-scale climate variability on pinot noir phenolic composition. *Agricult. For. Meterol.* 151, 1556–1567. doi: 10.1016/j.agrformet.2011.06.010

Op, De Beeck, M., Lievens, B., Busschaert, P., Declerck, S., Vangronsveld, J., et al. (2014). Comparison and validation of some ITS primer pairs useful for fungal metabarcoding studies. *PLoS ONE* 9:e97629. doi: 10.1371/journal.pone.0097629

Pallman, C. L., Brown, J. A., Olineka, T. L., Cocolin, L., Mills, D. A., and Bisson, L. F. (2001). Use of WL medium to profile native flora fermentations. *Am. J. Enol. Viticult.* 52, 198–203.

Pastore, C., Allegro, G., Valentini, G., Muzzi, E., and Filippetti, I. (2017). Anthocyanin and flavonol composition response to veraison leaf removal on Cabernet Sauvignon, Nero d'Avola, raboso piave and sangiovese *Vitis vinifera* L. cultivars. *Sci. Horticult.* 218, 147–155. doi: 10.1016/j.scienta.2017.01.048

Peter, J., De Chiara, M., Friedrich, A., Yue, J. X., Pflieger, D., Bergstrom, A., et al. (2018). Genome evolution across 1011 *Saccharomyces cerevisiae* isolates. *Nature* 556, 339–344. doi: 10.1038/s41586-018-0030-5

Pollastri, S., and Tattini, M. (2011). Flavonols: old compounds for old roles. *Ann. Bot.* 108, 1225–1233. doi: 10.1093/aob/mcr234

Pretorius, I. S. (2000). Tailoring wine yeast for the new millennium: novel approaches to the ancient art of winemaking. *Yeast* 16, 675–729. doi: 10.1002/1097-0061(20000615)16:8<675::aid-yea585>3.0.co;2-b

Price, S. F., Breen, P. J., Valladao, M., and Watson, B. T. (1995). Cluster sun exposure and quercetin in pinot noir grapes and wine. *Am. J. Enol. Viticult.* 46, 187–194.

Rantsiou, K., Marengo, F., Englezos, V., Torchio, F., Giacosa, S., Rolle, L., et al. (2017). *Saccharomyces cerevisiae* biodiversity in monferrato, North West Italy, and selection of indigenous starter cultures for barbera wine production. *Ital. J. Food Sci.* 29, 518–536.

Redzepovic, S., Orlic, S., Sikora, S., Majdak, A., and Pretorius, I. S. (2002). Identification and characterization of *Saccharomyces cerevisiae* and *Saccharomyces paradoxus* strains isolated from Croatian vineyards. *Lett. Appl. Microbiol.* 35, 305–310. doi: 10.1046/j.1472-765x.2002.01181.x

Richards, K. D., Goddard, M. R., and Gardner, R. C. (2009). A database of microsatellite genotypes for *Saccharomyces cerevisiae*. *Antonie Van Leeuwenhoek* 96, 355–359. doi: 10.1007/s10482-009-9346-3

Roby, G., Harbertson, J. F., Adams, D. O., and Matthews, M. A. (2004). Berry size and vine water deficits as factors in winegrape composition: anthocyanins and tannins. *Austr. J. Grape Wine Res.* 10, 100–107. doi: 10.1111/j.1755-0238.2004.tb00012.x

Rosenberg, N. A. (2004). DISTRUCT: a program for the graphical display of population structure. *Mol. Ecol. Notes* 4, 137–138. doi: 10.1046/j.1471-8286.2003.00566.x

Savoi, S., Wong, D. C. J., Degu, A., Herrera, J. C., Bucchetti, B., Peterlunger, E., et al. (2017). Multi-omics and integrated network analyses reveal new insights into the systems relationships between metabolites, structural genes, and transcriptional regulators in developing grape berries (*Vitis vinifera* L.) Exposed to Water Deficit. *Front. Plant Sci.* 8:1124. doi: 10.3389/fpls.2017.01124

Schacherer, J., Shapiro, J. A., Ruderfer, D. M., and Kruglyak, L. (2009). Comprehensive polymorphism survey elucidates population structure of *Saccharomyces cerevisiae*. *Nature* 458, 342–U103. doi: 10.1038/nature07670

Scholl, C. M., Morgan, S. C., Stone, M. L., Tantikachornkiat, M., Neuner, M., and Durall, D. M. (2016). Composition of *Saccharomyces cerevisiae* strains in spontaneous fermentations of Pinot Noir and Chardonnay. *Austr. J. Grape Wine Res.* 22, 384—-390. doi: 10.1111/ajgw.12221

Schuller, D., Cardoso, F., Sousa, S., Gomes, P., Gomes, A. C., Santos, M. A. S., et al. (2012). Genetic diversity and population structure of *Saccharomyces cerevisiae* strains isolated from different grape varieties and winemaking regions. *PLoS ONE* 7:e32507. doi: 10.1371/journal.pone.0032507

Senese, D. M., Wilson, W., and Momer, B. (2012). "The Okanagan wine region of British Columbia," in *The Geography of Wine: Regions, Terroir and Techniques*, Chap. 5, ed. P. H. Dougherty (Dordrecht: Springer), 81–91.

Setati, M. E., Jacobson, D., Andong, U. C., and Bauer, F. F. (2012). The vineyard yeast microbiome, a mixed model microbial map. *PLoS ONE* 7:e52609. doi: 10.1371/journal.pone.0052609

Singleton, P., and Sainsbury, D. (1987). *Dictionary of Microbiology and Molecular Biology*. Chichester: John Wiley & Sons.

Sipiczki, M. (2016). Overwintering of vineyard yeasts: survival of interacting yeast communities in grapes mummified on vines. *Front. Microbiol.* 7:212. doi: 10.3389/fmicb.2016.00212

Spayd, S. E., Tarara, J. M., Mee, D. L., and Ferguson, J. C. (2002). Separation of sunlight and temperature effects on the composition of vitis vinifera cv. merlot berries. *Am. J. Enol. Viticult.* 53, 171–182.

Styger, G., Prior, B., and Bauer, F. F. (2011). Wine flavor and aroma. *J. Ind. Microbiol. Biotechnol.* 38, 1145–1159.

Su, Y., Origone, A. C., Rodriguez, M. E., Querol, A., Guillamon, J. M., and Lopes, C. A. (2019). Fermentative behaviour and competition capacity of cryotolerant *Saccharomyces* species in different nitrogen conditions. *Int. J. Food Microbiol.* 291, 111–120. doi: 10.1016/j.ijfoodmicro.2018.11.020

Teixeira, A., Eiras-Dias, J., Castellarin, S. D., and Geros, H. (2013). Berry phenolics of grapevine under challenging environments. *Int. J. Mol. Sci.* 14, 18711–18739. doi: 10.3390/ijms140918711

Tello, J., Cordero-Bueso, G., Aporta, I., Cabellos, J. M., and Arroyo, T. (2011). Genetic diversity in commercial wineries: effects on farming system and vinification management on wine yeasts. *J. Appl. Microbiol.* 112, 302–315. doi: 10.1111/j.1365-2672.2011.05202.x

Tofalo, R., Perpetuini, G., Schirone, M., Fasoli, G., Aguzzi, I., Corsetti, A., et al. (2013). Biogeographical characterization of *Saccharomyces cerevisiae* wine yeast by molecular methods. *Front. Microbiol.* 4:166. doi: 10.3389/fmicb.2013.00166

Tosi, E., Azzolini, M., Guzzo, F., and Zapparoli, G. (2009). Evidence of different fermentation behaviours of two indigenous strains of *Saccharomyces cerevisiae* and *Saccharomyces uvarum* isolated from Amarone wine. *J. Appl. Microbiol.* 107, 210–218. doi: 10.1111/j.1365-2672.2009.04196.x

Trouillas, P., Sancho-Garcia, J. C., De Freitas, V., Gierschner, J., Otyepka, M., and Dangles, O. (2016). Stabilizing and modulating color by copigmentation: insights from theory and experiment. *Chem. Rev.* 116, 4937–4982. doi: 10.1021/acs.chemrev.5b00507

Valero, E., Cambon, B., Schuller, D., Casal, M., and Dequin, S. (2007). Biodiversity of Saccharomyces yeast strains from grape berries of wine-producing areas using starter commercial yeasts. *FEMS Yeast Res.* 7, 317–329. doi: 10.1111/j.1567-1364.2006.00161.x

Valero, E., Schuller, D., Cambon, B., Casal, M., and Dequin, S. (2005). Dissemination and survival of commercial wine yeast in the vineyard: a large-scale, three-years study. *FEMS Yeast Res.* 5, 959–969. doi: 10.1016/j.femsyr.2005.04.007

van Leeuwen, C. (2010). "Terroir: the effect of the physical environment on vine growth, grape ripening and wine sensory attributes," in *Managing Wine Quality*, ed. A. G. Reynolds (Cambridge: Woodhead Publishing), 273–315. doi: 10.1533/9781845699284.3.273

van Leeuwen, C., and Seguin, G. (2006). The concept of terroir in viticulture. *J. Wine Res.* 17, 1–10. doi: 10.1080/09571260600633135

Varela, C., and Borneman, A. R. (2017). Yeasts found in vineyards and wineries. *Yeast* 34, 111–128. doi: 10.1002/yea.3219

Vaudano, E., Quinterno, G., Costantini, A., Pulcini, L., Pessione, E., and Garcia-Moruno, E. (2019). Yeast distribution in grignolino grapes growing in a new vineyard in Piedmont and the technological characterization of indigenous *Saccharomyces* spp. strains. *Int. J. Food Microbiol.* 289, 154–161. doi: 10.1016/j.ijfoodmicro.2018.09.016

Viel, A., Legras, J. L., Nadai, C., Carlot, M., Lombardi, A., Crespan, M., et al. (2017). The geographic distribution of *Saccharomyces cerevisiae* isolates within three italian neighboring winemaking regions reveals strong differences in yeast abundance, genetic diversity and industrial strain dissemination. *Front. Microbiol.* 8:1595. doi: 10.3389/fmicb.2017.01595

Willwerth, J. J., Reynolds, A. G., and Lesschaeve, I. (2010). Terroir factors: their impact in the vineyard and on the sensory profiles of riesling wines. *Le Progres Agricole et Viticole* 8, 159–168.

Wong, D. C., Lopez Gutierrez, R., Dimopoulos, N., Gambetta, G. A., and Castellarin, S. D. (2016). Combined physiological, transcriptome, and cis-regulatory element analyses indicate that key aspects of ripening, metabolism, and transcriptional program in grapes (*Vitis vinifera* L.) are differentially modulated accordingly to fruit size. *BMC Genomics* 17:416. doi: 10.1186/s12864-016-2660-z

Yamane, T., Jeong, S. T., Goto-Yamamoto, N., Koshita, Y., and Kobayashi, S. (2006). Effects of temperature on anthocyanin biosynthesis in grape berry skins. *Am. J. Enol. Viticult.* 57, 54–59.

Yan, Y., Song, C., Falginella, L., and Castellarin, S. D. (2020). Effect of temperature regimes on flavonoids accumulation in 'Merlot' (*Vitis vinifera* L.) grapes. *Food Chem.* doi: 10.3389/fpls.2020.01095

Yang, P., Yuan, C., Wang, H., Han, F., Liu, Y., Wang, L., et al. (2018). Stability of anthocyanins and their degradation products from cabernet sauvignon red wine under gastrointestinal pH and temperature conditions. *Molecules* 23:354. doi: 10.3390/molecules23020354

Zarrouk, O., Francisco, R., Pinto-Marijuan, M., Brossa, R., Santos, R. R., Pinheiro, C., et al. (2012). Impact of irrigation regime on berry development and flavonoids composition in aragonez (syn. tempranillo) grapevine. *Agric. Water Manage.* 114, 18–29. doi: 10.1016/j.agwat.2012.06.018

Zhang, H. Y., Richards, K. D., Wilson, S., Lee, S. A., Sheehan, H., Roncoroni, M., et al. (2015). Genetic characterization of strains of Saccharomyces uvarum from New Zealand wineries. *Food Microbiol.* 46, 92–99. doi: 10.1016/j.fm.2014.07.016

Zhu, L., Huang, Y., Zhang, Y., Xu, C., Lu, J., and Wang, Y. (2017). The growing season impacts the accumulation and composition of flavonoids in grape skins in two-crop-a-year viticulture. *J. Food Sci. Technol.* 54, 2861–2870. doi: 10.1007/s13197-017-2724-3

Conflict of Interest: The authors declare that the research was conducted in the absence of any commercial or financial relationships that could be construed as a potential conflict of interest.

Advantages of publishing in Frontiers

OPEN ACCESS
Articles are free to read for greatest visibility and readership

FAST PUBLICATION
Around 90 days from submission to decision

HIGH QUALITY PEER-REVIEW
Rigorous, collaborative, and constructive peer-review

TRANSPARENT PEER-REVIEW
Editors and reviewers acknowledged by name on published articles

Frontiers
Avenue du Tribunal-Fédéral 34
1005 Lausanne | Switzerland

Visit us: www.frontiersin.org
Contact us: frontiersin.org/about/contact

REPRODUCIBILITY OF RESEARCH
Support open data and methods to enhance research reproducibility

DIGITAL PUBLISHING
Articles designed for optimal readership across devices

FOLLOW US
@frontiersin

IMPACT METRICS
Advanced article metrics track visibility across digital media

EXTENSIVE PROMOTION
Marketing and promotion of impactful research

LOOP RESEARCH NETWORK
Our network increases your article's readership